

***INTERNATIONAL CONFERENCE
SYNCHROTRON RADIATION
INSTRUMENTATION
SRI '94***

RECEIVED
OCT 12 1994
OSTI

Hosted by the
National Synchrotron Light Source
Brookhaven National Laboratory
at the
State University of New York at Stony Brook

JULY 18 - 22, 1994

Conference Chair:	Denis B. McWhan
Program Chair:	J. B. Hastings
Local Committee Chair:	Gwyn P. Williams

Program Committee:

J. Als-Nielsen	ESRF	J. Kirz	SUNY
C.T. Chen	AT&T Bell Labs	K. Kohra	Tokyo
W. Eberhardt	Julich	G. Materlik	DESY
J. Galayda	Argonne	T. Matsushita	KEK
M. Hart	U. Manchester	P. Thiry	LURE
K. Hodgson	Stanford U.	A.H. Walenta	U. Siegen

MASTER

DISCLAIMER

This report was prepared as an account of work sponsored by an agency of the United States Government. Neither the United States Government nor any agency thereof, nor any of their employees, nor any of their contractors, subcontractors, or their employees, makes any warranty, express or implied, or assumes any legal liability or responsibility for the accuracy, completeness, or usefulness of any information, apparatus, product, or process disclosed, or represents that its use would not infringe privately owned rights. Reference herein to any specific commercial product, process, or service by trade name, trademark, manufacturer, or otherwise, does not necessarily constitute or imply its endorsement, recommendation, or favoring by the United States Government or any agency, contractor or subcontractor thereof. The views and opinions of authors expressed herein do not necessarily state or reflect those of the United States Government or any agency, contractor or subcontractor thereof.

DISCLAIMER

Portions of this document may be illegible in electronic image products. Images are produced from the best available original document.

INTERNATIONAL ADVISORY COMMITTEE

Prof. C. Goncalves da Silva	LNLS, Campinas, Brasil
Prof. E. Tang	BSRL, Beijing, People's Republic of China
Prof. Liu Nasquan	NSRL, People's Republic of China
Prof. Yuen-Chung Liu	SRRC, Taiwan ROC
Prof. E. Uggerhoj	Institute for Synchrotron Radiation, Denmark
Prof. Y. Petroff	ESRF, France
Prof. R. Comès	LURE, France
Prof. W. Gudat	BESSY, Germany
Prof. J. Hormes	BONN II, Germany
Prof. J. R. Schneider	HASYLAB, Germany
Prof. E. Iarocci	INFN-LNF, Italy
Prof. R. Rosei	ELETTRA, Italy
Prof. H. Kamitsubo	SPring-8, Japan
Prof. N. Kosugi	UVSOR, Japan
Dr. E. Toyota	AURORA, Japan
Prof. T. Ishii	SRL-ISSP, Japan
Prof. M. Kihara	Photon Factory, Japan
Prof. T-N. Lee	Pohang Light Source, Korea
Dr. R. Nyholm	MAX, Sweden
Prof. J. Bordas	SRS, United Kingdom
Dr. D. Moncton	APS, United States
Dr. V. Saile	CAMD, United States
Dr. B. Kincaid	ALS, United States
Prof. B. Batterman	CHESSE, United States
Dr. R. Madden	SURF-II, United States
Prof. A. Bienenstock	SSRL, United States
Prof. D. Huber	SRC, United States
Prof. I.M. Karnauchov	Kharkov, Ukraine
Prof. S. T. Belyaev	KSRS, Russia
Prof. G. Kulipanov	SSRC, Russia

Time	MONDAY, JULY 18, 1994																																		
MATERIALS CHARACTERIZATION / BIOLOGY																																			
MoA Staller Center Chairpersons: J. Chikawa (Himeji); D. McWhan (NSLS)																																			
8:30	Dr. John H. Marburger, President, SUNY at Stony Brook																																		
8:45	Dr. Nicholas P. Samios, Director, Brookhaven National Laboratory																																		
9:00	T. Blundell (Birbeck College)																																		
9:45	<i>X-rays in Biology</i>																																		
9:45	S.K. Sinha (Exxon)																																		
10:30	<i>Materials Characterization</i>																																		
10:30	Coffee Break																																		
<table border="1" style="width: 100%; border-collapse: collapse;"> <thead> <tr> <th data-bbox="199 825 343 1038"></th> <th data-bbox="343 825 882 1038" style="text-align: center;"> MoB Staller Center Chairpersons: J. Kirz (SUNY SB) T. Matsushita (PF) </th> <th data-bbox="882 825 1445 1038" style="text-align: center;"> MoC Student Union Chairpersons: B. Lengeler (ESRF) A. Savoia (ELETTRA) </th> </tr> </thead> <tbody> <tr> <td data-bbox="199 1038 343 1070">11:00</td> <td data-bbox="343 1038 882 1070">S. Williams (SUNYSB)</td> <td data-bbox="882 1038 1445 1070">P. Pianetta (SSRL)</td> </tr> <tr> <td data-bbox="199 1076 343 1108"></td> <td data-bbox="343 1076 882 1108"><i>Scanning x-ray microscopy</i></td> <td data-bbox="882 1076 1445 1108"><i>Impurity characterization in</i></td> </tr> <tr> <td data-bbox="199 1115 343 1146"></td> <td data-bbox="343 1115 882 1146"></td> <td data-bbox="882 1115 1445 1146"><i>semiconductors</i></td> </tr> <tr> <td data-bbox="199 1153 343 1185">11:20</td> <td data-bbox="343 1153 882 1185">N. Sakabe (PF)</td> <td data-bbox="882 1153 1445 1185">J. Reffner (Spectra Tech)</td> </tr> <tr> <td data-bbox="199 1191 343 1223"></td> <td data-bbox="343 1191 882 1223"><i>Weissenberg camera at PF</i></td> <td data-bbox="882 1191 1445 1223"><i>IR microscopy</i></td> </tr> <tr> <td data-bbox="199 1229 343 1261">11:40</td> <td data-bbox="343 1229 882 1261">G. Schmal (Gottingen)</td> <td data-bbox="882 1229 1445 1261">G. Zachmann (Hamburg)</td> </tr> <tr> <td data-bbox="199 1268 343 1300"></td> <td data-bbox="343 1268 882 1300"><i>Phase contrast x-ray microscope</i></td> <td data-bbox="882 1268 1445 1300"><i>Polymer fibers</i></td> </tr> <tr> <td data-bbox="199 1306 343 1338">12:00</td> <td data-bbox="343 1306 882 1338">N. Allinson (York)</td> <td data-bbox="882 1306 1445 1338">B. Tonner (Wisconsin)</td> </tr> <tr> <td data-bbox="199 1344 343 1376"></td> <td data-bbox="343 1344 882 1376"><i>Instrumentation for protein</i></td> <td data-bbox="882 1344 1445 1376"><i>Magnetic Imaging</i></td> </tr> <tr> <td data-bbox="199 1383 343 1415"></td> <td data-bbox="343 1383 882 1415"><i>crystallography</i></td> <td data-bbox="882 1383 1445 1415"></td> </tr> </tbody> </table>				MoB Staller Center Chairpersons: J. Kirz (SUNY SB) T. Matsushita (PF)	MoC Student Union Chairpersons: B. Lengeler (ESRF) A. Savoia (ELETTRA)	11:00	S. Williams (SUNYSB)	P. Pianetta (SSRL)		<i>Scanning x-ray microscopy</i>	<i>Impurity characterization in</i>			<i>semiconductors</i>	11:20	N. Sakabe (PF)	J. Reffner (Spectra Tech)		<i>Weissenberg camera at PF</i>	<i>IR microscopy</i>	11:40	G. Schmal (Gottingen)	G. Zachmann (Hamburg)		<i>Phase contrast x-ray microscope</i>	<i>Polymer fibers</i>	12:00	N. Allinson (York)	B. Tonner (Wisconsin)		<i>Instrumentation for protein</i>	<i>Magnetic Imaging</i>		<i>crystallography</i>	
	MoB Staller Center Chairpersons: J. Kirz (SUNY SB) T. Matsushita (PF)	MoC Student Union Chairpersons: B. Lengeler (ESRF) A. Savoia (ELETTRA)																																	
11:00	S. Williams (SUNYSB)	P. Pianetta (SSRL)																																	
	<i>Scanning x-ray microscopy</i>	<i>Impurity characterization in</i>																																	
		<i>semiconductors</i>																																	
11:20	N. Sakabe (PF)	J. Reffner (Spectra Tech)																																	
	<i>Weissenberg camera at PF</i>	<i>IR microscopy</i>																																	
11:40	G. Schmal (Gottingen)	G. Zachmann (Hamburg)																																	
	<i>Phase contrast x-ray microscope</i>	<i>Polymer fibers</i>																																	
12:00	N. Allinson (York)	B. Tonner (Wisconsin)																																	
	<i>Instrumentation for protein</i>	<i>Magnetic Imaging</i>																																	
	<i>crystallography</i>																																		
12:30	LUNCH																																		
2-5:30	MATERIALS/BIOLOGY POSTERS (MoD)																																		
6:00	DINNER																																		
7:00	FACILITY POSTERS																																		
10:00	COOPERATIVE PHENOMENA POSTERS (MoE)																																		

Session MoB - Invited Talks

Weissenberg camera for macromolecules with imaging plate data collection system at the Photon Factory

Present status and future plan

N.Sakabe¹⁾, K.Sakabe²⁾, T.Higashi³⁾, A.Nakagawa⁴⁾, N.Watanabe⁴⁾, S. Adachi⁵⁾, S. Ikemizu¹⁾ & K. Sasaki⁶⁾. 1) Institute of Applied Biochemistry, University of Tsukuba, Tsukuba, Ibaraki, 305 Japan. 2) Department of Chemistry, Faculty of Science, Nagoya University, Chikusa, Nagoya 464 Japan. 3) Rigaku Corporation, Matsubara, Akishima, Tokyo 196 Japan. 4) Photon Factory, National Laboratory for High Energy Physics, Tsukuba, 305 Japan. 5) The Institute of Physical and Chemical Research (RIKEN), Hirosawa 2-1, Wako, Saitama, 351-01 Japan. 6) College of Medical Technology, Nagoya University, Nagoya 461 Japan.

The photon Factory is operating at 2.5GeV and 300mA. There are two data collection systems for macromolecular crystallography at BL6A and BL18B, consisting of Weissenberg camera, imaging plate (IP), image reader (BA100 & BAS2000), data reduction program "WEIS" and auto-indexing program. The optical system of BL6A is equipped with bent plane fused quartz mirror and triangular bent asymmetric cut Si(111) monochromator and that of BL18B is equipped with 1m long fused quartz bent cylindrical Pt coated mirror with 1:1 focusing and a double-crystal monochromator which can be changed either using Si(111) or Ge(111) without opening the mirror house.

The main basic ideas of Weissenberg camera for macromolecular crystallography are 1) Film cassette should be designed cylindrical to get higher resolution data nicely, 2) the radius(r) of film cassette must be the larger the better because background noise will decrease approximately proportional to r^2 ; on the other hand, Bragg reflections do not be affected so much by r^2 . 3) About ten times more reflection data will be recorded on a film than those of just oscillation method, when the Weissenberg geometry will be applied. 4) Bijvoet pairs are recorded with high accuracy on the same film as simultaneous reflections. 5) Almost all X-

ray pass should be filled with helium gas to reduce the scattering and absorption by air.

The fundamental requirements for the detection of X-ray diffraction from protein crystals are : 1) high detective quantum efficiency, 2) wide dynamic range, 3) linearity of response, 4) high spatial resolution, 5) large detective area, 6) uniformity of response, 7) high counting rate capability and 8) low back ground noise. A X-ray integrated-type area detector, called an imaging plate (IP) is one of the most suitable detectors for the data collection of X-ray diffraction from protein crystals. The combination with the camera, IP and SRX-ray becomes a very powerful (N. Sakabe, Nucl. Instr. and Meth., 1991, A303. 448).

The camera type III was designed for PF users at BL6A station. Normally, one data set around an axis is recorded on 10-30 IP sheets with consuming only one or two crystals and 5-10 sets of data are collected in 24 hours. The size of IP which we are using is 400x200mm. Strong demanding of the large size of IP, we have developed 800x400mm and 400x400mm IPs and its reader. This reader is a drum type and is a linear scale to 262,144 steps. The linearity of the scanner is observed $1-1 \times 10^5$ photons per a pixel (0.1x0.1 mm) by using monochromatized Cu $K\alpha$ X-ray radiation. We will open this scanner to our users from the next October. We are developing a new type camera taken with Weissenberg photograph using monochromatic beam and time resolved Laue photograph using polychromatic beams. This camera has 430mm and 1,290mm radius cassette, and IP is fixed to the cassette by reduced pressure. Number of the proposal to BL6A and BL18B is 71 in domestic and 41 from overseas. Because the stations are so busy that we can only allocate two days for each proposal per one year. We want to built another beam line for protein crystallography as early as possible.

SR Instrumentation for Optimised Anomalous Scattering and High Resolution Crystal Structure Studies of Proteins and Nucleic Acids

A Deacon¹, J Habash¹, S J Harrop¹, J R Helliwell¹, W N Hunter¹, G A Leonard¹, M Peterson¹, A Hadener², A J Kalb (Gilboa)³, N M Allinson⁴, C Castelli⁴, S McSweeney⁵, A Gonzalez⁶ and A W Thompson⁶.

University of Manchester¹, University of Basle², Weizmann Institute³, University of York⁴, Daresbury Laboratory⁵ and EMBL/ESRF Grenoble⁶.

Crystal structure solution by anomalous dispersion methods has been greatly facilitated using the rapidly tunable station 9.5 at Daresbury (1, 2, 3). We have successfully used SIROAS and MAD techniques in the structure solution of a brominated nucleotide and a seleno-deaminase respectively. Data were recorded with an online image plate device. The brominated nucleotide required two data sets involving slow and quick exposures so as to acquire the full dynamic intensity range of these data. The seleno-deaminase MAD data collection involved multiple wedges of data as is the case with this approach. The data collection times were considerably lengthened by the duty cycle of the detector. Hence, the instrument represents a considerable step forward but improvements can be made in the methodology to accelerate the number of projects that can be accommodated.

Detailed structure refinement pushes the limits of resolution and quality of data. In a study of the lectin protein, concanavalin A, by using very short wavelengths (0.7Å), the image plate device referred to above and crystal freezing, data have been collected on 9.5 for the sugar free form to 1.4Å resolution. A total of 250,000 reflections have been measured from two crystals. Again a slow and quick pass are required to capture the dynamic range of the data. The duty cycle of the detector is not the limiting factor for the slow pass data but rather the beam intensity. There are also data seen to 1.2Å and beyond for a pure Mn substituted form of the protein. A higher intensity still is required to actually record these weak data at the highest resolution possible. Even shorter wavelengths (e.g. 0.5Å or less) will essentially remove sample absorption errors. These data might therefore be considered ideal. The provision of a new source like the ESRF will allow such data to be collected routinely.

Possibilities at ESRF offer further impetus for the field (4). These include more intense rapidly tunable beams for anomalous dispersion based structure solution and higher resolution data collection and reactivity studies. A detailed design for such a station on an ESRF bending magnet is described in ref. 5 (BL19). Facilities on BL19 are to include a system for freezing and storing crystals at cryogenic temperatures, so that data can be recorded from the same frozen crystal on different runs.

In all these categories of data collection the detector can certainly be improved upon whereby the DQE of the image plate at weaker signals and the poor duty cycle are serious limitations. A columnar based CsI scintillator coupled CCD offers enhanced PSF, DQE and duty cycle performance [6]. These advantageous properties have to be realised without sacrificing overall aperture, an important characteristic of the image plate, and so require designs involving the butting of several CCD devices together.

References

1. Brammer, R, Helliwell, J R (1988) Nucl. Instrum. & Methods, A271, 678–687.
2. Thompson, A W, Nave, C, et al. (1992) Rev. Sci. Inst., 63(1), 1062–1064.
3. McSweeney, S, et al. (1994) Proceedings of this meeting.
4. Helliwell, J R (1987) ESRF Red Book, pp 329–340.
5. Kvick, A and Thompson, A W (1992) ESRF Internal Report to the Science Advisory Committee.
6. Allinson, N M, et al. (1994) Proceedings of this meeting.

Session MoC - Invited Talks

Total Reflection X-Ray Fluorescence Spectroscopy Using Synchrotron Radiation for Wafer Surface Trace Impurity Analysis

P. Pianetta, S. Brennan, W. Tompkins, and N. Takaura, SSRL

S. S. Laderman, R. Smith, and A. Fischer-Colbrie, Hewlett Packard Company

M. Madden, Intel Corporation

J. B. Kortright, Lawrence Berkeley Laboratory

D. C. Wherry, Fisons Instruments

A. Shimazaki, K. Miyazaki, M. Kaneko, and T. Matsumura, Toshiba Corporation

Trace impurity analysis is essential for the development of competitive silicon circuit technologies. Current best methods for chemically identifying and quantifying surface and near surface impurities include grazing incidence x-ray fluorescence techniques using rotating anode x-ray sources. To date, this method falls short of what is needed for future process generations. However, the work described here demonstrates that with the use of synchrotron radiation, total reflection x-ray fluorescence (TRXRF) methods can be extended to meet projected needs of the silicon circuit industry through at least the remainder of this century. The present results represent over an order of magnitude improvement in detection limit over what has been reported previously.

In the past twelve months, we have tested three synchrotron radiation TRXRF experimental configurations in order to build and quantify the performance of the best arrangement. The three experimental configurations were: 1) bending magnet radiation from SPEAR ($E_c = 4.8$ keV) modified only with a focusing mirror to give a high energy cut off at 15 keV and filters to reduce the flux below 9 keV; 2) a single multilayer monochromator on BL 4-2 at SSRL (8 pole 1.8 Tesla wiggler); and 3) a double multilayer monochromator on BL10-2 (32 pole, 1.4 Tesla wiggler). The detection limits obtained from the experiments with the single multilayer and the focused bending magnet radiation are 2×10^9 atoms/cm² and 2×10^{10} atoms/cm² respectively. The sensitivities in these experiments were primarily limited by the scattered radiation found under the fluorescence peaks. In the case of the single multilayer monochromator, the scatter came from the small but finite reflectivity of the multilayer for energies below the primary Bragg peak. In the case of the filtered, focused bending magnet radiation, the scatter was due to the significant amount of radiation at the same energies as the fluorescent peaks that could not be completely eliminated by the filters.

The double multilayer monochromator eliminated the parasitic radiation and with the higher flux from the BL10, 32 pole wiggler gave a detection limit for Ni of 3×10^8 atoms/cm². This data was from a sample intentionally contaminated with 10^{11} atoms/cm² Fe, Ni, and Zn. This is to be compared with a detection limit of 5×10^9 atoms/cm² obtained with a rotating anode system. This is due to the greatly improved signal to noise in the case of the synchrotron. Furthermore, there is a clear path to improving the synchrotron case to reach a detection limit of 5×10^7 atoms/cm². According to the published trends of the Si VLSI industry associations, this detection limit is sufficient to meet the needs of the industry until at least the year 2000. Furthermore, the tunability of the synchrotron radiation makes it possible to achieve this very high sensitivity for nearly all the atoms in the periodic table.

Abstract

FT-IR MICROSCOPICAL ANALYSIS WITH SYNCHROTRON RADIATION: THE MICROSCOPE OPTICS AND SYSTEM PERFORMANCE

John A. Reffner,* Pamela A. Martoglio,* and Gwyn P. Williams**

*Spectra-Tech, Inc.; 652 Glenbrook Rd.; Stamford, CT 06906

**Brookhaven National Laboratory; Upton, NY 11973

When a Fourier transform infrared microspectrometer (IMS) was first interfaced to the National Synchrotron Light Source (NSLS), a 40-fold increase in S/N was achieved for spectra from a 12 x 12 μm area. The synchrotron's high brightness increases the performance at the IMS' diffraction limit. The NSLS has found that this source was 100 - 1,000 times brighter than thermo-emission sources.

A Spectra-Tech/Nicolet IR μs [®] was interfaced to the U2B beam line at the NSLS. This extraction port emits a beam with a source size of 0.2 x 0.4 mm. The interface for extracting the IR beam (developed by L. Carr and G. Williams) has a KBr window that provides a transparent, high-vacuum seal between the storage ring and the microspectrometer. Beyond this window, the beam was contained in a tube purged with dry nitrogen. The optics of both the interface and the microscope will be presented.

The source size at the sample was calculated to be 6 x 12 μm for the 15X Objective (NA = 0.58) and 3 x 6 μm for the 32X Objective (NA = 0.65). For 10- μm -wavelength radiation, the calculated diffraction-limited resolution was 10.7 μm (15X) and 9.6 μm (32X). The synchrotron source was imaged at or below the microscope's optical diffraction limit for mid-IR radiation. The IR beam's profile, obtained using a 12.5- μm aperture stepped in 10- μm increments along two directions, showed that the beam width is 12 μm at half maximum. In fact, 65% of the total beam's intensity was transmitted through a 12.5- μm -diameter circular aperture in the specimen plane. This beam profile demonstrated that the system was operating at the diffraction limit for IR radiation.

To test the resolution and performance of the IR microprobe with synchrotron radiation, a multi-layered laminate film was analyzed. The laminate selected was a five-layer polymer film on a paper backing. The thicknesses of the five polymer layers were 6, 4, 4, 8, and 32 μm . A series of IR absorbance spectra were recorded across the layers of the film at 1- μm intervals, with a 6 x 6 μm dual-confocal-apertured sample area. The variations in chemical composition across the layers were readily detected. Spectra were collected over the range 4,000 - 650 cm^{-1} at a resolution of 8 cm^{-1} , and 16 scans were co-added for each spectrum. The total acquisition time was about 5 sec per spectrum. This series of spectra profiles the composition across a visibly-sharp boundary between these layers. In the IR region, the observed spreading (or blur) equalled the calculated diffraction-limited beam's diameter, which is 5.4 μm (1740 cm^{-1}).

IMS analyses are S/N-limited. The spectrum of a 6-x-6- μm sample area, collected at 8 cm^{-1} resolution with 16 scans co-added, had an S/N ratio of 250:1. This S/N level is 40 times higher than could be obtained with a conventional source. The improved S/N performance was the direct result of using synchrotron radiation.

SIMULTANEOUS MEASUREMENTS OF SMALL ANGLE X-RAY SCATTERING, WIDE ANGLE X-RAY SCATTERING AND LIGHT SCATTERING DURING PHASE TRANSITIONS OF POLYMERS

C. Wutz, J. Cronauer, R. Döhrmann and H.G. Zachmann

Institut für Technische und Makromolekulare Chemie, University of Hamburg, Bundesstr. 45, D-20146 Hamburg, Germany

By means of simultaneous measurements of small angle X-ray scattering (SAXS), wide angle X-ray scattering (WAXS) and light scattering (LS) important new informations of the mechanism of crystallization and melting of polymers may be obtained. WAXS is used to determine the overall change in the fraction of crystallized materials. SAXS reveals in which way this change takes place, for example whether by growth of already existing crystals or by formation of new crystals within the lamellar stacks of crystalline and amorphous regions. LS, finally, indicates how far crystallization is related to the growth of morphological units such as spherulithes.

To perform such measurements two different experimental set-ups are used at the polymer beamline at HASYLAB (DESY, Hamburg). In one of the set-ups the SAXS and WAXS are measured by two one-dimensional Gabriel counters positioned at different locations (Fig. 1). In the other set-up (Fig. 2), by a luminescent screen, the WAXS is transformed to visible light which is reflected on a vidicon, while the SAXS passes through a hole in this screen and is detected by a two-dimensional Gabriel counter. The second set-up has the advantage that two-dimensional WAXS can be detected, however the resolution of the WAXS is not so good as in the first set-up.

Different polymers have been investigated and it is shown, in particular, that different processes take place during secondary crystallization.

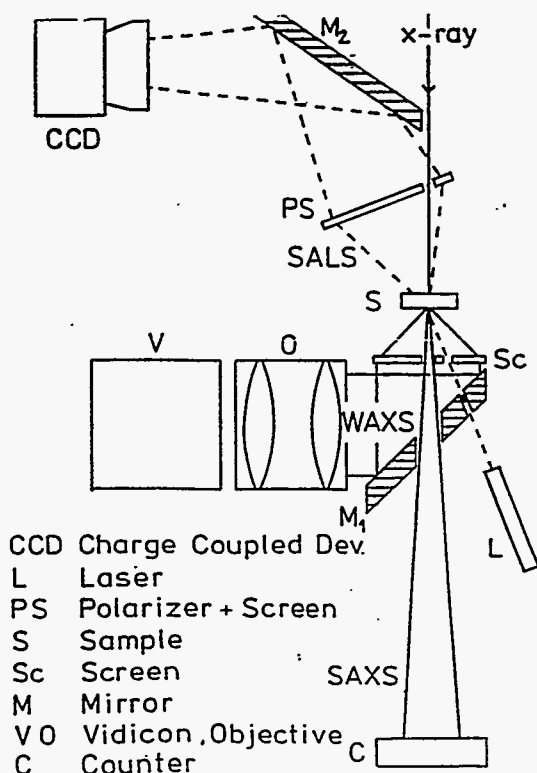


Fig. 1

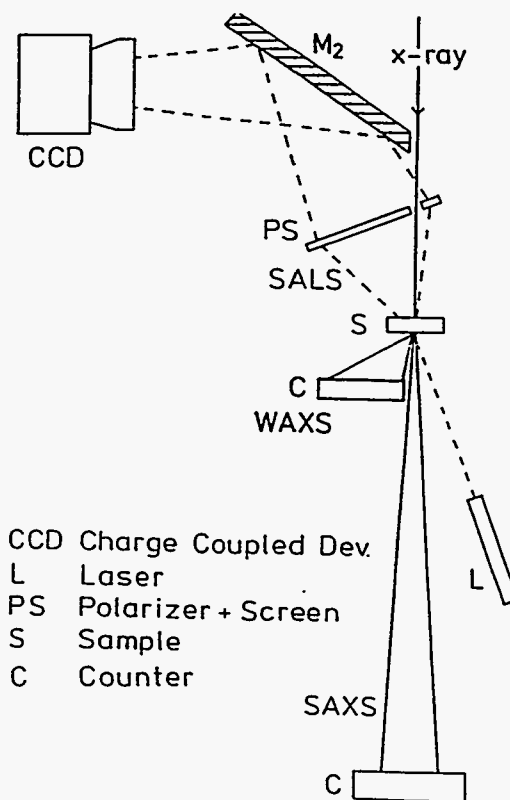


Fig. 2

Spin-sensitive Microscopy with Circularly Polarized X-rays

Brian Tonner
Synchrotron Radiation Center
University of Wisconsin-Madison
Stoughton, WI 53589

Magnetic circular dichroism is the difference in absorption coefficient when the relative orientation of sample magnetization and incident helicity are changed. At the L edges of transition metals, the soft X-ray magnetic dichroism (XMCD) effect is very large, approaching 50%, which allows it to be exploited for studying magnetic phenomena in ultrathin films and layered magnetic nanostructures. In addition to being very large, the XMCD signal can be quantitatively interpreted to measure the vector spin direction, and the relative contributions of spin and orbital moment of the total magnetic moment. Recently, it has been shown that the large XMCD effects can be used as a new form of image contrast, to create maps of surface magnetization. Because of the inherent elemental selectivity of X-ray spectroscopy, X-ray dichroism microscopy is a unique imaging tool for surface magnetism. Recent results will be shown, and projections for future development with linear and circularly polarized beamlines, using both electron imaging and scanned photon beam techniques, will be discussed.

Materials/Biology Posters

(Session MoD)

- MoD1 Beno, M.A., Knapp, G.S., Armand, P., Price, D.L., Saboungi, M.-L. Application of a New Synchrotron Powder Diffraction Technique to Anomalous Scattering from Glasses.
- MoD2 Bliss, N., Bordas, J., Fell, B.D., Harris, N.W., Helsby, W.I., Mant, G.R., Smith, W., Towns-Andrews, E. W16.1 A New Fixed Wavelength Diffraction Station at the SRS Daresbury.
- MoD3 Bras, W., Mant, G.R., Derbyshire, G.E., Ryan, A.J. Multiple Simultaneous Time Resolved Experimental Techniques.
- MoD4 Brister, K. CO₂ Laser Heating Instrumentation at CHESS.
- MoD5 Buckley, C.J. The Measurement and Mapping of Calcium in Mineralised Tissues by Absorption Difference Imaging.
- MoD6 Buckley, C.J., Bellamy, S.J., Khaleque, N., Zhang, X., Downes, S. The NEXAFS of Biological Calcium Phosphates at the Calcium L Edge and the Potential for Chemical State Imaging.
- MoD7 Arfelli, F., Barbiellini, G., Cantatore, G., Castelli, E., Dalla Palma, L., Longo, R., Poropat, P., Rosei, R., Sessa, M., Tromba, G., Vacchi, A. Digital Mammography With Synchrotron Radiation.
- MoD8 Chapman, D., Thomlinson, W., Gmur, N., Dervan, J.P., Stavola, T., Giacomini, J., Gordon, H., Rubenstein, E., Lavender, W., Schulze, C., Thompson, A.C. Effects of Spatial Resolution and Spectral Purity on Transvenous Coronary Angiography Images.
- MoD9 Chapman, H.N., Jacobsen, C., Williams, S. Applications of a CCD Detector in a Scanning Transmission X-Ray Microscope.
- MoD10 Chen, J.H., Kikegawa, T., Yaoita, K., Shimomura, O. DDX Diffraction System: A Combined Diffraction System with EDX and ADX for High Pressure Structural Studies.
- MoD11 Chernov, V.A., Chkhalo, N.I., Mytnichenko, S.V. Bragg Reflection from Molecular Crystals at the Core Anisotropic Resonances: Soft X-Ray Polarization Applications.
- MoD12 Clark, S.M. A New High Pressure Diffraction Facility at the SRS.
- MoD13 Clark, S.M., Nield, A., Evans, J.S.O., Francis, R.J., O'Hare, D. Development of Large Volume Reaction Cells for Kinetic Studies Using Energy-Dispersive Powder Diffraction.
- MoD14 Clark, S.M., Rathbone, T., Irvine, P., Flaherty, J. Development of a New High Temperature Cell for Powder Diffraction Using Induction Heating.
- MoD15 Craievich, A.F., Alves, O.L., Barbosa, L.C. In situ Synchrotron Radiation SAXS Study of the Kinetics of Growth of CdTe Nanocrystals in Borosilicate Glass.
- MoD16 Denlinger, J.D., Rotenberg, E., Warwick, T., Visser, G., Nordgren, J., Guo, J.H., Skytt, P., Kevan, S.K., McCutcheon, S., Shuh, D., Bucher, J., Edelstein, N., Tobin, J.G., Tonner, B.P. First Results From the SpectroMicroscopy Beamline at the Advanced Light Source.
- MoD17 Denlinger, J.D., Warwick, T., Ade, H., Tonner, B.P. Design of a Tandem Soft X-Ray Microscope for High Spectral and Spatial Resolution Spectromicroscopy Under Ultra-High Vacuum or Ambient Conditions.
- MoD18 Dilmanian, F.A., Wu, X.Y., Chen, Z., Slatkin, D.N., Chapman, D., Shleifer, M., Staicu, F.A., Thomlinson, W. Multiple Energy Computed Tomography (MECT) at the NSLS: Status Report.
- MoD19 Dragun, G.N., Mezentsev, N.A., Kolesnikov, K.A., Kuzin, M.V., Nesterov, S.I., Pindyurin, V.F., Zelentsov, E.L. Preliminary Results of Animal Lymphatic System Study at the VEPP-3 Angiography Station.

- MoD20 Engstrom, P., Fiedler, S., Riekkel, C. The Microdiffraction Instrumentation and Experiments on Microfocus Beamline at ESRF.
- MoD21 Gaponov, Yu.A., Evdokov, O.V., Sukhorukov, A.V., Tolochko, B.P. A Computer Controlled System for Studying the Gas-Solid State Reactions in X-Ray Diffraction Experiments.
- MoD22 Garrett, R.F., Cookson, D.J., Foran, G.J., Sabine, T.M., Kennedy, B.J., Wilkins, S.W. Powder Diffraction Using Imaging Plates at the Australian National Beamline Facility at the Photon Factory.
- MoD23 Gehrke, R., Bark, M., Lewin, D., Cunis, S. Ultra Small Angle X-Ray Scattering at the HASYLAB Wiggler Beamline BW4.
- MoD24 Gmur, N.F., Chapman, D., Thomlinson, W., Thompson, A.C., Levender, W.M., Scalia, K., Malloy, N., Mangano, J., Jacob, J. NSLS Transvenous Coronary Angiography Beamline Upgrade and Advanced Technology Initiatives.
- MoD25 Hasegawa, M., Ninomiya, K. Total Photoelectron Imaging of Sub-micron Stripe Patterns Using Soft X-Ray Microbeam Formed by Wolter-Type Mirror.
- MoD26 Sakata, O., Hashizume, H. Ultrahigh Vacuum Diffractometer for Grazing-Angle X-Ray Standing-Wave Experiments at a Vertical-Wiggler Source.
- MoD27 Hirsch, G. Biological Imaging with a New Type of Soft X-Ray Microscope.
- MoD28 Holldack, K., Kachel, T., Gudat, W. Element Specific Imaging of Structural and Magnetic Domains Using Linear and Circular Polarized Light.
- MoD29 Horii, Y., Tomita, H., Komiya, S. New Diffractometer for Thin Film Structure Analysis Under Grazing Incidence Condition.
- MoD30 Iida, A., Noma, T., Miyata, H., Hirano, K. Micro X-Ray Diffraction Technique for Analysis of the Local Layer Structure in the Ferroelectric Liquid Crystal.
- MoD31 Iketaki, Y., Watanabe, T. Feasibility of Photo-Excitation Imaging in Soft X-Ray Microscopy Using the Transition to π^* -Orbits in Biological Molecules
- MoD32 Illing, Gz., Heuer, J., Reime, B., Lohmann, M., Schildwachter, L., Dix, W.R., Graeff, W. A Double Beam Bent Laue Monochromator for Coronary Angiography.
- MoD33 Tamura, K., Inui, M., XAFS Measurements at High Temperatures and Pressures.
- MoD34 Itai, Y., Takeda, T., Akatsuka, T., Maeda, T., Hyodo, K., Uchida, A., Yuasa, T., Kazama, M., Wu, J., Ando, M. High Contrast Computed Tomography With Synchrotron Radiation.
- MoD35 Iwasaki, H., Chen, J.H., Kikegawa, T. Structural Study of the High Pressure Phases of Bismuth Using High Energy Synchrotron Radiation.
- MoD36 Jennings, G., Lee, P.L. EX6AFS: A Data Acquisition System for High Speed Dispersive EXAFS Measurements Implemented Using Object-Oriented Programming Techniques.
- MoD37 Jia, J.J., Calcott, T.A., Yurkas, J., Ellis, A.W., Himpfel, F.J., Samant, M.G., Stohr, J., Ederer, D., Carlisle, J.A., Hudson, E.A., Terminello, L.J., Perera, R.C.C., Shuh, D.K. First Results from the IBM/Tennessee/Tulane/LLNL/LBL Undulator Beam Line at the Advanced Light Source.
- MoD38 Johansson, U., Nyholm, R., Tornevik, C., Plodstrom, A. The VUV Scanning Spectromicroscope at MAX-Lab.
- MoD39 Wang, J., Kagoshima, Y., Miyahara, T., Ando, M., Aoki, S., Watanabe, N., Anderson, E., Attwood, D., Kern, D.,

- Shinohara, K., Kihara, H. A Zone Plate Soft X-Ray Microscope at the Beamline NE1B of the TRISTAN Accumulation Ring.
- MoD40 Kawasaki, K., Iwasaki, H. Rapid Projection of Crystal Grain Orientation Distribution by Synchrotron X-Ray Diffraction.
- MoD41 Kawata, H., Mori, K. X-Ray Magnetic Bragg Scattering Topography from Fe₃O₄.
- MoD42 Kovalchuk, M.V., Kazimirov, A.Y. X-Ray Multiple Dynamical Diffraction Experiments With Synchrotron Radiation.
- MoD43 Kirkland, J.P., Kovantsev, V.E., Dozier, C.M., Gilfrich, J.V., Gibson, W.M., Xiao, Q.F., Umezawa, K. Wavelength-Dispersive X-Ray Fluorescence Detector.
- MoD44 Kirz, J., Jacobsen, C., Williams, S., Wirick, S., Zhang, X., Ade, H., Rivers, M. Instrumentation Developments in Scanning Soft X-Ray Microscopy at the NSLS.
- MoD45 LaFontaine, B., MacDowell, A.A., Tan, Z., White, D.L., Taylor, G.N., Wood III, O.R., Bjorkholm, J.E., Tennant, D.M., Hulbert, S.L. Real-Time, Sub-Micron, Soft X-Ray Fluorescence Imaging.
- MoD45 Kitajima, Y. Fluorescence Yield XAFS Measurements in the Soft X-Ray Region.
- MoD46 Ko, C.H., Kirz, J., Ade, H., Johnson, E., Hulbert, S., Anderson, E. Development of a Second Generation XPS-Based Scanning Photoemission Microscope with a Zone Plate Generated Microprobe at the National Synchrotron Light Source.
- MoD47 Kojima, S., Kudo, Y., Kawado, S., Ishikawa, T., Matsushita, T. A New Technique for Time-Resolved X-Ray Diffraction Measurements in the Single Bunch Operation Applied to Laser Annealing.
- MoD48 Zheludeva, S.I., Kovalchuk, M.V., Novikova, N.N., Sosphenov, A.N. Long Periodic X-Ray Standing Wave for Characterization of Heat Treatment Effects on Ni/C Layered Synthetic Microstructures.
- MoD49 Kulipanov, G.N., Makarov, O.A., Mezentseva, L.A., Milyokhin, A.G., Nazmov, V.P., Pindyurin, V.F., Sinyukov, M.P., Zarodyshev, A.V. The Use of SR From VEPP-3 Storage Ring for Fabrication of Micromechanic Elements by Deep X-Ray Lithography.
- MoD50 Kulipanov, G.N., Makarov, O.A., Mezentseva, L.A., Mishnev, S.I., Nazmov, V.P., Pindyurin, V.F., Redin, O.A., Skrinsky, A.N., Artamonova, L.D., Gashtold, V.N., Deis, G.A., Prokopenko, V.S., Reznikova, E.F., Chesnokov, V.V., Cherkov, G.A. Fabrication and Preliminary Testing of the Regular Microporous Membranes Manufactured by Deep X-Ray Lithography at the VEPP-3 Storage Ring.
- MoD51 Lamble, G.M. Design and Operation of a UHV Double-Bounce Harmonic Rejection Mirror for XAFS Studies.
- MoD52 Lee, P.L., Beno, M.A., Ogata, C.M., Knapp, G.S., Jennings, G. Diffraction Applications Using the Energy Dispersive Beamline, X6A, at NSLS.
- MoD53 Lessmann, A., Schuster, M., Brennan, S., Materlik, G., Riechert, H. X-Ray Standing Wave and High-Resolution Diffraction Measurements on III-V Compound Superlattices.
- MoD54 Mahadev, V., Gunshor, R.L., Liedl, G.L. Atomic Structure and Ordering at the ZnSc/GaAs Interface.
- MoD55 McNulty, I., Haddad, W.S., Trebes, J., Anderson, E.H., Yang, L. Soft X-Ray Scanning Microtomography with Submicron Resolution.
- MoD56 Momose, A., Takeda, T., Itai, Y. Phase-Contrast X-Ray Computed Tomography for Observing Biological Specimens and Organic Materials.

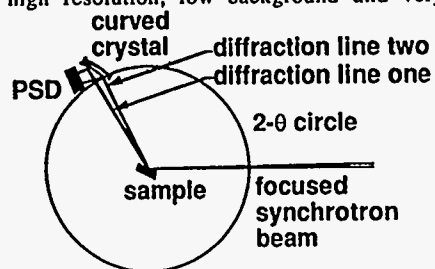
- MoD57 Murata, T., Nakagawa, K., Kimura, A., Otoda, N. Design of a Cell and Transportation System for the X-Ray Absorption Study of Supercritical Fluid Material.
- MoD58 Nakajima, T., Suzuki, H., Suzuki, T., Suzuki, H. Low Temperature Diffractometer Below 1K by a ^3He - ^4He Dilution Refrigerator Used for Synchrotron Radiation X-Ray Diffractometry and Topography.
- MoD59 Nakajima, T., Yoshizawa, M. Astatic Magnets Producing Arbitrarily Directed Magnetic Fields With Goniometric Control Used for X-Ray Diffraction.
- MoD60 Ng, W., Singh, S., Solak, H., Cerrina, F. Progress Report on the Soft X-Ray Scanning Photoemission Microscope: MAXIMUM.
- MoD61 Novikov, D.V., Gog, T., Griebenow, M., Materlik, G. Synchrotron Radiation Plane Wave GID Topography.
- MoD62 Ohsumi, K., Hagiya, K., Miyamoto, M., Ohmasa, M. Development of Micro-Area Diffraction System by Polychromatic SR with Laue Method.
- MoD63 Oku, Y., Hyodo, K., Aizawa, K., Ando, M. Simulation of Scattering X-Rays for Improving Image Quality in SR Coronary Angiography.
- MoD64 Rivers, M.L., Sutton, S.R. A Wavelength Dispersive Detector for Synchrotron X-Ray Fluorescence Microprobe Analysis.
- MOD65 Rivers, M.L., Sutton, S.R., Rarback, H. A Multielement Ge Detector with Complete Spectrum Readout for X-Ray Fluorescence Microprobe and Microspectroscopy.
- MoD66 Rodricks, B. Time Resolved X-Ray Scattering Program at the Advanced Photon Source.
- MoD67 Belsky, A.N., Kulipanov, G.N., Mikhailin, V.V., Pustovarov, V.A., Rogalev, A.L., Shepel, G.T., Vasiliev, A.N., Zinin, E.I. Subnanosecond-Resolved XEOL Spectroscopy Using a Dissector.
- MoD68 Slatkin, D.N., Dilmanian, F.A., Spanne, P., Gebbers, J.O., Archer, D.W., Laissue, J.A. Design of a Multislit, Optional Width Collimator for Microplanar Beam Radiotherapy.
- MoD69 Snigirev, A., Snigireva, I., Engstrom, P., Suvorov, A., Chevallier, P., Legrand, F., Soullie, G. Testing of Sub-micrometer Fluorescence Microprobe Based on Bragg-Fresnel Crystal Optics at the ESRF.
- MoD70 Stephenson, J.D., Hentschel, M.P., Lange, A. SR-Hard-X-Ray Diffraction Microscopy of Carbon Fibre Reinforced Plastic.
- MoD71 Sutton, S.R., Bajt, S., Schulze, D., Tokunaga, T. Oxidation State Mapping Using Micro-XANES.
- MoD72 Suzuki, Y., Uchida, F. Dark Field Imaging in Hard X-Ray Scanning Microscopy.
- MoD73 Takeda, T., Maeda, T., Ito, T., Kishi, K., Wu, J., Kazama, M., Yuasa, T., Hyodo, K., Akatsuka, T., Itai, Y. Fluorescent Scanning X-Ray Computed Tomography With Synchrotron Radiation.
- MoD74 Tanaka, K., Ikeura, H., Sekiguchi, T., Sekitani, T., Tinone, M.C.K. Photon Stimulated Ion Desorption Studies Using Pulsed Synchrotron Radiation.
- MoD75 Thiel, D.J., Walter, R.L., Ealick, S.E., Bilderback, D.H., Gruner, S.M., Eikenberry, E.F. Macromolecular Crystallographic Results Obtained Using a CCD Detector at CHESS.
- MoD76 Toellner, T., Fullerton, E., Sturhahn, W., Alp, E. Nuclear Resonant Diffraction from a $^{57}\text{Fe}/\text{Cr}$ Antiferromagnetic Multilayer.

- MoD77 Bessergenev, A.V., Tolochko, B.P., Sheromov, M.A., Mezentsev, N.A. Simultaneously Two Energy Powder Diffraction Method Using the Effect of Anomalous Scattering.
- MoD78 Suchorukov, A.V., Tolochko, B.P., Gavrilov, N.G., The Cutting Mashing for Investigation of the Relaxation Process by Synchrotron Radiation Diffraction.
- MoD79 Urakawa, S., Ohno, H., Umesaki, N., Igarashi, K., Shimomura, O. X-Ray Diffraction Analysis of Molten KCl under High Pressures.
- MoD80 vanDorssen, G.E., Roper, M., Padmore, H.A., Derst, G., Greaves, G.N. Core Excitons in Silicon and Silicon Oxides.
- MoD81 Vartanyants, I.A., Kovalchuk, M.V. The Possibilities of X-Ray Standing Wave Method for Investigation of the Structure of Real Crystals. Theory and Applications.
- MoD82 Iketaki, Y., Watanabe, T. Feasibility of Photo-Excitation Imaging in Soft X-Ray Microscopy Using the Transition to π^* Orbits in Biological Molecules.
- MoD83 Nikulin, A.Yu., Stevenson, A.W., Hashizume, H., Wilkins, S.W., Cookson, D., Foran, G. High Resolution Triple-Crystal X-Ray Diffraction Experiments Performed at the Australian National Beamline Facility at the Photon Factory.
- MoD84 Will, G., Hoffner, C. A Newly Developed Hydraulic Modular Squeezer for High Pressure Experiments Using Synchrotron Radiation.
- MoD85 Hirschmugl, C.J., Williams, G.P. Signal to Noise Improvements with a New Far-IR Rapid-Scan Michelson Interferometer.
- MoD86 Wu, Z., Dai, P., Ehrlich, S.N., Taub, H. Structure and Growth of Hexane Films Adsorbed on the Ag(111) Surface.
- MoD87 Dai, P., Wu, Z., Ehrlich, S.N., Taub, H. Stacking Faults and Characterization of the Film-Vacuum Interface in Multilayer Xe Films Adsorbed on the Ag(111) Surface.
- MoD88 Xie, X.S., Jia, C.Z., Zhao, Y.F., Shang, L., Deng, J.F., Wang, G.Q., Zhang, J.Y. Soft X-Ray Microscopy Project at NSRL.
- MoD89 Haibin, P., Xu, P., Lu, E., Yang, F., Xia, A., Zhang, X. Alkali Doped C_{60} : The Movement of the Fermi Energy.
- MoD90 Chu, B., Yeh, F., Li, Y., Harney, P.J., Rousseau, J., Darovsky, A., Siddons, D.P. Construction of a Multiwavelength Bonse-Hart Ultrasmall-Angle X-Ray Scattering Instrument.
- MoD91 Carr, G.L. Performance of an Infrared Microspectrometer at the NSLS.
- MoD92 Yamada, T., Yuri, M., Onuki, H., Ishizaka, S. Development of Circularly Polarizing Microscope with a Polarizing Undulator.
- MoD93 Johnson, E.D., Siddons, D.P., Guckel, H. Precision Micro-Machining with Hard-X-Rays
- MoD94 Hecht, M., Brennen, R., Manion, S., Pianetta, P., Stowe, T., Kenny, T., Bonivert, W., Hachman, J. Fabrication of Xray Collimators for Solar Physics Using LIGA at SSRL.
- MoD96 Kelly, L.A., Trunk, J.G., Polewski, K., Sutherland, J.C. Simultaneous Resolution of Spectral and Temporal Properties of UV and Visible Fluorescence Using Single-Photon Counting with a Position-Sensitive Photomultiplier
- MoD97 Hodeau, J.L., Vacinova, J., Garreau, Y., Fontaine, A., Hagelstein, M., Elkaim, E., Lauriat, J.P., Prat, A., Wolfers, P. D.A.F.S. Measurements by Using an "Energy/Angular Dispersive Diffraction" Experimental Set-Up.

Application of a New Synchrotron Powder Diffraction Technique to Anomalous Scattering from Glasses

M. A. Beno, G. S. Knapp, P. Armand, D. L. Price, and M.-L. Saboungi
Materials Science Division, Argonne National Laboratory, Argonne IL 60439

A synchrotron powder diffraction technique which uses a curved perfect crystal analyzer to simultaneously diffract multiple powder lines into a position sensitive detector has been shown¹⁻³ to possess high resolution, low background and very high counting rates. High



quality diffraction data resulting from the application of this method to anomalous scattering from amorphous materials⁴ will be presented. Highly accurate diffraction data is required since the anomalous scattering

results are derived from differences in large values. The use of a rapid sample changer allows the scattering from the sample and a standard material (a material not containing the anomalous scatterer) to be measured alternately at each angle. This measurement strategy provides excellent energy resolution and high data rates while minimizing systematic errors resulting from factors such as detector non-linearity, beam instability or sample misalignment.

Work at Argonne National Laboratory is supported by the US Department of Energy, Office of Basic Energy Science, Division of Materials Sciences, under contract W-31-109-ENG-38.

1. M.A. Beno, G. S. Knapp, Rev. Sci. Instrum. 63, 4134(1992).
2. G. S. Knapp, M. A. Beno, G. Jennings, M. Engbretson, M. Ramanathan, Adv. X-Ray Analysis, 36, 653(1993).
3. G. S. Knapp, M. A. Beno, G. Jennings, M. Ramanathan, Mat. Res. Soc. Symp. Proc. 307, 317(1993).
4. P. Armand, A. J. G. Ellison, M. A. Beno, G. S. Knapp, M.-L. Saboungi, D. L. Price, Meeting of the American Physical Soc., Pittsburgh, PA, March 21-25, 1994.

MoD1

W16.1 A New Fixed Wavelength Diffraction Station at the SRS Daresbury

**N Bliss, J Bordas, B D Fell, N W Harris, W I Helsby,
G R Mant, W Smith, E Towns-Andrews.**
DRAL Daresbury Laboratory, UK

W16.1 is a high flux high intensity fixed-wavelength diffraction station. It has been designed primarily for the study of non-crystalline materials, both biological and non-biological. The station has been optimised at a wavelength of 1.4Å and is capable of both high angle and low angle dynamic measurements. In order to achieve the high X-ray intensities required by these types of experiment it has been constructed on the new 6T superconducting wiggler magnet at the SRS. The station has been positioned at an angle of 46 mrad defined from the centre of the wiggler magnet. This allows 12 mrad of horizontal aperture to be focused onto the sample.

As a consequence of the high thermal loads, produced by the wiggler, the optical layout of the station has some novel design features. Notably, a bent triangular Ge 111 asymmetric cut crystal with a liquid gallium interface, to dissipate heat, to a cooled copper block. The monochromator not only compresses the beam, but also focuses it horizontally at a variety of distances. Vertical focusing is achieved using a 1.2 m bent platinum coated ultra low expansion glass mirror.

For the low angle measurements an extremely clean background has been achieved by a series of horizontal and vertical collimating slits. In addition a Kratky style aperture has been included in the front end of the beamline to minimise scatter in the vertical plane. The experimental optics and camera system is highly configurable utilising a linear guide rail support arrangement. Data can be collected from 2Å to ca.7000Å with a time resolution of 1 µsec.

The beamline motor control system comprises of recently developed Daresbury VME stepper motor controllers interfaced to a conventional drive system. A number of detector systems are available for data collection. The data acquisition system associated with these has been configured with several recently developed VME modules designed and constructed at Daresbury. Amongst these is a novel TAC/ADC system which includes a sliding scale correction for the ADCs and a pile-up rejection system. This has been shown to give an overall resolution of 2048 x 2048 pixels and a data rate in excess of 1 MHz.

A detailed design of the beamline and preliminary results will be presented during the meeting.

MoD2

Multiple simultaneous time resolved experimental techniques

W. Bras[#], G.R.Mant, G.E.Derbyshire, A.J.Ryan[‡]

Daresbury Laboratory, Warrington WA4 4AD, UK

[#] also Netherlands Organisation for Scientific Research (NWO)

[‡] also University of Manchester Institute for Science and Technology

Abstract

The desire to eliminate experimental artefacts arising from the correlation of several independent time resolved experiments has been the impetus to perform several simultaneous experimental techniques on a single sample. Combinations of Small and Wide Angle X-ray Scattering or fibre diffraction, together with a variety of other experimental techniques have been combined into a single experiment, rendering for instance both structural as well as thermodynamic information. A versatile system has been developed that allows for instance the interfacing of Differential Scanning Calorimetry, Fourier Transform Infrared Spectroscopy or Raman spectroscopy to X-ray scattering experiments covering wide q -range ($0.007 < q < 2.1 \text{ \AA}^{-1}$) with a sub second time resolution and a high spatial resolution.

CO₂ LASER HEATING INSTRUMENTATION AT CHESS

Keith Brister

CHESS, Cornell University

Laser heating instrumentation for experiments using diamond anvil cells will be presented. This system allows powder diffraction from samples at simultaneous high pressures and high temperatures. The system consists of a beam delivery system and incandescent light collection optics to analyze the resulting graybody spectra, see the figure for details. A portion of the incandescent light is used to control which multichannel analyzer group the x-ray diffraction pattern is collected in so that variations in temperature do not compromise the quality of the diffraction spectra. Examples of experiments which have used this system will be presented, including recent work by Gu, Vohra and Brister (Accepted for publication in Scripta. Met.).

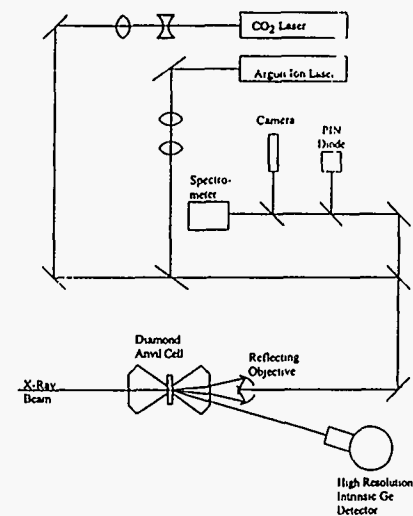


Figure. Schematic diagram of the optical system for laser heating and pressure measurements for the dedicated High Pressure Facility at CHESS. Light from either the CO₂ laser or the argon ion laser is focused onto the sample through a combination of beam expanders and a reflecting objective lens. Light from the sample from 600 to 900 nm is focused on a PIN diode, a camera, and a 0.28 meter spectrometer equipped with a diode array detector.

**The Measurement and Mapping of Calcium in Mineralised
Tissues by Absorption Difference Imaging**

C.J. Buckley

Department of Physics, King's College, the Strand, London WC2R 2LS, UK.

This paper reviews the mapping of calcium in mineralised tissues by absorption difference imaging using scanning x-ray microscopy at the calcium L edge. In particular, the mapping of embedded and sectioned mineralised tissues is considered. Here, the technique is discussed in detail, and the detection limits are evaluated with and without corrections.

In principle, the calcium concentration at any point in a thin specimen can be measured by measuring the incident and transmitted x-ray flux at two energies close the L absorption edge (350eV). These two energies are chosen such that there is a large difference in absorption cross-section. If only a general indication of the relative calcium concentration is required, the error introduced to the measurement by effects such as changes in the transmission of the other elements in the specimen can be ignored. However, where it is important to obtain a quantitative linear measurement of the concentration, then corrections must be applied to avoid sizeable errors.

The effect of the other specimen-elements on the measurement of the calcium concentration is assessed. Also evaluated are the errors introduced by; detector non-linearity, photon statistics, specimen registration, resolving power, thickness effects and the uncertainty in absorption cross-section values. Techniques which have been developed to minimise artefact introduced by these phenomena are presented, and comparative results are shown.

MoD5

**The NEXAFS of Biological Calcium Phosphates at the Calcium L edge
and the Potential for Chemical State Imaging**

C.J. Buckley[†], S.J. Bellamy[†], N. Khaleque[†], X. Zhang^{††} and S. Downes^{†††}

[†] Department of Physics, King's College, The Strand, London WC2R 2LS, UK.

^{††} Department of Physics, SUNY at Stony Brook, Stony Brook, NY 11795, USA.

^{†††} Institute of Orthopaedics, Brockley Hill, Stanmore, MIDDX HA7 4LP, UK.

An important development in x-ray microscopy has been the advent of imaging which is sensitive to the chemical state of an element^{1,2}, with a spatial resolution capability of 50nm. Results thus far have determined the distribution of specific molecules by using shifts in the near edge x-ray absorption spectra (NEXAFS) peaks of carbon K edge structure at 280eV. These π^* resonance peaks arise from double or triple bonds in the molecules (C=C, C=N, and C=O, etc, at C K-edge), where the peak position is strongly affected by the bond's environment and the peak magnitude represents the bond concentration.

In crystalline materials, the NEXAFS signature of an atom can be strongly influenced by the electrostatic field exerted on the atom in question by the surrounding ions. This effect has been investigated by de Groot *et al*³ for calcium and other atoms in octahedral symmetry. These results suggest that differences in the crystal structure of different mineral-phase calcium phosphates will alter both the magnitude and position of the calcium L edge NEXAFS peaks.

These changes in the NEXAFS signature lead to the possibility of imaging calcified tissues with sensitivity to the mineral phase at the sub-micron level. This would have considerable impact in the areas of mineralisation disorders, such as arthritis, and also in the understanding of bone re-modelling⁴. We have attempted to characterise the NEXAFS signatures of biologically important calcium phosphates (such as calcium hydroxy apatite), and have evaluated the potential for mapping the mineral phases in calcified tissues using the scanning x-ray microscope.

References

- 1 H. Ade, X. Zhang, S. Cameron, C. Costello, J. Kirs and S. Williams "Chemical contrast in X-ray microscopy and spatially resolved XANES spectroscopy of organic specimens". *Science* 258 972-5 (1992)
- 2 X. Zhang *et al* " Mapping DNA and Protein in Biological Samples using STXM". *Proc. Conf. Mic. Soc. Am.* 1994 (In press).
- 3 F.M.F. de Groot, J.C. Fuggle, B.T. Thole and G.A. Sawatsky " $L_{2,3}$ x-ray absorption edges of d^0 compounds K^+ , Ca^{2+} , Sc^{3+} and Ti^{4+} in O_h (octahedral) symmetry". *Phys Rev B* 41(5) 928-37 (1990)
- 4 C.J. Buckley, S. Downes, N. Khaleque, S.J. Bellamy and X. Zhang. " Mapping the density and mineral phase of calcium in bone at the interface with biomaterials using scanning x-ray microscopy" *Proc. Conf. Mic. Soc. Am.* 1994 (In press).

MoD6

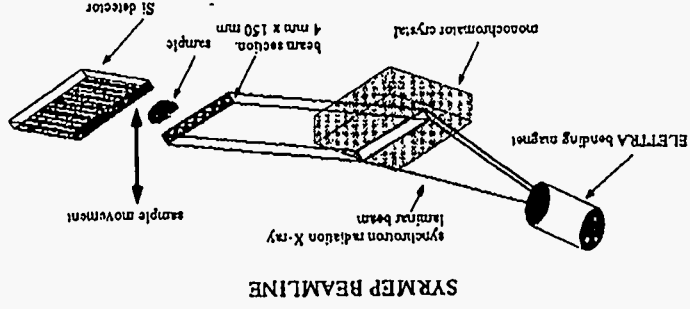
DIGITAL MAMMOGRAPHY WITH SYNCHROTRON RADIATION

F. Arfelli, G. Barbini, G. Camarero, E. Caselli, L. Dalla Palma, R. Longo, P. Poropat, R. Rossi, M. Sessa, G. Tromba, A. Vacchi (Universita', INFN and Sincrotrone - Trieste, Italy)

The Synsep (Synchrotron Radiation in Medical Physics) Collaboration is planning to use a beam of monochromatic X-rays provided by Elettra, the synchrotron radiation facility under construction in Trieste (Italy), in conjunction with a novel silicon pixel detector to conduct research in digital mammography.

A beamline dedicated to mammography is presently under construction in Trieste. It will provide at a distance of about 20 m from an Elettra bending magnet (see Figure below), a monochromatic, laminar-section ($150 \times 4 \text{ mm}^2$), X-ray beam. This beam will illuminate in vitro samples and will be detected by a fixed Si microstrip device forming a matrix of pixels. Digital images of phantoms having a size ($150 \times 150 \text{ mm}^2$) common in the diagnostic practice can be then produced by scanning the sample itself in front of the detector.

A prototype detector with a sensitive area of $7.5 \times 0.5 \text{ mm}^2$ and pixels of $0.5 \times 0.5 \text{ mm}^2$ has been built and tested. We present the current status of the SYRMEP beamline and digital images of test objects exposed to a radioactive X-ray source obtained with our prototype detector.



Measurements have been made on the National Synchrotron Light Source (NSLS) Coronary Angiography X17B2 beamline under ideal and real imaging conditions to investigate the optimal imaging conditions for spatial resolution and spectral purity. The spatial resolution tests were performed using two multielement Si(Li) detectors (600 element, 0.5mm pixel-pixel spacing; 1200 element, 0.25mm pixel-pixel spacing [1]). Images were taken of phantoms containing iodine contrast agent over a wide range of incident beam absorption conditions. Patient images were also obtained using the same viewing projection with both detectors. Harmonics present in the imaging beam can be reduced by operating the superconducting wigglers source at reduced field strength. At regions of high absorption in the patient, the harmonics present can contribute to the detected signal [2]. Iodine phantom images were obtained at a wiggler field strength of 3 Tesla ($E_c=13.3 \text{ keV}$) and 4 Tesla ($E_c=17.8 \text{ keV}$) for the comparison. As before, patient images were obtained using the same projection at both wiggler fields. Results of the detector resolution and wiggler field measurements will be presented for the phantoms as well as the patient scans.

1. A.C. Thompson et al, *A 1200 Element Detector System for Synchrotron-Based Coronary Angiography*, Nuclear Instruments and Methods, in press (1994).
2. H.D. Zeman and H.R. Moulin, *Removal of Harmonic Artifacts from Synchrotron Radiation Angiography*, IEEE Transactions on Nuclear Science, Vol. 39, No. 5, pp. 1431-1437 (October 1992).

This work was supported by the U.S. Department of Energy Contract No. DE-AC02-66CH00016 (BNL); DOE Contract No. DE-FG03-87ER60527-M011 (Giacomini).

(Submitted for International Synchrotron Radiation Instrumentation Conference SRI'94; July 18-11, 1994)

Effects of Spatial Resolution and Spectral Purity on Transvenous Coronary Angiography Images

D.Chapman, W. Thomlinson, N.F. Gmlr

National Synchrotron Light Source, Brookhaven National Laboratory, Upton, NY 11973-5000, USA

J.P. Dervan, T. Stavola

Division of Cardiology, Health Sciences Center T17-020, SUNY at Stony Brook, NY 11794-8171, USA

J. Giacomini, H. Gordon, E. Rubenstein

Department of Medicine, Stanford University, Stanford, CA 94305, USA

W. Lavender

Hansen Experimental Physics Laboratory, Stanford University, Stanford, CA 94305, USA

C. Schulze

European Synchrotron Radiation Facility, BP 220, 38043 Grenoble Cedex, France

A.C. Thompson

Center for X-Ray Optics, Lawrence Berkeley Laboratory, Berkeley, CA 94720, USA

Applications of a CCD detector in a scanning transmission x-ray microscope

Henry N. Chapman, Chris Jacobsen, and Shawn Williams.

Department of Physics, SUNY at Stony Brook, Stony Brook, NY 11794-3800, USA.

In the conventional set-up of the Stony Brook scanning transmission x-ray microscope (STXM) at the NSLS, a specimen is scanned through a beam that has been focussed by a zone plate and a proportional counter detects the total x-rays transmitted through the specimen. A back-illuminated, thinned, 512²-element CCD detector has been used on the STXM to obtain angular resolution of the transmitted x rays. The CCD detects the x rays directly and has high quantum efficiency and excellent linearity. The CCD is housed in a vacuum chamber and is liquid-nitrogen cooled to minimise noise. A small aluminium-coated silicon nitride window admits x rays to the detector. The distance from the focus to the detector plane may be varied, but is usually placed to accept a 300 mrad angle, in any row or column, which corresponds to about three times the numerical aperture of the zone plate. Either the proportional counter or CCD may be easily selected as the detector without the need for further microscope adjustments.

Several applications of this detector have been investigated: (1) A configured detector for differential phase-contrast or dark-field imaging. In this mode a CCD frame or sub-frame is recorded at each position of the specimen as it is scanned. The form of the configured detector may be chosen after the experiment by summing over regions of the CCD frames or by multiplying the arrays with a mask function. Direct comparisons may be made between various configurations. (2) For selected area diffraction or convergent beam diffraction, in which microdiffraction patterns are recorded at various positions on a sample. (3) For imaging with phase-retrieval and super-resolution via Wigner-distribution deconvolution. As in (2) this involves collecting a frame for each point in a scan, however processing is carried out by deconvolving the Wigner-distribution function of the zone plate from the four-dimensional data set. (4) For testing zone-plate optics, such as measuring diffraction efficiency as a function of focal order and zone radius, or by performing a Foucault test. (5) As a quick alignment tool for the microscope. Optimisation of the beamline and microscope optics can be made easily when the CCD is read out repeatedly at a rapid rate.

MoD9

DDX Diffraction System : A Combined Diffraction System with EDX and ADX for High Pressure Structural Studies

J. H. Chen*, T. Kikegawa, K. Yaoita¹⁾ and O. Shimomura

Photon Factory, National Laboratory for High Energy Physics
Tsukuba, Ibaraki 305, Japan

¹⁾ National Institute for the Research of Inorganic Materials
Tsukuba, Ibaraki 305, Japan

A Dual Dispersive X-ray (DDX) diffraction system which combines Energy Dispersive X-ray (EDX) diffraction with Angle Dispersive X-ray (ADX) diffraction has been developed on the cubic-type multi-anvil press MAX80 at the NE5C beam line of the TRISTAN Accumulation Ring (6.5GeV) at the Photon Factory. With the DDX diffraction system, quick recording of the diffraction pattern is made in the EDX diffraction mode for pressure determination and sample identification, and high-quality diffraction patterns with reliable diffraction intensities are obtained in the ADX diffraction mode for structural analyses. It requires only three minutes to switch between the EDX and ADX diffraction modes.

Figure 1 shows the layout of the DDX diffraction system. The same optical system with a Solid State Detector (SSD) is used in both the EDX and ADX diffraction modes. A retractable double crystal [Si(111)] monochromator is used in the ADX diffraction mode and the data collection is made by angular step-scanning with the SSD.

The structural relation between BiIII and BiIII' which was suggested by previous researcher was investigated with this system. The volumetric compressibility was obtained by the EDX diffraction mode and the atomic arrangement was determined from the data collected in the ADX diffraction mode. No significant change was found around the suggested transition pressure. The crystal structure of BiIII' is therefore determined to be identical to that of BiIII.

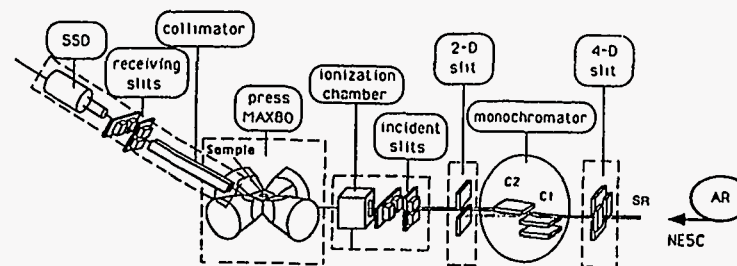


Figure 1 The layout of the DDX diffraction system.

* Present address: Center for High Pressure Research and Department of Earth and Space Sciences, State University of New York at Stony Brook, Stony Brook, NY 11794-2100, USA.

MoD10

BRAGG REFLECTION FROM MOLECULAR CRYSTALS AT THE CORE
ANISOTROPIC RESONANCES: SOFT X-RAY POLARIZATION APPLICATIONS

Vladimir A. Chernov, Nikolay I. Chkhalo, Sergey V. Mytnichenko
Siberian SR Center at Budker INP, 630090, Novosibirsk, Russia
Telex: 133116 ATOM SU. Fax: (3832)35-21-63

The simple theory and potential applications of a new structural technique to study molecular crystals, anomalous scattering at the core excited anisotropic molecular resonances, will be presented. In the SX range (0.1-1 keV) the discrete resonance strengths of light elements (B,C,N,O,F) are well known to be extremely strong. Another important feature of these resonances is the strong polarization anisotropy resulted from the low symmetry of functional chemical groups. Since each functional group has its own characteristic resonance energy, one can analyze diffraction at the isolated group by tuning the beam energy [1].

The diffraction and scattering in resonant conditions are essentially anisotropic and have unusual polarization properties. For example, a sigma-polarized incident beam can be transformed into a pi-polarized one and vice versa; in another cases only a circularly polarized beam is reflected, etc [2]. Thus this phenomena can be applied not only to study the structure of crystals, but to analyze or transform the beam polarization properties as well.

To check theoretical predictions we have revised the previous experimental reflectivity data of commonly used in SX-range phthalate crystals [3]. To ensure our conclusions we have first studied the properties of the forbidden by a screw-axis 21 rule (001) reflection from NAP crystal near the carbon K-edge. The reflectivity versus energy measurements have shown a violation of the extinction rule and the strong resonance-like reflectivity behaviour near the K-edge. Besides, the reflected beam intensity varies with azimuthal angle according to the theoretical predictions and indicate full scale modulation [4]. Moreover the polarization measurements have shown remarkable conversion of the beam from sigma-polarization to pi-polarization and vice versa going on in the diffraction [5].

1. V. A. Chernov, S. V. Mytnichenko, in Proc. International Conference on Anomalous Scattering, Malente/Hamburg, Germany, 1992; V. A. Chernov, S. V. Mytnichenko, Preprint No. 93-16, Budker INP, Novosibirsk, 1993.
2. V. A. Dmitrienko, Acta Cryst. A39, 29, 1983.
3. V. A. Chernov, S. V. Mytnichenko, X-Ray Sci. and Techn., 1994, in press.
4. V. A. Chernov, N. I. Chkhalo, S. V. Mytnichenko, Preprint No. 94-52, Budker INP, Novosibirsk, 1994; to be submitted in Acta Cryst.
5. V. A. Chernov, N. I. Chkhalo, S. V. Mytnichenko, to be published

MoD11

A new high pressure diffraction facility at the SRS.

S.M. Clark

DRAL, Daresbury Laboratory, Warrington, WA4 4AD, UK.

A new high pressure diffraction facility is under construction at the Daresbury Laboratory Synchrotron Radiation Source. High pressures will be generated by a 1000 ton hydraulic press in a novel horizontal configuration. Samples will be contained in a Walker type high pressure cell which will achieve pressures in excess of 250kbar at temperatures greater than 2000°C. Both monochromatic and white beam experiments are planned with this equipment. Details of the beam definition apparatus, press and Walker cells, detector table and detector systems will be given together with the first results from this facility.

MoD12

Development of Large Volume Reaction Cells for kinetic studies using energy-dispersive powder diffraction.

S.M. Clark, A. Nield, J.S.O. Evans *, R.J. Francis* and D. O'Hare*.

DRAL, Daresbury Laboratory, Warrington, WA4 4AD, UK.

*Inorganic Chemistry Laboratory, South Parks Road, Oxford, OX1 3QR, UK.

The measurement of the rates of chemical reactions is of fundamental importance to chemistry. Powder diffraction offers a powerful method of measuring reaction rates for processes that involve crystalline materials. The well established techniques of multiphase quantitative analysis are used on a series of powder diffraction spectra collected during the course of a chemical reaction to determine the amount of each crystalline component as a function of time. This method is of particular importance when a number of processes are occurring simultaneously since the powder method can determine the amount of each phase in a mixture of phases and hence each rate. One problem however lies in the small amount of material that is usually sampled by the X-ray beam which could be unrepresentative of the bulk reaction. To overcome this problem we have developed a multi-slit energy-dispersive powder diffraction system together with a range of large volume reaction cells. We shall present the basic experimental layout and describe three types of large volume cell: a high temperature cell, a cell for air sensitive samples and a hydrothermal cell. Data collected at the energy-dispersive powder diffraction facility of the Daresbury synchrotron source will illustrate the use of each cell.

MoD13

Development of a new high temperature cell for powder diffraction using induction heating.

S.M. Clark, T. Rathbone, P. Irvine and J. Flaherty.

DRAL, Daresbury Laboratory, Warrington, WA4 4AD, UK.

A new spinning flat plate induction furnace for powder diffraction studies has been developed at the Daresbury Laboratory Synchrotron Radiation Source. The furnace, which is capable of temperatures in excess of 2000°C, uses a carbon sample holder that couples to a surrounding induction coil. A magnetic coupling is used to connect the sample holder to an external DC motor for rotation. The powder sample is held in a rotary pump vacuum. Details of the furnace, induction heater and control system will be given together with data from some recent high temperature structural studies.

MoD14

In situ synchrotron radiation SAXS study of the kinetics of growth of CdTe nanocrystals in borosilicate glass

A. F. Craievich

National Laboratory for Synchrotron Light/CNPq, Campinas, SP and Institute of Physics/USP, São Paulo, Brazil

O. L. Alves

Institute of Chemistry, UNICAMP, Campinas, SP, Brazil

and

L. C. Barbosa

Institute of Physics, UNICAMP, Campinas, SP, Brazil

A number of materials doped with semiconductor nanocrystals exhibit interesting non-linear optical properties associated with the existence of quantum electronic confinement effects. The most investigated composites of this type are glass matrices containing CdSe nanocrystals⁽¹⁾. The optical properties of these materials depend on the nature, average size and dispersion in size of the semiconductor nanocrystals. Recently it was demonstrated that CdTeS nanocrystals immersed in borosilicate glasses also exhibit confinement effects⁽²⁾. A first small-angle x-ray scattering (SAXS) study of this system indicated that the dispersion in the sizes of nanocrystals exhibits a minimum during annealing at a constant temperature⁽³⁾. The present communication reports an *in situ* SAXS study using synchrotron radiation of binary CdTe and CdTe(S) quasi-binary semiconductor-glass composites. The purpose of the investigation is to determine the correlation between: i) annealing and pre-annealing treatments of the samples, ii) structural features (average size and dispersion in size of the nanocrystals) and iii) optical absorption properties. *In situ* experiments were performed using a high temperature cell⁽⁴⁾ to maintain the semiconductor-glass composites at a constant temperature during SAXS measurements. From the experimental SAXS results, the geometric average and geometric standard deviation of crystal size distribution were determined for increasing annealing times at 570 C. This allowed us to characterize the structural variations associated with nanocrystal growth. The average radius of the nanocrystals (assumed spherical) ranges from 20 to 50 Å. Similar experiments were carried out using "as quenched" glass samples and samples pre-treated at a lower temperature. Optical absorption spectra of both types of samples showed a clear correlation with the nanocrystal structural characterization. The experimental SAXS curves exhibit, in addition to the contribution attributed to nanocrystals, a sharp increase for decreasing scattering angle in the very low angle range. This feature of SAXS intensity is produced by heterogeneities in electronic density whose average size is several hundreds Å. Since the nature of these rather large heterogeneities could not be unambiguously established from the present investigation, additional experiments using the anomalous SAXS technique are planned.

(1) Ekimov, A. I. and Efros, A. E., Soc. Phys. Semicond. **16**, 772 (1982).

(2) Medeiros Neto, J. A., Barbosa, L. C., Cesar, C. L., Alves, O. L. and Galembeck, F., Appl. Phys. Lett. **59**, 2715 (1991).

(3) Craievich, A. F., Alves, O. L. and Barbosa, L. C., J. de Physique IV, C8, **3**, 373 (1993).

(4) Bagnato, O. and Augusto, N. V., LNLS Technical Manual 03/92.

First results from the SpectroMicroscopy Beamline at the Advanced Light Source

J.D. Denlinger^{1,7}, E. Rotenberg^{1,4}, T. Warwick¹, G. Visser², J. Nordgren³, J.-H. Guo³, P. Skytt³, S. D. Kevan⁴, K. S. McCutcheon⁴, D. Shuh⁵, J. Bucher⁵, N. Edelstein⁵, J. G. Tobin⁶, and B. P. Tonner⁷

¹Advanced Light Source, Lawrence Berkeley Laboratory, Berkeley, CA 94720

²Department of Physics, University of California, Berkeley, CA 94720

³Uppsala University, Uppsala, Sweden S-75121

⁴Department of Physics, University of Oregon, Eugene OR 97403

⁵Chemical Sciences Division, Lawrence Berkeley Laboratory, Berkeley, CA 94720

⁶Chemistry and Materials Science Department, Lawrence Livermore National Laboratory, Livermore CA 94550

⁷Department of Physics, Univ. of Wisconsin-Milwaukee, Milwaukee, WI 53211

The SpectroMicroscopy Beamline at the Advanced Light Source is comprised of a 5 meter, 5-cm-period undulator and a 10,000-resolving-power spherical grating monochromator covering the spectral range from 100 to 1300 eV. Through the use of adaptive optics, this beamline focuses to a 25µm spot for experiments such as ultra-ESCA (small-area, high-resolution, time-resolved core-level photoemission), photoelectron diffraction, soft X-ray fluorescence, and soft X-ray microscopy which are optimal for high-brightness sources. Within only two months of operation we have already met significant performance goals in spectroscopy. Examples will be given of high resolution fluorescence spectroscopy, ultra-ESCA from sub-nanogram, microscopic actinide compounds, and high resolution photoemission core-level studies.

This paper should be considered for a POSTER. Contact:

Dr. Jonathan Denlinger

MS 7-222 Lawrence Berkeley Laboratory, Berkeley, CA 94720.

Tel. (510) 486-5648 Fax (510)486-7696

Design of a tandem soft X-ray microscope for high spectral and spatial resolution spectromicroscopy under ultra-high vacuum or ambient conditions

J. D. Denlinger^{1,3}, T. Warwick¹, H. Ade², and B. P. Tonner³

¹Advanced Light Source, Lawrence Berkeley Laboratory, Berkeley, CA 94720

²Department of Physics, North Carolina State University, Raleigh, NC 27695

³Department of Physics, Univ. of Wisconsin-Milwaukee, Milwaukee, WI 53211

We present the design of a new soft X-ray photoemission microscope which is under construction on the SpectroMicroscopy Beamline at the Advanced Light Source, which includes independent stations in tandem for imaging either in ultra-high vacuum (UHV) or atmospheric pressure. The microscope facility includes a 5 meter long, 5 cm period undulator, a spherical grating monochromator with 10,000 resolving power and moving exit slit, adaptive refocusing optics which provide a stigmatic monochromatic beam at a fixed aperture location, a micro-zoneplate intended for operation near the diffraction limit, and a high transmission electron energy analyzer. The design philosophy for the UHV microscope has been to provide the experimenter with the flexibility expected in ordinary synchrotron photoemission spectroscopy, such as sample temperature control and 0.1 eV energy resolution, while at the same time providing imaging capability with spatial resolution well below 100 nm. Results from characterization of the adaptive optics, spectral resolution, and analyzer performance will be presented.

This paper should be considered for a POSTER. Contact:

Dr. Jonathan Denlinger

MS 7-222 Lawrence Berkeley Laboratory, Berkeley, CA 94720.

Tel. (510) 486-5648 Fax (510)486-7696

MoD17

**Multiple Energy Computed Tomography (MECT) at the NSLS:
Status Report**

F. A. Dilmanian, X. Y. Wu, Z. Chen, and D. N. Slatkin
Medical Department

D. Chapman, M. Shleifer, F. A. Staicu, and W. Thomlinson
National Synchrotron Light Source
Brookhaven National Laboratory, Upton, New York 11973

A monochromatic computed tomography (CT) system called multiple energy computed tomography (MECT) for imaging the human head and neck is being developed at the X17 wiggler beam line of the NSLS. It employs a horizontal fan beam and an upright (seated) subject rotating about a vertical central body axis. MECT's potential is based on the beam's narrow energy bandwidth ($\approx 0.2\%$, compared to $\approx 50\%$ in conventional CT), which eliminates beam-hardening effects and allows the efficient use of the following energy-selective methods: K-Edge Subtraction (KES) of iodine and of other high-Z elements, and Dual Photon Absorptiometry (DPA). A prototype of MECT has provided images of phantoms, and of live rats, gerbils, and rabbits. These images show that a) the image contrast resolution obtained from a single-energy beam using monochromatic synchrotron radiation is higher than that obtained from conventional CT; b) the advantages of KES and DPA MECT lie not only in the quantification of the contrast but also in the enhancement of the image contrast resolution, although the concomitant increase of image noise is not negligible; and c) the combination of the high sensitivity of the method for density measurement of the low-Z-element group and the large amount of oxygen in the bone should make also the low-Z-element image useful in the diagnosis of the bone disorders, besides the intermediate-Z image which is used for bone mineral densitometry. This latter two-viewed DPA CT may find applications in bone disorders such as osteomalacia in which both the low-Z and the intermediate-Z element groups are affected.

The clinical MECT system is being constructed while its prototype components are progressively upgraded as indicated below.

a. The clinical MECT's monochromator has two independent Laue-Laue monochromators, in tandem, to provide the low- and the high-energy beams for DPA. The energy-switching time is designed as 2 s. The system's first section is a prototype now, and will be tested soon.

b. The new 480-element detector is composed of linear-array modules of CdWO₄, having 32 elements with 0.5 mm center-to-center spacing, coupled to PIN diode modules of corresponding geometry. The detector is expected to be ready in June 1994.

c. The new data acquisition system, which is now being commissioned, employs a fast interface to the host DEC Alpha computer. The interface allows sustained data collection at a rate of 1.4 Mbyte/s for several hundred seconds, the rate and measurement duration necessary for helical CT.

The clinical MECT system is expected to be functional in late 1995 when the patient chair, additional beamline components, and the safety control system will be ready. The first images of human subjects are expected in 1996, with a 20 cm field of view.

This research has been supported by Department of Energy contract DE AC02-76CH00016.

MoD18

PRELIMINARY RESULTS OF ANIMAL LYMPHATIC SYSTEM STUDY
AT THE VEPP-3 ANGIOGRAPHY STATION

G. N. Dragun*, N. A. Mezentsev, K. A. Kolesnikov, M. V. Kuzin,
S. I. Nesterov, V. F. Pindyurin, E. L. Zelentsov*

Budker Institute of Nuclear Physics,
630090 Novosibirsk, Russia

*Tomography Centre, 630090 Novosibirsk, Russia

Preliminary results of an X-ray visualization the lymphatic nodes of alive rats are presented. The lymphatic nodes were contrasted *in vivo* by iodine containing agent at low concentrations. The technique of digital subtraction angiography at the K-absorption edge of iodine was applied to visualize the lymphatic nodes.

Experiments were performed at the angiography station of the VEPP-3 storage ring. The station is based on the dedicated double-beam X-ray monochromator [1] and the double one-coordinate X-ray detector [2]. Brief description of used experimental instrumentation are given as well.

References:

1. V.P. Barsukov, I.P. Dolbnya et al. Nuclear Instruments and Methods in Physics Research, V. A308, N 1/2 (1991) 419.
2. E.N. Dementiev, I.P. Dolbnya et al. Review of Scientific Instruments, V. 60, Pt. 2, N 7 (1989) 2264.

MoD19

**The microdiffraction instrumentation and experiments
on microfocus beamline at ESRF.**

P. Engström, S. Fiedler, C. Rickel

ESRF, B.P. 220, F-38043 Grenoble, France.

The micro focus beamline (BL1) at ESRF is designed to have as high flux as possible in a $10 \mu\text{m}$ by $10 \mu\text{m}$ focal point and to be used for microdiffraction experiments. This is done by focusing the full low- β undulator beam with an ellipsoidal mirror which should give a flux of 10^{12} photons with a bandwidth of $2 \cdot 10^{-4} \Delta E/E$.

There has also been a number of tests with other kinds of optics to get a smaller focal spot, in the order $1 \mu\text{m}$ or less. Optics like tapered capillaries, crystal based bragg fresnel and others has been tested. The work on the bragg fresnel optics will be covered by another paper at the conference.

The experimental setup consist of: 1/ a low- β undulator with a K_{max} of 2.2, 2/ either a tunable (6.5 to 16 keV) liquid nitrogen cooled Si(111) channel cut monochromator with bandwidth of $2 \cdot 10^{-4} \Delta E/E$ or a multilayer monochromator used at 8 keV or 17 keV, 3/ slits to define the beam, 4/ either a focusing ellipsoidal mirror with a demagnification ratio of 10:1 or a capillary.

The performance of the different combinations and some diffraction experiment (thin metal-layers and biological samples) will be given.

MoD20

A computer controlled system for studying the gas - solid state reactions in X-ray diffraction experiments.

Gaponov Yu.A., Evdokov O.V., Sukhorukov A.V., Tolochko B.P.
Institute of Solid State Chemistry, Novosibirsk, 91, Russia.

An automated system for controlling the temperature and pressure in reaction chamber during solid state reactions studied by X-ray methods with use SR was developed and realized in Siberian Synchrotron Radiation Center (BINP, Novosibirsk). Computer algorithm of controlling the temperature in reaction chamber with use CAMAC-based subsystems was developed and realized. Test experiments for definition of thermal characteristics of reaction chamber was carried out in the range of pressure 0-0.2MPa, temperature 293-800K with accuracy 0.01MPa and 1-3K respectively. The system was adjusted and tested in experiments on studying the thermal decomposition of same metal organic systems.

MoD21

POWDER DIFFRACTION USING IMAGING PLATES AT THE AUSTRALIAN NATIONAL BEAMLINE FACILITY AT THE PHOTON FACTORY

*R. F. Garrett, D. J. Cookson and G. J. Foran and T. M. Sabine,
Australian Nuclear Science and Technology Organisation,
PMB 1, Menai, NSW, 2234, Australia.*

*B. J. Kennedy,
School of Chemistry,
University of Sydney,
NSW, 2006, Australia.*

*S. W. Wilkins
CSIRO-Division of Materials Science and Technology
Locked Bag 33, Clayton, Vic, 3168, Australia.*

A novel X-ray diffractometer was installed at the Australian National Beamline Facility at the Photon Factory, Japan, in October 1993. One of the major capabilities of the instrument is high speed high resolution powder diffraction using Imaging Plate detectors. The diffractometer combines a two circle goniometer and a large cassette in which Imaging Plates can be loaded covering 320° of 2θ . The diffractometer is enclosed in a large vacuum chamber and can be operated in air, vacuum or helium. Powder diffraction data can also be collected using a conventional scintillation detector mounted on the two circle goniometer.

Recently, powder data has been obtained from rutile (TiO_2) at wavelengths from 0.67 to 1.9 Angstroms using Imaging Plates, and has been used to characterise the performance of the instrument. The data has been refined using the Rietveld method and R values of under 2% obtained. The resolution of the system varies from a minimum of about 0.04° to around 0.2° at 2θ angles above 120° , which is the equal of most synchrotron based powder diffractometers, and only slightly worse than that obtained using an analyser crystal and scintillation detector. However, using the Imaging Plates, 160° of data is simultaneously acquired in an exposure of about 10 minutes, compared to conventional counter diffractometer scans which routinely exceed 10 hours.

The performance of the powder diffractometer will be described in detail, and future plans, including utilising the high speed of data collection in a time resolved mode, will be discussed.

MoD22

Ultra Small Angle X-Ray Scattering at the HASYLAB Wiggler

Beamline BW4

R. Gehrke, M. Bark, D. Lewin, S. Cunis

HASYLAB at DESY, Hamburg, University of Ulm

Time resolved USAXS measurements using position sensitive detectors are preferably performed with pinhole collimating systems. A system of this type has been constructed at HASYLAB at one of the new insertion device beamlines of DORIS III. The basic layout of this instrument has been published at the beginning of the construction phase together with theoretical performance calculations. In the meantime the instrument was extensively tested and first measurements have been carried out. In the presented paper a summary of this first experiment is given. It includes a description of the instrument, the characterization of the focal spot produced by the optics (i.e. double crystal monochromator and toroidal mirror), the performance of an especially constructed collimating slit system using adjustable single crystal blades, and the achievable resolution of the instrument in terms of the largest observable correlation length which is limited to about 600 nm at 8 keV photon energy.

Some scientific results are illustrating the practical use of the beamline in the field of material science and the attained improvements compared with previously existing SAXS instruments at synchrotron radiation sources. For the first time the complete scattering patterns of SBS blockcopolymer superstructures could be observed and the formation of crazes in different polymer materials during mechanical deformation could be measured. Anomalous scattering was used for contrast variation in zeolites in order to detect the growth of extended metal clusters inside the material.

R. Gehrke, Rev. Sci. Instrum. **63**, 466 (1992)

MOD23

NSLS Transvenous Coronary Angiography Beamline Upgrade and Advanced Technology Initiatives

N.E. Gmlt, D. Chapman and W. Thomlinson

National Synchrotron Light Source, Brookhaven National Laboratory, Upton, NY 11973-5000, USA

A.C. Thompson

Center of X-Ray Optics, Lawrence Berkeley Laboratory, Berkeley, CA 94720, USA

W.M. Laverder

Hansen Experimental Physics Laboratory, Stanford University, Stanford, CA 94305, USA

K. Scailia and N. Malloy

Advanced Acoustic Concepts, Inc., Ronkonkoma, NY 11779-6820, USA

J. Mangano and J. Jacob

Science Research Laboratory, Inc., Somerville, MA 02143, USA

Since October 1990, the coronary anatomies of 16 male and female patients have been imaged as part of the Digital Subtraction Transvenous Coronary Angiography research program. This program takes place in the National Synchrotron Light Source (NSLS) Synchrotron Medical Research Facility (SMERF) on the X17B2 wiggler beamline. Encouraged by the success of the initial patient images, the NSLS has recently embarked on an ambitious upgrade effort. This effort covers all aspects of the X17B2 beamline and includes improved radiation shielding, a Laue monochromator assembly, a computer-controlled 5-axis patient scanning chair assembly, a fast low-noise image acquisition system, and a modularized patient safety system. These improvements will allow major advances in imaging patients based on ECG signal gating and multiple view imaging. Two advanced technology initiatives are underway with industrial collaborators. One will develop real-time image acquisition and display of the subtracted digital images. The second will develop a compact x-ray source for medical imaging. The source will be a linear electron accelerator creating characteristic radiation line emissions.

This work was supported by the US Department of Energy Contract No. DE-AC02-76CH00016, the Advanced Research Projects Agency, and NIH grant 1 R01 HL 39253-04.

MOD24

(Submitted for International Synchrotron Radiation Instrumentation Conference SR194; July 18-22, 1994)

Total Photoelectron Imaging of Sub-micron Stripe Patterns Using Soft X-ray Microbeam Formed by Wolter-type Mirror

Masaki Hasegawa and Ken Ninomiya

Central Research Laboratory, Hitachi, Ltd., Kokubunji, Tokyo 185, Japan

Photoelectron microscopes are promising tools for microanalysis both in surface science and in industrial applications. We have been developing a scanning photoelectron microscope using a Wolter-type grazing incidence mirror.¹ In the present study, we have performed one-dimensional imaging of sub micron-sized stripe patterns by detecting total photoelectron signals.

The design of the Wolter-type mirror is shown in Fig. 1. The demagnification of the mirror is 1/29.8. The mirror was fabricated by using vacuum replication and its mirror surface was then reproduced with epoxy resin.² The mirror was installed in the bending-magnet soft x-ray beamline (BL-8A) at the Photon Factory (KEK-PF) in Tsukuba. A 30- μm pinhole was positioned at F_1 and we generated about 1 μm sized soft x-ray microbeam with energy of 150 eV. Photon flux was $\sim 10^4$ photons/s. The microbeam was scanned on a sample surface in one-direction. The samples were several sets of Al stripe patterns formed on a SiO_2 layer on a Si wafer. Each set consisted of 5-10 Al stripes with the same width and spacing ranging from 4 to 0.7 μm . Photoelectrons emitted from the sample were detected with a microchannel plate.

The variations of total photoelectron intensity are shown in Figs. 2(a)-(c) when the microbeam was scanned on the 4 μm (Fig. 2(a)), 1 μm (2(b)) and 0.7 μm (2(c)) stripes. Arrows in the figures denote the center of the Al stripes. As shown in the figures, each stripe was clearly detected with modulations of 0.33, 0.12, and 0.08, respectively. We have achieved the highest lateral resolution in one-dimensional photoelectron imaging performed by grazing incidence mirrors. This work has been performed under the approval of the Program Advisory Committee of Photon Factory (Proposal No. 93-Y003) of the National Laboratory for High Energy Physics.

References

1. K. Ninomiya, M. Hasegawa, A. Aoki, and K. Suzuki, *Jpn. J. Appl. Phys.* **30**, 2889 (1991).
2. M. Hasegawa and K. Ninomiya, *Rev. Sci. Instrum.* (to be published).

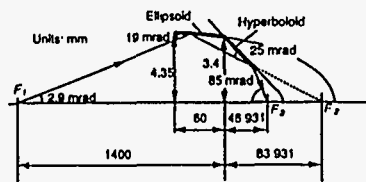


Fig. 1 Wolter-type mirror design.

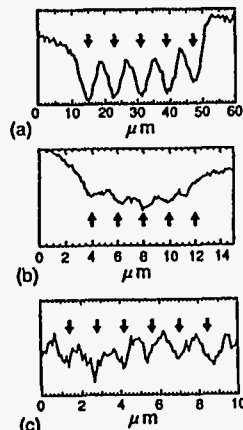


Fig. 2 Photoelectron intensity variation of scanned on stripe pattern. Stripe widths are (a) 4 μm , (b) 1 μm , and (c) 0.7 μm .

ULTRAHIGH VACUUM DIFFRACTOMETER FOR GRAZING-ANGLE X-RAY STANDING-WAVE EXPERIMENTS AT A VERTICAL-WIGGLER SOURCE

O. Sakata and H. Hashigume, Research Laboratory of Engineering Materials, Tokyo Institute of Technology, Nagatsuta, Midori, Yokohama 227, Japan

A ultrahigh vacuum diffractometer has been designed for grazing-angle X-ray standing-wave studies of surface structures. It features the horizontal diffraction-vector configuration for use with vertically polarized X-rays from the vertical-wiggler source of the Photon Factory. A sample is mounted on a horizontal holder, of which inclination angles and translations are controlled by crossed swivels in air via a flexible bellows joint. This varies glancing-incidence angle ϕ of X-rays on the sample surface with a 5- μrad accuracy (Fig. 1). A load-lock system mounted at the top of the chamber allows the sample to be received from a portable vessel under high vacuum condition. Beryllium windows allow the specular reflected beam and the Bragg diffracted beam to reach separate X-ray detectors, and the fluorescent X-rays to enter an energy-sensitive semiconductor detector. A base pressure of 4×10^{-7} Pa is maintained by an ion-sputter pump and a titanium getter pump. The whole assembly, weighing some 55 kg, sits on the high-precision rotary table at beamline 14B, which controls the sample ω angle with a reproducibility better than 0.5 μrad .

The instrument was successfully applied to the collection of X-ray standing-wave data from an arsenic-adsorbed $\text{Si}(111) 1 \times 1$ surface [1]. Samples prepared in the authors' institute by As deposition on clean silicon 7×7 surfaces were transported to the synchrotron radiation site in a pumped vessel. 16.8-keV photons obtained from a silicon monochromator were guided onto the sample surface at grazing angles to meet the Bragg condition on the perpendicular (220) planes. Data were collected by scanning the sample ω axis for fixed ϕ angles near the critical angle for total external reflection (1.85 mrad). The observed As fluorescence profiles are well explained by the model indicating a bulk-like surface with threefold-coordinated As atoms in the first layer. Fits of the specular-reflection profiles determined the absolute values of the ϕ angles, which were used to evaluate the two-dimensional crystalline order of As atoms from the fluorescence data. Very high in-plane coherent fractions close to 0.9 were consistently observed for the As atoms.

The instrument was also used to confirm the shallow penetration of X-rays in the grazing-angle geometry. Sr fluorescences observed from a 100 \AA -thick CaSrF_2 epilayer on a GaAs substrate are predominantly modulated by the X-ray standing waves generated by the CaSrF_2 overlayer. This provides a possibility of studying the surface structures of very thin epitaxial crystals with the grazing-angle XSW technique.

- [1] O. Sakata *et al.* *Phys. Rev. B* **48** 11408 (1993).

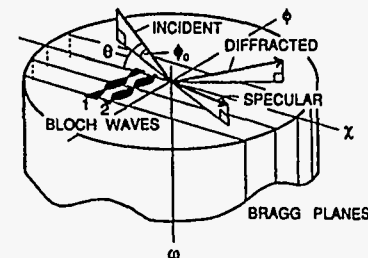


Fig. 1 Geometry for grazing-angle X-ray standing-wave measurements.

BIOLOGICAL IMAGING WITH A NEW TYPE OF SOFT X-RAY MICROSCOPE

Gregory Hirsch
Hirsch Scientific
365 Talbot Avenue, Suite D8
Pacifica, CA 94044

The operation of a new type of soft x-ray microscope at SSRL is described. This microscope represents a significant simplification over existing x-ray microscopes and has the potential to be a valuable tool for biological research and, possibly, clinical use. The technique is a variation of the photoelectron contact method [1] and the basic principles have been previously described [2]. The geometry of the instrument is very similar to the field emission microscope. As in field emission microscopy, an emitter is placed in a vacuum chamber, facing a microchannel plate detector. Instead of the usual solid emitter, the instrument uses a special cone-like hollow emitter. The specimen to be examined is placed *inside* the hollow emitter tip. To produce an image, soft x-rays are beamed down the axis of the hollow cone from the open end, through the specimen, and onto the hemispherical emitter tip membrane. An x-ray contact image is thereby produced on the emitter tip, corresponding to the x-ray absorption of the specimen. The emitter tip is transparent to soft x-rays and is coated with a high efficiency photoemissive layer. Photoelectrons are liberated into the vacuum, outside the emitter tip, in a pattern corresponding to the contact image of the specimen. The electrons are accelerated radially to the detector by a high voltage placed on the emitter. A magnified, high resolution, real-time image results. The specimen can remain at atmospheric pressure, wet, unstained and unsectioned. The instrument had previously demonstrated a resolution of roughly 1000Å with non-biological test objects [3]. More recently, imaging of dry biological specimens with a similar resolution was accomplished. Microscope operation is currently being extended to the imaging of wet biological specimens. It is expected that routine microscopy of wet specimens with a resolution below 1000Å will be accomplished in the near future. The advantages, limitations and ultimate performance of the technique will be discussed.

This work was partially supported by NIH SBIR grants 1 R43 RR07941-01 and 9 R44 GM51669-02. Work done partially at SSRL, which is operated by the Department of Energy, Office of Basic Energy Sciences.

[1] F. Polack, S. Lowenthal, D. Phalippou, P. Fournet in *X-ray Microscopy II*, D. Sayre, M. Howells, J. Kirz, H. Rarback eds. (Springer-Verlag, Berlin, 1988), 220 (1988)

[2] G. Hirsch, U.S. Patent 4,829,177 (1989)

[3] G. Hirsch, Stanford Synchrotron Radiation Laboratory 1991 Activity Report, 121 (1992)

Element Specific Imaging of Structural- and Magnetic Domains using Linear and Circular Polarized Light

K.Holldack, T.Kachel, W.Gudat
BESSY GmbH Berlin, Lentzeallee 100
14195 Berlin, Germany

The commercial photoelectron microscope ESCASCOPE (Fisons Ltd.) had been installed at the SX 700/III monochromator at a bending magnet of the BESSY storage ring. In addition to its high electron energy resolution the spectromicroscope allows to take photoelectron images of surfaces with a lateral resolution of 10 µm. The photoelectrons were excited in a spectral range from 10eV up to 2000eV photon energy with adjustable helicity and polarization degree up to 90%.

Examples illustrating the possibilities and the limits of the set-up will be presented: Linear polarized light was used to image lateral distributions of nitrogen interstitials in Si₃N₄ films and to image stripped hydrogen in organic films by resonant photoabsorption (participant- and spectator electron detection) /1/.

Circular polarized light has been used to image magnetic domains of Fe(100) using the Auger-yield imaging method which was developed by one of us in preliminary experiments /2/.

The antiferromagnetic coupling of rare earth monolayers (Gd,Tb) on Fe(100) substrate was directly observed using Auger-imaging and resonant photoemission imaging, respectively.

Exploitation of these techniques by applying different spectroscopic modes and photon energies allows image information based on chemical- structural- magnetic- and even molecule symmetry contrasts. A comparison with other imaging techniques will be given.

/1/ K.Holldack, M.Grunze, M.Kinzler, C.M.Brundle: *J.Electon.Spectr.Rel.Phen.* (submitted)

/2/ C.M.Schneider, K.Meinel, J.Kirschner, K.Holldack, M.Kinzler, M.Grunze: *J.Appl.Phys.*, 63, 1993, 2432

New Diffractometer for Thin Film Structure Analysis

under Grazing Incidence Condition

Yoshimasa HORII, Hirofumi TOMITA and Satoshi KOMIYA

FUJITSU LABORATORIES Ltd.

10-1, Morinosato-Wakamiya Atsugi, Kanagawa, 243-01, JAPAN

Grazing incidence X-ray diffraction (GIXD)¹⁻³ is an effective technique to characterize the structures of crystal near the surface and applied on semiconductor thin film layer. Furthermore, it has already known that the penetration depth of X-ray can be controlled as changing the grazing incident angle.³ In the present paper, we will describe a structure and an accuracy of our designed GIXD goniometer and a few application for material analysis.

FIGURE 1 shows the new diffractometer under GIXD condition. The monochromatized X-ray incidents the goniometer through a slit. A grazing angle is controlled by the horizontal rotation axis of ψ . A sample and a detector rotate around the θ and 2θ axes, respectively, and they are orthogonal to the ψ . The detector also moves around the circular arm on the 2θ table, that is defined as μ rotation. The goniometer for the θ - 2θ and μ scanning is set on the goniometer for the ψ rotation. The sample goniometer for fine adjustment is also set on the θ table. Since the ψ axis is perpendicular to the θ - 2θ axes and they are independently controllable, the angle of the incident beam to the surface of a sample, ψ , is kept constant during the θ - 2θ scanning. So that, we can measure the θ - 2θ diffraction for the lattice planes perpendicular to the surface of a sample on any incident condition. Furthermore, X-ray diffraction for the lattice planes inclined to the sample surface⁴ is measured by the ψ - 2μ rotation.

The GIXD experiment was carried out on the beam line 17C of Photon Factory (PF). It was applied the θ - 2θ measurement for TiSi_2 which has two phase structure silicidation (C49 and C54). They are clearly identified in relation to annealed conditions. The ψ - 2μ measurement was performed for thin film GaAs (20 mono-layers) on Si. From the GaAs (224) diffraction, it is obtained the mismatch between the inclined lattice planes. Furthermore, the lattice distortion of 20 mono-layer GaAs on Si is evaluated from the (224) and (220) lattice mismatch.

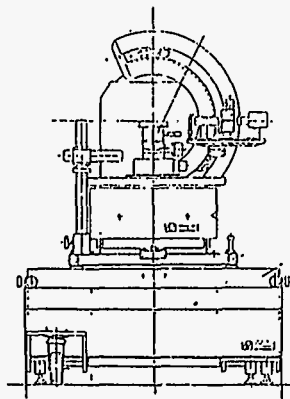


FIG.1. Schematic view of the diffractometer

References

- 1 W.C. Marra, P. Eisenberger and A.Y. Cho, J. Appl. Phys. 50, 6927(1979)
- 2 H. Dosch, Phys.Rev. B35, 2137(1987)
- 3 H. Dosch, B.W. Batterman and D.C. Wack, Phys.Rev. Lett. 56, 1144(1986)
- 4 S. Kishino, J. Phys. Soc. Jpn. 31, 1168(1971)

MICRO X-RAY DIFFRACTION TECHNIQUE FOR ANALYSIS OF THE LOCAL LAYER STRUCTURE IN THE FERROELECTRIC LIQUID CRYSTAL

A. Iida, T. Noma,* H. Miyata* and K. Hirano

Photon Factory, National Laboratory for High Energy Physics, Japan

*Canon Research Center, Canon Inc., Atsugi, Japan

Hard X-ray microprobes having less than a few μm spatial resolution have been realized at several SR facilities. The X-ray microbeam is characterized not only by the beam size but also by a photon flux, an energy resolution and an angular divergence. In this presentation, we describe the characteristics of X-ray microbeam system developed for small angle X-ray diffraction and its application to the determination of the local layer structure (LLS) of the surface stabilized ferroelectric liquid crystals (SSFLC).

An X-ray microprobe system was developed at the Photon Factory (BL-4A) using a multilayer monochromator in combination with X-ray focusing mirrors (Kirkpatrick-Baez type).¹⁾ The beam size at the sample was about $5 \times 5 \mu\text{m}$ and the angular divergence was about 0.5 mrad and 0.2 mrad in horizontal and vertical directions, respectively. The sample SSFLC cell was mounted on X-Z translation stages to determine the analyzing position and also on a θ rotation stage to obtain the rocking curve. A scintillation detector was also on X-Z translation stages.

The layer structure in thin SSFLC cells is characterized by the "chevron" structure. A zig-zag defect is the local layer structure defect observed in SSFLC and corresponds to walls between the two possible chevron directions²⁾. No direct experimental evidence of the LLS has been reported due to the complicated cell structure. A series of the rocking curves was measured by changing the analyzing position across the defect boundary. In addition to sharp peaks corresponding to the chevron structure, new peaks appearing at around $\theta=0$ indicated that the pseudo-bookshelf structure was realized at the boundary. Temperature dependence and the effect of the applied electric field were also investigated. Present results is the first direct observation of the zig-zag defect boundary in SSFLC cells.

1)A.Iida and T.Noma, Nucl. Instrum. and Methods, B82(1993)129

2)N.Clark and T.P.Rieker, Phys. Rev. A37(1988)1053

FEASIBILITY OF PHOTO-EXCITATION IMAGING IN SOFT X-RAY MICROSCOPY USING THE TRANSITION TO π^* -ORBITS IN BIOLOGICAL MOLECULES

Yoshinori Iketaki¹ and Tsutomu Watanabe¹

Res. Dev. Corporation of Japan (JRDC) 2-45-13 Honcho, Nakano-ku, Tokyo 164 Japan
¹Dept. of Phys., International Christian Univ., Mitaka-shi, Tokyo 181 Japan

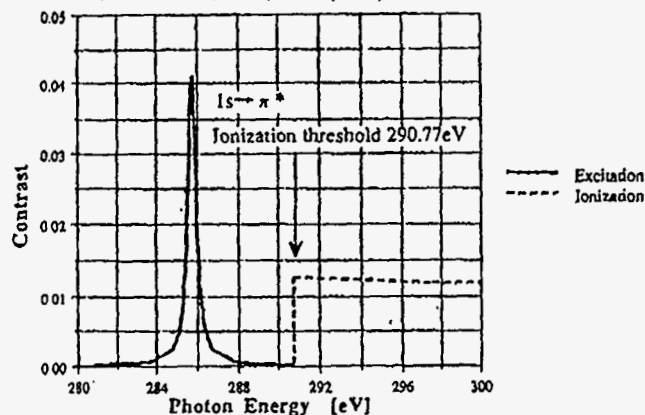
Usual X-ray microscopy for wavelengths within the water window is carried out using an absorption process caused by the *photo-ionization* of 1s electrons in carbon or nitrogen[1]. Recently, soft X-ray microscopy using inner shell *photo-excitation* was proposed by J. H. Klems [2]. This soft X-ray microscopy technique consists of a uv laser and an X-ray source. Uv laser is used for the production of unoccupied π -character orbit. It is expected that a more sensitive soft X-ray microscopy would be realized by utilizing inner-shell excitation, because the photo-excitation cross sections are generally larger than the photo-ionization cross sections by one or two orders of magnitude in this wavelength region.

Since DNA and RNA in biological cells contain innumerable bases which have unoccupied π^* -character molecular orbits. It is also expected that another type of soft X-ray microscopy would be proposed based on the use of the excitation process to unoccupied π^* -character molecular orbits. In this paper we estimate the photo-absorption cross section caused by the transition of 1s electrons to π^* -character molecular orbits and discuss the feasibility of X-ray microscopy based upon transition to unoccupied π^* -character orbits.

The figure below displays the calculated photo-absorption contrast of T4-phage as a function of photon energy

References

1. J. Kirz and H. Rarback, *Rev. Sci. Instrum.*, **56**, 1 (1985)
2. J. Klems, *Phys. Rev.*, **A42**, 2041 (1991).



¹ On leave from Olympus Optical Co. Ltd. Hachioji-shi, Tokyo 192 Japan

A Double Beam Bent Laue Monochromator for Coronary Angiography

G. Illing, J. Heuer, B. Reime, M. Lohmann, L. Schildwächter, W.-R. Dix and W. Graeff

Hamburger Synchrotronstrahlungslabor HASYLAB at DESY, Notkestr.85, 22603 Hamburg

High photon fluxes are crucial in dichromatic Digital Subtraction Angiography with line scan systems to allow for high scan speed and thus omit image blurring due to the motion of the heart. To obtain images wide enough and with sufficient vertical resolution each of the two beams used has to be at least 100 mm wide but only 0.5 mm high at the patient's heart with the beam energies bracketing the iodine K-edge at 33.17 keV [1].

Following an idea in ref. [2] a new monochromator in Laue transmission geometry has been developed, successfully tested at beamline ID11 of the ESRF and is now in use at the angiography wiggler beamline W2 at HASYLAB.

The monochromator consists of two almost identical goniometer heads in a He-filled housing which are closely mounted but independently controlled in position and angle.

Within each head a vertically bent silicon single crystal extracts a beam with a bandwidth of 180 eV from the 1.85 mm high white wiggler beam and focuses it to the patient. The crystals are 112 mm by 22 mm in size and their active part is 0.6 mm thick. The angle of asymmetry is 35.26° and the (111) reflection is used. The monochromator is located at a distance of 31.6 m from the source. With a bending radius of 10.3 m the beams are vertically focused to the patient sitting 3.8 m behind the monochromator thus also increasing intensity compared to an unbent crystal. Vertical bending is set via two motor driven lever springs fixed at both sides of the top of the crystal.

For reasons of thermal and mechanical stability the crystals are double-T shaped with thick top and bottom parts. With the bottom they are glued to a water cooled copper base. A copper tube is glued to the top which is connected to the cooling circle via flexible silicon tubes. The temperature of the cooling water is kept constant within 0.5°C.

With a storage ring current of 50 mA the new monochromator provides $0.8 \cdot 10^{11}$ ph/mm²/s in front of the patient which is an increase by a factor of 6 compared to the former used Bragg design. Also it is remarkably more stable against variations of the input power load.

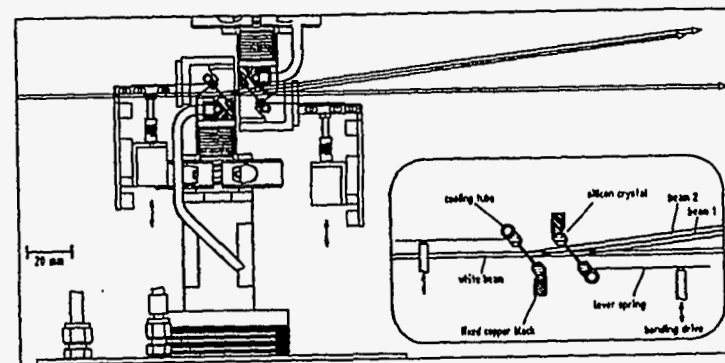


Fig. 1: Partial cut and simplified side view of the the monochromator system. The inset shows only substantial parts.

References:

- [1] W.-R. Dix, K. Engelke, W. Graeff, C. Hamm, J. Heuer, B. Kaempf, W. Kupper, M. Lohmann, B. Reime, R. Reumann, *NIM A314* (1992) 307.
- [2] P. Suortti and W. Thomlinson, *NIM A269* (1989) 639.

XAFS Measurements at High Temperatures and Pressures

Kozaburo Tamura and Masanori Inui
Faculty of Integrated Arts and Sciences,
Hiroshima University, Higashi-hiroshima 724, Japan

Shinya Hosokawa
Faculty of Science, Hiroshima University, Higashi-hiroshima 724, Japan

The method of the XAFS measurements at high temperatures and pressures for supercritical fluids with high critical-constants have been developed. Figure 1 shows the side view of an internally heated high-pressure vessel made of super-high-tension steel, where a poly crystalline sapphire cell of our own design is set up. The vessel is pressurized by high purity grade He gas and it permits XAFS measurement up to 800bar. The experiments were carried out at high temperatures up to 1600°C, and high pressures up to 150 bar. The XAFS spectra of liquid Se at 1300°C and 150bar, and dense Se vapor at 1600°C and 150bar have been obtained. The amplitude of oscillations decreases with increasing temperature. However the oscillations are observable at these temperatures. These results suggest that a chain molecule or a Se dimer consisting of covalently bonded atoms remains at the extreme high temperature.

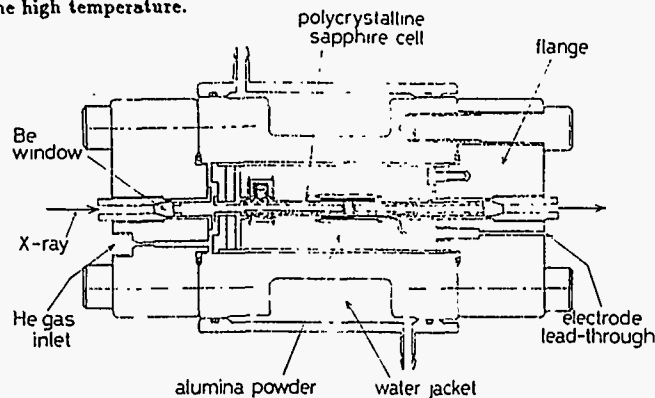


Fig. 1

REFERENCES

- 1) S. Hosokawa, K. Tamura, M. Inui, M. Yao, H. Endo and H. Hoshino, J. Chem. Phys. **97**, 786 (1992).
- 2) S. Hosokawa, K. Tamura, M. Inui and H. Endo, Jpn. J. Appl. Phys. **32**, Suppl. 32-2, 703 (1993).
- 3) S. Hosokawa, K. Tamura, M. Inui and H. Endo, J. Non-Cryst. Solids **156-158**, 712 (1993).

HIGH CONTRAST COMPUTED TOMOGRAPHY WITH SYNCHROTRON RADIATION

Yuji ITO, Tohoru TAKEDA, *Takao AKATSUKA, *Tomokazu MAEDA,
**Kazuyuki Hyodo, *Akira UCHIDA, *Tetsuya YUASA, Masahiro KAZAMA,
Jin WU, **Masami ANDO.

Institute of Clinical Medicine, University of Tsukuba.
1-1-1 Tennodai, Tsukuba-shi, Ibaraki-ken 305 Japan

*Department of Electrical and Information Engineering, Yamagata University, Yamagata 905 Japan

**Photon Factory, National Laboratory for High Energy Physics, Tsukuba, Ibaraki 305 Japan

Monochromatic X-ray computed tomography (CT) with synchrotron radiation (SR) is being used to analyze fine structures of material by means of its sufficient X-ray flux and tunability of energy spectrum from 1990. We are studying on a SR-CT biomedical diagnose system to obtain clear image and to detect tracer material for quantitative functional evaluation of the organs. Now, a new SR-CT system is being constructed.

The computed tomographic system is set at the beam line of NE-5 of the Tristan Accumulation Ring in Tsukuba (6.5 GeV, 20-30 mA, 1 T bending magnet). This system consists of a rotating X-ray shutter, a silicon (220) and silicon (511) double monochromator, X-ray slits system and an X-ray linear array sensor (Fig.1). The energy of monochromatic X rays can be changed from 33.0 to 37.0 keV without high order energy contamination by monochromator adjustment. The X-ray linear array sensor consists of BGO scintillator and silicon photo-diode array (153.6 mm long and 3.2 mm wide, 768 channel). The dynamic range of this sensor is 60000 and the spatial resolution is 0.2 mm. Image data was digitized by a 16 bit A/D converter and led to the computer. Exposure time of each projection can be changed from 10 to 1000 ms. Slice thickness of the object can be also changed from 0.1 to 3.2 mm.

Here, we present the detail structures and the first experimental results of this new SR-CT system.

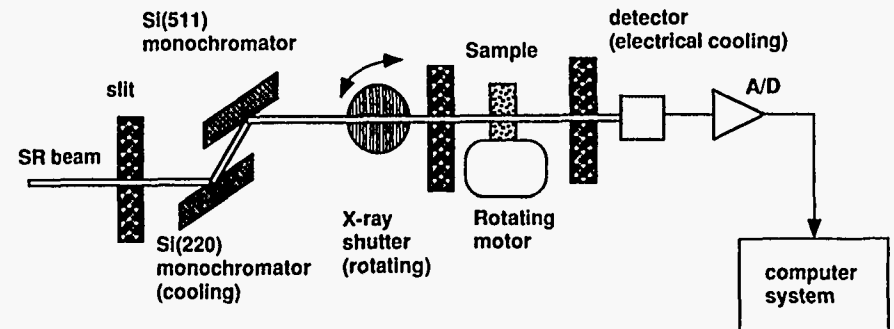


Fig.1 Diagram of SR-CT system

Structural Study of the High Pressure Phases of Bismuth Using High Energy Synchrotron Radiation

H. Iwasaki*, J.H. Chen and T. Kikegawa

Photon Factory, National Laboratory for High Energy Physics
Tsukuba, Ibaraki 305, Japan

Bismuth of the atomic number 83 is known to undergo structural phase transition under high pressure. There exist, however, no reliable structural data for the high pressure phases, BiIII, BiIII' and BiIV. We have made a diffraction study of these phases using high energy synchrotron radiation that has a high penetrating power for the heavy element. Diffraction measurements were carried out at the Beamline NE-5C at the TRISTAN Accumulation Ring (6.5 GeV). High pressure apparatus employed was a cubic type multi-anvil press MAX80 and powdered sample was compressed with a liquid medium. Radiation from the bending magnet was monochromatized by reflection from the double Si(111) crystals and diffraction patterns were recorded using an Imaging Plate. Angular step-scan recording was also made using a solid state detector.

Figure 1 shows a diffraction pattern of BiIV taken at 3.9 GPa and 503 K. The energy of monochromatized radiation was 50 keV. Thirty-five diffraction peaks are clearly recognized and they can be indexed in terms of a monoclinic unit cell containing eight atoms. Analysis based on the observed intensities led to the atomic arrangement that can be regarded as a distorted BCC structure. Crystal structure of BiIII was solved at 3.8 GPa to be tetragonal with ten atoms in the unit cell. It can be regarded as another kind of distorted BCC structure. BiIII' has been shown to have the crystal structure identical to that of BiIII.

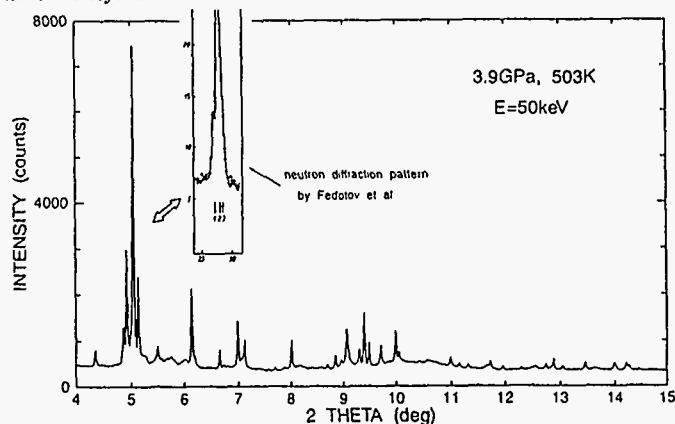


Fig.1. Diffraction pattern of BiIV.

* Present address : Department of Physics, Faculty of Science and Engineering, Ritsumeikan University, Kusatsu, Shiga 525, Japan

EX6AFS : a data acquisition system for high speed dispersive EXAFS measurements implemented using Object-Oriented Programming techniques.

Guy Jennings and Peter L. Lee

Materials Science Division, Argonne National Laboratory,
9700 S. Cass Ave. Argonne, IL 60439

In this paper we describe the design and implementation of a computerized data acquisition system for high speed energy dispersive EXAFS experiments on the X6A beamline at NSLS. The acquisition system drives the stepper motors used to move the components of the experimental setup and controls the readout of EXAFS spectra. The detector used is a linear photodiode array detector with 1024 discrete channels, capable of readout rates of 250,000 channels/second.

The system runs on a Macintosh IIx computer and is written entirely in the object-oriented language C++. Large parts of the system are implemented by means of commercial class libraries, specifically the MacApp application framework from Apple, the Rogue Wave class library and the HDF data file format library from NCSA. This reduces the amount of code which must be written and enhances reliability.

The system makes use of several advanced features of C++ : Multiple Inheritance allows the code to be decomposed into independent software components and the use of Exception handling allows the system to be much more reliable in the event of unexpected errors.

Using Object-Oriented techniques allows the program to be extended easily as new requirements develop. All sections of the program related to a particular concept are located in a small set of source files.

The program will also be used as a prototype for future software development plans for the BESSRC CAT beamlines being designed and built at the Advanced Photon Source.

Work at Argonne National Laboratory is supported by the US Department of Energy (DOE), Office of Basic Energy Sciences, Division of Material Sciences, under contract W-31-109-ENG-38

First Results from the
IBM/Tennessee/Tulane/LLNL/LBL
Undulator Beam Line at the Advanced Light
Source

L. JIA, T. A. CALLCOTT, U. Tennessee, Knoxville, TN 37996, J. YURKAS, A. W. ELLIS, F. J. HIMPSEL, IBM T. J. Watson Research Center, POB 218, Yorktown Heights, NY 10598, M. G. SAMANT, J. STOHR, IBM Almaden Res. Center, 650 Harry Rd., San Jose, CA 95120-6099, D. L. EDERER, Tulane University, New Orleans, LA 70118, J. A. CARLISLE, E. A. HUDSON, and L. J. TERMINELLO, Lawrence Livermore National Laboratory, Livermore, CA 94550, R. C. C. PERERA and D. K. SHUH, Lawrence Berkeley Laboratory, Berkeley, CA 94720.

The Advanced Light Source at Lawrence Berkeley Laboratory is one of the first high-brightness, third generation synchrotron radiation sources that use undulators to boost the spectral brilliance beyond second generation sources by four orders of magnitude. We present the first photoabsorption and fluorescence data obtained from a beam line, which combines a 5 cm, 89 period undulator with a 70 m spherical grating monochromator and two end stations, one for fluorescence, the other for photoemission. The spectral range of 70-1200 eV covers the sharpest core levels of all elements with optimum surface sensitivity and resolution.

We will present performance results from our beam line that will include photon flux, focusing, and undulator harmonic behavior. Along with these measurements we will present experimental results obtained from higher fullerenes, metal oxides, conductive polymers, oxynitride growth on silicon, and buried heterointerface detection. Prospects for other high brightness experiments will be discussed.

This work was conducted under the auspices of the US Department of Energy, Office of Basic Energy Sciences, Division of Materials Science, by the Lawrence Livermore National Laboratory under contract No. W-7405-ENG-48.

MoD37

The VUV Scanning Spectromicroscope at MAX-lab.

U. Johansson¹, R. Nyholm¹, C. Törnevik² and A. Flodström².

¹ Department of Synchrotron Radiation Research, Institute of Physics, Lund University, Sölvegatan 14, S-223 62 Lund, Sweden.

² Department of Physics, Material Science, Royal Institute of Technology, S-104 00 Stockholm, Sweden.

The design and performance of a scanning photoelectron microscope at the MAX synchrotron radiation laboratory is presented. The main use of the instrument is for high energy resolution core level photoelectron spectroscopy with a lateral resolution in the micrometer range.

The system consists of an undulator, a plane grating monochromator and a focusing stage with a ring-shaped ellipsoidal mirror giving a micrometer-sized light spot on the sample surface [1].

The monochromator is equipped with two interchangeable gratings in order to cover a photon energy range from 15 eV to 150 eV with an energy resolution of about 0.2 eV or better. The diffracted radiation is focused by a Kirkpatrick-Baez objective onto a circular exit aperture which defines the bandwidth of the monochromator and also serves as an entrance aperture for the last ellipsoidal focusing mirror.

The system is capable of producing a micrometer-sized final focal spot with a photon flux in the range 10^9 to 10^{10} s⁻¹ [2]. This allows high energy resolution ($\Delta E \sim 0.1$ - 0.2 eV) photoemission experiments to be performed with reasonably high count-rates in the photon energy range of 15 to 150 eV.

Recent results of high resolution photoelectron spectra demonstrating the capabilities of the system will be presented.

1. R. Nyholm, M. Eriksson, K. Hansen, O-P. Sairanen, S. Werin, A. Flodström, C. Törnevik, T. Meinander and M. Sarakontu, Rev. Sci. Instrum. 60, 2168, 1989.

2. MAX-LAB Activity Report 1991, p100 and 1992, p96.

MoD38

A zone plate soft x-ray microscope at the beamline NE1B of the TRISTAN Accumulation Ring

J. Wang,¹ Y. Kagoshima,^{1,2} T. Miyahara,^{1,2} M. Ando,^{1,2} S. Aoki,³ N. Watanabe,³ E. Anderson,⁴ D. Attwood,⁴ D. Kern,⁵ K. Shinohara,⁶ and H. Kihara⁷

¹Department of Synchrotron Radiation Science, The Graduate University for Advanced Studies, Japan

²Photon Factory, National Laboratory for High Energy Physics, Japan

³Institute of Applied Physics, University of Tsukuba, Japan

⁴Center for X-ray Optics, LBL, USA

⁵Institut für Angewandte Physik, Universität Tübingen, FRG

⁶Tokyo Metropolitan Institute of Medical Science, Japan

⁷Kansai Medical University, Japan

An imaging zone plate soft x-ray microscope has been constructed at the beamline NE1B of the TRISTAN Accumulation Ring (AR) in KEK, National Laboratory for High Energy Physics. An insertion device named the Elliptic Multipole Wiggler#NE1 is in operation in the AR of which storage energy is 6.5 GeV. When it operates in the helical undulator mode, it produces circularly polarized soft x rays. The NE1B is equipped with a 10 m vertical-dispersion grazing incidence spherical grating monochromator and a post focusing mirror.¹ The microscope has been installed behind the post focusing mirror. The spectral resolution of the monochromator is roughly around 500. Since it meets the monochromaticity requirement of the zone plate we used, the chromatic aberration can be neglected. The microscope aims at the real time observation at present and microscopic application of circular polarization in the future.

The optical system of the microscope is composed of a 500 $\mu\text{m}\phi$ pre-pinhole, a condenser zone plate ($r_1=15.8 \mu\text{m}$, $N=1000$), a 20 $\mu\text{m}\phi$ pinhole, and an objective zone plate ($r_1=1.41 \mu\text{m}$, $N=200$). The condenser zone plate was fabricated by NTT and the objective zone was fabricated as part a collaboration between LBL and IBM.² A visible optical prefocus unit consisting of two microscope objectives has been developed and introduced into the x-ray microscope for a quick, easy, and precise adjustment of the optical system.

Our microscope has been applied to a test pattern and some dry biological specimens at a wavelength of 2.37 nm. The test pattern used was a zone plate with the same parameters as the condenser zone plate. Its outer zones with about 250 nm widths were able to be observed clearly. An enlarged x-ray image of dry diatoms was also obtained. These images were barely observable in real time in spite of poor monochromatized photon flux. Therefore, our system will provide high resolution real time observation when combined with sources of higher brilliance.

References

¹ Y. Kagoshima *et al.*, in this conference.

² E. Anderson and D. Kern, in *X-ray microscopy III*, edited by A. G. Michette, G. R. Morrison and C. J. Buckley (Springer-Verlag, Berlin, 1992) pp. 75-78.

Rapid Projection of Crystal Grain Orientation Distribution by Synchrotron X-ray Diffraction

Koichi Kawasaki¹ and Hiroshi Iwasaki²

1. Advanced Materials & Technology Research Laboratories, Nippon Steel Corp., Nakahara-ku, Kawasaki 211, Japan

2. Photon Factory, National Laboratory for High Energy Physics, Tsukuba, Ibaraki 305, Japan

Taking advantage of the high brightness of synchrotron radiation, a system was developed for rapid recording of the crystal grain orientation distribution, the pole figure, in polycrystalline materials. It consists of an X-ray two-circle diffractometer and a translating Imaging Plate holder. The sample in the form of sheet is fixed on the sample stage of the diffractometer and a screen with an arc-shaped window to accept a part of the diffraction cone of a particular reflection is fixed behind the sample stage. A monochromatized X-ray beam is incident on the sample which is rotated so that the surface of the sphere of the poles of the selected reflection is scanned, while the Imaging Plate is translated with an angular velocity that is synchronized with that of the sample rotation. It is possible to project the intensity distribution over an extended angle range of the surface onto the Imaging Plate within a short period of time. The pattern recorded also carries an information on the size distribution of crystal grains.

Measurements were made at the beamline BL-3A at the Photon Factory. Fig. 1 (a) shows the result of projection of the [111] poles of the cold-rolled sheet of an aluminum alloy. The wavelength of radiation used was 0.06 nm and the angle of sample rotation was 40 deg. It took 80 s to take the pattern. It can be seen that the orientation distribution is continuous with a high density of the poles around the north pole of the sphere (top of the pattern). When the sheet was annealed to induce recrystallization, the pattern was changed, as shown in Fig. 1(b). It consists of a number of tiny diffraction spots, indicating the growth of crystal grains. It can be seen that the distribution of the poles has been changed by annealing.

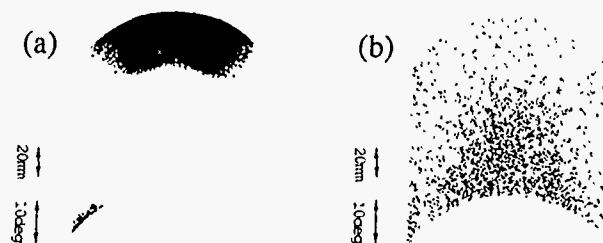


Fig. 1 The orientation distribution of the [111] poles of an aluminum alloy sheet. (a), as cold rolled, and (b), after recrystallization.

X-ray Magnetic Bragg Scattering Topography from Fe₃O₄

Hiroshi KAWATA, and Koichi MORI*

Photon Factory, National Laboratory for High Energy Physics, Oho, Tsukuba 305,
JAPAN

*JAERI, Tokai, Ibaraki 319-11, JAPAN

X-ray Bragg scattering topography gives us information of the crystal defect, strain distribution, domain structure etc. in a crystal. In the case of the domain structure on ferro-electric material, X-ray topography reveals not only the presence of domain structure, but also the direction of the spontaneous polarization by using departures from Friedel's law which appears with the anomalous scattering. In the case of the domain structure on ferro- or Ferri-magnetic materials, however, it is impossible to reveal the direction of the spontaneous magnetization within the charge scattering X-ray topography.

Recently, X-ray magnetic Bragg scattering rapidly developed. Especially, by using a resonant effect, the magnetic effect (asymmetrical ratio) can be enhanced. Therefore, it is possible to reveal the direction of the spontaneous magnetization, if we take a magnetic Bragg scattering X-ray topography. In this paper, we present a first success of the magnetic Bragg scattering X-ray topography from Fe₃O₄ single crystal.

The experiment was carried out at the beamline 15B of Photon Factory. The experimental arrangement was same to the resonant magnetic Bragg scattering except the detector. In a case of the topography work, we used a nuclear plate as a detector. Figure 1 shows the magnetic asymmetrical ratio of 444 diffraction; $(I^+ - I^-)/(I^+ + I^-)$ (black dots) and the intensity of fluorescent X-ray (open circles) through the Fe K-absorption edge. As shown in this figure, there is a large magnetic effect. Especially, at the pre-edge peak, the magnetic effect changes the value +2.5 % to -3.9 %, when the photon energy changes just 1 eV (marked by arrows in Fig. 1).

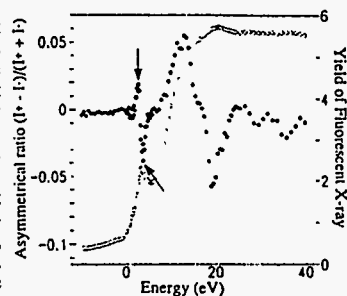


Fig. 1

We took two topographies at these energies and made a image subtraction in order to reduce strain images at these topographies. The subtracted image is shown in Fig. 2(a). It is possible to see some vertical stripe images in this picture. In order to identify the domain formation we took a normal charge scattering topography (Fig. 2(b)), whose scattering vector is 606. As compared with these two pictures, the vertical stripe images well corresponds to the domain itself. Finally, the magnetization direction of each domain can be determined as the drawing which is shown in Fig. 2(c) from this domain contrast.

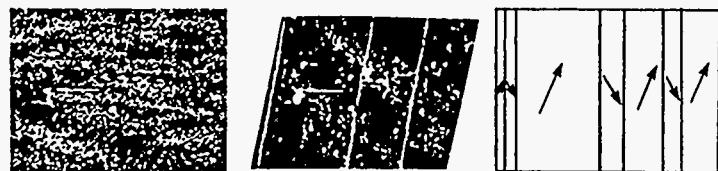


Fig. 2(a) 444 diffraction, Fig. 2(b) 606 diffraction, Fig. 2(c) Domain structure

X-ray Multiple Dynamical Diffraction Experiments with Synchrotron Radiation

M.V.Kovalchuk, A.Yu.Kazimirov

*Institute of Crystallography, Russian Academy of Sciences,
Moscow 117333, Russia*

Two-beam dynamical diffraction effects have been the subject of intensive investigations since perfect crystals such as silicon and germanium appeared more than thirty years ago. Many X-ray diffraction methods to study the structure of surfaces, surface layers and bulk of nearly perfect crystals have been developed. Dynamical diffraction is used as a basis for X-ray crystal optics for synchrotron radiation.

Multiple dynamical diffraction when more than two crystallographic planes are involved in the diffraction process provides new opportunities for observation of interesting physical phenomena and possible practical applications. However, experiments in this field were hampered by various practical problems and the most serious among them is a requirement of two-dimensional collimation of incident X-ray beam which leads to drastic intensity reduction. Only high intensity of SR sources made possible such experiments in recent years.

In this paper we review results of experiments performed at the Photon Factory and the Daresbury Laboratory with participation of the authors. These experiments on perfect and nearly perfect crystals include direct measurements of anomalous transmission of X-rays under conditions of six-beam diffraction, X-ray standing wave measurements under conditions of three-beam diffraction, development of phase-sensitive diffractometry of surface layers. Different X-ray optical arrangements for two-dimensional angular collimation (based on channel-cut crystals, crystal-slits combinations and phenomena of anomalous transmission in six-beam Laue case) are analyzed. Future experiments in this field will make possible development of new multiple diffraction methods for crystal structure characterization as well as new X-ray optics schemes which may be used in other diffraction experiments on intense SR X-ray sources.

Wavelength-Dispersive X-Ray Fluorescence Detector

J.P. Kirkland¹, V.E. Kovantsev², C.M. Dozier³, J.V. Gilfrich¹,
W.M. Gibson⁴, Qi-Fan Xiao², and K. Umezawa⁴

¹ SFA Inc., 1401 McCormick Dr., Landover, MD 20785

² X-Ray Optical Systems, Inc., 90 Fuller Rd., Albany, 12205

³ Naval Research Laboratory, Condensed Matter Physics Branch, Washington, DC 20375

⁴ Center for X-Ray Optics, University at Albany, SUNY, Albany NY 12222

Fluorescence XAFS using energy-dispersive solid-state detectors is becoming more difficult to do on synchrotron sources as the incident photon flux increases. Multi-element detectors that are being developed now can barely cope with fluxes common on second-generation synchrotron sources. The number of elements and the speed of A/D conversion in these detectors is slowly, linearly going up; whereas, the flux available from new beam lines, insertion devices, and synchrotron sources is going up by orders of magnitude. It seems unlikely that the technology for energy-dispersive discrimination will improve sufficiently to keep up with the new sources. The alternative is to find a way to wavelength discriminate fluorescence photons. After that has occurred, they can be counted by almost any detector, i.e. ionization chamber, PIN photo diode, or scintillation detector, and these can handle nearly limitless flux. Unfortunately, to be able to select particular wavelengths with crystals, the photons must be collimated. Fluorescence photons radiate in all directions, just the opposite of collimation.

One possible solution to this problem has been developed. A prototype wavelength-dispersive fluorescence detector using capillary optics has been tested on the Naval Research Laboratory's X-23B beam line at the NSLS. A polycapillary lens was designed to collect and collimate x-rays emanating from a small area. The photons emerging from the lens were incident on a crystal. The crystal was chosen to have a rocking curve width similar to the divergence of the light exiting the lens. A scintillation detector was used to count the photons diffracted from the crystal.

The detector had a resolution of less than 150eV at 8 keV using a stressed LiF (200) crystal, and was easily able to discriminate between Zn K α (8.620 keV) and Cu K β (8.905 keV) x-rays emitted from a brass sample. The (400) reflection had a resolution of approximately 60 eV, but ten times less intensity.

Instrumentation developments in scanning soft x-ray microscopy at the NSLS*

Janos Kirz[®], Chris Jacobsen, Shawn Williams[®], Sue Wirick, Xiaodong Zhang
Physics Department, SUNY, Stony Brook, NY 11794-3800

Harald Ade

Physics Department, North Carolina State University, Raleigh, NC 27695-8202.

Mark Rivers

CARS, University of Chicago, 5640 S. Ellis Ave. Chicago, IL 60637

The scanning transmission soft x-ray microscope has been operating on the X1A beamline, with zone plates fabricated by E. Anderson (Center for X-ray Optics, LBL). The X1 soft x-ray undulator serves as the bright tuneable source and the zone plate forms a microprobe that provides the 50 nm resolution of the instrument. (1)

In routine operation the specimen is scanned and the transmitted fraction of the incident x-rays is used to form the image. The following new instrumentation developments have added significantly to the capabilities of the microscope:

1/ XANES microscopy. By scanning the monochromator with the x/y scan stopped an absorption spectrum can be taken from a small (submicron) specimen area. Because the zone plate is highly chromatic (focal length proportional to photon energy), the focus must track the monochromator to keep the exposed spot in focus. Based on resonant structure observed in the spectra, one selects characteristic energies at which to image the specimen to map its chemical components. Applications to polymer morphology were the first to bear fruit (2); however, applications to biological specimens (3) and to coal (4) soon followed.

2/ Scanning luminescence microscopy. If the x-ray probe is used to excite labels that emit visible light, the location of some labels can be determined with the resolution of STXM, (which is about five times better than the resolution of the confocal microscope) for immunolabeling (5). Initial experiments using inorganic phosphors and organic dyes showed promising results (6). More recently Moronne et al. have shown that terbium chelates have superior resistance to radiation-bleaching compared to all-organic labels. (7).

3/ Dichroism microscopy. The undulator output is linearly polarized. To the extent that the absorptivity of a component of the specimen depends on its orientation relative to the plane of polarization (dichroism), the image will change if the relative orientation changes. Ade and Hsiao have recently imaged sections of Kevlar fiber, rotating the specimen in the plane perpendicular to the beam between images. The pattern of absorptivity provides clear indication of the molecular orientation within the specimen (8).

* Supported in part by the NSF and by the DOE OHER

@ On leave during 1993-94, part time at the NSLS, part time at the ALS

Address, starting 6/1/94: Dep. Molecular Biophysics and Biochemistry, Yale University, New Haven CT

1. C. Jacobsen, et al., *Opt. Comm.* **86**, 351 - 364 (1991).
2. H. Ade, et al., *Science* **258**, 972 - 975 (1992).
3. X. Zhang, et al., *Nucl. Instrum. Meth.* (to be published), (1994).
4. R. E. Botto, et al., *Energy & Fuels* **8**, 151 - 154 (1994).
5. C. Jacobsen, et al., *J. Microscopy* **172**, 121 - 129 (1993).
6. C. J. Jacobsen, et al., in *SPIE Proc.* 1741, (1993), pp. 223 - 231.
7. M. M. Moronne, et al., *J. Microscopy* in preparation (1994).
8. H. Ade, B. Hsiao, *Science* **1427 - 1429**, (1993).

Fluorescence Yield XAFS Measurements in the Soft X-Ray Region

Yoshinori Kitajima

Photon Factory, National Laboratory for High Energy Physics
Oho 1-1, Tsukuba, Ibaraki 305, Japan

In the soft x-ray region under 4keV, various electron yield (EY) techniques have been employed in X-ray Absorption Fine Structure measurements of bulk materials. Fluorescent x-ray yield (FY) is also utilized for samples of low concentration such as surface adsorbates. FY has several advantages compared to EY; a higher signal-to-background ratio and applicability to insulating material, but it has not been thought suitable to concentrated materials. Recently, it has been shown in the oxygen *K*-edge EXAFS spectrum of NiO single crystal that FY is also applicable to bulk materials through correction of the self-absorption effect under some special conditions[1].

Here we will discuss the case in the higher energy range of several keV. According to the formalism in Ref.[1], the self-absorption effect is negligible only at the sampling depth smaller than 100Å in oxygen *K*-edge of NiO, however, it becomes larger than 300Å in silicon *K*-edge of Si crystal with 100% concentration. It is because the decreased absorption cross section at the increased *K*-edge energy so that we can get bulk information without any correction from the EXAFS measurements by selecting the experimental geometry of very grazing emission.

We will present some typical fluorescent yield EXAFS spectra of concentrated materials such as silicon wafer, quartz crystal and so on. As for silicon wafer, we have observed more prominent feature of surface natural oxide in the simultaneously-recorded total electron yield spectrum which may affect the smooth background subtraction. We have got a nice spectrum of insulator quartz which can never be taken by EY.

[1] L. Tröger et al., Phys. Rev. B 46, 3283 (1992).

Development of a second generation XPS-based scanning photoemission microscope with a zone plate generated microprobe at the National Synchrotron Light Source

Cheng-Hao Ko and Janos Kirz
Department of Physics, SUNY, Stony Brook, NY 11794
Harald Adc
Department of Physics, NCSU, Raleigh, NC 27695
Erik Johnson and Steve Hulbert
National Synchrotron Light Source, Brookhaven National Laboratory, Upton, NY 11973
Erik Anderson
Center for X-ray Optics, Lawrence Berkeley Laboratory, CA 94720

For the past few years, we have been developing an instrument that combines the techniques of X-ray Photoelectron Spectroscopy (XPS) and zone plate microfocusing for doing spectromicroscopy. The X1A undulator provides a bright photon source in the soft x-ray range with a high degree of spatial coherence, a requirement for zone plate focusing. A spherical grating monochromator selects the desired photon energy in the 280-800 eV range. Fresnel zone plate focusing is based on diffraction and the first order focus, which has the highest efficiency, is used to form the microprobe. Other diffraction orders are blocked by an order sorting aperture placed between the sample and the zone plate. An electron energy analyzer acquires photoelectron spectra from the small irradiated area. In this way, spatially resolved XPS spectra, element-specific or chemical-state-specific images of the surface can be obtained.

The microprobe instrument makes use of a flexure stage for precise sample scanning, a Hemispherical Sector Analyzer (HSA), with a multi-channel detector, for electron spectroscopy and a positioning device to control the focusing optics (the zone plate and the order sorting aperture). A custom-designed ultra-high vacuum chamber, installed in the short wavelength branch of the beamline X1A, incorporates these major components into an integrated system. The positioning device for the focusing optics allows separate control of the zone plate and the order sorting aperture. In this way, when a different photon energy is used for XPS analysis, we are able to compensate for the change in focal length of the zone plate (which is proportional to the photon energy) by repositioning the focusing optics to keep the beam focused on the sample. The multi-channel detector of the HSA enables the system to simultaneously acquire multiple images as the sample is scanned, with each image corresponding to a different photoelectron energy (bandwidth and energy separation between channels are determined by the pass energy of the HSA). With this parallel detection scheme, the acquisition time for mapping multiple chemical or structural states on the surface is greatly reduced. Besides photoelectrons, sample current (related to total electron yield) and transmitted flux (to measure the absorption of thin samples) are also monitored to form images.

A new technique for time-resolved x-ray diffraction measurements in the single bunch operation applied to laser annealing

S. Kojima,^{1,4)} Y. Kudo,¹⁾ S. Kawado,¹⁾ T. Ishikawa²⁾ and T. Matsushita^{3,4)}

1) Sony Corporation Research Center, Hodogaya-ku, Yokohama 240, Japan
2) Faculty of Engineering, The University of Tokyo, Bunkyo-ku, Tokyo 113, Japan

3) Photon Factory, KEK, Oho, Tsukuba, Ibaraki 305, Japan

4) Department of Synchrotron Radiation Science, The Graduate University for Advanced Studies, Oho, Tsukuba, Ibaraki 305, Japan

We propose a new technique that is applicable to the time-resolved measurement of deformation on silicon surface during pulsed laser annealing in the single bunch operation of the Photon Factory. In general, there are jitters between the external trigger pulse and the laser firing in the external trigger operation of laser equipment. When a time standard pulse is made by the 312-divided RF-ring pulse which is synchronous with the positron bunch, the laser firing time based on the time standard in the single bunch operation is distributed because the laser equipment has the jitters. The jitters clearly make the time-resolved measurement inaccurate for the x-ray intensity change caused by the laser irradiation.

To overcome this disadvantage, a time-resolved measurement system that utilizes the jitters has been developed. The block diagram of this system is shown in Fig. 1. The external trigger pulse to the laser equipment was made from the external oscillator (DG-535) pulse and the 312-divided RF-ring pulse through the coincidence unit. The time distribution of the bunch (event number), which was synchronous with the laser trigger, and the time distribution of the intensity of the x-rays diffracted from the silicon surface were measured by TAC1 and TAC2, respectively. The respective signals were then accumulated in MCA1 and MCA2. The time course of the diffraction intensity before and after the laser irradiation was obtained by normalizing the time distribution of the intensity of the diffracted x-rays with the time distribution of the event number.

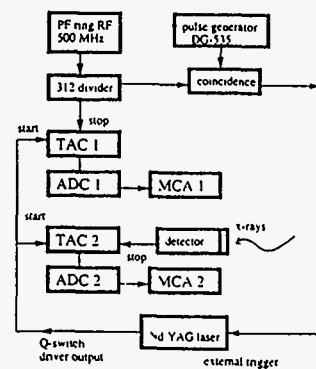


Fig. 1

LONG PERIODIC X-RAY STANDING WAVE FOR CHARACTERIZATION OF HEAT TREATMENT EFFECTS ON Ni/C LAYERED SYNTHETIC MICROSTRUCTURES

S.I. Zheludeva, M.V. Kovalchuk, N.N. Novikova, A.N. Sosphanov
Institute of Crystallography Academy of Sciences of Russia, Leninsky pr. 59, Moscow 117333, Russia.

Layered synthetic microstructures of metal-carbon combination (LSM) consisting of alternating ultra-thin layers with high and low electron density (metal-carbon or metal-silicon) are in fact artificial diffracting elements with controllable period ranging from tens to hundreds of angstroms. Since the properties of multilayers can be easily tailored to any desired X-ray application, such structures offer quite new possibilities for soft X-ray and UV optics. The classical problem which restricts to a large extent the practical application of multilayer optical elements is the instability of these structures to high intensity radiation and temperature. The behavior of the metal-carbon multilayer as it undergoes heat treatment has been extensively studied using X-ray diffraction, electron microscopy and EXAFS techniques. But a lack of precise knowledge of thermally induced changes in LSM has motivated considerable experimental activity in this field.

Recently new high precision nondestructive technique has been developed for structural characterization of LSM measuring the secondary radiation (characteristic fluorescence or photoelectron yield) excited by evanescent long-periodic X-ray standing wave field [1-3]. We have applied this technique for investigation of heat treatment effect on ultra thin Ni/C bilayer ($d_{Ni} = 38\text{\AA}$, $d_C = 68-90\text{\AA}$) deposited on Cr/C LSM [4]. It was demonstrated that thermally induced changes in the thickness and density of Ni/C bilayer can be determined unambiguously and with angstrom-level precision by the XRSW fluorescence measurements.

In the present paper the behavior of Ni/C LSM as it undergoes the heat treatment has been studied by long-periodic modification of XRSW technique. Ni/C LSM was deposited by laser beam evaporation on glass substrate and annealed at temperature from 200° to 300° C. Fluorescence measurements were performed in the angular range including TER and first order Bragg reflection from Ni/C LSM. The series of experiments presented here have demonstrated the possibilities of XRSW method for the determination of the parameters of ultra-thin layers comprising multilayers and for the investigation of the dynamic behavior of these layers under heat treatment.

1. Barber T.W. and Warburton W.K., Matter Lett. 3 (1984) p.17.
2. Zheludeva S.I., Kovalchuk M.V., Novikova N.N., Buzhebanov I.N., Salashenko N.N., Akhsakhalyan A.D. and Platonov Yu.Ya., Rev.Sci.Instrum., 1992, 63, p. 1519
3. Zheludeva S.I., Kovalchuk M.V., Novikova N.N., Sosphanov A.N., Malysheva N.E., Salashenko N.N., Akhsakhalyan A.D. and Platonov Yu.Ya., Thin Solid Films, 1993, 232, p. 252
4. Zheludeva S.I., Kovalchuk M.V., Novikova N.N. and Sosphanov A.N., J.Phys.D: Appl Phys., 1993, 26, p. A206

The use of SR from VEPP-3 storage ring for fabrication of micromechanic elements by deep X-ray lithography

G.N.Kulipanov, O.A.Makarov, L.A.Mezentseva, A.G.Milyokhin (*), V.P.Nazmov,
V.F.Pindyurin, M.P.Sinyukov (*), A.V.Zarodyshev
Budker Institute of Nuclear Physics,
630090 Novosibirsk, Russia
(* Institute of Semiconductor Physics,
630090 Novosibirsk, Russia

Deep X-ray lithography with using of SR from the VEPP-3 storage ring is applied for fabrication of test specimens of micromechanic elements. The PMMA layers were used as an X-ray resist in order to produce the 1 mm-height regular structures with lateral sizes of tens microns repeated in two directions. The electroplating was used to obtain a copper replica of resist pattern.

This copper plates with formed microstructure arrays can be used as IR filters and spinnered plate. The results of investigation of the specimens by scanning electron microscopy and IR transmittance are given.

MoD49

Fabrication and preliminary testing of the regular microporous membranes manufactured by deep X-ray lithography at the VEPP-3 storage ring

G.N.Kulipanov, O.A.Makarov, L.A.Mezentseva, S.I.Mishnev, V.P.Nazmov,
V.F.Pindyurin, O.A.Redin, A.N.Skrinsky
Budker Institute of Nuclear Physics
630090 Novosibirsk, Russia
L.D.Artamonova, V.N.Gashtold, G.A.Deis, V.S.Prokopenko, E.F.Reznikova,
V.V.Chesnokov, G.A.Cherkov
"VOSTOK" Company, 276 D.Kovalchuk str.,
630075 Novosibirsk, Russia

The technique of deep X-ray lithography at the VEPP-3 storage ring was used for fabrication the regular microporous membranes. Intensive and high collimated beams of synchrotron radiation (SR) are ideally suitable for this purpose.

The 2.5, 3, 6 and 10 micron mylar films were used as a membrane support media. The regular filters with a pore of 0.3 - 0.5 micron in diameter spaced by 1 micron steps in two directions were obtained. The X-ray masks have 0.6 micron-thick gold absorber electroplated on 2 micron-thick silicon membrane with the pattern area of 2.3×2.5 sq mm.

Fabricated membranes were tested by the methods of scanning electron microscopy, by measuring of gas conductivity and electrical conductivity in electrolytes. Results were taken in comparison with nuclepore filters. Filters of 2.5 micron-thick mylar with 30 mm diameter can stand under pressures up to 3500 Pa without any additional supports. Data on gaseous conductivity correspond to theoretical calculations taking into account the parameters obtained by the scanning electron microscopy. The results of the all methods have satisfactory agreement between each other.

Filters have geometrical transparency about 15%. The value of this parameter can be increased up to more than 50% by choosing the appropriate pattern of an X-ray mask. Apart from nuclepore filters, the regular microporous membranes have no dispersion of pore sizes caused by merged holes.

MoD50

Design and Operation of a UHV Double-Bounce Harmonic Rejection Mirror for XAFS Studies

G.M. Lamble

Brookhaven National Laboratory, Upton, N.Y. 11973, USA.

A simple but effective harmonic rejection system has been installed on beamline X-11B at the NSLS. The system includes a parallel pair of nickel coated float glass mirrors, that allows a constant off-set and an angle-independent exit beam. They are housed within a UHV chamber and situated 1 meter upstream of the sample position and 8 meters downstream of a double crystal monochromator. The angle of the mirror pair is adjusted by a single stepper motor. The double-bounce system works for energies between about 2 and 8 keV. For harmonic rejection of energies higher than this, the whole device may be repositioned to permit a single bounce of the X-ray beam from one of the mirrors. The features and operation of this simple device are discussed.

This work was supported by the U.S. Department of Energy under contract Nos. DE-FG05-89ER45384 and DE-AC02-76CH00016.

MoD51

Diffraction Applications Using the Energy Dispersive Beamline, X6A, at NSLS

P.L. Lee*, M. A. Beno*, C. M. Ogata**, G. S. Knapp*, G. Jennings*

*Materials Science Division, Argonne National Laboratory, Argonne, Illinois 60439

**Howard Hughes Medical Institute, X4, NSLS, Brookhaven National Laboratory, Upton, NY 11973

The newly constructed energy dispersive beamline, X6A¹, employs a curved crystal monochromator (polychromator) to focus a range of x-ray energies (bandwidth ~1 keV) into a narrow (100-120 μm) line image. This beamline will primarily be used for time dependent EXAFS experiments. However, we have begun to explore the use of this energy dispersive instrument for diffraction experiments. One of these, a newly developed d-space matching technique, Continuous Energy Diffraction Spectroscopy (CEDS)², allows us to record single crystal diffraction intensities for the full energy spectrum of the polychromator, simultaneously without crystal or detector motion. This method creates new opportunities for time resolved single crystal diffraction experiments. The basic theory of CEDS and its application for single crystal DAFS experiments will be discussed. Diffraction data derived from thin film and powder samples will also be presented.

The highly focused polychromatic x-ray beam at this beamline can also be used for diffraction studies of macromolecular crystals. The tuneability ($E = 6.5 \text{ keV}$ to 21 keV) and flexibility ($\Delta E = 100\text{-}1000 \text{ eV}$) of the instrument makes the beamline ideal as a test bed for polychromatic protein diffraction techniques. The first of these, the use of this instrument for oscillation data measurements³ and limited energy range Laue diffraction⁴ experiments, will be presented.

Work at Argonne National Laboratory is sponsored by the US Department of Energy, Office of Basic Energy Sciences, Division of Materials Sciences, under contract W-31-109-ENG-38.

1. P.L. Lee, et al., Rev. Sci. Instrum. **65**, 1 (1994).
2. P.L. Lee, et al., Rev. Sci. Instrum., in press.
3. U.W. Arndt, et al., Nature **298**, 835 (1982).
4. V.P. Thomas, J. Appl. Cryst., **5**, 83 (1972).

MoD52

X-ray standing wave and high-resolution diffraction measurements on III-V compound superlattices

A. Lessmann^a, M. Schuster^b, S. Brennan^a, G. Materlik^c and H. Riechert^b

^a Stanford Synchrotron Radiation Laboratory, Stanford, CA 94306, USA

^b Siemens AG, ZFE BT MR 3, D-81739 Munich, Germany

^c Hamburger Synchrotronstrahlungslabor HASYLAB, D-22607 Hamburg, Germany

In X-ray diffraction (XRD), the measurement of the reflected intensity is the usual way to study the structural parameters of heteroepitaxial layers. A natural extension of this method offers the simultaneous registration of inelastic channels, as it is done in the X-ray Standing wave (XSW) method. By recording the X-ray fluorescence or the photo or Auger electron yield from the sample it is possible to determine the phase of the X-ray wave and by that the position of the excited atoms. To study the possible applications we performed XRD/XSW measurements using AlAs/GaAs superlattices on GaAs(001) substrates as well as InGaAsP/InP quantum well structures on InP(001). The AlAs/GaAs samples consist of short-period superlattices with several hundred periods and typical bilayer thicknesses of 3 nm.

The radiation from a SPEAR bending magnet was collimated and monochromatized at $h\nu \approx 5$ keV using Ge(004) (+,-) symmetric/asymmetric reflections. For the detection of a surface related signal, the sample was placed in a He atmosphere and the X-ray induced photo electron current was detected. Due to secondary excitations in the gas, the contribution of higher energy electrons to the total current is much larger than in total yield measurements, where most of the current results from thermal electrons with long mean free paths in the solid. Consequently, the information depth of this signal is smaller, which was also confirmed by an XSW measurement on a clean GaAs(001) crystal. With this signal, characteristic phase shifts of the thickness fringes with respect to the reflected intensity were observed.

The X-ray fluorescence was monitored with a thin window Si(Li) detector. The much larger sampling depth of this signal resulted in strong differences of the XSW induced modulation compared to the photo electron yield. Differences were also observed between the Al-K, Ga-L and As-L fluorescence. On the superlattices, measurements were not only performed in the region of the substrate (004) reflection and the 0th order satellite but also in grazing incidence geometry using the 1st order superlattice reflection. These experiments were carried out at another beamline at higher photon energy and monitoring the Ga-K fluorescence. In the discussion of the applicability of these results to the study of superlattices, the data will be compared with numerical calculations based on the Takagi-Taupin theory.

ATOMIC STRUCTURE AND ORDERING AT THE ZnSe/GaAs INTERFACE

Y. Mahadev, R. L. Gunshor^{*} and G. L. Liedl

School of Materials Engineering

^{*}School of Electrical Engineering
Purdue University

West Lafayette, IN 47907

Heterojunctions of II-VI/III-V semiconductors offer wide combinations of band gaps for systems that are nearly lattice matched. This provides possibilities for the formation of several novel electronic devices such as light emitting devices. One example of such a material system is the ZnSe/GaAs system. However, in developing such systems large variations in the interface state densities were observed for varying As coverages on the surface by capacitance-voltage measurements¹. ZnSe/GaAs heterostructures formed by growing ZnSe on As deficient GaAs produced a highly stable interface structure with excellent electronic properties². Tu and Khan³ proposed a compound formation at the interface to explain the observed electronic properties. Otsuka *et al.*⁴ used high resolution transmission electron microscopy and imaging techniques to show the formation of vacancy ordered Ga₂Se₃ type compound at the interface.

X-ray total external reflection-Bragg diffraction technique⁵ was used for the first time in conjunction with normal Bragg diffraction to probe the atomic structure and the degree of order at the interface of MBE grown ZnSe/GaAs heterostructures. Availability of a very intense synchrotron x-ray beam over a wide range of wavelengths allowed us to probe varying depths of the samples. Two samples viz., ZnSe grown over (i) As deficient and (ii) Ga deficient GaAs, were utilized for this study. Our results indicate the formation of a very well developed reconstruction at the interface on the ZnSe grown on As deficient GaAs sample.

This research was supported by DOE (DE-FG02-85ER45183) and utilized the MATRIX (X-18A) beamline at the National Synchrotron Light Source at Brookhaven National Laboratory.

References

- 1 Q. D. Qian, J. Qiu, M. R. Melloch, J. A. Cooper, Jr., L. A. Kolodziejski, M. Kobayashi and R. L. Gunshor, *Appl. Phys. Lett.*, 54, (1989), 1359.
- 2 J. Qiu, Q. D. Qian, R. L. Gunshor, M. Kobayashi, D. R. Menke, D. Li, and N. Otsuka, *Appl. Phys. Lett.*, 56, (1990), 1272
- 3 D. W. Tu and A. Khan, *J. Vac. Sci. Technol.*, A3, (1985), 922
- 4 N. Otsuka, D. Li, J. Qiu, M. Kobayashi and R. L. Gunshor, *Mater. Trans, JIM*, 31(7), (1990), 622
- 5 W. C. Marra, P. Eisenberger and A. Y. Cho, *J. Appl. Phys.* 50, 6927, (1979)

Soft X-ray Scanning Microtomography with Submicron Resolution

L. McNulty,^a W.S. Haddad,^b J. Trebes,^b E.H. Anderson,^c and L. Yang^a

^aAdvanced Photon Source, Argonne National Laboratory, Argonne, IL 60439

^bLawrence Livermore National Laboratory, Livermore, CA 94550

^cCenter for X-ray Optics, Lawrence Berkeley Laboratory, Berkeley, CA 94720

Scanning soft x-ray microtomography was used to obtain high-resolution three-dimensional (3D) images of a microfabricated test object. The object consisted of two gold patterns separated by 4.5 μm and supported on transparent silicon nitride membranes. The features in the patterns were 100-300 nm wide and 65 nm thick. Using the scanning transmission x-ray microscope (STXM) at the X1A Beamline at the National Synchrotron Light Source,¹ we recorded nine two-dimensional projections of the 3D test object over an angular range of -50° to $+55^\circ$. The x-ray wavelength was 3.6 nm and the radiation dose to the object per projection was approximately 2×10^6 Gy. The STXM utilizes a Fresnel zone plate to form a diffraction-limited focal spot under which the sample is scanned; the zone plate used provided a focal spot radius of 75 nm and working distance of 2.3 mm. The instrument was modified for tomography experiments by adding a precision specimen rotation stage. We reconstructed a volumetric data set of the test object from the 2D projections using an algebraic reconstruction technique (ART) code.² The test object is clearly resolved in transverse and longitudinal extent in 3D images rendered from the volumetric set. Despite the limited number of projections used in the reconstruction, the images exhibit a low degree of artifact. This work indicates that zone-plate-based scanning microtomography is promising for high resolution 3D imaging.

¹ C. Jacobsen *et al.*, *Opt. Commun.* **86**, 351 (1991)

² D. Verhoeven, *Appl. Opt.* **32**, 3736 (1993)

* This work supported by the U.S. Department of Energy, under Basic Energy Sciences contracts W-31-109-ENG-38, W-7405-ENG-48 and DE-AC03-76SF0098.

The submitted manuscript has been authored by a contractor of the U.S. Government under contract No. W-31-109-ENG-38. Accordingly, the U.S. Government retains a nonexclusive, royalty-free license to publish or reproduce the published form of this contribution, or allow others to do so, for U.S. Government purposes.

Phase-Contrast X-Ray Computed Tomography for Observing Biological Specimens and Organic Materials

Atsushi Momose, Tohoru Takeda*, and Yuji Itai*

Advanced Research Laboratory, Hitachi, Ltd., Hatoyama, Saitama 350-03, Japan
* Institute of Clinical Medicine, University of Tsukuba, Tsukuba, Ibaraki 305, Japan

X-ray computed tomography (CT) reveals structure inside an object nondestructively; the origin of the image contrast is heavy elements with high X-ray absorbance. Organic substances with low X-ray absorbance therefore cannot be observed with conventional X-ray CT without staining them with contrast medium. In contrast, X-ray phase-contrast imaging using an X-ray interferometer is sensitive to organic substances because phase shifts by light elements are still detected as X-ray interference patterns while their absorption coefficients are almost zero.

We will present phase-contrast X-ray computed tomography (PCX-CT) for observing the inside of organic substances three-dimensionally. It was necessary to input the X-ray phase shift caused by a specimen into a CT algorithm. We therefore used subfringe analysis methods to read the phase shift from the interference patterns.

Figure 1 shows a schematic view of a PCX-CT apparatus using an X-ray interferometer. We used 0.92- \AA X-rays from a bending section of a 2.5-GeV storage ring of Photon Factory at the National Laboratory for High Energy Physics (KEK). As shown in the inset of Fig. 1, the specimen was rotated in liquid instead of being exposed to air. A wedge-shaped phase shifter was inserted in a reference beam path for reading the X-ray phase shift with subfringe analysis methods.

We used PCX-CT to observe a cerebellum and a liver cancer tumor extirpated from a rat. Figure 2(a), for example, is a PCX-CT image of a rat cerebellar specimen fixated in 10% formalin, and in it the molecular layer, granular layer, and white matter can be distinguished. For comparison, an absorption-contrast CT image obtained at the same X-ray dose as that for the PCX-CT image is also shown in Fig. 2(b). It is easy to see that PCX-CT is much more sensitive.

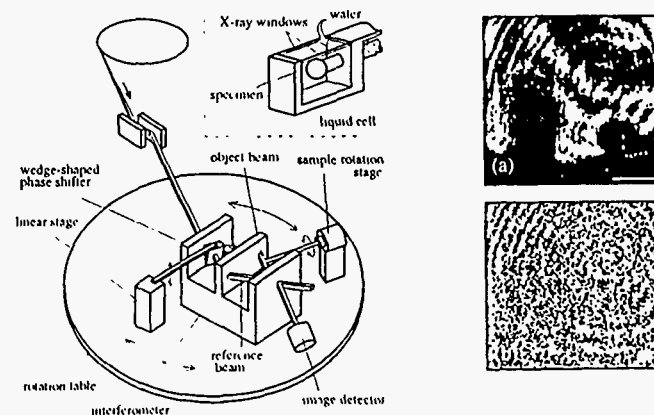


Fig. 1 Schematic view of PCX-CT. The specimen was rotated in a liquid cell, as shown in the inset.

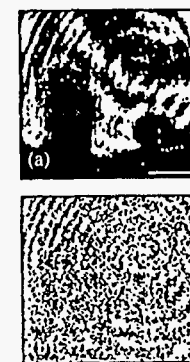


Fig. 2 CT images of a rat cerebellar specimen: (a) phase contrast, and (b) absorption contrast. Bar = 0.5 mm

**Design of a Cell and Transportation System
for the X-ray Absorption Study of Supercritical Fluid Material**

T. Murata, K. Nakagawa¹, A. Kimura¹, N. Otsuda¹

Department of Physics, Kyoto Univ. of Education,
Fushimi, Kyoto 612, Japan

¹Division of Natural Environment, Faculty of Human Development,
Kobe University, Nada, Kobe 657, Japan

The local structure of supercritical fluid (SCF) state, i.e. the state beyond the critical temperature and pressure, is an interesting subject which is not well understood yet. In the SCF state it is known that clusters of a few molecules are formed. The material in this state often show an interesting phenomena such as high solubility for a certain solute, which is widely utilized in industry such as the decaffeining process from coffee. We have designed and developed a cell and transportation system of material to study the SCF state by means of x-ray absorption spectroscopy. The cell was made of stainless steel with a pair of Be windows (3 mm thick for each). The x-ray path can be controlled by changing the distance between two Be windows. Electric cartridge heaters are embedded in the cell to control the temperature. With this system we have studied the SCF state of CF_3Br , whose critical point is 67°C and 39 atm. X-ray absorption measurements for Br K-edge EXAFS for gas, liquid, and SCF states of the sample were performed at BL-6B and BL-7C EXAFS stations in the Photon Factory. The performance of the transportation system and the cell are presented together with the result of the absorption measurements.

MoD57

**LOW TEMPERATURE DIFFRACTOMETER BELOW 1K BY A ^3He - ^4He DILUTION REFRIGERATOR
USED FOR SYNCHROTRON RADIATION X-RAY DIFFRACTOMETRY AND TOPOGRAPHY**

TETSUO NAKAJIMA^a, HARUHIKO SUZUKI^b, TAKAYOSHI SUZUKI^c and HIDEJI SUZUKI^d

^aPhoton Factory, National Laboratory of High Energy Physics, Tsukuba-shi,
Ibaraki-ken, 305 Japan.

^bDepartment of Physics, Faculty of Science, Kanazawa University,
Kanazawa-shi, 920 Japan

^cInstitute of Industrial Science, University of Tokyo, Minato-ku, Tokyo,
108 Japan

^dFaculty of Engineering, Tokyo Engineering University, Hachioji-shi,
192 Japan

The direct observation of variations in the crystal structure at ultra-low temperatures plays very important roles in gaining a better understanding of the mechanism of the phase transformation and stability of the phase as a ground state. For these purposes, two sets of ^3He - ^4He dilution refrigerators (model 200NS, hereafter abbreviated DR) with a top-loading facility were installed at BL-3C₂ and 6C₁ of the Photon Factory.

The DR in BL-3C₂ is used exclusively for taking topographs from quantum crystals of solid ^3He , ^4He and their mixtures for studies of lattice defects. In this case, it fulfills the following requirements:

- (1) It can resist up to at least 100atm below 4K, to prepare solid helium.
- (2) Incident and scattered X-ray can pass through with moderate attenuation.
- (3) A capillary tube of helium inflow and thermometer should be fitted.
- (4) The goniometric adjustment of the position and orientation of a single crystal should be feasible to take Laue patterns.

For crystal positioning, only the ω and χ rotation mechanism of the sample cell with a limit of $\pm 20^\circ$ in each were established by modifying the top-loading facility.

Typical examples of solid ^3He and ^4He topographs, among which ^3He indicates a remarkable annealing effect, which might be understood in terms of a quantum tunneling effect, are presented. The disappearance of downward diffraction Laue spots ($2\theta_p=90^\circ$), which is orthogonal projection of images in Laue spots is discussed based on the temperature factor and others as one of peculiarities in solid helium.

The DR in BL-6C₁ is widely used for X-ray diffraction studies of crystalline solids. The DR, which weighs about 180kg, is set on the three circle goniometer ($\omega, 2\theta, \chi$ -circle), which resist up to 500kg. Top-loading facility is extremely useful for exchange of specimen.

An observation of a splitting of the Laue spots from $\text{Cs}_2\text{NaHoCl}_6$ below 150mK as an evidence of a cooperative Jahn-Teller transition of the first kind, which was only observed in the decreasing temperature process, is briefly explained as an example of diffractometry. In the increasing process, the transition could not be found up to about 1K, which shows good agreement with an observation of a Schottky-type specific-heat. This is a peculiar structural transformation at ultra-low temperature.

Detailed construction and test experiment will be presented.

MoD58

ASTATIC MAGNETS PRODUCING ARBITRARILY DIRECTED MAGNETIC FIELDS WITH GONIO-METRIC CONTROL USED FOR X-RAY DIFFRACTION.

Tetsuo Nakelima^a and Masami Yoshizawa^b

^aPhoton Factory, National Laboratory for High Energy Physics, Oho-machi, Tsukuba-shi, Ibaraki, 305 Japan.

^bSaitama Institute of Technology, Okabe-machi, Ohsato-gun, Saitama, 369-02 Japan.

Following a fashion of the goniometric control of magnetic fields, the superconductive and normal conductive magnets (hereafter abbreviated to SCM and NCM) were constructed, in which a given direction of magnetic fields astatically generated by a set of 3 pair coils was goniometrically controlled by 3 bipolar power sources. Hence, AC and DC magnetic fields applied to a crystal are able to varied from one direction $[h_1k_1l_1]$ to other direction $[h_2k_2l_2]$ keeping parallel to an arbitrary curved surface. The working of this magnet is very useful for taking dynamic characteristic of magnetic crystals by X-ray diffraction, including topographs.

In the SCM, the equipollent three pair split coils are made of NbTi single wire. Their coil constants lie in $0.012597A^{-1}$. Strength of magnetic fields is up to 0.87T with 2.4% homogeneity over 10ϕ mm sphere volume. The sectional view of the SCM is shown in Fig. 1. In the used cryostat, beryllium thin plates in size of $140\phi \times 1.2$ and $80\phi \times 0.5$ in mm unit for X-ray transmission are sealed by In-coated metal O-ring "Helicoflex".

The components H_x , H_y and H_z of the orthogonal three magnetic fields were measured at the same instant by 3-channel GPIB Gauss meter (model 9900) with Hall generator of two plate type (BHT-921) and one cylinder type (BHA-921) used at low temperatures manufactured by F.W.Bell Inc. in U.S.A. The simultaneous measurement of H_x , H_y and H_z is essential for control of above mentioned specification.

Both magnets are driven by two kinds of 3 bipolar electric power sources, i.e., rating output ($\pm 16V$, $\pm 82A$) and ($\pm 43V$, $\pm 82A$) ranging from DC to 100 Hz. Hence, the fields are changed by stepwise cycle of H_x , H_y and H_z closely along the concerned path by the current control by PC-9801RA5 of NEC.

The sectional view of the NCM is shown in Fig. 2. The maximum field of three coils (A, B and C coil) is up to about 0.03T by 30A exciting current with $1 \cdot 10^{-4}$ homogeneity over 10ϕ mm sphere volume. As a trial use, the NCM was used for taking white X-ray topographs of Fe-3%Si single crystals in magnetic fields swept in the (110) plane from $[200]$ via $[222]$ $[110]$, $[222]$, $[200]$ to $[200]$.

Details of the construction and the test experiments will be presented.

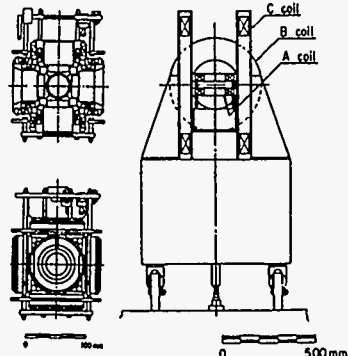


Fig. 1

Fig. 2

Progress Report on the Soft X ray Scanning Photoemission Microscope: MAXIMUM

W. Ng, S. Singh, H. Solak, F. Cerrina

Center for X-ray Lithography, University of Wisconsin-Madison
3731 Schneider Dr., Stoughton, WI 53589.

ABSTRACT

We will present a progress report from the soft x-ray scanning photoemission microscope: MAXIMUM. The microscope is installed at the U41 undulator at the Synchrotron Radiation Center at the University of Wisconsin. The instrument is based on a multilayer-coated Schwarzschild objective, and it is now operating at $h\nu = 135eV$. It has demonstrated spatial resolution 900\AA and electron energy resolution of $250meV$. We will discuss the implementation and performance of the new 135eV multilayer mirror. We will also present recent data from the different experimental programs that are being conducted on MAXIMUM.

Synchrotron Radiation Plane Wave GID Topography

D.V.Novikov, T.Gog, M.Griebenow, G.Materlik

Hamburger Synchrotronstrahlungslabor HASYLAB
at Deutsches Elektronen-Synchrotron DESY
Notkestr. 85, D-22607 Hamburg, Germany

X-ray diffraction topography is a traditional tool for investigating the real structure of crystals and provides high sensitivity to lattice constant variations with a good space resolution. However, recent advances in technology and the growing importance of surface regions of single - crystals and multilayer systems require new approaches to this method, which are made possible by the high brightness and wide tunability of synchrotron radiation.

In this work the SR plane-wave grazing-incidence diffraction (GID) topography is discussed as an effective tool for depth-resolved investigations of near surface defect structure in single crystals and epitaxial layers. The favorable properties of synchrotron radiation enable one to avoid usual limitations on applicability of this diffraction geometry and investigate all classes of defects in real materials

The experiments were performed at the beamlines ROEMO1 and CEMO of HASYLAB, using double-crystal Ge / asymmetric Si monochromators. The image formation of near-surface dislocations and the effects of refraction on rough surfaces were investigated.

Oblique diffraction planes were used to compare the topography in skew inco-planar and coplanar geometries. The latter is shown to be more effective, as it utilizes the wavelength tunability of SR and allows to vary the diffraction conditions in a wide range from usual highly asymmetric to grazing-incidence below the critical angle of total external reflection (and the penetration depth from hundreds to tens of nanometer) without off-plane rotations and provides pictures free of complicated geometrical distortions.

The dislocation images at different diffraction conditions proved to be qualitatively the same for near-surface defects, while the structure distortions, produced by the defects in the underlying layers become invisible at grazing incidence, due to both depth resolution of the method and inevitable loss of lattice parameter resolution. This might be a substantial advantage for characterization of films on substrates with a low perfection.

Thus, SR based plane-wave GID topography provides all the features of usual asymmetric topography and has substantial advantages for surface defect analysis.

MoD61

DEVELOPMENT OF MICRO-AREA DIFFRACTION SYSTEM BY POLYCHROMATIC SR WITH LAUE METHOD

K.Ohsumi¹⁾, K.Hagiya²⁾, M.Miyamoto³⁾ and M.Ohmasa²⁾

1) Photon Factory, KEK, 1-1, Oho, Tsukuba, Ibaraki, 305 Japan.
2) Life Sci., Himeji Inst.Tech., 3) Miner. Inst., Univ.Tokyo.

An equipment and software system was developed using Laue method combined with polychromatic synchrotron radiation, in order to analyze micro-textures in complicated crystal aggregates, and to refine structures of submicrometer-sized crystal particles or twinned domains. This development was carried out at beamline 4B(BL-4B) of the Photon Factory(PF), KEK and was successfully applied to some inorganic specimens. The minimum volume of specimen from which diffraction intensities were used for observed values in a structure refinement was $0.02\mu\text{m}^3$. This size of specimen beyond the limits of optical microscopy, and it is difficult to handle such small specimens under an optical microscope. In the case of using a second generation SR light source, therefore, micro-areas of a larger specimen can now be analyzed by an X-ray diffraction method. Micro-area diffraction studies will play an important role in the era of third generation SR light sources. The equipment is described briefly below.

Due to the limited space around BL-4B of PF, a micro-beam is produced by using a micro-pinhole which is set at a distance of 10mm before a specimen. At first we produced a micro-pinhole with a diameter of 8 μm . Using this micro-pinhole, a structure of olivine ((Fe,Mg)₂SiO₄) in a thin section of a Yamato meteorite was successfully refined including site occupancies of Fe and Mg in both M1 and M2 sites. Since then several micro-pinholes have been made by the authors. Their diameters were measured by scanning an ion chamber with a slit using polychromatic SR, and their shapes were confirmed to be circular from film images(Radocolor film: Nitto Elec. Co.Ltd. and Polaroid film). Micro-pinholes with diameters of 2.4 and 3.5 μm full width at half maximum are now available. The divergence of the obtained micro-beams after the pinholes were measured to be 26 and 15 μrad respectively. Two other pinholes with a diameter of 50 μm were installed in the beamline 2350mm apart from each other. The downstream 50 μm pinhole was approximately 1000mm from the sample. The newly developed equipment was designed to incorporate an imaging plate (200x400mm, Fuji Co.Ltd.) read out system. An imaging plate is set on a cylindrical cassette with a radius of 100mm, and covers -60 to 165 degrees in 2θ . The diffraction experiment is carried out in a vacuum chamber to minimize air scattering. To account for the varying path lengths of diffracted X-rays through non-irradiated parts of the sample and the subsequent variation in absorption, the software system was revised with respect to absorption correction of the integrated intensities of Laue spots.

Laue patterns of olivine and diamond in thin sections of meteorites with a 3.5 μm pinhole were successfully recorded and will be shown together with crystallographic analyses.

MoD62

SIMULATION OF SCATTERING X-RAYS FOR IMPROVING IMAGE QUALITY IN SR CORONARY ANGIOGRAPHY

Y. Oku, K. Hyodo*, K. Aizawa, and M. Ando*
Akashi Technical Institute, Kawasaki Heavy Industries, Ltd.
*Photon Factory, National Laboratory for High Energy Physics

Coronary angiography by intravenous injection of contrast material using synchrotron radiation is a safe and easy method for diagnosis of coronary arteries. In Japan, a two-dimensional imaging system for coronary angiography is being developed[1]. It benefits the ability to evaluate coronary arteries that are actually functioning as well as to do diagnosis in measuring blood flow or checking heart wall motion. However in the case of two-dimensional imaging, there exists a problem: Image contrast and visibility deteriorate due to harmful scattering x-rays which are made when passing through a patient's body.

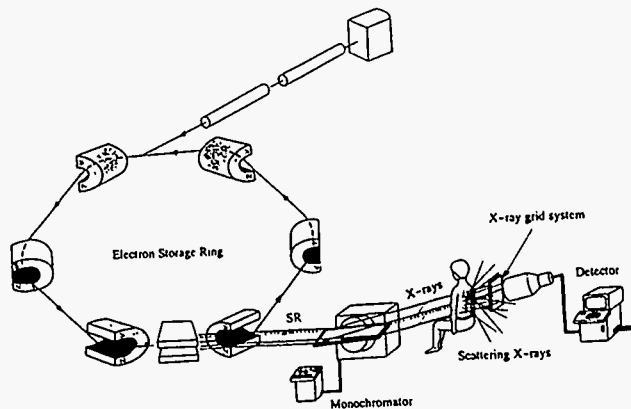
X-ray grids, which are used in conventional x-ray imaging systems to decrease the scattering x-rays in images, are considered to be very useful for improving the image quality taken by the two-dimensional SR imaging system. But direct x-rays for making images are also decreased considerably by absorption when passing through an x-ray grid.

Therefore, we have developed a simulation program in order to study x-ray scattering behavior in a subject using monochromatic x-rays and to find a way to decrease the scattering x-rays in images using x-ray grids. The calculated results concerning the scattering x-rays using the simulation program were compared with experimental results using monochromatic x-rays at 33.17keV from synchrotron radiation. The experiments were performed using an acrylic plate phantom and an imaging plate as a detector.

We will improve the concept of a compact SR source dedicated to medical applications as proposed by these authors et al.[2] using these results.

References

- [1] K.Hyodo, K.Nishimura, and M.Ando : Handbook on Synchrotron Radiation, Vol.4, 55 (ed. by S.Ebashi, M.Koch and E.Rubenstein Elsevier Science Publishers, Amsterdam, 1991)
- [2] Y.Oku, K.Aizawa, S.Nakagawa, M.Ando, K.Hyodo, and S.Kamada : Proceedings of the 1993 Particle Accelerator Conference, Vol.2, 1468 (1994)



Proposal of a Coronary Angiography System using a Compact Storage Ring

A Wavelength Dispersive Detector for Synchrotron X-ray Fluorescence Microprobe Analysis

Mark L. Rivers, Stephen R. Sutton
Dept. of Geophysical Sciences and Consortium for Advanced Radiation Sources, The University of Chicago, Chicago IL USA

The synchrotron x-ray fluorescence (SXRF) microprobe has proven to be a valuable tool for trace element research. It permits analysis down to a few parts-per-million of many elements in a spot size of less than 10 microns. Existing SXRF microprobes are using energy dispersive detectors (EDS), either Si(Li) or intrinsic Ge diodes. Such detectors have the advantage of collecting the entire fluorescence spectrum at once. They can also be positioned to collect a relatively large solid angle. However, EDS detectors suffer from several significant problems: resolution at Fe K α is about 150 eV, which is roughly 60 times the natural line width; the maximum count rate is less than 20,000 counts/second in the entire spectrum; there is significant low-energy background due to scattering and incomplete charge collection in the device. For geochemical analyses these limitations preclude trace element analyses in the presence of a large amount of a high atomic number element: for example trace element studies of galena (PbS) and zircon (ZrSiO₄), or measurements of Cr or Ti in minerals with more than a few percent Fe or Mn. The poor energy resolution prevents the measurement of small amounts of rare-earth elements in samples with significant concentrations of first-row transition elements.

Wavelength dispersive spectrometers, based upon Bragg diffraction from a bent crystal, have several distinct advantages over EDS detectors. The resolution at Fe K α is about 10 eV, or only 4 times the natural line width. This permits the analysis of rare-earth elements and also lowers the background which improves detection limits to the 0.1 ppm range. The WDS spectrometer only detects a single energy at once, so it is possible to measure trace elements in the presence of intense fluorescence of a major element.

We have installed a commercial wavelength dispersive spectrometer¹ on the X-26A microprobe beamline at the NSLS. The spectrometer can scan the range from 33°-135° 2 θ . It contains 4 analyzing crystals (TAP, PET, LiF200, LiF220) mounted on a motor-driven turret, which cover the energy range from 1-17 keV. The detector is equipped with tandem proportional counters: a thin-window flow counter (P-10 gas) followed by a Be-windowed sealed Xe counter. A remotely adjustable exit slit is located just before the flow counter. This slit can be used to trade off count rate for energy resolution. Measured resolution at Fe K α is 11 eV. The peak/background ratio on Fe metal is 10⁵, which is roughly 100 times better than with a Si(Li) detector. The measured collection efficiency varies from roughly 10⁻³-10⁻⁴, which is a factor of 3 to 10 lower than that for the Si(Li) detector as it is normally used at X-26A.

The X-26A microprobe has been configured to allow simultaneous use of both the WDS and Si(Li) detector. The detectors complement each other nicely, with the Si(Li) providing an overview of the entire spectrum and the WDS available to study selected peaks with significantly better energy resolution and sensitivity.

¹ Model WDX-3PC from Microspec Corp., Fremont CA

A Multielement Ge Detector with Complete Spectrum Readout for X-ray Fluorescence Microprobe and Microspectroscopy

Mark L. Rivers, Stephen R. Sutton, Harvey Raback
Dept. of Geophysical Sciences and Consortium for Advanced
Radiation Sources, The University of Chicago, Chicago IL USA

Multielement Ge and Si(Li) detectors have been used in recent years to improve increase count rate capability and to improve the solid-angle efficiency in fluorescence x-ray absorption spectroscopy (XAS). Such systems have typically been equipped with one or more single-channel analyzers (SCAs) for each detector element. Such SCA-based electronics are sufficient when only the counts in one or two well-resolved peaks are of interest. For the fluorescence (XRF) microprobe at beamline X-26A at the NSLS, SCA-based electronics were not a satisfactory solution for two reasons: 1) for XRF experiments the entire fluorescence spectrum is required; 2) for micro-XAS studies of trace elements in complex systems the fluorescence peak often sits on a significant background or partially overlaps another fluorescence peak, requiring software background subtraction or peak deconvolution.

We have designed an electronics system which permits collection of the entire fluorescence spectrum from each detector element. The system is made cost-effective by the use of analog multiplexors, reducing the number of analog-to-digital converters (ADCs) and multichannel analyzers (MCAs) required. The system was manufactured by Canberra Industries and consists of:

- 13 element Ge detector (11 mm diameter detector elements)
- 13 NIM spectroscopy amplifiers with programmable gains
- 4 analog multiplexors with maximum of 8 inputs each
- 4 ADCs with programmable offsets and gains and 800 nsec conversion time
- 2 MCAs with Ethernet communications ports and 2 ADC inputs each

The amplifiers have shaping times which are adjustable from 0.5-12 microseconds. The analog multiplexors were modified to perform pileup rejection. The analog multiplexing does not significantly reduce the count rate capability of the system, even at the shortest amplifier shaping times. The average detector resolution is 170 eV at 12 μ s shaping time and 200 eV at 4 μ s shaping time. The maximum aggregate count rate is 400 kHz with 0.5 microsecond shaping time.

The system is controlled by software based upon a package from Canberra and another commercial package (IDL), both running on a VAXstation 4000/90. The software automatically adjusts the gains of the amplifiers and offsets of the ADCs so that the spectra from each detector have identical calibrations and can be added channel-for-channel. The overhead to read a 1024 channel spectrum from each of the 13 elements and sum them is about 2 seconds. The software allows a range of options for data storage, from saving the complete spectrum for each of the 13 detectors elements (>50,000 bytes/point) to saving only the net counts under a single fluorescence peak summed over all the detector elements (4 bytes/point). These data can be stored at each pixel in an elemental map or at each point in a monochromator scan. The system has been commissioned and is being used for XRF and micro-XAS studies.

**Time-Resolved X-Ray Scattering Program At
The Advanced Photon Source**

Brian Rodricks
Advanced Photon Source
Argonne National Laboratory
9700 South Cass Avenue
Argonne, IL 60439

The Time-Resolved Scattering Program's goal in the development of instruments and techniques for time-resolved studies. This entails the development of wide bandpass and focusing optics, high-speed detectors, mechanical choppers, and components for the measurement and creation of changes in samples. Techniques being developed are pump probe experiments, single bunch scattering experiments, high-speed white and pink beam Laue scattering, and nanosecond to microsecond synchronization of instruments. This program will be carried out primarily from a white beam bend magnet source experimental station, IBM-B, that immediately follows the First Optics Enclosure (IBM-A). This paper will describe the experimental station and instruments under development to carry out the program.

Subnanosecond-resolved XEOL spectroscopy using a dissector

A.N.Belsky¹⁾, G.N.Kulipanov²⁾, V.V.Mikhailin¹⁾, V.A.Pustovarov³⁾,
A.L.Rogalcy⁴⁾, G.T.Shepel²⁾, A.N.Vasil'ev¹⁾, E.I.Zinin²⁾

1) *Synchrotron Radiation Laboratory, Moscow State University, 117234 Moscow*

2) *Budker Institute of Nuclear Physics, 630090 Novosibirsk*

3) *Ural Politechnical Institute, 620002 Ekaterinburg*

4) *European Synchrotron Radiation Facility, B.P. 220, F-38043 Grenoble Cedex*

The experimental set-up for subnanosecond time-resolved X-ray Excited Optical Luminescence (XEOL) spectroscopy of solids is described. This instrument has been developed and installed at the white beam wiggler beam line of the VEPP-3 storage ring. Short X-ray synchrotron radiation pulses with a FWHM of about 1 ns and a repetition period of 248.1 ns are used for excitation of luminescence. The emission in the spectral range from 200 nm to 800 nm is detected by using a stroboscopic version of electron-optical chronography based on a dissector having apparatus time resolution better than 20 ps. The stroboscopic mode of operation of the dissector in combination with the temporal structure of SR from VEPP-3 storage ring enabled three types of measurements to be performed: i) steady-state luminescence spectra; ii) emission decay curves at different emission wavelength. Decay times could be determined from the experimental data with a temporal resolution about of a 100 ps which is limited by the duration of the excitation pulses; iii) time-resolved XEOL spectra recorded simultaneously in six temporal windows of 50 ps separated by 41.35 ns. The time position of the windows could be varied relative to the excitation pulses within 41.35 ns.

The emission spectra (steady-state or time-resolved) and decay curves can be measured as well as a function of externally variable parameters, e.g. sample temperature. Decay data analysis is done by the modulating functions technique or by iterative deconvolution.

The performance of the experimental set-up is demonstrated with two examples of current interest, the non-exponential kinetics of emission of some inorganic scintillating crystals and the time-resolved measurement of the emission of high-temperature superconductor thin films.

MoD67

DESIGN OF A MULTISLIT, OPTIONAL WIDTH COLLIMATOR FOR MICROPLANAR BEAM RADIOTHERAPY

D.N. Slatkin, F.A. Dilmanian, and P. Spanne (Medical Department, Brookhaven National Laboratory, Upton, New York); J.-O. Gebbers (Pathologisches Institut des Kantonsspitals, Luzern, Switzerland); D.W. Archer and J.A. Laissue (Pathologisches Institut der Universität, Bern, Switzerland).

It has been shown that microplanar beam (microbeam) radiation therapy [MRT], initially proposed to treat human brain tumors (1), can palliate or ablate large (~ 4 mm-diameter), otherwise imminently and inexorably lethal (median residual lifespan [MRL] ~7 d) right frontocerebral brain tumors in rats (2). A horizontally propagated, 4-mm high, 25 μ m-wide, 0.25 mm Gd-filtered (median energy ~49 keV) microplanar beam was used in the X17B1 hutch of the National Synchrotron Light Source [NSLS] at Brookhaven National Laboratory [BNL] to irradiate 100 3-tiered, 12 mm-high x 25 μ m-wide, quasiparallel, microplanar fields in the rat head, separated from each other by 100 μ m intervals, field center-to-field center. Skin-entrance absorbed dose [SED] rates were ~ 400 Gy·s⁻¹. Using a sequential pattern of 300 exposures to irradiate these fields, straddling tumors anteroposteriorly with SED = 625 Gy/exposure, 4/14 rats were alive 99 d after irradiation (MRL = 28 d). Moreover, 9/15 or 8/15 rats were alive 99 d after such tumors were crossfired first anteroposteriorly and then transversely from right to left using that pattern twice with SED = 625 or 312 Gy/exposure, respectively.

As optimal beam widths and interbeam intervals for various conditions of MRT are unknown, an optional width collimator would be useful. Our present collimator design is for a pair of identical, parallel stacks, each stack comprised of 100 μ m- or 150 μ m-thick tungsten foils alternating with 100 μ m- or 50 μ m-thick beryllium foils, respectively. Translation of one stack parallel to the fixed, identical stack, each stack perpendicular to the beam line, should yield arrays of quasiparallel microplanar beams at 200 μ m intervals, beam center-to-beam center, with optional microplanar beam widths in the 0-100 μ m or 0-50 μ m range, respectively. Two exposures, the second after a 100 μ m translation of either the collimator or the target parallel to the stacks, would result in 100 μ m intervals between microplanar beams, center-to-center. Improvements in construction techniques may allow beryllium to be replaced by more radiolucent materials such as air. A mechanism for cooling the collimator and its frame may be incorporated into the device, if required.

1. D.N. Slatkin, P. Spanne, F.A. Dilmanian, and M. Sandborg. Microbeam radiation therapy. *Med. Phys* 19, 1395-1400 (1992).
2. D.N. Slatkin, P. Spanne, F.A. Dilmanian, H.M. Nawrocky, J.-O. Gebbers, and J.A. Laissue. Microplanar beam radiotherapy [MRT] of malignant brain tumors in rats. In *National Synchrotron Light Source 1993 Annual Report*, Brookhaven National Laboratory, Upton, New York.; BNL-52415 (In press, 1994).

We are grateful to the staffs of the NSLS and Medical Departments of BNL for their invaluable help. J.A.L. and D.W.A. acknowledge the University of Bern, and J.-O.G. acknowledges the Cantonal Hospital of Lucerne, for sponsorship. This study is supported primarily by the U.S. Dept. of Energy through its prime contract DE-AC02-7600016 with BNL.

MoD68

TESTING OF SUB-MICROMETER FLUORESCENCE MICROPROBE BASED ON BRAGG-FRESNEL CRYSTAL OPTICS AT THE ESRF

A.Snigirev, I.Snigireva, P.Engström
ESRF, B.P. 220, F-38043 Grenoble, France

A.Suvorov
Institute for Microelectronics Technology, Russian Academy of Sciences,
142342 Chernogolovka, Moscow Region, Russia

P.Chevallier, F.Legrand, G.Soullie
LURE, University Paris-Sud, Bat.209D, F-91405, Orsay, France

The performance of the fluorescence microprobe based on Bragg-Fresnel lens is tested at the ESRF Microfocus beamline (Fig.1). A low- β undulator with the source size $150 \times 90 \mu\text{m}^2$ was located at a distance of 36m. The 7.6 keV and 13.5keV monochromatic beam was selected by a N₂-cooled channel-cut Si monochromator and was focused on a sample by a circular Ge BFL using 444- and 777-reflections in nearly backscattering geometry.

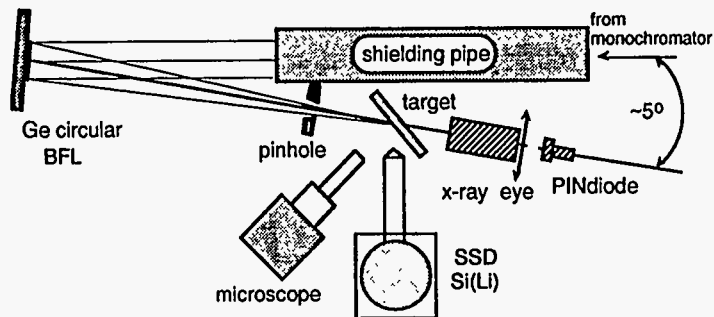


Fig.1 Optical set-up for sub μm fluorescence microprobe, top view.

A Cr mask with 80nm thickness was used as a test object to measure the resolution and sensitivity of the microprobe. The fluorescence signal was recorded with a Si(Li)-detector. The knife-edge scan data show a focal spot of $0.7 \mu\text{m}$. The intensity in the focal spot was measured to 10^8 ph/s. The developed sub-micrometer fluorescence microprobe was applied for mapping $100 \mu\text{m}$ size micrometeorite. Some aspects of sample preparation and sample alignment for sub- μm fluorescence microprobe will be considered as well.

We gratefully acknowledge the support of C. Riekel, M. Kocsis, S. Lequien, A. Freund, M. Idir and S. Engrand.

SR-Hard-X-Ray-Diffraction-Microscopy of Carbon Fibre Reinforced Plastic

By J.D.Stephenson, M.P.Hentschel and A.Lange¹

Div.6.22 Federal Inst. of Material Research and Testing, Unter den Eichen 87, 12206 Berlin, FRG.

The characterization of carbon fibre reinforced plastics (CFRP) requires high resolution (non destructive) X-ray techniques which differentiate between fibre bundle-layers and -inner structure within the bulk material. As an example, we examined a (pseudo hexagonal) CFRP, composed of fibres, approximately 6μ in diameter \bar{a} -axis along- and \bar{c} -axis perpendicular to the fibre length) which were unidirectionally arranged in layers approximately 100μ apart.

Alternate planar layers were preferentially orientated and bonded together in an epoxy matrix forming a high strength/light weight material, designed for helicopter- and turboprop-blades, primary and secondary structures for advanced aircraft fuselages, automobile components, medical architecture and other peripheral (sport) devices. The perfection of such advanced materials is marred by defects within the composite material (pores, microbuckling, delamination) and a careful quality control is therefore paramount for the advancement of these materials.

As the eyepiece 'E' (00.2) X-ray quantum efficiency yield from a (1mm thick) sample is very low (10^{-7} at $\approx 8\text{KeV}$) a SR-'straight through' microscope has been designed to improve the spatial resolution of an earlier characteristic X-radiation model². The much higher intensity and smaller emittance from the SR-source made it possible to design an objective 'O' (formed by accurately aligned (crossed) tantalum slits, $480 \mu\text{m}$ (V) and $20 \mu\text{m}$ (H)). The eyepiece 'E' was formed by similar slits $15 \mu\text{m}$ (V) and $25 \mu\text{m}$ (V) and separated to fully accept the (00.2) diffracted intensity into the detector 'D'. Two test experiments were carried out at HASYLAB (Hamburg) using a) WSR and b) Monochromatic (7.77KeV) Wiggler-SR. In both cases the same (cross ply) CFRP laminate ($\approx 1 \mu\text{m}$ thick, 1.25mm wide, containing 12 bundle layers) was used.

We will show the results of the two experiments where;

1. The WSR intensity scans have the disadvantage that the (00.2)-reflection is highly wavelength dispersed causing E to accept a range of diffracted wavelengths from different parts of the sample. The signal-noise modulation in this case was $\approx 10\%$ giving a spatial resolution of $100 \mu\text{m}$ without computer processing.
2. The use of Si-(220) monochromatised SR (FWHM = 5.3arcsec) has the advantage of non wavelength dispersed (00.2)-diffraction. The signal-noise modulation in this case was 70% which improved the spatial resolution to $\approx 25 \mu\text{m}$. This was at the expense of reducing the signal intensity to a tenth of that obtained in 1).

Again the scanned data did not need to be deconvoluted, instead only the top (highly resolved) signal region was used reclaiming the true inherent resolution.

¹NIM (B), (1994) in press

²K.W. Harbich, M.P Hentschel and A Lange, Kunststoffe/ German Plastics, 83,22, (1993), 9

Oxidation State Mapping using Micro-XANES

S. R. Sutton¹, S. Bajt¹, D. Schulze² and T. Tokunaga³

¹ Department of the Geophysical Sciences and Center for Advanced Radiation Sources, The University of Chicago, Chicago, IL 60637, USA; ² Agronomy Department, Purdue University, W. Lafayette, IN 47907, USA; ³ Earth Sciences Division, Lawrence Berkeley Laboratory, Berkeley, CA 94720 USA.

X-ray absorption near edge structure (XANES) is a valuable technique for studying the electronic structure of specific elements in complex materials. In principle, XANES applied with x-ray microprobe instrumentation can be used to obtain this information in a spatially-resolved manner. Examples of problems which might benefit from micro-XANES include:

- redox states and mineralogical associations of toxic species in contaminated sediments and waste encapsulation materials.
- oxygen fugacity determinations based on partitioning of trace elements in specific valence states between co-existing phases in earth and extraterrestrial materials.
- redox state of the Earth's interior based on valence determinations on micro-crystals within diamonds from the mantle.
- redox chemistry of Mn at the root-soil interface and its role in agriculturally-relevant plant diseases.

The basic approach in oxidation state mapping is to make multiple, 2-dimensional x-ray fluorescence (elemental) maps of the specimen using monochromatic radiation where the monochromatic energy for each map is chosen to preferentially excite particular oxidation states of the element of interest. The distributions of individual oxidation states are then determined by deconvolution of these maps.

This method was used to map selenium oxidation states in water-saturated sediment containing decomposing roots of *Scirpus*, a common wetland plant [1]. Selenium was introduced homogeneously as selenate (Se^{6+}). The resulting oxidation state map clearly showed that soluble Se^{6+} was reduced to the less mobile Se^{4+} and insoluble Se^0 in the regions of high microbial activity, i.e., immediately adjacent to the decaying roots. In another application, Mn oxidation state maps of wheat roots growing in agar amended with Mn^{2+} and infected with the take-all fungus *Gaeumannomyces graminis* var. *tritici*. Abstracts - 10th Inter. Clay Conf. Adelaide, Australia. [3] Schulze, D., S. R. Sutton and S. Bajt (1994) Measurement of Mn oxidation state in soils using x-ray absorption near edge structure (XANES) spectroscopy. *Soil Science Society of America Journal*, in preparation.

Acknowledgments: This research was supported in part by the following grants: US DOE DE-F602-92ER14244 (SRS), DE-AC02-76CH00016 (BNL).

References: [1] Tokunaga, T., S. Sutton, and S. Bajt (1994) Mapping of selenium concentrations in soil aggregates with synchrotron x-ray fluorescence microprobe. *Soil Science*, submitted. [2] Micro-XANES spectroscopy of Mn-oxide precipitates around wheat roots infected with the take-all fungus *Gaeumannomyces graminis* var. *tritici*. Abstracts - 10th Inter. Clay Conf. Adelaide, Australia. [3] Schulze, D., S. R. Sutton and S. Bajt (1994) Measurement of Mn oxidation state in soils using x-ray absorption near edge structure (XANES) spectroscopy. *Soil Science Society of America Journal*, in preparation.

Dark Field Imaging in Hard X-ray Scanning Microscopy

Yoshio Suzuki and Fumihiko Uchida¹

Advanced Research Laboratory, Hitachi Ltd.,

¹ Central Research Laboratory, Hitachi Ltd.,

In x-ray microscopy, image contrast is produced by transmission contrast or fluorescent x-ray yield. Although the fluorescence yield method provides dark field imaging, other kinds of contrast are possible, such as diffraction, scattering, reflection, refraction, and phase contrast. We will discuss some of these dark field imaging (DFI) methods used in hard x-ray scanning microscopy.

Our microbeam optical system is essentially the same as that discussed in an earlier paper[1]. SR from PF 2.5GeV storage ring is monochromatized through a Si double crystal monochromator and focused by a pair of elliptical total-reflection mirrors (elliptical Kirkpatrick-Baez optics[2]). With this optical system, a focus spot of about 1 μm has been achieved. For DFI, scattered x-rays, reflected x-rays, diffracted x-rays and fluorescent x-rays are detected with a NaI scintillation counter or a Ge solid state detector. A beam stop is located behind the sample to absorb the directly transmitted x-rays.

An example of DFI is shown in Fig. 1. GaAs hetero-epitaxial film on Si is used as the model sample. Crystal structure imaging of GaAs film and substrate Si is obtained by detecting diffracted x-rays (scanning X-ray diffraction microscopy, or scanning diffraction topography). Defects in the GaAs film can be observed, as shown in Fig. 1a, and lattice strain images of the underlying Si substrate can also be seen (Fig. 1b). Uniformity in the GaAs film is confirmed by elemental mapping observation by means of fluorescent x-ray detection (Ga $K\alpha$ and As $K\alpha$ x-rays). We will also discuss other types of DFIs, edge contrast by reflected x-ray detection, and imaging of light elements by scattered x-ray detection.

1) Y. Suzuki and F. Uchida, *Rev. Sci. Instr.* 63 (1992) 578 (proceedings of SRI91).

2) P. Kirkpatrick and A. V. Baez, *J. Opt. Soc. Am.* 38 (1948) 766.



Fig.1a. GaAs on Si.

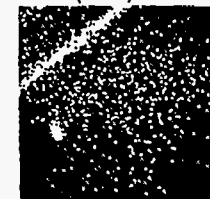


Fig.1b. Si substrate.

FLUORESCENT SCANNING X-RAY COMPUTED TOMOGRAPHY WITH SYNCHROTRON RADIATION.

Tohoru TAKEDA, *Toshikazu MAEDA, Tatsuo ITO, Kenichi KISHI, Jin WU, Masahiro KAZAMA, *Tetsuya YUASA, **Kazuyuki HYODO, *Takao AKATSUKA, Yuji ITAI

Institute of Clinical Medicine, University of Tsukuba, Tsukuba, Ibaraki 305 Japan

*Faculty of Engineering, Yamagata University, Yamagata 992 Japan

**Photon Factory, National Laboratory for High Energy Physics, Tsukuba, Ibaraki 305 Japan

INTRODUCTION: From analysis of fluorescent X-ray, we can obtain several characteristics of the material and biological specimen. But these specimens are thin slice section and measures surface scanning of the object. A new fluorescent scanning X-ray computed tomography (FS X-ray CT) is developed to detect tracer material (an iodine and gadolinium) of living object. Here, the concept of the system and preliminary results of this FS X-ray CT experiment will be reported.

METHOD: FS X-ray CT consists of silicon (111) channel cut monochromator, X-ray shutter, X-ray slit system, a scanning table for target organ and an X-ray detector with germanium which detects fluorescent X-ray excited by SR (Fig.1). Experiment was carried out at bending beam line of BLNE-5A of the Tristan accumulation ring (6.5 GeV, 10-30 mA) in Tsukuba, Japan. The energy of monochromatic X-ray beam was adjusted to 33.17 ± 0.2 keV. Data acquisition time was 50 s at each scanning point.

Phantom filled with various concentration of an iodine contrast material was scanned. Beam size for excitation was collimated in 1×2 mm² and the fluorescent X-ray detection site was also collimated 2×2 mm². The small circular phantom (20 mm in diameter) was scanned using relatively large excitation and detected size ($2 \times 2 \times 2$ mm³).

RESULTS: The 50 µg/ml of an iodine contrast agent was detected sufficiently by this preliminary FS X-ray CT system. The observation area by excitation was only 4 mm³. The image of cylindrical phantom filled with 2 mg/ml iodine was demonstrated (Fig.2). The image quality was now poor probably because scanning size was relatively large, however contrast agent was detected. FS X-ray CT might be available to detect contrast agent with low concentration and to reveal its distributions.

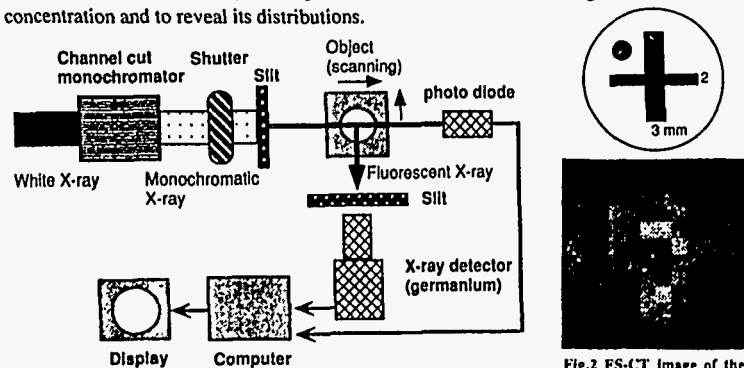


Fig.1 Diagram of fluorescent scanning X-ray CT

Fig.2 FS-CT Image of the phantom
above: shape of phantom
below: FS-CT image

MoD73

Photon Stimulated Ion Desorption Studies Using Pulsed Synchrotron Radiation

Kenichiro Tanaka^{1,2,4}, Hiromi Ikeura², Tetsuhiro Sekiguchi³, Tetsuji Sekitani¹, and Marcia C. K. Tinone⁴

1. Photon Factory, Nat'l Lab. for High Energy Phys., Oho, Tsukuba, 305 Japan

2. Dept. of Chem., Univ. of Tokyo, Hongo, Tokyo, 113 Japan

3. SR Facility Project Team, Japan Atomic Energy Res. Inst., Tokai, 319-11 Japan

4. Dept. of SR, Grad. Univ. for Adv. Studies, Oho, Tsukuba, 305 Japan

Recently, inner-shell electron energy loss spectroscopy (ISEELS) and near-edge x-ray absorption fine structure (NEXAFS) spectroscopy have been successfully applied to the characterization of molecular and electronic structure of various kinds of molecules. However, subsequent reactions after the inner-shell excitation have not necessarily been investigated in detail. Among such reactions, photon stimulated ion desorption (PSID) is a relatively simple process and is efficiently observed by inner-shell excitation.

In this work, a simple ion time-of-flight (TOF) spectrometer was designed and installed in the soft x-ray beamlines BL11A and BL13C, in order to investigate the mechanism of PSID initiated by soft x-ray. During single bunch operation of the Photon Factory 2.5 GeV storage ring, soft x-ray pulses with period of 624 ns and width of 100 ps were irradiated on the sample. Due to the very good time reproducibility of the SR pulses, heavy ions which have flight times longer than 624 ns can also be measured. Therefore, in this work, we were able to investigate the PSID of both small molecules (H₂O and DCOOD) and large molecules (polymer thin films).

Chemisorbed Small Molecules

PSID of H₂O/Si(100) and DCOOD/Si(100) have been examined at the oxygen K-edge and the carbon K-edge regions, respectively. The results are summarized as follows: O⁺ ions from H₂O exhibit a delayed threshold at ca. 570 eV which is interpreted in terms of the primary excitation and the modification of number of charge of desorbing species. D⁺ and CDO⁺ ions from DCOOD strongly depend on the primary excitation, and are selectively enhanced at the C 1s to σ_{C-D}^* and σ_{C-O}^* excitations, respectively.

Polymer Thin Films

PSID of Poly(methylmethacrylate) and Poly(methylacrylate) have been examined at both the carbon and the oxygen K-edge regions. It was found that the ion desorption occurs specifically around the site of the atom where the primary excitation takes place. The efficient production of CH⁺, CH₂⁺ and CH₃⁺ ions at 288 eV and 538 eV are considered to be a result of the localized excitation of C 1s and O 1s in the methoxy group to the $\sigma_{O-CH_3}^*$ state, respectively. CDO⁺ ions are also site-specifically enhanced at 539 eV excitation which is assigned to the transition from methoxy O 1s to the $\sigma_{C-OCH_3}^*$ state.

MoD74

MACROMOLECULAR CRYSTALLOGRAPHIC RESULTS OBTAINED USING A CCD DETECTOR AT CHESS

D. J. Thiel, R.L. Walter, S. E. Ealick, Section of Biochemistry, Cell and Molecular Biology and D. H. Bilderback, Cornell High Energy Synchrotron Source (CHESS), Cornell University, Ithaca NY 14853; S. M. Gruner, Department of Physics, Princeton University, Princeton NJ 08544; and E. F. Eikenberry, Robert Wood Johnson Medical School, Piscataway NJ 08854.

The development of large format, low noise charge-coupled devices (CCD's) is beginning to exert an impact on macromolecular crystallography. Results from various macromolecular crystallography experiments are presented showing the effectiveness of a recently installed CCD detector at the Cornell High Energy Synchrotron Source (CHESS). The detector [1] uses a 1024 x 1024 CCD array directly coupled to a phosphor with a fiber optic taper. The pixel size at the phosphor (50 microns) results in an effective spatial resolution of about 80 microns. Even with the relatively small active area, about 150 orders of diffraction can be resolved across the detector face. With this detector format, well-resolved diffraction data have been collected from unit cells with edges as large as 300 Å. In an offset configuration, the detector has been used to collect extremely high resolution data (1 Å). A number of data sets have been collected having R_{sym} values in the 4-6% range; in the case of room-temperature lysozyme, an R_{sym} value as small as 2.0 was obtained for a 2.0 Å resolution data set. In addition to fixed wavelength studies, the detector has also been used to collect MAD data. In all cases, the use of this detector has proven to be more efficient than using standard image plates. An oscillation data frame is displayed shortly after the exposure, and while the data set is being collected, a fast program transforms the data by subtracting the background, removing distortion effects, and correcting the intensities as a function of both phosphor position and obliquity angle of the diffracted x-rays. Entire data sets were collected and preprocessed over the period of a few fills, each lasting 60 minutes. In ideal cases, a data set is collected in one 60 minute fill. Based upon resolution and crystallographic statistics, the quality of the presented data shows a marked improvement over data previously recorded with other detection devices.

[1] M. Tate, E. Eikenberry, S. Barna, M. Wall, J. Lowrance, and S. Gruner, "A Large Format, High Resolution Area Detector Based on a Directly Coupled CCD", in preparation.

Nuclear Resonant Diffraction from a ⁵⁷Fe/Cr Antiferromagnetic Multilayer

T. Toellner, E. Fullerton, W. Sturhahn, and E. Alp
Argonne National Laboratory, Argonne, IL 60439

We report the observation of nuclear resonant diffraction of synchrotron radiation from a ⁵⁷Fe/Cr multilayer. The multilayer consist of 25 ⁵⁷Fe(15Å)/Cr(10Å) bilayers which was chosen so as to exhibit antiferromagnetic coupling of the ⁵⁷Fe layers. Due to the coupling, the magnetic periodicity of the multilayer is twice the electronic periodicity. Nuclear resonant diffraction from the multilayer shows a pure nuclear resonant Bragg reflection corresponding to this magnetic periodicity of the ⁵⁷Fe layers. The pure nuclear Bragg reflection presents a means of filtering synchrotron radiation to the level of 10⁻⁸eV at the nuclear resonance energy of 14.4 keV. For the future it demonstrates the potential for probing thin film magnetic structures containing ⁵⁷Fe with synchrotron radiation.

This work is supported by US-DOE, BES Materials Science, under contract No: W-31109-ENG-38.

Simultaneously two energy powder diffraction method using the effect of anomalous scattering.

A.V.Bessergenev, B.P.Tolochko
Institute of Solid-State Chemistry, Novosibirsk, Russia
M.A.Sheronov, N.A.Mezentsev
Institute of Nuclear Physics, Novosibirsk-90, Russia

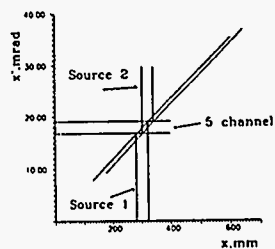


Fig. 1

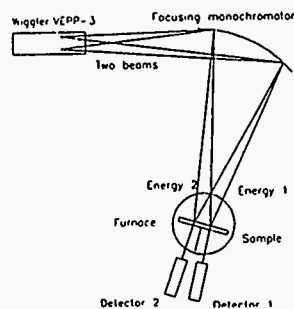


Fig. 2

The using of synchrotron radiation from VEPP-3 wiggler gives the possibility to work with two beams a different energy simultaneously. The different beams appears from electron trajectory in wiggler which corresponding to ellipse at phase diagram. At fig.1 show only part of ellipse ($z=17$ m), related to the aperture of 5-th beam line were this work was made. For the fifth beam line the distance between this sources of SR is equal 1.14 sm. This space distance between sources lead to different incidence angles on the monochromator (in horizontal monochromatization scheme) and finally to the appearing two monochromatized beams with different energies. Due to the divergence of the SR the beams overlapping (fig 1). Using the focusing monochromator (fig.2), we separated this radiations in the space. The difference between energies of this beams was 18 eV for K K-edge energy. The difference between first energy and energy of K edge of absorption was 15 eV.

Using the beams with different energies gives the possibility to use the anomalous scattering effect in the "in situ" experiments.

In order to test our method we measured the intensities of reflections from mixture NiO and MoO₃ with position sensitive detector. We obtained, that the change of intensity of reflection from NiO (reflection (111)) was 18 %, and the intensities of reflections from MoO₃ don't change. This method was used for the study of the solid state chemical reaction: $NiO + MoO_3 \rightarrow NiMoO_4$

The cutting mashing for investigation of the relaxation process by synchrotron radiation diffraction..

A.V.Suchorukov*, B.P.Tolochko*, N.G.Savrilov**
Institute of solid state chemistry,
Novosibirsk-91, Russia(*)
Institute of nuclear physics,
Novosibirsk-90, Russia(**)

The cutting mashing was design for fast deformation of the metal wire and registration of diffraction pattern immediately after cutting proses.

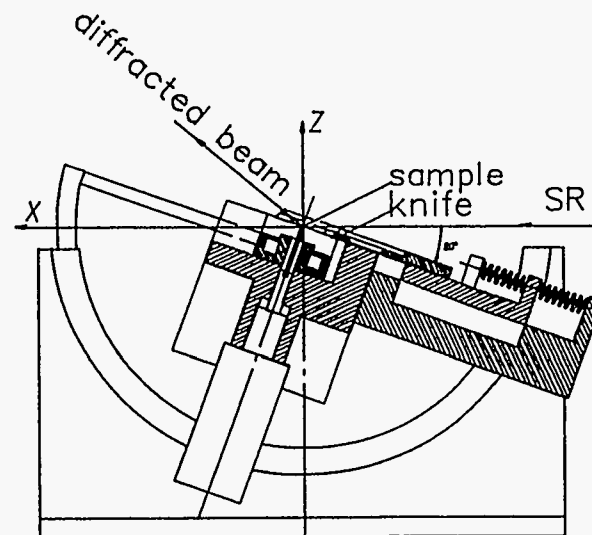
Every act of cutting realized by knife which move under the spring force. After that knife return to the stop position by motor and press the spring at the same time.

During the cutting process the knife cover the sample. For overcoming this problem, in the knife prepare the special slit. Through this slit the synchrotron radiation penetrate at the sample. Diffracted radiation go out through the same slit and registered by position sensitive detector

The registration system was synchronize with the end of cutting process with accuracy 1 ms. It work in accumulation mode and store information from hundreds cutting process.

The cutting mashing has a temperature stabilization system and can work in region (-50) - (+200) C.

The cutting mashing was used for investigation of relaxation process in copper, silver and nickel.



X-Ray Diffraction Analysis of Molten KCl under High Pressures

Satoru Urakawa¹⁾, Hideo Ohno²⁾, Norimasa Umesaki³⁾,
Kazuo Igarashi⁴⁾ and Osamu Shimomura⁵⁾

- 1) Okayama University, Okayama 700, Japan
- 2) Japan Atomic Energy Research Institute, Tokai 319-11, Japan
- 3) Government Industrial Research Institute Osaka, Ikeda 563, Japan
- 4) Government Industrial Research Institute Nagoya, Nagoya 462, Japan
- 5) National Laboratory for High Energy Physics, Tsukuba 305, Japan

Combined with a large volume high pressure apparatus, synchrotron radiation has the potential to reveal the structure of molten salt, such as alkali halide, under high pressures. Solid KCl has a relatively high compressibility and it transforms into CsCl structure from NaCl structure around 2 GPa (Figure 1). Thus it is expected that the structure of molten KCl will also be changed by increasing pressure. Here we report the results of X-ray diffraction experiments on molten KCl up to 4 GPa.

Experiment has been conducted at the wiggler beamline (BL-14C) in Photon Factory by the energy dispersive method with white beam (30-120keV). SSD is fixed at $2\theta=4, 5, 6, 7, 8, 10, 12, 15, 20$ and 25° to cover the Q range from 1 \AA^{-1} to 15 \AA^{-1} . High pressure is generated by using the cubic-type apparatus MAX90. Data are collected just above the melting point of KCl up to 4 GPa (Figure 1). The analysis method of obtained data is identical to that described in reference (1).

Structure factor $S(Q)$ for KCl is shown in Figure 2. Principal feature of $S(Q)$ curve is identical among four data. Two peaks are detected at $Q=2.3 \text{ \AA}^{-1}$ and 4.5 \AA^{-1} , and a subpeak is observed at high Q side of first peak. However, the first peak becomes sharp and high with increasing pressure. According to molecular dynamics simulation, this can be explained by the continuous increase of coordination number of nearest neighbor with increasing pressure.

(1) Tuji, K., Yacita, K., Imai, M., Shimomura, O. & Kikegawa, T. (1989), *Rev. Sci. Instrum.*, **60**, 2425-2428.

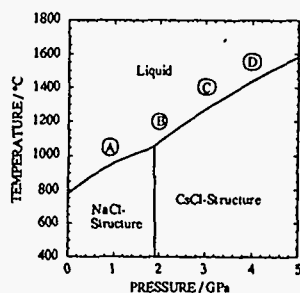


Figure 1. Phase diagram of KCl. The experimental conditions are shown as A, B, C and D.

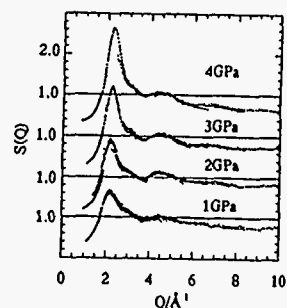


Figure 2. Structure factor for molten KCl.

Core Excitons in Silicon and Silicon Oxides

G.E. van Dorssen¹, M. Roper, H.A. Padmore², G. Derst, G.N. Greaves

DRAL Daresbury Laboratory, Warrington WA4 4AD, UK

¹DRAL Daresbury Laboratory, Warrington WA4 4AD, U.K. and NWO, P.O.
Box 93138, 2509 AC The Hague, The Netherlands

²Advanced Light Source, Lawrence Berkeley Laboratory, Berkeley CA 94720,
USA

Measurements have been carried out on two different stations of the Daresbury SRS in order to determine the binding energy of core level excitons in silicon compounds. Near edge structures at the Si L-edge have been measured on undulator station 5U.1, and Si K-edge EXAFS data has been measured on station 3.4. All measurements have been performed in reflection mode, using two soft X-ray reflectometers.

From the EXAFS data the local environment of the Si atoms can be determined. The position of the K-edge combined with literature values for the K fluorescence radiation gives the energy of the conduction band minimum (CBM) [1]. The position of the exciton peaks in the spectrum of the L-edge data in combination with the CBM gives the exciton binding energy.

When using a Wannier model to describe the core excitons the effective mass of the exciton can be determined. Comparing the values of the exciton binding energy and effective mass with literature values [2,3] we find that they are in good agreement. For crystalline quartz we find a binding energy of 0.7 ± 0.1 eV, compared with a literature value of 0.6 ± 0.1 eV [3]. In this work we have shown that it is possible to combine the data obtained on two different stations, and measure the parameters of core excitons with sufficient accuracy needed to compare the data with literature values. We have also shown that it is possible to carry out reflectivity measurements with the resolution necessary for the determination of the exciton parameters. Comparison with literature values shows that a rigid Kramers-Kronig analysis of the data is not needed for the determination of the exciton parameters, and the structural data determined from the EXAFS measurements also agree with known values.

References

1. C. Sugiura, *J. Phys. Soc. Jpn.* **62**, 585 (1993).
2. R.D. Carson and S.E. Schnatterly, *Phys. Rev. Lett.* **59**, 319 (1987).
3. W.L. O'Brien *et al.*, *Phys. Rev. B* **44**, 1013 (1991).

THE POSSIBILITIES OF X-RAY STANDING WAVE METHOD
FOR INVESTIGATION OF THE STRUCTURE OF REAL
CRYSTALS.

THEORY AND APPLICATIONS.

Vartanyants I.A., Kovalchuk M.V.,

A.V. Shubnikov Institute of Crystallography RAS, Leninsky pr. 59, 117333
Moscow, Russia.

The X-ray Standing Wave (XSW) method now is a powerful tool for determining the structure of surfaces and the position of adsorbed atoms on the top of the crystals. In the most of applications of XSW method dynamical theory of X-ray propagation in a perfect crystal is used. However this method can be successfully applied also for investigation of the structure of the real crystals for e.g. crystals with deformed surface layers. It gives also an opportunity to determine the position of the impurity atoms in that structures. General theory of XSW method in real crystals is presented. The possibilities of the method are demonstrated on several examples. Investigation of the implanted crystals: structure of Si crystals implanted by Fe and Ni atoms. Investigation of artificial nanometer-scale materials: structure of (InAs) (GaAs) layered crystals. Combination of XSW and High Precision Diffraction methods opens the possibilities for phase analysis and gives an opportunity for the unique determination of the profile of deformation of the crystal surface. Special attention would be paid for investigation of bent crystals that are widely used as X-ray monochromators at synchrotron radiation sources, as X-ray microscopes and focusing spectrometers for plasma analysis with XSW methods.

MoD81

FEASIBILITY OF PHOTO-EXCITATION IMAGING IN SOFT
X-RAY MICROSCOPY USING THE TRANSITION TO π^* -ORBITS
IN BIOLOGICAL MOLECULES

Yoshinori Iketaki¹ and Tsutomu Watanabe¹

Res. Dev. Corporation of Japan (JRDC) 2-45-13 Honcho, Nakano-ku, Tokyo 164 Japan
¹Dept. of Phys., International Christian Univ., Mitaka-shi, Tokyo 181 Japan

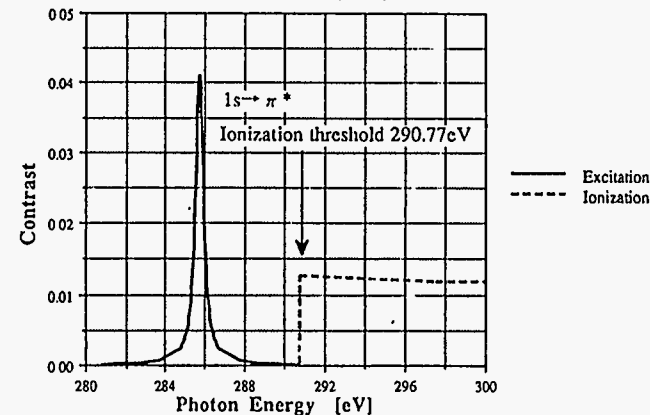
Usual X-ray microscopy for wavelengths within the water window is carried out using an absorption process caused by the *photo-ionization* of 1s electrons in carbon or nitrogen[1]. Recently, soft X-ray microscopy using inner shell *photo-excitation* was proposed by J. H. Klems [2]. This soft X-ray microscopy technique consists of a uv laser and an X-ray source. Uv laser is used for the production of unoccupied π -character orbit. It is expected that a more sensitive soft X-ray microscopy would be realized by utilizing inner-shell excitation, because the photo-excitation cross sections are generally larger than the photo-ionization cross sections by one or two orders of magnitude in this wavelength region.

Since DNA and RNA in biological cells contain innumerable bases which have unoccupied π^* -character molecular orbits. It is also expected that another type of soft X-ray microscopy would be proposed based on the use of the excitation process to unoccupied π^* -character molecular orbits. In this paper we estimate the photo-absorption cross section caused by the transition of 1s electrons to π^* -character molecular orbits and discuss the feasibility of X-ray microscopy based upon transition to unoccupied π^* -character orbits.

The figure below displays the calculated photo-absorption contrast of T4-phage as a function of photon energy

References

1. J. Kirz and P. Barback, Rev. Sci. Instrum., 56, 1 (1985).
2. J. Klems, Phys. Rev., A42, 2041 (1991).



¹On leave from Olympus Optical Co. Ltd. Hachioji-shi, Tokyo 192 Japan

MoD82

High-resolution Triple-crystal X-ray Diffraction Experiments Performed at the Australian National Beamline Facility in Japan

A.Yu. Nikulin¹, A.W. Stevenson², H. Hashizume³, S.W. Wilkins²,
D. Cookson⁴, G. Foran⁴ and R.F. Garrett⁵

¹School of Physics, University of Melbourne, Parkville, Vic. 3052, Australia

²CSIRO Division of Materials Science & Technology, Private Bag 33, Rosebank MDC, Clayton, Vic. 3169, Australia

³Research Laboratory of Engineering Materials, Tokyo Institute of Technology, Nagatsuta, Midori, Yokohama 227, Japan

⁴Australian National Beamline Facility, Photon Factory, National Laboratory for High Energy Physics, 1-1 Oho, Tsukuba-shi, Ibaraki-ken 305, Japan

⁵Australian National Beamline Facility, ANSTO Building 22, Private Mail Bag 1, Menai, N.S.W. 2234, Australia

The X-ray diffraction results reported here are from the first high-resolution triple-crystal experiments to be performed at the Australian National Beamline Facility (ANBF) at the Photon Factory. Heart of the facility is a multi-purpose two-axis high-resolution vacuum diffractometer (BIGDIFF)¹ capable of use for high-resolution powder diffraction (using both conventional scintillation detectors and imaging plates), protein crystallography, reflectometry as well as single-crystal diffractometry.

The present experiments were conducted on BIGDIFF in triple-crystal diffraction mode with a monolithic channel-cut Si monochromator (supplied by Prof. M. Hart), a single-crystal Si sample, and a four-reflection monolithic channel-cut Si analyzer crystal. The Si (111) sample is a part of a wafer which had been implanted with 100 keV B⁺ ions (doses 1×10^{15} and 5×10^{15} cm⁻²) through a one-dimensional 0.5 μ m thick oxide strip pattern with a 5.83 μ m period and 4 μ m open region. The triple-crystal data were collected in the form of two-dimensional intensity maps in the vicinity of the 111 Bragg peak, varying the sample rotation (ω) and the analyzer/scintillation detector rotation (2θ). The first results were collected in air both with the as described sample and after the oxide layer had been removed. Certain slice scans (one-dimensional sections of the two-dimensional intensity maps) were also collected with a vacuum of 1 Torr and reveal considerable improvement in signal to background.

The data will be compared with a recent similar study² performed on BL-14B at the Photon Factory. The new data collected in air indicate that lattice distortion may be mapped with a resolution of approximately 160 \AA , to a depth of approximately 1.0 μ m, providing valuable quantitative information on ion diffusion in such implanted materials. The slice scans collected in vacuum indicate that a depth resolution of 50 \AA is certainly achievable using BIGDIFF. The data show the excellent potential of BIGDIFF for extremely good signal-to-noise and very high resolution in such experiments, and the advantages of working entirely in vacuum.

¹Barnea, Z. et al. (1992). *Rev. Sci. Instrum.* 63, 1069.

²Nikulin, A.Yu. et al. (1994). *J. Appl. Cryst.* 27, in press.

A NEWLY DEVELOPED HYDRAULIC MODULAR SQUEEZER FOR HIGH PRESSURE EXPERIMENTS USING SYNCHROTRON RADIATION

G. Will and Ch. Höffner

Mineralogical Institute, University Bonn, Poppelsdorfer
Schloß, 53115 Bonn, Germany

In order to reach high pressures in the Mbar-range for synchrotron diffraction experiments diamond anvil squeezers are regularly used. In order to guarantee such pressures without destroying the diamonds special care has to be taken to guarantee exact parallel movements of the diamonds, since large forces, especially shear forces act on the diamonds. We have developed and built a modular system, which can be incorporated in diamond anvil squeezers as well as in other devices. As an example we have built a high pressure cell driven by hydraulic forces.

The modular system consists of a long cylinder, made of maraging steel which guarantees parallel movement. The diamonds are mounted inside this cylinder. The exact parallel positions is first adjusted by using AgJ powder, which changes color at two phase transitions, 2.9 and 4.7 kbar. Parallel colored rings are seen if the diamonds are parallel.

For the extreme pressure ranges in the Mbar-range we use the direct interference in air, known as Newton rings. Thereby the diamonds are in direct contact. A small misalignment acts like a wedge yielding the well known colors.

The system was used to determine the compressibility of iron and gold in the pressure range up to 1.1 Mbar. About 240 runs have been made and evaluated. The compressibility data have been fitted by the Murnaghan equation and K_0 and K_0' has been determined.

Signal to Noise Improvements with a New Far-IR Rapid-Scan Michelson Interferometer.

C.J. Hirschmugl and G.P. Williams, National Synchrotron Light Source, Brookhaven National Laboratory, Upton, NY 11973 USA.

In this paper we discuss signal to noise issues in the infrared spectral region, presenting an update on instrumentation developments that have focused on this topic. We have been able to achieve reproducibilities in the 0.01% range for spectra measured in around 1 minute on samples with an area of 1 mm² illuminated with an #10 beam. The main thrust of these studies has been based on removing noise caused by beam motion. This has been done both by reducing the motion itself and by immunizing the measuring system from any residual motions. The former is achieved with a sophisticated feedback system and the latter by employing a Michelson interferometer running in the rapid-scan mode. The principle of this is that if the interferogram (which represents the spectrum of interest) is measured rapidly compared to any beam motion, then the latter can only introduce a relatively slow modulation to the interferogram and will be eliminated when the Fourier Transform is performed. This system has been widely developed to deal with low frequency noise found in a conventional laboratory, and is ideally suited for reducing noise due to electron beam motion in a storage ring. The latter is mostly confined to lower frequencies (<300Hz) due to the fact that it is impossible to drive a magnetic field through the metal vacuum chamber wall at higher frequencies. Higher frequencies are sometimes present, however, and come from audio frequency side-bands of the main ring radio frequency drive. They give rise to specific signatures in the Fourier Transform and can be identified by the predictable shifts with changing mirror velocity.

For these new studies, a Nicolet™ Impact 400 rapid scan Michelson Interferometer was modified by Pike Technologies and installed in vacuum at the U4IR infrared beamline at the NSLS. The instrument is capable of scanning at an optical retardation rate of 3.2 cm/sec, and of a data collection frequency of 50 kHz triggered by the co-linear reference beam of a HeNe laser. A proprietary Nicolet™ solid-state beamsplitter was used to cover the range from 10-2500 cm⁻¹. Spectra were taken at grazing incidence off a single crystal Cu surface in ultra-high vacuum using liquid helium cooled detectors of the photoconductive type (Cu/Ge) or bolometric type (B/Si). The sample throughput for this system was 0.01 mm² steradians. Combining this with the ring feedback system we obtained the reproducibilities mentioned at the beginning of the abstract.

MoD85

Structure and Growth of Hexane Films Adsorbed on the Ag(111) Surface

Z. Wu,^(a) P. Dai,^(a) S. N. Ehrlich,^(b) and H. Taub^(a)

(a) U. of Missouri Columbia, (b) Purdue U

Knowledge of the structure of organic films adsorbed on metal surfaces is fundamental to the technology of catalysis, lubrication, and adhesion. As a starting point for investigating such technologically important systems by synchrotron x-ray diffraction, it is of interest to consider a relatively short-chain hydrocarbon film such as the *n*-alkane hexane [C₆H₁₄ (CH₂)₄CH₃] adsorbed on the close-packed Ag(111) surface [1]. Such experiments naturally follow our earlier investigations of the multilayer structure and growth of the simpler adsorbate, xenon, on the same Ag(111) surface [2,3].

Thus far, we have demonstrated x-ray monolayer sensitivity by observing two Bragg peaks of a single hexane layer on the Ag(111) surface. Indexing of the peaks is consistent with a rectangular unit cell containing two molecules with the same area per molecule of 83.7 Å² as for the herringbone structure of monolayer hexane on graphite [4]. Hexane coverage of one and two layers can be determined independently of the x-ray measurement by use of a low-energy electron diffraction (LEED) apparatus within the specially designed ultra-high vacuum chamber [2]. While dosing the substrate with hexane at a constant rate, a step-like attenuation occurs in the Ag(10) LEED spot intensity at monolayer and bilayer condensation.

At higher coverages, we observe Bragg peaks corresponding to epitaxially grown bulk hexane which has the (101) plane of the bulk triclinic structure parallel to the Ag(111) surface. We have monitored the hexane film growth at an ambient hexane pressure of 1.0 × 10⁻⁸ Torr by observing the intensity evolution at the anti-Bragg point on the specular rod associated with the bulk hexane (101) plane (Q_z = 0.858 Å⁻¹) [1]. As the substrate is cooled below 170 K, the intensity decreases due to destructive interference between the fluid hexane monolayer and Ag substrate. A further small intensity decrement results from the density change upon monolayer freezing at T = 155 K. As the substrate is cooled to 130 K, a second solid hexane layer begins to grow resulting in an increase in the reflected intensity. The bare Ag reflectivity is nearly recovered upon completion of the second layer at T = 120 K. Above two hexane layers, the intensity at the anti-Bragg point again drops and approaches a constant value at a temperature of ~100 K.

Specular reflectivity scans can be conducted with our chamber when the diffractometer is operated in a five-circle mode [5]. At a temperature of ~100 K and a hexane coverage of ~3 layers estimated from the deposition time, a sharp peak first appears at Q_z = 1.72 Å⁻¹ corresponding to the (101) reflection of bulk hexane. Our tentative interpretation is that a bilayer film coexists with the preferentially oriented bulk hexane. The structure of the second film layer is yet to be determined.

1. Z. Wu, P. Dai, S. N. Ehrlich, and H. Taub, NSLS Annual Report 1993; *Bull. Am. Phys. Soc.* 39, 455 (1994); and to be published.
2. J. R. Dennison, S.-K. Wang, P. Dai, T. Angot, H. Taub, S. N. Ehrlich, *Rev. Sci. Instrum.* 63, 3835 (1992).
3. P. Dai, T. Angot, S. N. Ehrlich, S.-K. Wang, and H. Taub, *Phys. Rev. Lett.* 72, 685 (1994); and P. Dai, Z. Wu, T. Angot, S. N. Ehrlich, S.-K. Wang, and H. Taub, unpublished.
4. H. Taub, in *The Time Domain in Surface and Structural Dynamics*, edited by G. J. Long and P. Grandjean, NATO Advanced Study Institute Series, Vol. C-238, (Kluwer, Dordrecht, 1988), p. 467.
5. S.-K. Wang, P. Dai, and H. Taub, *J. Appl. Crystallogr.* 26, 697 (1993).

Supported by NSF Grant Nos. DMR-9011069 and DMR-9311245 and DOE Grant No. DE-FC02-85ER45183 of the MATRIX PFC at the NSLS.

MoD86

Stacking Faults and Characterization of the Film-Vacuum Interface in Multilayer Xe Films Adsorbed on the Ag(111) Surface

P. Dai,^(a) Z. Wu,^(a) S. N. Ehrlich,^(b) and H. Taub^(a)
(a) U. of Missouri-Columbia; (b) Purdue U.

Although rare gases physisorbed on single-crystal metal surfaces offer some of the simplest films to model theoretically, synchrotron x-ray diffraction studies of the structure and growth of these films have lagged behind those on semiconductor and metal surfaces. Using a specially designed ultra-high vacuum chamber [1], we have overcome some of the difficulties previously encountered and have been able to investigate the structural perfection of multilayer Xe films adsorbed on a Ag(111) surface under different growth conditions [2].

The Xe films are grown by two different methods: 1) "quasiequilibrium" growth during which the Xe film is in near equilibrium with a constant flux of Xe gas as the substrate is slowly cooled [1-3]; and 2) "kinetic" growth in which the the substrate is maintained at a lower temperature while being exposed to a lower Xe flux [2,4]. For nominal monolayer and bilayer films, we can compare the Xe-vacuum interface profile under these different growth conditions. In addition, for kinetically grown films, we are able to investigate the stacking sequence in films grown at different substrate temperatures as well as the dependence of film roughness on the average film thickness.

Specular reflectivity scans can be conducted with our chamber when the diffractometer is operated in a three-circle mode [5]. Analysis of these scans at coverages of nominally 1 and 2 layers shows that Xe films grown under quasiequilibrium conditions have significantly smaller occupancies of 2nd and 3rd layers, respectively, than those grown kinetically. The number of partial layers increases in kinetically grown films as the nominal thickness increases from 1 to 4 layers. When specular reflectivity scans are taken as a function of time on the same kinetically grown film, we find the mean-square surface roughness to increase with average film thickness in the range 10 to 30 layers.

Diffraction scans along the (10) Xe rod were used to determine the stacking sequence in three and four layer films grown kinetically. For films grown at 33 K, we find evidence of a large number of stacking faults corresponding to 'ABA' stacking. However, the 'ABA' fraction decreases substantially in films grown at higher temperatures.

1. J. R. Dennison, S.-K. Wang, P. Dai, T. Angot, H. Taub, S. N. Ehrlich, *Rev. Sci. Instrum.* **63**, 3835 (1992).
2. P. Dai, T. Angot, S. N. Ehrlich, S.-K. Wang, and H. Taub, *Phys. Rev. Lett.* **72**, 685 (1994).
3. J. Unguris, I. W. Bruch, E. R. Moog and M. B. Webb, *Surf. Sci.* **87**, 415 (1979)
4. P. Dai, Z. Wu, H. Taub, and S. N. Ehrlich, *Bull. Am. Phys. Soc.* **39**, 454 (1994); and P. Dai, Z. Wu, T. Angot, S. N. Ehrlich, S.-K. Wang, and H. Taub, unpublished.
5. S.-K. Wang, P. Dai, and H. Taub, *J. Appl. Crystallogr.* **26**, 697 (1993).

Supported by NSF Grant Nos. DMR-9011069 and DMR-9314235 and DOE Grant No. DE-FG02-85ER45183 of the MATRIX PRT at the NSLS.

MoD87

SOFT X-RAY MICROSCOPY PROJECT AT NSRL

X. S. Xie, C. Z. Jia, Y. F. Zhao, L. Shang, J. F. Deng,
G. Q. Wang and J. Y. Zhang

University of Science and Technology of China
Hefei 230026, P. R. China

Soft x-ray microscopy project has been planned at Hefei National Synchrotron Radiation Laboratory since 1984^[1]. The Hefei Synchrotron Radiation Source was operated and available for experiments at the end of 1991. One of the first beamlines U12A is dedicated to soft x-ray imaging studies.

A prototype scanning transmission x-ray microscope has been installed in beamline U12A. In the first generation of our instrument the x-ray probe is formed by a 2 μ m pinhole. We have tested this scanning x-ray microscope and obtained the real time x-ray image using synchrotron radiation^[2]. The effort of constructing a new x-ray scanning microscope is undertaken. In the next generation of the instrument a high resolution micro zoneplate with outermost zonewidth 45nm which was fabricated at IBM^[3] will be used to focus the x-rays. An improved scanning stage and an x-ray image processing system also will be made.

Studies of soft x-ray contact microscopy have been performed using synchrotron. A exposure chamber can be connected with beamline U12A and worked well. Some biological and medical specimens have been chosen for examination^[2]. A new wet specimen chamber is designed and will be tested.

We are greatly indebted to Dr. E. Anderson and Prof. D. Attwood of Center for X-Ray Optics at LBL and Prof. J. Kirz of SUNY at Stony Brook for their help and support to our x-ray microscopy project.

References

1. X. S. Xie et al., *Nucl. Instrum. Meth. A* **246**, 698(1986)
2. C. Z. Jia et al., To be published in the Proc. of the 4th Int. Conf. on X-ray Microscopy. (1994)
3. E. Anderson et al., In *X-ray Microscopy 111*, ed. by A. G. Michette, G. R. Morrison and C. J. Buckley (Springer-Verlag, 1992). P. 75.

MoD88

Alkali Doped C₆₀: the Movement of the Fermi Energy

Pan Haibin, Xu Pengshou, Lu Erdong, Yang Fengyuan, Xia Andong, Zhang Xinli
National Synchrotron Radiation Laboratory, University of Science and Technology of China,
Hefei, 230029, China

Recently, fullerene C₆₀ has caused intense interest in theoretical and experimental aspect due to its physical and chemical properties [1,2,3,4]. Using synchrotron radiation light, we have performed photoemission spectra of alkali doped C₆₀ to reveal the electron structure. Chromatographically purified C₆₀ powder is evaporated from a crucible and condensed onto cleaved GaAs(110) in ultrahigh vacuum. The photon energy used is from 60eV to 150eV with a resolution $E/\Delta E$ of 1000. When Rb is doped, at first the spectra moves to the high binding energy side for about 0.5eV. As doping continues, the spectra move to low binding energy side again. The Fermi energy retrieves to the original position when the stoichiometry reaches about 1. This phenomenon has not been reported in other alkali doped C₆₀ systems. Takashi Takahashi [4] came to the conclusion that the forward movement (to the high binding energy side) because of the occupation of the gap states by electrons donated from Rb atoms. But he did not explain the backward movements. We suggest that the backward movements is due to the formation of the RbC₆₀ phase. At the first stage of doping, the system forms the α -C₆₀ phase (when the stoichiometry is less than 0.1)[5]. The Rb atoms do not reaction with C₆₀ atoms. Instead they only act as a diluted solid solution. Because the radius of the Rb atom is big enough to change the C₆₀ film structure, the Rb will act as the origin of imperfection. As doping continues, Rb and C₆₀ will form RbC₆₀ phase. The film now will recover the imperfection and perform an orderly structure. Most of the electrons of Rb will donate to C₆₀. The lowest unoccupied states of C₆₀ begin to accept electrons donated from Rb. This will be domination to the system compare to the defect states and the Fermi energy will move backwards again.

References:

- [1] S. Saito, A. Oshiyama, Phys. Rev. Letters 66, 2837 (1991)
- [2] P. J. Benning, J. L. Martins, J. H. Weaver, L. P. F. Chibante and R. E. Smalley, Science 252, 1417 (1991)
- [3] P. J. Benning, D. M. Porrier, T. R. Ohno, Y. Chen, M. B. Jost, F. Stepniak, G. H. Kroll, J. H. Weaver, J. Fure and R. E. Smalley, Phys. Rev. B 45, 6899 (1992)
- [4] T. Takahashi, Comments Cond. Mat. Phys. 16, 133 (1992)
- [5] D.M.Poirier and J.H.Weaver Phys. Rev. B 47,10959 (1993)

MoD89

Construction of a Multiwavelength Bonse-Hart Ultrasmall-Angle X-Ray Scattering Instrument

Benjamin Chu, Fengji Yeh, Yingjie Li, Paul J. Harney and Jean Rousseau
Department of Chemistry, State University of New York at Stony Brook,
Long Island, New York 11794-3400

Alex Darovsky
SUNY X3 Beamline, National Synchrotron Light Source,
Brookhaven National Laboratory, Upton, New York 11973

D. P. Siddons
National Synchrotron Light Source,
Brookhaven National Laboratory, Upton, New York 11973

ABSTRACT

A Bonse-Hart ultrasmall-angle x-ray scattering (USAXS) instrument, employing a synchrotron x-ray source for variable wavelength, has been designed, constructed and tested. Solid as well as suspensions of polystyrene and poly(chloro-styrene) latex spheres were used as reference standards in order to demonstrate the range of this instrument. The USAXS results measured at both $\lambda = 0.06573$ nm and $\lambda = 0.154$ nm were compared with those from another calibrated Bonse-Hart instrument operating at $\lambda = 0.154$ nm, by means of a rotating anode x-ray generator using the standard Cu K α radiation as well as the synchrotron x-ray source at NSLS. The crystals were supported by super Invar mechanical elements making the high temperature experiments feasible. Moreover, an x-rays wavelength of 0.06573 nm permits us to combine USAXS with laser light scattering by using the same cylindrical glass sample cell as, for many polymer systems, the optimal sample thickness at $\lambda = 0.066$ nm is increased to ~ 10 mm and thin-walled (0.3 mm thick) glass windows become acceptable. The main hurdle for performing simultaneous static and dynamic light scattering as well as USAXS experiments on polymer solutions and gels with the same sample has been resolved. This capability should open up new frontiers in structural and dynamical studies of systems involving a large range of length scales from Angstroms to microns.

MoD90

Performance of an Infrared Microspectrometer at the NSLS

G.L. Carr, Advanced Development Center, M.S. AO1-26, Grumman Corporation, Bethpage, NY 11714 USA, J. Reffner, Spectra-Tech, Inc. 652 Glenbrook Rd. Bldg. 8, PO Box 2190-G, Stamford, CT 06906, USA, and G.P. Williams, National Synchrotron Light Source, Brookhaven National Laboratory, Upton, NY 11973 USA

An infrared microspectrometer was installed and tested on the two NSLS VUV ring beamlines presently supporting infrared research programs. Attention was paid to evaluating the performance of the instrument in terms of beam spot size (spatial resolution) and signal to noise. The results compare closely with those expected theoretically.

The microspectrometer was a Spectra-Tech IR μ s™, modified to allow the collimated infrared synchrotron beam to enter at the back. The beam is delivered to - and collected from - the sample using a confocal arrangement with redundant aperturing and reflective Schwarzschild optics. The instrument has an integral Michelson interferometer to allow full spectral analysis at the sample focus, and can operate in either transmission or reflection mode. The standard KBr beamsplitter and HgCdTe detector yield a useful spectral range of 650 cm^{-1} to 5000 cm^{-1} with a resolution up to 1 cm^{-1} . Mapping is achieved by scanning the sample, the minimum step interval being 1 micron in either x or y.

The NSLS VUV source is roughly 1000 times brighter than a conventional 1000K black body source in the infrared spectral region. Assuming a source size of 1000 microns (larger than the intrinsic size due to the collection angle and diffraction effects) emitting into $\pi/100$, one expects the beam to be demagnified to a 10 micron size spot at the focus of the IR μ s™ #1 sample optics. Furthermore we would expect the flux through a 10 micron aperture to be approximately the same as that through a 100 micron aperture with a conventional source. These expectations were indeed realized.

The two infrared beamlines on which the microscope was tested were a conventional VUV port delivering 15 milliradians horizontally by 10 milliradians vertically, and a custom infrared port that delivering 90X90 milliradians. The demagnification of the source was similar for both beamlines, and thus produced comparable brightness at the sample location. However, the custom infrared port extracted a larger flux, and illuminated an area 20 times larger. Spectra taken with redundant aperturing for a 10 micron spot in 15 seconds at 8 cm^{-1} resolution had noise of <1%. Spatial resolution was consistent with the diffraction limit.

Development of Circularly Polarizing Microscope with a Polarizing Undulator

Toru Yamada, Masatada Yuri, Hideo Onuki, and Shozo Ishizaka*
Electrotechnical Laboratory, Tsukuba-shi, Ibaraki 305, Japan, *Toyama University of International Studies, Ohyama-machi, Toyama 930-12, Japan

A circularly polarizing microscope has been constructed in the beam line of the polarizing undulator which had been installed in the electron storage ring NIJI-II in the Electrotechnical Laboratory. By the circularly polarizing microscopy, we intend to image with CD or CIDS (Circular Intensity Differential Scattering) in order to observe structures and distribution of biomolecules such as DNA and Proteins.

Figure 1 shows the schematic diagram of the instrument. This microscope is a type of scanning micro-beam microscope. The illumination light source is a polarizing undulator with crossed and retarded magnetic field having fifteen periods, which was proposed by Onuki¹⁾ and developed by Onuki et al²⁾. In order to conserve the degree of polarization in focusing circularly polarized radiation from the undulator, it is necessary to use a symmetric optical system with respect to light axis. Also, less of chromatic aberration is needed because of a quasi-monochromatic incident light in which the FWHM of power spectrum is about ten percents. So we have constructed a Schwarzschild type mirror system combined with a convex mirror positioned in front of the undulator. The size of the focused beam was from 0.7 microns in the wavelength at 200nm up to 0.9 microns at 400nm. A sample stage can be scanned by piezoelectric translators in 3D axes and a photomultiplier is positioned on the back of the sample stage. Transmitted and scattered light intensities are measured by the photomultiplier with two different masks, respectively.

Using the circularly polarizing microscope, we have obtained some images of transmitted or scattered light from some kinds of biomolecules such as DNA and Proteins. We are trying imaging with CD and CIDS by the alternation of the right and left handed circularly polarized radiations from the undulator.

- 1)H.Onuki: Nucl. Instr. and Method, A246, 94 (1986)
- 2)H.Onuki, N.Saito, and T.Saito: Appl. Phys. Lett., 52, 178 (1988)

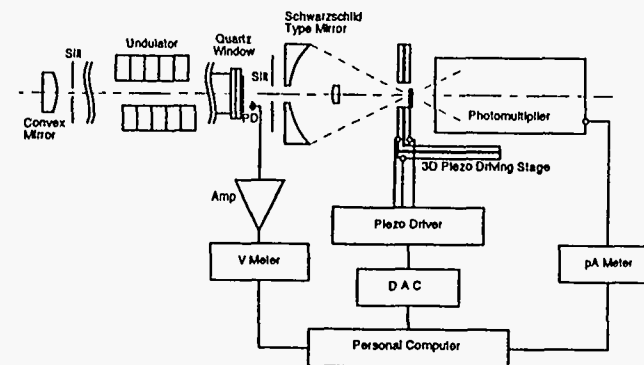


Fig.1: Schematic diagram of the circularly polarizing microscope

Precision Micro-Machining with Hard X-rays

Erik D. Johnson and D. Peter Siddons
Brookhaven National Laboratory, National Synchrotron Light Source
Upton, Long Island New York 11973-5000

Henry Guckel
University of Wisconsin Madison, Department of Electrical and Computer Engineering
Madison, Wisconsin 53706

ABSTRACT

We have performed a series of experiments which demonstrate the potential of hard x-rays as a lithographic tool for the fabrication of precision structures possessing fully three dimensional geometries. Samples produced thus far cover a wide range of configurations. We have fabricated various solids of rotation, including some possessing re-entrant geometries, a fixture with multiple 300μ square channels traversing 1 cm of plastic and joining in the center of the piece, and a variety of very high aspect ratio parts of up to 10 cm in thickness. Aspects of the techniques employed to produce these samples, their advantages, and potential pitfalls will be discussed.

*Work performed under the auspices of the U.S. Department of Energy, under contract DE-AC02-76CH00016.

Fabrication of X-Ray Collimators for Solar Physics Using LIGA at SSRL*

Michael Hecht, Reid Brennen, Steven Manion
Center for Space Microelectronics
Jet Propulsion Laboratory, Pasadena, CA

Piero Pianetta
Stanford Synchrotron Radiation Laboratory, Stanford, CA

Tim Stowe, Tom Kenny
Stanford University, Stanford, CA

William Bonivert, John Hachman
Sandia National Laboratory, Livermore, CA

A LIGA exposure facility has been established at the Stanford Synchrotron Radiation Laboratory (SSRL) to complement exposure and developing facilities at the Advanced Light Source, mask fabrication capabilities at the Jet Propulsion Lab, and electroplating resources at Sandia Livermore Labs. The bending magnet beam lines at SSRL have a characteristic energy of 4.7 keV, making it an ideal source for exposure of LIGA structures in the 1-10 mm thickness range. A particular advantage of the bending magnet spectrum is that x-ray masks can be fabricated on self-supporting silicon wafers using conventional thick resist optical lithography. The immediate objective of this work is the fabrication of x-ray optical elements for a proposed NASA mission, the High Energy Solar Imager (HESI). LIGA will be used to make high aspect ratio collimators for the HESI telescope, which will perform spectroscopic Fourier x-ray imaging of the sun from 5 keV to > 1 MeV.

* Work supported by NASA and work was partially done at SSRL which is operated by the Department of Energy, Office of Basic Energy Sciences.

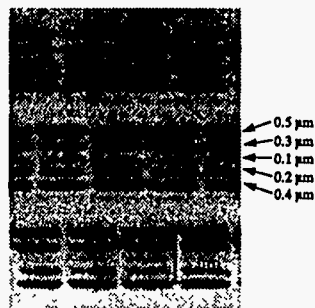
Real-time, sub-micron, soft x-ray fluorescence imaging

Bruno La Fontaine, Alastair A. MacDowell, Zhengquan Tan
AT&T Bell Laboratories, 510E Brookhaven National Laboratory, Upton NY 11973
Don L. White, Gary N. Taylor
AT&T Bell Laboratories, 600 Mountain Ave., Murray Hill NJ 07974
Obert R. Wood II, John E. Bjorkholm, Don M. Tennant
AT&T Bell Laboratories, 101 Crawfords Corner Road, Holmdel NJ 07733
and Steven L. Hulbert
National Synchrotron Light Source, 725D Brookhaven National Laboratory, Upton NY 11973

A new technique using single crystal phosphors has been used to observe, in real time, soft x-ray images with features as small as 100 nm. This fluorescence imaging scheme takes advantage of the high fluorescence yield, high index of refraction, short absorption depth of extreme ultraviolet (EUV) light ($\lambda \sim 134\text{\AA}$) and excellent optical properties of single crystals activated with rare earth ions. We will present the characteristics of these crystals and the results of resolution studies performed with a EUV Schwarzschild camera.

The experiments were carried out at the National Synchrotron Light Source, Brookhaven National Laboratory, using the U13 undulator insertion device on the VUV ring as a source. The third harmonic, at 139\AA , was used to illuminate a patterned mask which was imaged using a multi-layer coated Schwarzschild camera, with a reduction factor of 20. The maximum resolution afforded by this camera, over a $(25\ \mu\text{m})^2$ field, is 100 nm limited by a numerical aperture of 0.088. A STI-F10G crystal was placed at the image plane of this camera, converting the incident EUV light into green light. The resulting visible light image was then observed with a high power microscope (with a numerical aperture of 1.25) and viewed with an intensified CCD camera or directly through an eyepiece.

The accompanying figure exemplifies the results obtained. This is a fluorescent image of patterned EUV radiation at the image plane of the Schwarzschild, which was composed of several groups of 5 lines that varied in width from 500 nm to 100 nm.



This new technique could prove extremely useful for deep or extreme ultraviolet lithography, where real time, in-situ optimization of the lithography exposure tools is required. One can also envisage using a similar arrangement for x-ray microscopy. Finally, we believe that it could be useful for a variety of experiments using ultraviolet light or x-rays.
[SRI-94,SUNY-StonyBrook,NY]

Simultaneous Resolution of Spectral and Temporal Properties of UV and Visible Fluorescence Using Single-Photon Counting with a Position-Sensitive Photomultiplier

Lisa A. Kelly, John G. Trunk, Krzysztof Polewski and **John C. Sutherland**,
Biology Department, Brookhaven National Laboratory, Upton, New York 11973

A new fluorescence spectrometer has been assembled at the U9B beamline of the National Synchrotron Light Source to allow multi-wavelength, time-resolved fluorescence detection, as well as spatial imaging of the sample fluorescence. The spectrometer employs monochromatized, tunable UV and visible excitation light from a synchrotron bending magnet and an imaging spectrograph equipped with a single-photon sensitive emission detector. The detector is comprised of two microchannel plates in series, with a resistive anode for encoding the position of the photon-derived current. The centroid position of the photon-induced electron cascade is analyzed in a position computer from the four signals measured at the corners of the resistive anode. Spectral information is obtained by dispersing the fluorescence spectrum across one dimension of the detector photocathode. Timing information is obtained by monitoring the voltage divider circuit at the second MCP detector. The signal from the MCP is used as a "start" signal to perform a time-correlated single photon counting experiment. The analog signal representing the position, and hence wavelength, is digitized concomitantly with the start/stop time difference and stored in the two-dimensional histogramming memory of a multi-parameter analyzer. This system is advantageous in recording fluorescence in systems composed of multiple emitting species, as emission spectra spanning different wavelength ranges and possessing different excited state lifetimes can be simultaneously characterized.

D.A.F.S. MEASUREMENTS BY USING AN "ENERGY/ANGULAR DISPERSIVE DIFFRACTION" EXPERIMENTAL SET-UP.

J.L. Hodeau⁽¹⁾⁽³⁾, J. Vacinová⁽¹⁾, Y. Garreau⁽²⁾, A. Fontaine⁽²⁾, M. Hagelstein⁽³⁾,
E. Elkaim⁽²⁾, J.P. Lauriat⁽²⁾, A. Prat⁽¹⁾, P. Wolfers⁽¹⁾

⁽¹⁾ Laboratoire de Cristallographie CNRS, BP 166, F-38042 Grenoble Cedex, France

⁽²⁾ LURE CNRS, Bat. 209D, F-91405 Orsay Cedex, France

⁽³⁾ ESRF, BP 220, F-38043 Grenoble Cedex, France

Herein we present a combined "Energy/Angular Dispersive" experimental set-up which has been used for D.A.F.S. (Diffraction Anomalous Fine Structure) experiments on a Hexaferrite single crystal. Intensity variations of eight Bragg reflections over a spectral range of 250eV have been measured using energy dispersive focusing optics and a two dimensional detector. We have also performed the same measurements by using classical double crystal optics and we compare both results.

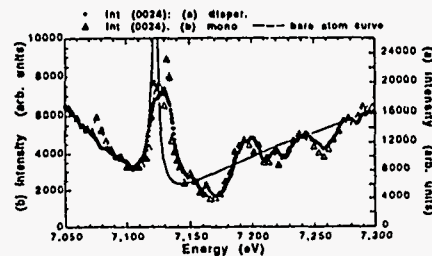
D.A.F.S. oscillations were first observed a long time ago [1] and recently it was shown that these oscillations can be used for experimental determination of site selective EXAFS or XANES spectra [2-3]. For such experiments, diffraction intensities at about one hundred discrete photon energies with a step width of a few eV have to be collected. In order to decrease the beam time, both the whole spectral range and the diffraction profile can be measured simultaneously [4,5].

We have performed experiments at the energy dispersive EXAFS station (XAS10) at DCI-LURE. The sample crystal was mounted on a remotely controlled goniometer and placed in the polychromatic focus point. D.A.F.S. spectra were directly recorded on an image plate detector, oscillating the sample crystal. Afterwards, the X.A.F.S. spectrum was recorded in transmission geometry using a powdered sample

D.A.F.S. experiments were performed in the vicinity of the Fe K_{α} absorption edge on a single crystal of Y-type hexaferrite $BaZnFe_6O_{11}$ to distinguish Fe cations contributions on tetrahedral sites and on octahedral ones. This compound contains four octahedral sites occupied by Fe cations and two tetrahedral sites occupied by Fe and Zn cations. We have measured several (00 l) reflections where we have clearly observed the absorption edge and D.A.F.S. oscillations. Theoretical intensity variations fit experimental data. On weak reflections, D.A.F.S. oscillations are much more pronounced since these reflections are more sensitive to f' and f'' variations.

In order to evaluate the data quality, a similar experiment has been performed on the diffraction station WDIF4C at DCI-LURE by using a double crystal monochromator. Diffraction intensities and the X-ray fluorescence spectrum have been collected simultaneously. Both data sets, recorded with the different techniques, compare well and this shows high possibilities of the "energy/angular dispersive" set-up for multi-wavelength diffraction research.

Comparison of (0024)
Bragg reflection DAFS
spectra recorded by using
a) energy dispersive
focusing optics,
b) double crystal
monochromatic optics



[1] Y. Cauchois, C. Bonnelle, C. R. Acad. Sci., 242, 1596 (1956)

[2] I. Arcon *et al.*, J. de Phys. supp. 48, 391 (1987)

[3] H. Stragier *et al.*, Phys. Rev. Lett., 21 (69) 3064 (1992)

[4] J.L. Hodeau *et al.*, E S R.F. User Meeting, Sept. 1993, Beam Line 8 Satellite Meeting

[5] K.D. Finkelstein, M. Sutton, preprint

Facility Posters

- Fac. Jiang, X., Tang, E., Xian, D. Beijing Synchrotron Radiation Facility.
- Fac. Ishii, T. The Present Status of SRL-ISSP.
- Fac. Masui, S., Amano, D., Kato, T., Zhang, Y., Yamada, H. Applications of the Superconducting Compact Ring "AURORA".
- Fac. Korchuganov, V. Status and Prospects of SR Source Siberia-2.
- Fac. Zhang, X. Some Progresses in NSRL.
- Fac. Kim, Y.S., Han, K.S., Namkung, W., Lee, T.N., Kim, H. Present Status of the Pohang Light Source.

Beijing Synchrotron Radiation Facility

Xiaoming Jiang, Esheng Tang and Dingchang Xian

Synchrotron Radiation Laboratory, Institute of High Energy
Physics, P.O.Box 918, Beijing, 100039, P.R. China

Abstract

The storage ring for the Beijing Synchrotron Radiation Facility (BSRF) is the 1.6-2.8 GeV Beijing Electron-Positron Collider (BEPC), which was constructed for China's first project on high energy physics research. The storage ring was designed to be operated either in the colliding mode or the dedicated synchrotron radiation mode. The project was approved by the Chinese government at the end of 1983. The ground breaking took place in October of 1984 and the project was completed in 1989.

The Beijing Synchrotron Radiation Laboratory (BSRL) was founded in July of 1985, and the construction of the first beam line was completed in 1989. The first phase construction of BSRF was finished in 1991, three beam ports, seven beam lines and nine experimental stations were constructed. Since 1991, BSRF has been opened to users from all over the country.

The description of the beam lines and experimental stations and the present research activities is given in this paper. The second phase construction of BSRF as well as the plan of constructing a third generation synchrotron radiation source, the Beijing Light Source (BLS), in adjacent to BSRF, are described.

THE PRESENT STATUS OF SRL-ISSP

T. Ishii

Institute for Solid State Physics, University of Tokyo
7-22-1 Roppongi, Minato-ku, Tokyo 106, Japan

The Synchrotron Radiation Laboratory of the Institute for Solid State Physics, University of Tokyo (SRL-ISSP) owns SOR-RING, a 0.38 GeV electron storage ring with five beam lines for spectroscopy. The SRL-ISSP has its Branch Laboratory in the Photon Factory at Tsukuba. The status of the SRL-ISSP before 1992 was reported at the SRI '91 conference.¹⁾

Since 1992, effort to improve the performance of SOR-RING has been made. Four beam position monitors and beam steering magnets have been installed. The beam position is measurable quite accurately now. By the use of the beam steering magnets, the variation of the betatron function and the distortion of chromaticity have been measured. Using the beam position monitor system the closed orbit distortion was measured. The CODs were corrected and subsequently the optical elements in the beam lines were readjusted. The beam lifetime has been almost doubled by changing operating points and using a ion clearing electrodes.

Five experimental stations associated with SOR-RING are working well. Two of them are for photoemission experiments and mainly used for materials science. One station is for absorption and reflection measurements in the photon energy region below 30 eV. Remaining two are for radiation biology experiments and a free port. About 200 users are carrying out experiments within a total beam time of about 2000 hours per year.

In Tsukuba Branch Laboratory, two experimental stations out of three are open to outside users. In one station, angle-resolved photoemission measurements on metal and semiconductor surfaces are underway. In this beam line, light from an ordinary bending magnet section is used. The experimental system is comprised of a VG-ADES 500 spectrometer connected to a constant deviation monochromator. An overall resolution of 35 meV is the champion data achieved so far. In one station, spin- and angle-resolved photoemission experiments are being carried out. Light from a revolver undulator is used. A Mott detector is used for spin analysis. The third beam line, which is not yet open to outside users, is also for spin-resolved photoemission experiments. In this beam line, a SPLEED spin detector is used. Light from the revolver undulator is used by time-sharing basis. This beam line is also intended to be shared with soft X-ray fluorescence measurements. The measurement system has already been built and tested in other beam lines, BL-2 and -3, in the PF-ring and showed excellent performance.

Reference: T. Ishii: Rev.Sci.Instr. 63 1589 (1992)

Applications of the superconducting compact ring 'AURORA'

Shin Masui, Daizo Amano, Takanori Katoh, Yanping Zhang, and Hironari Yamada^{a)}

Quantum Technology Research Section, Sumitomo Heavy Industries, Ltd. 2-1-1 Yato-Cho, Tanashi-City, Tokyo 188, Japan

Since the first SR light was observed in 1989, AURORA has been raising its performance. At present it is easy to accumulate the current of 500 mA and the lifetime reaches 16 hours at 300 mA. By the help of thick iron yoke which functions as a radiation shielding, SR exposures can be carried out at the distance just less than 2 m away from the source point. Consequently high photon density can be obtained. Our facility can offer many possibilities for scientific researches as well as for industrial applications. Several application programs have been under way. Those are as follows:

- 1) X-ray lithography
- 2) X-ray microscopy
- 3) Reflectance measurement in the range of soft X-ray
- 4) Solid phase epitaxy of amorphous Si
- 5) Total reflection X-ray fluorescence analysis
- 6) LIGA
- 7) White topography

In X-ray lithography, for example, we have already obtained 0.2 μm line-and-space patterns. In X-ray microscopy, we attained the spacial resolution of 0.19 μm at a wavelength of 136 \AA using Schwarzschild objective. Initially AURORA was designed as a soft X-ray source optimized for X-ray lithography, but we are extending the applications to the hard X-ray range. For LIGA, we attained the lithography as deep as 700 μm in reasonable irradiation time using more than 2 keV photons. In white topography, we confirmed the structural deficits of Si with 10.5 keV diffraction. We have installed a double crystal monochromator to promote the applications of hard X-ray. we intend to try EXAFS and X-ray diffraction in the near future. We will present the latest results.

a) present occupation : Ritsumeikan University

STATUS AND PROSPECTS OF SR SOURCE SIBERIA-2

V. Korchuganov

Budker Institute of Nuclear Physics

630090 Novosibirsk, Russia

ABSTRACT

The dedicated SR source, a 2.5 GeV electron storage ring SIBERIA-2 was designed and manufactured at the Budker Institute of Nuclear Physics (Novosibirsk) for the Kurchatov Institute (Moscow). Besides SIBERIA - 2, a facility includes a small ring SIBERIA-1 (450 MeV), that can be used both as a SR source in the VUV and soft X-ray ranges and as a booster for the main ring, a 80 MeV linac and two transport lines. Now the injection part is in operation, the electron beam was transferred from the booster to the main ring. All systems of the SIBERIA-2 were mounted on the site and high precision geodetical alignment is in underway. In this paper the status and commissioning plans are described.

Some Progresses in NSRL

Zhang Xinyi

*National Synchrotron Radiation Laboratory
University of Science and Technology of China
Hefei, 230029, China*

Abstract

The National Synchrotron Radiation Laboratory(NSRL, former HESYRL) began to be open for the users in the month of April, 1993, and since then, the synchrotron radiation facility of the NSRL, as a dedicated light source, works well. The lifetime has reached 13 hours at a beam current of 150 mA. A brief description about the status of NSRL will be reported in this paper.

Some experimental results are chosen, as examples, to be introduced in various fields including the photoemission, soft X-ray microscopy, VUV spectroscopy, photoionization processes in molecules and X-ray lithography.

A new project called "NSRL-phase II" is under the way of consideration. The main task of this project is (a) to construct about 26 beamlines and 30 experimental stations, and (b) to construct 3 insertion devices: one combine undulator, one superconducting wiggler and one free electron laser. A brief introduction of this project is also given in this report.

Present Status of the Pohang Light Source

Y. S. Kim, K. S. Han, W. Namkung, T. N. Lee, and H. Kim
Pohang Accelerator Laboratory
Pohang University of Science and Technology

The Pohang Light Source (PLS) project is now in its final year of construction phase. The machine consists of a full energy(2 GeV) linac injector, a storage ring with a 12-period TBA structure, and 32 eventual beamlines from insertion devices and bending magnets. The commissioning of the injector linac is under progress and it has reached to electron energy of 1.5 GeV. The machine integration of the storage ring is nearly completed and the commissioning of the PLS is expected to take place by the fall of this year. The facility will provide high brightness, tunable radiation in a wide spectral range up to 30 keV of photon energy and will serve national and international users starting from mid 1995.

Cooperative Phenomena Posters

(Session MoE)

- MoE1 Bajt, S., Hanson, A.L. An Investigation of the Iron Pre-Edge XANES Structure.
- MoE2 Bajt, S., Sutton, S.R., Delaney, J.S. Quantification of Mixed Fe Valence States Using the Energy of the Pre-edge Peak in K XANES.
- MoE3 Snell, G., Kuntze, R., Muller, N., Heinzmann, U., Hergenahn, U., Viefhaus, J., Wehlitz, R., Becker, U. Spin-Resolved Time-of-Flight Electron Spectroscopy Following Excitation with Circularly Polarized Synchrotron Radiation.
- MoE4 Bedzyk, M. The Effect of Coherence on the Visibility of X-Ray Interference Fringes.
- MoE5 Belyakov, V.A. Coherent Inelastic Mossbauer Scattering of Synchrotron Radiation.
- MoE6 Belyakov, V.A., Zhadenov, I.V. Mossbauer Filtration of Synchrotron Radiation at Isotope Interface.
- MoE7 Brauer, S., Stephenson, G.B., Sutton, M., Mochrie, S.G.J., Dierker, S., Flemming, R., Pindak, R., Robinson, I.K., Grubel, G., Als-Nielsen, J., Abernathy, D. Asymmetrically-Cut Crystals as Optical Elements for Coherent X-Ray Beams.
- MoE8 Carr, G.L. Nanosecond Time-Resolved Spectroscopy Using a Pulsed Laser Diode and Infrared Synchrotron Radiation.
- MoE9 Daimon, H., Nakatani, T., Imada, S., Suga, S., Kagoshima, Y., Miyahara, T. Circularly-Polarized-Light Induced Dichroism in Photoelectron Diffraction Observed With Display-Type Spherical Mirror Analyzer.
- MoE10 DiFonzo, S., Muller, B.R., Jark, W., Gaupp, A., Schafers, F., Underwood, J.H. Multilayer Transmission Phase-Shifters for the Carbon K-Edge and the Water Window.
- MoE11 Ehrlich, S.N., Angot, T., Dai, P., Wang, S.K., Dennison, J.R., Taub, H. Ultra-High Vacuum Chamber for Synchrotron X-Ray Diffraction From Films Adsorbed on Single-Crystal Surfaces.
- MoE12 Wong, J., Froba, M., Frahm, R. A Critical Assessment of the QEXAFS Method.
- MoE13 deBergevin, F., Vettier, C., Malgrange, C., Giles, C., Grossi, F., Grubel, G. X-Ray Polarimetry with Phase Plates.
- MoE14 Gog, Th., Hille, A., Bahr, D., Materlik, G. Extremely Dispersive X-Ray Standing Wave Measurements.
- MoE15 Hamalainen, K., Krisch, M., Sette, F., Kao, C.C., Caliebe, W., Hastings, J.B. A High Resolution X-Ray Spectrometer Based on a Cylindrically Bent Crystal in Non-Dispersive Geometry.
- MoE16 Hiraya, A., Watanabe, M., Sham, T.K. Electron and X-Ray Fluorescence Yield Measurements of the Cu L_{2,3} Edge X-Ray Absorption Fine Structures (XAFS): A Comparative Study.
- MoE17 Chang, S.L., Hung, H.H., Sheu, H.S., Liu, J.Y. A Multi-Purpose X-Ray Diffractometer for Synchrotron Radiation at SRRC.
- MoE18 Itchkawitz, B.S., Kempgens, B., Koppe, H.M., Feldhaus, J., Bradshaw, A.M. Absolute Photoabsorption Cross-Section Measurements of Simple Molecules in the Core Level Region.
- MoE19 Kagoshima, Y., Wang, J., Miyahara, T., Aoki, S., Ando, M. A Scanning X-Ray Microscope Using Circularly Polarized Radiation at the TRISTAN Accumulation Ring and Its Application to Observation of Magnetic Structure.
- MoE20 Kamada, M., Sakai, K., Tanaka, S-I., Ohara, S., Kimura, S-I., Hiraya, A., Hasumoto, M., Nakagawa, K., Ichikawa, K., Soda, K., Fukui, K., Fujii, Y., Ishiguro, E. Monochromator for Circularly Polarized Synchrotron Radiation in the Energy Range of 5-250 eV.

- MoE21 Lang, J.C., Srajer, G. Bragg Transmission Phase Plate for the Production of Circularly Polarized X-Rays.
- MoE22 Ma, Y., Blume, M. Interference of Fluorescence X-Rays and Coherent Excitation of Core Levels.
- MoE23 Macrander, A.T., Kushnir, V.I., Blasdel, R.C. Performance of Spherical Focusing Ge(444) Backscattering Analyzer for Inelastic X-Ray Scattering.
- MoE24 Aleksandrov, Yu.M., Kirikova, N.Yu., Klimenko, V.E., Kolobanov, V.N., Makhov, V.N., Syrejschikova, T.I., Yakimenko, M.N. Experimental Facility for Luminescence Studies of Solids at the S-60 Synchrotron Radiation Source.
- MoE25 Giles, C., Malgrange, C., Goulon, J., Bergevin, F.de., Vettier, C., Fontaine, A., Dartyge, E., Pizzini, S., Baudalet, F., Freund, A. Perfect Crystal and Mosaic Crystal Quarter-Wave Plates for Circular Magnetic X-Ray Dichroism Experiments.
- MoE26 Meyer, M., Lacoursiere, J., Simon, M., Morin, P. Fluorescence-Photoion-Coincidence Spectroscopy on Inner Shell Excited Molecules.
- MoE27 Miyahara, T., Park, S.Y., Hanyu, T., Hatano, T., Muto, S., Kagoshima, Y. Comparison Between 3p MCD and 2p MCD in Transition Metals and Alloys: Is the Sum Applicable to Itinerant Magnetic System?
- MoE28 Ivanov, S.N., Mikhailin, V.V., Mikheeva, M.N., Moryakov, V.P., Nazin, V.G., Naumov, I.V., Svishchev, A.V., Tarasov, Y.F., Tsetlin, M.B. Photoemission Station for Crystal and Film Investigation Down to 10 K.
- MoE29 Nordgren, J., Wassdahl, N., Guo, J.H., Skytt, P., Duda, L.C., Butorin, S., Englund, C.J., Ma, Y. Polarization and Excitation Energy Selective Soft X-Ray Fluorescence Spectroscopy Using Synchrotron Radiation.
- MoE30 Pahl, R. Collimation and Polarization of Synchrotron Radiation Using Multiple-Beam Diffraction Optics.
- MoE31 Quinn, F.M., Seddon, E.A. Facilities for Spin Resolved Photoemission at the SRS.
- MoE32 Kortright, J.B., Rice, M., Frank, K.D. A Tunable Multilayer EUV/Soft X-Ray Polarimeter.
- MoE33 Saito, T., Yuri, M., Onuki, Hideo. Application of Oblique Incidence Detector to VUV Polarization Analyzer.
- MoE34 Sasaki, S. Fe²⁺ and Fe³⁺ Ions Distinguishable for X-Ray Anomalous Scattering: Method and Its Application to Magnetite.
- MoE35 Schneider, J.R., Bouchard, R., Bruckel, T., Lippert, M., Neumann, H.-B., Poulsen, H.F., Rutt, U., Schmidt, T., von Zimmermann, M. High Energy Synchrotron Radiation a New Probe for Condensed Matter Research.
- MoE36 Schulke, W., Kaprolat, A., Fischer, Th., Hoppner, K., Wohlert, F. A Spectrometer for High Resolution Resonant Inelastic X-Ray Scattering.
- MoE37 Schulke, W., Kaprolat, A., Gabriel, K.J., Schell, N., Burkel, E., Simmons, R.O. First IXSS Measurement of the Dynamic Structure Factor S(Q,w) of Electrons in a Solid Noble Gas (He).
- MoE38 Shastri, S.D., Finkelstein, K.D., Shen, Q., Batterman, B.W., Walko, D.A. Undulator Test of a Bragg Reflection Elliptical Polarizer at ~7.1 keV.
- MoE39 Shin, S., Agui, A., Fujisawa, M., Tezuka, Y., Ishii, T. A Soft X-Ray Emission Spectrometer for Undulator Radiation.
- MoE40 Ferrand-Tanaka, L., Simon, M., Thissen, R., Lavollee, M., Morin, P. New Experimental Set-Up Devoted to the Auger Electron Ion Multiple Coincidences Spectroscopy.

- MoE41 Suzuki, M., Hanmura, K., Kotani, T., Yamaguchi, N., Kobayashi, M., Misu, A. Direct Measurement of Magnetic Circular Dichroism and Kerr Rotation Spectra in VUV Using Four Mirror Polarizer.
- MoE42 Yagi, K., Yuri, M., Onuki, H. Polarization Modulation Spectroscopy for MCD Study Using Polarizing Undulator.
- MoE43 Yanagihara, M., Goto, Y. A Soft-X-Ray Emission Spectrometer Equipped with a Multilayer Rotating Analyzer for Polarized Emissions.
- MoE44 Belyakov, A.V. Xray Mossbauer Optics of High Angular and Frequency Resolution.
- MoE45 Johnson, E.D. Simple UHV Compatible Electromagnet for Magnetic Scattering Studies
- MoE46 Hochst, H., Pulicke, P., Nelson, T., Middleton, F. Performance Evaluation of a Soft Xray Quadruple Reflection Circular Polarizer
- MoE47 Beck, L., Bizeuil, C., Stemmler, P., LeGrand, F. Measurement of the Xray Spectrometric Properties of Cesium Hydrophthalate (CsAP) Crystal with the Synchrotron Radiation.

An Investigation of the Iron Pre-Edge XANES Structure*

S. Bajt,¹ and A. L. Hanson²

¹Department of Geophysical Sciences and Center for Advanced Radiation Sources, The University of Chicago, ²Department of Advanced Technology, Brookhaven National Laboratory

The XANES spectra of iron compounds exhibit a pre-edge structure as a function of the incident x-ray energy. This structure contains small peaks the centroids of which depend on the oxidation state and/or coordination of the iron. This fact has been used to determine relative concentrations of the different iron oxidation states in geological samples [1]. In order to utilize these pre-edge peaks for quantitative purposes, the cause of these energy shifts must be understood. The pre-edge structure of XANES spectra are the results of x-rays scattered by the x-ray internal transition scattering process. Such an internal transition is constituted of two parts, a resonant part when the transition takes place through a real state and non-resonant part that is due to a transition through a virtual state. This paper will report on investigations of this scattering with respect to the energy of the pre-edge peaks. The scattered x-rays were studied with both high and low energy resolution spectrometers.

[1] Bajt, S., S. R. Sutton, and J. S. Delaney, (1994) submitted to *Geochim. Cosmochim. Acta*.

*This work was supported by U.S. Department of Energy under Contract DE-AC02-76CH00016.

Quantification of Mixed Fe Valence States using the Energy of the Pre-edge Peak in K XANES

S. Bajt¹, S. R. Sutton¹, and J. S. Delaney²

¹ Department of the Geophysical Sciences and Center for Advanced Radiation Sources, The University of Chicago, Chicago, IL 60637, USA, ² Department of Geological Sciences, Rutgers University, New Brunswick, NJ 08903, USA.

Oxygen fugacity is an important parameter that influences phase equilibria and geochemical kinetics in the formation of natural rocks. We are exploring the possibility of determining the oxygen fugacity of geological and cosmochemical systems from the valence states of multivalent elements in these materials [1]. A crucial step in this method is the ability to quantify the amount of different valence states in specific mineral grains within a rock. The pre-edge peak energy of K-edge XANES spectra is a promising parameter for this purpose.

Experiments are being done at the NSLS (x-ray microprobe beamline X26A) where K-edge XANES spectra are collected in fluorescence mode [2]. This beamline offers a 50-100 micron focused monochromatic beam which is essential to study single crystals in-situ within polymineralic materials. Our initial work has concentrated on Fe K-edge XANES mainly because iron is a ubiquitous element in earth materials and three Fe valence states (Fe⁰, Fe²⁺ and Fe³⁺) are known to occur in nature.

3d-transition metals exhibit a pre-edge peak in their K-edge XANES spectra due to electronic transitions from core to unoccupied bound states. This pre-edge peak is a few eV below the main absorption edge and its intensity is typically only a few percent of the main absorption edge step. Pre-edge peaks are rarely used for valence quantification purposes because of this low intensity. On the other hand, these pre-edge peaks are well-suited for valence state studies because bound state transitions are involved. Consequently, the energy of pre-edge peaks is less affected by the local bonding environment than the main absorption edge energy or the energies of multiple scattering features.

We have observed that the pre-edge peak energy in well-characterized samples (silicates and oxides) with known Fe oxidation states was a linear function of ferric/ferrous ratio demonstrating the suitability of this approach [3]. The demonstrated detection limit is 100 ppm Fe. The technique is being applied to various minerals from terrestrial and extraterrestrial rocks and additional research on matrix and self-absorption effects is in progress.

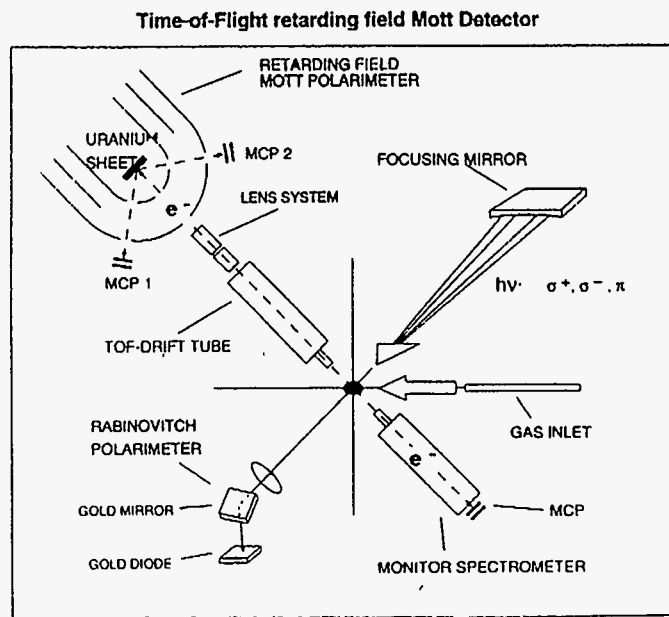
Acknowledgments: This research was supported by the following grants: NASA NAG9-106 and NAGW-3651 (SRS) and NAG9-304 (JSD), US DOE DE-F602-92ER14244 (SRS) and DE-AC02-76CH00016 (BNL).

References: [1] Delaney, J. S., Sutton, S. R., and Bajt, S. (1994) An oxygen fugacity grid for nebular and planetary geochemistry, *LPSC XXV*, 323-324. [2] Sutton, S. R., Jones, K. W., Gordon, B., Rivers, M. L., Bajt, S., and Smith, J. V. (1993) Reduced chromium in olivine grains from lunar basalt 15555: X-ray Absorption Near Edge Structure (XANES), *Geochim. Cosmochim. Acta* 57, 461-468. [3] Bajt, S., Sutton, S. R., and Delaney, J. S. (1994) submitted to *Geochim. Cosmochim. Acta*.

Spin-resolved time-of-flight electron spectroscopy following excitation with circularly polarized synchrotron radiation

G. Snell, R. Kuntze, N. Müller and U. Heinzmann,
 (Fakultät für Physik, Universität Bielefeld, 33501 Bielefeld),
 U. Hergenhan, J. Viehhaus, R. Wehlitz and U. Becker,
 (Fritz-Haber-Institut der Max-Planck-Gesellschaft, 14195 Berlin)

A new type of spectrometer for the spin-polarization sensitive analysis of electrons has been developed. This instrument allows for multichannel detection by employing a retarding-field Mott polarimeter along with a time-of-flight analyzer for the energy selection of the incoming electrons. This method is particularly advantageous for spectra with many lines spread over a wide range of energies, as the whole spectrum can be recorded simultaneously. Such conditions are common for most cases of inner-shell photoionization, where in addition to the photolines a large variety of corresponding Auger lines occurs. The spectrometer was particularly designed to study such processes. First measurements were taken at the crossed-field undulator beamline U2 at BESSY. We obtained results for the Xe 5p photoelectrons in the photon energy range between 42 and 60 eV and for Xe 4d photoelectrons and the following NOO Auger decay at 95 eV.

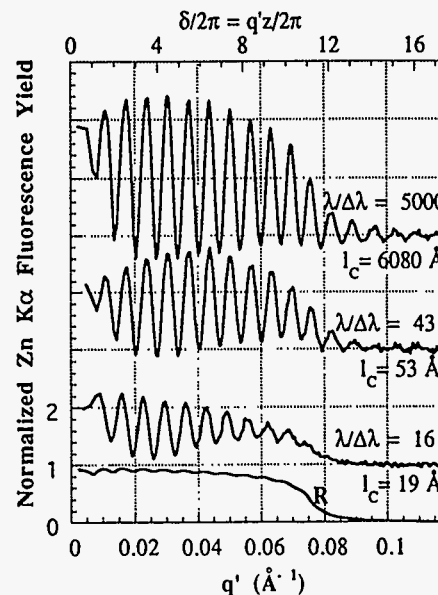


MoE3

The Effect of Coherence on the Visibility of X-ray Interference Fringes

Michael J. Bedzyk, Northwestern University and Argonne National Laboratory,
 Materials Science Division, Argonne, IL 60439

During total external reflection (TER), the superposition of the incident and reflected x-ray beams produces x-ray interference fringes above the reflecting surface. The observation of this x-ray standing wave (XSW) can be made by monitoring the fluorescence yield from a layer of heavy atoms suspended in a low-density film which coats the mirror surface.^{1,2} If the spatial and temporal coherence properties of the incident photon beam are well known, this observation can be used to determine the spatial distribution of the fluorescent atom species within the film. We have recently demonstrated that the converse condition can also be used. Namely, if the spatial distribution of the fluorescent atom species is known, the observation of the x-ray interference fringes can be used to characterize the longitudinal and transverse coherence lengths of the incident photon beam. Shown below are three separate TER XSW measurements taken at $\lambda = 1.21 \text{ \AA}$ with three different longitudinal coherence lengths (l_c). The data is for a gold mirror coated with a Langmuir-Blodgett multilayer film that is terminated with a zinc arachadate bilayer at $z = 923 \text{ \AA}$ above the Au mirror surface. As expected, the fringe visibility as observed by the Zn K α fluorescence is not affected by a reduction in l_c until the phase lag ($\delta/2\pi$) due to the path length difference between the two beams at z approaches the value of the monochromaticity $\lambda/\Delta\lambda$. The top curve corresponds to a nearly ideal plane wave condition produced by using a Si(111) monochromator. The lower two curves correspond to much wider band-pass incident beams which used Bragg diffraction from two different multilayers. Curve R is the measured reflectivity from the Au mirror with $\lambda/\Delta\lambda = 5000$. $q' = 4\pi\sin\theta'/\lambda$ is the magnitude of the standing wave vector in the film.



MoE4

Work at Argonne National Laboratory is supported by DOE/BES under contract No. W-31-109-ENG-38.

¹ M.J. Bedzyk, G.M. Bommarito, and J.S. Schildkraut, Phys. Rev. Lett. 62, 1376 (1989).

² J. Wang, M.J. Bedzyk, T.L. Penner, and M. Caffrey, Nature 354, 377 (1991).

V.A.Belyakov, Surface and Vacuum Research
Centre, Kravchenko str., 8, 117331 Moscow, Russia

An overview of different phenomena connected with a coherent emission of γ quanta in crystals accompanied by an energy change of the emitted quanta in comparison with the energy of the quanta initiating the process [1] is presented. As specific examples of the mentioned phenomena are examined coherent inelastic Mossbauer scattering connected with absorption or emission of phonons in a crystal lattice, coherent Coulomb excitation of Mossbauer transitions, coherent excitation of a Mossbauer gamma-cascade and influence of the inelastic coherent scattering on the Mossbauer absorption and conversion electron spectra. The common features of the mentioned processes distinguishing them from the analogous processes involving interaction of radiation only with electrons of crystals are connected with a very long time of resonant interaction of gamma quanta with nuclei compared with the time of their interaction with electrons in crystals and typical crystal lattice times. As a consequence of this difference, for example, the angular distribution of quanta in the coherent inelastic Mossbauer scattering in a contrast to the X-ray scattering does not depend on the wave vector of a phonon accompanying the scattering process [2]. Another typical features of the processes are examined. The possibilities of experimental observation of the mentioned phenomena at modern dedicated synchrotron radiation sources and in conventional Mossbauer spectroscopy are discussed and the relevant recently performed experiments are analyzed.

1. V.A.Belyakov, Diffraction Optics of Complex-Structured Periodic Media, N.Y., Springer Verlag, 1992.
2. V.A.Belyakov, Yu.M.Aivazian, Nucl.Instrum.Methods A 282, 628, (1989).

V.A.Belyakov and I.V.Zhadenov, Surface and Vacuum Research
Centre, Kravchenko str., 8, 117331 Moscow, Russia

Mossbauer filtration of Synchrotron Radiation (SR) due to the resonant Mossbauer scattering at an isotope interface (a plane interface between different isotopes of the same chemical element) under conditions of a total internal reflection is theoretically investigated. The mentioned scheme of Mossbauer filtration of SR allows one to suppress the background connected with the nonresonant SR scattering because of absence of reflection at the isotope interface if there is no resonant scattering. Calculations of the reflection coefficient at the Fe56/Fe57 isotope interface versus the SR energy and the incidence angle are performed. It is shown that due to the sharp resonant dependence of the total reflection critical angle for an isotope interface on the SR energy the choice of the incidence angle and of the divergence of the incident SR beam allows one to change in a great extent an energy line width of the filtrated SR. Because in any real experiment other interfaces except of the isotope one are inevitably present and generate a nonresonant background special geometries of these interfaces which allow to suppress the background are examined. The main idea of the suppressing of the background by a choice of the interfaces geometry reduces to the choice of such geometries in which the isotope interface is nonparallel to the another ones. This allows to separate the scattering direction at the isotope interface from the background scattering directions from the other interfaces with a simultaneous background intensity reduction because the nonisotope interfaces occur to be far away from the total reflection condition. A vacuum - non-Mossbauer isotope interface of a saw-like profile combined with a planar isotope interface is examined in details. Numerical calculations illustrating advantages of the proposed scheme of SR Mossbauer filtration in comparison with the others [1] are carried out for a Fe56/57Fe isotope interface.

1. V.A.Belyakov, Diffraction Optics of Complex-Structured Periodic Media, N.Y., Springer Verlag, 1992, Chpt.X.

Asymmetrically-cut Crystals as Optical Elements for Coherent X-ray Beams

S. Brauer, G.B. Stephenson *IBM Research Division*, M. Sutton *McGill University*, S.G.J. Mochrie *Massachusetts Institute of Technology*, S. Dierker *University of Michigan*, R. Flemming, R. Pindak *AT&T Bell Laboratories*, I.K. Robinson *University of Illinois*, G. Grübel, J. Als-Nielsen, D. Abernathy *European Synchrotron Radiation Facility*.

In forming a coherent beam of hard x-rays, one must select an angular collimation which is much smaller than the angular acceptance (Darwin width) of a typical crystal monochromator. To evaluate how these highly collimated beams are affected by perfect crystal optics, it is necessary to understand the optical behavior on a scale which is finer than the Darwin width. The utility of such optics for altering the shape of the coherence volume, or enhancing the useful coherent flux, can then be assessed. By considering the position and orientation of the crystal truncation rod in reciprocal space, the relationship between the exact incidence and exit angles can be determined as a function of wavelength and crystal surface orientation. The properties of both Bragg (reflection) and Laue (transmission) diffraction geometries can then be assessed with the aid of DuMond diagrams. One of the most important cases is for highly collimated, polychromatic radiation incident on a crystal, as is typical in synchrotron studies with coherent beams. Under these conditions, for Laue and asymmetric Bragg geometries, the exit divergence is increased much beyond that of the symmetric Bragg case. This results from an inherent chromatic aberration which is worst in Laue geometries. For coherence studies, the Laue and asymmetric Bragg geometries are generally undesirable since the enhanced divergence corresponds to a loss of useful coherent flux.

Nanosecond Time-Resolved Spectroscopy Using a Pulsed Laser Diode and Infrared Synchrotron Radiation

G.L. Carr, Advanced Development Center, M.S. AO1-26, Grumman Corporation, Bethpage NY 11714 USA.

Photo-excited electron-hole pairs in semiconductors and broken Cooper pairs in superconductors are two example system that can relax on a nanosecond time scale. Far-infrared spectroscopy is well-suited to the characterization of such photo-excitations since the electronic collision time for many materials falls in the 10^{-12} to 10^{-14} second range, leading to frequency dependent properties that allow the plasma frequency and scattering rate to be separately determined. The photon energy for breaking superconducting pairs also falls in this spectral range. Nanosecond time resolution is needed to follow the spectral properties of the excitations during the relaxation process. Therefore, a pump-probe technique has been developed for performing infrared spectroscopy with nanosecond time resolution.

The pump-probe method requires a pulsed light source for photo-excitation and another for spectroscopy, with a variable time-delay between. The NSLS VUV ring provides sub-nanosecond infrared probe pulses, and is a proven source for high quality spectroscopy. A laser diode system has been developed for pump pulses, delivering from 100 mW to 1W peak power. Pulse repetition frequencies from 5 MHz to over 50 MHz are possible using a fast electronic pulse generator that is readily triggered with the synchrotron's RF signal. The present diode operates at a photon energy of 1.47 eV (i.e. a wavelength of about 845 nm).

The nanosecond time-resolved IR spectroscopy system has been used to follow the decay of photocarriers in GaAs. Measurements reveal a scattering rate that evolves over a 20 ns time scale (during the decay process). A model, based on the different electron and hole decay times and scattering rates, may account for the result.

Circularly-Polarized-Light Induced Dichroism in Photoelectron Diffraction Observed with Display-type Spherical Mirror Analyzer

H. Daimon, T. Nakatani, S. Imada, S. Suga, Y. Kagoshima¹, and T. Miyahara¹
 Dept. of Material Phys., Fac. of Engineering Sci., Osaka Univ., Toyonaka, Osaka 560 Japan
¹PF, National Lab. for High Energy Physics, Tsukuba, Ibaraki 305 Japan

Circular dichroism (CD) in 2-dimensional photoelectron diffraction patterns was observed for the first time for the photoelectron from the Si 2p core on the Si(001) surface using a display-type spherical mirror analyzer, Fig.1.[1], developed by ourselves. The emitted direction of the energy-selected photoelectrons can be directly observed on the screen without distortion. The experiment was performed at the NE1-B beamline of the 6.5-GeV accumulation ring at KEK, Tsukuba. The circularly polarized synchrotron radiation was monochromatized and incident perpendicularly to the surface.

Figure 2 shows a typical CD pattern obtained as a difference of the patterns obtained for the left and right helicity lights at the photoelectron kinetic energy (E_k) of 400 eV. Strong CD is found, although this Si(001) surface has no chirality and magnetism.

One can recognize strong CD even in the original photoelectron diffraction patterns. Fig. 3 shows original patterns at $E_k = 250$ eV excited by left and right helicity light. The peaks in the pattern rotate in the same direction as the rotational direction of the electric field of the light. This rotation of the peak was explained by the rotation of the propagating vector of photoelectrons around the nuclei, whose angular momentum was selected by the circularly-polarized light. The peaks in these patterns are well recognized as the forward focusing (0-th order diffraction) peaks in the propagation of photoelectrons by near-neighbour atoms around the emitting atom. The small full crosses in these figures show the quantum-mechanically predicted peak positions, which correspond to the direction of the propagating vector at the scatterer[2]. This is the first direct observation of the rotation of the photoelectrons.

This result is a new type of CDAD (CD in angular distribution)[3,4] of photoemission for nonchiral and nonmagnetic materials. This phenomenon can be used to measure the polarization of the circularly polarized light in situ because the asymmetry is large(about 16%).

- [1] H. Daimon and S. Ino, Rev. Sci. Instrum. 61 (1990) 57.
- [2] H. Daimon, et al., Jpn. J. Appl. Phys. 32 (1993) L1480.
- [3] G. Schönhense, Phys. Scr. T31 (1990) 255.
- [4] J. Bansmann, et al., Phys. Rev. B 46 (1992) 13496.

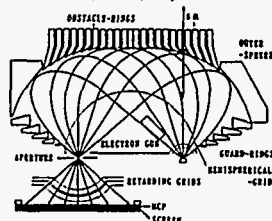


Fig. 1 Display-type spherical mirror analyzer.



Fig. 2 CD pattern at $E_k = 400$ eV.



Fig. 3 Original patterns at $E_k = 250$ eV.

Multilayer transmission phase-shifters for the carbon K-edge and the water window.

S. Di Fonzo, B. R. Müller, W. Jark,
 SINCROTRONE TRIESTE, Padriciano 99, I-34012 Trieste, Italy
 A. Gaupp, F. Schäfers
 BESSY, Lentzeallee 100, D-14195 Berlin, Germany
 and J. H. Underwood
 Center for X-Ray Optics, LBL, Berkeley CA 94720, USA

In this report we will present the comparison between the theoretical predictions [1] and experimental results [2] that we obtained for the phase-shifting close to the carbon K-edge in a Cr/C multilayer transmission filter. For arriving at a good agreement experiment-theory one needs to assume an interface roughness of 0.65 nm rms, which is a realistic value supported also by reflectivity measurements. The filter has been characterised at the SX700/3 beamline at BESSY providing circularly polarized light. The measurements were performed during two measuring shifts separated by 7 months in the first case in single bunch operation with low current and later in multi-bunch operation with high current. The phase-shifting of the filter was found to be unaltered after the stand-by period. The observed phase-shifting was sufficient for a use of the filter also for a complete polarization characterization of the beamline. Even though the storage ring parameters were rather different the output characteristics of the monochromator were found to not have changed as far as its polarization characteristics are concerned.

With additional model calculation we will show in how far multilayer transmission phase-shifters can be applied in the water window.

- [1] S. Di Fonzo and W. Jark, Rev. Sci. Instrum. 63, 1375 (1992)
- [2] S. Di Fonzo, W. Jark, F. Schäfers, H. Petersen, A. Gaupp and J. H. Underwood, Synchrotron Radiation News Vol. 6, No. 2, 16 (1993) and accepted for publication in Appl. Opt.

Ultra-high Vacuum Chamber for Synchrotron X-ray Diffraction from Films Adsorbed on Single-crystal Surfaces

S. N. Ehrlich,^(a) T. Angot,^(b) P. Dai,^(b) S. K. Wang,^(b) J. R. Dennison,^(c) and H. Taub^(b)

(a) Purdue U.; (b) U. of Missouri-Columbia; (c) Utah State U.

An ultra-high vacuum chamber has been developed for structural analysis of adsorbed films on single-crystal surfaces using synchrotron x-ray diffraction [1]. It is particularly well suited for investigations of physisorbed and other weakly bound films. The chamber is small enough to transport and mount directly on a standard four-circle Huber diffractometer and can also be used independently of the x-ray diffractometer. A low-current, pulse-counting low-energy electron diffraction (LEED)/Auger spectroscopy system with a position-sensitive detector enables *in situ* characterization of the film and substrate while the sample is located at the x-ray scattering position. A closed-cycle He refrigerator and electron bombardment heater provide substrate temperatures from 40 K to 1300 K. The chamber is also equipped with an ion sputter gun, a quadrupole mass spectrometer, and a gas handling system.

Recently, the chamber operation has been improved by including a novel sample rotator which allows manual rotation of the sample about its surface normal and good thermal contact with the sample at low temperatures after completion of the rotation. In addition, the Huber diffractometer [1] has been modified to achieve five-circle capability [2] by mounting the x-ray detector on a linear drive moving perpendicular to the vertical scattering plane. Both of these modifications increase the volume of reciprocal space accessible in surface scattering experiments; and, in particular, the linear drive permits specular reflectivity measurements useful in film growth experiments. Also, centering of the sample at the x-ray scattering position has been facilitated with a computer-controlled stepper motor, enabling precision translational motion of the sample perpendicular to the incident x-ray beam. Details of the design and operation of the instrument are described. Thus far, the chamber has been used to investigate the layer-by-layer structure of xenon [1,3] and hexane [4] films adsorbed on a Ag(111) substrate.

1. J. R. Dennison, S.-K. Wang, P. Dai, T. Angot, H. Taub, S. N. Ehrlich, *Rev. Sci. Instrum.* **63**, 3835 (1992).
2. S.-K. Wang, P. Dai, and H. Taub, *J. Appl. Crystallogr.* **26**, 697 (1993).
3. P. Dai, T. Angot, S. N. Ehrlich, S.-K. Wang, and H. Taub, *Phys. Rev. Lett.* **72**, 685 (1994); and P. Dai, Z. Wu, T. Angot, S. N. Ehrlich, S. K. Wang, and H. Taub, unpublished.
4. Z. Wu, P. Dai, S. N. Ehrlich, and H. Taub, *NSLS Annual Report 1993*, *Bull. Am. Phys. Soc.* **39**, 455 (1994); and to be published.

Supported by U.S. NSF Grant Nos. DMR-8304366, DMR-8704438, and DMR-9011069, DOE Grant No. DE-FC02-85ER45183 of the MATRIX PRT at the NSLS, University of Missouri Multicampus Weldon Springs Awards, and a Research Council Grant of the University of Missouri-Columbia.

A Critical Assessment of the QEXAFS Method.

Joe Wong^a, Michael Fröba^a, and R. Frahm^b ^aLawrence Livermore National Laboratory, PO Box 808, Livermore, CA 94551, USA ; ^bHASYLAB am DESY, D-22603 Hamburg, Germany.

The idea of recording an x-ray absorption spectrum "on the fly" when a mechanically stable monochromator is being slewed smoothly and continuously over a given energy range has been proposed and successfully demonstrated by one of us in 1988¹. This procedure constitutes what is now known the QEXAFS method. The question of *How quick is QEXAFS?* has been examined in some detail at the Kobe conference². Thus, the QEXAFS technique provides a novel characterization tool to study the bonding and local atomic structure in materials with a time resolution of the order of seconds. In the present paper, we provide a critical assessment of this technique in terms of spectral quality and resolution as a function of various QEXAFS experimental parameters such as scan rate, integration time, type of monochromator used, as well as an experimentally definable energy window over which a QEXAFS data point is collected. Model compounds with well defined shape pre-edge XANES and whiteline features and long k-range EXAFS are used as test systems to arrive at a set of practical experimental parameters. The versatility, application and limitations of this time-resolved spectroscopic tool will be discussed.

References

- ¹R. Frahm, *HASYLAB Ann. Report* (1987), p. 374; *Nucl. Instrum. Meth. A270*, 578 (1988)
- ²R. Frahm and Joe Wong, *Jpn. J. Appl. Phys.* **32**, Suppl. 32-2, 188 (1993)

X-ray polarimetry with phase plates

F. de Bergevin^{1,3}, C. Vettier¹, C. Malgrange², C. Giles¹, F. Grossi¹, G. Grübel¹

1. European Synchrotron Radiation Facility, B.P. 220, F-38043 Grenoble Cédex, France

2. Laboratoire de Minéralogie-Cristallographie, associé CNRS, Universités de Paris 6 et 7, case 115, Tour 16, 4, Place Jussieu, 75252 Paris Cédex 05, France

3. Laboratoire de Cristallographie, B.P. 166, F-38042, Grenoble Cédex 09, France

Diamond crystals have been used as x-ray quarter-wave plates (QWP) and half-wave plates (HWP) in the Bragg and Laue transmission geometry to produce circularly and vertical linearly polarized beams from an undulator source (ID10) at the ESRF. The linear polarization (analyzed by a linear polarimeter) could be set at any direction by the combination of two QWP with a variable azimuthal angle between them. Also, the second QWP and the linear polarimeter were used to completely characterize the polarization state of the circularly polarized beam after the first QWP. High rates of circular polarization (98%) and of linear polarization in the vertical (97%) and at 45° planes (95%), were achieved by reducing the tails of the 9.1 keV monochromatic beam from a C111 asymmetric Laue monochromator using a Si 111 channel-cut crystal with its diffraction plane at 45° from the horizontal plane. The use of the diamond plate in an asymmetric Laue geometry allowed the increase of the transmitted intensity from 10% (symmetric Bragg geometry) to 40%, keeping high efficiencies as QWP and HWP.

MoE13

Extremely Dispersive X-Ray Standing Wave Measurements

Th. Gog, A. Hille, D. Bahr, G. Materlik

Hamburger Synchrotronstrahlungslabor HASYLAB am

Deutschen Elektronen-Synchrotron DESY, 22603 Hamburg, Germany

In the last decade X-ray standing waves (XSW) have become a routine tool in the study of surface- and bulk structures of perfect or nearly perfect crystals. Conventional x-ray standing wave (XSW) measurements are performed in a "non-dispersive" mode where sample and monochromator reflections arise from identical diffraction plane spacings, generating one single standing wave field at the sample with a well defined phase for any particular angle of incidence. In contrast, extremely dispersive set-ups with non-matching reflections lead to a simultaneous generation of standing wave fields with all possible phases, obscuring standing wave yields and decreasing the resolution of the experiment. Nevertheless, useful structural information can be gained through dispersive XSW, as is demonstrated in this work for sample / monochromator combinations of Ge(111) / Ge(111), Ge(111) / Ge(333) in (+1,-1), and Ge(111) / Ge(111) in (+1,+1) configuration. Rocking curves in these cases are reminiscent of the angular distribution of intensity in the incident x-ray beam, which needs to be modeled from given source parameters and should then be included in the data analysis. Highly asymmetric monochromators can help recover some of the lost resolution, as should decreased divergences in the incident synchrotron beam, which one expects from 3rd generation sources.

MoE14

A High Resolution X-ray Spectrometer based on a cylindrically bent crystal in non-dispersive geometry

K. Hämäläinen¹, M. Krisch², F. Sette², C.-C. Kao³, W. Caliebe³ and J. B. Hastings³

¹ Department of Physics, P.O. Box 9, FIN-00014 University of Helsinki, Finland

² European Synchrotron Radiation Facility, BP 220, F-38043 Grenoble Cedex, France

³ National Synchrotron Light Source, BNL, Upton NY 11973, USA

High resolution X-ray inelastic scattering is an old method coming back to fashion, thanks to the availability of intense synchrotron radiation sources as wigglers and undulators. Experimentally, the major challenge lies in the development of efficient spectrometers. Usually, they are based on crystal analyzers employing reflections close to backscattering angles in order to provide good energy resolution with large angular acceptance. So far, typical methods are based either on spherically or cylindrically bent crystal. In the first case, the crystal in Rowland geometry provides a monochromatic point focus, while in the second case it provides an energy dispersed line focus in the scattering plane. In the present communication we present a spectrometer based on a cylindrically bent crystal in Rowland geometry, which provides an energy dispersed line focus in the plane perpendicular to the scattering plane. The advantage of this geometry is to provide an energy dispersion which is only an order of magnitude larger than the energy resolution, allowing to optimize the count rate in the energy window of interest and to preserve the advantage associated with the practical realization of a cylindrically bent crystal. Experiments were performed at 8 keV incident photon energy on beamline X21 at the NSLS, monitoring the elastically scattered radiation from a plastic foil. A Si(111) crystal bent to a radius of 1 m provided a total energy resolution of 0.6 eV using the (444) reflection at 80.2 degrees Bragg angle and an energy dispersion of about 4 eV, using a linear energy dispersive detector positioned along the line focus. We will present these experimental results, and discuss the formalism to calculate the energy dispersion, as well as how the energy window can be optimized by rotating the focusing plane with respect to the scattering plane.

Electron and X-ray Fluorescence Yield Measurements of the Cu L_{2,3}-Edge X-ray Absorption Fine Structures (XAFS): A Comparative Study

A. Hiraya¹, M. Watanabe^{1,2} and T.K. Sham³

¹ UVSOR, Institute for Molecular Science, Myodaiji, Okazaki, 444, Japan

² Tohoku University, Aoba-ku, Sendai, 980 Japan

³ Department of Chemistry, University of Western Ontario, London, N6A 5B7 Canada

The Cu L_{2,3}-edge XAFS of a series of Cu compounds (ambient and in situ scraped Cu metal, Cu oxides, and Cu-Au alloys) have been recorded at the BL1A beamline (a double-crystal monochromator beamline with beryl crystals) of UVSOR using both electron yield and X-ray fluorescence yield techniques. Cu L_{2,3} edge XAFS were simultaneously recorded in three modes: total electron yield (TEY) with specimen current, total electron yield with a multichannel plate (MCP) and X-ray fluorescence yield (FLY) with an Ar/CH₄ gas proportional counter. While both TEY measurements produce essentially identical spectra, a comparison between TEY and FLY results exhibits a drastic difference in the sensitivity of the techniques towards sampling depth. This is illustrated with the Cu L_{2,3} XAFS of an ambient sample of pure Cu in the figure below. These results and their potential applications will be discussed.

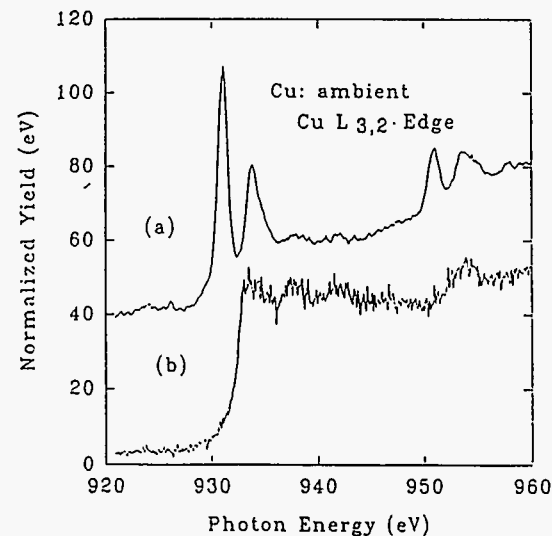


Fig. Cu L_{2,3}-edge XAFS of an ambient Cu sample recorded with (a) electron yield and (b) X-ray fluorescence yield.

A Multi-purpose X-ray Diffractometer for Synchrotron Radiation at SRRC

Shih-Lin Chang, Hsueh-Hsing Hung, Hwo-Shuenn Sheu, Jin-Yen Liu
Synchrotron Radiation Research Center, Hsinchu 30077, Taiwan, ROC

A multi-purpose x-ray diffractometer for synchrotron radiation is reported. Compared to the conventional Hüber six-circle diffractometer, the present specially designed eight-circle, or ψ -scan [K. Hümmer, E. Weckert, and H. Bondza, *Acta Cryst. A*45 (1989) 182-187], diffractometer has two additional degrees of freedom for sample rotation and detector motion. This arrangement make possible crystal rotation around any scattering vector and detector motion in any plane. Therefore, the diffractometer can be set for horizontal- as well as vertical-axis diffraction geometry [H. H. Hung, *Appl. Cryst.* 25 (1992) 761-765] which is capable of performing with ease grazing-incidence diffraction and ψ -scan multiple diffraction. In addition, with 5-phase stepping motors and large-ratio gear reducers implemented on the diffractometer, standing wave stimulated fluorescence measurements can also be carried out.

Details about the geometry of the diffractometer and some measurement results are also reported.

Absolute photoabsorption cross-section measurements of simple molecules in the core level region

B.S. Itchkawitz, B. Kempgens, H.M. Köppe, J. Feldhaus, A.M. Bradshaw, Fritz-Haber-Institut der Max-Planck-Gesellschaft, Faradayweg 4-6, D-14195 Berlin, Germany, and W.B. Peatman, BESSY, Lentzeallee 100, D-14195 Berlin, Germany.

The absolute photoabsorption cross-sections in the core level region of about 15 simple molecules in the gas phase have been measured both on the HE-TGM-1 beamline at BESSY and with high resolution on the undulator-based X1B spectroscopy beamline at the National Synchrotron Light Source. In particular, high resolution spectra were obtained for CH₄, C₂H₂, C₂H₄, and their deuterated isotopomers in the threshold region which includes C 1s \rightarrow π^* resonances, core-excited valence (double) excitations, and Rydberg states.

Higher order light from monochromator gratings normally hinders optical spectroscopy measurements of absolute photoabsorption cross-sections. Measurements near the C 1s threshold are particularly difficult on typical soft x ray beamlines such as HE-TGM-1 and X1B since there are significant second and third order components. In addition, the elimination of structure due to carbon contamination of the optical components becomes more difficult. In this work the higher order radiation has been reduced to acceptable levels by using a compact optical system after the exit slit. This high-order light suppressor consists of two plane mirrors mounted parallel to one another, which reflect the incident radiation twice at grazing angles yielding a high transmission of light at the desired energy. By varying the angle of incidence and the materials of the reflecting surfaces, the cut-off energy can be changed to achieve suppression factors of 10:1 to 100:1 for the second order relative to the first order. The subsequent photoabsorption measurements have much larger signal-to-noise ratios than do inner-shell electron energy loss measurements. Furthermore, the absolute cross-section determinations can be made from photoabsorption measurements in a straightforward way, without the background subtraction, kinematic correction, and scaling procedures necessary in the electron energy loss measurements.

A scanning x-ray microscope using circularly polarized radiation at the TRISTAN Accumulation Ring and its application to observation of magnetic structure

Y. Kagoshima ¹⁾, J. Wang ²⁾, T. Miyahara ¹⁾, S. Aoki ³⁾ and M. Ando ¹⁾

¹⁾ Photon Factory, National Laboratory for High Energy Physics, Tsukuba, Ibaraki 305, Japan

²⁾ Department of Synchrotron Radiation Science, The Graduate University of Advanced Studies, Tsukuba, Ibaraki 305, Japan

³⁾ Institute of Applied Physics, University of Tsukuba, Tsukuba, Ibaraki 305, Japan

Magnetic circular dichroism (MCD) measurements are actively performed at some synchrotron radiation facilities to study magnetism of magnetic thin films and bulks including alloys. The current MCD measurements give spectroscopic information mostly as an averaged value over the whole irradiated area on a sample. If a microscopic technique is introduced, MCD measurements with high spatial resolution can be performed. J. Stöhr *et al* have recorded images of magnetic domains of a recording disk at spatial resolution of 1 μ m using an electrostatic microscope with circularly polarized x rays ¹⁾.

We have constructed a scanning x-ray microscope at the beamline NE1B ²⁾ which is for circularly polarized soft x rays from a helical undulator ³⁾ aiming at the imaging of magnetic structures as well as at the spatially resolved spectroscopy of magnetic materials. The microscope consists of interchangeable pre-pinholes, a reducing optical system using a zone plate, an order selecting aperture, samples, a scanning stage, a detector to measure photoelectron yield, an MCP for optical alignment, and a micro-computer to control the system.

The microscope has been applied to observation of the magnetic structure. A size of a focused spot, namely a spatial resolution, was set to be 1.5 μ m. The focused beam was incident at an angle of 30° from the surface of the sample. Measuring photoelectron yield from the sample using a channeltron, the sample was scanned two dimensionally. Two dimensional mapping of the photoelectron yield was displayed as an microscopic image. A sample used was a piece of video tape, and its magnetic layer is an evaporated one with its component of Co:Ni=80:20. Images of the same field were taken at different photon energies of 778eV (L_3), 793eV (L_2), and 798eV (higher than L_2). It was found that the contrast between two images at L_3 and L_2 was reversed. Further, the image at 798eV exhibited no apparent structures. These results show that the magnetic structure was observed by our microscope.

References

- 1) J. Stöhr, Y. Wu, B. D. Hermsmeier, M. G. Samant, G. R. Harp, S. Koranda, D. Dunham and B. P. Tonner, *Science* 259(1993)658.
- 2) Y. Kagoshima *et al.*, in this conference.
- 3) S. Yamamoto, H. Kawata, H. Kitamura, M. Ando, N. Sakai, and N. Shiotani, *Phys. Rev. Lett.* 62, 2672(1989).

Monochromator for Circularly Polarized Synchrotron Radiation in the Energy Range of 5-250 eV.

Masao Kamada, Kusuo Sakai, Shin-ichiro Tanaka, Shigeo Ohara, Shin-ichi Kimura, Atunari Hiraya, Masami Hasumoto, Kazumichi Nakagawa,^{a)} Kouichi Ichikawa,^{b)} Kazuo Soda,^{b)} Kazutoshi Fukui,^{c)} Yasuo Fujii,^{d)} and Eiji Ishiguro^{d)}

Institute for Molecular Science, Okazaki 444, Japan

a) Kobe University, Kobe 657, Japan

b) University of Osaka Prefecture, Sakai 593, Japan

c) Fukui University, Fukui 909, Japan

d) Osaka City University, Osaka 558, Japan

A new Spherical Grating Monochromator with Translational and Rotational Assembly Including a Normal incidence mount (SGM-TRAIN) is under construction at BL 5A of the UVSOR Facility, IMS, and its design concept is reported. The following points have been taken into account in the design: (1) energy range of 5-250 eV, (2) use both of undulator and bending radiations, (3) linear and circular polarizations, (4) spectral purity, (5) resolution, and (6) length of beam line.

The SGM-TRAIN is an improved version of a constant deviation monochromator proposed by Ishiguro *et al.* (*Rev. Sci. Instr.* **60**, 2105 (1989)). Its main optical components are a spherical grating, a plane mirror, and fixed slits. The radii of the gratings are about 25 and 7.3 m for the deviation angles of 172 and 152°, respectively. The distance between the entrance and exit slits is 3.5 m. Two driving modes of the monochromator, standard and high resolution modes, are available by a computer control system. A normal incidence mount is also included in the monochromator to supply a well-polarized light with small second-order component in the low energy region (<25 eV).

It should be stressed that the SGM-TRAIN is useful for the experiments where circularly polarized synchrotron radiation is used. Moreover, the SGM-TRAIN has an advantage that small emittance of a storage ring and large space for a long beam line are not necessary.

**Bragg Transmission Phase Plate for the Production of
Circularly Polarized X-rays***

J.C. Lang and G. Srajer
Argonne National Laboratory
Advanced Photon Source
Argonne, IL 60439, USA

A Si (400) X-ray phase plate of the bragg transmission type has been constructed. The variation in the degree of circular polarization as a function of off-bragg position has been observed. Left- and right-handed circular polarizations as high as $P_c=0.75\pm 0.05$ were measured using a multiple beam diffraction method. The application of these type of phase plates for resonant absorption and diffraction measurements will be discussed.

*This work is supported by the U.S. DOE Contract No. W-31-109-Eng-38.

MoE21

Interference of Fluorescence X-rays and Coherent Excitation of Core Levels

Yanjun Ma
Physics Department, University of Washington, Seattle, WA 98195 and Pacific
Northwest Laboratories, Richland, WA 99352

M. Blume
Brookhaven National Laboratory, Upton, NY 11973

The question of coherence in inelastic x-ray absorption and fluorescence processes will be considered for molecules and solids. It is argued that the absorption-decay processes on equivalent but identical atoms are generally coherent. As a result, fluorescence x-rays or other secondary particles such as Auger electrons emitted from individual atoms can exhibit interesting interference effects.

We discuss the conditions for the observation of the interference effects in terms of various time scales, such as the core hole life time, the vibrational relaxation time, and the detection time. As in the classical Young's double-slit experiment, the primary requirement for the existence of the interference effect is that one cannot determine which atom had undergone the excitation-decay process. Recent experimental evidence supporting such a coherent excitation and decay picture, including the excitation energy dependence of the valence band emission spectra and the anisotropy of the Si $K\beta$ emission, will be discussed.

This view of the excitation-decay process opens experimental possibilities in synchrotron radiation research including *momentum resolved* x-ray absorption and emission spectroscopies. One might also use the interference effect to determine interatomic distances in molecules.

MoE22

PERFORMANCE OF SPHERICAL FOCUSING Ge(444) BACKSCATTERING ANALYZER
FOR INELASTIC X-RAY SCATTERING.*

A.T. Macrander, V.I. Kushnir, and R.C. Blasdell
Experimental Facilities Division
Advanced Photon Source
Argonne National Laboratory

Abstract

A spectrometer designed to use an undulator source and having a targeted resolution of 0.2 eV will operate at the APS. We have constructed analyzers for use on this spectrometer, and we have tested them at NSLS beamline X21 using focused wiggler radiation and at CHESS using the CHESS-ANL undulator. Analyzers were constructed by pressing and gluing 90 mm diameter (111) oriented wafers into concave glass forms having a radius near 1 m. An overall inelastic scattering resolution of 0.3 eV using the (444) reflection was demonstrated at CHESS. Recent results at X21 revealed a useful diameter of 74 mm at 87 deg Bragg angle with an overall inelastic scattering resolution of 0.7 eV. We will present data for the figure perfection, efficiency of collection, and resolution of such analyzers as measured in a variety of ways with a variety of scattering samples. In addition, we will present inelastic spectra recently obtained at X21 with such an analyzer for SiC and TiC single crystals.

*This work is supported by the U.S. DOE Contract No. W-31-109-Eng-38..

EXPERIMENTAL FACILITY FOR LUMINESCENCE STUDIES OF
SOLIDS AT THE S-60 SYNCHROTRON RADIATION SOURCE

Yu.M.Aleksandrov¹⁾, N.Yu.Kirikova¹⁾, V.E.Klimenko¹⁾, V.N.Kolobanov²⁾,
V.N.Makhov¹⁾, T.I.Syrejshchikova¹⁾ and M.N.Yakimenko¹⁾.

¹⁾ Lebedev Physical Institute, Moscow 117924, Russia

²⁾ Moscow State University, Moscow 117234, Russia

A new station for time-resolved luminescence studies of solids was installed at the S-60 synchrotron radiation (SR) source. High-intense ($>10^{14}$ photons/s/cm²) "white" direct SR beam (parameters of spectrum after 5 μ Be-foil: $h\nu \sim 1$ keV, HWHM ~ 0.5 keV) illuminates the sample installed right after the slit diaphragm being at the same time an entrance slit of the analyzing monochromator (0.5 m Seya-Namioka type). Time-resolved emission spectra (in the photon energy range 2.3-10.5 eV at temperatures 80-300 K) and emission decay curves can be measured at this station under pulsed SR excitation using single-photon counting technique. Due to high intensity of exciting soft X-ray SR beam this setup permits to measure emission characteristics of specimens with low quantum yields. Additional advantage of the mounting is that the spectral response function of the apparatus was measured in the direct SR beam. Another station that has been working at the S-60 SR source for more than 10 years allows to measure time-resolved excitation spectra (in the range 5-30 eV at temperatures 80-400 K) and thermally stimulated luminescence glow curves (in the range 80-400 K) as well as transmission and reflection spectra (in the same spectral range). Thus in fact a full range of luminescence characteristics can be measured using a combination of these two stations. A program of time-resolved studies of the nature and properties of fast emission in solids is now in progress at the facility. Several classes of fast inorganic scintillators including so-called crossluminescence crystals and cerium fluoride were studied at the S-60 SR source and recommendations concerning their using in fast scintillating detectors, in particular in high-counting rate X-ray detectors were given [1,2].

[1] Yu.M.Aleksandrov, V.N.Makhov and M.N.Yakimenko, Rev.Sci.Instrum. 63 (1992) 1466.

[2] V.N.Makhov, Proc. "Crystal-2000" Int. Workshop, September 22-26, 1992, Chamonix (France), p.167.

Perfect crystal and mosaic crystal quarter-wave plates for Circular Magnetic X-ray Dichroism experiments

C.Giles¹, C.Malgrange², J.Goulon¹, F.de Bergevin^{1,3}, C.Vettier¹, A.Fontaine⁴, E.Dartyge⁴, S. Pizzini⁴, F. Baudelet⁴, A.Freund¹

1. European Synchrotron Radiation Facility, B.P. 220, F-38043 Grenoble Cédex, France
2. Laboratoire de Minéralogie-Cristallographie, associé CNRS, Universités Paris 6 et 7, case 115, tour 16, 4 place Jussieu, 75252 Paris Cédex 05, France
3. Laboratoire de Cristallographie, B.P. 166, F-38042, Grenoble Cédex 09, France
4. LURE, Laboratoire mixte CNRS-CEA-MEN, Bâtiment 209 D, F-91405 Orsay Cédex, France

Diamond and beryllium crystals have been used successfully as x-ray quarter-wave plates to detect Circular Magnetic X-ray Dichroism (CMXD) from ferromagnetic samples with an energy dispersive absorption spectrometer. CMXD signals have been obtained at LURE (Orsay-France) using the linearly polarized x-ray beam in the orbit plane and the quarter-wave plate (QWP) (fig.1a and 2a). They are compared to those obtained using the elliptically polarized beam below the orbit plane (Fig.1b and 2b). The polarization rate and the intensity are higher with the QWP. The QWP technique makes then possible to create circularly polarized x-rays from a planar undulator. The energy bandpass, proportional to the size of the crystal reaches 180 eV for the diamond crystal and 250 eV for the beryllium. The wavelength tunability has been demonstrated by recording dichroic spectra at different rare-earths absorption edges from Pr L_{II} (6440 eV) to Tm L_{III} (8648 eV). Finally, the sign of the photon helicity can be easily changed by switching the crystal from one side of the rocking curve to the other. This property has been used to obtain a dichroic spectra keeping the magnetic field fixed and flipping the helicity from right to left which opens new fields of experiments.

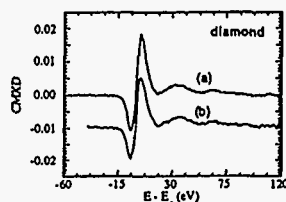


Figure 1

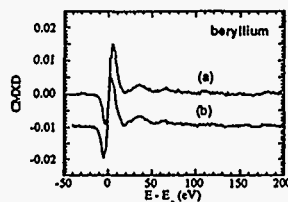


Figure 2

CMXD signals obtained for HoFe₂ at the Ho L_{III} edge (a) with the QWP (diamond in fig.1 and beryllium in fig.2) (b) below the orbit plane.

Fluorescence-Photoion-Coincidence Spectroscopy on Inner Shell Excited Molecules

M. Meyer (a), J. Lacoursière (a,b), M. Simon (a,b) and P. Morin (a,b)

- (a) Laboratoire pour l'Utilisation du Rayonnement Electromagnétique, Bâtiment 209D, Université Paris-Sud, F-91405 ORSAY Cedex, France
(b) Commissariat à l'Energie Atomique, DRECAM, SPAM, CEN Saclay, F- 91191 Gif-sur-Yvette Cedex, France

A new experimental set-up for measuring PIFCO (PhotoIon-photon of Fluorescence-Coincidence) spectra of inner shell excited molecules will be presented. The technique has been invented some years ago for the determination of lifetimes and quantum yields of the radiative emission of molecular ions (e.g. [1]) produced by discharge lamps. In the following it has been used in combination with synchrotron radiation to detect excited doubly charged ions (e.g.[2]). Since studies of inner shell resonances suffer quite often from low counting rates, we have improved the fluorescence detection efficiency by the installation of an elliptical mirror collecting about 60% of the total solid angle and have adapted a modified time-of-flight analyser for the ion detection. In contrast to the well established PhotoElectron-PhotoIon-PhotoIon-Coincidence (PEPIPICO) method (e.g. [3,4]) the coincidences with a fluorescence photon represents a new approach probing particularly the excited, fluorescing final states. Internal energies of the excited fragments as well as their relative abundance can be determined. The present set-up enables us to measure also fluorescence-photoion-photoion coincidences allowing to study the dissociation mechanisms producing excited fragments. The performed experiments on some simple molecules (N₂, N₂O, ICN and OCS) photoexcited in the N 1s, I 4d and S 2p shell, respectively, provide supplementary, specific information about the dynamics of dissociation of inner shell excited molecules investigated already in great detail by the more general PEPIPICO technique. In the PIFCO spectra taken upon resonant excitation a high intensity due to excited atomic ions was found, whereas till now only the emission from the molecular parent ion has been observed in the spectra of the dispersed fluorescence [5].

- [1] J.H.D. Eland, M. Devoret, and S. Leach, Chem.Phys.Lett.43, 97 (1976)
- [2] L. Hellner, M.J. Besnard, G. Dujardin, and Y. Malinovich, Chem.Phys.119, 391 (1988)
- [3] J.H.D. Eland, in "Vacuum Ultraviolet Photoionisation and Photodissociation of Molecules and Clusters", ed. C.Y. Ng, World Scientific (1991)
- [4] M. Simon, T. Lebrun, P. Morin, M. Lavollee, and J.L. Marechal, Nucl.Instrum.Meth. B62, 167 (1991)
- [5] E.D. Poliakov, L.A. Kelly, L.M. Duffy, B. Space, P. Roy, S.H. Southworth, and M.G. White, J.Chem.Phys.89, 4048 (1988) and Chem. Phys. 129, 65 (1989)

Comparison between 3p MCD and 2p MCD in transition metals and alloys: Is the sum applicable to itinerant magnetic system?

Tsuneaki Miyahara, Serng-Yerl Park, Takaaki Hanyu¹, Tadashi Hatano, Sadatsugu Muto², and Yasushi Kagoshima

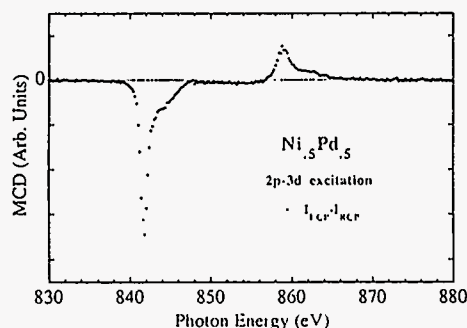
The Photon Factory, National Laboratory for High Energy Physics, Oho 1-1, Tsukuba-shi, Ibaraki 305 JAPAN

¹*Faculty of Science, Tokyo Metropolitan University, Minamiosawa 1-1, Hachiohji-shi, Tokyo 192-03 JAPAN*

²*Present address: National Institute for Fusion Science, Furo-cho, Chikusa-ku, Nagoya-shi, 464-01 JAPAN*

We measured magnetic circular dichroism (MCD) on Ni, Co, and Fe metals, and Ni-Pd, Co-Pd, Fe-Pd alloys in the 3p-3d and 2p-3d excitation regions of the transition metals, and 4p-4d and 3p-4d excitation region of Pd. An example of the results is shown in the figure. The results have shown that the orbital moments of Ni, Co, and Fe estimated through the sum rule, together with the number of 3d hole increase when they are diluted with Pd. Quantitatively, however, the above increases are more conspicuous in the 2p-3d excitation than in 3p-3d excitation. This should be ascribed to the difference between the initial states, 2p and 3p of the transition metal. In fact excitation of a deeper core electron would make MCD spectra more atomic, increasing the apparent orbital contribution.

Interpretation of the observed increase in the number of 3d holes is not so simple when we consider only the difference between the initial states. We will discuss a possibility to explain the results in terms of RKKY interaction and hybridization between 3d and ligand orbitals, and also the limitation of applicability of the sum rule.



MoE27

Photoemission Station for Crystal and Film Investigation down to 10 K.

Ivanov S.N., Mikhailin V.V., Mikheeva M.N., Moryakov V.P., Nazin V.G., Naumov I.V., Svishchev A.V., Tarasov Y.F., Tsetlin M.B.
RRC "Kurchatov Institute, Moscow, Russia

We designed new photoelectron station for in situ complex investigation of thin films, multilayer structures and cleaved single crystals. This PES station is positioned at the I.V. Kurchatov Institute of Atomic Energy at the "Siberia" synchrotron radiation (SR) source. Structurally, the PES station consists of a VUV radiation monochromator and a spectrometer. We use monochromator with two optical schemes: first scheme is normal incidence scheme for the spectral region of 4 ÷ 40 eV (resolution ~1 Å) and second is grazing incident scheme which extends the energy range of the monochromator operation up to 100 eV [1]. Both schemes are without of an entrance slit and have vertical plane of dispersion. For first scheme there is in use concave 3 meters spherical grating and for second - the plane grating with an additional focusing toroidal mirror. For both schemes diffracted beam is focused to the same exit slit and at the same angle. Optical schemes can be replaced without breaking the vacuum.

Spectrometer consists of a research chamber, a preparatory chamber and ion sputtering unit. The ultimate vacuum amounts to, approximately, 10⁻⁹ Pa in the research chamber and to 10⁻⁸ Pa in the preparatory one. The spectrometer is equipped with a locking unit intended for fast reloading of investigated samples as well as with a system of manipulators for transportation of samples. A LEED system and double-pass cylindrical mirror type energy analyzer with preretardation (for UPS and EELS) are located in the research chamber. The energy analyzer is similar to [2] and can operate with the angular resolution mode (in a limited range of angles). There is electron gun inside first analyzer cascade with preliminary electron beam monochromatization about 0.1 eV using 180° spherical deflector. Electron gun energy range is from 5 to 2500 eV. Samples can be placed at high precision manipulator or at liquid helium cryostat. The cryostat can hold 8 samples. All the preparatory operations involving extensive escape of gas are performed within the chamber of sample preparation. The preparatory chamber contains Auger spectroscopy module for chemical analysis of the sample surfaces, crystal cleavage stage, ion gun and thermoheating evaporation source. The sputtering unit is connected to preparatory chamber with transportation system to move substrates and condensed films to research chamber. This unit has two calibrated evaporation sources and one can produce multilayer systems or admixed two component alloy of two materials.

The spectrometer allows one to perform the following operations: ion beam cleaning of the sample surfaces; film deposition of practically any substances; checking the content of samples by using the Auger spectroscopy method; measuring of specimen conductance in the research chamber; surface structure investigation using low electron energy diffraction (LEED) method; optical reflectivity measurements of samples; study the luminescence spectra of samples. All investigations can be performed within the temperature range from 10 to 1300 K.

To control all functions of above mentioned facility IBM PC computer is used. All measured spectra are collected and then treated by standard methods such as subtraction of background, peak decomposition etc.

1. Ivanov S.N. et al., Pribori i Tekhnika Eksperimenta, 1988, N 4, 231.
2. Knapp J.A. et al., Rev. Sci. Instrum., 1982, v. 53, 781.

MoE28

POLARISATION AND EXCITATION ENERGY SELECTIVE SOFT X-RAY
FLUORESCENCE SPECTROSCOPY USING SYNCHROTRON RADIATION.

J. Nordgren, N. Wassdahl, J.-H. Guo, P. Skytt, L.-C. Duda, S. Butorn, C.J. Englund,
Uppsala University, Physics Department, Box 530, S-751 21 Uppsala, Sweden.

Y. Ma,
Molecular Science Research Center, Pacific Northwest Laboratories,
Richland, Washington 99352

The development of high brightness synchrotron radiation (SR) sources has opened up new interesting possibilities for soft x-ray emission spectroscopy, traditionally pursued with electron beam or broad band x-ray tube excitation. Energy and polarisation selective excitation provided by synchrotron radiation has facilitated soft x-ray emission studies of core electron resonances, multiple excitation and satellite free partial density of states (PDOS)¹, resonant inelastic scattering processes², site selective PDOS³, magnetic circular dichroism⁴, and surface adsorbate bonding⁵. The realisation of these experiments has been facilitated by a development of spectroscopic instrumentation including both soft x-ray high resolution detectors and other end station facilities, along with the SR source development. In the present paper we present an end station for polarisation and excitation energy selective soft x-ray fluorescence spectroscopy using synchrotron radiation.

The end station for soft x-ray fluorescence spectroscopy includes an experiment chamber which is rotatable 90° under UHV conditions around the incoming synchrotron radiation beam, and which is provided with a high resolution soft x-ray spectrometer. A manipulator allowing three axes of rotation, three directions of translation, as well as LN₂ cooling and resistive heating is mounted to the chamber and serves as the sample holder. Samples can be transferred under vacuum between the experiment chamber and two other chambers, one for sample preparation and one load lock chamber for introducing new samples and for sample storage.

The end station has been used at two different synchrotron radiation laboratories, at BW3 at HASYLAB in Hamburg and at BL7.0 at ALS in Berkeley. Polarisation dependent and angular resolved, selectively excited x-ray emission studies have been made of ordered as well as non-ordered systems, e.g. high T_c systems, diamond, fullerenes and molecular ices. The experimental system will be presented along with some recent scientific results.

¹N. Wassdahl, et al. AIP Conference Proc 215, 451 (1990)

²Y. Ma et al. Phys Rev Lett 69, 2598 (1992)

³S. Butorn et al. Phys Rev B, 49 (Jan 1, 1994)

⁴L. Duda et al. Proc Mat Res Soc, April 1993

⁵N. Wassdahl et al. Phys Rev Lett 69, 812 (1992)

Collimation and Polarization of Synchrotron Radiation Using
Multiple-beam Diffraction Optics

R. Pahl

CHES and Dept. of Applied and Engineering Physics
Cornell University, Ithaca, NY 14853

The collimation and polarization effects on X-rays by multiple-beam diffraction (MBD) have been studied for Laue and Bragg geometry. Using the dynamical theory of multiple-beam diffraction a significant enhancement in the reflected intensity relative to the normal two-beam case was found for several reflections. Specific Laue diffractions also result in high collimation in directions parallel and normal to the main reflection plane simultaneously. The reflected transmitted beam shows linear polarization in these cases.

Experiments on silicon and germanium crystals performed at the Cornell High Energy Synchrotron Source (CHES) are in accordance with the theoretical calculations. Applications of the MBD-effects in SR will be discussed.

* Supported by the NSF under Award No. DMR-9311772 and the Alexander von Humboldt Foundation, Germany.

Facilities for Spin resolved Photoemission at the SRS

E. M. Quinn, E. A. Seddon,
Daresbury Laboratory, Warrington, WA4 4AD, United Kingdom

Polarisation analysis of photoemitted electron beams at Daresbury is carried out using either a conventional high-energy Mott polarimeter or a conical retarding potential Mott polarimeter (the micro-Mott polarimeter). The high-energy Mott polarimeter is a fixed feature of Station 1.2. The micro-Mott polarimeter can be used on Stations 1.1, 5U.1, 3.3 or 6.1. This combination of beamlines, spectrometers and polarimeters provides the research community with the capability of performing spin resolved photoemission from both gases and solids over the photon energy range 6 eV to 1500 eV.

First results have been obtained from the dedicated spin polarised photoemission Station 1.2. A full discussion of these data from Ni(110) will be given along with a description of the station's unique characteristics and performance.

Photoemission from the 4d levels of xenon was used as a first test of the microMott polarimeter. It has since been used to perform photoemission studies of fcc Fe on Cu(100). A summary of the spin resolved spectra for a range of film thicknesses around 10 ML will be given.

We will also give an outline of ongoing instrumental developments relevant to the application of these polarimeters in the areas of thin film magnetism and metallic glasses.

A Tunable Multilayer EUV/Soft X-ray Polarimeter

J.B. Kortright, M. Rice, and K.D. Frank
Center for X-ray Optics
Lawrence Berkeley Laboratory
Berkeley, CA 94720

A tunable polarimeter using multilayer interference coatings as both reflection polarizer and transmission retarder has been constructed. The portable device bolts onto existing chambers and its rotation axis is precisely aligned to the beam. The upstream transmission phase retarder is tunable by varying its incidence angle, and the downstream reflection polarizer is tunable by translating a laterally graded multilayer. Together these two optical components allow an unambiguous determination of the polarization state of any collimated beam entering the polarimeter with energies ranging from 50 eV to at least 800 eV. The device is useful both to characterize the polarization of synchrotron sources and beamlines, and to perform polarization resolved studies of the interaction of x-rays with matter. Early studies using the polarimeter will be described.

This work was supported by the Director, Office of Energy Research, Office of Basic Energy Sciences, Materials Sciences Division, of the U.S. Department of Energy under Contract AC03-76SF00098.

Application of Oblique Incidence Detector to VUV Polarization Analyzer

Terubumi Saito, Masatada Yuri and Hideo Onuki
Electrotechnical Laboratory
1-1-4, Umezono, Tsukuba-shi, Ibaraki 305, JAPAN

It is well-known that a polarization property arises when a photon beam hits obliquely upon photosensitive surface of a detector. However, very little work was reported on the polarization property of a oblique incidence detector, especially in the VUV region. In this report, we present experimental characterization of a oblique incidence detector as a VUV polarization analyzer together with a model calculation.

Figure 1 shows a VUV ellipsometer constructed employing a semiconductor photodiode as an analyzer. Monochromatic radiation hits a sample specimen at the angle of incidence of 67.5° (or 45°). The reflected beam is detected by an inclined semiconductor photodiode. The angle of incidence to the photodiode is approximately 40° . The entire ellipsometer chamber can be rotated around the axis of the incident beam (angle α). In addition, the analyzer can be rotated around the reflected beam (angle β). Intensity measurements in the several combinations of α and β make it possible to completely determine the Stokes parameters of the incident radiation, optical constants of the sample and the detector polarization characteristics.

It has been shown that this method has an advantage in simplifying the structure of the instrument and in increasing the signal intensity compared to the case like a triple-reflection type analyzer.

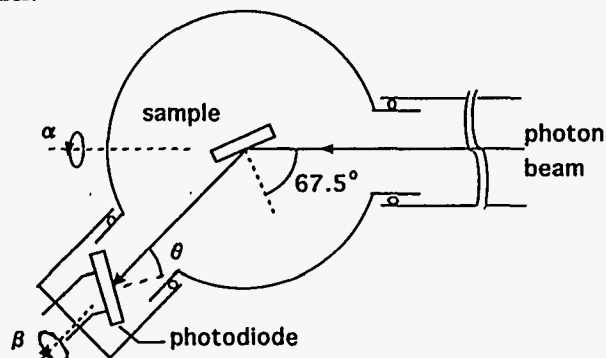


Fig. 1 Schematic layout of the polarization analyzer employed in a VUV ellipsometer.

MoE33

Fe²⁺ and Fe³⁺ ions distinguishable by X-ray anomalous scattering: method and its application to magnetite

Satoshi Sasaki

Research Laboratory of Engineering Materials, Tokyo Institute of Technology,
Nagatsuta 4259, Midori-ku, Yokohama 227, Japan

Anomalous scattering effect is useful to distinguish between elements with very similar atomic numbers. This effect also makes possible to distinguish and evaluate different valence states of the same element, if the f' values can be estimated accurately at the XANES region of an absorption edge. Valence-state refinements on theoretical f basis have been performed by powder diffraction.¹⁾

From the observation of XANES absorption spectra of FeO and Fe₂O₃ at the Photon Factory BL-3A, the chemical shift of about 5 eV was found between ferrous and ferric ions which coordinate octahedrally with the neighboring oxygen atoms in the respective structures. The spectrum of magnetite (Fe₃O₄; space group $Fd\bar{3}m$, $a = 8.356(3)$ Å, $Z = 8$) was confirmed to have an intermediate pattern between those of FeO and Fe₂O₃. The chemical shift reflects the difference of electronic states corresponding to Fe²⁺: $1s \rightarrow 3d(4p)$ and Fe³⁺: $1s \rightarrow 3d(4p)$. The linear absorption coefficient can be represented using f'' which is connected with f' by the Kramers-Kronig dispersion relation. In order to obtain the observed f' values, the cross section data were partially replaced with observed ones near and at the Fe K absorption edge in the Cromer and Liberman's calculation.²⁾ Beam conditions such as the energy resolution were taken into account for adjusting experimental difference. Finally, the maximum difference in scattering factor between Fe²⁺ and Fe³⁺ was estimated to be about 2.3 at an appropriate wavelength near the Fe²⁺ edge.

Synchrotron X-ray diffraction data from an Fe₃O₄ single crystal were collected using a vertical-type four-circle diffractometer at the Photon Factory BL-10A. An Si(111) monochromator was used to select several wavelengths at the XANES region of the Fe K absorption edge. Of a total 160 reflections measured up to $2\theta = 120^\circ$, 21 averaged reflections with $F \geq 3\sigma_F$ were used in each f' analysis. Difference Fourier syntheses based on two extremities of $\rho_{\text{obs}} - \rho_{\text{calc}}[\text{Fe}^{2+}$ in octahedral and tetrahedral sites] and $\rho_{\text{obs}} - \rho_{\text{calc}}[\text{Fe}^{3+}$ in the sites] were very helpful to detect the spatial distribution of ferric and ferrous ions. The s dependency of residual structure factors may suggest orbital spreading of K -shell electrons.

[1] e.g. J.P. Attfield: Nature, 343, 46 (1990); J.K. Warner et al.: J. Am. Chem. Soc., 114, 6074 (1992).

[2] D.T. Cromer and D. Liberman: J. Chem. Phys. 53, 1891 (1970).

MoE34

**High Energy Synchrotron Radiation
A New Probe for Condensed Matter Research**

J.R. Schneider, R. Bouchard, T. Brückel, M. Lippert,
H.-B. Neumann, H.F. Poulsen, U. Rütt, T. Schmidt and
M. von Zimmermann

Hamburger Synchrotronstrahlungslabor HASYLAB at
Deutsches Elektronen-Synchrotron DESY,
Notkestr. 85, D 22603 Hamburg, Germany

The absorption of 150 keV synchrotron radiation in matter is weak and, as normally done with neutrons, bulk properties are studied in large samples. However, the k-space resolution obtained with a Triple Crystal Diffractometer (TCD) for high energy synchrotron radiation is about one order of magnitude better than in high resolution neutron diffraction.

The technique has been applied to measure the structure factor $S(Q)$ of amorphous solids up to momentum transfers of the order of 32 \AA^{-1} , to study the intermediate range Ortho-II ordering in large, high quality $\text{YBa}_2\text{Cu}_3\text{O}_{6.5}$ single crystals and for investigations of the defect scattering from annealed Czochralski grown silicon crystals. Magnetic superlattice reflections have been measured in MnF_2 demonstrating the potential of the technique for high resolution studies of ground state bulk antiferromagnetism. Recently the question of two length scales in the critical scattering at the 100 K phase transition in SrTiO_3 was studied.

At the PETRA storage ring, which serves as an accumulator for the HERA electron-proton storage ring at DESY and which is actually operated at electron energies between 7 and 12 GeV, an undulator beam line is currently under construction and should be available in summer 1995. It opens up exciting new research opportunities for photon energies from about 20 to 150 keV.

MoE35

**A Spectrometer for High Resolution Resonant
Inelastic X-Ray Scattering**

W.Schülke, A. Kaprolat, Th. Fischer, K. Höppner and F. Wohlert

Institute of Physics, University of Dortmund, D-44221 Dortmund, Germany

High resolution resonant inelastic X-ray scattering is on the way to become a powerful tool for investigating element specifically and Bloch-k-vector sensitively the excitation of valence electrons in solids /1/, where for spin ordered systems the utilization of resonant exchange scattering /2/ might provide access to the dynamic of spin correlation. Moreover, this method offers the possibility for measuring the near-edge fine structure free of core-hole lifetime broadening /3/.

In order to obtain an appropriate energy and k-space resolution, one needs an overall resolution of better than 1 eV both for the passband of the exciting radiation and for the analyzing spectrometer, together with a q-resolution (q = momentum transfer) of the order of $\Delta q/q = 0.03$. Both the exciting passband and the analyzer passband have to be tunable. In order to achieve these goals, we have equipped the existing setup for $S(q, \omega)$ -measurements /4/ at HASYLAB with an additional tunable analyzing spectrometer. We have chosen a full Rowland geometry spectrometer with doubly bent Si crystals in order to use horizontal and vertical focussing. The full Rowland geometry has been realized by mechanically coupling the detector translation both with the θ -rotation of the analyzing crystal and the 2θ -rotation of the detector arm and by installing a computer-controlled variation of the sample to analyzing crystal distance. At the detector position either a linear position sensitive gas-filled proportional counter or a solid state detector can be used. In the first case the analyzer resolution is mainly determined by the spatial resolution of the counter, in the latter case by the lateral size of the illuminated area on the sample. This full Rowland geometry spectrometer was connected to the fixed-exit sagittally focussing double crystal monochromator of the Wiggler-beamline W2 of HASYLAB.

The results of test measurements both of high resolution resonant Raman scattering on Cu and of the Cu- and Ni-K-edges in the light of the resonant scattered radiation will be presented. The Cu-K-edge, free of the core-hole lifetime broadening, exhibit a much better resolved near-edge fine structure compared with absorption measurements and indications for a quadrupole transition induced pre-edge structure. The necessity of a careful selfabsorption correction of these edge spectra is stressed.

/1/ Y. Ma, N. Wassdahl, P. Skytt, J. Guo, J. Nordgren, P.D. Johnson, J.-E. Rubensson, T. Boske, W. Eberhardt, and S.D. Kevan, Phys. Rev. Lett. 69, 2598 (1992)

/2/ P. Hannon, G.T. Trammel, M. Blume, and D. Gibbs, Phys. Rev. Lett. 61, 1245 (1988)

/3/ K. Hämäläinen, D.P. Siddons, J. B. Hastings and L.E. Berman, Phys. Rev. Lett. 67, 2850 (1991)

/4/ A. Berthold, S. Mourikis, J.R. Schmitz, W. Schülke and H. Schulte-Schrepping, Nucl. Instr. and Meth. A317, 373 (1992)

MoE36

First IXSS-Measurement of the Dynamic Structure Factor $S(q,\omega)$ of Electrons in a Solid Noble Gas (He)

W. Schülke, A. Kaprolat and K.J. Gabriel

Institute of Physics, University of Dortmund, D-44221 Dortmund, Germany

N. Schell and E. Burkel

Institute of Applied Physics, University of Erlangen, D-91054 Erlangen, Germany

R.O. Simmons

University of Illinois, Urbana, IL 61801, USA

Inelastic X-ray scattering spectroscopy (IXSS) yields information about the dynamic structure factor $S(q,\omega)$ of electrons, which in turn is related to the dielectric function $\epsilon(q,\omega)$, thus providing information about collective and individual excitation of electrons. To the knowledge of the authors up to now no measurements of $S(q,\omega)$ on single crystals of solid noble gases have been performed, because these samples require a pressure cell providing pressure within the kbar regime and temperatures of several Kelvin, so that only hard X-rays can probe the excitation spectrum. Nevertheless, when measuring $S(q,\omega)$ by means of inelastic hard X-ray scattering, the signal will be contaminated by the contributions of the pressure cell, so that a measurement of the empty cell must be subtracted appropriately from the spectra of the filled cell in order to extract the sample signal.

We present first IXSS-measurements on single crystal solid He, performed at the Compton spectrometer of the Wiggler W2-beamline of HASYLAB /1/. The He single crystal (hcp) was grown in a pressure cell made of Be under a pressure of 600 bar and held at a temperature between 5 and 7 Kelvin /2/. The primary energy was 13.8 keV. The measurement was carried out with $q \parallel c$ -axis and $q=0.45$; 0.97 and 1.24 at. units. The achieved energy resolution was 2 eV, the countrate in the profile maxima 50 cts./s. The subtraction of the empty cell spectrum from the filled cell spectrum has been performed after normalizing both spectra according to the Johnson f-sum rule. The Fig.1 shows the pure He- $S(q,\omega)$ spectrum for $q=0.97$ at. units. One can clearly see a prominent structure around $\Delta E=22$ eV (clearly visible also in the other spectra), which can be ascribed to an excitonic excitation separated by 2.6 eV from the He absorption edge.

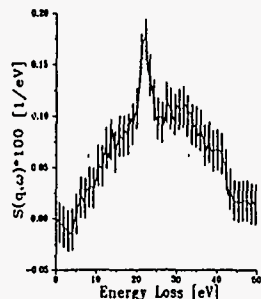


Fig.1 Pure solid He $S(q,\omega)$ spectrum for $q=0.97$ at. units

/1/ A. Berthold, S. Mourikis, J.R. Schmitz, W. Schülke and H. Schulte-Schrepping, Nucl. Instr. and Meth. A317, 373 (1992)

/2/ N. Schell, R.O. Simmons and E. Burkel, HASYLAB Annual Report 1993, p.963

Undulator Test of a Bragg Reflection

Elliptical Polarizer at ~ 7.1 keV

S.D. Shastri, K.D. Finkelstein, Qun Shen, B.W. Batterman

Cornell High Energy Synchrotron Source

and the School of Applied and Engineering Physics,

Cornell University, Ithaca, New York 14853

and

D.A. Walko

Physics Department, University of Illinois at Urbana-Champaign,

Urbana, Illinois 61801

Abstract

A method employing perfect crystal diffraction optics for the generation of elliptically polarized X-rays was tested at CHESS beamline A2 under the high-brightness conditions of a standard undulator. In this method, polarization state selection is achieved by precise control of the incident angle of a collimated, approximately 45°-linearly pre-polarized beam of X-rays entering a symmetrically cut, 4-bounce Bragg reflection channel-cut Ge(220) crystal. In addition to the efficiency of the device, the full polarization state of the output beam as a function of incident angle, including the purity of circular polarization P_3 , was measured directly using the multiple-beam Bragg reflection technique with a GaAs crystal polarimeter. The reversibility of the circular helicity by changing the incident angle and the ability to scan the optics in energy was demonstrated at the vicinity of the Fe K-edge at 7.1 keV.

A soft x-ray emission spectrometer for undulator radiation

S. Shin, A. Agui, M. Fujisawa, Y. Tezuka, and T. Ishii

*Synchrotron Radiation Laboratory, Institute for Solid State Physics,
The University of Tokyo, 3-2-1 Hongo, Tanashi, Tokyo 188, Japan*

An experimental system for soft x-ray emission spectroscopy (SXES) using undulator beam line was made. By this system, high resolution SXES and photoelectron emission spectroscopy (PES) can be measured at the same time. The experimental system is designed to be attached to the undulator beam lines, BL2B, BL16u, and BL19B at Photon Factory.

Spectrometer uses the Rowland circle geometry in which input slit, concave grating, and multichannel detector lie on the focal circle. Three holographic ion-etched gratings are changeable in the vacuum. The Rowland circle radii of gratings are 5 m, 7 m, and 10 m and their line densities are 600, 1200, and 2400 l/mm, respectively. The detector is positioned tangentially to the Rowland circles by precision movement in a three-axis coordinate system of two translations and one rotation. The size of the multichannel detector is 30x80 mm². It consists of CsI-coated multichannel plates (MCP) and a position-sensitive detector. In addition, a retarding screen is mounted in front of the MCP in order to increase the quantum efficiency of the detector. The resolution $E/\Delta E$ is about 1400~340 for 100 μ -input-slit width for the photon energy region from 30 eV to 1000 eV.

MoE39

New experimental set-up devoted to the Auger Electron Ion multiple coincidences spectroscopy

Laurence FERRAND-TANAKA^(1,2), Marc SIMON^(1,2), Roland THISSEN^(1,3), Michel LAVOLLEE⁽¹⁾ and Paul MORIN^(1,2)

- (1) LURE, Bt 209d, Centre Universitaire, 91405 Orsay Cédex, France
- (2) CEA/ DRECAM/ SPAM, CEN Saclay, Bt 522, 91191 Gif Cédex, France
- (3) LSP, Université de Liège, Sart Tilman B6, 4000 Liège, Belgium

Much work has been devoted to the dissociation of inner shell excited molecules¹ and the understanding of the processes is now quite good² but smeared out by the very large number of formed electronic states of the ion. The dissociation measurement of those selected states is an attractive purpose²⁻⁵. Taking advantage of the pulsed character of the synchrotron radiation light, we have recently developed an original experimental set up combining an electron analyser with a time of flight mass spectrometer without angular discrimination, operated with a strong pulsed electrostatic field. This allows high counting rates for multiple coincidence measurements Auger Electron PhotoIon PhotoIon COincidences. We will focus our contribution on the experimental set up and show new results obtained with core excited N₂O and demonstrate how we get more insight into the relaxation dynamics by the selection of the excited state combined with the selection of the final state. The "break down curve" of very excited singly charged ion obtained by resonant Auger ion spectroscopy exhibits interesting effects such as scrambling of the atoms within the core excited molecule before dissociation.

References

- (1) M. Simon, T. Lebrun, P. Morin, M. Lavollée and J. L. Maréchal, N. I. M. B 62, 167 (1991)
- (2) T. Lebrun, M. Lavollée, M. Simon and P. Morin, J. Chem. Phys. 98, 2534 (1993)
- (3) R. Murphy and W. Eberhardt, J. Chem. Phys., 89, 4054 (1988)
- (4) D. Hanson, C. I. Ma, K. Lee, D. Lapiano-Smith and D. Y. Kim, J. Chem. Phys. 93, 9200 (1990)
- (5) K. Ueda, H. Chiba, Y. Sato, T. Hayaishi, E. Shigemasa and A. Yagishita, Phys. Rev. A 46, R5 (1992)

MoE40

Polarization modulation spectroscopy for MCD study using polarizing undulator

K. Yagi, M. Yuri, and H. Onuki

Electrotechnical Laboratory, Tsukuba-shi, Ibaraki 305, Japan

Direct Measurement of Magnetic Circular Dichroism and Kerr Rotation Spectra in VUV using Four-Mirror Polarizer

M. Suzuki, K. Hanmura, T. Kotani, N. Yamaguchi, M. Kobayashi, and A. Misu

Department of Physics, Science University of Tokyo,
1-3 Kagurazaka, Shinjuku-ku, Tokyo 162, Japan

For magneto-optical measurements in the VUV region, we have constructed a four-mirror reflection type polarizer which is reasonably superior as an optical component. Fig. 1 sketches the polarizer. The polarizer consists of two pairs of parallel plane gold mirrors spaced with thickness gauge blocks. The incident angle of each mirror was set at 79° , and the polarizer was found to work as a quarter-wavelength plate in a relatively wide photon energy region from 5 to 40 eV. The aperture is 12×9 mm for parallel rays, and the angular aperture is about 6° .

The optical properties of the polarizer were measured with the visible light. Since the high accuracy of the parallelism 1.6×10^{-4} rad of the pair mirrors was archived, the direction of an incident ray changes only by 0.33 mm per one meter. With the light of Na D line, relative transmittance $\rho^2 = T_p / T_s$ and relative phase retardation $\delta = \delta_p - \delta_s$ were measured for parallel rays and for convergent rays of full aperture. The measured values of ρ^2 and δ for the convergent rays were respectively coincident with those for the parallel rays within the experimental accuracy. The four-mirror polarizer was easy to set into any optical path and worked perfectly as a polarizer.

The polarization characteristics were measured at Photon Factory, KEK. The ρ^2 and the δ were obtained in the VUV with the convergent rays of projection angle 2° . The polarizer produces circular polarization which is used in magnetic circular dichroism (MCD) measurement, but it can not be used as a circular polarizer around 5 eV because the δ is close to 180° . On the other hand, the ρ^2 is less than 0.35 over the measured photon energy range, and the instrument works as a quasi-linear analyzer for Kerr rotation (KR) measurement. The intensity of the transmitted light was sufficient for our purpose.

We measured the MCD and the KR spectra of yttrium iron garnet (YIG) using the four-mirror polarizer in the range from 24 to 36 eV. The magnetic field modulation technique with an AC electromagnet was used. It is the first experiment that the conjugate magneto-optical spectra, MCD and KR, are obtained in the photon energy range where no transmission type optical component works. The Kramers-Kronig relation between the MCD and KR was exactly obtained, and it was shown that our instruments gave correct results.

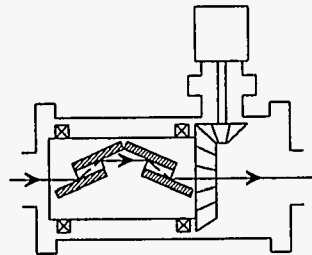


Fig.1 The sketch of the four-mirror polarizer presently constructed.

We developed a polarization modulation spectroscopy in the XUV region for magnetic circular dichroism (MCD) measurements. We used a polarizing undulator with crossed and retarded magnetic fields which was proposed by Onuki¹⁾. It enables us to obtain radiation adjusting the polarization states arbitrarily and rapidly. It is expected to be very useful in polarization modulation spectroscopy for MCD study in the XUV region.

Up to now MCD measurements have been restricted to the region from visible to ultraviolet. Recent advances in synchrotron radiation instrumentation have made possible the utilization of high quality circularly polarized light in the XUV region. Various experiments and calculations have established magnetic x-ray circular dichroism (MXCD) as an important technique for investigating magnetic materials. The previous experiments designed to measure MXCD spectra using synchrotron radiation were all fixed polarization instruments. No MXCD experiment has apparently reported yet using the polarization modulation technique. In order to reveal fine structures in the spectra, the polarization modulation method has to be applied to the MCD measurement.

The experiments were performed at the storage ring TERAS of the Electrotechnical Laboratory. Fig.1 shows schematic diagram of the polarization modulation experimental setup. The degree of circular polarization P_c of the radiation depends on the phase difference of two crossed magnetic fields. It can be varied in a range of $-0.9 < P_c < 0.9$ and modulated with frequencies up to 3 Hz. The elliptical radiation generated by the undulator is quasi-monochromatic. The photon energy is selected by varying the electron energy or the magnetic field intensity of the undulator by the change of gap of its magnet arrays. The photon energy of the undulator radiation is tuned to the output photon energy of the monochromator by adjusting the undulator magnet gap in order to make effective use of the undulator radiation. The monochromator is a grazing incidence toroidal grating monochromator. A sample was attached directly to the Nd-Co-B permanent magnet producing 0.4 T at the position of the sample. The fractional change in reflectivity caused by the polarization was measured with a technique of phase sensitive detection, which can detect a relative difference of reflectivity of circularly polarized photons as small as 0.1%.

We successfully measured the MCD of $Y_3Fe_5O_{12}$ (YIG) in the vacuum ultraviolet region between 22 eV and 40 eV. Strong MCD features were observed for the inner core transitions of Y^{3+} from $4p^6$ to $4p^5(4d+5s)$ levels, even though its ground state has $J=0$.

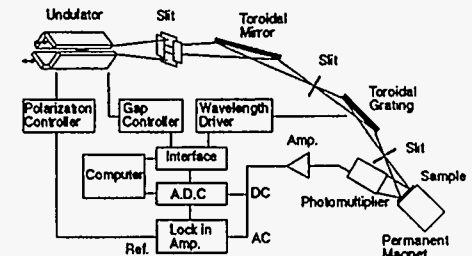


Fig.1: Schematic diagram of the polarization modulation experimental setup. The polarizing undulator that was installed in the storage ring TERAS of ETL enables us to obtain polarized radiation of any ellipticity and modulate with frequencies up to 3Hz. The photon energy of the undulator radiation is tuned to the output photon energy of the monochromator by adjusting the undulator magnet gap. The fractional change in reflectivity caused by the polarization was measured with a technique of phase sensitive detection.

1) H.Onuki, Nucl. Instrum. Methods. A246, 94 (1986)

A Soft-X-Ray Emission Spectrometer Equipped with a Multilayer Rotating Analyzer for Polarized Emissions

M. Yanagihara and Y. Goto

Research Institute for Scientific Measurements, Tohoku University
2-1-1 Katahira, Aoba-ku, Sendai 980-77, Japan

From the definite dependence of C K-emission spectra of diamond on the energy of the excitation photons, Ma et al.¹ recently proposed that the absorption-emission process should be treated as a coherent inelastic scattering process. To verify this proposal, we should examine the polarization degree of the x-ray emission while exciting with linearly polarized photons. We have so far developed multilayer mirrors for soft x-rays (SXR's), and found that they are the most useful polarizing elements in the SXR region at around 45° angle of incidence,² i.e., the Brewster angle. We have recently made a new instrument for SXR emission spectroscopy. The spectrometer consists of a flat-field grating and a multichannel detector (Fig. 1a). A rotating analyzer mounted with a SXR multilayer is equipped to measure polarization degree of the SXR emission (Figs. 1a and 1b). Figure 2 shows (a) B K-emission spectrum of h-BN and (b) spectral reflectance of a Ru/B₄C 199-layer coating. The peak at 194 eV in Fig. 2a is due to the scattered excitation light, which is completely filtered off with the multilayer before the microchannel plate (MCP). Using this instrument we ascertained that the B K-emission from h-BN is partially polarized. This polarization is due to mostly the anisotropic property of the h-BN crystal.³ For a sintered B₄C sample we observed slight polarization, which is probably attributable to the coherent scattering process.

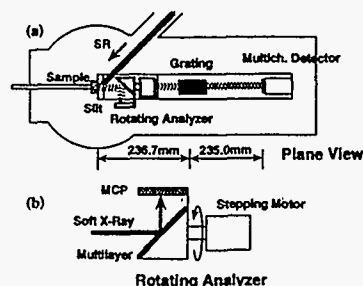


Fig. 1

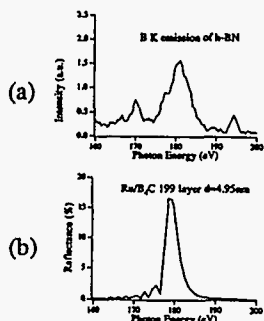


Fig. 2

References

1. Y. Ma et al., Phys. Rev. Lett. 69 (1992) 2598.
2. M. Yanagihara et al., Rev. Sci. Instrum. 63 (1992) 1516.
3. E. Tegeler et al., Phys. Stat. Sol. (b) 91 (1979) 223.

X-RAY MOSSBAUER OPTICS OF HIGH ANGULAR AND FREQUENCY RESOLUTION

V.A.Belyakov

Surface and Vacuum Research Centre, Kravchenkoko str.8,
117331 Moscow, Russia

Application of synchrotron radiation (SR) dedicated sources to Mossbauer spectroscopy opens new possibilities in the field of Mossbauer experiments, in particular, and in the field of gamma- and X-ray optics in general [1]. These possibilities are connected as well with fundamental research in physics [2] so with applied researches in solid state physics and with development of gamma and X-ray spectroscopy of extremely high (sub millielectronvolt) resolution [3]. An overview of the recent progress in the field of X-ray SR optics of solids containing Mossbauer nuclei is presented. The main topics of the overview are: nuclear resonant magnetic Bragg diffraction of SR, coherent inelastic Mossbauer scattering of SR, different approaches to Mossbauer filtration of SR including the filtration at an isotope interface and with the help of surface guided Mossbauer modes, polarization peculiarities of the SR Mossbauer optics. Related to the problem recent experimental results are discussed and the perspectives of the further development of SR Mossbauer optics are evaluated.

References

1. V.A.Belyakov "Diffraction Optics of Complex Structured Media", Springer Verlag, New York, 1992.
2. Yu.Kagan, A.M.Afanas'ev, V.G.Kohn, Phys.Lett.A 68, 339 (1978); J.Phys.Ser.C 12, 615 (1979).
- 3.V.A.Belyakov, Sov.Phys.Usp.30, 331 (1987).

Simple UHV Compatible Electromagnet for Magnetic Scattering Studies

Erik D. Johnson
Brookhaven National Laboratory National Synchrotron Light Source
Upton, Long Island New York 11973-5000

ABSTRACT

For our soft x-ray magnetic reflectivity measurements, we often require some means to magnetize our samples. Since our experiments are typically performed with photon energies below 1 keV the scattering apparatus must be operated in vacuum. In the past, we have utilized electromagnets with soft iron pole pieces and solenoid windings of 22 gauge copper wire insulated with teflon tubing or fiberglass braid. These magnets could be slow to pump down in spite of the relatively low number of windings. The old magnet would provide a comparatively modest field of only 400 Gauss for a 10 A current, which deposited nearly 13 W in the windings. In a new design described in this paper, we have substituted conductors fashioned from sheets of 0.025" thick copper for the copper wire previously employed. The cross section of these windings is comparable to that of 6 gauge wire hence higher current operation is possible with much lower heating. In addition, the windings are separated from each other using small diameter alumina spacers, hence the design is much more vacuum compatible than our original conventional magnet. The current design provides a field of 900 Gauss at 10 A with a power dissipation the order of 1 W.

*Work performed under the auspices of the U.S. Department of Energy, under contract DE-AC02-76CH00016.

Performance Evaluation of a Soft X-ray Quadruple Reflection
Circular Polarizer

Hartmut Höchst, Peter Bulicke, Tom Nelson and Fred Middleton+
Synchrotron Radiation Center, University of Wisconsin-Madison
3731 Schneider Dr., Stoughton WI 53589.

and

+Physical Sciences Laboratory, University of Wisconsin-Madison
3731 Schneider Dr., Stoughton WI 53589.

We have built a quadruple reflection polarizer which can be used in the energy range $h\nu=8-130$ eV to convert linearly polarized synchrotron radiation into circularly polarized light of either left or right handedness. The conversion efficiency can be tailored by selecting different reflector coating materials to enhance the optical throughput over a certain energy range. The polarizer is part of a new variable polarization beamline consisting of a stigmatic PGM and a 48 period linear undulator which are currently under construction at SRC. The concept of converting linearly polarized light by means of an optical phase shifter is expected to deliver at least an order of magnitude more flux and significantly higher degrees of circular polarization as one might expect from a x-field undulator design.

We have tested the optical performance and phase shifting properties of a prototype quadruple reflector polarizer up to $h\nu=130$ eV using a bending magnet beamline. Our design permits independent adjustment of the angle of reflection θ as well as the angle of rotation α along the light axis. These adjustments allow to operate the polarizer at a given energy in a mode where either the degree of circular polarization $P_{\text{circ}}=S_3/S_0$ or the modified throughput or figure of merit TP_{circ}^2 is maximized.

We present first data on the conversion efficiency and measurements determining the degree of circular polarization. The experimental results are in good agreement with our extensive model calculations.

MoE46

Measurement of the X-ray spectrometric properties of cesium hydrophthalate (CsAP) crystal with the synchrotron radiation

L. BECK, C. BIZEUIL, P. STEMMLER et F. LEGRAND
CEA/Service CEM
BP 12
91680 Bruyères-le-Châtel
FRANCE

Abstract

Single crystals of hydrophthalates have been often investigated by several authors [1, 2] for their high resolution as analyser crystals in spectrometers. Seidl et al. [3] advanced the hypothesis that in principle it is possible to attain the greatest reflective capacity for X-rays with the heaviest cation available in that structure : Cs+. Therefore, there is only little information in the literature of the performance of the crystal of CsAP. For that reason we tested one sample of that crystal at 1000 and 2500 eV on the beamline SB3 at the Super ACO storage ring (LURE-Orsay). In the BL-SB3 we can select several types of double-crystal monochromators; we used beryl crystals at 1000 eV and Si crystals to work at higher energy. In both cases we performed absolute measurement of the rocking curves. We compared the performance of CsAP to other crystals which are isostructural : KAP, RbAP and TIAP. Our results confirm the predictions of Seidl et al.: we observe that the CsAP crystal has the best integrated reflectivity.

In addition we compare the experimental values with a simulation based on the improved version [4] of Shadow [5] developed in our laboratory. This version allows to simulate rocking curves of any crystal structures. In that case, the results are also in remarkable agreement.

-
- [1] P.G. Burkhalter et al., *J. Appl. Phys.* 52(7) (1981)
 - [2] A. J. Burek et al., *Astrophys. J.* 191, 533 (1974)
 - [3] P. Seidl et al., *Appl. Opt.* 16, 578 (1977)
 - [4] F. Legrand et al., to be published in the proceedings of "Sources cohérentes et incohérentes, Nouan-le-Fuzelier, Annales de Physique, (1994)
 - [5] B. Lai et F. Cerrina, *NIM A246*, 337, (1986)

MoE47

Time	TUESDAY, JULY 19, 1994																																		
COOPERATIVE PHENOMENA																																			
TuA Staller Center Chairpersons: J. Schneider (HASYLAB); T. Ishii (Tokyo)																																			
8:30	B. J. Birgeneau (MIT)																																		
	<i>Cooperative Phenomena: Scattering</i>																																		
9:15	G.A. Sawatsky (Groningen)																																		
	<i>Cooperative Phenomena: Spectroscopy</i>																																		
10:00	Coffee Break																																		
<table border="1" style="width: 100%; border-collapse: collapse;"> <thead> <tr> <th data-bbox="212 793 358 884"></th> <th data-bbox="358 793 862 884" style="text-align: center;"> TuB Staller Center Chairpersons: D. Mills (APS) C. Malgrange (Paris) </th> <th data-bbox="862 793 1404 884" style="text-align: center;"> TuC Student Union Chairpersons: P. Thiry (LURE) S.T. Belyaev (KSRS) </th> </tr> </thead> <tbody> <tr> <td data-bbox="212 999 358 1031">10:30</td> <td data-bbox="358 999 862 1031">T. Ishikawa (PF)</td> <td data-bbox="862 999 1404 1031">A. Fontaine (LURE)</td> </tr> <tr> <td></td> <td data-bbox="358 1031 862 1062"><i>X-ray phase retarders</i></td> <td data-bbox="862 1031 1404 1062"><i>Dispersive XAFS</i></td> </tr> <tr> <td data-bbox="212 1073 358 1104">10:50</td> <td data-bbox="358 1073 862 1104">Q. Shen (CHESS)</td> <td data-bbox="862 1073 1404 1104">W. Drube(HASYLAB)</td> </tr> <tr> <td></td> <td data-bbox="358 1104 862 1136"><i>X-ray polarization analysis</i></td> <td data-bbox="862 1104 1404 1136"><i>Non-radiative X-ray Res-Raman scattering from solids</i></td> </tr> <tr> <td data-bbox="212 1188 358 1220">11:10</td> <td data-bbox="358 1188 862 1220">T. Brückel(HASYLAB)</td> <td data-bbox="862 1188 1404 1220">J. Andersen(MAXLAB)</td> </tr> <tr> <td></td> <td data-bbox="358 1220 862 1293"><i>High Q Res. Scattering with high energies</i></td> <td data-bbox="862 1220 1404 1293"><i>High resolution photo-emission</i></td> </tr> <tr> <td data-bbox="212 1304 358 1335">11:30</td> <td data-bbox="358 1304 862 1335">E. Vlieg (FOM)</td> <td data-bbox="862 1304 1404 1335">B. Sinkovic (NYU)</td> </tr> <tr> <td></td> <td data-bbox="358 1335 862 1367"><i>Surface Diffraction</i></td> <td data-bbox="862 1335 1404 1367"><i>Spin polarized photo-emission</i></td> </tr> <tr> <td data-bbox="212 1377 358 1409">11:50</td> <td data-bbox="358 1377 862 1409">W. Schülke (Dortmund)</td> <td data-bbox="862 1377 1404 1409">H. Hochst (SRC)</td> </tr> <tr> <td></td> <td data-bbox="358 1409 862 1482"><i>Inelastic Scattering: Medium Resolution</i></td> <td data-bbox="862 1409 1404 1482"><i>VUV Circular Polarizers</i></td> </tr> </tbody> </table>				TuB Staller Center Chairpersons: D. Mills (APS) C. Malgrange (Paris)	TuC Student Union Chairpersons: P. Thiry (LURE) S.T. Belyaev (KSRS)	10:30	T. Ishikawa (PF)	A. Fontaine (LURE)		<i>X-ray phase retarders</i>	<i>Dispersive XAFS</i>	10:50	Q. Shen (CHESS)	W. Drube(HASYLAB)		<i>X-ray polarization analysis</i>	<i>Non-radiative X-ray Res-Raman scattering from solids</i>	11:10	T. Brückel(HASYLAB)	J. Andersen(MAXLAB)		<i>High Q Res. Scattering with high energies</i>	<i>High resolution photo-emission</i>	11:30	E. Vlieg (FOM)	B. Sinkovic (NYU)		<i>Surface Diffraction</i>	<i>Spin polarized photo-emission</i>	11:50	W. Schülke (Dortmund)	H. Hochst (SRC)		<i>Inelastic Scattering: Medium Resolution</i>	<i>VUV Circular Polarizers</i>
	TuB Staller Center Chairpersons: D. Mills (APS) C. Malgrange (Paris)	TuC Student Union Chairpersons: P. Thiry (LURE) S.T. Belyaev (KSRS)																																	
10:30	T. Ishikawa (PF)	A. Fontaine (LURE)																																	
	<i>X-ray phase retarders</i>	<i>Dispersive XAFS</i>																																	
10:50	Q. Shen (CHESS)	W. Drube(HASYLAB)																																	
	<i>X-ray polarization analysis</i>	<i>Non-radiative X-ray Res-Raman scattering from solids</i>																																	
11:10	T. Brückel(HASYLAB)	J. Andersen(MAXLAB)																																	
	<i>High Q Res. Scattering with high energies</i>	<i>High resolution photo-emission</i>																																	
11:30	E. Vlieg (FOM)	B. Sinkovic (NYU)																																	
	<i>Surface Diffraction</i>	<i>Spin polarized photo-emission</i>																																	
11:50	W. Schülke (Dortmund)	H. Hochst (SRC)																																	
	<i>Inelastic Scattering: Medium Resolution</i>	<i>VUV Circular Polarizers</i>																																	
12:30	LUNCH																																		
2-5:30	BEAMLIN POSTERS																																		
6:00	DINNER																																		
7:00-10:00	SOURCES POSTERS																																		

Session TuA - Invited Talks

ROLE OF X-RAY SPECTROSCOPY IN THE UNDERSTANDING OF COOPERATIVE PHENOMENA

G.A. Sawatzky, Laboratory of Applied and Solid State Physics, Materials Science Centre, University of Groningen, Nijenborgh 4, 9747 AG Groningen, The Netherlands

Some of the most interesting areas of research in condensed matter science involve materials and phenomena in which the cooperative behaviour of electrons and magnetic moments play the most important role. Examples are the high T_c superconductors, magnetic materials in thin film and multilayer structures, Kondo and heavy fermion systems and C_{60} compounds. X-ray spectroscopies have and are playing an extremely important role in obtaining a basic understanding of the electronic structure and related physical properties of these systems. Starting with a brief introduction to the electronic structure of strongly correlated systems I will describe with the use of examples some of the ways in which x-ray spectroscopies have and will help us to understand these systems. I will concentrate on systems with quite atomic like open shells like the 3d transition metal compounds and rare earths. Various forms of x-ray spectroscopies like core level photoemission valence band photoemission, x-ray absorption resonant photoemission, magnetic x-ray dichroism, Auger-photoelectron coincidence spectroscopy, x-ray fluorescence, etc. will be discussed with examples of new science which has resulted and some new techniques which have been and are being developed. Surprising to many of us is the discovery that x-ray spectroscopic techniques can be used to obtain detailed information on ground state and low energy scale properties of magnetic materials. The use of x-ray spectroscopies to study magnetic materials as thin films and their surfaces will be demonstrated and some possible future developments discussed.

Session TuB - Invited Talks

Development and Application of X-Ray Phase Retarders

Keiichi HIRANO, Tetsuya ISHIKAWA* and Seishi KIKUTA*

Photon Factory, KEK, Oho, Tsukuba, Ibaraki 305, Japan

**Department of Applied Physics, Faculty of Engineering, The University of Tokyo,
7-3-1 Hongo, Bunkyo-ku, Tokyo 113, Japan*

Development of X-ray phase retarders (XPR's) has opened up new possibilities to control and analyze polarization of SR in the X-ray region. One of the advantages to use XPR's for polarization control of SR (from practical point of view, production of circularly polarized X-rays (CPX) is important) is that well-defined polarization is supplied to a sample since an XPR is usually the last optical component before the sample and no depolarization is introduced by other optics.

Up to date, we have mainly used Si crystal for a Bragg-transmission type XPR [1-5]. However, the performance of the Bragg-transmission type XPR is greatly enhanced if light crystals such as diamond, LiF and so on is employed instead of Si crystal [6]. The polarization conversion properties of the diamond XPR was studied at BL-15C of the Photon Factory. A horizontally polarized beam monochromatized with a Si(111) double crystal ($\lambda=1.48\text{\AA}$) was directly converted to CPX in the 1mm-thick diamond (100) crystal plate in Bragg geometry with conversion efficiency of 25%. Laue-transmission type XPR using diamond crystal was also investigated.

In the higher energy X-ray region, XPR using Ge crystal in Laue geometry is available. Mills et al. developed XPR using diffracted beam [7], but the dynamic theory of X-ray diffraction shows that forwardly-diffracted beam is also available for the XPR [8]. One of the advantages to use forwardly-diffracted beam instead of diffracted beam is that both of beam position and direction are kept constant during polarization conversion. Fast switching of photon helicities is easily performed by making use of the symmetry of XPR crystal.

Polarization properties of the elliptical multipole wiggler (EMPW), which was recently installed on BL-28B at the Photon Factory, was characterized by an X-ray polarimeter composed of an XPR and an analyzer crystal. At the downstream of the beamline optics, polarization states are completely determined including the ratio of unpolarized-light component. Further, polarization states of the light radiated from the EMPW were estimated taking the depolarization at the double crystal monochromator into consideration.

Some novel optics to produce high quality CPX with high throughput will be presented.

- [1] K. Hirano et al.: Jpn. J. Appl. Phys., **30** (1991) L407.
- [2] T. Ishikawa et al.: Rev. Sci. Instrum., **63** (1992) 1098.
- [3] K. Hirano et al.: J. Appl. Cryst., **25** (1992) 531.
- [4] K. Hirano et al.: Jpn. J. Appl. Phys., **31** (1992) L1209.
- [5] T. Ishikawa et al.: J. Appl. Cryst., **24** (1991) 982.
- [6] K. Hirano et al.: Nucl. Instrum. & Methods Phys. Res. A **336** (1993) 343.
- [7] D. M. Mills et al.: *private communication*
- [8] K. Hirano et al.: Jpn. J. Appl. Phys., *to be published*.

Complete Determination of Stokes Polarization Parameters for X-rays

Qun Shen, K.D. Finkelstein, and S. Shastri
Cornell High Energy Synchrotron Source (CHESS)
and School of Applied and Engineering Physics
Cornell University, Ithaca, New York 14853, USA.

The ability to completely analyze the polarization state, especially the degree of circular polarization, of an x-ray beam is of great scientific interest in many areas of synchrotron radiation and materials research. It plays an important role in evaluating the performance of special insertion devices and crystal phase plates, as well as in x-ray spectroscopy and scattering experiments involving magnetic and resonant interactions in various materials.

In this paper we present the basic experimental techniques of determining a full set of polarization parameters, i.e. Stokes parameters, that characterize the general polarization of an x-ray beam. We will focus on the newly developed method of using multiple-beam Bragg diffraction (MBD) on a noncentrosymmetric crystal. Due to the *phase-sensitive interference* between the multiple Bragg reflections and the *polarization mixing* that occurs when the multiple reflections are not coplanar, an MBD intensity profile is sensitive to the *phase* between the σ and π wave fields and thus can be used to measure the degree of circular polarization in the incident beam. A simple formalism has been developed and a versatile polarimeter has been constructed based on this principle to allow for relatively easy measurements of all Stokes parameters in a broad x-ray energy range. Several experiments using this new MBD polarimetry will be presented to illustrate its applications.

This work is supported by the National Science Foundation through CHESS under grant number DMR 93-11772.

Diffraction of High Energy Synchrotron Radiation

Th. Brückel, R. Bouchard, T. Köhler, M. Lippert, H.-B. Neumann, H.F. Poulsen, U. Rütt,
T. Schmidt, J.R. Schneider and M. von Zimmermann

Hamburger Synchrotronstrahlungslabor HASYLAB at
Deutsches Elektronen-Synchrotron DESY
Notkestr. 85, D-22603 Hamburg, Germany

Diffraction of high energy synchrotron radiation at energies above 100 keV combines advantages of conventional X-ray diffraction and neutron diffraction. For hard X-rays absorption in matter is weak with typical mean free paths of several mm. Bulk properties are studied on large samples. With a three crystal diffractometer an excellent \underline{k} -space resolution of about 10^{-4} \AA^{-1} transversal and 10^{-3} \AA^{-1} longitudinal is achieved.

In this contribution we discuss the particularities of hard X-rays, present the instrumental set-up and the \underline{k} -space resolution. The potential of the new method will be demonstrated on two examples: magnetic diffraction from MnF_2 and the structural phase transition of SrTiO_3 .

Session TuC - Invited Talks

**INSTRUMENTATION and KEY-ELEMENTS of the DISPERSIVE X-ray
ABSORPTION SPECTROMETER for ACCURATE MEASUREMENTS**

A. Fontaine, F. Baudalet*, E. Dartyge, J.M.Dubuisson, C. Giorgetti, Stefania Pizzini+,
D.Andrault‡, F.Farges‡, G.Fiquet‡, J.P.Itié@, A.Polian@, A.San Miguel°@, H.Tolentino

LURE (CNRS-CEA-MESR) Bât. 209D, 91405 Orsay, France

and + Laboratoire Louis Néel BP 166 F38042 Grenoble

**Lab.de Phys.des Solides, Univ. de Nancy I, 56 Vandoeuvre les Nancy, France*

Now at ESRF F38043 Grenoble

@Lab de la Physique des Milieux Condensés Paris VI

‡IPG Paris VI

°Lab Nacional de Luz Sinchrotron Campinas 13081

Measurement of very small differences of the total cross-section is the current demand for the spectrometers dedicated to time-dependent experiments carried out under various time-ramped parameters. The dispersive optics and more precisely the full X-ray Absorption Spectrometer is mechanical movement-free during data collection which can last over 12 hours at LURE-DCI to be sensitive to relative change of the absorption of the order of 10^{-5} . In this range, artefacts due to the drift of silicon lattice spacing under temperature change of the crystal, and drifts of the detector position because of liquid nitrogen evaporation contained in the cryostat are sources of errors which have been identified and cured or ... by-passed. The accuracy in difference measurements is now of the order of 10^{-5} for a total cross-section measured equal to 1. In term of optics stability a difference signal of 10^{-4} out of 1 can be generated by an absorption edge shift caused by a 0.05K drift of the temperature of the silicon crystal at 7 KeV. These performances are essential for the measurement of XMCD in the hard X-ray range. Water cooling of the dynamically bent crystal reduces dramatically the change of the Si temperature. Adequate geometry makes the spatial drift of the position of the photodiode array much less concerning. The focusing efficiency is also a key-parameter to push high pressure X-ray absorption spectroscopy (55 GPa), and high temperature XAS (2000K), and the combination (15 GPa, 800K). Simple devices, taking advantage of the focusing geometry, have been successfully tested these last two years.

Non-Radiative X-Ray Resonant Raman Scattering from Solids

W. Drube, R. Treusch and G. Materlik

Hamburger Synchrotronstrahlungslabor HASYLAB
am Deutschen Elektronen-Synchrotron DESY
Notkestr. 85, 22603 Hamburg, Germany

High-intensity synchrotron radiation is a powerful tool to study photon-electron scattering phenomena involving resonantly excited inner-shell electrons. A basic process is the X-ray resonant Raman effect which dominates the radiative and non-radiative emission in the threshold region. The one-step nature of the transition from the initial ground state to the final scattering state results in peculiar characteristics of the emission spectrum, e.g. a Raman-type dispersion of emission lines and lifetime suppression of the intermediate hole states. This has been studied mostly in the radiative channel for atoms, molecules and solids. Data on the accompanying electron emission, however, are still scarce, especially for solids. We concentrate on the various aspects of radiationless scattering and present experimental results on resonant Auger electron emission from solid 4d metals at the L_3 excitation threshold.

High Resolution Photoemission

Jesper N. Andersen,
Department of Synchrotron Radiation Research, Institute of Physics, Lund
University,
Sölvegatan 14, S-223 62 Lund, Sweden.

High resolution core level photoemission has, due to the sensitivity of the core level binding energy to the chemical surroundings of the emitting atom, found extensive use in the study of the electronic structure of bulk materials and of surfaces and interfaces. As a result of major improvements in recent years in monochromator and analyzer design the technique has matured almost to the point where it is often limited more by the inherent properties of the samples studied (core hole lifetime, vibrational broadening, sample perfection, etc.) than by the experimentally obtainable energy resolution and intensity. In the present talk I will firstly describe a beamline at MAXLAB which due to the unique monochromator-analyzer combination has shown an excellent performance in terms of energy resolution and throughput. Secondly, I will give a number of examples of the present state-of-the-art of high resolution core level photoemission studies of surfaces and interfaces and will comment on some of the developments of the field that may result from the large increase in photon flux expected at the new third generation storage rings presently starting to operate.

Spin Polarized Photoemission

B. Sinkovic, New York University, Dept. of Physics

Spin analysis of photoemitted electrons offers an unique perspective for the study of magnetic solids, their surfaces and atomically engineered thin magnetic films. The strength of spin polarized photoemission (SPPE) is that it directly measures the spin polarization of electronic structure which is responsible for ferromagnetism¹. In particular, angle resolved SPPE measurements of valence electrons have been able to probe spin dependent band dispersion of ferromagnets² which allows the most stringent test of the current theories of magnetic solids. Similar SPPE experiments on atomically layered magnetic films have recently identified spin polarized interface (quantum well) states³ which are responsible for magnetic coupling in 3d metallic magnetic superlattices. The application of spin analysis to photoemitted core-level electrons has also been fruitful, since the first observation of non-zero spin polarization of these levels.⁴ Spin Polarized version of Electron Spectroscopy for Chemical Analysis (SPESCA) technique is able to distinguish magnetic states of elements in different valence states with an atomic layer sensitivity.⁵ In addition to spectroscopic measurements, spin polarized core-electrons have been employed in electron diffraction. Such spin polarized photoelectron diffraction measurements offer a unique way for study of short range magnetic order around a given photoemitter.⁶

The inherent difficulty in performing SPPE is the low efficiency of electron spin detectors.⁷ Most of the electron detection schemes rely on spin the dependence in electron-surface scattering with efficiency factor of only $\sim 10^{-4}$. This limitation is usually compensated for by the use of photon sources that are capable of producing extremely high fluxes, and most of SPPE experiments today are performed using undulator radiation. The energy tunability and the polarization characteristics of synchrotron radiation are also being explored for further enhancement of SPPE technique. The increase in flux, brightness and control of polarization of radiation expected from third generation synchrotron sources are welcome development for SPPE. Together with possible improvements in spin detector efficiency,⁸ more novel SPPE experiments are anticipated.

- 1) M. Campagna, D.T. Pierce, P. Meier, K. Sattler, and H.C. Siegmann, *Adv. Electron. Electron Phys.* **41**, 113 (1976).
- 2) E. Kisker, K. Shroder, W. Gudat, M. Campagna, *Phys. Rev. B* **31**, 329 (1985).
- 3) N.B. Brookes, Y. Chang, and P.D. Johnson, *Phys. Rev. Lett.* **67**, 351 (1991).
- 4) C. Carbone and E. Kisker, *Solid State Commun.* **65**, 1107 (1988).
- 5) B. Sinkovic, P.D. Johnson, N.B. Brookes, A. Clarke, and N.V. Smith, *Phys. Rev. Lett.* **65**, 1647 (1990).
- 6) B. Sinkovic, B. Hermsmeier, and C. S. Fadley, *Phys. Rev. Lett.* **55**, 1227 (1985).
- 7) D.T. Pierce, R.J. Cellota, M.K. Kelly, and J. Ungris, *Nucl. Instrum. Methods A* **266**, 550 (1988).
- 8) D. Tillmann, R. Thiel, and E. Kisker, *Z. Phys. B* **77**, 1 (1989).

Optical Converters for Circularly Polarized VUV and Soft X-ray Radiation

Hartmut Höchst

Synchrotron Radiation Center, University of Wisconsin-Madison
3731 Schneider Dr., Stoughton WI 53589.

During the last few years considerable effort was spent at various laboratories to evaluate the possibilities of optical devices to generate circularly polarized synchrotron radiation. These instruments convert linearly polarized radiation by utilizing the phase shifting properties of multiple reflectors or multilayer transmission optics. In the VUV and soft x-ray range, the figure of merit TP^2 , where P is the degree of circular polarization and T the optical transmission, of specially tailored reflection coatings or multilayer structures can be considerably higher than what can be achieved with conventional insertion devices such as the crossed field undulator.

In addition to being considerably less expensive, the various optical designs have the great advantage of not being an integral part of the storage ring and as such completely transparent to the operation and other users of the storage ring.

Various phase shifter designs will be discussed in terms of their performance, eg. optical throughput, degree of polarization and capabilities to modulate between left and right circular light. Recent MCD experiments utilizing optical phase shifters not only demonstrate the proof of principle, but also provide strong evidence of the potential capabilities of "optical insertion" devices as an alternative tool to generate variably polarized synchrotron radiation.

Beamline Posters

(Session TuD)

- TuD1 Abrami, A., Barnaba, M., Battistello, L., Brena, B., Cautero, G., Cocco, D., Comelli, G., Contrino, S., DeBona, F., DiForzo, S., Fava, C., Finetti, P., Galimberti, A., Gambitta, A., Giuressi, D., Godnig, R., Jark, W., Lizzit, S., Mazzolini, F., Melpignano, P., Paolucci, G., Pugliese, R., Qian, S.N., Rosei, R., Sandrin, G., Savoia, A., Sergio, R., Sostero, G., Tommasini, R., Tudor, M., Zanini, F. Super ESCA: First Beamline Operating at ELETTRA.
- TuD2 Aksela, S., Kivimaki, A., Sairanen, O.-P., Naves de Brito, A., Nommiste, E. The Finnish Beamline at Max-Laboratory: Progress in Photon Energy Resolution.
- TuD3 Amenitsch, H., Bernstorff, S., Laggner, P. High Flux Beamline for SAXS at ELETTRA.
- TuD4 Asfaw, A., Ederer, D.L., Marchang, S.A., Morikawa, E., Smith, W.S., Callcott, T.A., Jia, J.J., Lin, L., Osborn, K., Zhou, L., Miyano, K.E. Performance and Preliminary Results of the SXR Beamline at CAMD-LSU.
- TuD5 Barraza, J., Shu, D. Experimental Station Support Systems for the Advanced Photon Source.
- TuD6 Bilsborrow, R.L., Bliss, N., Cernik, R.J., Clark, G.F., Clark, S.M., Collins, S.P., Dobson, B.R., Fell, B.D., Grant, A.F., Harris, N.W., Smith, W., Towns-Andrews, E., Bordas, J. Five New Experimental Stations at the SRS Daresbury from a 6 Tesla Superconducting Wiggler Magnet.
- TuD7 Bosecke, P. The High-Brilliance Beamline at the ESRF.
- TuD8 Brite, C., Shu, D., Nian, T., Wang, Z., Haeffner, D., Alp, E., Parry, R., Kuzay, T. Modular Filter Design for White Beam Undulator/Wiggler Beamlines at the Advanced Photon Source.
- TuD9 Carr, G.L., Hanfland, M., Williams, G.P. The Mid-Infrared Beamline at the NSLS Port U2B.
- TuD10 Cerino, J., Rabedeau, T., Sabersky, A. A Photon Beam Position Monitor for SSRL Beamline 9.
- TuD11 Chang, J., Shu, D., Nian, T., Kuzay, M., Job, P.K. Design of Integral Shutters for the Beamlines of the Advanced Photon Source.
- TuD12 Chantler, C.T., Staudenmann, J.-L. Energy Dependences of Absorption in Beryllium Windows and Argon Gas.
- TuD13 Chung, S.-C., Chen, C.-I., Tseng, P.-C., Lin, H.-F., Dann, T.-E., Song, Y.-F., Huang, L.-R., Chen, C.-C., Chuang, J.-M., Tsang, K.-L., Chang, C.-N. Soft X-Ray Spectroscopy Beam Line 6m-HSGM at SRRF: Optical Design and First Performance Tests.
- TuD14 Tseng, P.-C., Lin, H.-J., Chung, S.-C., Chen, C.-I., Lin, H.-F., Dann, T.-E., Song, Y.-F., Hsieh, T.-F., Tsang, K.-L., Chang, C.-N. Current Status of the 6m-LSGM Beam Line at SRRC.
- TuD15 Bernstorff, S., Busetto, E., Lausi, A., Olivi, L., Zanini, F., Savoia, A., Colapietro, M., Portalone, G., Camalli, M., Pifferi, A., Spagna, R., Barba, L., Cassetta, A. The Macromolecular Crystallography Beamline at ELETTRA.
- TuD16 Comin, F. Six Degree-of-Freedom Scanning Supports and Manipulators Based on Parallel Robots.
- TuD17 Drube, W., Schulte-Schrepping, H., Schmidt, H.-G., Treusch, R., Materlik, G. Design and Performance of the High-Flux X-Ray Wiggler Beamline BW2 at HASYLAB.
- TuD18 Eisert, D.E., Stott, J.P., Fisher, M.V., Bissen, M., Hochst, H. Computer Control of the SRC High Resolution Beamline.
- TuD19 Ferrer, S., Comin, F. The Surface Diffraction Beamline at ESRF.
- TuD20 Frahm, R., Weigelt, J., Meyer, G., Materlik, G. The X-Ray Undulator Beamline BW1 at DORIS III.

- TuD21 Gambitta, A., Poloni, C., Visintin, A., Zanini, F. Comparison of Numerical and Experimental Simulation of a Beryllium Window Under Intense Heat Load.
- TuD22 Garrett, R.F., Cookson, D.J., Davey, P., Janky, S., Wilkins, S.W. DC-Servo-Motor Controlled Four-Jaw Slits for Synchrotron Radiation.
- TuD23 Garrett, R.F., Cookson, D.J., Foran, G., Creagh, D.C., Wilkins, S.W. The Australian National Beamline Facility at the Photon Factory.
- TuD24 Gavrilov, N.G., Evdokov, O.V. Wave Transmission, High Precision (0.03") Rotation Stage for Synchrotron Radiation Instrumentation.
- TuD25 Grubel, G., Als-Nielsen, J., Abernathy, D. The TROIKA Beamline at ESRF.
- TuD26 Huang, K.G., Ramanathan, M., Montano, P.A. The ANL X6B Beamline at NSLS: A Versatile Facility.
- TuD27 Iwazumi, T., Koyama, A., Sakurai, Y. New Beamline (BL-28B) for Circularly Polarized X-Rays at the Photon Factory.
- TuD28 Jiang, X., Zhang, W., Wu, J., Jing, Y., Liu, G. Performance of Beamline 4W1C for X-Ray Diffuse Scattering Station at Beijing Synchrotron Radiation Facility.
- TuD29 Kagoshima, Y., Muto, S., Park, S.Y., Wang, J., Miyahara, T., Yamamoto, S., Kitamura, H. Construction and Performance of the Beamline NE1B for Circularly Polarized Soft X-Rays in the TRISTAN Accumulation Ring.
- TuD30 Kao, C.C., Hamalainen, K., Krisch, M., Siddons, D.P., Hastings, J.B., Oversluisen, T. Optical Design and Performance of the Inelastic Scattering Beamline at the National Synchrotron Light Source.
- TuD31 Kamiya, N., Uruga, T., Kimura, H., Yamaoka, H., Kashihara, Y., Yamamoto, M., Kawano, Y., Ishikawa, T., Kitamura, H., Ueki, T., Iwasaki, H., Tanaka, N., Hamada, K., Moriyama, H., Miki, K., Tanaka, I. Conceptual Design of the High Energy Undulator Pilot Beamline for Macromolecular Crystallography at the SPring-8.
- TuD32 Kikuchi, T., Takagi, Y., Sasaki, S., Mori, T., Kohzu, H. A New Mechanism to Balance Moment of Inertia Induced in a Goniometer Axis.
- TuD33 Kirkland, J.P., Elam, W.T. The Naval Research Laboratory's New Hard X-Ray Beam Line at the National Synchrotron Light Source.
- TuD34 Knapp, G.S., You, H. On the Use of Electronic Tilt Sensors as Angle Encoders for Synchrotron Applications.
- TuD35 Konishi, H., Yokoyama, A., Motohashi, H., Ohno, H. Beamline BL-27 for Radioactive Materials Researches at the Photon Factory.
- TuD36 Krumrey, M., Kvick, A., Schwegle, W. Optics of a High Power Wiggler Beamline at the ESRF.
- TuD37 Derossi, A., Lama, F., Piacentini, M., Prosperi, T., Zema, N. High Flux and High Resolution Beamline for Elliptically Polarized Radiation in the Vacuum Ultraviolet and Soft X-Ray Range.
- TuD38 LeGrand, A.D., Pradervand, C., Schildkamp, W., Bourgeois, D., Wulff, M. An Ultra-Fast Mechanical Shuttering System for Separating Single X-Ray Pulses From a Synchrotron.
- TuD39 Park, B.-J., Rah, S.-Y., Park, Y.-J., Lee, K.-B. PLS Bending Magnet X-Ray Beamline 3C2.
- TuD40 Lequien, S., Goirand, L., Lesimple, F. A New Conceptual Design for the Anomalous Scattering Beamline at the ESRF.

- TuD41 Liu, C., Nielsen, W., Kruy, T.L., Shu, D., Kuzay, T.M. Vacuum Tests of a Beamline Front End Mock-up at the Advanced Photon Source.
- TuD42 Mazzolini, F., Fava, C., DeBona, F., Sandrin, G., Gambitta, G. A New Kind of UHV Piezotranslator.
- TuD43 McClain, D.B., Pflibsen, K.P., Goetz, A.J. Virtual Threaded Language (VTL): A Scientist's Computer Language for Instrument Control.
- TuD44 McMillin, P., Baker, T., Berry, B. Six DOF Hexapod Actuation System for Beam Control Mirrors.
- TuD45 Bjorneholm, O., Federmann, F., Beutler, A., Fossing, F., Larsson, C., Hahn, U., Rieck, A., Moller, T. Performance of the XUV High Resolution Undulator Beamline BW3 at HASYLAB: First Results and Time-of-Flight Spectroscopy.
- TuD46 McSweeney, S.M., Buffey, S.G., Atkinson, P.A., Duke, E.M.H., Nave, C., Gonzales, A., Thompson, A., Kinder, S.H. A Protein Crystallography Beamline for Multiwavelength Anomalous Dispersion at the SRS Daresbury.
- TuD47 Nian, H.L.T., Shu, D., Kuzay, T.M. Thermo-Mechanical Analysis of the White Beam Slits for an Undulator Beamline at the Advanced Photon Source.
- TuD48 Padmore, H.A., Earnest, T., Kim, S.H., Thompson, A.C., Robinson, A. A Beamline for Macromolecular Crystallography at the ALS.
- TuD49 Panchenko, V.E. SR Beamlines at the VEPP-4 - 6 GeV Storage Ring.
- TuD50 Paul, D.F. Design of an X-Ray Beamline on a Bending Magnet at the ESRF for Magnetic and High Resolution Diffraction.
- TuD51 Perera, R.C.C., Jones, G., Lindle, D.W. High-Brightness Beamline for X-Ray Spectroscopy at the Advanced Light Source.
- TuD52 Jones, G., Ryce, S., Lindle, D.W., Karlin, B.A., Woicik, J.C., Perera, R.C.C. Design and Performance of the ALS Double-Crystal Monochromator.
- TuD53 Quaresima, C., Perfetti, P., Ottaviani, C., Capozzi, M., Rinaldi, S., Matteucci, M., Crotti, C., Antonini, A., Prince, K., Savoia, A., Astaldi, C., Zacchigna, M. The HERP Beam Line.
- TuD54 Rah, A.Y., Kang, T.H., Chung, Y., Kim, B., Lee, K.B. Bending Magnet VUV Beamline 2B at PLS.
- TuD55 Ramanathan, M., Montano, P.A. A Versatile Double Crystal Fixed Exit Monochromator for X-Ray Synchrotron Radiation.
- TuD56 Randall, K.J., Gluskin, E., Xu, Z. Spectroscopy Beamline for the Photon Energy Region from 0.5 to 3 keV at the Advanced Photon Source.
- TuD57 Fajardo, P., Rev-Bakaikoa, V. Control of Six Degree of Freedom Parallel Manipulators for Synchrotron Radiation Applications.
- TuD58 Robinson, A.W., D'Addato, S., Finetti, P., Dhanak, V.R., Thornton, G. Performance of the IRC SEXAFS beamline at Daresbury SRS.
- TuD59 Robinson, I.K., Graafsma, H., Kwick, A., Linderholm, J. First Testing of the Fast Kappa Diffractometers at NSLS and ESRF.
- TuD60 Rosenbaum, G., Westbrook, E.M. Design of the Structural Biology Center Beamlines at the APS.

- TuD61 Ruan, Y., Meron, M. Transient and Steady State Thermal and Stress Analysis of an ID Beam Shutter for the APS.
- TuD62 Sakurai, Y., Oura, M., Sakae, H., Usui, T., Konishi, T., Shiwaku, H., Nakamura, A., Amamoto, H., Harami, T., Kimura, H., Oikawa, Y., Kitamura, H. Conceptual Design of SPring-8 Front Ends.
- TuD63 Sakurai, Y., Yamaoka, H., Kimura, H., Marechai, X., Ohtomo, K., Ishikawa, T., Kitamura, H., Kashihara, Y., Harami, T., Tanaka, Y., Kawata, H., Shiotani, N., Sakai, N. Design of an EMPW Beamline for High Energy Inelastic Scattering at the SPring-8.
- TuD64 Petersen, H., Senf, F., Schafers, F., Bahrtdt, J. Monochromators for the U49 Undulator at the BESSY II Storage Ring.
- TuD65 Shimada, H., Matsubayashi, N., Imamura, M., Sato, T., Yoshimura, Y., Hayakawa, T., Takehira, K., Toyoshima, A., Tanaka, K., Nishijima, A. Performance of a Material Science Facility at the Photon Factory: A Soft X-Ray Beamline BL-13C Coupled with a Multi-Purpose Analytical Apparatus.
- TuD66 Shu, D., Li, Y., Ryding, D., Kuzay, T.M., Brasher, D. Explosion Bonding and Its Applications in the Advanced Photon Source Front End and Beamline Component Designs.
- TuD67 Shu, D., Yun, W., Lai, B., Barraza, J., Kuzay, T.M. A Double Multilayer Monochromator Using Modular Design for the Advanced Photon Source.
- TuD68 Shu, D., Brite, C., Nian, T., Yun, W., Haeffner, D.R., Alp, E.E., Ryding, D., Collins, J., Li, Y., Kuzay, T.M. Design of Precision White Beam Slits Design for the High Power Density X-Ray Undulator Beamlines at the Advanced Photon Source.
- TuD69 Shu, D., Tsheskidov, V., Nian, T., Haeffner, D.R., Alp, E.E., Ryding, D., Collins, J., Li, Y., Kuzay, T.M. Design of High Heat Load White Beam Slits for Wiggler/Undulator Beamlines at the Advanced Photon Source.
- TuD70 Shu, D., Barraza, J., Brite, C., Sanchez, T., Tcheskidov, V. Design of the Beamline Standard Components at the Advanced Photon Source.
- TuD71 Suortti, P., Tschentscher, Th. High Energy Scattering Beamlines at ESRF.
- TuD72 Takagi, Y., Kikuchi, T., Mizutani, T., Imafuku, M., Sasaki, S., Mori, T. A Triple-Axis/Four-Circle Diffractometer at PF-BL3A (II).
- TuD73 Tolentino, H., Durr, J., Cusatis, C., Mazzaro, I., Udron, D. Two and Four Crystal Reflections Monochromators.
- TuD74 Trakhtenberg, E.M., Gluskin, E.S., Xu, S. Vacuum System for APS Insertion Devices.
- TuD75 Tsang, K.-L., Lee, C.-H., Jean, Y.-C., Dann, T.-E., Chen, J.-R. The Wiggler X-Ray Beam Lines at SRRC.
- TuD76 Tseng, P.-C., Hsieh, T.-F., Song, Y.-F., Lee, K.-D., Chung, S.-C., Chen, C.-I., Lin, H.-F., Dann, T.-E., Huang, L.-R., Chen, C.-C., Chuang, J.-M., Tsang, K.-L., Chang, C.-N. Performance of the 1m-SNM Beam Line at SRRC.
- TuD77 van Silfhout, R.G., Hermes, C. X-Ray Instrumentation for a Focused Wiggler Beamline at the EMBL Outstation Hamburg.
- TuD78 Vlieg, E., Bijleveld, J.H.M., Glastra van Loon, D., van der Heide, U.A., Kronenburg, M., Levine, Y.K. Conceptual Design of the Dutch-Belgian Beamline at the ESRF.
- TuD79 Wang, Z., Kuzay, T.M. A Variable Thickness Window: Thermal and Structural Analyses.

- TuD80 Warwick, T., Heimann, P., Mossessian, D., Padmore, H. Performance of a High Resolution, High Flux Density SGM Undulator Beamline at the ALS.
- TuD81 Watanabe, N., Adachi, S., Nakagawa, A., Sakabe, N. New Macromolecular Crystallography Station BL-18B at Photon Factory.
- TuD82 Wei, W., Wu, J., Gu, X., Sheng, W., Jin, M., Li, C., Zhao, N., Wang, K., Zhao, F., Wang, W., Zheng, D. The 3B1B Biology Spectroscopy Station at BSRF.
- TuD83 Xu, Z., McNulty, I., Randall, K.J., Yang, L., Gluskin, E., Johnson, E.D., Oversluizen, T. X13A: A Versatile Soft X-Ray Undulator Beamline.
- TuD84 Xu, P.S., Yu, X.J., Lu, E.D., Wang, Q.P., Xu, S.H. Commissioning and Operation of Beam Line for Photoelectron Spectroscopy in NSRL.
- TuD85 Yamamoto, M., Fujisawa, T., Nakasako, M., Tanaka, T., Uruga, T., Kimura, H., Yamaoka, H., Inoue, Y., Iwasaki, H., Ishikawa, T., Kitamura, H., Ueki, T. Conceptual Design of SPring-8 Contract Beamline for Structural Biology.
- TuD86 Zhang, Y., Shi, C., Xu, P., Xie, X., Hu, Y. Progresses of Synchrotron Radiation Applications at the NSRL.
- TuD87 Montano, P.A., Bedzyk, M.J., Ramanathan, M., Beno, M.A., Jennings, J., Cowan, P.L., Gluskin, E., Trakhtenberg, E., Vasserman, I.B., Ivanov, P.M., Franchon, D., Moog, E.R., Turner, L.R., Shenoy, G.K. Elliptical Motion Wiggler Beamline at the Advanced Photon Source.
- TuD88 Pflibsen, K.P., Goetz, A.J., McClain, D. A Systems Approach to Optimizing Synchrotron Beamline Performance.
- TuD89 Sugiyama, H. X-Ray Undulator Beamline and Experimental Station for the Feasibility Study at TRISTAN Main Ring.
- TuD91 Murray, P.K., Collins, S.J., Emerich, H., Mardalen, J., Pattison, P., Weber, H.P. Design and Construction of a General Purpose Bending Magnet Beamline at the ESRF.
- TuD92 Nian, H.L.T., Sheng, I.C., Shu, D., Kuzay, M. Thermo-Mechanical Analysis of the White Beam Slits for a Wiggler/Undulator Beamline at the Advanced Photon Source.

SuperESCA: First beamline operating at ELETTRA

A. Brami, M. Barnaba, L. Battistello, B. Brena, G. Cautero, D. Cocco, G. Comelli, S. Contino, F. DeBona, S. Di Fonzo, C. Fava, P. Finetti, A. Galimberti, A. Gambitta, D. Giuressi, R. Godnig, W. Jark, S. Lizzit, F. Mazzolini, P. Melpignano, G. Paolucci, R. Pugliese, S.N. Qian, R. Rosei, G. Sandrin, A. Savoia, R. Sergo, G. Sostero, R. Tommasini, M. Tudor, F. Zanini

Sincrotrone Trieste S.C.p.A., Padriciano 99, I-34012 Trieste

Abstract

First spectra are presented from the soft X-ray beamline SuperESCA, the first beamline which received monochromatic light in the experimental chamber at the 2 GeV storage ring ELETTRA in Trieste. Besides of gas phase spectra presenting the resolution of the monochromator SX700 we are also presenting first experimental results with the high resolution of the beamline operated at the design electron energy of 2.0 GeV and with electron currents around 100 mA. This beamline is served by a 5.6 cm-81 periods undulator, which provides very brilliant radiation, starting from 100eV, in the whole soft x-ray range. The beamline optical layout is based on a modification of the original SX700 monochromator designed by Petersen in 1982 [1]. In our configuration the slope error problem, due to the presence of aspherical surfaces, has been reduced considerably applying a sagittally focusing configuration. In addition by introducing a prefocusing mirror this monochromator creates a stigmatic monochromatic image in the fixed exit slit [2]. This beamline, coupled with the experimental chamber, will allow the experimentalist to perform photo-emission experiments with high photon flux and high resolving power (>10.000 at 200 eV).

Alignment and characterisation of the beamline were started in February 1994, and the first monochromatic beam was brought within a few shifts to the experimental chamber. Before Easter a resolution in excess of 2000 was achieved. Further fine alignment is still in progress.

[1] H. Petersen, Opt. Comm. 40, 402 (1982); Nucl. Instr. Methods A 246, 260 (1986)

[2] W. Jark, Rev. Sci. Instr. 63, 1241 (1992).

THE FINNISH BEAMLINE AT MAX-LABORATORY: PROGRESS IN PHOTON ENERGY RESOLUTION

S. Aksela, A. Kivimäki, O.-P. Sairanen, A. Naves de Brito, and E. Nömmiste
*Department of Physics, University of Oulu, FIN-90570 Oulu, Finland,
and the Finnish Synchrotron Radiation Facility at MAX-lab,
University of Lund, S-22100 Lund, Sweden*

S. Svensson

Department of Physics, Uppsala University, S-75121 Uppsala, Sweden

The Finnish beamline (BL51) [1] at MAX-laboratory has been designed principally for gas phase studies. It uses synchrotron radiation from a short-period narrow-gap undulator in the photon energy range of about 60-600 eV. Synchrotron radiation is monochromatized with a modified SX-700 plane grating monochromator, equipped with a plane elliptical focusing mirror whose slope errors are ≤ 0.4 arcsec (rms). After the monochromator, the beamline has a permanent differential pumping section that decreases the pressure from the order of 10^{-5} mbar used in typical gas phase experiments to the ultra high vacuum of the monochromator. This section includes also a toroidal refocusing mirror that provides a spot size of about $\varnothing \approx 1$ mm into the experimental station.

Resolution tests done after the final alignment of the monochromator reveal very high photon energy resolution. The total linewidths recorded with the total-ion-yield technique for the Kr $3d_{5/2} \rightarrow 5p$ ($h\nu=91.2$ eV: $\Gamma_{\text{tot}}=84$ meV) and Ar $2p_{3/2} \rightarrow 4s$ ($h\nu=244.4$ eV: $\Gamma_{\text{tot}}=121$ meV) resonances are the sharpest that have been reported. The latter result suggests that the natural linewidth of the Ar $2p_{3/2} \rightarrow 4s$ excitation could be narrower than 116 meV, as obtained with electron energy-loss spectroscopy [2]. Total ion yield measurements at higher photon energies, at CO $C1s \rightarrow \pi^*$ ($h\nu=287.4$ eV: $\Gamma_{\text{tot}}=113$ meV) and $N_2 N1s \rightarrow \pi^*$ ($h\nu=401$ eV: $\Gamma_{\text{tot}}=164$ meV) resonances, show less exceptional values but, nevertheless, indicate the high photon energy resolution of the monochromator. All these measurements were done at the first diffraction order but with partly masked optics.

[1] S. Aksela, A. Kivimäki, A. Naves de Brito, O.-P. Sairanen, S. Svensson, J. Väyrynen, Rev. Sci. Instrum., in press.

[2] D.A. Shaw, G.C. King, F.H. Read, and D. Cvejanovic, J. Phys. B: At. Mol. Phys. 15, 1785 (1982).

High Flux Beamline for SAXS at ELETTRA

H.AMENITSCH¹⁾, S.BERNSTORFF²⁾ and P.LAGNER¹⁾

¹⁾ Institute for Biophysics and X-ray Structure Research, Austrian Academy of Science, Steyregg, 17, 8010 Graz, Austria

²⁾ Sincrotrone Trieste, Padriciano 99, 34012 Trieste, Italy

A double-focusing high-flux beamline dedicated for SAXS (Small-Angle X-ray Scattering) is presently under construction at the 2 GeV Electron Storage Ring ELETTRA. The instrument is mainly intended for time-resolved studies of fast structural transitions in the submillisecond time region in solutions and partly ordered systems. The primary goal is to obtain structural information during relaxations from nonequilibrium states in supramolecular assemblies, such as gels, liquid crystals and (bio-)polymers. A multi-purpose sample stage¹ will include various devices to study such transitions. Apart from the SAXS it will be possible to perform simultaneously wide angle X-ray scattering experiments (WAXS) between 5 and 10 Å.

The source of the instrument will be a 57-pole wiggler (critical energy: 4.1 keV), which is shared simultaneously with the Macromolecular Crystallography Beamline. The SAXS-beamline will be situated 1.25 mrad off wiggler axis and will have an acceptance of 1.0×0.3 mrad² (horizontal x vertical). The optics consists of a flat double-crystal monochromator deflecting vertically with a fixed exit beam, and a downstream toroidal focusing mirror. In the monochromator three interchangeable pairs of asymmetric cut Si (111) crystals with grazing angles of $1 - 2^\circ$ will be used optimised for the energies 5.4, 8, and 16 keV (2.3, 1.54 and 0.77 Å), respectively. The 1.5 m long toroidal mirror consists of two segments, is coated with Pt and has a grazing angle of 4.8 mrad.

The performance of the optics has been optimised by ray tracing calculations. The spot size at the detector is about 1.1×0.7 mm² with a sample size of 4.2×2 mm². For 8 keV photons the calculated maximal SAXS-resolution will be about 400×1400 Å² d-spacing assuming an optimal distance between detector and sample of 1.8 m. If necessary, this can be improved by reducing the horizontal acceptance of the beamline. Assuming an horizontal acceptance of 1 mrad a photon flux in the order of 10^{13} ph/s has been estimated for 8 keV photons (2 GeV, 400 mA).

The monochromator will be built in two phases; the commissioning for the 8 keV - instrument will start beginning of 1995.

¹ M.Kriechbaum, M.Steinhard, P.Laggner, manuscript in preparation

Performance and Preliminary Results of the SXR Beamline at CAMD-LSU

A. Asfaw, D. L. Ederer, S. A. Marchant

Department of Physics, Tulane University, New Orleans, La, 70118

Eizi Morikawa, W. S. Smith

Center for Advanced Microstructures and Devices-LSU, Baton Rouge, La, 70803

T. A. Callcott, J. J. Jia, Lin Lin, K. Osborn, L. Zhou

Department of Physics, University of Tennessee, Knoxville, TN, 37996

K. E. Miyano

Department of Physics, Brooklyn College, Brooklyn, NY, 11210

A new soft x-ray beamline has been recently placed in operation at the Center for Advanced Microstructures and Devices (CAMD). The beamline features a plane grating monochromator utilizing a variable groove spaced grating, which operates in the spectral region 50-800 eV, and a high sensitivity soft x-ray spectrometer that is used to measure fluorescence excited by monochromatized soft x-rays. The monochromator also features simple optic scanning motion, and high throughput and good resolution. The spectrometer achieves high sensitivity through the use of toroidal gratings and a position sensitive detector using a resistive anode. The beamline performance and preliminary results will be presented.

Experimental Station Support Systems for the Advanced Photon Source*

J. Barraza and D. Shu

Experimental Facilities Division
Advanced Photon Source
Argonne National Laboratory
Argonne, IL 60439

ABSTRACT

Support systems have been designed for the experiment stations of the Advanced Photon Source at Argonne National Laboratory. These systems utilize modular precision positioning slides and stages arranged in 3-point kinematic-mount fashion for optimum mechanical stability. Through the use of novel configurations, these systems can achieve large linear motions, six degree-of-freedom motion, and large load capacities without sacrificing valuable experimental station space. This paper will discuss the designs and specifications of the positioning systems developed.

The submitted manuscript has been authored by a contractor of the U.S. Government under contract No. W-31-109-ENG-38. Accordingly, the U.S. Government retains a nonexclusive, royalty-free license to publish or reproduce the published form of this contribution, or allow others to do so, for U.S. Government purposes.

*Work supported by the U. S. Department of Energy BES Materials Science under contract W-31-109-ENG-38.

TuD5

Five New Experimental Stations at the SRS Daresbury from a 6 Tesla Superconducting Wiggler Magnet

R L Bilsborrow, N Bliss, R J Cemik, G F Clark, S M Clark, S P Collins,
B R Dobson, B D Fell, A F Grant, N W Harris, W Smith, E Towns-Andrews, J Bordas,
DRAL Daresbury Laboratory, UK

Daresbury Laboratory is currently completing the construction and commissioning of five new experimental research stations utilising high flux hard X-ray radiation from a 6T superconducting wiggler with a critical wavelength of 0.77 Å.

The new 6T superconducting wiggler magnet was commissioned in the SRS in early 93 with the first diagnostic X-ray beams successfully commissioned in July 93.

The broad areas of science covered by the new stations and the novel features are as follows.

* **A high flux high intensity fixed-wavelength station** primarily for dynamic and time resolved studies of non-crystalline materials. A bent triangular Ge 111 asymmetric cut single crystal monochromator is used for focusing and selecting a wavelength of 1.4 Å. The crystal has a novel liquid gallium interface to enable the high thermal loading to be transferred to a cooled copper block. The vertical focusing is achieved using a 1.2 m bent platinum coated ultra low expansion glass mirror.

* **A solid and liquid interface diffraction station** is being constructed to study solid-solid, liquid-liquid and solid-liquid surfaces. The station will be optimised for three fixed wavelengths within the range 0.5 to 1.3 Å. The beamline consists of a complex optical arrangement with three monochromators and a bent 1.5 m toroidal mirror. The experimental station will house a heavy-duty diffractometer / reflectometer to accommodate environmental cells.

* **A materials diffraction station** to study for example phase transitions and critical scattering, magnetic diffraction, lattice distortions and charge density waves within the wavelength range 0.3 to 1.5 Å. The initial optical arrangement will be for high Q resolution mode utilising a Si 111 channel cut crystal monochromator and analyser with a six circle diffractometer designed to achieve an angular accuracy of 0.1 mdeg. and a total sphere of confusion at the sample of less than 50 µm. For weak scattering studies a second monochromator employing a sagittally bent crystal is planned.

* **A high energy powder diffraction station** which uses white beam for studying reaction kinetics and phase transitions. There will be an emphasis on high pressure and high temperature studies on large volume samples as required for studies on the structure of mantle rocks. The main feature of the experimental equipment is a 1000 tonne hydraulic press as the prime mover for producing pressures up to 250 Kbar with temperatures up to 2000° C in a Walker cell.

* **A ultra-dilute spectroscopy station** designed to allow X-ray absorption studies of ultra-dilute elements with K or LIII absorption edges in the energy range 7 to 25 KeV. The optical arrangement includes a pre-mirror for vertical focusing, a double crystal monochromator and post-mirror. The monochromator 1st crystal is water cooled and the 2nd crystal is mounted on inchworm piezo electric translators for harmonic rejection. The monochromator is driven by a dc servo motor controlled by output from an encoder position to 0.1 mdeg. Fluorescence from dilute samples is collected with a 30 element solid state detector provided with novel signal processing electronics which permit very high count rates without loss of linearity.

The most salient instrumentation aspects of this project will be presented during the meeting.

TuD6

The High-brilliance Beamline* at the ESRF

Peter Bösecke†, Olivier Diat†, Bjarne Rasmussen‡

† ESRF, B.P. 220, F-38043 Grenoble Cedex

‡ EMBL, Grenoble Outstation, B.P. 156, F-38042 Grenoble Cedex

The ESRF High-brilliance Beamline is under commissioning and will become officially available to users in September 1994. Currently, the actual performance of the beamline is under test. The experimental results are in very good agreement with previous calculations [1]. In this paper a comparison will be presented.

The main components of the beamline are,

- an undulator at a high- β section of the ESRF storage ring,
- a cryogenically cooled Sill channel cut monochromator operating between 8 keV and 24 keV with fixed vertical beam offset of 30 mm,
- a 1:1 focusing toroidal mirror (<17 keV),
- an endstation for biocrystallography and
- an endstation for time-resolved small-angle X-ray scattering.

Along the beamline a series of simple diagnostic tools are permanently installed, e.g. a calorimeter and a number of photodiodes. The position of the monochromator is controlled by three vertical linear actuators. They allow control of the scattering angle, the height and the rotation around the primary beam. Both crystal surfaces have slightly different asymmetric cuts. By adjusting the height of the crystal the vertical displacement between the incident and the exiting beam can be kept constant in the energy range between 8 keV and 24 keV. A closed liquid nitrogen loop is used for cooling the monochromator crystal to about -190°C. A problem is the clamping of the monochromator block to the cooling blocks. A too loose clamping reduces the heat transfer while a too tight clamping induces deformation on the crystal block. This problem has been solved with manual skill. Monochromator rocking curves have been measured. Cryogenic cooling is now in routine use at the beamline.

For work above 17 keV the mirror can be removed. This will result in a loss of photon flux density at the sample position by a factor 10 to 20 compared to the focused beam.

The biocrystallography endstation consists of a high-precision 5-circle diffractometer and, initially, of a 2d on-line imaging-plate detector system.

The time-resolved small-angle X-ray scattering station consists of an xyz-sample-stage and a 12 m long vacuum pipe, in which a 2d-gasfilled detector is travelling.

[1] Peter Bösecke, *The High-flux Beamline at the ESRF*, Rev. Sci. Instrum. **63** (1992), pp. 438-441.

* The original name of this beamline was "High-flux Beamline".

Modular Filter Design for White Beam Undulator/Wiggler Beamlines at the Advanced Photon Source*

C. Brite, D. Shu, T. Nian, Z. Wang, D. Haeffner, E. Alp, R. Parry, and T. Kuzay

Experimental Facilities Division
Argonne National Laboratory
Advanced Photon Source
Argonne, IL 60439

ABSTRACT

A new filter has been designed at Argonne National Laboratory. It is intended for the use in undulator/wiggler beamlines at the Advanced Photon Source. The water cooled frame allows up to four individual filter foil banks simultaneously in the beam path. Additionally the bottom of each frame holds two thin (20 μ m) uncooled carbon filters in tandem for low energy filtering. Therefore a maximum of 625 filter selection combinations is theoretically possible. The design is intelligent, compact and modular, with great flexibility for the users. To prevent accidental movement of the filter, effort has been taken to provide a mechanically locked, fail-safe actuator system. Programming aspects are under development as part of our general personal and equipment protection system.

Design and operational principles aspects of the filter are presented in this paper.

* This work was supported by the U.S. Department of Energy, BES-Materials Science under contract W-31-109-Eng-38.

A PHOTON BEAM POSITION MONITOR FOR SSRL BEAMLINE 9

J. Cerino, T. Rabedeau, A. Säbersky

Stanford Synchrotron Radiation Laboratory, Stanford University,
Stanford, CA.

The Mid-Infrared Beamline at the NSLS Port U2B

G.L. Carr, Advanced Development Center, M.S. AO1-26, Grumman Corporation, Bethpage, NY 11714 USA; M. Hanfland, Geophysical Laboratory, Carnegie Institute of Washington, Washington, DC USA; G.P. Williams, National Synchrotron Light Source, Brookhaven National Laboratory, Upton, NY 11973 USA

A new infrared beamline has been developed on a conventional dipole bending magnet port of the VUV ring at the National Synchrotron Light Source. The port provides approximately 15 milliradians horizontal and 10 milliradians vertical aperture, which limits the high-brightness spectral range to wavelengths less than 20 μm . The short wavelength limit is about 300 nm, due to mirror coatings and a KBr vacuum window. Though the total flux is less than from the standard mid-infrared spectrometer source, a 1000K to 1500K blackbody, the calculated brightness of synchrotron radiation is several orders of magnitude greater. Also, the synchrotron light is delivered in sub-nanosecond pulses. The beamline was designed for simplicity, compactness, and low cost. Most components, including the mirrors, were available off-the-shelf. The infrared is transported to a commercial interferometric spectrometer system appropriate for wavelengths between 1 μm and 20 μm . Tests of the beamline's performance confirm the high source brightness. In particular, the transmitted flux (and consequently the signal-to-noise) through a 50 μm aperture was nearly two orders of magnitude greater than that for the conventional (blackbody) infrared source. The developing experimental program includes studies of hydrogen and other materials at extremely high pressures, time-resolved studies of various infrared sensor materials, and scanning microspectroscopy.

TuD9

ABSTRACT

Beamline 9 at SSRL is presently under construction. It is an insertion device beamline designed for use in structural molecular biology research. We will report results of preliminary tests of a new photon beam position monitor concept for use on the beamline.

Beam position and angle stability is a major consideration when performing high resolution experiments using synchrotron radiation. The benefits of high source brightness and low source emittance cannot be fully exploited unless the direction of the radiation can be very precisely controlled.

Since the present SPEAR beam steering system cannot independently control beam position and angle, locating the position monitor as near the experiment as possible offers the best method to control these parameters. Photo-emission and ion chamber monitors, in downstream locations are subject to mislocation of the beam due to shadows cast by upstream apertures as well as scattered low energy radiation from upstream objects such as mirrors, slits and stoppers.

We propose a position monitor which uses x-ray fluorescence from a copper target struck by the beam. The fluorescence is viewed at a large angle to the primary beam by two silicon photodiodes. The field of view of each diode is obstructed such that one diode views only the portion of the target above the median plane and the other views the portion below. Vertical motion of the beam on the target unbalances the flux onto the diodes, providing a signal to feed back to the beam steering system.

Because the monitor uses secondary radiation, only the copper target need be inside the beam transport vacuum. The detectors, and aperture defining slits can be mounted outside a beryllium window for easy adjustment and maintenance. No in-vacuum motions are required and the detectors can easily be shielded from stray radiation.

We will report on the concept and results of early tests of a prototype on Beamline 2 at SSRL.

TuD10

Design of Integral Shutters for the Beamlines of the Advanced Photon Source*

J. Chang, D. Shu, T. Nian, T. M. Kuzay, and P. K. Job

Argonne National Laboratory
Advanced Photon Source
Argonne, IL 60439

ABSTRACT

An integral shutter is a device that integrates a white-beam stop, mono-beam shutters, a safety stop, and a collimator into one assembly to save space in the photon beamline. Various typical integral shutters have been developed as standard components for the beamlines of the Advanced Photon Source. The integral shutters are designed to be operated in several different modes: white-beam pass; white-beam stop; or mono-beam pass. Each mode of operation is secured by locking certain devices at their up or down positions. Some of the devices of the integral shutters share designs similar to the front-end shutters. Design detail of the integral shutter is presented.

*This work was supported by the U.S. Department of Energy, BES-Materials Science, under contract W-31-109-Eng-38.

The submitted manuscript has been authored by a contractor of the U.S. Government under contract No. W-31-109-ENG-38. Accordingly, the U.S. Government retains a nonexclusive, royalty free license to publish or reproduce the published form of this contribution, or allow others to do so for U.S. Government purposes.

TuD11

Energy Dependences of Absorption in Beryllium Windows and Argon Gas

C. T. Chantler and J.-L. Staudenmann

National Institute of Standards and Technology

Quantum Metrology Division

Building 221, Room A141

Gaithersburg, MD 20899

In part of an ongoing work on x-ray form factors, new absorption coefficients are being tabulated for all elements, across the energy range from below 100 eV to above 100 keV. These new coefficients are applied herein to typical problems in synchrotron radiation stations, namely the use of beryllium windows and argon gas detectors. Results are compared with those of other authors. The electron-ion pair production process in ionization chambers is discussed, and the effects of 3d-element impurities are indicated.

TuD12

Soft x-ray spectroscopy beam line 6m-HSGM at SRRC: Optical design and first performance tests

S.-C Chung, C.-I. Chen, P.-C. Tseng, H.-F. Lin, T.-E. Dann, Y.-F. Song, L.-R. Huang, C.-C. Chen, J.-M. Chuang, K.-L. Tsang, and C.-N. Chang*

SRRC, No.1, R and D Rd., Hsinchu Science Based Industrial Pk., Hsinchu, Taiwan, ROC

* also at National Taiwan Normal University.

The layout and first data on the performance of the soft x-ray bending magnet beam line 6 meter High energy Spherical Grating Monochromator (6m-HSGM) at SRRC are described. The 6m-HSGM beam line, which covers photon energies from 110 to 1500 eV, is based on the Dragon concept with spherical gratings, movable exit slit. During the first performance tests core-excitation thresholds of Ar, and Ne and K thresholds of N, and O for gas phase CO, N₂ and O₂ have been recorded with resolution reached so far one of the bests in the soft x-ray region.

TuD13

Current status of the 6m-LSGM beam line at SRRC

P.-C Tseng, H.-J. Lin, S.-C Chung, C.-I. Chen, H.-F. Lin, T.-E. Dann, Y.-F. Song, T.-F. Hsieh, K.-L. Tsang, and C.-N. Chang*

SRRC, No.1, R and D Rd., Hsinchu Science Based Industrial Pk., Hsinchu, Taiwan, ROC

* also at Taiwan National Normal University

The six meter Low energy Spherical Grating Monochromator (6m-LSGM) beam line at SRRC is at its commission stage. The 6m-LSGM beam line, which covers photon energies from 15 to 200 eV, is based on Dragon concept with spherical gratings and movable exit slit. Some of the commission data will be presented in this paper.

TuD14

The Macromolecular Crystallography Beamline at ELETTRA

S. Bernstorff, E. Busetto, A. Lausi, L. Olivi, F. Zanini and A. Savoia
SINCROTRONE TRIESTE, Padriciano 99, Trieste, Italy

M. Colapietro and G. Portalone
Dipartimento di Chimica, Univ. "La Sapienza", Rome, Italy

M. Camalli, A. Pifferi and R. Spagna
Istituto di Strutturistica Chimica, CNR, Montelibretti, Rome, Italy

L. Barba and A. Cassetta
Istituto di Strutturistica Chimica, CNR, Padriciano 99, Trieste, Italy

ELETTRA is a low emittance (7×10^{-9} mrad at 2 GeV) synchrotron radiation facility currently under commissioning at Trieste. The electron energy is 1.5-2 GeV, and electron currents of up to 400 mA have been stored. One of the 11 insertion devices is a 4.5 m long, 57 poles permanent magnet wiggler. With a peak magnetic field of 1.55 T it has a characteristic energy of 4 keV (at 2 GeV) and delivers a usable photon flux up to 25 keV ($\approx 0.5 \text{ \AA}$).

The optics in this wiggler beamline is designed to deliver both monochromatic or white light. In order to obtain a higher flux on the sample a mirror collects 2.8 mrad horizontally and 0.23 mrad vertically and focuses X-rays up to 25 keV with a demagnification factor of 1.5. The SR can be monochromatized in the range 4-25 keV (0.5-3 Å) by means of a fixed-exit double-crystal monochromator containing two interchangeable pairs of Si(111)- or Si(220)-crystals in a nondispersive parallel setting. The first monochromator crystal will be internally water cooled. During the white beam mode, a rotating beam chopper can be used to reduce the sample illumination time according to the required short measuring times in order to keep the total energy deposited on the mirror, on the beamline exit window and also on the sample (on which up to 415 W/mm² would arrive) within safe limits. A cooled N₂-stream will also be available to cool the sample crystal.

The experimental station is equipped with both a Mod. 5020 Huber 4-circle diffractometer and an imaging plate detector system from Marresearch (diameter 180 mm). The diffractometer is driven by 5-phase stepper motors with an angular resolution of 0.001° for each circle. A kinematic table allows to align the instrument with respect to the beam using a closed-loop electronic control based on a X-ray sensitive CCD. The diffractometer is controlled by a personal computer through a plug-in board interface developed by us. The program system CS has been written to carry out single crystal diffraction experiments and a great effort has been made to make it user friendly, highly flexible and easy to modify as an "open instrument". The imaging plate system is controlled by a VAX station 3100 using the software supplied by the factory and shares the beam with the diffractometer. For data analysis and molecular structure determination the most powerful packages are available.

The commissioning of the entire beamline will take place during late spring / early summer of 1994. First results will be presented during the conference.

Six degree-of-freedom scanning supports and manipulators based on parallel robots

Fabio Comin

ESRF

The exploitation of third generation SR sources heavily relies on accurate and stable positioning and scanning of samples and optical elements. In some cases active feedback is also necessary. Normally these tasks are carried out by serial addition of individual components, each of them providing a well defined excursion path. On the contrary, the exploitation of the concept of parallel robots, structures in close cinematic chain, permits to follow any given trajectory in the six dimensional space with a large increase in accuracy and stiffness. At ESRF the parallel robot architecture, conceived few tens of years ago for flight simulators has been adapted to both actively align and operate optical elements of considerable weight and position small samples in Ultra High Vacuum. The performance of these devices resulted far superior the initial specification and a variety of drive mechanism have been developed to fit the different needs of the ESRF beam lines.

Design and Performance of the High-Flux X-Ray Wiggler Beamline BW2 at HASYLAB

**W. Drube, H. Schulte-Schrepping, H.-G. Schmidt,
R. Treusch and G. Materlik**

**Hamburger Synchrotronstrahlungslabor HASYLAB
am Deutschen Elektronen-Synchrotron DESY
Notkestr. 85, 22603 Hamburg, Germany**

After its first year of full operation the X-ray wiggler beamline BW2 has proven to be a powerful instrument for state-of-the-art X-ray experiments requiring high monochromatic photon flux. It is designed to cover a wide energy range from 2.02 to 35 keV for a variety of experimental X-ray techniques such as surface diffraction, photoemission, absorption, micro-tomography, standing waves etc.

Briefly, the white beam produced by a 56-pole hybrid wiggler (maximum total power 7 kW at 100 mA) is monochromatized by a fixed-exit Si(111) double crystal arrangement operated under vacuum. A cooled plane pre-mirror in combination with a demagnifying toroidal mirror in the monochromatic beam is used to achieve a well focused beam up to 12 keV. The thermal distortion of the first crystal is minimized by means of direct water-cooling. In order to provide high photon flux also at the lowest accessible energies – for uhv-compatible experiments – the beamline is windowless except for a carbon-foil (20 μ) at the monochromator entrance. For photon energies above 12 keV the beamline is operated without mirrors.

Details of the optical design, monochromator, beam position and intensity diagnostics, and beamline control are presented. The high performance is demonstrated by measurements of its beam characteristics and selected results of recent scientific experiments obtained at this beamline.

TuD17

Computer Control of the SRC High Resolution Beamline

**David E. Eisert, John P. Stott, Mike V. Fisher, Mark Bissen, and Hartmut Höchst
Synchrotron Radiation Center, University of Wisconsin-Madison
3731 Schneider Drive, Stoughton, Wisconsin 53589-3097, U.S.A.**

We discuss the complexity in controlling the new high-resolution soft X-ray beamline^{1,2,3,4} at the University of Wisconsin Synchrotron Radiation Center. A monochromator at the heart of the beamline utilizes a combined rotation and translation of a variable line spaced grating to minimize major aberration terms. A rotational accuracy of 0.12 arc seconds and a translational accuracy of 10 micrometers are required for the combined motions to obtain the desired resolution. A rotational resolution better than 0.01 arc seconds was achieved with the use of a laser interferometer and piezoelectric actuator for sub-micrometer feedback control. The translation control uses a linear encoder with a resolution of 0.1 micrometers and a motorized feedback loop. A calculation speed of less than 100 microseconds per step in scan energy was obtained using a spline fit to accurately "approximate" the required rotational and translation positions. In all there are five stepping motors, one optical encoder, one piezoelectric actuator, one laser interferometer and several status indicators controlled from a five-slot VME system. This beamline VME system controls the monochromator as well as the entrance and exit slits. A PC is used to collect data from the scan and handle the user interface to the beamline control. This PC also has an ethernet connection to the storage ring VME system which allows the PC to collect real-time information from the storage ring computers as well.

- [1] H. Höchst, M. Bissen, M.A. Englehardt and D. Crossley, "Design study of a high resolution soft X-ray monochromator with a movable variable groove density grating", Nucl. Instr. and Meth. A 319 121 (1992).
- [2] Optical systems based on the combined translation and rotation of a varied line space grating are protected by US Patent no.4 991 934 issued to M.C. Hettrick and licensed to SRC by Hettrick Scientific Inc., P. O. Box 8046, Kensington, CA 94707.
- [3] M.V. Fisher, N. Steinhauser, D.E. Eisert, B. Winter, B. Mason, F. Middleton, H. Höchst "Combining rotation and translation in a variable line space high-resolution soft X-ray monochromator: design requirements and performance evaluation of a novel grating mount", In press, Nucl. Instr. and Meth.
- [4] M. Bissen, M.V. Fisher, G. Rogers, D.E. Eisert, K. Kleman, T. Nelson, B. Mason, F. Middleton, and H. Höchst "First test results of SRC's new high energy variable line density grating monochromator", These proceedings.

TuD18

THE SURFACE DIFFRACTION BEAMLINE AT ESRF

Salvador Ferrer and Fabio Comin
ESRF, BP 220, 38043 Grenoble Cedex. France

The Surface Diffraction beamline is installed in a low beta section of the electron orbit at the exit of a standard ESRF undulator of 44 mm of period with a fundamental energy of 3 keV and a critical energy of 11.8 keV. The beam position and shape are visualized with two position monitors described elsewhere in these proceedings.

The first active optical element is a Si (111) double crystal monochromator cryogenically cooled and sagittally focusing. Characteristic figures of merit are the following. The FWHM angular widths of the transmitted intensity of the (333) reflection measured by rocking the second crystal through the Bragg angle (21 degrees) are 7 μ rad and 11 μ rad for the thermal loads on the first crystal of 3 and 143 watt respectively. Also, horizontal focusing of the beam down to 150 μ m at the sample position (45 m from the source) has been achieved at 16 keV without significant loss of intensity (see these proceedings for details).

The end station is based on a six circle diffractometer with its main axis horizontal. The sample surface sits in a vertical plane in UHV and can be oriented by three circles (ϕ, χ, θ) in air. The pressure gradient is maintained with a specially designed rotary feedthrough. The detector has two degrees of freedom: one in the vertical plane and another in the horizontal plane. A vertical rotation axis along the sample surface allows to define the angle of incidence.

The diffraction chamber has two beryllium windows which allow a maximum in plane scattering angle of 150 degrees and a maximum X-ray outgoing angle of 46 degrees. The sample, while sitting in the X-ray scattering position, may be monitored with RHEED and with Auger Electron Spectroscopy by means of a retractable Cylindrical Mirror Analyzer. Also, it can be ion sputtered and exposed to the flux of several deposition cells for in situ growth studies. Adjacent to the main chamber, a UHV preparation chamber allows storing, cleaning and outgasing samples before transferring them into the main chamber.

Measurements on the Ge(001) 1x2 reconstructed surface performed during the commissioning phase give counting rates of 10^5 photons per second for the (0,1.5, 0.2) surface reflection for a stored beam current of 100 mA and a photon energy of 16 keV.

TuD19

The X-Ray Undulator Beamline BW1 at DORIS III

R. Frahm, J. Weigelt, G. Meyer and G. Materlik

Hamburger Synchrotronstrahlungslabor HASYLAB at DESY
Notkestr. 85, D-22603 Hamburg, Germany

The BW1 X-ray undulator beamline at HASYLAB is well suited for advanced applications of synchrotron radiation requiring high intensities like QEXAFS or X-ray diffraction on surfaces, DAFS, experiments with standing waves or scattering studies of amorphous materials using anomalous dispersion. Such an experimental setup has to cope with high heat loads from the insertion device and has to have a high precision monochromator.

The X-ray undulator at the positron storage ring DORIS III is a 4m long device with 127 periods ($\lambda = 3.14$ cm) and a variable magnetic gap ranging from 15 to 25 mm (maximum magnetic field 0.49 T). At 4.5 GeV ring energy this corresponds to a photon energy range from about 9 to 15 keV in the 3rd harmonic of the undulator. The tuning range of the 1st harmonic can be accessed by using thin diamond- or graphite windows along the beamline.

There are four operating modes: i) focussing the white beam using two mirrors with a cut-off energy of approximately 11 keV, ii) focussed monochromatic beam using both mirrors with a cut-off energy of ≈ 12 keV and a double crystal monochromator, iii) unfocussed monochromatic beam using the monochromator without mirrors and iv) focussed monochromatic beam using the monochromator without mirrors using a sagittally focussing second monochromator crystal. The monochromator is a (+,-) double crystal fixed exit monochromator under high vacuum. The first crystal is directly water cooled to reduce the distortion induced by the high heat load of the white beam. Each crystal is mounted on a piezo-driven micro-goniometer in order to stabilize the intensity of the monochromatic beam. A feedback system with absolute position readout corrects for the hysteresis of the piezo crystals.

A universal X-ray multicircle diffractometer is installed at beamline BW1. This device offers an extraordinary large number of degrees of freedom for sample adjustments and independent movements of two detectors.

All movements of the beamline components are performed by a total of up to 48 stepper motors, which are controlled by a μ VAX. Most of the experiment control and data acquisition is done using CAMAC hardware using a universal data collection software designed at HASYLAB.

Typical scientific investigations performed at this beamline like surface studies or DAFS measurements will be presented to demonstrate the capabilities of the whole setup.

TuD20

**COMPARISON OF NUMERICAL AND EXPERIMENTAL
SIMULATION OF A BERYLLIUM WINDOW UNDER INTENSE
HEAT LOAD**

A. Gambitta (1), C. Poloni (2) , A. Visintin (2) and F. Zanini (1,3)

- (1) Sincrotrone Trieste, Trieste (Italy)
- (2) Dip. di Energetica, Università di Trieste; Trieste (Italy)
- (3) I.N.F.N., Sezione di Trieste, Trieste (Italy)

Beryllium windows are widely used in synchrotron radiation beamlines as filters to absorb photons in the lower energy region or used as an interface between two different vacuum environments. In the X-Ray Diffraction beamline at Elettra the UHV environment of the front-end is decoupled from the high vacuum of the beamline by means of two different beryllium windows. The first one act as a prefilter and will absorb most of the heat load, while the second is a safety, bent window against a possible overpressure due to accidental venting in the high vacuum part of the beamline. We focalize our attention on the first window to evaluate its resistance to thermal loads by means of a finite element method analysis and an experimental test with an electron gun assembly. This subject has already been studied by some research groups who have usually found a large discrepancy between experimental results and theoretical predictions, finding a higher resistance to thermal loads. To overcome this discrepancy, non-linear analysis in the plastic region of the material is developed taking into account the behaviour of the material as a function of temperature.

TuD21

**DC-SERVO-MOTOR CONTROLLED FOUR-JAW
SLITS FOR SYNCHROTRON RADIATION**

R. F. Garrett, and D. J. Cookson
Australian Nuclear Science and Technology Organisation,
PMB 1, Menai, NSW, 2234, Australia.

P. Davey, S. Janky and S. W. Wilkins
CSIRO-Division of Materials Science and Technology
Locked Bag 33, Clayton, Vic, 3168, Australia.

A four jaw slit system and controller has been constructed and is in use at the Australian National Beamline Facility at the Photon Factory. The slits can be actuated by motorised or manual micrometers, and are designed such that the jaws are only driven open, avoiding the problem of jamming the jaws together. Two models were built, a free standing slit and one built into the main vacuum flange of the diffractometer. Due to the vacuum operation of the diffractometer, DC motors were preferred over stepper motors.

In several configurations of operation, up to 16 DC motors are installed in the diffractometer. This relatively large number presented problems if commercially available DC servo controllers were used: most are either PC bus or serial communication devices, and operating four or five from a PC is difficult at best. Our solution was to construct an 8 axis controller which is designed to be used in conjunction with the popular E500 camac stepper motor control module. This is accomplished using a DC controller chip manufactured by the Galil company. In this way, the DC servo motors and other stepper motors used at the beamline are controlled via the same hardware (E500s). The other advantage is that the E500 controller has the facility to download an arbitrary motor position (when slits are swapped for example); this function is not available in commercial DC controllers to our knowledge.

Design details of the slits and controller will be presented, and the operational experience gained with the devices will be described.

TuD22

**THE AUSTRALIAN NATIONAL BEAMLINE
FACILITY AT THE PHOTON FACTORY**

*R. F. Garrett, D. J. Cookson and G. Foran
Australian Nuclear Science and Technology Organisation,
PMB 1, Menai, NSW, 2234, Australia.*

*D. C. Creagh
Physics Department,
Australian Defence Forces Academy,
Campbell, ACT, 2600, Australia.*

*S. W. Wilkins
CSIRO-Division of Materials Science and Technology
Locked Bag 33, Clayton, Vic, 3168, Australia.*

The Australian National Beamline Facility has been installed at the Photon Factory, Tsukuba, Japan. The construction and operation of the facility has been funded by a consortium of Australian research organisations, universities and government funding agencies. with the aim of providing Australian scientists with routine access to synchrotron radiation in the hard X-ray region. The first experiments were performed at the ANBF in November 1992.

The facility consists of a general purpose X-ray beamline, including a simple two-crystal monochromator, delivering either monochromatic X-rays (range 5-20 keV) or white radiation to the experimental hutch. The main experimental instrument, a multi-configuration diffractometer, has recently been installed at the beamline. This unique instrument combines vacuum operation and Imaging Plate detectors, and can be configured for high resolution powder diffraction (including a time resolved mode), protein crystallography and triple axis experiments. In addition, the white or monochromatic beam can pass through the diffractometer to a secondary experimental table, where experiments such as EXAFS, Laue diffraction, topography and micro-beam measurements are performed.

Details of the beamline, monochromator and diffractometer optics and performance will be described, and an overview will be given of the experimental capabilities of the facility.

TuD23

Wave transmission, high precision (0.03") rotation stage for synchrotron radiation instrumentation.

N.G.Gavrilov*, O.V.Evdokov**

Institute of nuclear physics,
Novosibirsk-90, Russia(*)
Institute of solid state chemistry,
Novosibirsk-91, Russia(**)

There are many problems connected with using precise device for linear and angular translation in synchrotron radiation beam lines. New experiments need more and more high precision technic.

The most using gear transmission mechanism has essential defect - the inconstant instantaneous transmission ratio. This defect is especially strong during rotation at small angles (in range of 0.1 - 0.2 degree of arc) and can reach 3"-10" in this region. Therefore we used absolutely different principle of transmission of rotation which has not such failing.

This defect was overcome in rotation stage developed in BINP and ISSC, in which rotating mechanism made on basis of wave transmission.

In the report will be show how this and same type mechanism works. The rotation from step motor and gear transmission is transfer to wave generator. This rotation deform the elastic circle and generate wave of deformation in it. The rotation of flange with crystal-monochromator, install on inside circle of gliding bearing happen because of the difference of diameter of internal circle of bearing and elastic circle. The external circle of self-grease gliding bearing fasten on the body of mechanism. Ending and radial beat of self-grease gliding bearing are 0.002 mm on the diameter 140 mm ($2.8 \cdot 10^{-5}$ rad). Calculating angle of rotation by one impulse of step motor is 0.06". Calculating error from the inconstant instantaneous transmission ratio of gear transmission are 0.03".

Therefore the error in rotation was decrease more then 100 times in compare with usual gear transmission mechanism.

Moment of rotation - 200 N/cm
The sizes of rotation stage 180x180x50 mm.

TuD24

The TROIKA BEAMLINE at ESRF

G. Grübel, J. Als-Nielsen and D. Abernathy
European Synchrotron Radiation Facility
B.P. 220
F-38043 Grenoble
France

The Troika beamline at ESRF is based on the concept of beam multiplexing by using x-ray transparent diamond and/or beryllium monochromators. The favorable thermal and crystallographic properties of perfect diamond are well matched to the characteristics of the new low emittance undulator sources. A series of such transmission monochromators can use the same white beam and supply several experimental stations simultaneously with monochromatic x-rays of slightly different energies. The first experimental station of the Troika beamline is operating and the multiplexing mode has been tested successfully. First experiments including Protein Crystallography, Resonant Magnetic Scattering, Liquid Surface Diffraction and Scattering with Coherent X-Rays were carried out during the commissioning period and the results demonstrate the wide potential of third generation synchrotron sources.

TuD25

THE ANL X6B BEAMLINE AT NSLS: A VERSATILE FACILITY

K.G. Huang, M. Ramanathan, and P.A. Montano

Materials Science Division, Argonne National Laboratory, Argonne, IL 60439, USA

The Argonne National Laboratory (ANL) X6B beam line has been completed at a bending magnet port at the National Synchrotron Light Source (NSLS). The main components of the X6B beamline include premonochromator slits, a double-crystal fixed-exit monochromator, a double-focusing mirror, and a six-circle HUBER diffractometer. With high intensity, high energy resolution, high-q resolution, and energy tunability, the X6B beam line has become a versatile facility for a variety of diffraction, scattering, and spectroscopy experiments.

The monochromator, positioned 9.8 m from the source, consists of two nondispersive silicon (111) or (220) crystals and delivers monochromatic beams with a fixed offset of 1° [1]. The cylindrical rhodium-coated fused silica mirror is located 12 m from the source (1:1 focusing) and is bent to focus the x-ray beam both vertically and horizontally. At 1:1 focusing, the incident beam with 5.0 mrad horizontal divergence and 0.33 mrad vertical divergence can be focused into a spot with a FWHM of 0.65 mm in diameter. A total intensity of 3×10^{11} photons/sec was obtained at 8 keV and 100mA electron current, and the corresponding area intensity is nearly three orders of magnitude higher than that of an unfocused beam at the same energy.

The beam line can be operated in either focused beam or unfocused beam modes depending on the experimental requirements. With focused beam, many experiments have been carried out such as x-ray reflectivity and diffuse scattering, surface diffraction, powder diffraction, energy dispersive diffraction, diffraction anomalous fine structure (DAFS), and XAFS, while the unfocused beam has been used for coherent scattering and dynamical diffraction experiments. We describe the x-ray optics and beamline performance, and present selected experimental results to demonstrate the flexibility and important features of the X6B beam line as a versatile facility.

This work has been supported by the U.S. Department of Energy (DOE), Office of Basic Energy Sciences, Division of Materials Sciences, under contract W-31-109-ENG-38.

[1] M. Ramanathan *et al.* these proceedings.

TuD26

New Beamline (BL-28B) for Circularly Polarized X-rays at the Photon Factory

Toshiaki IWAZUMI, Atsushi KOYAMA and Yoshiharu SAKURAI*

Photon Factory, National Laboratory for High Energy Physics, Oho, Tsukuba, Ibaraki 305, Japan

*JAERI-RIKEN SPring-8 Project Team, Honkomagome 2-28-8, Bunkyo, Tokyo 113, Japan

In the Photon Factory, there are two insertion devices to generate the intense circularly polarized synchrotron radiation, EMPW#28 and EMPW#NE1. Both devices are complementary each other on the radiated energy range. Beamlines, NE1A2 (6 ~ 100 keV), NE1B (240 ~ 1500 eV) and 28A (5 ~ 300 eV), were already commissioned in 1991.

Design and construction of new beamline BL-28B for the experiments using the EMPW#28 in the multipole wiggler mode were done from the spring of 1991 to Feb. of 1993. Designed specifications are as follows;

#Photon Energy: 2 ~ 10 keV,
#Beam Acceptance: 4.0 mrad(H) x 0.2mrad(V),
#Pre-Mirror: 18.8 m from source point,
16 mrad reflection, Pt-coated Si & Ni-coated Si,
Bent cylinder, Indirect water cooling,
#Double crystal monochromator:
29.0 m from source point, Fixed exit beam position,
Several kinds of crystals, Indirect water cooling,
#Post-Mirror: 30.5 m from source point,
16 mrad reflection, Pt & Ni-coated SiO₂, Bent plane,
#Focusing Point: 34.5 m from source point.

Photon beams were successfully transported into the experimental hutch in 15 Feb. '93. Obtained specifications at focusing point in the present stage are as follows;

#Focusing Size: 2.4 mm(H) x 0.3 mm(V),
#Photon Flux: 3×10^{10} photons/sec at 9 keV,
#Energy Resolution: 2 eV at 6.3 keV,
#Degree of Circular Polarization:
0.46 at 8.3 keV, 0.41 at 7.7 keV, 0.30 at 6.5 keV.

All above data were taken using Pt-coated pre-mirror, Si(220) monochromator crystals and Pt-coated post-mirror.

TuD27

Performance of Beamline 4W1C for X-ray Diffuse Scattering Station at Beijing Synchrotron Radiation Facility

X. Jiang, W. Zheng, J. Wu, Y. Jing, and G. Liu
Synchrotron Radiation Laboratory, Institute of High Energy Physics,
P. O. Box 918, 100039 Beijing, P. R. China

4W1C is a branch of the beamline 4W1B at Beijing Synchrotron Radiation Facility^[1,2], therein monochromatic X-rays are focused by a bent triangular crystal monochromator (horizontally) and cylindrical mirror (vertically) onto the sample about 5m far away in the diffuse scattering station. Three different oriented Si crystals cut with oblique-cut angle 12.16° were located at a distance of 13.8m from the wiggler source to satisfy the Guinier condition^[3]. Focused monochromatic X-rays of wavelengths 2.52Å, 1.54Å, and 0.89Å are available by Si(111), Si(220) and Si(422) crystals respectively.

During the recent SR dedicated operation of BEPC, the performances of the beamline with the bent triangular crystal and the mirror were tested.

The measured horizontal dimension of the focused beam spot was 1.4mm and the maximum photon density reached 2.0×10^7 photons/mm²·mA·s at the sample position. Diffraction pattern of the standard Si powder was acquired to check the alignment of the 5-circle diffractometer. The interplanar spacings obtained from the diffraction pattern fitted to the standard ASTM values with the maximum relative error $|\Delta d/d| \leq 2 \times 10^{-3}$. The resolution of the monochromatic beam was measured as 4.3×10^{-4} through the rocking scanning of a Si(333) crystal.

The cylindrical mirror, located after the bent triangular crystal to focus the beam vertically, is made of Al substrate coated with 500 Å Pt film and of the size of 800×80mm². The second harmonic X-rays were suppressed to less than 2×10^{-4} in the reflected beam at glancing angle of 0.31°. Reflectivities of the mirror with the 1.54Å X-rays were obtained experimentally as 86% and 83% under the incident angles of 0.17° and 0.30°. These experimental data are consistent with calculations based on the Fresnel formula for the Pt coated mirror with surface roughness of 20Å. Furthermore, the vertical dimension of the focused beam reached as small as 0.1 mm at the glancing angle of 0.30° as the mirror was curved to cylindroid.

The beamline 4W1C and attached diffuse scattering station is now being prepared to pass acceptance of the state. Recent experiments in nonspecular X-ray scattering from amorphous multilayers, characterization of superlattice structures and diffuse X-ray scattering of irradiated crystals will be discussed.

References:

- [1]. X. Jiang, Y. Fang, D. Liu, and D. Xian, Proceedings of the International Conference on Synchrotron Radiation Applications. (USTC Press, 1990)P409
- [2]. Y. Jing, S. Xia, Q. Zhang, Y. Zhang, C. Liu, and D. Xian, Rev. Sci. Instrum. 63, 1077(1992)
- [3]. G. Rosenbaum, and K. C. Holmes, in *Synchrotron Radiation Research*, Chapter 16. Ed. H. Winick, and S. Doniach, Plenum Press, New York, 1980.

TuD28

Construction and performance of the beamline NE1B for circularly polarized soft x-rays in the TRISTAN Accumulation Ring

Y. Kagoshima¹⁾, S. Muto²⁾, S.-Y. Park²⁾, J. Wang²⁾, T. Miyahara¹⁾, S. Yamamoto¹⁾ and H. Kitamura¹⁾

¹⁾ Photon Factory, National Laboratory for High Energy Physics, Tsukuba, Ibaraki 305, Japan

²⁾ Department of Synchrotron Radiation Science, The Graduate University of Advanced Studies, Tsukuba, Ibaraki 305, Japan

The NE1B has been designed and constructed mainly for research studies on circular dichroism (CD) or magnetic circular dichroism (MCD) of various materials including biological materials, magnetic thin films and molecules adsorbed on surfaces in an energy region of soft x-rays. It serves us with circularly polarized synchrotron radiation produced by a helical undulator operation mode of an insertion device named "Elliptical Multipole Wiggler #NE1 (EMPW #NE1)"¹⁾, which is a combination of a horizontal and a vertical arrays of permanent magnets. The commissioning of a hard x-ray branch was already finished²⁾.

The radiation is firstly deflected into a soft x-ray branch, namely NE1B, by a water-cooled SiC plane mirror about 20 m apart from a center of the EMPW#NE1 and deflected again by a SiO₂ variably bendable cylindrical mirror about 10 m apart from the first mirror, and then introduced into a vertical dispersion grazing incidence grating monochromator. It is of the inverse Vodar type with two interchangeable gratings with groove densities of 1200 lines/mm and 2400 lines/mm. The radius of curvature of the gratings is 10.31 m. The monochromatized light is post-focused by a toroidal mirror. The focused spot size is approximately 0.2 mm (V) x 0.8 mm (H).

In order to evaluate the spectral resolution of the monochromator, well-known K-edge absorption spectrum of gas phase N₂ has been measured with a grating with groove density of 1200 lines/mm and with 10 μ m-10 μ m slit openings. At least five vibration structures have been clearly observed. Compared with the results obtained at other facilities, the achieved energy resolution may be better than 90 meV ($E/\Delta E \sim 4400$). Since the ray tracing shows that the achievable spectral resolution reaches 10000 in $E/\Delta E$, the result has not reached the designed resolution. From the photoelectron yield of I_0 monitor, the photon flux under the above resolution has been evaluated to be about 5×10^8 photons/s.

We have already measured the magnetic circular dichroism of Ni, Ni_x/Pd_{1-x}, Co_x/Pd_{1-x} and Fe_x/Pd_{1-x} alloys in 2p-3d excitation region of Ni, Co and Fe, and in 3p-4d excitation region of Pd, respectively, by detecting total photoelectron yield. The results and analysis will be given elsewhere³⁾.

A soft x-ray microscope using zone plates has been also performed. Micrographs of test patterns and some dry biological specimens has been obtained under the spatial resolution of about 130 nm and the optical magnification of about 1000. The results will be also given elsewhere⁴⁾. Another microscope, to which magnetic circular dichroism is applied, is also under commissioning. Its instrumentation and preliminary result will also be given elsewhere⁵⁾.

References

- 1) S. Yamamoto, H. Kawata, H. Kitamura, M. Ando, N. Sakai, and N. Shiotani, Phys. Rev. Lett. 62, 2672(1989).
- 2) H. Kawata, T. Miyahara, S. Yamamoto, T. Shioya, H. Kitamura, S. Sato, S. Asaoka, N. Kanaya, A. Iida, A. Mikuni, M. Sato, T. Iwazumi, Y. Kitajima and M. Ando, Rev. Sci. Instrum. 60, 1885(1989).
- 3) S.-Y. Park *et al.*, in preparation.
- 4) J. Wang *et al.*, in this conference.
- 5) Y. Kagoshima *et al.*, in this conference.

Optical design and performance of the inelastic scattering beamline at the National Synchrotron Light Source

C.-C. Kao, K. Hamalainen, M. Krisch, D.P. Siddons, J.B. Hastings, T. Overluisen

National Synchrotron Light Source, Brookhaven National Laboratory

Upton, New York 11973

Phase I of the X21 beamline at the National Synchrotron Light Source was commissioned during 1993. The research program at the X21 beamline is focused on the study of electronic excitations on the scale of 0.1 eV to 1.0 eV. The source is a 27 pole hybrid wiggler. A water-cooled horizontal focusing Si(220) monochromator and a spherically bent Si(444) analyzer were installed and commissioned. The monochromator accepts the full vertical opening of the beam, 0.25 mrad, and 0.5 mrad in the horizontal direction. At 8 keV, the energy resolution of the monochromator is about 0.7 eV, the focused beam size is about 0.2mm(H) x 10mm(V). The photon flux delivered onto the sample is about 2×10^{11} per second at 100 mA ring current. The analyzer is bent to about 1 meter radius with an effective diameter of 35 mm. The energy resolution of the analyzer is about 0.1 eV. Several demonstration experiments will also be reported.

* Supported by US DOE under contract #DE-AC02-76CH00016.

Conceptional Design of the High Energy Undulator Pilot Beamline for Macromolecular Crystallography at the SPring-8

N. Kamiya^{*1}, T. Uruga^{*1}, H. Kimura^{*1}, H. Yamaoka^{*1}, Y. Kashihara^{*2},
M. Yamamoto^{*1}, Y. Kawano^{*1}, T. Ishikawa^{*1}, H. Kitamura^{*1}, T. Ueki^{*1},
H. Iwasaki^{*1}, N. Tanaka^{*3}, K. Hamada^{*4}, H. Moriyama^{*3}, K. Miki^{*5} and I. Tanaka^{*6}.

^{*1}The Institute of Physical and Chemical Research (RIKEN), Hirosawa 2-1, Wako 351-01, Japan. ^{*2}Japan Synchrotron Radiation Research Institute, Minatojima-Nakamachi, Chuo-ku, Kobe 650, Japan. ^{*3}Tokyo Institute of Technology, Nagatsuda 4259, Midori-ku, Yokohama 227, Japan. ^{*4}Shimane University, Nishikawatsu 1060, Matsue 690, Japan. ^{*5}Kyoto University, Sakyo-ku, Kyoto 606-01, Japan. ^{*6}Hokkaido University, Kita 10 Nishi 8, Kita-ku, Sapporo 060, Japan.

SPring-8 (Super Photon ring-8GeV) is a third-generation synchrotron radiation facility of Japan for basic science and advanced technology, and is under construction by the JAERI-RIKEN SPring-8 project team at Harima Science Garden City in Hyogo prefecture. (Commissioning of the storage ring will be started early at 1997.) The SPring-8 project team adopted our proposal as one of the two pilot beamlines for standardizing the beamline elements. X-ray crystallography of biological macromolecules is a most powerful technique to determine their three-dimensional structures, and contributes very much to a recent progress of biology. However, the technique is limited now on the complicated process of multiple isomorphous replacement phasing, and on the data collections for small crystals less than 100 μm or for very large macromolecules such as ribosomal particles. All of these limitations are due to the available energy range of X-rays and its brilliance. The light source of our beamline is an in-vacuum type undulator of magnetic periodicity of 3.2 cm, which emits highly brilliant X-rays in the energy range between 9 and 38 keV. One of the most serious problems is high heat load up to 5 kW from the light source. The highest power density is 300 kW/mrad². To handle the tremendous power density of the undulator light, grazing incidence diffraction with variable glancing angle will be used for the first crystal of a fixed-exit double crystal monochromator. Compatibility of grazing incidence and fixed-exit is achieved by introducing an additional crystal rotation axis to the so-called inclined diffraction geometry being developed in APS. To focus the high energy X-rays up to 38 keV, two super mirrors (Ovonic Synthetic Materials Co.) will be installed in this beamline to get quasi-isotropic and small beam profile of about 100 μm at focal position. For recording the diffraction patterns of sample crystals, imaging plate (Fuji Photo Film Co.) will be used as the X-ray detector in the experimental station.

TuD31

A NEW MECHANISM TO BALANCE MOMENT OF INERTIA INDUCED IN A GONIOMETER AXIS

Toshiharu Kikuchi, Yasuo Takagi^{*}, Satoshi Sasaki^{**}, Takeharu Mori^{***}, and Hiroyuki Kohzu^{****}
Advanced Materials and Technology Research Laboratories,
Nippon Steel Corporation, 1618 Ida, Nakahara-ku, Kawasaki 211, JAPAN.
^{*}Advanced Materials and Technology Research Laboratories, Futtsu Branch,
Nippon Steel Corporation, 20-1 Shintomi, Futtsu, Chiba 299-12, JAPAN
^{**}Research Laboratory of Engineering Materials, Tokyo Institute of Technology, 4259 Nagatsuta, Midori-ku, Yokohama 227, JAPAN.
^{***}Photon Factory, National Laboratory for High-Energy Physics (KEK), 1-1 Oho, Tsukuba 305, JAPAN.
^{****}Kohzu Seiki, Co., Ltd., 2-27-37 Misyuku, Setagaya-ku, Tokyo 154, JAPAN

A new mechanism to balance moment of inertia being generated at a rotation center of goniometers during its rotation were installed to the 2θ axis of the four-circle/triple-axis diffractometer, SIN-1 at PF-BL3A(1) - 3) in order to avoid serious mechanical troubles such as hunting of motors and wear of gears, and to increase accuracy of its movements and life time.⁴⁾ A new moment, L_a , which is adjustable corresponding to a successive change of the moment (L_i) due to the motion of the axis was generated, and applied to the axis in order to balance the moment. The system consists of two pair of a sequence of a wire, a displacement gauge, a linearizer, an electropneumatic controller, and an air-cylinder, as described in a flow chart in Figure. The wire is hooked to a pin fixed onto the 2θ axis to apply F_a to the axis by the tension of the wire. The displacement gauge detects the wire position which reflects the 2θ -axis position. The output voltage of the sensor is transformed to the air cylinder pressure appropriate to balance the value of L_i through the linearizer and the electropneumatic controller. The air pressure is finally converted to the wire tension, and generate L_a . The linearizer function, G was determined and adjusted by calculation, depending on the weight of the equipments mounted on the axis. By this mechanism, 2θ axis can be scanned as fast as 100°/min when the L_i is as large as 500 Nm.

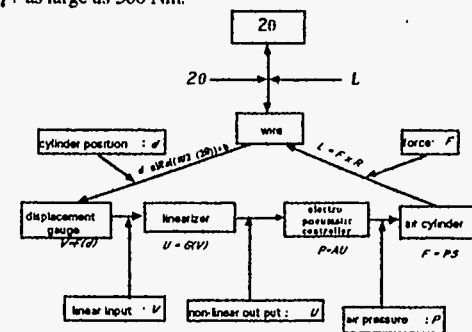


Figure The mechanism of detecting intrinsic moment, and generating applied moment.

REFERENCES

- 1) K Kawasaki, Y Takagi, K Nose, H Morikawa, S Yamazaki, T Kikuchi and S Sasaki Rev. Sel. Instrum., 63(1992)1023
- 2) Y Takagi, T Kikuchi, T Mizutani, K Kawasaki, S Sasaki and T Mori Photon Factory Activity Report 10(1992)43
- 3) Y. Takagi, T. Kikuchi, T. Mizutani, M. Imafuku, S. Sasaki, and T. Mori Rev. Sel. Instrum., to be published, (in this volume).
- 4) T. Kikuchi, Y. Takagi, S. Sasaki, T. Mori, and H. Kohzu Photon Factory Activity Report, 10(1992)44

TuD32

The Naval Research Laboratory's New Hard X-ray Beam Line at the
National Synchrotron Light Source

J.P. Kirkland

SFA Inc., 1401 McCormick Dr., Landover, MD 20785

W.T. Elam

Naval Research Laboratory, Condensed Matter
Physics Branch, Washington, DC 20375

The Naval Research Laboratory is currently redesigning our beam line at the NSLS. The energy range of the beam line will be increased from the present range of 3.5 to 10.5 keV to a range of 2.5 to 30 keV. The present optical system will be entirely replaced. The current beam line optics include a dynamically-bent flat mirror that vertically collimates the synchrotron radiation, a fixed-exit two-crystal monochromator, and a dynamically-bent cylindrical mirror that focuses the light horizontally. These optics will be replaced by a two flat mirrors configured to give a fixed-exit beam over grazing incidence angles that may vary from 10 mrad down to 2.5 mrad. The first mirror of the pair can be dynamically bent to either collimate or focus the light vertically. The mirror system removes all second and third order harmonics for energies above 6 keV. The mirrors will be followed by a fixed-exit two-crystal monochromator with a sagittally focusing conical second crystal. A conical crystal allows the Bragg condition to be met over a wide horizontal acceptance angle with a focal spot approximately 1 x 1 mm. The horizontal acceptance of the line will be increased from 6 mrad to 18 mrad. The flux is expected to increase by a factor of 10 to 30 due to improved mirror surfaces, elimination of the second reflecting surface, and increased horizontal acceptance. The beam line is used for XAFS, diffraction, and DAFS, all of which will benefit from the improved focusing, higher flux, and increased energy range.

TuD33

On the Use Of Electronic Tilt Sensors as angle encoders for Synchrotron
Applications

G. S. Knapp and H. You

Materials Science Division, Argonne National Laboratory, Argonne IL 60439

Gary R. Holzhausen

Applied Geomechanics Incorporated, Santa Cruz, CA 95062

The accurate measurement of angles is difficult in the hostile environment in which monochromators, mirrors and other beam line components must operate. In many cases the angle encoder must be insensitive to high radiation environments, may need to be ultrahigh vacuum compatible, should be quite sensitive and reproducible, and should have a reasonable time response. We have tested some electrolytic tilt sensors produced by Applied Geomechanics Inc. These sensors operate on the principle that a bubble, suspended in a liquid-filled case is always bisected by the vertical gravity vector. As the case tilts, the case moves around the bubble, linearly changing the electrical resistance measured through the electrolyte. A pair of $\pm 40^\circ$ sensors, model number 757-1122, were tested by mounting them on the Chi circle of a Huber 4 circle diffractometer. The angles were scanned in 1° intervals over a range of $\pm 38^\circ$. Under ideal test conditions such detectors have a repeatability and resolution of ± 1 arc second. In the Huber tests the resolution was about ± 1 arc second but the repeatability was about ± 5 arc second after large angle changes. The time for the detectors tested to settle to ± 1 arc second was of order of 10 seconds. The tested sensors are high vacuum compatible since they are constructed from Al, Glass and a zirconium silicate ceramic potting compound with Teflon insulated wires. They are bakeable to 100°C . Such tilt sensors have been tested in high radiation environment of 0.08 megarad/hour to a total dose of 9.76 megarads and the sensors continued to function normally. The wide angle tilt sensor discussed above may be too slow as a primary angle encoder for a monochromator or diffractometer, but for a system run by stepping motors, they would prove quite useful as secondary angle encoders. These sensors need not be on or near the center of rotation to be accurate. Other models which have better sensitivity would be useful in setting and tuning focusing mirrors. A detector with a range of ± 8 mrad is repeatable to $1\ \mu\text{rad}$. Using a pair of such sensors the angle of a mirror could be set to $1\ \mu\text{rad}$ and bending radius of the mirror could be set to about 1%. Other applications will be discussed.

Work at Argonne National Laboratory is supported by the US Department of Energy, Office of Basic Energy Science, Division of Materials Sciences, under contract W-31-109-ENG-38.

TuD34

Beamline BL-27 for Radioactive Materials Researches at the Photon Factory

Hiroyuki Konishi, Akinari Yokoya, Haruhiko Motohashi and Hideo Ohno
JAERI-RIKEN SPring-8 Project Team, Honkomagome 2-28-8, Bunkyo-ku, Tokyo 113, Japan

Katsumi Kobayashi
Photon Factory, National Laboratory for High Energy Physics, Tsukuba, Ibaraki 305, Japan

We designed and constructed a new beamline, BL-27, at the Photon Factory (PF), the National Laboratory for High Energy Physics. This beamline is in full operation at present. The aim of construction is to study unsealed radioactive materials, to obtain the know-how on design and installation of a beamline and to investigate necessary optics and instrumental specifications of the SPring-8 beamline for radioactive material researches

The BL-27 is designed to accept radiation's emitted from a bending magnet. The basic design of the front end is similar to those of the conventional type in the PF. It is divided into two branch beamlines by means of a water-cooled copper mask. One is a soft X-ray [1.6-6 keV] beamline, BL-27A, which adopts optical focusing system with a bent-cylindrical CVD-SiC mirror and an InSb (111) flat double-crystal monochromator. The first crystal of the monochromator is cooled using a heat pipe. The BL-27A has two tandem experimental stations. The upstream station is located at halfway to the focusing point and available for irradiation in radiation biology studies. The downstream station is located at the focus point to be used for photoelectron spectroscopy. The other is an X-ray [4-17keV] beamline, BL-27B. It has vacuum-tight Be windows and a Si (111) double-crystal monochromator with optical focusing system by second-crystal bending (sagittal focusing system). On this branch beamline, one can perform absorption spectroscopy and X-ray diffraction experiments

There are new design concepts for the beamline different from those of conventional beamlines. Two monitor chambers (RI ports) for an eventual radioactive contamination are installed in the ultra high vacuum section. The radioactivity of those monitors is checked at regular intervals. To protect the vacuum of the beamline in the case of vacuum failure, two additional fast closing valves (FCV) are installed in the ultra high vacuum section, and a piece of polyimide thin film (Kapton) mounted on SUS wires of 200 meshes is inserted at the upstream end of the experimental area of the BL-27A.

TuD35

Optics of a high power wiggler beamline at the ESRF

M. Krumrey, Å. Kvik and W. Schwegle
European Synchrotron Radiation Facility, B.P. 220, F-38043 Grenoble, France

The materials science beamline ¹ at the ESRF can provide monochromatic or white radiation in the energy range from 5 up to 100 keV. The source is a 24 pole wiggler with a critical energy of up to 29 keV, producing a radiant power of 5 kW at 20 mm wiggler gap and a storage ring current of 100 mA. This would create an extremely high heat load on the first monochromator crystal if it would be the first optical element. Depending on the required photon energy, the bandpass of the radiation can be tailored and the total power reduced by adjusting the wiggler gap and by using movable attenuators and a premirror at variable angle which is also used for collimating the beam.

The premirror is a 1 m long single crystal of Si with Pt coating. The surface is continuously monitored by a wavefront sensor and thermal deformations can be corrected by piezoelectric actuators on the backside of the mirror.² Even under these conditions the incident power on the monochromator is up to 1.5 kW.

The monochromator is a HASYLAB-type double crystal monochromator, using two totally independent Si (111) crystals that are rotated and translated by UHV stepper motors. To avoid thermal deformations of the first monochromator crystal, it is cooled down to liquid nitrogen temperature where the thermal expansion coefficient of Si is close to zero and the thermal conductivity is very high. The monochromatic beam is focused in the horizontal plane by the second monochromator crystal using a sagittal bender and in the vertical plane by a second mirror that can be bent using piezoelectric actuators. Behind the second mirror, the monochromatic beam is again horizontal and 20 mm below the orbital plane so that high energy background can easily be separated. This is also possible for the white beam reflected by both mirrors.

The paper will present the general layout as well as the performance of the beamline that will be in user operation for the materials science community from September 1994.

1. Å. Kvik and M. Wulff, Rev. Sci. Instrum. 63, 1073 (1992)

2. J. Susini, M. Krumrey, R. Baker and Å. Kvik, this conference

TuD36

ABSTRACT

HIGH FLUX AND HIGH RESOLUTION BEAMLINE FOR
ELLIPTICALLY POLARIZED RADIATION IN THE VACUUM
ULTRAVIOLET AND SOFT X-RAY RANGE

A. Derossi[®], E. Lama[®], M. Piacentini[#], T. Prosperi^{*}, N. Zema[§]

[®] Consorzio INFN, via Dodecaneso 33, Genova, Italy

^{*} Istituto di Chimica dei Materiali/CNR, Montelibretti (Rome), Italy

[§] Istituto di Struttura della Materia/CNR via E. Fermi 38 00044 Frascati, Italy

[#] Università di Roma "La Sapienza", Dip. di Energetica, via A. Scarpa 14, Roma, Italy

The dependence of the optical properties and of the photoelectrons spectra of magnetic materials on the photon polarization has raised an increasing interest in the use of elliptically polarized synchrotron radiation.

A dedicated beam line with a broad energy range of photons and with high flux and a high degree of polarization has been designed for the ELETTRA storage ring.

The beamline exploits the elliptically polarized radiation produced by an electromagnetic elliptical wiggler with a switching rate of about 50 Hz [1].

The requirements of covering the photon energy range 5-1200 eV with a resolving power better than 5000 and with an average photons flux of 1×10^{13} [photons/s/0.1% bw] are satisfied by two independent spherical grating monochromators sharing the entrance and the exit slits. The low energy range 5-35 eV is covered by a normal incidence monochromator equipped with two holographically corrected gratings. The high energy range 30-1200 eV monochromator is based on a Padmore-like design [2], without defocusing on the fixed exit slits. The optical elements have been designed taking into account the high thermal load due to the high power source. The reduction of the degree of circular polarization estimated at the sample is always less than 20% with respect to that at the source, over the entire energy range.

[1] R. P. Walker and B. Diviacco, Rev. Sci. Instrum. 63-1 (1992) 332.

[2] H. A. Padmore, Rev. Sci. Instrum. 60-7 (1989) 1608.

TuD37

An ultra-fast mechanical shuttering system for separating single
x-ray pulses from a synchrotron

Alan D. LeGrand, Claude Pradervand, and Wilfried Schildkamp
Consortium for Advanced Radiation Sources,
The University of Chicago, Chicago, Illinois 60637

Dominique Bourgeois and Michael Wulff
ESRF, Grenoble, France

We have developed a mechanical shutter system for conducting time resolved experiments at the APS and ESRF storage rings which is suitable for use with white and monochromatic x-ray beams. The system is able to isolate single x-ray pulses from the APS and ESRF when they operate in single bunch mode and can provide an experimental trigger accurate to within 2 ns of the arrival time of the x-ray pulse. The system consists of three components: a slotted rotating disk which opens for 3 μ s every 2 ms, a fast magnetic shutter which can open and close in less than 1.5 ms, and dedicated electronics which monitors the arrival of the x-rays from the storage ring and the opening of the slotted disk shutter. This information is used by the electronics to predict when the opening of shutter will coincide with the arrival of an x-ray pulse. When the prediction is made the electronics generates an experimental trigger and opens the magnetic shutter to allow the x-ray pulse through.

This system has been tested at both the CESR and the ESRF storage rings and has been used to collect Laue data from four crystals: a mineral sample, a small organic molecule, and from two forms of the protein lysozyme. We will present the principles behind the shutter system's operation and results from our experimental tests.

TuD38

PLS Bending Magnet X-ray Beamline 3C2

B.-J. Park, S.-Y. Rah, Y.-J. Park and K.-B.Lee
Pohang Accelerator Laboratory
Pohang University of Science and Technology

The design of the 3C2 beamline at the Pohang Light Source(PLS) is described. The beamline is designed for x-ray scattering studies with x-ray photons over an energy range of 4 -12 keV. A Cylindrical Pt-coated silicon mirror intercepts a photon beam up to 3 mrad at a distance of 16 m from a source point and focuses the beam sagittally at the sample position with a magnification of 1:1. For the vertical focussing it will be dynamically bent by the mirror holder. A double crystal monochromator of two Si(111) crystals with a fixed exit beam geometry provides monochromatic photons and is located in front of the experimental hutch to reduce the motion of the beam position. The hutch is equipped with a 6-circle diffractometer and various photon detection electronics for x-ray scattering experiments. The future use of this beamline for various x-ray scattering experiments is presented.

TuD39

A NEW CONCEPTUAL DESIGN FOR THE ANOMALOUS SCATTERING BEAMLINE AT THE E.S.R.F

S. LEQUIEN, L. GOIRAND, F. LESIMPLE
E.S.R.F, B.P 220, F-38043 GRENOBLE, FRANCE

The tunability of synchrotron radiation allows anomalous scattering techniques to be easily applied to the study of atomic arrangements in the area of materials science. The ESRF will construct a public beamline which will combine anomalous dispersion and mainly diffuse scattering. The two original features of this beamline are that SAXS and WAXS experiments might be carried out on the same spectrometer without moving the sample and also under vacuum.

An insertion device (ID) with a 46 pole wiggler of critical energy $\epsilon_c = 17.4$ keV and a maximum deflection parameter $K = 4.7$ has been chosen. It is optimized to give the maximum integrated flux over the continuous energy range specification. Because the power of a wiggler ID is proportional to K , this low- K choice allows to reduce as much as possible the heat load problem ($P = 2.1$ kW for a nominal current of 100 mA) and reaches an undulator regime if the gap is set to large values.

The optics will consist of two mirrors located before and after a double-crystal monochromator. This arrangement provides a fixed-exit monochromatic beam and allows to maintain the focal spot constant during energy tuning. The x-ray fan will be vertically reflected by Si-premirror. It will make the beam almost parallel in order to match the vertical divergence to the acceptance of the first flat Si monochromator. These two first optical elements will be liquid nitrogen cooled. The full horizontal divergence of the source will be accepted by the second Si crystal which will sagittally focus. Finally meridional focusing will be achieved by the second Si-mirror which will also be used to reject the harmonics. The mirror surfaces will be composed of three tracks corresponding to (i) uncoated, (ii) Rh coated and (iii) Pt coated in order to cover the 235 keV energy range just by translating the mirrors. The Si crystals will have the orientations (111), (311) or (511) depending on the working energy.

Diffuse scattering being generally weak compared to Bragg diffraction, experiments will be performed in an evacuable hutch ($p = 5 \cdot 10^{-3}$ Torr) in order to decrease the background to the lowest possible level. With the same aim beryllium windows will be removed although air scattering is in fact up to now one of the limitations in diffuse scattering experiments. Anyway this is necessary to work at low energies, i.e below 5 keV. The insulation from the storage ring will be assured by differential pumping stages and valves.

A 6-circle diffractometer will be set up in this evacuable hutch to perform scattering experiments either in the vertical scattering plane or in the horizontal one. An analyzer assembly will be mounted on the detector arm to provide high-Q resolution when necessary. Si, Ge or HOPG crystal analyzers will be available. Single or ID detectors are planned to be used in connection with the analyzer.

For the SAXS measurements, a movable 2D detector will be mounted in a tube 5 m long. It will be possible to move the detector close to the sample ($d \cong 0.5$ m) to allow diffraction experiments at high energy. With these conditions a 10^{-2} \AA^{-1} lower limit can be reached for the Q value whatever the incident energy.

The conceptual design including ID, ray-tracing studies and layout of the beamline will be presented.

TuD40

Vacuum Tests of a Beamline Front End Mock-up at the Advanced Photon Source*

C. Liu, R. W. Nielsen, T. L. Krzy, D. Shu, and T. M. Kuzay

Experimental Facilities Division
Advanced Photon Source
Argonne National Laboratory
Argonne, IL 60439

ABSTRACT

A mock-up has been constructed to test the functioning and performance of the Advanced Photon Source (APS) front ends. The mock-up consists of all components of the APS insertion-device beamline front end with a differential pumping system. Primary vacuum tests have been performed and compared with finite element vacuum calculations. Pressure distribution measurements using controlled leaks demonstrate a better than four decades of pressure difference between the two ends of the mock-up. The measured pressure profiles are consistent with results of finite element analyses of the system. The safety-control systems are also tested. A closing time of ~20 ms for the photon shutter and ~12 ms (?) for the fast closing valve have been obtained. Experiments are in process for shock-wave flight time measurements.

The submitted manuscript has been authorized by a contractor of the U.S. Government under contract No. W-31-109-ENG-38. Accordingly, the U.S. Government retains a nonexclusive, royalty free license to publish or reproduce the published form of this contribution, or allow others to do so, for U.S. Government purposes.

*Work supported by the U. S. Department of Energy BES Materials Science under contract W-31-109-ENG-38.

TuD41

A new kind of UHV Piezotranslator.

F. Mazzolini, C. Fava, F. De Bona, Sandrin, G., Gambitta, G.
Sincrotrone Trieste, Scientific Division

A new kind of UHV compatible micro displacement actuator has been developed. It is based on a piezoelectric translator bakeable up to 150 °C, encapsulated in a stainless steel housing. A metal bellows allows the movement of the actuator and it gives a suitable preload to compensate the vacuum load.

This new actuator has a very low outgassing rate, due to the external stainless steel surface of the casing and to the UHV electrical feedthrough. The mechanical characteristics (resolution, load capability, stiffness) are similar to that available with standard not UHV compatible piezos.

This new kind of UHV compatible micro displacement actuator can be used in a UHV environment without any remarkable effect on the Ultra High Vacuum. The vacuum test and the accuracy test in UHV have been performed and will be detailed reported.

TuD42

**Virtual Threaded Language (VTL):
A Scientist's Computer Language for Instrument Control**

D.B. McClain, K.P. Pflibsen, A.J. Goetz
EODC, Kaman Aerospace Corporation, Tucson, AZ

Until the standard operating modes of modern beam-lines have been determined, there is a need for a very flexible computer control system that permits ad-hoc experimentation and quickly programmed operating sequences. A completely interactive computer system that can control every aspect of beam steering, mirror surface control, monochromator wavelength tuning, and loop control beam sensors is desirable.

Such a development environment is described that offers scientists intuitive and interactive control of laboratory instruments. It presents a threaded language environment whose syntax closely parallels the HP-48 calculator languages. The language offers a variety of abstract data types such as lists, tables, arrays, etc., as well as simple numeric types. Underlying the user level is an easily extended object-oriented C++ core in which working high-level prototype code can be recast for speed and then continue to be called from the user level as a new primitive of the language. This permits indefinite extensibility as well as speed and fully interactive control.

The use of VTL to construct an advanced third-generation beam-line control system is described with block diagrams displaying the computer control network architecture. Short code excerpts are presented that demonstrate the advantages of a completely interactive instrument diagnostic and debugging capability for real-time debugging without resorting to conventional breakpoint debugging that would otherwise interfere with overall system performance.

TuD43

Title: Six DOF Hexapod Actuation System for Beam Control Mirrors

Patrick McMillin, Todd Baker, Britt Berry
EODC, Kaman Aerospace Corporation, Tucson, AZ

An external actuation control system for positioning a grazing incidence mirror mounted in an ultra-high vacuum chamber is described. The support system, given the name HEXAPOD is a heavily coupled, kinematic arrangement of six telescoping actuators in parallel which provide high stiffness and minimal hysteresis. The experimenter has remote control of the actuation of the mirror and chamber over translation in any axis of up to ± 8 cm and rotation about any axis of up to ± 9 deg. These ranges and motions are obtained with micron and microradian accuracies in a stable system exhibiting first mode resonant frequencies over 50 Hz. The system eliminates the need for large volume vacuum chambers and high vacuum qualified moving parts.

TuD44

**PERFORMANCE OF THE XUV HIGH RESOLUTION
UNDULATOR BEAMLINE BW3 AT HASYLAB: FIRST
RESULTS AND TIME-OF-FLIGHT SPECTROSCOPY**

O. Björneholm, F. Federmann, A. Beutler*, F. Fössing*, C. Larsson, U. Hahn,
A. Rieck, and T. Möller

*Hamburger Synchrotronstrahlungslabor HASYLAB at Deutsches
Elektronensynchrotron DESY 22607 Hamburg, Notkestr. 85, FR Germany*

**II. Inst. für Experimentalphysik, Universität Hamburg, Luruper Chaussee 149,
22761 Hamburg, FR Germany*

The XUV-beamline BW3 at Hasylab is a state of the art beamline for the energy range 15-2000 eV which consists of a triple undulator equipped with a modified high-flux SX-700 plane grating monochromator [1,2]. The first three optical elements of the beamline are made of graphite coated with SiC to withstand the high heatload at the 4.5 GeV storage ring DORIS III. Excellent spectral resolution of the order of 10^4 at the nitrogen K-edge at 400 eV is obtained by replacing the elliptical focusing mirror of the original SX-700 design [3] by a spherical mirror with very small tangent errors and with a large focal length in order to suppress spherical aberrations. In the energy range 50 -1700 eV a photon flux of 10^{11} - 10^{13} /s is obtained in a band pass of 0.1%. Photoionisation and photoemission measurements on atoms, molecules and clusters making use of time-of-flight techniques demonstrate the excellent performance of the beamline [4]. The time structure of DORIS III (192 -960ns bunch distance) can be directly used for the determination of the mass of photoions with a very short time-of-flight mass spectrometer up to 2000 amu. This feature opens up a new field for the study of clusters.

[1] R. Reininger, V. Saile, Nucl. Instr. Meth. A 288, 343 (1990)

[2] C.U.S. Larsson, A. Beutler, O. Björneholm, F. Federmann, U. Hahn, A. Rieck, S. Verbin, T. Möller, Nucl. Instr. Meth. A 337 (1994)

[3] H. Petersen, Opt. Commun. 40, 402 (1982)

[4] F. Federmann, O. Björneholm, A. Beutler, T. Möller, to be published

TuD45

**A Protein crystallography beamline for
Multiwavelength Anomalous Dispersion
at the SRS Daresbury.**

S.M. McSweeney, S.G. Buffey, P.A. Atkinson, E.M.H. Duke,
C. Nave, A. Gonzales, A. Thompson and S.H. Kinder.

Abstract

A beamline has been developed for multiwavelength anomalous dispersion on the SRS wiggler1 at Daresbury. The instrumentation consists of a toroidal focussing mirror, a channel cut double crystal monochromator and an on line image plate detector. Software has been developed which allows automatic collection of multiwavelength diffraction data. This paper will deal with the design of the beamline for operation in multiwavelength mode. Examples of the beamline's performance will be drawn from recent successful MAD experiments.

TuD46

Thermo-Mechanical Analysis of the White Beam Slits for an Undulator Beamline at the Advanced Photon Source¹

H. L. Thomas Nian, D. Shu, and Tuncer M. Kuzay
Argonne National Laboratory, 9700 S. Cass Ave., Argonne, IL 60439

A set of precision horizontal and vertical white beam slits has been designed for an undulator beamline at Advanced Photon Source (APS). Due to the powerful x-ray heat flux emitted by the undulator, it is difficult to control the thermal distortion at the desired range of 1-2 microns. We analyzed many conceptual designs in an attempt to minimize the thermal distortion of the slits. The grazing incidence angle was fixed at 2.5° due to limited space. Even with 1-mm-thick low-Z material (graphite) coated on the heating surface of the slit, the maximum thermal distortion is over 25 microns. A three-piece slit was designed that consists of one large block, two tungsten knife edges, and an OFHC cooling tube (filled with copper mesh) brazed inside the large block. Both TZM (vacuum arc-cast molybdenum-0.5% titanium-0.1% zirconium alloy) and tungsten were considered for the block material. The thermal distortion at the knife edge of this three-piece slit has a maximum deflection of less than 3 microns.

With a heat transfer coefficient, $h=2\frac{W}{cm^2\cdot^{\circ}C}$, the maximum temperature of the large block is about 380°C if tungsten is used, and about 425°C if TZM is used. Because, at these temperatures, tungsten will start annealing, we have decided to use TZM.

The calculation shows that increasing the h (convective heat transfer coefficient) from $1\frac{W}{cm^2\cdot^{\circ}C}$ to $2\frac{W}{cm^2\cdot^{\circ}C}$ will not only reduce the interface (between the TZM block and the OFHC tube) temperature from 191°C to 138°C (which keeps the OFHC from annealing and helps to retain its yield strength), but it will also reduce the thermal distortion from 110 microns to 90 microns. Enhanced heat transfer technology was used to increase the convective heat transfer coefficient from $1\frac{W}{cm^2\cdot^{\circ}C}$ to about $2-3\frac{W}{cm^2\cdot^{\circ}C}$ for the OFHC tube.

¹This work was supported by the U.S. Department of Energy, BES-Materials Science, under contract W-31-109-Eng-38

The submitted manuscript has been authored by a contractor of the U.S. Government under contract No. W31109-ENG-38. Accordingly, the U.S. Government retains a nonexclusive, royalty-free license to publish or reproduce the published form of this contribution or allow others to do so, for U.S. Government purposes.

A beamline for macromolecular crystallography at the ALS

H. A. Padmore, T. Earnest, S-h Kim, A. C. Thompson and A. Robinson

Advanced Light Source
Lawrence Berkeley Laboratory
Berkeley, CA 94720

A beamline for macromolecular crystallography has been designed for the ALS. The source will be a 37 pole, 2 T multipole wiggler and it will feed three beamlines, each receiving a horizontal angular width of up to 3 mrad of radiation. The central beamline will primarily be used for multiple wavelength anomalous dispersion (MAD) measurements in the wavelength range from 4 to 0.9 Å. A rapid scanning double plane crystal monochromator will be used, and will be preceded by a vertically collimating mirror and followed by a toroidal refocusing mirror. This arrangement will allow the system to operate at high energy resolution at full vertical aperture, and in addition gives a simple mechanism for changing to a focused Laue mode of operation. The side stations will be used primarily for fixed wavelength crystallography in the range from 1.5 to 0.95 Å. They will be essentially identical, each consisting of a vertically focusing mirror followed by an asymmetrically cut curved crystal monochromator. This system will be arranged to allow coupled crystal rotation and bending as well as sample stage and detector rotation and translation, thus giving a limited MAD capability. Details of the mechanical and optical arrangements will be presented.

This arrangement, in which we will use beam compressing crystal optics for the side stations, is dictated by the optical properties of the multipole wiggler source, for which the apparent optical source size is a strong function of the source depth and aperture position. We have studied these effects using phase space descriptions of the source, and used the same methods to fully optimize the optical systems. We will also present a comparison of presently operating and planned crystallography beamlines with the ALS using phase space techniques to calculate the expected flux accepted by typical protein crystals.

*This work was supported by the Director, Office of Energy Research, Office of Basic Energy Sciences, Materials Sciences Division, of the U.S. Department of Energy, under Contract No. DE-AC03-76SF00098.

SR BEAMLINES AT THE VEPP-4 - 6 GEV STORAGE RING

Panchenko V. E.

Institute of Nuclear Physics,
630090 Novosibirsk, Russia

The report is devoted to the complex of the SR beamlines which are now being projected and made for a N(I) semi-ring of the VEPP-4 storage ring. The complex consists of the beamlines themselves; the control, interlock and signalling system (CISS) of the beamlines and experimental stations; shielding arrangements and structures. There is detailed description of the complex geometry, the electron orbit sections which are concerned with the SR complex, a structure of beamlines, their vacuum system, functional and constructional peculiarities of all the elements of beamlines, shaping of SR beams for beamlines, collimation of bremsstrahlung and showers, the forced filtration of SR beams by beryllium foils which divide the vacuum volumes of storage ring and beamlines, coupling of beamlines with experimental stations, and requirements to radiation shielding of stations. Particular attention is given to radiation shutters for an operative "intercept" of SR beams. Various radiation factors and origin of them are described in detail. Technical and organizing aspects of radiation safety as well as guaranteeing of the last by means of the CISS are discussed. The effective sizes of the SR sources vs an azimuth are presented. Unavoidable complications as well as contribution to the work of each of the researchers, designers, engineers and laboratory assistants are carefully mentioned

TuD49

Design of an X-ray Beamline on a Bending Magnet at the E.S.R.F. for Magnetic and High Resolution Diffraction

DF Paul

Dept. of Physics, University of Warwick, Coventry CV4 7AL, UK

We propose constructing a bending magnet station at the ESRF for investigations of magnetic structure, magnetic and structural phase transitions and critical phenomena, etc. principally through work on single crystals. The general requirement is for a design able to deliver: high flux onto the sample; a compact focal spot on the sample often available, only as very small crystals; high wavevector and energy resolution; usable flux in the 3-4 keV range and an upper limit of 15 keV; capability for polarisation analysis.

Two designs are compared and contrasted. The first comprises a toroidal mirror, formed by bending a straight cylinder, followed by a fixed exit monochromator formed from a pair of flat silicon crystals. The mirror approximates to an ellipsoid to provide 1:1 focusing. The second consists of two paraboloidal mirrors sandwiching the monochromator. The mirrors, which are bent straight sector cones ensure that a truly parallel beam is incident upon the monochromator and then focused by the second mirror. This second design, which has not been implemented elsewhere, offers higher energy resolution at the expense of some complication.

In addition to the choice of beamline optics the ESRF bending magnet source can be viewed at either its "soft" or "hard" end, the two critical energies being 9.6 and 19.1 keV respectively.

This paper reviews the advantages and disadvantages of the options for magnetic high resolution x-ray diffraction and vindicates the chosen design.

TuD50

High-Brightness Beamline for X-Ray Spectroscopy at the Advanced Light Source

R. C. C. Perera and G. Jones
Advanced Light Source,
Lawrence Berkeley Laboratory,
Berkeley, CA 94720

D. W. Lindle,
Department of Chemistry,
University of Nevada, Las Vegas,
Las Vegas, NV 89154-4003

Beamline 9.3.1 at the Advanced Light Source (ALS) is a windowless beamline, covering the 1-6 keV photon-energy range, designed to achieve the goals of high energy resolution, high flux, and high brightness at the sample. When completed later this year, it will be the first ALS monochromatic hard-x-ray beamline, and its brightness will be an order-of-magnitude higher than presently available in this energy range. In addition, it will provide flux and resolution comparable to any other beamline now in operation. To achieve these goals, two technical improvements, relative to existing x-ray beamlines, have been incorporated. First, a somewhat novel optical design for x-rays, in which matched toroidal mirrors are positioned before and after the double-crystal monochromator, was adopted. This configuration allows for high resolution by passing a collimated beam through the monochromator, and for high brightness by focussing the ALS source on the sample with unit magnification. Second, a new "Cowan type" double-crystal monochromator based on the design^{1,2} used at NSLS Beamline X-24A has been developed. The measured mechanical precision of this new monochromator shows significant improvement over existing designs, without using positional feedback available with piezoelectric devices. Such precision is essential because of the high brightness of the radiation and the long distance (12 m) from the source (sample) to the collimating (focusing) mirror. This combination of features will provide a bright, high resolution, and stable x-ray beam for use in the x-ray spectroscopy program at the ALS.

References:

1. J.A. Golovchenko, R.A. Levesque and P.L. Cowan, Rev. Sci. Instr. 52, 509 (1981).
2. P.L. Cowan, J.B. Hastings, T. Jach, and J.P. Kirkland, Nucl. Instr. and Meth. 208, 349 (1983).

This work is supported by U.S. DOE under Contract No. DE-AC03-76SF00098.

TuD51

Design and Performance of the ALS Double-Crystal Monochromator

G. Jones*, S. Ryce*, D. W. Lindle#, B.A. Karlin+, J.C. Woicik®, and
R. C. C. Perera*

*Advanced Light Source, Lawrence Berkeley Laboratory,
Berkeley, CA 94720

#Department of Chemistry, University of Nevada, Las Vegas,
Las Vegas, NV, 89154

+National Synchrotron Light Source, Brookhaven National Laboratory,
Upton, NY 11973

®National Institute of Standard and Technology,
Gaithersburg, MD 20899

A working double-crystal monochromator based on the boomerang design^{1,2} used at NSLS Beamline X-24A has been developed for the beamline 9.3.1 at the ALS, a windowless UHV beamline covering the 1-6 keV photon energy range, designed to achieve the goals of high energy resolution, high flux, and high brightness at the sample. We have simplified the mechanical design and included recent improvements in technology. The measured mechanical precision of this new "Cowan type" monochromator shows significant improvement over existing designs, without using positional feedback available with piezoelectric devices. Such precision is essential because of the high brightness of the radiation and the long distance (12 m) from the source (sample) to the collimating (focusing) mirror. This monochromator will provide a bright, high resolution, and stable x-ray beam for use in the x-ray spectroscopy program at the ALS.

References:

1. J.A. Golovchenko, R.A. Levesque and P.L. Cowan, Rev. Sci. Instr. 52, 509 (1981).
2. P.L. Cowan, J.B. Hastings, T. Jach, and J.P. Kirkland, Nucl. Instr. and Meth. 208, 349 (1983).

This work is supported by U.S. DOE under Contract No. DE-AC03-76SF00098.

TuD52

ABSTRACT

THE HERP BEAM LINE

C. Quaresima[§], P. Perfetti[§], C. Ottaviani[§], M. Capozzi[§], S. Rinaldi[§], M. Matteucci[§], C. Crotti[§], A. Antonini[§], K. Prince[Ⓢ], A. Savoia[Ⓢ], C. Astaldi[Ⓢ], M. Zacchigna[Ⓢ]

[§] Istituto di Struttura della Materia/CNR via E. Fermi 38 00044 Frascati, Italy.

[Ⓢ] Sincrotrone Trieste, Padriciano 99, 34012 Trieste, Italy.

The Italian beamline HERP (High Energy Resolution Beamline for VUV and Soft X-ray Photoemission Spectroscopy) is now under commissioning at the Trieste storage ring ELETTRA.

The beamline optics is designed following the well tested, high resolution and high flux, DRAGON scheme.

The line collect the central portion of the radiation emitted from a 12.5 cm period undulator, which gives an usable photons energy range from 15 eV to 800 eV. The radiation emitted from the undulator is focused, in the dispersion direction, onto the cooled entrance slit via a Kirkpatrick-Baez pre optics. Three, type IV, holographic, spherical gratings diffract the radiation in the 60-800 eV photon energy range with an included angle of 173°, while two other, type IV, holographic, spherical gratings cover the photons energy range 15-120 eV with an included angle of 160°. Optimum focus condition is maintained with the use of a moveable exit slit. After the exit slit a last mirror, with a toroidal shape, focuses the radiation onto the sample. The achievable resolving power is more than 10000 in all the range with an average photon flux of 10^{14} photons/(s 0.1 % bw). The experimental chamber is a commercial station equipped with two electron analyzers to perform angle integrated and angle resolved photoemission experiments. We will present and discuss the first test results obtained with the HERP beamline.

TuD53

S.-Y. Rah, T.-H. Kang, Y. Chung, B. Kim and K.-B. Lee

Pohang Accelerator Laboratory

Pohang University of Science and Technology

A bending magnet VUV beamline with two branches, SGM(2B1) and NIM(2B2), at Pohang Light Source(PLS) is described. The SGM branch, designed for photoemission spectroscopy, accepts photon beam 10 mrad horizontally and 2 mrad vertically. The condensing system composed of horizontal and vertical mirrors focus the beam at the sample position and at the entrance slit, respectively. The grating chamber houses 5 gratings to cover photon range of 10 eV to 1230 eV. The monochromator employs a fixed entrance slit and a movable exit slit to satisfy focusing conditions. The beamline is designed to obtain the resolution of 4,000 - 10,000 in 10 eV - 225 eV region and 3,000 - 5,000 in 170 - 1230 eV region. The NIM branch is designed for gas-phase experiments with 2 eV - 30 eV photons. A spherical grating monochromator to be installed in a standard 3 m normal incident, off-Rowland circle mount. The focusing to the entrance slit is done by a mirror system composed of a plane mirror, a spherical mirror and a toroidal mirror. The dispersed photon beam will be refocused by a toroidal mirror at the sample position. A gas-phase experimental station, equipped with differential pumping stages and diagnostic instruments, is to be installed.

TuD54

A VERSATILE DOUBLE CRYSTAL FIXED EXIT MONOCHROMATOR FOR X-RAY SYNCHROTRON RADIATION

Mohan Ramanathan, and Pedro A. Montano
Materials Science Division, Argonne National Laboratory
9700 S. Cass Ave, Argonne, IL 60439

The Materials Science Division at Argonne National Laboratory has a multipurpose X-ray beam line (X6B) at the NSLS x-ray ring facility at Brookhaven National Laboratory. The beam line was built to accommodate a wide range of experiments from scattering to spectroscopy. With this goal in mind a versatile monochromator system was designed and built for the X6B beam line. The monochromator consists of two separate crystals of the same type. The monochromator covers a wide angular range from 58 to 5.1 degrees which is equivalent to an energy range of 2.3 to 22 keV with Si<111> crystals. For the full angular range, a constant offset of 1 inch is maintained between incident white radiation and the exiting monochromatic radiation. The monochromator employs a simple mechanism, where both crystals are rotated by a single drive mechanism and the first crystal is translated along the direction of the radiation such that center of the first crystal is always at the center of the beam. The translation is accomplished by a mechanical link. The first crystal is 1 inch long while the second crystal is 5 inches in length. The Bragg diffracted beam from the first crystal walks on the second crystal, however the exit beam is at a fixed offset from the incident beam. The energy tuning is obtained with a single stepping motor driving the rotary stage of the monochromator. The second crystal has two vacuum inchworm and a PZT device for alignment. The monochromator is housed inside a stainless steel vacuum chamber and is currently operating in high vacuum environment. All the drive mechanism are located inside the vacuum system with the exception of the stepping motor, which is connected through a vacuum feed through to the drive mechanism. The monochromator is capable of accepting an horizontal span of 5.5 mrad of radiation. Due to the heat load from the synchrotron radiation the first monochromator crystal is water cooled. A complete characterization of the monochromator has been performed. For a typical x-ray absorption energy scan (over a range of 1.5 keV) one needs to move only the stepping motor. The parallelism between the two crystals is maintained well within the rocking curves over a very large range of energy (typically 10 keV). A feedback system is not required to run this monochromator. Data can also be taken during the motion of the monochromator, thereby acquiring a complete EXAFS spectra in a matter of about 20 seconds.

Work at Argonne National Laboratory is supported by the US Department of Energy (DOE), Office of Basic Energy Sciences, Division of Material Sciences, under contract W-31-109-ENG-38.

TuD55

Spectroscopy beamline for the photon energy region from 0.5 to 3 keV at the Advanced Photon Source.

K.J. Randall, E. Gluskin, Z. Xu

Advanced Photon Source, Argonne National Laboratory,
9700 S. Cass Ave, Argonne, IL60439

Interest in the 0.5 to 3 keV, intermediate x-ray, energy region has recently intensified as this spectral region covers, among others, the important L and M edges of transition metal and rare earth magnetic materials, respectively. Third generation synchrotron facilities with their inherent high brightness have the unique potential to cover this energy region with high resolution, high flux x-ray beams ideal for spectroscopic studies. A 5.5 cm period, planar undulator to be installed on the 7 GeV Advanced Photon Source will produce a high brightness source of intermediate energy X-rays. The 0.5 to 3 keV spectroscopy beamline is based on the Spherical Grating Monochromator design which has already been shown to yield high resolution and throughput in the soft X-ray region, below 1 keV. The beamline has been designed to cover the entire region with a peak resolving power of 6000 to 10000. Photon Flux at the sample is calculated to be in the range from 10^{11} to 10^{12} photons/second into a spot size of 1 mm². A refocussing mirror will be used to further demagnify the image size at a second experimental station. As a second phase to the spectroscopy program, an elliptically polarized insertion device will be used. The polarization preserving nature of the grazing incidence optical elements in the SGM is crucial to obtain X-rays of well defined polarization. The beamline layout, together with calculations of resolution, throughput, power loading and high harmonic suppression will be presented. The photoemission experimental station, UHV goniometer and UHV polarimeter designed specifically for the spectroscopy station will also be described.

This research was supported by the U.S. Department of Energy, BES Materials Sciences under contract #W-31-109-ENG-38

The submitted manuscript has been authored by a contractor of the U.S. Government under contract No. W-31-109-ENG-38. Accordingly, the U.S. Government retains a nonexclusive, royalty-free license to publish or reproduce the published form of this contribution or allow others to do so for U.S. Government purposes.

TuD56

Control of six degree-of-freedom parallel manipulators for synchrotron radiation applications

P. Fajardo, V. Rey-Bakaikoa
European Synchrotron Radiation Facility, B.P. 220, 38043 Grenoble Cedex, France

ABSTRACT

This high precision parallel manipulator is a well adapted support for optical instrumentation in synchrotron radiation beamlines. It consists of a single moving element that obtain its six degrees of freedom from the combined movement of six independent actuators. This arrangement offers new control possibilities, together with fewer constraints for instrument mounting and alignment. Control of this kind of manipulator requires a special approach in order to exploit its full capabilities while keeping a reasonable simplicity of operation.

In this paper we present the details of the control procedure and associated software package. Special emphasis is given to the geometry: definition and ability to follow smooth trajectories, optimized calculations and special interface features like the possibility of defining virtual axes: logical motors associated with any particular rotation or translation of the instrument. By defining adequate virtual axes it is now simple to execute sequence of movements that were difficult with serial manipulators. The program includes special help for the alignment and calibration process and global instrument security features. It was written in a modular way, so that it can be easily adapted to different geometries, motor controllers and other site-dependent parameters.

At present three ESRF beamlines have installed and used these programs and around ten new installations are foreseen.

TuD57

Performance of the IRC SEXAFS beamline at Daresbury SRS

A. W. Robinson, S. D'Addato¹, P. Finetti, V. R. Dhanak and G. Thornton²

Surface Science Research Centre, University of Liverpool, P. O. Box 147, Liverpool L69 3BX, UK.

¹Present address: Dipartimento di Fisica, Università di Modena, Italy.

²Also: Department of Chemistry, University of Manchester, Manchester M13 9PL, UK.

We report on the performance of a new beamline, designated BL 4.2 at the SRS Daresbury laboratory UK, which forms a part of a dedicated research facility for the Interdisciplinary Research Centre for Surface Science (IRC). The beamline covers the energy range between 1 and 10 keV using a double crystal monochromator. A novel feature is the use of a premirror system in which the energy cutoff is changed by selecting different optical coatings on the plane mirror and the sagittal focusing cylindrical mirror [1,2]. In this report the design parameters and layout of the beamline will be reviewed. The performance of the beamline is illustrated by reference to a NEXAFS study of thiophenecarboxylic acid on Cu(110) and a SEXAFS study of Ni(110)c(2x2)S.

NEXAFS data indicate a resolution of 1 eV at a photon energy of 2470 eV, sufficient to resolve the two leading resonances associated with the thiophene ring. In general, the use of SEXAFS has previously been limited to the study of the first and second coordination shell geometry, a restriction which is usually imposed by the limited data range and experimental signal to noise ratio. Here, by a careful selection of the coatings on the premirror system to reject higher order light contributions and using a fluorescence yield detector, the S K-edge data from Ni(110)c(2x2)S extend to a k-range of 13 \AA^{-1} , which corresponds to a photon energy range of 650 eV.

References.

1. G. Van der Laan and H. Padmore, Nucl. Instr. and Meth. A291 (1990) 225.
2. V. R. Dhanak, A. W. Robinson, G. Van der Laan and G. Thornton, Rev. Sci. Instrum. 63 (1992) 1342.

TuD58

First Testing of the Fast Kappa Diffractometers at NSLS and ESRF

I. K. Robinson

Department of Physics
University of Illinois at Urbana-Champaign
1110 West Green St, Urbana, IL 61801, USA

H. Graafsma and A. Kvick

European Synchrotron Radiation Facility,
B.P. 220, 38043 Grenoble, France

J. Linderholm
Risø National Laboratory, DK 4000 Roskilde, Denmark

We present the design and first results of the performance of a new 4-circle x-ray diffractometer featuring the less-common "kappa" geometry originally used on the CAD-4 instrument. This geometry permits access to all reciprocal-space settings while the mechanical supports remain entirely on one side of the beam; this is very useful for split ports on bending-magnet beamlines. Our design is able to carry heavy loads, such as a Displex-type cryostat, and operates at relatively high speeds because it uses direct-drive servomotors. Considerable attention has been given to the distribution of loads which is optimised for horizontal-axis operation. A sphere of confusion of 50 μ m was achieved fairly easily for the mutual alignment of the axes, and this can probably be improved. The equations for the conversion from the Kappa geometry to the more familiar Eulerian geometry are given.

The initial tests show that accurate alignment of crystals can be achieved, and reliable measurements have been made on a number of experimental systems. Rocking curves of Silicon have been measured, but these are at the limit of the setting accuracy. Arbitrary settings are achieved in about 1 second, but an additional 1 sec settling time is needed for high accuracy work.

TuD59

Design of the Structural Biology Center Beamlines at the APS Gerd Rosenbaum and Edwin M. Westbrook

The Structural Biology Center (SBC) Collaborative Access Team (CAT) will develop and operate a sector of the Advanced Photon Source (APS) as a user facility for studies in macromolecular crystallography. Crystallographically determined structures of proteins, nucleic acids and their complexes with proteins, viruses, and complexes between macromolecules and small ligands have become of central importance in an increasing number of research programs of molecular and cellular biologists.

The two major design goals for the SBC beamlines are

- to make the extremely high brilliance of the APS available to perform studies that cannot be done elsewhere, and,
- achieve a high throughput of less demanding studies.

The crystal samples we expect to see at the SBC will include

- extremely small crystals
- crystals with large unit cells (viruses, ribosomes, etc.)
- ensembles of closely similar crystal structures for drug design, protein engineering, and similar endeavors.

The techniques applied will include multiple-energy anomalous dispersion (MAD) phasing and polychromatic (I α) data collection. Data will be recorded on a high resolution CCD-area detector and optionally on image plates.

The SBC will develop two beamlines, one for radiation from insertion devices and one for radiation from a bending magnet. The active insertion device is either an undulator (APS type A) or a wiggler (APS type A) which are installed in series.

The X-ray optics is highly demagnifying in order to match the focal size with the sizes of the sample and the resolution element of the detector. This provides the best flux in brilliance driven experiments, e.g. small crystals with large unit cells. Vertical focusing is achieved by a flat, cylindrically bent vertically deflecting mirror which also serves to reject higher harmonics. Horizontal focusing is achieved by sagittally bending the second crystal of a double crystal monochromator.

The double crystal monochromator has a constant exit height output beam. In order to satisfy both, the high-flux requirement for standard crystallography and the narrow bandwidth requirement for MAD-phasing, three crystals (Si-111, Si-220, Si-400) are mounted side-by-side on the first crystal stage and translated into the beam as required. The sagittally focusing second crystal has to be exchanged manually. A in-vacuum crystal changer is planned as a future upgrade. On the BM-line the first crystals are cooled. On the ID-line the double-crystal monochromator is preceeded by a high heat load element which is at current planning a double inclined crystal monochromator (Si-111-orientation) with liquid gallium cooling developed by the APS.

Great attention has been paid to the degrading effects on the usable brilliance at the sample due to slope errors and aberrations of the mirror and vibrations of the monochromator. Demagnification facilitates shorter distances between optics and specimen. Medium length mirrors reduce aberrations. Both measures help to prevent a considerable increase of the beam size at the sample. Vibrations of the monochromator will be greatly reduced by isolating the optical components from the tank and supporting them from a vibration isolation base.

TuD60

Conceptual Design of SPring-8 Front-ends

Transient and Steady State Thermal and Stress Analysis of an ID Beam Shutter for the APS

Yifei Ruan
Mati Meron

Consortium for the Advanced Radiation Source
The University of Chicago

This paper describes a conceptual design of an ID beam shutter for the Advanced Photon Source (APS). Various aspects of the design such as geometry, cooling arrangement and material selection are optimized based on thermal and stress finite element analysis. The goal of the optimization is to assure survivability while maintaining reasonably compact physical size.

The analysis is performed using the finite element software ANSYS. The power envelope is obtained from the output of the program POWER [1] which is based on a formula derived by K. J. Kim [2]. In addition, calculations utilizing some simple approximations of the power envelope are performed. It turns out that the temperature and stress distributions are not very sensitive to the details of the power distribution and depend primarily on the total power in the beam and the peak power density.

As could be expected, optimal thermal behavior of the shutter is obtained using high heat conductivity materials and the choice of material is OFHC (oxygen free high conductivity) copper. However, it turns out that OFHC copper can not withstand the large stresses which appear at the center of the heat load footprint area. Therefore, our design utilizes a dispersion strengthened copper (Glidcop) face plate which acts as a thermal structural barrier to prevent material yielding. The face plate is brazed to an OFHC body after the cooling channels have been machined. This design combines ease of manufacturing with excellent thermal and mechanical performance.

While the optimization is performed at steady state condition, transient thermal analysis is needed to assure that no unduly high thermal gradients are generated in the shutter's face plate during the initial heating stage before equilibrium is obtained. The results of such analysis show that: given our choice of geometry and materials, the peak thermal gradients and stresses during the transient stage are always lower than the steady state values. This remains true even under the worst condition using the APS Undulator A beam at closed gap.

References:

- [1] A.M. Khounsary and B. Lai "Power Distribution Profiles for APS Bending Magnets and Insertion Devices" APS/LS-198, July 1992
- [2] K. J. Kim "Angular Distribution of Undulator Power for an Arbitrary Deflection Parameter K" Nuclear Instruments and Methods in Physics Research A246 (1986) 67-70

Y.Sakurai, M. Oura, H.Sakae, T.Usui, T.Konishi*, H.Shiwaku*,
A.Nakamura*, H.Amamoto*, T.Harami*, H.Kimura, Y.Oikawa
and H.Kitamura

JAERI-RIKEN SPring-8 Project Team, The Institute of Physical and
Chemical Research (RIKEN), Wako, Saitama 351-01, Japan.

*JAERI-RIKEN SPring-8 Project Team, Japan Atomic Energy Research
Institute, Tokai, Ibaraki 319-11, Japan.

The SPring-8 is a third generation synchrotron radiation (SR) facility constructing in Japan. The electron or positron beam with an energy of 8 GeV is stored up to a current of 100 mA in the storage ring with a circumference of 1435.95 m. Of 44 straight sections, 38 sections are used to accommodate an insertion device. The insertion devices produce SR with higher power and lower emittance than those of second generation SR facilities. Thus, handling the power and SR beam position is a major challenge in the engineering of the front-end components.

The undulator emits angular power density of 500kW/mrad² and the MPW produces total power of about 50kW at the highest.

The fixed mask and heat absorber which are made of the Gridcop, intercept completely the SR at a grazing angle of several degrees to reduce the input heat power below 10W/mm² on the receiving surface.

The slits confine the size of the SR. The beam is received by a block of the Super-Graphite which has excellent thermal conductivity in the a-b plane. The block is holed by a water cooled Cu block and the thermal contact is enhanced by inserting In-Ga liquid alloys between them.

An assembly of two Be windows with a thickness of 250μm each are placed at the end of the front-ends. A graphite filter with a thickness of 100μm at least is necessary to protect the windows. The Super Graphite is used as filter material. The foils with a thickness of 100μm are attached to a water-cooled Cu holder, and are cooled radiatively and conductively.

The SPring-8 front-ends must be standardized. Thus, three kinds of front-ends are being developed, which are for the undulators, MPWs and BMs.

Design of an EMPW Beamline for High-energy Inelastic Scattering at the SPring-8

Y.Sakurai, H.Yamaoka, H.Kimura, X.Marechal, K.Ohtomo, T.Ishikawa
and H.Kitamura,

*JAERI-RIKEN SPring-8 Project Team, The Institute of Physical and Chemical
Research(RIKEN), Wako, Saitama 351-01, Japan.*

Y.Kashihara and T.Harami,

*JAERI-RIKEN SPring-8 Project Team, Japan Atomic Energy Research Institute,
Tokai, Ibaraki 319-11, Japan.*

Y.Tanaka,

*The Institute of Physical and Chemical Research(RIKEN), Wako,
Saitama 351-01, Japan.*

H.Kawata,

*Photon Factory, National Laboratory for High Energy Physics, 1-1 Oho, Tsukuba,
Ibaraki 305, Japan,*

N.Shiotani,

Tokyo University of Fisheries, Kounan, Minato, Tokyo 108, Japan

N.Sakai,

*Faculty of Science, Himeji Institute of Technology, 1479-1 Kanaji, Kamigohri,
Ako-gun, Hyogo 678-12, Japan.*

Compton scattering experiments provide the information of the momentum distribution of electrons. Further, the magnetic Compton scattering of circularly polarized x-rays gives that of magnetic electrons in ferromagnetic materials. For these experiments the use of higher than 100keV x-rays is certainly appreciated, but have never been achieved in the synchrotron radiation facility.

An elliptic multipole wiggler (EMPW) beamline for these experiments with use of such high energy x-rays is decided to be constructed as one of pilot beamlines at the SPring-8 and will be completed in 1997.

Two experimental stations will be constructed; one is for the high-resolution experiments using 100-150 keV x-rays, another is mainly for the magnetic Compton scattering using circularly polarized 300 keV x-rays. Doubly bent monochromator or combination of an asymmetric Johann monochromator and a single d-spacing W/B₄C multilayer are being developed for both vertical and horizontal focusings as a optics of the former experiments. An asymmetric Johann monochromator will be used for the optics of the latter experiments.

TuD63

Monochromators for the U49 Undulator at the BESSY II Storage Ring

H. Petersen, F. Senf, F. Schäfers, J. Bahrtdt
BESSY GmbH, Lentzeallee 100, D - 14195 Berlin, Germany

Two beamlines have been designed for use on the undulator U49, which will be one of the first insertion devices operational at the new 1.7 GeV BESSY II storage ring. The monochromators will be a plane grating monochromator using the proven plane grating focusing condition [1] and an exact focusing spherical grating monochromator with a variable angle of deviation across the grating and fixed exit slits [2]. The optical designs as well as results of detailed numerical calculations will be presented. These include radiation simulation with the code SMUT [3] for the undulator, which has 84 periods of 49 mm length each. Subsequent ray tracing with the code RAY [4], which includes slope errors and reflectivity and grating efficiency calculations, provides detailed information about photon flux, spectral resolution and transmission across the broad photon energy range covered by the U49 (135 eV - 1516 eV in the first, third and fifth harmonic). Reaching an energy resolution between 12000 and 17000 at the oxygen K-edge a flux of still more than 10¹¹ phot./sec·100 mA can be maintained. The overall efficiency of the beamlines varies between 0.1 % and 6 % while up to 95 % of the radiation emitted by the U49 is geometrically accepted by the beamline optics. Our calculations are supported by the excellent experimental results obtained with these two types of monochromators at BESSY and in other SR-laboratories.

References

- [1] H. Petersen, Optics Commun. 40, 402 (1982) and H. Petersen, C. Jung, C. Hellwig, W. Peatman, W. Gudat, Rev.Sci.Instr. (in press)
- [2] W. Peatman, J. Bahrtdt, A. Gaupp, F. Schäfers, F. Senf, BESSY Ann. Report 1992, p. 49
- [3] C. Jacobson, H. Rarback, SPIE Vol. 582, Int.Conf.on Insertion Devices for Synchrotron Radiation, Stanford 1985, p. 201
- [4] RAY, J. Feldhaus, HASYLAB, Hamburg; F. Schäfers, BESSY, Berlin

TuD64

Performance of a Material Science Facility at the Photon Factory: A Soft X-ray Beamline BL-13C Coupled with a Multi-Purpose Analytical Apparatus

H. SHIMADA*, N. MATSUBAYASHI*, M. IMAMURA*, T. SATO*, Y. YOSHIMURA*, T. HAYAKAWA*, K. TAKEHIRA*, A. TOYOSHIMA**, K. TANAKA**, and A. NISHIJIMA*

*National Institute of Materials and Chemical Research, 1-1, Higashi, Tsukuba, Ibaraki 305, Japan

**Photon Factory, National Laboratory for High Energy Physics, Oho, Tsukuba, Ibaraki 305, Japan

We reported the detailed designs of BL-13C¹⁾ and a multi-purpose analytical apparatus²⁾ in the past SRI meetings. The present paper introduces the fundamental performances of the facility as well as some applications to material and surface science.

BL-13C, a Dragon-type beamline on a 13-pole undulator, covers an energy range between 150 and 1200 eV by the use of a mechanically ruled grating with 750 gr/mm. High resolution with moderate flux or high flux with moderate resolution soft x-rays can be chosen depending on the slit width. The highest resolution at 400 eV is about 70 meV with a slit width of 10 μ m, when vibrationally resolved photoionization spectra of gaseous nitrogen are obtained. For the XAFS analyses of bulk materials, sufficient resolution of about 0.4 eV at 400 eV is achieved at a slit width of 100 μ m when a photon flux more than 10¹²/sec is obtained. B, C, N, or O K-edge XAFS spectra can be obtained by means of total or partial electron yields, sample drain current, fluorescent x-ray yields and Auger electron yields at the same time.

Another important feature of the facility lies in the use as an energy-variable x-ray photoelectron spectrometer using a hemispherical electrostatic analyzer. The exit slit of the beamline is moved corresponding to the x-ray energy to obtain the best energy resolution. Non-destructive depth analysis on not only composition but also chemical state is performed by changing photoelectron escape depth. Figure 1 shows the O_{1s} photoelectron spectra of a perovskite-type oxidation catalyst, La_{0.6}Sr_{0.4}CoO_{3-x}, at various incident x-ray energies (E_i in Fig. 1). With the decrease in the incident x-ray energy, the signal from the surface is enhanced.

The peak at 527.8 eV is ascribed to lattice oxygen, while the peak at 530.7 eV arises from surface oxygen species which is supposed to play an important role in catalysis. The present system has significant advantages over other depth profiling methods such as detection angle alteration or surface erosion by ion bombardment in respects of high depth resolution and chemical state preservation.

References

- 1) N. Matsubayashi, H. Shimada, K. Tanaka, T. Sato, Y. Yoshimura, and A. Nishijima, Rev. Sci. Instrum., 63 (1992) 1363.
- 2) N. Matsubayashi, I. Kojima, M. Kurahashi, A. Nishijima, A. Itoh, and T. Utaka, Rev. Sci. Instrum., 60 (1989) 2533.

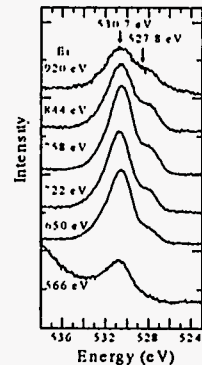


Fig 1 O_{1s} photoelectron spectra of La_{0.6}Sr_{0.4}CoO_{3-x}.

Explosion Bonding and Its Applications in the Advanced Photon Source Front End and Beamline Component Designs *

D. Shu, Y. Li, D. Ryding and T. M. Kuzay

Experimental Facilities Division
Advanced Photon Source
Argonne National Laboratory
Argonne, IL 60439, U.S.A.

and

Dave Brasher

Northwest Technical Industries, Inc.
547 Diamond Point Rd. Sequim, WA 98382, U.S.A.

ABSTRACT

Explosion bonding is a bonding method in which the controlled energy of a detonating explosive is used to create a metallurgical bonding between two or more similar or dissimilar materials.

Since 1991, a number of explosion-bonded joints have been designed for high-thermal-load, ultrahigh-vacuum (UHV) compatible components in the Advanced Photon Source. A series of standardized explosion bonding joint units has also been designed and tested, such as oxygen-free copper (OFHC) to stainless steel vacuum joints for slits and shutters, Glidcop to stainless steel vacuum joints for fixed masks and Glidcop to OFHC thermal and mechanical joints for shutter face-plates et al.

The design and test results for the explosion-bonded components in the Advanced Photon Source front ends and beamlines are discussed in this paper.

The submitted manuscript has been authored by a contractor of the U.S. Government under contract No. W-31-109-ENG-38. Accordingly, the U.S. Government retains a nonexclusive, royalty-free license to publish or reproduce the published form of this contribution, or allow others to do so, for U.S. Government purposes.

*Work supported by the U. S. Department of Energy BES Materials Science under contract W-31-109-ENG-38.

A Double-Multilayer Monochromator Using a Modular Design for the Advanced Photon Source *

D. Shu, W. Yun, B. Lai, J. Barraza and T. M. Kuzay

Experimental Facilities Division
Advanced Photon Source
Argonne National Laboratory
Argonne, IL 60439, U.S.A

ABSTRACT

A novel double-multilayer monochromator has been developed for the Advanced Photon Source X-ray undulator beamline at Argonne National Laboratory. The monochromator consists of two ultrahigh-vacuum-compatible modular vessels with a sine-bar driving structure and a water-cooled multilayer holder. A high precision X-Z stage has been used to provide a compensation motion for the second multilayer from outside of the vacuum so that this monochromator can fix the output monochromatic beam direction and the angle during the energy scan in a narrow range.

The design details for this monochromator are presented in this paper.

The submitted manuscript has been authored by a contractor of the U.S. Government under contract No. W-31-109-ENG-38. Accordingly, the U.S. Government retains a nonexclusive, royalty free license to publish or reproduce the published form of this contribution, or allow others to do so, for U.S. Government purposes.

*Work supported by the U. S. Department of Energy BES Materials Science under contract W-31-109-ENG-38.

TuD67

Design of Precision White-Beam Slits for the High Power Density X-ray Undulator Beamlines at the Advanced Photon Source *

D. Shu, C. Brite, T. Nian, W. Yun, D.R. Haeflner, E.E. Alp,

D. Ryding, J. Collins, Y. Li and T. M. Kuzay

Experimental Facilities Division
Advanced Photon Source
Argonne National Laboratory
Argonne, IL 60439, U.S.A

ABSTRACT

A set of precision horizontal and vertical white-beam slits has been designed for the Advanced Photon Source X-ray undulator beamlines at Argonne National Laboratory. There are several new design concepts applied in this slit set, including a grazing-incidence, knife-edge configuration to minimize the scattering of x-rays downstream, enhanced-heat-transfer tubing to provide water cooling, and a secondary slit to eliminate the thermal distortion on the slit knife edge.

The novel aspect of this design is the use of two L-shaped knife-edge assemblies, which are manipulated by two precision X-Z stepping linear actuators.

The design details and preliminary test results for this slit set are presented in this paper.

The submitted manuscript has been authored by a contractor of the U.S. Government under contract No. W-31-109-ENG-38. Accordingly, the U.S. Government retains a nonexclusive, royalty free license to publish or reproduce the published form of this contribution, or allow others to do so, for U.S. Government purposes.

*Work supported by the U.S. Department of Energy BES Materials Science under contract W-31-109-ENG-38.

TuD68

**Design of High Heat Load White-Beam Slits for
Wiggler/Undulator Beamlines at the Advanced Photon Source ***

D. Shu, V. Tcheskidov, T. Nian, D.R. Haeffner, E.E. Alp

D. Ryding, J. Collins, Y. Li and T. M. Kuzay

Experimental Facilities Division
Advanced Photon Source
Argonne National Laboratory
Argonne, IL 60439, U.S.A

ABSTRACT

A set of horizontal and vertical white-beam slits has been designed for the Advanced Photon Source wiggler/undulator beamlines at Argonne National Laboratory. While this slit set can handle the high heat flux from one APS undulator source, it has large enough aperture to be compatible with a wiggler source also. A grazing-incidence, knife-edge configuration has been used in the design to eliminate downstream X-ray scattering. Enhanced heat transfer technology has been used in the water cooling system. A unique stepping parallelogram driving structure provides precise vertical slit motion with large optical aperture.

The full design detail is presented in this paper.

The submitted manuscript has been authored by a contractor of the U.S. Government under contract No. W-31-109-ENG-38. Accordingly, the U.S. Government retains a nonexclusive, royalty free license to publish or reproduce the published form of this contribution, or allow others to do so, for U.S. Government purposes.

*Work supported by the U. S. Department of Energy BES Materials Science under contract W-31-109-ENG-38.

TuD69

Design of the Beamline Standard Components at the Advanced Photon Source *

D. Shu, J. Barraza, C. Brite, T. Sanchez, V. Tcheskidov

Experimental Facilities Division
Advanced Photon Source
Argonne National Laboratory
Argonne, IL 60439

ABSTRACT

This paper provides an overview of the design of the standard beamline components for the Advanced Photon Source.

The submitted manuscript has been authored by a contractor of the U.S. Government under contract No. W-31-109-ENG-38. Accordingly, the U.S. Government retains a nonexclusive, royalty free license to publish or reproduce the published form of this contribution, or allow others to do so, for U.S. Government purposes.

*Work Supported by the U.S. Department of Energy BES Materials Science under contract W-31-109-ENG-38.

TuD70

High Energy Scattering Beamlines at ESRF

P. Suortti and Th. Tschentscher
European Synchrotron Radiation Facility, B.P. 220, F-38043 Grenoble, France

Beamlines for high energy x-ray scattering are under commissioning at the ESRF. Two insertion devices will be available in the same straight section: a 7-period asymmetrical permanent magnet wiggler is used in the initial operation, and it will be complemented by a superconducting wavelength shifter. The critical energies are 43 keV and 100 keV, respectively. The basic concept is to use the white radiation several times by placing semi-transparent monochromators in the beam. The monochromators are bent Si crystals, which focus the beams to the side stations, while white beam is available at the center station. The stations have separate slits, beam position monitors and shutters, and they can be operated independently. One of the side stations, S on the starboard side, is dedicated for inelastic scattering and designated as Beamline 25, while the center station B and the station on the port side, P, form Beamline 5, which is dedicated for diffraction and imaging.

The monochromators are either of Bragg (reflection) or Laue (transmission) type. They are cylindrically bent, and different focusing conditions and bandwidths are achieved by varying the bending radius. The thermal load on the crystal is reduced by an upstream Al absorber, which cuts off radiation below 20 keV, and a new way of cooling the crystal is introduced. The crystal is attached by Ga-In eutectic to the bender, which has an opening in the middle for the transmitted beams and horizontal water channels along the edges of the crystal. The bender is attached to a frame by one end, and it is bent by applying a torque at the free end. Prototype benders have been used at the Materials Science Beamline of the ESRF, and the results indicate large intensity gains due to focusing and kinematic rather than dynamical diffraction by a bent crystal.

Biological protection is based on local shielding of the beamline components. The strongly scattering common elements of the beamlines, the beam limiter/splitter, attenuators, and primary slits are encased in 20 mm to 50 mm of lead shielding. The hutches for white beam scattering have wall thickness of 12 mm of lead, but still local shielding of the experiments is foreseen. Scattering from air is about 2% per meter at high photon energies, so that the beam path in air is minimized by He-filled or vacuum tubes.

The principal instrument at BL 25 is a scanning-type x-ray spectrometer. It will be used mostly for Compton scattering, but also studies of other inelastic scattering is foreseen. The sample stage is designed to support large weights, such as cryomagnets. The white beam station of BL 5 is equipped with a high-precision 3-axis diffractometer, which can be used for studies of crystal imperfections, domain structures, phase transitions and measurements of structure factors in different sample environments. This station is also served by special monochromators in the second optics hutch, which allows different pilot studies in high-energy scattering and imaging. The side station P will be used for diffraction under various experimental conditions, such as high pressures and temperatures.

Results of first test measurements at are shown. These characterize the performance of the beamlines in terms of the monochromatic flux at the sample and the degree of circular and linear polarization. Detailed reports of these experiments will be published separately.

A TRIPLE-AXIS/FOUR-CIRCLE DIFFRACTOMETER AT PF-BL3A (II)

Yasuo Takagi, Toshiharu Kikuchi*, Toshiyuki Mizutani*, Muneyuki Imafuku*, Satoshi Sasaki**, and Takeharu Mori***

Advanced Materials and Technology Research Laboratories, Futtsu Branch,
Nippon Steel Corporation, 20-1 Shintomi, Futtsu, Chiba 299-12 JAPAN

*Advanced Materials and Technology Research Laboratories,
Nippon Steel Corporation, 1618 Ida, Nakahara-ku, Kawasaki 211, JAPAN
**Research Laboratory of Engineering Materials, Tokyo Institute of Technology,
4259 Nagatsuta, Midori-ku, Yokohama 227, JAPAN

***Photon Factory, National Laboratory for High-Energy Physics (KEK),
1-1 Oho, Tsukuba, Ibaraki 305, JAPAN

Several new goniometer systems were installed to the triple-axis/four-circle diffractometer at PF-BL3A to improve data acquisition ability and beam collimation.^{1) & 2)} The most prominent improvement is the installation of a three-circle goniometer system which was designed to mount various x-ray detectors such as an imaging plate (IP) and a multi-element solid-state detector (multi-SSD) to acquire diffraction and/or fluorescence data over a wide range of the scattering angles. As is shown in Figure, the new goniometer system and the original four-circle goniometer system has a common rotation center. It can be operated independently to the four-circle goniometer system for a wide range of the solid-angles close to 4π . The new system consists of a tandem combination of a translation stage, ξ , and two circle goniometers, κ and η . Their coordinates correspond to (ρ, θ, ϕ) , respectively in a polar coordinate. By using the new goniometer system, data acquisition with the detectors such as IP and/or multi-SSD became possible for a wide range of the scattering angle close to 4π .

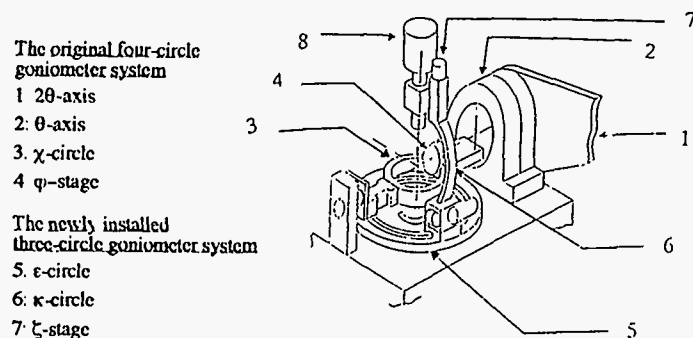


Figure The original and new goniometer systems of the triple-axis/four-circle diffractometer at PF-BL3A

REFERENCES

- 1) K. Kawasaki, Y. Takagi, K. Nose, H. Morikawa, S. Yamazaki, T. Kikuchi and S. Sasaki: *Rev. Sci. Instrum.*, **63**(1992)1023.
- 2) Y. Takagi, T. Kikuchi, T. Mizutani, K. Kawasaki, S. Sasaki and T. Mori: *Photon Factory Activity Report*, **10**(1992)43

Two and four crystal reflections monochromators

H. Tolentino and J. Durr

Laboratório Nacional de Luz Síncrotron - LNLS/CNPq
C.P. 6192, 13081-970 Campinas (SP) Brazil

C. Cusatis, I. Mazzaro and D. Udron

Universidade Federal do Paraná - Dept. of Physics
C.P. 19091, 81504-000 Curitiba (PR) Brazil

ABSTRACT

Two and four crystal reflections monochromators, developed at LNLS (Campinas-Brazil)¹, were tested and used at the synchrotron radiation facility LURE (Orsay-France). We report on their performance in terms of stability, reliability and energy resolution. The important characteristic of these devices is simplicity: they are based on monolithic mechanics and compactness, crucial for reaching good stability and high energy resolution. In addition, we report on a new design for the two-crystal monochromator, where the first crystal is fixed in the center of rotation, and is water-cooled, while the second crystal is mounted on a "crossed elastic translator". Both monochromators will be used in the XAFS and Diffraction beamlines in construction for LNLS.

¹ Proceedings of the 4th International Conference on Synchrotron Radiation Instrumentation (Chester, UK); Rev. Sci. Instrum. 63(1) (1992) p. 896, p. 946.

TuD73

Vacuum System for APS Insertion Devices

E.M. Trakhtenberg, E.S. Gluskin, Shenglan Xu
Argonne National Laboratory, Argonne, IL

Abstract

A vacuum system for the APS insertion devices was designed; a prototype of this system was manufactured and successfully tested. The system consists of two vacuum chamber sections with distributed vacuum pumps, two boxes contained vacuum pumps, vacuum analyzers and special transition sections, and finally two support structure sections. The vacuum chambers are made of extruded aluminum, the wall thickness of the insertion devices vacuum chamber section is 1 mm in the area of the insertion device's magnetic gap on the length of 2.4 meters. An ultimate pressure better than 5.5×10^{-11} torr was achieved in the prototype that contains the insertion device vacuum chamber section with the 12 mm vertical aperture.

This work was supported by the US Department of Energy BES material sciences, under contract W-31109-ENG-38

The submitted manuscript has been authored by a contractor of the U.S. Government under contract No. W-31109-ENG-38. Accordingly, the U.S. Government retains a nonexclusive, royalty free license to publish or reproduce the published form of this contribution, or allow others to do so, for U.S. Government purposes.

TuD74

The wiggler x-ray beam lines at SRRC

K.-L. Tsang, C.-H. Lee, Y.-C. Jean, T.-E. Dann, J.-R. Chen,

Synchrotron Radiation Research Center, Hsinchu, Taiwan, ROC

K. L. D'Amico

X-ray Analytics Ltd, PO Box 678, Upton, NY 11973.

and

T. Oversluisen

National Synchrotron Light Source, Upton, NY 11973

We have designed three x-ray beam lines extracted out from one 25 poles 1.8 tesla wiggler insertion device. This wiggler insertion device at the SRRC 1.3 GeV storage ring will increase the usable x-ray photons with an energy up to 15 KeV. In order to satisfy the big x-ray user community at Taiwan, we need to have at least three different types of beam lines to cover various kinds of experiments. Due to the limitation of radiation source and space, we have specially designed three x-ray beam lines sharing the 13 mrad horizontal radiation output from the insertion device. The design and construction of these three beam lines will be described in this paper.

TuD75

Performance of the 1m-SNM beam line at SRRC

P.-C. Tseng, T.-F. Hsieh, Y.-F. Song, K.-D. Lee, S.-C. Chung, C.-I. Chen, H.-F. Lin, T.-E. Dann, L.-R. Huang, C.-C. Chen, J.-M. Chuang, K.-L. Tsang, and C.-N. Chang*

SRRC, No. 1, R and D Rd., Hsinchu Science Based Industrial Pk., Hsinchu, Taiwan, ROC

* also at National Taiwan Normal University

The performance of the 1 meter Seya-Namioka Monochromator (1m-SNM) beamline at SRRC has been measured and reaches the designed goal. The beam line throughput (photon flux) has been measured by a calibrated SiO₂ photodiode and is close to the theoretical values. The resolving power of this beam line has been measured from the studies of the core absorption of Ar and the Rydberg states of Mg vapor gas, and has reached the theoretical values. The improvement of the cooling system of the first mirror is also described.

TuD76

X-ray Instrumentation for a focused Wiggler Beamline at the EMBL Outstation Hamburg.

R.G. van Silfhout and C. Hermes

EMBL, Notkestr. 85, D-22603 Hamburg, Germany

A flexible set-up consisting of two independent water-cooled X-ray monochromators providing radiation for two separate beamlines and experimental stations (A & B) has been installed on the multipole Wiggler BW7 at the DORIS III storage ring.

The first optical element of both lines is a Rh-coated SiC mirror to reduce the heat load on subsequent energy defining elements.

Line B, which will be predominantly used for Protein Crystallography, is optimised for flux and employs a triangular monochromator and segmented glass mirror for horizontal and vertical focusing respectively; it can be operated in a wavelength range from 0.8 -1.3 Å.

In contrast Line A is optimised for energy resolution and fast energy scans. This is achieved by a fixed exit, non-dispersive double monochromator followed by a segmented glass mirror. It will mainly be used for Anomalous scattering, EXAFS and SAD experiments.

The use of encoders, intelligent stepper/DC-motor controllers and position sensitive beam monitors allow a comfortable and fast alignment of all axes. Both experimental hutches are equipped with large motorized optical tables, offering a versatile and convenient experimental surface.

CONCEPTUAL DESIGN OF THE DUTCH-BELGIAN BEAMLINE AT THE ESRF

E. Vlieg¹⁾, J.H.M. Bijleveld²⁾, D. Glastra van Loon¹⁾, U.A. van der Heide³⁾, M. Kronenburg³⁾ and Y.K. Levine³⁾

¹⁾ FOM-Institute AMOLF, Kruislaan 407, 1098 SJ Amsterdam, The Netherlands

²⁾ NIKHEF, Kruislaan 411, 1098 SJ Amsterdam, The Netherlands

³⁾ Debye Institute, University of Utrecht, Buys Ballot Laboratory, Princetonplein 5, 3584 CC Utrecht, The Netherlands

The conceptual design of the proposed Dutch-Belgian CRG beamline (DUBBLE) at the ESRF will be presented. DUBBLE is designed as a multi-purpose beamline, providing facilities for four different techniques: small-angle X-ray scattering (SAXS), interface diffraction, X-ray absorption spectroscopy (XAS) and high-resolution powder diffraction. In order to accommodate these experimental techniques with their own optical demands, the beamline will be split into two fully focused branches. Each branch will utilise 2 mrad of the available horizontal radiation fan of 6 mrad. The branch accommodating experimental facilities for SAXS and interface diffraction will make use of a sagittally focusing monochromator followed by a meridionally-focusing mirror. The optics of the branch for XAS and high-resolution powder diffraction experiments will consist of a collimating mirror followed by a monochromator and with a toroidal mirror as the last element. This branch will operate in two modes depending on the energy range required for the experiments. The low-energy operational mode will make use of the toroidal mirror. This mirror will be removed for the high-energy mode and sagittal focusing will be accomplished through the monochromator.

The choice for a beamline with two fully focusing branches imposes strong boundary conditions on the spatial layout of the beamline and the size of its optical components. We have chosen the SAXS/interface diffraction experimental station to be the end station, because these techniques demand the largest experimental space. The available space in the experimental hutch containing the facilities for XAS and powder diffraction will be limited in one direction by the beam pipe of the other branch. These techniques, however, require less experimental room, so this will hardly limit the type of experiments that can be performed.

A Variable Thickness Window: Thermal and Structural Analyses

Zhibi Wang, Tuncer M. Kuzay

Experimental Facilities Division
Advanced Photon Source
Argonne National Laboratory
9700 South Cass Avenue
Argonne, IL 60439

A novel idea that uses a variable thickness window for a synchrotron radiation insertion device is proposed here. The main advantages of using a variable thickness window are as follows: (1) to make it possible to design a window without filters and therefore make more low energy photons available to the users; (2) to increase the heat conduction area without increasing the thickness in core area so that the maximum temperature in the window can be significantly decreased; (3) to increase the safety margin of window system due to the increasing structural integrity, especially the buckling load in thin windows, which also increases the structural integrity of window against shock due to sudden loss of vacuum; (4) to increase the window size under the same operating condition. Compared to a uniform Be window, the variable thickness Be window reduces the likelihood of the catastrophic break.

The finite difference formulations for variable thickness thermal analysis and variable thickness plane stress analysis are presented. In the thermal analysis, radiation effects and temperature-dependent thermal conductivity have been taken into account. Thermal stress analysis has considered the thermal expansion coefficient as temperature dependent. An application of the variable thickness window to the APS beamline is presented.

This work is supported by the U.S. Department of Energy, BES-Materials Sciences, under contract no. W-31-109-ENG-38.

TuD79

Performance of a High Resolution, High Flux Density SGM Undulator Beamline at the ALS

Tony Warwick, Phil Heimann, Dmitry Mossessian,
Wayne McKinney and Howard Padmore.
Lawrence Berkeley Laboratory, Berkeley, CA 94720, USA

ALS beamline 7.0 is designed for high resolution operation with maximum photon flux and a small spot size at the sample, matched to the acceptance of the experiment spectrometers. The performance of the beamline will be described, as measured during the first few months of operation. The system has operated fully in accordance with the design goals, with the undulator gap varying from $K=0.5$ to $K=2.2$.

We will report on the focussing of the first optic, which can deliver all of the useful radiation through the entrance slit of the monochromator at $25\mu\text{m}$. Beam stability measurements will be shown; the image of the source shakes and drifts by only a small fraction of its size, and fill-to-fill reproducibility is excellent. The spherical grating monochromator has operated at resolving powers in excess of 7000. The refocus optics are in operation, giving a spot at two interchangeable sample stations with a diameter of $50\mu\text{m}$, containing all of the resolved flux across the entire operational range of photon energy. Intensity measurements at the experimental stations correlate well with the predictions for the resolved flux. The scientific program is underway, with several experiments taking advantage of the high flux density of resolved photons at the sample.

This work was supported by the Director, Office of Energy Research, Office of Basic Energy Sciences, Materials Sciences Division of the U.S. Department of Energy, under Contract No. DE-AC03-76SF00098

This paper should be considered as a possible INVITED TALK contact:

*Dr. Tony Warwick, 2-400 Lawrence Berkeley Laboratory,
Berkeley, CA 94720.
Tel. (510) 486 5819 Fax (510) 486 7696*

TuD80

NEW MACROMOLECULAR CRYSTALLOGRAPHY STATION BL-18B
AT PHOTON FACTORY.

N. Watanabe¹⁾, S. Adachi²⁾, A. Nakagawa¹⁾, and N. Sakabe¹⁾,

1) Photon Factory, National Laboratory for High Energy Physics, Tsukuba, Ibaraki 305, 2) The Institute of Physical and Chemical Research (RIKEN), Wako, Saitama 351-01, JAPAN.

A new experimental station, BL-18B, has been constructed on the bending-magnet beamline at the Photon Factory to extend its capability for macromolecular crystallography. The branch beamline is equipped with a 1m long fused quartz bent cylindrical mirror with 1:1 focusing, located 13.75m from the source. The surface of the focusing mirror is cylindrically polished and platinum coated with a sagittal radius of 41.3mm, and bent to a radius of ca. 4,500m. The glancing angle of the X-ray beam with the mirror is set to about 3mrad, which gives a cut-off wavelength of approximately 0.4Å. The mirror can focus the X-ray beam to about 0.4mm (vertical) × 1.2mm (horizontal), which is consistent with the expected focus size simulated by the raytracing technique. Total power of focused white x-ray beam estimated using a calorimeter was 800mW per 300mA. The monochromator is a fixed-exit double-crystal, located 23.1m from the source. The monochromator consists of two kinds of flat crystals, usually Si(111) and Ge(220), mounted parallel on the goniometer. The two types of crystals are therefore interchangeable without opening the vacuum chamber. Photon flux of the monochromatic beam estimated using an ionization chamber was 4×10^{10} Photons/sec at 1.07Å, Si(111), and 1×10^{10} Photons/sec at 0.72Å, Ge(220), at the sample position when the PF ring was operated at 2.5GeV, 300mA and the acceptance of the first slit was 0.2mrad, vertical, and 2.0mrad, horizontal. BL-18B has been built as an end station in order to have enough space available for installing a large camera and other instruments in the experimental hutch. In addition to increasing the experimental time available for users of Weissenberg camera, BL-18B provides a point focused white beam. This feature gives the station milli-second time-resolved Laue capability. Special Image Plates (IP) and IP scanner are also being developed to allow more effective exposures using Weissenberg and Laue cameras at the station. The dimensions of the new IP are 400mm×400mm and 400mm×800mm. Response of the scanner was tested and the nonlinearity between the input x-ray photons and the measured intensity is negligible from 1 to 1×10^5 photons per pixel. The beamline has been opened for general users from April 1994.

TuD81

THE 3B1B BIOLOGY SPECTROSCOPY STATION AT BSRF

Wang Wei, Wu Jian-wu, Gu Xiang-ming, Sheng Wei-fan, Jin Ming,
Li Chong-ci*, Zhao Nan-sheng**, Wang Ke-bin†, Zhao Fu-hong†,
Wang Wen-qing††, Zheng Duo-kai†

Institute of High Energy Physics, CAS P.O.Box 918 Beijing 100039

*Beijing Agricultural University **Beijing Planetarium

†Institute of Botany, CAS ††Beijing University †Institute of Medica, CAMS

ABSTRACT

In June, 1993 the 3B1B Biology Spectroscopy Station at Beijing Synchrotron Radiation Facility (BSRF), located in the beamline 3B1B, is gotten into commission. The main apparatus of this station is a Circular Dichroism (CD) Spectroscopy. It consists of Seya-Namioka ARC VM-502 monochromator, Photo-Elastic Modulator (PEM-80), Sample chamber and detector etc. The synchrotron radiation monochromatic beam with the wavelength ranging from 170 nm to 500 nm is focused on the sample. The system could be operated as the Beijing Electron-Positron Collider (BEPC) run either in parasitic or dedicated mode, and either in normal atmospheric or in vacuum (10^{-2} torr) environmental condition.

During the period of dedicated running mode in this summer (June 17-30), the CD spectra for 11 biological and medicinal samples with molecules having chirality were measured on the system and good results were obtained. It is the first time in China that CD spectra of D-phenylalanine, Androsterone, Camphor Sulfonic Acid and a symmetric CD curve of D- and L- leucine is obtained using synchrotron radiation.

The station is being improved. Researchers in the field of biology or physics are welcome to this station.

TuD82

X13A: A VERSATILE SOFT X-RAY UNDULATOR BEAMLINE

Z. Xu, I. McNulty, K. J. Randall, L. Yang, E. Gluskin

Advanced Photon Source, Argonne National Laboratory
9700 S. Cass Ave, Argonne, IL 60439

E. D. Johnson, and T. Overslizen

National Synchrotron Light Source, Brookhaven National Laboratory
Upton, Long Island, NY 11973

The undulator based beamline X13A at NSLS has been commissioned recently. The X13 undulator has an 8 cm period, with a first harmonic in the energy range of 200-700 eV at the nominal ring energy of 2.5 GeV. The beamline uses horizontally diffracting optics. It consists of a SiC plane mirror, a water cooled entrance slit, a spherical grating monochromator, and two fixed position exit slits. A peak intensity of more than 10^{11} photons per second at ~450 eV has been measured with a calibrated aluminum oxide photo diode with a 200 μm entrance slit, a 500 μm exit slit, and a ring current of 122 mA. A VF_3 absorption spectrum shows the estimated energy resolution of 1000 at ~500 eV with 40 μm entrance slit and exit slit, which is in agreement with the calculated results. The X13A beamline will be used for the studies of x-ray coherence, spectroscopy, and multilayer reflectivity as well as the diagnostics of x-ray instrumentation.

This research was supported by the U.S. Department of Energy, BES Materials Sciences, under contract No. W-31-109-ENG-38 and DE-AC02-76CH0016.

TuD83

Commissioning and Operation of Beam Line for Photoelectron Spectroscopy in NSRL

P. S. Xu, X. J. Yu, E. D. Lu, Q. P. Wang, S. H. Xu

National Synchrotron Radiation Laboratory,
Univ of Sci. & Tech. of China, Hefei, Anhui 230026, P. R. of China

The grazing incidence spherical grating monochromator(SGM) for photoelectron spectroscopy has been designed and set up in NSRL[1].

The horizontal and vertical prefocussing mirrors intercept up to 15 mrad and 2.5 mrad of SR beam respectively. Four spherical laminar gratings separate SR beam to two optical branches for soft X-ray (62-1000eV) and VUV(10-60eV). Wave length scan in the monochromator is achieved by the rotation of grating and the translation of a pair of slits driven by stepping motors.

The gratings are installed at the end of 1992. In 1993 we started to commission and operate the beam line.

We aligned the movement of slits and sin bar with laser interferometer. The wave length was calibrated and the errors were corrected. The output flux of gratings has been measured with photoelectron current of a detector.

We have developed the software based on the spectrometer of VSW company in order that it could be used with EDC, CFS and CIS mode.

Some experiments have been done in our experimental station using the monochromator[2,3]. The results are satisfied and the resolution power could be obtained from 500 to 1000($E/\Delta E$) with 50 μm of slits in a wide range of photon energy. The improvement of the beam line performance is continuing.

Reference

- (1) D M Shu et al, Nucl. Instr. and Meth. A291(1990)168
- (2) X F Jin et al, Phys. Rev. B submitted
- (3) P S Xu et al, The 22nd International Conference on The Physics of Semiconductors, August, 1994, Vancouver, Canada, submitted

TuD84

Conceptual Design of SPring-8 Contract Beamline for Structural Biology

M. Yamamoto, T. Fujisawa, M. Nakasako, T. Tanaka, T. Uruga, H. Kimura,
H. Yamaoka, Y. Inoue, H. Iwasaki, T. Ishikawa, H. Kitamura and T. Ueki
The Institute of Physical and Chemical Research (RIKEN)
Hirosawa 2-1, Wako, Saitama, Japan

From the viewpoint of Structural Biology, three-dimensional structures of biological macromolecules are essential for understanding biological functions and mechanisms. X-ray crystallography and small angle X-ray scattering (SAXS) are the important techniques for Structural Biology. At SPring-8, the contract beamline for Structural Biology is being designed and developed by the Institute of Physical and Chemical Research (RIKEN).

This beamline is simultaneously operated with two experimental stations: SAXS and protein crystallography. In order to use both stations simultaneously, dichromatic synchrotron radiation emitted from tandem vertical undulator is branched by the transparent diamond monochromator. The SAXS station uses the monochromatized undulator beam that enables us to obtain the data with high-spatial resolution and high flux as well. The structure of proteins in solution under various conditions will be studied in this station.

The protein crystallography station is newly designed to optimize for MAD (Multiwavelength Anomalous Diffraction) methods. Anomalous dispersion effects are so weak that the accuracy of multiwavelength data collection is the most important role for MAD-phasing. Therefore the simultaneous three-wavelengths data collections are planned using the same protein crystal and same setting. Diamond "Trichromator" that co-linearly introduces three wavelengths to the sample is under development based on the transparent fixed exit diamond monochromators. The most remarkable feature of this beamline concept is most effectively utilizing anomalous dispersion effects by neglecting the systematic errors of data collection.

TuD85

Progresses of Synchrotron Radiation Applications at the NSRL

Yunwu Zhang, Chaoshu Shi, Pengshou Xu, Xingshu Xie and Yiguan Hu

National Synchrotron Radiation Laboratory, University of Science and Technology of China
Hefei, Anhui 230026, P. R. China

The Hefei 800MeV electron storage ring was completed in the end of 1991. Then it was taken about one year for testing operation, beamline calibration and in-house use. It has been open to users all over the country since April 1 last year.

At present five beamlines and corresponding experimental stations are under operation. Synchrotron radiation research includes photoemission, fluorescence, photochemistry, soft x-ray microscopy and x-ray lithography. Up to now one hundred twenty proposals of users have been approved and about forty of them carried out. We report some results in this paper.

Photoemission spectroscopy Interface of $M_n/G_aA_5(100)$ was studied by SR photoemission spectroscopy. It is realized that the magnetic ordering exists in the ultra-thin overlayer of M_n . In addition, interfaces of $K/G_aA_5(100)$, $K/I_nP(100)$ and $K/Cd_{0.96}Zn_{0.04}Te$ were also studied.

Fluorescence spectroscopy The VUV reflection spectrum of C_{60} in the wavelength range from 50nm to 200nm was measured. It shows three shoulders without obvious reflection peaks, which means that the electrons in the empty states of conduction band are delocalized. The reflection spectra of different wBN samples prepared by shock-wave method and heat-treated at 100C and 500C in the wavelength range from 100nm to 240nm were measured and the optical constants of the wBN samples determined.

Photochemistry Photoionization studies of molecules such as C_2H_3Cl , NH_3 , N_2 , O_2 and clusters such as $(CH_3CN)_n(C_2H_3Cl)_m$, $(CH_3CN)_n(NH_3)_m$ were carried out under super-sonic molecular beam conditions. Photoionization potentials and dissociation energies were determined and autoionization of Rydberg states observed from the photoionization curves for some molecules and clusters.

Soft x-ray microscopy The contact imaging microscope has been built but the scanning one is being developed. Specimens studied include wings of flyings and mosquitoes, onion skin and cancer cells of esophagus etc. The resolution of the contact imaging microscope has reached 80 μ m.

X-ray lithography Basic studies of superfine structure fabrication and LIGA technology are emphasized. Surface sonic wave devices, optical elements and gearwheels with diameter of 35-300 μ m and height of 50 μ m were fabricated.

TuD86

Elliptical Motion Wiggler Beamline at The Advanced Photon Source

P. A. Montano^{1,2}, M. J. Bedzyk^{1,3}, M. Ramanathan¹, M. A. Beno¹, G. Jennings¹ and P. L. Cowan⁴, G. S. Knapp¹, E. Gluskin⁵, E. Trakhtenberg⁵, I.B. Vasserman⁵, P. M. Ivanov⁵, D. Frachon⁵, E. R. Moog⁵, L. R. Turner⁵, and G. K. Shenoy⁵

1. MSD, Argonne National Laboratory, Argonne IL 60439; 2. University of Illinois, Chicago; 3. Northwestern University, Evanston, IL 60208; 4. Physics Division, Argonne National Laboratory, Argonne IL 60439; 5. APS, Argonne National Laboratory, Argonne IL 60439.

Magnetic scattering experiments require a high photon flux and defined polarization. The APS is an ideal source of X-ray radiation for such studies. We present a description of the Elliptical Motion Wiggler (EMW)¹ beam line to be constructed at the APS. The beamline consists of three stations operating in tandem with only one station receiving x-rays at any one time. The three stations have three distinct functions; namely Compton Scattering, Magnetic Scattering, and Surface Scattering. The optics going from downstream to upstream will consist of a vertically focussing mirror, a steering mirror, a premonochromator, and an optional post monochromator in the front end of each station. The EMW period will be $\lambda_u=15$ cm, the number of Periods=16 and total length of 2.1 m. The hybrid magnetic structure produces the vertical magnetic field with $K=14$ and the electromagnet provides horizontal magnetic field with $K=1-2$. The frequency of the horizontal field change is up to 10 Hz. This device has been chosen for reasons of tunability and special polarization properties. The first mirror will be used to vertically focus (or collimate) the wiggler beam. It will also be used to reduce the power load on the downstream premonochromator. The mirror will have an upper energy cut off of 23 keV. Above 23 keV, the mirror will be lowered out of the beam and a filter will serve to reduce the heat load on the premonochromator. The meridional radius of the mirror will be adjustable and allow for vertical focusing of the beam at all three downstream stations. Collimation will be important for spectroscopy experiments where we want an energy resolution that is limited only by the Darwin width of the monochromator crystals and not by the angular divergence of the source. The second mirror will serve the purpose of steering the beam back to a horizontal direction. It will be identical in construction to the first. For high energy experiments both mirrors will be translated vertically out of the beam. The premonochromator, which is in a high vacuum chamber, will be a double crystal monochromator. The second crystal will have the option of sagittal focusing. Special considerations will be made to insure the proper control of the polarization when using circular polarized light. The first experimental station will be dedicated to magnetic and non-magnetic Compton scattering. The second station will be used for magnetic scattering and XAS. The end station will be used for surface science, XSW and magnetic scattering from thin films. The design of the elliptical multipole wiggler beam line will follow an approach very close to that developed by Kawata et al². Our objective is to obtain a high photon flux with energies above 40 keV and well characterized polarization.

1. S. Yamamoto, H. Kawata, H. Kitamura, M. Ando, PRL. 62 (1989) 2672.

2. H. Kawata, T. Miyahara, S. Yamamoto, T. Shioya, H. Kitamura, S. Sato, S. Asaoka, N. Kanaya, A. Lida, A. Mikuni, M. Sato, T. Iwazumi, Y. Katijima, M. Ando, Rev. Sci. Instr. 60 (1989) 1885.

Work at Argonne National Laboratory is supported by the US Department of Energy (DOE), Office of Basic Energy Sciences, Division of Material Sciences, under contract W-31-109-ENG-38.

A Systems Approach to Optimizing Synchrotron Beamline Performance

K. P. Pflibsen, A. J. Goetz, D. McClain
EODC, Kaman Aerospace Corporation, Tucson, Az

Current developments in synchrotron radiation sources and the fabrication of synchrotron radiation optics and beamline components make possible spectral and spatial resolutions, photon energies, and throughputs which have not been previously attainable. These advances necessitate a corresponding improvement in the overall performance of synchrotron beamlines. Such improvements can be most effectively achieved when the performance requirements are systematically flowed down to each of the beamline subsystems with careful attention paid to cost / performance tradeoffs.

In developing an optimal synchrotron beamline control approach the disturbances, monitoring methods and control architectures must be conscientiously balanced. The nature and sources of external and internal beam position disturbances and the requirements on the scientific quality synchrotron radiation influence the choice of beam position monitoring and control methods. Improvements in fabrication of synchrotron radiation optical components now make it possible to increase the requirements on optical design performance. These changes in requirements have spawned the development of synchrotron mirror figure sensing and control techniques so that the full potential of current generation optics can be achieved. The complexity and quality of third generation synchrotron radiation research facilities are causing changes in the information exchange which is required between the central facility control systems and the individual beamlines. We will discuss a number of the trade-offs associated with arriving at a functional integrated beamline. The relative significance of various approaches to achieving a desired level of performance will be provided and a rationale for selecting a given approach discussed.

X-ray Undulator Beamline and Experimental Station for The Feasibility Study at TRISTAN Main Ring

Hiroshi SUGIYAMA

Tristan Super Light Facility, Photon Factory, National Laboratory for High Energy Physics, Japan

A feasibility study will be carried out for SR experiments using the TRISTAN Main Ring (MR) as a super brilliant x-ray source ^{1), 2)} in the autumn of 1995. Here we describe a design of the test beamline BL-BW-TL that is to be constructed for the feasibility study. It will be installed in a north-west-side tunnel of the Tsukuba experimental hall of TRISTAN. In this beamline, super brilliant radiation from electrons which pass through the x-ray undulator, XU#MR0 is used.

Important characteristics of the beamline structure are described below.

a) We use beam ducts with 35 mm in diameter which are connected by ICF70 flanges since the beam size is very small.

b) In order to curtail a number of vacuum pumps, we find an optimum design of pumping-power distribution on the basis of a principle of differential pumping and obtain an optimum pressure distribution: 10^{-9} Torr at the most upstream point of the beamline and 10^{-7} Torr at the most downstream point.

c) We need to align the beamline with an accuracy less than ± 1 mm throughout it. For this purpose we can use the quadrupole magnets of the MR as targets for this alignment since the beamline is placed along the long straight section of the MR within about 2m.

d) In order to monitor the light beam position, graphite-wire beam position monitors (BPMs) are installed at three points. Development of this type of BPM is in progress in the BL-NE3 in TRISTAN Accumulation Ring.

e) A water-cooled shutter and a γ -ray shutter are placed at 17.5- and 19-m points from emission point, respectively. Only a single set of these shutters are used unlike usual cases at PF in which two sets are used for spares.

f) A fast closing valve (FCV) is installed between the water-cooled shutter and the γ -ray shutter. This is to protect the vacuum of the MR against accidental leak at the lower reaches of the beamline. To protect a valve plate of the FCV against the high heat load radiation from the XU#MR0, we have to put a thermal protective object which closes faster than the FCV, or we have to turn off the power of the RF cavity when the FCV is closed.

g) Whereas the MR itself is located at the third basement, a room which can be used for the SR experimental station is located at the fourth basement. The SR beam is led to the experimental station after it is kicked down 4.5 m by a double crystal monochromator. By using this room we can avoid a large-scale construction work such as construction of radiation shield.

h) The monochromator has a special structure to meet the above aim. The first crystal of the monochromator is set on third basement, and the second crystal is put on the experimental station on fourth basement.

i) The first crystal of the monochromator is cooled by liquid nitrogen in vacuum. The second crystal is put in helium gas isolated by beryllium windows.

References

- 1) The Tristan Super Light Facility, Conceptual Design Report 1992, KEK Progress Report No. 92-1 (1993).
- 2) "The Tristan Super Light Facility", Photon Factory Activity Report 1992 #10, S-1, (1993).

TuD89

A Simple In-hutch Mirror Assembly for X-ray Harmonic Suppression

Matthew J. Latimer,^{1,§} Annette Rompel,^{1,§} James H. Underwood,⁴ Vittal K. Yachandra,[§] and Melvin P. Klein[§]

Department of Chemistry,¹ Structural Biology Division,[§] Lawrence Berkeley Laboratory and Center for X-ray Optics,² Lawrence Berkeley Laboratory, University of California, Berkeley, CA 94720

Harmonic contamination of a monochromatized beam can result in serious distortions of the data in an X-ray absorption experiment. In experiments at the manganese K-edge (>6.5 KeV) we have encountered a particularly troubling case of harmonic contamination in samples containing considerable amounts of bromine. We observed a drop in Mn fluorescence midway through a Mn EXAFS (Extended X-ray absorption fine structure) scan due to absorption of the harmonic energy X-rays by Br (K-edge 13.47 KeV).

There are several ways to minimize harmonic content of the beam; Si $\langle 111 \rangle$ crystals will not pass this harmonic, but they possess an unacceptable glitch pattern for our experiments. We use Si $\langle 220 \rangle$ which also pass this harmonic. Monochromator detuning by rocking one crystal relative to the other results in reduction of harmonics due to the narrower rocking curve of the harmonic relative to the fundamental. However, we were unable to achieve sufficient harmonic rejection through detuning to 10% of the maximum flux and our extremely dilute Mn samples made further reductions in flux untenable. Finally, harmonics can be suppressed through the use of an X-ray mirror, but the beamline used, VII-3 at Stanford Synchrotron Radiation Laboratory, does not have a mirror.

To circumvent these problems we have designed and built a simple tabletop double mirror harmonic suppressor to be used in the X-ray hutch. Each mirror is a 285 x 25.4 mm strip of float glass coated with gold. The two mirrors are mounted in a face-to-face ("periscope") orientation spaced 1 mm apart and are further offset to allow a vertical entrance aperture of 2 mm at a glancing reflection angle of 0.4 degrees. This angle was chosen to achieve an optimum balance between second harmonic suppression and fundamental transmission through the use of the critical angle cutoff for gold. The double mirror design results in a vertical displacement of the beam, but the exit beam remains parallel to the entering beam. We have demonstrated that the mirror apparatus described here is much more effective than monochromator detuning, allowing much greater rejection of harmonics without a drastic reduction in flux of the fundamental. The harmonic suppressor can be used over a range of energies by rotating it to new angles and is generally useful for a variety of applications.

This work was supported by grants from the National Science Foundation (DMB91-04104) and by the Director, Division of Energy Biosciences, Office of Basic Energy Sciences, Department of Energy, under contract DE-AC03-76SF00098. Synchrotron radiation facilities and additional technical assistance were provided by the Stanford Synchrotron Radiation Laboratory which is supported by the U.S. Department of Energy.

TuD90

Design and construction of a general-purpose bending magnet beamline at the ESRF

by

P.K.Murray, S.J.Collins, H.Fmerich, J.Mardalen, P.Pattison and H.-P.Weber

Swiss-Norwegian Beamline at ESRF, BP. 220, F-38043 Grenoble, France.

Abstract

The Swiss-Norwegian Beamline (SNBL) is now being installed on a bending magnet source at the ESRF in Grenoble. The beamline will provide synchrotron radiation for scientists from Switzerland and Norway, as well as to public users of the ESRF. Experimental facilities include single crystal diffraction (inorganic, small molecule and protein crystallography), powder diffraction, EXAFS and white-beam topography. In order to accommodate this wide range of techniques, two experimental stations can operate independently. One station provides 1mrad of unfocussed white or monochromatic beam, while the other station receives focussed, monochromatic beam from a 2.5mrad horizontal fan of radiation. A general description of the beamline design and construction techniques is presented.

Thermo-Mechanical Analysis of the White Beam Slits for a Wiggler/Undulator Beamline at the Advanced Photon Source¹

H. L. Thomas Nian, I.C. Sheng, D. Shu, and Tuncer M. Kusay
Argonne National Laboratory, 9700 S. Cass Ave., Argonne, IL 60439

A set of horizontal and vertical white beam slits has been designed for a wiggler/undulator beamline at the Advanced Photon Source (APS). The design uses a grazing incidence knife edge to minimize the scattering, which induces a much higher temperature and thermal stress due to the "wedge heating" effect. The slits consist of a main tungsten block and an OFHC cooling channel (filled with copper mesh) inside the tungsten block. We analyzed many conceptual designs in order to

1. reduce the maximum temperature of the tungsten block to under 400°C (to avoid annealing),
2. reduce the maximum temperature of the OFHC to under 175°C (to avoid annealing),
3. reduce the maximum thermal distortion to 50 microns.

The final design is achieved by adding material to reduce the wedge effect and by moving the cooling channel closer to the heating surface. Enhanced heat transfer technology was used to increase the convective heat transfer coefficient from $1 \frac{W}{cm^2 \cdot ^\circ C}$ to about $2-3 \frac{W}{cm^2 \cdot ^\circ C}$ for a plain tube. The calculation shows that increasing the h (convective heat transfer coefficient) from $1 \frac{W}{cm^2 \cdot ^\circ C}$ to $2 \frac{W}{cm^2 \cdot ^\circ C}$ will

1. reduce the maximum thermal distortion from 60 microns to 45 microns,
2. reduce the maximum effective interface (between tungsten block and OFHC cooling tube) stress from 282 MPa to 178 MPa, which will make certain that OFHC cooling tube remain in elastic deformation during application,
3. reduce the maximum interface temperature from 150°C to about 110°C,
4. reduce the maximum temperature of tungsten from 420°C to about 380°C.

The submitted manuscript has been authored by a contractor of the U.S. Government under contract No. W-31-109-ENG-38. Accordingly, the U.S. Government retains a nonexclusive, royalty-free license to publish or reproduce the published form of this contribution, or allow others to do so, for U.S. Government purposes.

¹This work was supported by the U.S. Department of Energy, BES-Materials Science, under contract W-31-109-Eng-38.

Sources Posters

(Session TuE)

- TuE1 Anashin, V.V., Evstigneev, A.B., Lysenko, A.P., Malyshev, O.B., Osipov, V.N. The Set for Synchrotron Radiation Stimulated Desorption Study on Collider's Vacuum Chamber Prototypes.
- TuE2 Andersson, A., Eriksson, M., Lindgren, L.J., Rojssel, P., Werin, S. The New 1.5 GeV Storage Ring for Synchrotron Radiation: MAX-II.
- TuE3 Bandyopadhyay, P., Boyanov, B., Bunker, G., Mitrovic, V. Numerical Simulations of Flux Density Spectra of Tapered Undulators.
- TuE4 Biscardi, R., Ramirez, G., G.P. Williams. Effects of RF Side-Bands on Spectral Reproducibility for Infrared Synchrotron Radiation.
- TuE5 Cai, Z., Lai, B., Yun, W., Gluskin, E., Dejus, R., Ilinski, P. Phase-Space Measurement of Stored Electron Beam at Cornell Electron Storage Ring Using a Combination of Slit Array and CCD Detector.
- TuE6 Carr, R., Lidia, S., Kortright, J., Rice, M., Coffman, F. Performance of the Elliptically Polarizing Undulator on SPEAR.
- TuE7 Lidia, S., Carr, R. Faster Magnet Sorting with a Threshold Acceptance Algorithm.
- TuE8 Chavanne, J., Elleaume, P. Insertion Devices at the ESRF.
- TuE9 Chubar, O.V. Precise Computation of Electron Beam Radiation in Non-uniform Magnetic Fields as a Tool for the Beam Diagnostics.
- TuE10 Dejus, R.J., Vasserman, I., Moor, E.R., Gluskin, E. Phase errors and Predicted Spectral Performance of a Prototype Undulator.
- TuE11 Diviacco, B., Walker, R.P. Initial Operation of Insertion Devices in ELETTRA.
- TuE12 Fajardo, P., Ferrer, S. Beam Monitor for Undulator White Radiation in the Hard X-Ray Range.
- TuE13 Fajardo, P., Ferrer, S. UHV-Compatible Position and Shape Monitor for High Brilliance Synchrotron Radiation Beams.
- TuE14 Gluskin, E., Ivanov, P., Medvedko, E., Trakhtenberg, E., Turner, L., Vasserman, I., Gavrilov, N., Erg, G., Kulipanov, G., Petrov, S., Popik, V., Vinokurov, N., Friedman, A., Krinsky, S., Rakowsky, G. A Status of the Elliptical Multipole Wiggler Project.
- TuE15 Gottschalk, S.C., Robinson, K.E., Quimby, D.C. Gap Independent Passive End Field Optimization Methods for W wigglers and Undulators.
- TuE16 Heimann, P., Mossessian, D., Warwick, A., Gullikson, E., Wang, C., Marks, S., Padmore, H. Experimental Characterization of ALS Undulator Radiation.
- TuE17 Holldack, K., Peatman, W., Schroeter, Th. Vertical Photon Beam Position Measurement at Bending Magnets Using Lateral Diodes.
- TuE18 Katoh, M., Hori, Y., Nakamura, N., Kitamura, H., Kobayakawa, H. Upgrade of the Photon Factory Storage Ring for a High Brilliance Configuration.
- TuE19 Hoyer, E., Akre, J., Humphries, D., Marks, S., Minamihara, Y., Pipersky, P., Plate, D., Schlueter, R. Advanced Light Source Elliptical Wiggler.

- TuE20 Hoyer, E., Akre, J., Chin, J., Gath, W., Hassenzahl, W.V., Humphries, D., Kincaid, B., Marks, S., Pipersky, P., Plate, D., Portmann, G., Schlueter, R. Advanced Light Source - First Undulators.
- TuE21 Hoyer, E., Marks, S., Pipersky, P., Schlueter, R. Multiple Trim Magnets, or "Magic Fingers".
- TuE22 Humphries, D., Goetz, F., Kownacki, P., Marks, S., Schlueter, R. A Multiple Objective Magnet Sorting Algorithm for the Advanced Light Source Insertion Devices.
- TuE23 Ilinski, P., Yun, W., Lai, B., Gluskin, E., Cai, Z. Absolute Flux and Spatial Intensity Distribution Measurements of the CHESS Undulator.
- TuE24 Izawa, M., Koseki, T., Kamiya, Y., Toyomasu, T. Characteristics of SiC Microwave Absorber for Damped Cavity.
- TuE25 Kamada, S., Fukuma, H., Yoshioka, K., Nakajima, K., Ogata, A., Mitsunobu, T., Isawa, M., Nakamura, N., Sakanaka, S., Tobiyama, M., Ohmi, K., Kurokawa, S., Kanazawa, K., Kubo, T., Egawa, K., Mimashi, T., Kobayashi, M., Mizuno, H., Furuya, T., Mitsunobu, S., Ieiri, T., Tejima, M., Katsura, T. Accelerator Plan for the Light Source Study at the Tristan MR
- TuE26 Kudo, H., Nagatsuka, T., Shinoe, K., Takaki, H., Koseki, T., Nakamura, N., Kamiya, Y. Beam Position Control of SOR-RING.
- TuE27 Kimura, H., Miyahara, T., Goto, Y., Mayama, K., Yanagihara, M., Yamamoto, M. Polarization Measurement of SR From a Helical Undulator Using Quarter-Wave Plate for 12.7 nm Wavelength.
- TuE28 Kimura, H., Tanaka, T., Marechal, X., Kitamura, H. Helical Undulator Systems for Rapid Switching of Helicity.
- TuE29 Tanaka, T., Marechal, X., Kitamura, H. Vertical Undulators for SPring-8.
- TuE30 Koide, T., Shidara, T., Miyahara, T., Yuri, M. Polarization Characterization of Elliptically-Polarized VUV-Soft X-Ray Helical Undulator Radiation.
- TuE31 Erg, G., Korchuganov, V., Levichev, E., Philipchenko, A., Sajev, V., Ushakov, V. Multipole Wiggler Performance for the Siberia-2 SR Source.
- TuE32 Koseki, T., Izawa, M., Kamiya, Y. A Damped Structure Cavity for a High Brilliant VUV and SX Storage Ring.
- TuE33 Polewski, K., Kramer, S.L., Kolber, Z.S., Trunk, G., Monteleone, D.C., Sutherland, J.C. Time Resolved Fluorescence Using Synchrotron Radiation Excitation: A Powered Fourth-Harmonic Cavity Improves Pulse Stability.
- TuE34 White, D., Wood, O., Spector, S., MacDowell, A., LaFontaine, B. Modification of the Coherence of Undulator Radiation.
- TuE35 Marcelli, A., Nucara, A., Calvani, P., Sanchez del Rio, M. DAΦNE As a Source of Synchrotron Radiation: An Estimate of the Source Size and of the Brilliance in the Infrared Region.
- TuE36 Marechal, X.M., Tanaka, T., Kitamura, H. An Elliptical Wiggler for SPring-8.
- TuE37 Marks, S., McKinney, W., Padmore, H., Young, A. Optimization Design Study for an Elliptical Wiggler at the Advanced Light Source.
- TuE38 Melcher, M.E., Saffarnia, A. Performance of a Diagnostic Imaging Beamline at the Advanced Light Source.
- TuE39 Borovikov, V.M., Vobly, P.D., Mezentsev, N.A., Shkaruba, V.A., Sukhanov, S.V., Fedurin, M.G. Power Supply and Quench Protection System for Superconducting 7.5 Tesla Wiggler.

- TuE40 Kulipanov, G.N., Mezentsev, N.A., Wobly, P.D., Shkaruba, A., Ruvinsky, S.G., Sukhanov, S.V., Khlestov, B.V., Koo, Y.M., Kim, D.E., Sohn, Y.U. Superconducting 7.5 Tesla Wiggler for PLS.
- TuE41 Vasserman, I., Moog, E.G. A Passive Scheme for ID End Correction.
- TuE42 Pfluger, J., Heintze, G., Vasserman, I. Search for Possible Radiation Damage on a NdFeB Permanent Magnet Structure After Two Years of Operation.
- TuE43 Pinayev, I.V., Popik, V.M., Shaftan, T.V., Sokolov, A.S., Vinokurov, N.A., Vorobyov, P.V. Experiments with Undulator Radiation of a Single Electron.
- TuE44 Quimby, D.C., Jander, D.R., Robinson, K.E. Control System for a 1.8 Tesla Wiggler.
- TuE45 Robinson, K.E., Gottschalk, S.C., Jander, D.R., Quimby, D.C., Valla, A.S. Development of a 1.8 Tesla Permanent Magnet Wiggler System.
- TuE46 Sasaki, S., Hashimoto, S. A Concept of Quasi-Periodic Undulator.
- TuE47 Schildkamp, W., Pradervand, C. Position Monitor and Read-Out Electronics for Undulator and Focused Bending Magnet Beamlines.
- TuE48 Sugiyama, S., Ohgaki, H., Mikado, T., Yamazaki, T., Isojima, S., Usami, H., Suzawa, C., Masuda, T., Hosoda, Y. Design and Manufacture of a 10 T Superconducting Wiggler Magnet for the TERAS.
- TuE49 Suzuki, H., Yonehara, H., Aoki, T., Tani, N., Kaneda, T., Ueyama, Y., Sasaki, Y., Nagafuchi, T., Hayashi, S., Yokomizo, H. Status of the Booster Synchrotron for Spring-8.
- TuE50 Nakanishi, T., Ikegami, K., Kodera, I., Maruyama, A., Matsuda, T., Nakagawa, T., Nakamura, S., Nakata, S., Oishi, N., Okuda, S., Takeuchi, T., Tanaka, H., Tsukishima, C., Yamada, T. Construction and Beam Experiment of a Compact Storage Ring at MELCO.
- TuE51 Tanaka, H., Nakanishi, T. Studies of Beam Dynamics of a Compact Storage Ring Using Superconducting Bending Magnets.
- TuE52 Tarazona, E., Elleaume, P. Emittance Measurement at the ESRF.
- TuE53 Hartman, Ya., Tarazona, E., Elleaume, P., Snigireva, I., Snigirev, A. Emittance Monitors Based on Bragg-Fresnel Lenses.
- TuE54 Toyofuku, F., Tokumori, K., Nishimura, K., Saito, T., Endo, M., Takeda, T., Itai, Y., Hyodo, K., Ando, M., Naito, H., Uyama, C. Development of a Fluorescent X-Ray Source for Medical Imaging.
- TuE55 van Dorssen, G.E., Padmore, H.A. The Optimisation of Multipole Wigglers as Sources of Polarised Radiation for X-Ray Experiments.
- TuE56 Warwick, T. Performance of Photon Position Monitors for Undulator Beams at the Advanced Light Source.
- TuE57 Winick, H. The LCLS - A 4th Generation Light Source Using the SLAC Linac.
- TuE58 Zhang, X., Hiroshi, S., Masami, A., Xia, S., Hideaki, S. A Wire Scanning SR Position Monitor for Insertion Devices.
- TuE59 Yagi, K., Computer Simulation Study of Undulator Radiation.
- TuE60 Yamamoto, S., Shioya, T., Tsuchiya, K., Kitamura, H. A Super-Brilliant X-Ray Undulator for the Tristan Super Light Facility.

- TuE61 Baryakhtar, V., Bulyak, B., Gevchuk, A., Gladkikh, P., Karnaukhov, I., Kononenko, S., Molodkin, V., Mytsykov, A., Nemoshkalenko, V., Shcherbakov, A., Shpak, A., Zelinsky, A. Design of the ISI 800 for the Ukrainian National Synchrotron Center
- TuE62 Karnaukhov, I., Kononenko, S., Molodkin, V., Nemoshkalenko, V., Shcherbakov, A., Shpak, A., Tarasenko, A. A Combined Magnet Lattice of the Synchrotron Light Source.

The set for synchrotron radiation stimulated desorption study on collider's vacuum chamber prototypes

V.V.Anashin, A.B.Evstigneev, A.P.Lysenko, O.B.Malyshev and V.N.Osipov
Budker Institute of Nuclear Physics,
Novosibirsk, Russia
I.L.Maslennikov and V.Turner
Superconducting Super Collider Laboratory *
Dallas, USA

At design of new accelerator it's very important to know a pressure dynamic inside beamline chamber. One of more preferable way is to test the beamline chamber prototypes irradiating by synchrotron radiation. For this aim on area of Budker Institute of Nuclear Physics (Novosibirsk, Russia) at collaboration with Superconducting Super Collider Laboratory (Dallas, USA), there were designed, mounted and installed two (high and low intensity) special sets to study photodesorption on beamline prototypes chamber with use VEEP-2M collider as synchrotron radiation source. There is possible to make measurements at different temperatures in range of 2 to 300 K. New sets are automatized and apply to control and operate with IBM PC use.

* The SSCL is operated by URA for the U.S. DOE Contract No. DE-AC02-89ER40486.

TuE1

The new 1.5 GeV storage ring for synchrotron radiation: MAX-II

Å. Andersson, M. Eriksson, L.-J. Lindgren, P. Rösjel and S. Werin

MAX-lab
Lund University
P.O. Box 118
S-221 00 Lund, Sweden

The MAX-laboratory at the Lund University, Sweden, operates today an accelerator system consisting of a 100 MeV racetrack microtron and a 550 MeV storage ring (MAX I). At the moment (April 1994) a new storage ring, MAX II, is near completion and will start first injections within 5 months.

This work gives an overview of the MAX II project with descriptions of both the accelerator system and the first beamlines.

MAX II is 1.5 GeV third generation light source optimised for the VUV and soft X-ray region. It consists of a 10 cell Double Bend Achromat lattice forming the 90 m circumference ring. Injection is done at 500 MeV from the existing storage ring MAX I, and ramping up to full energy will take place in MAX II. The straight sections have a length of 3.2 m and 8 sections are free to house insertion devices. At start up the ring will be equipped with one 7.5 T Super conducting wiggler and one 1.8 T Multipole wiggler. Two more undulators are ordered and under construction.

To be able to achieve the project a few shortcuts have been made in the design of the storage ring:

- Non zero dispersion is allowed in the straight sections.
- Chromaticity correction is built into the quadrupole magnets.
- Limiting the length of the straight sections to 3.2 m.

The project is progressing on time.

Extraction of an electron beam from the MAX I storage ring has been achieved and it has successfully been transported into the MAX II building. The MAX II ring is under assembly with most of the sections already mounted. First injection is planned to take place in August 1994

TuE2

Numerical Simulations of Flux Density Spectra
of Tapered Undulators

Pathikrit Bandyopadhyay, Boyan I. Boyanov, Grant B. Bunkor, Vesna F. Mitrovic
Illinois Institute of Technology, Chicago IL 60616

Calculations of the angular photon flux density distribution from tapered undulators were performed as a function of energy. Modulations in the on-axis brightness spectra vs. energy are correlated with modulations in the angular pattern of emitted photons. When the angular acceptance of the monochromator crystals is included, the alterations in the angular pattern arising from tapering may result in larger transmitted flux modulations than are apparent from on-axis brilliance or brightness spectra alone.

TuE3

Effects of RF Side-Bands on Spectral Reproducibility
for Infrared Synchrotron Radiation.

R. Biscardi, G. Ramirez and G.P. Williams
National Synchrotron Light Source
Brookhaven National Laboratory
Upton, NY 11973 USA

C. Zimba
Polaroid Corporation
750 Main St.
Cambridge, MA 02139 USA.

We have investigated the effects of audio side-bands from the main RF of the NSLS VUV storage ring on beam motion and specifically on spectral reproducibility in the infra-red region. For this spectral region it is advantageous to use Michelson interferometers because of their high throughput (Jacquinot advantage). A second advantage is that interferometers inherently give a multiplex or Fellgett advantage, since one is always looking at all the wavelengths for all of the measuring time, even though there is only one detector. In such instruments it is beneficial to scan the moving mirror at a fast rate so that any mechanical or other low frequency noise shows up as a slow modulation in the interferogram and disappears altogether in the Fourier transform from the spectral region of interest. In practice mirror scanning velocities are typically of the order of 5mm/sec, giving an optical retardation of 1cm/sec. This has the effect of considerably reducing noise in the data and improving reproducibility. It means that, for example a frequency of 2000 cm^{-1} or 5 microns wavelength, will be modulated and appear at the detector at a frequency of 2000 Hz in the audio range. In principle this should be well clear of any frequencies associated with beam motion in the storage ring. Due to the fact that the beam is circulating in a metal vacuum chamber, it is not possible to drive it at frequencies much above 100 Hz as higher frequency magnetic fields cannot penetrate the walls. However, audio frequency side-bands appear on the RF energy restoring cavity. These always occur at multiples of 60 Hz and can thus be readily identified. They can also be confirmed by changing the mirror velocity which changes where they appear in the spectra in a predictable way. In the present work, we measured spectra while simultaneously reducing and shifting the side bands in the RF and thus were able to correlate the effects and ultimately eliminate them as a source of noise. Ultimately we were able to achieve reproducibilities of <1% in 15 seconds of scanning time across the entire spectral region from 800 cm^{-1} to 4000 cm^{-1} with a sample throughput of only 10^{-10} meter² steradians.

TuE4

Phase-Space Measurement Of Stored Electron Beam At Cornell
Electron Storage Ring Using A Combination
Of Slit Array And CCD Detector

Z. Cai, B. Lai, W. Yun, E. Gluskin, R. Dejus and P. Ilinski

Advanced Photon Source, Argonne National Laboratory

Abstract

A new technique for fast phase-space measurement has been developed and tested during recent APS/CHESS undulator run. A measurement time of several seconds was obtained by using a slit array and a high resolution optical imaging system with a CdWO₄ scintillation crystal that replace two scanning slits in the conventional scanning/scanning two-slit method. Thus, contaminations due to instabilities of the electron beam can be avoided mostly. The vertical emittance at the Cornell Electron Storage Ring in single bunch and low current mode was measured and reasonable results for both source size and source divergence were obtained ($\sigma_y=75 \mu\text{m}$ and $\sigma_y=12.3 \mu\text{rad}$). It was also found that the effects due to finite size of and diffraction from the first slit are not negligible, and they have to be taken into account in data analysis.

This research was supported by the U.S. Department of Energy, BES Materials Sciences, under contract #W-31-109-ENG-38.

The submitted manuscript has been authorized by a contractor of the U.S. Government under contract No. W-31-109-ENG-38. Accordingly, the U.S. Government retains a nonexclusive, royalty free license to publish or reproduce the published form of this contribution, or allow others to do so, for U.S. Government purposes.

TuE5

Performance of the Elliptically Polarizing
Undulator on SPEAR

R. Carr¹, S. Lidia², J. Kortright³, M. Rice³, F. Coffman¹

1) Stanford Synchrotron Radiation Laboratory, Stanford CA 94309

2) Physics Department, University of California, Davis CA 95616

3) Center for X-Ray Optics, Lawrence Berkeley Laboratory, Berkeley, CA 94720

In the last year we have designed and built an Elliptically Polarizing Undulator (EPU) on the SPEAR storage ring at SSRL. [1] The undulator has four rows of magnets parallel to the axis of the electron beam; two rows in a plane above the beam, and two below. Each row generates a sinusoidal magnetic field on-axis, and each may be moved longitudinally, parallel to the axis. These 'phase' motions allow us to create horizontal and vertical plane magnetic fields, as well as left and right helical fields. Electrons passing through these fields generate vertically and horizontally plane polarized x-rays and left and right circularly polarized x-rays, respectively. Our design also allows us to vary the energy of the x-rays with phase motions, in addition to variation of the polarization. The EPU has 26 periods, each 6.5 cm long, of pure NdFeB magnets.

The fundamental x-ray energy of the of the EPU's circularly polarized light is variable from 550-950 eV, corresponding to the L-edges of the first row transition elements. Certain magnetic multilayers and biological molecules containing these elements exhibit magnetic circular dichroism, and the EPU will be useful to study their properties.

The first tests of the EPU were done to characterize its effect on the electron beam in SPEAR. Even at minimum gap (30 mm), variation of the phase of the EPU caused negligible changes in the tune or the steering of the electron beam, even with no compensation of the trim coils. This is an advantage of an adjustable phase device over an adjustable gap device. We can change the phases of the EPU at will, with no disturbance to other users at SPEAR.

The second tests of the EPU were of the polarization of the x-rays. We designed a polarimeter based on a 75 layer, 1.243 nm d-spacing B4C/W multilayer we grew at LBL. This multilayer's σ reflectivity was about 10^{-2} , while its π reflectivity was 10^{-6} . It could be rotated azimuthally while mounted at the 45° Brewster angle, for peak reflectivity at 700 eV. Using a silicon detector, we observed vertically and horizontally plane polarized x-rays from the EPU, and right and left circularly polarized x-rays. We can achieve almost 100% polarization in each of these modes.

This research was performed at SSRL which is operated by the Department of Energy, Office of Basic Energy Sciences. J.K and M.R. acknowledge the support of the Director, Office of Energy Research, Materials Sciences Division or the U.S. Department of Energy under contract number DEAC-76SF00098.

- [1] R. Carr and S. Lidia, Proceedings of the 1993 SPIE Conference on Electron Beam Sources of High Brightness Radiation #2013.

TuE6

Faster Magnet Sorting with a Threshold Acceptance Algorithm

Steve Lidia
Physics Department, University of California, Davis, CA 95616

Roger Carr
Stanford Synchrotron Radiation Laboratory, Stanford, CA 94309

We introduce here a new technique for minimizing the magnetic field errors in permanent magnet insertion devices. Simulated annealing has been used in this role, but we find the technique of threshold acceptance produces results of equal quality in much less computer time. Threshold annealing would be of special value in designing very long insertion devices, such as long FEL's.

Simulated annealing is the Monte Carlo technique of sorting that employs the Metropolis algorithm to explore a cost function space and find minimum values. In addition, the technique employs a synthetic temperature to control the range of exploration; when the temperature is lowered, the cost function converges.

Threshold acceptance is a similar Monte Carlo technique that retains the role of temperature, but uses an algorithm simpler than Metropolis's. In simulated annealing, changes in the sort are retained if they result in a lower cost function, or if they meet a Boltzman function random acceptance criterion. In threshold accepting, sort changes are retained if they are merely below a positive but decreasing threshold. Threshold accepting allows more active exploration of the configuration space, and converges faster to the global minimum.

Our application of threshold accepting to magnet sorting showed that it converged to equivalently low values of the cost function, but that it converged significantly more quickly. We present typical cases showing time to convergence for various error tolerances, magnet numbers, and temperature schedules.

This research was performed at SSRL which is operated by the Department of Energy, Office of Basic Energy Sciences.

J. Chavanne, P. Elleaume
ESRF, BP 220, 38043 Grenoble Cedex France

Two years after the first beam in the storage ring, fourteen undulators and wigglers are presently in operation at ESRF. Brilliance as high as $2 \cdot 10^{18}$ Ph/sec/.1%/mm²/mr² is routinely achieved around 1 Angstrom. The method of production of Insertion Devices (IDs) and of field measurement will be described. Emphasis is placed on a special shimming technique which allow a complete removal of all normal and skew multipoles as well as ensuring maximum Brilliance on the high harmonic of the spectrum. To satisfy the demand for circularly polarised radiation 4 exotic IDs have been produced. Two helical undulators have been built covering the range from 0.5 to 10 keV. Two asymmetric wigglers have been built with peak field of 1.0 and 1.8 T covering the range between 20 and 200 keV. An undulator with variable gap chamber is being manufactured which is intended to operate at a 7 mm gap allowing a brilliance increase of a factor 5 around 50 keV.

Precise Computation of Electron Beam Radiation in
Non-uniform Magnetic Fields as a Tool for the Beam Diagnostics

O.V.Chubar
RRC KURCHATOV INSTITUTE, Moscow

Visual range radiation emitted by ultrarelativistic electron beam at bending magnet edges and within elements of the beam optics (steering magnets, quadrupole lenses, etc.) in modern storage rings is very sensitive to horizontal and vertical angular divergences, transversal sizes, emittances, energy, position and trajectory tilts of the electron beam. Precise computation of the radiation intensity distributions with due regard for non-zero beam emittances, layout of storage ring magnet structure and peculiarities of a measurement scheme allows to obtain the electron beam parameters from measured intensity distributions of the radiation.

To realize the beam diagnostics, an effective method for calculation of the radiation intensity distributions was elaborated. In contrast to traditional methods incorporating non-zero beam emittances, the method does not use integral convolution technique and may be used even when this technique is not applicable (as it takes place in the case of radiation from quadrupole lenses).

In the report to be presented, the computation technique, as well as the software and the experimental equipment for the beam diagnostics on the Siberia-1 electron storage ring will be described. Experimental results on measurements of the radiation intensity distributions on the Siberia-1 ring and the correspondent electron beam parameters determined by the method under discussion, will be presented. The parameters obtained agree well with theoretical estimations and data from different Siberia-1 diagnostic systems.

The figures below illustrate the processing of experimental data on the radiation intensity distribution in order to determine beam divergences.

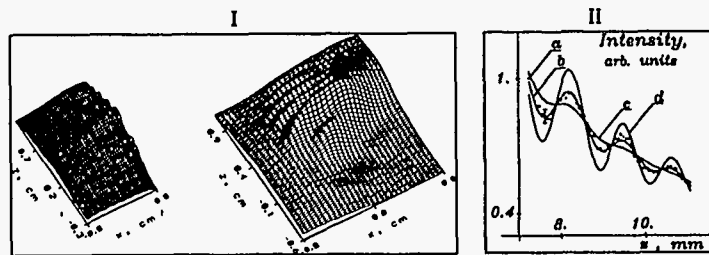


Figure captions

I- Intensity distribution of radiation emitted at bending magnet edges and within a steering magnet of Siberia-1: experiment (left) and computation best-fit (right).

II- Fitting over effective vertical angular divergence $\sigma'_{z,eff} = [\sigma_z'^2 + (\sigma_z/r)^2]^{1/2}$:

a- experimental points; b- best-fit curve: $\sigma'_{z,eff} = (\sigma'_{z,eff})_{fit} = 0.12 \text{ mrad}$;

c- $\sigma'_{z,eff} = 1.4 (\sigma'_{z,eff})_{fit}$; d- $\sigma'_{z,eff} = 0.6 (\sigma'_{z,eff})_{fit}$.

TuE9

Phase errors and predicted spectral performance
of a prototype undulator

Roger J. Dejus, Isaac Vasserman, Elizabeth R. Moog, and Efim Gluskin
Advanced Photon Source
Argonne National Laboratory
9700 S. Cass Ave
Argonne, IL 60439

A prototype undulator (3.3 cm-period permanent magnet hybrid device) has been used to study different magnetic end-configurations and shimming techniques for straightening the beam trajectory. Field distributions obtained by Hall probe measurements were analyzed in terms of trajectory, phase errors, and on-axis brightness over a large energy range for the purpose of correlating predicted spectral intensity with the calculated phase errors.

Two device configurations (shimmed and unshimmed) were analyzed. The unshimmed device had a full-strength first magnet at each end and the next-to-last pole was recessed to make the trajectory through the middle of the undulator parallel to the undulator axis. For the shimmed device, shims were added to straighten the trajectory. For this configuration the first permanent magnet at each end was replaced by a half-strength magnet to reduce the trajectory displacement and the next-to-last pole was adjusted appropriately.

Random magnetic field errors can cause trajectory deviations which will affect the optimum angle for viewing the emitted radiation and care must be taken to select the appropriate angle when calculating the phase errors. This angle may be calculated from the average trajectory angle evaluated at the location of the poles.

For the shimmed device, we find a phase error of 3° and 95% of the ideal value of on-axis brightness for the third harmonic (nominal gap is 11.5 mm and derived effective K is 2.26). In contrast, for the unshimmed device the third harmonic intensity is 68% of the ideal. The predicted reduction of intensity for the shimmed device is in good agreement with the simple model proposed by Walker.¹ For the shimmed device we have also analyzed the gap dependence of the phase errors and spectral brightness and have found that the phase errors remain small at all gap settings.

¹ R.P. Walker, Nucl. Instr. and Meth. A 335 (1993) 328.

The submitted manuscript has been authored by a contractor of the U.S. Government under contract No. W-31-109-ENG-38. Accordingly, the U.S. Government retains a nonexclusive, royalty-free license to publish or reproduce the published form of this contribution, or allow others to do so, for U.S. Government purposes.

* This work was supported by the U.S. Department of Energy, BES-Materials Sciences, under contract No. W-31-109-ENG-38.

TuE10

Initial Operation of Insertion Devices in ELETTRA

B. Diviacco and R.P. Walker
Sincrotrone Trieste, Padriciano 99, 34012 Trieste, Italy

The 1.5-2 GeV ELETTRA synchrotron radiation source has recently come into operation. Three insertion devices (IDs) are currently in operation including two pure-permanent magnet undulators and a hybrid multipole wiggler. All three devices have a nominal length of 4.5 m and are composed of 3 individually controllable sub-sections. A narrow gap vacuum chamber permits a nominal minimum gap of 25 mm in each case.

In this report we give details of the initial operation of each of the above devices, in particular the measured effects on the electron beam, and first spectral data. Comparisons are made with expectations based on the measured field distributions in both cases. Some details are also included about operational aspects such as the performance of the ID control system, use of correction elements, vacuum chamber protection interlock system and ID vacuum chamber performance.

Beam monitor for undulator white radiation in the hard x-ray range

P. Fajardo, S. Ferrer
ESRF, B.P. 220 38043 Grenoble Cedex, France

An instrument for white x-ray beam monitoring that is suitable for the undulator beams at ESRF is presented in this paper. It is based on a 500 μm thick beryllium single crystal that is interposed in the beam path. Most of the beam passes through the crystal due to its low absorption and a small part is diffracted. The image of a Bragg reflection is recorded by a x-ray camera at a such geometry that the image obtained reproduces the cross-section of the main beam and it is possible to obtain information about its shape and position. In order to monitor position changes or drifts, the image is digitalised and the center of gravity of the intensity distribution is calculated periodically. If the position is determined from only one video frame, the resolution is about 5 μm . This value is strongly limited by the internal noise of the camera and can be reduced to 1 μm or less by simple frame averaging. The mosaic spread and the defects of the beryllium crystal degrade the fidelity of the beam images but does not affect the resolution of the instrument as position monitor. Tests were performed at two different ESRF undulator beamlines with power densities of the order of 20 W/mm^2 and the heating effects were negligible. The major limitation comes from the unavailability of large enough Be crystals of good quality. In our prototype the small crystal size forced us to reduce the active area of the instrument to a 10 mm circular region.

**UHV-compatible position and shape monitor for high
brilliance synchrotron radiation beams**

P. Fajardo, S. Ferrer
ESRF, B.P. 220 38043 Grenoble Cedex, France

Most of the beam position monitors that are been currently used at synchrotron radiation beamlines are either not vacuum compatible or they intercept completely a part of the photon beam. An instrument conceived to monitor small beams in UHV environment is presented here along with the results of the first prototype. The instrument, initially conceived to monitor the position of monochromatic beams, has shown to be useful for white radiation too. In addition it provides information about the shape of the beam. The monitor measures the integrated profiles of the beam spatial distribution by scanning two perpendicular thin metallic wires across the detection area. The photoemission current is amplified and recorded as a function of the position of the wires by a data acquisition system. A computer calculates the beam position and displays the beam profiles. In this instrument the absolute accuracy and the resolution are of the same order of magnitude and depend on the scanning speed and the beam size. The prototype has been tested with undulator beams at ESRF and the measured resolutions ranged from 5 to 50 μm depending on the particular working conditions. Beryllium and tungsten wire of 50 and 100 μm diameter have been used for white and monochromatic beams respectively and typical peak current values are 50 nA and 400 pA. The minimum scan time is one second and therefore this instrument is not suitable for fast position corrections. On the other hand it is inherently free of electronics drift and it is well suited to monitor the beam during long unattended experiments.

TuE13

A STATUS OF THE ELLIPTICAL MULTIPOLE WIGGLER PROJECT

E. Gluskin, P. Ivanov, E. Medvedko, E. Trakhtenberg, L. Turner and I. Vasserman*
APS, Argonne National Laboratory, Argonne, IL 60439

N. Gavrilov, G. Erg, G. Kulipanov, S. Petrov, V. Popik, N. Vinokurov
Budker INP, Novosibirsk, Russia

A. Friedman, S. Krinsky, G. Rakowsky**
NSLS, Brookhaven National Laboratory, Upton, NY 11973

The Elliptical Multipole Wiggler (EMW) for the NSLS Xray ring is currently under construction. The EMW will be a source of the variable circular polarized x-rays at the X-13 beamline in the energy range from 1 up to 10 keV. The EMW vertical magnetic field is produced by the 5 periods of the hybrid magnetic structure and the horizontal one by the electromagnet. The device period length is 16 cm. With the peak field values of 8 kGs for the vertical and 1 kGs for the horizontal magnetic field the vertical and horizontal K- values of 10 and 1.5 respectively will be achieved.

The EMW electromagnet poles are fabricated from the laminated iron in order to operate with the switching frequency up to 100 Hz, but the current power supply switching frequency is limited by 10 Hz.

The EMW has an internal ends compensation system in order to control a first and second field integrals with the required accuracy.

It is planned to fabricate and complete the magnetic measurements of the device in the Fall of 1994 and install it at NSLS Xray ring by the end of 1994.

* This project was supported by the U.S. Department of Energy, BES Materials Science, under contract #W-31-109-ENG-38.

**Work performed under the auspices of the U.S. Department of Energy, under contract DE-AC02-76CH00016

TuE14

GAP INDEPENDENT PASSIVE END FIELD OPTIMIZATION METHODS
FOR WIGGLERS AND UNDULATORS

S.C. Gottschalk, K.E. Robinson, and D.C. Quimby
STI Optronics, Inc., Bellevue, Washington, USA

Wigglers and undulators require careful termination of the end fields in order to meet several requirements. Trajectories should remain as flat as possible, phase and multipole errors should be controlled and the extent of the good field region should be as large as possible. All of these requirements will need to be met over the gap operation range of the device. Ideally it is desirable to achieve all these goals by entirely passive means without the use of electromagnets or mechanical magnet adjustments as the gap is varied. We have used finite element analysis of wiggler/undulator end fields to determine an optimum passive end field configuration for devices with and without terminating field clamps. The presence or absence of field clamps significantly modifies the analysis results. The technique involves adjustments of the strengths of the first two magnets and if necessary, the heights of the first two poles. We have confirmed the analysis experimentally and demonstrated an essentially ideal wiggler entrance field over a gap to wavelength range of 0.22 to 0.60 on our test device, HUMMER, which does not include field clamps. We have excellent agreement between analysis and experimental data on the SRRC - 1.8 T wiggler, which is equipped with a field clamp, operating at a gap to wavelength ratio of 0.11. We will present additional experimental results covering a gap to wavelength range of 0.11 to 1.2.

TuE15

Experimental Characterization of ALS Undulator Radiation.

P.Heimann[†], D.Mossessian[†], A. Warwick[†], E.Gullikson^{*}, C.Wang[†], S.Marks^{**},
and H.Padmore[†].

[†]Advanced Light Source, Accelerator and Fusion Research Division

^{*}Center for X-Ray Optics, Materials Sciences Division

^{**}Engineering Division

Lawrence Berkeley Laboratory, Berkeley, CA 94720

The radiation from the 5 cm period undulator at the Advanced Light Source (ALS) has been characterized using a transmission grating spectrometer. Spectral and angular distributions were measured for deflection parameter K values between 0.45 and 2.12 at low storage ring current (0.1 - 0.5 mA). From the calibration of the spectrometer, the absolute flux density of the undulator harmonics has been determined together with the spectral linewidth. Comparison has been made with radiation calculations based upon the measured magnetic field data of the undulator.

The fifth harmonic peak intensity and linewidth has been used as a test standard for undulator performance. The linewidth of the fifth harmonic, $\Delta\lambda/\lambda$, was 1/213 for K=2.12, which is larger than the width in a single electron approximation, 1/445. However, the radiation calculations, which include magnetic field errors together with the emittance and energy spread of the electron beam, quantitatively reproduce the measured 5th harmonic.

The taper of the undulator was varied in small steps, and the effect on the undulator harmonics was observed. At a taper of 100 μm the fifth harmonic was significantly suppressed and broadened. On the other hand, this taper resulted in only small changes in the fundamental.

Two dimensional angular distributions were measured showing the central cone and the red-shifted radiation off axis. Near field effects were examined by analyzing the widening of the harmonics in the off-axis spectrum. The angular distribution of the red-shifted fundamental was used to determine the electron beam emittance. At low current the measured ALS emittance was $\epsilon_x \sim 5 \cdot 10^{-9}$ m-rad, $\epsilon_y < 2 \cdot 10^{-10}$ m-rad in agreement with the theoretical value and less than 5% horizontal-vertical coupling.

The direct radiation from an undulator has been measured at the ALS, a third generation storage ring. Including field errors, electron beam emittance and energy spread, good agreement is found between theoretically and experimentally determined harmonic widths and peak brightness.

TuE16

Vertical Photon Beam Position Measurement at Bending Magnets using Lateral Diodes

K.Hollack, W.Peatman, Th.Schroeter
 BESSY GmbH Berlin, Lentzeallee 100
 14195 Berlin, Germany

Commercial position sensitive diodes (PSD) which were designed for measurements with visible light have been used to measure beam position in a white light beamline exposing them to the hard X-ray part of the dipole spectrum. In preliminary studies the spectral response of the lateral diodes in the VUV and XUV range from 100 eV up to 2keV was tested at the plane grating monochromator HE-PGM 2 at BESSY. It was found that the quantum efficiency of the lateral diodes is comparable to dedicated Si XUV diodes. At 1.4 keV a quantum efficiency of about 100 electrons per photon was measured in the central position. No long-term drifts of the efficiency have been observed. The position sensitivity of the diodes is almost independent of photon energy.

Hence, in a white light beam a photon energy window was defined simply by a water cooled Al-absorber foil of 200 μm thickness. Behind the foil two lateral diodes were arranged at 3.5 m (15 mm length) and at 7m (30mm length) behind the source. The horizontal position of the diodes was staggered so that the first diode does not occlude the beam to the second one. Using the given absorber thickness which has to be chosen to prevent thermal distortion of the absorber, photocurrents of ca. 100 nA for 100 mA ring current were detected at the diodes. The position response of the diodes was calibrated by scanning them vertically through the beam using a stepping motor-controlled y-stage. After calibration the centre of the diodes was set to the actual vertical beam centre and position changes relative to this level can be read out every millisecond.

With this system, the source position in a dipole can be detected with 10 μm accuracy while the change in deflection angle can be detected down to values of 1.5 μrad .

TuE17

UPGRADE OF THE PHOTON FACTORY STORAGE RING FOR A HIGH BRILLIANCE CONFIGURATION

M. Katoh, Y. Iiori, N. Nakamura, H. Kitamura and H. Kobayakawa

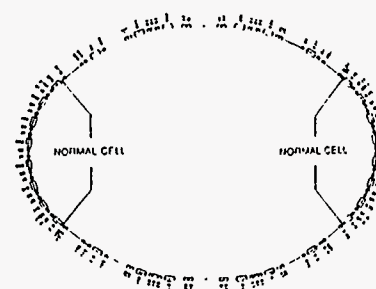
Photon Factory, National Laboratory for High Energy Physics
 1-1 Oho, Tsukuba, Ibaraki, 305 Japan

The 2.5-GeV Photon Factory storage ring has been steadily improved by decade-long research and development. Its performance, in particular the stored current, beam lifetime and beam stability has been achieved to the world highest level. A high brilliance configuration was designed and proposed as one of our recent activities. In the new configuration, the focusing magnets of the normal cells will be doubled. All the light-source points of the existing beamlines will not be changed, because all the bending magnets will be kept at their present locations. The beam emittance will be reduced to 27 nm-rad which is one fifth of the present value (130 nm-rad). The brilliance will be increased typically by a factor of ten.

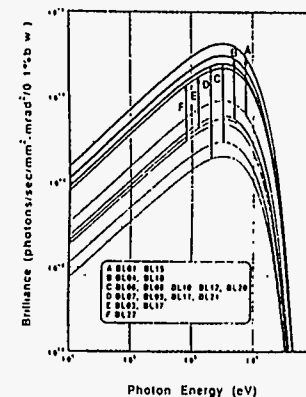
For this upgrade, improvements of vacuum chambers and front-ends of the beamlines are necessary on the normal cell sections. Also the injection scheme needs to be modified. All improvements are being designed and planned carefully to be achieved (1)with minimum influence to the existing beamlines, (2)in the shortest shutdown time and (3)by low cost.

The beam lifetime and the beam stability are discussed from a standpoint of the total effective brilliance. More than 40 hours of the beam lifetime is expected, and the light beam of each beamline will be stabilized by reinforcing the beam monitors and the orbit feedback system.

Details of the upgrade is described in this paper.



Designed arrangement of magnets for the upgrade of the PF ring.



Change of the brilliance at each bending magnet

TuE18

Advanced Light Source Elliptical Wiggler•

E. Hoyer, J. Akre, D. Humphries, S. Marks, Y. Minamihara, P. Pipersky, D. Plate, R. Schlueter

Advanced Light Source, Lawrence Berkeley Laboratory, University of California, Berkeley, Ca 94720

Abstract

A 3.5 m long elliptical wiggler, optimized to produce elliptically polarized light in the 50 eV to 10 keV range, is currently under design at the Advanced Light Source (ALS) at Lawrence Berkeley Laboratory (LBL). Spectral calculations show that the device will produce a polarization figure of merit, defined as flux times polarization squared, of greater than 10^{14} photons/sec/0.1%BW at photon energies up to 5 keV and greater than 10^{13} photons/sec/0.1%BW for photon energies between 5 and 10 keV, for a 5 mrad horizontal aperture with the ALS operating at 1.5 GeV and 400 mA.

This device features vertical and horizontal magnetic structures with 14 periods each. The period length is 20.0 cm. The vertical structure is a hybrid permanent magnet design with tapered poles and a peak field of 2.0 T. The horizontal structure is an electromagnetic design that is tucked between the upper and lower vertical magnetic structure sections. A maximum peak oscillating field of 0.10 T at a frequency up to 1 Hz will be achieved by excitation of the horizontal structure with a trapezoidal current waveform.

The vacuum chamber is an unconventional design that is removable from the magnetic structure, after magnetic measurements, for UHV processing. The chamber is fabricated from stainless steel to minimize the effects of eddy currents.

Spectral performance and device design are presented.

•The submitted abstract has been authored by a contractor of the U.S. Government under contract No. DE-AC03-76SF00098

TuE19

Advanced Light Source - First Undulators•

E. Hoyer, J. Akre, J. Chin•, W. Gath, W.V. Hassenzahl•, D. Humphries, B. Kincaid, S. Marks, P. Pipersky, D. Plate, G. Portmann, R. Schlueter

Advanced Light Source, Lawrence Berkeley Laboratory, University of California, Berkeley, Ca 94720

Abstract

At Lawrence Berkeley Laboratory's (LBL) Advanced Light Source (ALS), three 4.6 m long undulators have been completed, tested and installed. A fourth is under construction. The completed undulators include two 5.0 cm period length, 89 period devices (U5.0s) which achieve a 0.85 T effective field at a 14 mm minimum gap and a 8.0 cm period length, 55 period device (U8.0) that reaches a 1.2 T effective field at a 14 mm minimum gap. The undulator under construction is a 10.0 cm period length, 43 period device (U10.0) that is designed to achieve 0.98 T at a 23 mm gap.

Measurements show that the uncorrelated magnetic field errors are 0.23%, 0.24%, and 0.20% for the two U5.0s and the U8.0 respectively and that the field integrals are small over the 1 cm by 6 cm beam aperture.

Undulator magnetic gap variation (rms) is within 25 microns over the periodic structure length. Reproducibility of the adjustable magnetic gap has been measured to be within +/- 5 microns. Gap adjusting range is from 14 mm to 210 mm, which can be scanned in one minute.

The 5.1 m long vacuum chambers are flat in the vertical direction to within 0.74 mm and straight in the horizontal direction to within 0.08 mm over the 4.6 m magnetic structure sections. Vacuum chamber base pressures after UHV conditioning are in the mid 10^{-11} Torr range and storage ring operating pressures with full current are in the low 10^{-10} Torr range.

Device description, fabrication, and measurements are presented.

•The submitted abstract has been authored by a contractor of the U.S. Government under contract No. DE-AC03-76SF00098

•Retired

TuE20

Multiple Trim Magnets, or "Magic Fingers"•

E. Hoyer, S. Marks, P. Pipersky, R. Schlueter

Advanced Light Source, Lawrence Berkeley Laboratory, University of California,
Berkeley, Ca 94720

Abstract

Multiple Trim Magnets (MTM's), also known as "Magic Fingers", is an arrangement of magnets for reducing integrated magnetic field errors in insertion devices. The idea is to use transverse arrays of permanent magnets, hence the name "Multiple Trim Magnets", above and below the midplane, to correct both normal and skew longitudinal magnetic field integral errors in a device. MTM's are typically installed at the ends of an ID. Adjustments are made by changing either the size, position or orientation of each trim magnet.

Application of the MTM's to the ALS undulators reduced both the normal and skew longitudinal field integral errors, over the entire +/- 1 cm by +/- 3 cm "good field region", of the beam aperture by more than an order of magnitude. The requirements included corrections of field and gradients outside the multipole convergence radius. Additionally, these trim magnet arrays provided correction of the linear component of the integrated field gradients for particles with trajectories not parallel to the nominal beam axis.

The MTM concept, design method, tests that demonstrated feasibility and the application of the system to the ALS undulators is presented.

•The submitted abstract has been authored by a contractor of the U.S. Government under contract No. DE-AC03-76SF00098

TuE21

A Multiple Objective Magnet Sorting Algorithm for the Advanced Light Source Insertion Devices*

D. Humphries, F. Goetz, P. Kownacki, S. Marks, R. Schlueter

Advanced Light Source, Lawrence Berkeley Laboratory, University of California
One Cyclotron Road, Berkeley California 94720

Insertion devices for the Advanced Light Source (ALS) incorporate large numbers of permanent magnets which have a variety of orientation errors. These orientation errors can produce field errors which affect both the spectral brightness of the insertion devices and the storage ring electron beam dynamics.

In order to maintain the spectral quality of the light produced by the insertion devices, the poles of the device must be uniformly excited by the permanent magnets. Non-iterative algorithms have been previously developed and successfully applied to magnet populations to achieve uniform pole excitation. These algorithms primarily order and arrange magnets using the principal component of the magnetic moment (M_z).

Experience has shown that the minor components of the magnetic moments (M_x and M_y) may combine in the overall magnetic structure of a given insertion device to result in a non-uniform transverse distribution of integrated fields that may adversely affect electron beam dynamics. These error fields are typically large enough to require external correction to prevent beam lifetime and beta function effects.

A perturbation study was carried out to quantify the effects of particular magnetization minor components acting in a, hybrid magnetic structure. The results of this study were used to develop an iterative algorithm which acts on a limited parameter space to minimize undesirable integrated field errors.

This algorithm has been combined with the algorithm for uniform excitation to form a two stage magnet sorting. This algorithm has been incorporated into the program INSORT and applied to actual insertion device magnet data. The results show a significant reduction in integrated field errors and near elimination of excitation errors from permanent magnets.

Results of the perturbation study and the sorting algorithm are presented.

*This work was supported by the Director, Office of Energy Research, Office of Basic Energy Sciences, Materials Sciences Division, of the U.S. Department of Energy under Contract No. DE-AC03-76SF00098.

TuE22

Absolute flux and spatial intensity distribution measurements of the CHESS undulator

P. Ilinski, W. Yun, B. Lai, E. Gluskin, Z. Cai

Advanced Photon Source, Argonne National Laboratory,
9700 South Cass Avenue, Argonne, Illinois 60439

Abstract

Absolute radiation flux and polarization measurements of the APS undulators need to be made under high incident beam power and high incident beam power density conditions. A method that may circumvent the high heat load problem was examined during a recent APS/CHESS undulator run.

An experimental set-up to measure absolute flux and spatial intensity distribution of the intense undulator X-ray beam was developed and tested. The technique makes use of a Si(Li) energy-dispersive detector to measure X-ray scattering from a well-defined scattering volume at controlled pressure. This method was used to reduce high intensity of undulator radiation to the counting rate of the detector and allowed us to measure undulator spectrum in the 5 - 30 keV energy range with only Si(Li) detector need to be calibrated. The experimental results and data analysis will be presented and discussed.

* This work is supported by the Dept. of Energy, BES-Material Science, under contract no. W-31-109-ENG-38.

The submitted manuscript has been authored by a contractor of the U.S. Government under contract No. W-31-109-ENG-38. Accordingly, the U.S. Government retains a nonexclusive, royalty-free license to publish or reproduce the published form of this contribution, or allow others to do so, for U.S. Government purposes.

TuE23

Characteristics of SiC microwave absorber for damped cavity

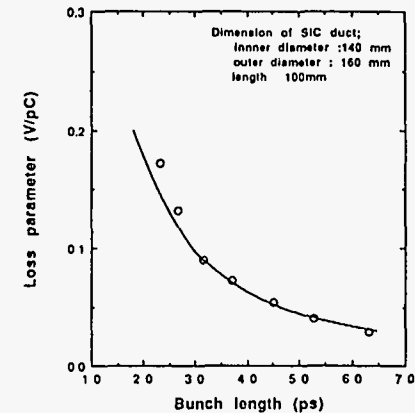
M. Izawa, T. Koseki^{a)}, Y. Kamiya^{a)}, and T. Toyomasu

National Laboratory for High Energy Physics,
1-1 Oho, Tsukuba-shi, Ibaraki, 305 Japan.

^{a)}The Institute for Solid State Physics, The University of Tokyo,
3-2-1 Midori-cho, Tanashi, Tokyo, 188 Japan

The microwave absorber is one of important elements of damped cavity. Many kinds of materials such as Ferrite¹⁾, Silicon carbide (SiC)²⁾, etc. are tried to absorb the electromagnetic field of higher-order-modes (HOM's) induced in a cavity. The SiC absorber is one of promising candidates since it has high thermal conductivity and the resistivity that we expect for the damped cavity being developed for the high brilliant ring in our labs. The effect of the SiC absorber on HOM's has already reported³⁾ and the recent development will be presented also in this conference⁴⁾.

In our damped cavity, the SiC absorber is used in a part of the beam duct. Therefore it is very important to investigate the characteristics of the SiC absorber to know the interaction between the beam and the SiC duct. The results of measurement of the dielectric constant and the permeability (both real and complex parts) at frequency range of 0.3 to 10 GHz and of the loss parameter of the SiC duct (shown below) are presented. The results of high power test of the SiC duct will be also presented.



Loss parameters of SiC duct (open circle : measured , solid line : calculated)

References

- 1) T. Tajima et al., KEK preprint 93-153. (presented at the 6th workshop on RF superconductivity, CEBAF, Virginia, U.S.A., Oct.4-8, 1993.
- 2) H. Matsumoto et al., Proceedings of the 8th linear accelerator meeting in Japan, p154, 1983 (in Japanese)
- 3) T. Koseki et al., Proc. of the 1993 Particle Accelerator Conference, Washington D.C., p930, 1993.
- 4) T. Koseki et al., 'A damped-structure cavity for a high-brilliant VUV and SX storage ring', to be presented in this conference.

TuE24

ACCELERATOR PLAN FOR THE LIGHT SOURCE STUDY AT THE TRISTAN MR

S.Kamada, H.Fukuma, K.Yoshioka, K.Nakajima, A. Ogata, T.Mitsuhashi, M.Isawa, N.Nakamura, S.Sakanaka, M.Tobiyama, K.Ohmi, S.Kurokawa, K.Kanazawa, T.Kubo, K.Egawa, T.Mimashi, M.Kobayashi, H.Mizuno, T.Furuya, S.Mitsunobu, T.Ieiri, M.Teijima and T.Katsura

KEK, National Laboratory for High Energy Physics, Tsukuba JAPAN

A three months operation with beam is scheduled in the autumn of 1995 at the TRISTAN main ring (MR) for the sake of light source development and research programs using it.

The lattice will be modified to install an undulator of 5.4m long and to reach very low emittance of 5nm at beam energy of 10GeV. The emittance damping wigglers will enhance radiation damping rate to stabilize coherent beam instabilities as well as to reduce emittance more.

Considerable numbers of cavities will be removed from the ring to minimize the impedance of higher order modes of accelerating cavities that may cause coupled bunch instabilities and limit the intensity of stored beam.

A beam emittance will be measured by detecting the angular distribution of Compton scattering of laser photons on beam electrons. Also adopted will be the image of visible synchrotron light to measure a beam emittance.

For the stability of light position, a local feedback system will be introduced to the stored electron beam.

TuE25

Beam Position Control of SOR-RING

H. Kudo, T. Nagatsuka, K. Shinoe, H. Takaki, T. Koseki,
N. Nakamura* and Y. Kamiya

ISSP, Tokyo University, Tanashi, Tokyo, 188 JAPAN.
* Photon Factory, KEK, Tsukuba, Ibaraki, 305 JAPAN

Recently, a global feedback of beam position was switched on at SOR-RING of Tokyo University. At a low beam current, the vertical orbit drift was suppressed almost always within a few μm which corresponds to a bit of steering's DAC [Fig. 1], and the horizontal orbit drift was within several μm . On the other hand, the suppression became worse at a high current and the fluctuation in beam position was within about ten μm or so, because the accuracy of BPM deteriorated due to a longitudinal instability.

In the 1992 summer shutdown, four beam position monitors (BPM's) and eight beam steerings were installed in the ring. The BPM system using PIN diode switches showed a good performance; the relative accuracy was 0.3 to 0.4 μm . The beam steerings consist of auxiliary coils wound on every pole of quadrupole magnets. With the BPM system, we measured the closed orbit distortion (C.O.D.) at the first time since the ring had been constructed; maximum values of C.O.D.'s were horizontally about 3 mm and vertically 4 mm. Then we corrected both horizontal and vertical C.O.D.'s much less than 1 mm by exciting the steerings and also by changing the RF frequency about 100 kHz. Continuous measurement of the beam orbit, however, revealed that the orbit slowly varies by the order of several tens of μm during a storage mode, and before and after injection it also jumps by several tens of μm . Now with the global feedback applied, both horizontal and vertical beam positions are controlled almost less than ten μm .

In order to find how the beam positions were fluctuating in a low frequency region, a BPM was connected to a hybrid circuit that was able to produce RF signals directly proportional to the beam positions. The RF signals were then fed into the BPM system and in turn into an FFT analyzer. When the electron synchrotron, ES, close to SOR-RING was operated with a repetition rate of 21 Hz, the 21-Hz frequency was clearly observed in the beam position spectra; horizontally 2.6 μm and vertically 0.6 μm . It was also observed that at 21 Hz the horizontal positions tend to fluctuate uniformly around the ring, i.e., monopole-like expansion and contraction, while the vertical positions have dipole-like fluctuation; a result expected if uniform magnetic field is impressed on the ring.

Presented in this paper are (1) long-term drift and low frequency spectra of beam positions at SOR-RING, (2) the global feedback system and (3) the suppression of orbit drift by the global feedback.

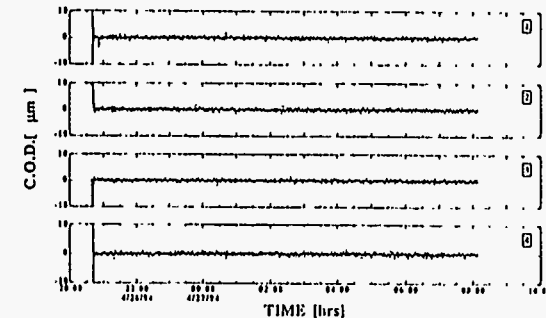


Fig. 1 Vertical orbit drift with a global feedback switched on. No. of BPM is denoted at the upper right corner.

TuE26

Polarization measurement of SR from a helical undulator using quarter-wave plate for 12.7-nm wavelength

H. Kimura¹⁾, T. Miyahara²⁾, Y. Goto³⁾, K. Mayama³⁾, M. Yanagihara³⁾
and M. Yamamoto³⁾

¹⁾Dept. SR Sci., The Grad. Univ. for Adv. Studies, KEK-PF, Tsukuba 305, Japan

²⁾Photon Factory, National Lab. for High Energy Physics, Tsukuba 305, Japan

³⁾Research Institute for Scientific Meas., Tohoku University, Sendai 980-77, Japan

We determined the polarization states of the circularly polarized light with 12.7-nm wavelength emitted from a helical undulator and monochromatized by a grating monochromator (KEK-PF BL-28A). A transmission-type multilayer phase shifter (Mo/Si 3.19 nm/ 6.03 nm 141L) and a multilayer mirror analyzer (Mo/Si 3.19 nm/6.03 nm 101L) were used in this study. The polarization characteristics of these elements were measured for the light with 12.7-nm wavelength beforehand. The ratio of the amplitude reflectance for the s- and p- components of the analyzer was evaluated to be 600. The retardation angle and the ratio of the amplitude transmittance for the s- and p-components of the phase shifter were evaluated to be 90 degrees and 1.1, respectively. This means that the phase shifter can be used as a quarter-wave plate. Using those, we measured all polarization parameters of highly circularly polarized SR, which are the degree of polarization (V), the ellipticity angle (ϵ) and the azimuth of the major axis of the polarization ellipse (δ).

The obtained polarization parameters are listed in Table 1. The degree of circular polarization through the grating monochromator is estimated to be 0.95 from these results. This value is much higher than that of the off-axis beam from a bending magnet and that of a beam from a crossed undulator in BESSY. The helical undulator is thus expected to provide MCD signals with high efficiency.

*)Present address: JAERI-RIKEN SPring-8 Project Team, The Institute of Physical and Chemical Research (RIKEN), Hirosawa 2-1, Wako, Saitama 351-01, Japan

Table 1. Parameters of the polarization state of the monochromatized light. The undulator gap was tuned to produce the 12.7-nm photons as the peak of first harmonics in helical undulator modes.

	Right-handed	Left-handed
V	0.97 ± 0.01	0.97 ± 0.01
$\epsilon(\text{deg})$	-46 ± 1	46 ± 1
$\delta(\text{deg})$	39 ± 2	40 ± 2

Abstract

Helical Undulator Systems for Rapid Switching of Helicity

H. Kimura, T. Tanaka, X. Maréchal and H. Kimura

JAERI-RIKEN SPring-8 Project Team

The Institute of Physical and Chemical Research (RIKEN)

Hirosawa 2-1 Wako, Saitama 351-01, Japan

To investigate the spin dependent phenomena in the vacuum ultraviolet or X-ray region, the circularly polarized radiation (CPR) from a helical undulator is required. Although several CPR sources have been constructed so far, most of them, except for HELIOS developed at ESRF, have the helicity fixed during the period between beam injections. In the near future, special helical undulator systems with rapid switching of helicity will be required to make modulation spectroscopy. In the paper, various undulator systems for the rapid switching including some new ideas will be reviewed.

Abstract

Vertical Undulators for SPring-8

T. Tanaka, X. Maréchal and H. Kitamura

JAERI-RIKEN SPring-8 Project Team
The Institute of Physical and Chemical Research (RIKEN)
Hirosawa 2-1, Wako, Saitama 351-01, Japan

The utilization of the vertical polarization is so important for special X-ray optics. The new undulator design for the vertical polarization is proposed in this work. As shown Fig.1, the undulator has a full aperture in the horizontal direction so that the vacuum duct with powerful pumps may be installed. In addition to that, the permanent magnet has a special structure for obtaining a good homogeneity of the field in the horizontal direction. In the paper, the performance of the vertical undulator design for SPring-8 will be reported.

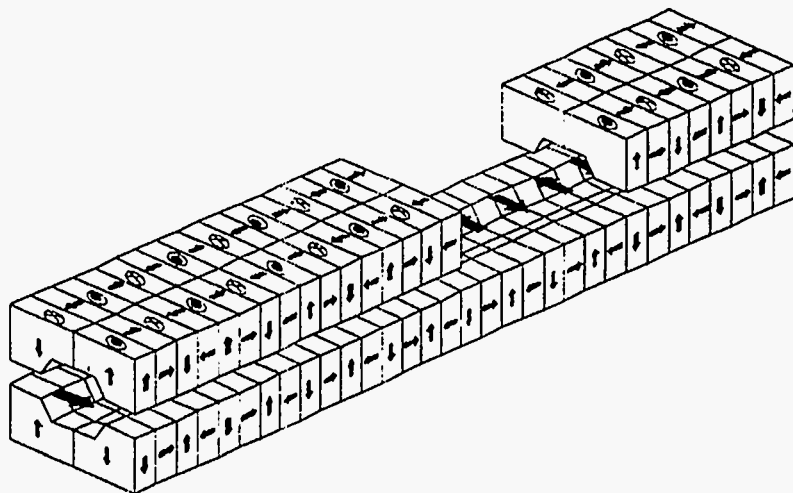


Fig.1 Schematic illustration of the vertical undulator design

Polarization Characterization of Elliptically-Polarized VUV-Soft X-Ray Helical Undulator Radiation

T. Koide^a, T. Shidara^a, T. Miyahara^a and M Yuri^b

^aPhoton Factory, National Laboratory for High Energy Physics,
1-1 Oho, Tsukuba, Ibaraki 305, Japan

^bTeikyo University of Technology, Ichihara, Chiba 290-01, Japan

A reflection polarimeter has been designed and constructed for monitoring the polarization state of elliptically polarized synchrotron radiation from a helical undulator installed on beamline BL-28 at the photon Factory. This polarimeter mainly comprises two triple-reflection polarizers each of which acts as a phase shifter and a quasi-linear polarization analyzer, and it is a renovated version of the polarimeter previously used for the polarization measurements of off-plane circular polarization on bending-magnet beamlines. The polarimeter allows one to make its axis adjustment to the beam axis with monochromatized light, which is to be polarization analyzed, under an ultrahigh vacuum.

All of the Stokes parameters have been measured using the polarimeter at given energies in the 50-80-eV region with the first harmonic peak energy ($h\nu_1$) of the undulator radiation kept at ~ 75 eV. The measured degree of circular polarization ($P_C = S_3/S_0$) exhibited high values ($\geq 90\%$) at $\sim h\nu_1$ and at lower energies within ~ 10 eV of $h\nu_1$. This indicates that only a small correction for P_C is necessary in order to analyze the experimental results such as MCD studies, as far as this energy region is concerned. However, the measured P_C rapidly decreased in regions higher than $h\nu_1$ and lower than ~ 65 eV. A correction for P_C would have a considerably important affect on the results of energy-scanning experiments in these regions.

We also made numerical calculations by taking into account the undulator-radiation characteristics alone, by considering the effect on the polarization of the reflection and diffraction on the beamline optical elements as well, and further by taking account of the influence of mixing of bending-magnet radiation. A comparison of the experimental results with the calculations showed that the effects on the polarization of both the beamline optics and the mixing of bending-magnet radiation cannot be neglected in the regions of low-intensity undulator radiation.

MULTIPOLE WIGGLER PERFORMANCE FOR THE SIBERIA-2 SR SOURCE

G. Erg, V. Korchuganov, E. Levichev, A. Philipchenko
V. Sajaev, and V. Ushakov
Budker Institute of Nuclear Physics
630090 Novosibirsk, Russia

ABSTRACT

For some experiments the radiation power distribution with good homogeneity along the sample is required. The multipole wiggler optimized for this purpose was designed and manufactured for the SIBERIA-2 X-ray ring. Here the design of the wiggler is described. The magnetic mapping results and wiggler radiation features are presented. The insertion effect on beam parameters and the matching procedure are considered.

A damped-structure cavity for a high-brilliant VUV and SX storage ring

T. Koseki, M. Izawa^{a)} and Y. Kamiya

Synchrotron Radiation Laboratory, The Institute for Solid State Physics, The University of Tokyo
3-2-1 Midori-cho, Tanashi, Tokyo, 188 Japan

^{a)} Photon Factory, National Laboratory for High Energy Physics,
1-1 Oho, Tsukuba, Ibaraki, 305 Japan

A third-generation VUV-SX storage ring with a low emittance of several nm-rad is being designed at the Institute for Solid State Physics, the University of Tokyo in collaboration with the Photon Factory at KEK [1]. As one of the R&D's for the storage ring, we have designed a new type of RF cavity which has a simple damped structure, and carried out its low power test on a prototype model. This paper presents the conceptual design of the cavity and the results of the low power test.

The specific feature of the cavity is that a beam duct with large diameter is attached to the cavity and a part of the beam duct is made of resistive material. Since the frequency of accelerating mode is much lower than the cutoff frequency of the beam duct, the accelerating field is fully trapped in the center of the cavity. On the other hand, the higher-order modes (HOM's), which can propagate out from the center of the cavity through the beam duct, are damped by the resistive part. Figure 1 shows the schematic of a quadrant of the designed cavity. The sintered SiC, named CERASIC-B (TOSHIBA CERAMICS), is used as the resistive material [2]. Its resistivity is about 20 Ωcm in the frequency region of 1.5 GHz to 4.5 GHz.

A prototype cavity was made of aluminum, and two types of beam-duct were prepared. One is made of aluminum and the other is CERASIC-B. Some RF characteristics (resonant frequency, Q-value, field distribution and shunt impedance) for fundamental mode and HOM's were measured with a network analyzer. Almost all measured values well agreed with the calculated ones, and the Q-values for most of HOM's were largely reduced in the case of the CERASIC-B duct. With this damped cavity, the coupled-bunch instabilities due to HOM's are expected to be sufficiently suppressed at the VUV-SX storage ring.

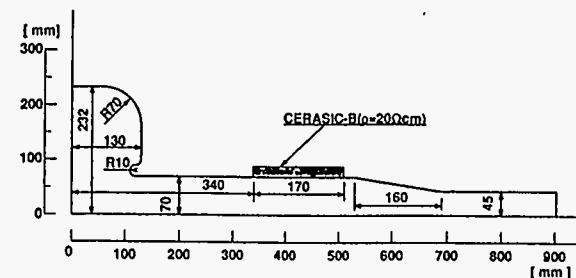


Figure 1: Schematic view of the cavity.

References

- [1] Y. Kamiya et al., "A future project of VUV and soft X-ray high-brilliant light source in Japan.", submitted to 4th European Particle Accelerator Conference.
- [2] M. Izawa et al., "Characteristics of SiC microwave absorber for damped cavity.", to be presented in this conference.

Time resolved fluorescence using synchrotron radiation excitation: a powered fourth-harmonic cavity improves pulse stability

Krzysztof Polewski,^{a,b)} Stephen L. Kramer,^{c)} Zbigniew S. Kolber,^{d)} John G. Trunk,^{a)} Denise C. Monteleone,^{a)} and John C. Sutherland^{d)}

Brookhaven National Laboratory, Upton, New York 11973-5000

- ^{a)} Biology Department
- ^{b)} Permanent address: Institute of Physics, Agricultural University, Poznan, Poland
- ^{c)} National Synchrotron Light Source Department
- ^{d)} Department of Applied Science

The pulsed nature or "time structure" of synchrotron radiation from electron storage rings is used to measure the kinetics of the decay of electronically excited states and is particularly useful because the wavelength of excitation can be chosen at will. However, changes in the length of the pulses of radiation from a storage ring resulting from the gradual decrease of current circulating in the ring during the course of a "fill" limit the duration of data collection, and hence photometric sensitivity. A fourth-harmonic cavity that was recently added to the VUV storage ring at the National Synchrotron Light Source slows the loss of current during a fill, and thus increases the total number of photons produced. When operated in a passive (unpowered) mode, however, the fourth-harmonic cavity increases both the average width of the photon pulses and the changes in width that occur during a fill, thus reducing the usefulness of the VUV ring in timing experiments. We demonstrate that operating the fourth-harmonic cavity in an active (powered) mode, while further increasing pulse duration, can stabilize pulse width, thereby restoring timing capabilities.

TuE33

Modification of the Coherence of Undulator Radiation

D.White¹, O.Wood II², S.Spector³ A.MacDowell⁴, B.La Fontaine⁴,

1. AT&T Bell Laboratories, 600 Mountain Av. Murray Hill, NJ 07974
2. AT&T Bell Laboratories, 101 Crawfords Corner Road, Holmdel, NJ 07733
3. State University of New York at Stony Brook, Stony Brook, NY 11974
4. AT&T Bell Laboratories, 510E Brookhaven Laboratory, Upton, NY 11973

Abstract

We have modified the spatial and temporal coherence of undulator radiation in a quantitative way, such that when imaging with undulator light of $\lambda=13\text{nm}$, the resultant images do not have the usual coherent artifacts of speckle and ringing. To achieve this, we made a soft x-ray scatter plate which, when inserted into the beam produces the required amount of divergence and phase shifting to fill the pupil of a 20:1 Schwarzschild camera operating at $\lambda=13\text{nm}$. Details of this soft x-ray scatter plate and its effect on imaging will be presented.

TuE34

DAΦNE AS A SOURCE OF SYNCHROTRON RADIATION:
AN ESTIMATE OF THE SOURCE SIZE
AND OF THE BRILLIANCE IN THE INFRARED REGION

A. Marcelli

Laboratori Nazionali di Frascati, INFN 00044 Frascati, Italy

A. Nucara and P. Calvani

Dipartimento Fisica, Universita' di Roma "La Sapienza", 00185 Roma, Italy

M. Sanchez del Rio

European Synchrotron Radiation Facility BP. 220, 38043 Grenoble Cedex, France

DAΦNE is a 0.51 GeV, 2 Amps, electron-positron collider under construction at Frascati, specially designed to be used as a meson factory. The technical characteristics of the rings make them also suitable as synchrotron radiation sources in the infrared (IR), vacuum ultraviolet (VUV) and soft x-ray energy domains. Here we present calculations showing that the electromagnetic radiation produced by DAΦNE bending magnets and wigglers is more brilliant in the infrared energy range 5-5000 μm, and also more intense in a narrower range, than black body radiation. Several effects have been taken into account in the estimate of the Actual Source Area (ASA). This parameter, which is a function of frequency, depends on the collecting solid angle, on the intrinsic divergence of the radiation, on the source geometry, and finally on the machine parameters. Basing on the ASA values thus obtained, the ratio between the brightness of the synchrotron source and the brightness of a blackbody, i.e. the Actual Brightness Ratio (ABR), has been calculated. Moreover, the results of ray-tracing calculations performed by SHADOW at different wavelengths, and for bending magnets belonging to different synchrotron sources, are compared and discussed.

An Elliptical Wiggler for SPring-8

X.M. MARÉCHAL¹, T. TANAKA, H. KITAMURA

JAERI-RIKEN SPring-8 Project Team

The Institute for Physical and Chemical Research (RIKEN)

Hirosawa 2-1, Wako-Shi, Saitama 351-01 JAPAN

This paper presents a study for the realization of an elliptical wiggler to be installed on the pilot beamline dedicated to material science (Compton scattering beamline) at SPring-8. Such a wiggler should meet the requirements of third generation synchrotron sources, i.e. use a planar structure (two jaws above and below the orbital plane of the electrons) which does not induce any modification on the vacuum chamber or the mechanical support (no horizontal constraints).

The performances of three possible designs proposed for this new elliptical wiggler are compared: two magnetic designs, based on the so-called APPLE concept developed by Sasaki et al. [1], and new type elliptical wiggler.

Magnetic and mechanical design (field and forces) as well as expected fluxes, polarization rates and power densities have been computed for the three magnetic arrangements. Effects on the electron beam are also discussed.

References

[1] K. Kakuno and S. Sasaki, "Conceptual design of a vertical undulator", JAERI-M 92-157, in Japanese.

1. This work has been realized with the support of the Japanese Science and Technology Agency.

Optimization Design Study for an Elliptical Wiggler at the Advanced Light Source*

S. Marks, W. McKinney, H. Padmore, A. Young

Advanced Light Source, Lawrence Berkeley Laboratory, University of California
1 Cyclotron Road, Berkeley, California 94720

This paper describes a design study that has been conducted for an elliptical wiggler which is to be installed in the Advanced Light Source (ALS). This device is to produce circularly polarized radiation in the energy range of 50 eV to 10 KeV. It consists of a variable-gap hybrid permanent magnet wiggler which produces a peak vertical field of 2.0 T, and an electromagnetic wiggler which produces a horizontal field with a peak deflection parameter, K_x , of 1.5. The horizontal magnetic structure is installed such that its peak field is 90° out of phase with the peak vertical field. The polarity of the horizontal field cycles at 1 Hz; this results in alternating left and right circularly polarized radiation.

The objective of the design study was to optimize performance over the operating range, and to evaluate the sensitivity of optimum set points to changes in parameter values. The quantity M which is optimized is defined as

$$M = P_c \sqrt{F} \quad (1)$$

where P_c is the degree of circular polarization and F is flux. This figure of merit is appropriate for experiments using single event counting to detect an asymmetry between effects of left and right circularly polarized radiation. The horizontal aperture was held fixed at a constant value while the vertical aperture was a free parameter. An optimum set point is characterized by values of the three parameters: peak vertical field B_y , horizontal deflection parameter K_x , and vertical aperture $\Delta\psi$. Optimum set points were calculated for photon energies throughout the 50 eV to 10 KeV range and for storage ring energies of 1.5 GeV and 1.9 GeV.

The stability of each optimum set point has been evaluated and compared with required engineering tolerances and with experimental operating requirements. The sensitivity of each solution has been evaluated for changing K_x and for steering errors. These results have been compared to the requirements of typical Magnetic Circular Dichroism (MCD) experiments and have been translated into engineering specifications.

A set of computer codes were developed by the authors for this study. The basis of these codes will be described in the paper.

*The submitted abstract has been authored by a contractor of the U.S. Government under contract No. DE-AC03-76SF00098

TuE37

Performance of a Diagnostic Imaging Beamline at the Advanced Light Source*

M. E. Melczer, A. Saffamia

Advanced Light Source
Lawrence Berkeley Laboratory
Berkeley, CA 94720
USA

The low emittance of the electron beam at the Advanced Light Source (ALS) in Berkeley prohibits imaging of the electron beam with visible light. High brightness and the diffraction limited nature of the beam required the design of a beamline that would image the beam in the soft x-ray region (>100 eV) and minimize the possible aberrations that are associated with grazing incidence optics.¹ A Kirkpatrick-Baez mirror system utilizing two crossed spherical mirrors with 1:1 imaging was employed to minimize coma and astigmatism. Use of a single crystal scintillator screen with conventional microscope optics and a high resolution CCD camera are employed to deliver the beam image to the ALS control room. Positional information, size, timing, and stability of the beam can be observed, captured, and analyzed. Factors such as thermal stability, mechanical stability, beam motion, and vibration from water cooled optics all relate to the final stability, aberrations, and resolution of the image. The current design of the diagnostic beamline and the characterization of its performance are discussed along with possible upgrades. These upgrades would improve its adjustability and expand the range of beam motions that it can accommodate during machine studies.

*This work was supported by the Director, Office of Energy Research, Office of Basic Energy Sciences, Materials Sciences Division, of the U. S. Department of Energy, under Contract No. DE-AC03-76SF00098.

¹ R.C.C. Perera, M.E. Melczer, A. Warwick, A. Jackson, B.M. Kincaid, Rev. Sci. Instrum., Vol. 63 no.1, pt. 11A, pp. 541-4 (Jan. 1992).

TuE38

Power supply and quench protection system for superconducting 7.5 Tesla wiggler

V.M.Borovikov, P.D.Vobly, N.A.Mezentsev, V.A.Shkaruba, S.V.Sukhanov, and
M.G.Fedurin
Budker Institute of Nuclear Physics
630090 Novosibirsk, Russia

The superconducting wiggler is powered by two current sources connected to different windings. The power supply system also includes quench protection. The results of the preburning of superconducting windings by superconductivity quenching in the windings are reported. The results of the measurements dealing with the dynamics of the normal zone in the windings are also given. The efficiency of reaching the external energy load by the wiggler field was measured.

Tue39

Superconducting 7.5 Tesla wiggler for PLS

G.N.Kulipanov, N.A.Mezentsev, P.D.Vobly, V.A.Shkaruba, S.G.Ruvinsky,
S.V.Sukhanov, V.B.Khlestov
Budker Institute of Nuclear Physics
630090 Novosibirsk, Russia
Y.M.Koo⁺, *D.E.Kim*⁺, and *Y.U.Sohn*⁺
(+)Pohang Institute of Science and Technology

The construction of a dedicated SR source - the 2 GeV PLS - is being completed in Korea. The superconducting 3-pole wiggler (shifter) with a 7.5 Tesla maximum field at the central pole, which is to be installed at the PLS storage ring was manufactured by the Institute of Nuclear Physics (Novosibirsk) in cooperation with the PLS Laboratory (POSTECH, Pohang). The magnetic field at the side poles does not exceed 1.6 Tesla in order to suppress the second source in the hard spectral section.

The basic parameters of the wiggler are given. The expected and experimental data on the magnetic field distribution are also presented. The data were derived after the wiggler was switched on in a special immersed cryostat. The major effects which are related to the influence of the magnetic field of the wiggler on the beam dynamics in the storage ring are discussed.

Tue40

Search for Possible Radiation Damage on a NdFeB Permanent Magnet Structure

after two Years of Operation

J. Pflüger, G. Heintze

DESY / HASYLAB , Notkestraße 85, 22603 Hamburg, Germany

I. Vasserman

ANL / APS, 9700 South Cass Avenue, Argonne IL 60439

A Passive Scheme for ID End Correction

I. Vasserman and E.R. Moog
Advanced Photon Source
Argonne National Laboratory
9700 S. Cass Ave
Argonne, IL 60439

Abstract

A passive end correction scheme used on the prototype for undulator A is described. This scheme allows the integrated field requirements to be met through the gap rang from 11.5 mm to 200 mm with no active correction. The main parameters that need to be adjusted are strength of the end magnets and the height of the next to last poles. The first field integral is stable to within 25 G-cm in the vertical direction and 50 G-cm in the horizontal direction. The second field integral is stable to within 10,000 G-cm². Results of magnetic measurements are presented.

This work was supported by the U.S. Department of Energy BES Material Sciences, under contract w-31-109-ENG-38

TuE41

The submitted manuscript has been authored by a contractor of the U.S. Government under contract No. W-31-109-ENG-38. Accordingly, the U.S. Government retains a nonexclusive, royalty-free license to publish or reproduce the published form of this contribution, or allow others to do so, for U.S. Government purposes.

Abstract

Recently there has been some concern about possible radiation damage due to ionizing particles present in high energy storage rings such as multi GeV electrons, fast neutrons or hard photons. Partial demagnetizing has been observed on undulators after missteering of injected electron beam.

Our interest was focused on possible radiation damage caused by the routine operation of a storage ring to a permanent magnet Insertion Device. Therefore we repeated the magnetic measurements on one of the three 4.0 m long DORIS III X Ray Wigglers, BW6, which is in operation since 1991 and compared the results to the data taken before installation.

The total dose was determined from measurements with thermoluminescence dosimeters and the known number of stored amperehours.

The results which show no significant degradations of the magnetic performance are presented and discussed.

TuE42

EXPERIMENTS WITH UNDULATOR RADIATION OF A SINGLE
ELECTRON

I. V. PINAYEV, V. M. POPIK, T. V. SHAFTAN,
A. S. SOKOLOV, N. A. VINOKUROV, P. V. VOROBYOV

A single electron circulating in a storage ring is a very peculiar object. Permanent emission of synchrotron radiation offers the possibility to observe the electron but also causes the "natural bunch length". In the quasiclassical treatment electron position uncertainties arise from the averaging of the energy and position of the point-like electron over many turns in the storage ring. Nevertheless a question about the electron localization remains open. The radiation from a long undulator permits to obtain "snapshots" of the electron longitudinal distribution. The experiments with a single electron on VEPP-3 optical klystron are discussed.

TuE43

CONTROL SYSTEM FOR A 1.8 TESLA WIGGLER

D. C. Quimby, D. R. Jander and K. E. Robinson
STI Optronics, Inc., Bellevue, Washington, USA

A personal-computer based control system has been developed for the SRRC 1.8 Tesla Wiggler. The system serves three major functions: gap monitoring and control, end-corrector adjustment and tracking, and interlock safety and monitoring. The end-correctors are programmed with a gap-following feature for compensation of the electron trajectory in both transverse planes at all gaps. Software and hardware interlocks are provided for overtravel limits and protection against excessive variation in gap from end-to-end. The system is designed for stand-alone operation as well as for compatibility with the SRRC central control system.

The system includes an IBM-compatible PC, four end-corrector power supplies, a Compumotor Model 4000 motion controller, two servo motors with motor drivers, and two linear encoders with 5 μm resolution. The PC provides the gap-following feature of the end correctors and enables the motor motion subject to all interlocks remaining within safe limits. The PC communicates with the programmable motion controller via a local GPIB bus. The end-corrector power supplies are under analog control and monitoring and the hardware interlocks function is completed via direct digital inputs and hardware cutoffs to the motion controller. Software limits are implemented utilizing the built-in capabilities of the motion controller with backup monitoring provided by the PC. The wiggler controller connects to the SRRC central control system via a separate GPIB interface and can receive commands and send information over this link.

TuE44

A Concept of Quasi-Periodic Undulator

DEVELOPMENT OF A 1.8 TESLA PERMANENT MAGNET WIGGLER SYSTEM

K.E. Robinson, S.C. Gottschalk, D.R. Jander, D.C. Quimby, and A.S. Valla

STI Optronics, Inc., Bellevue, Washington, USA

We present the design, development, and realization of a 1.8 tesla permanent magnet hybrid wiggler system. This 3.0 meter wiggler has a 200 mm period, operating at a minimum gap of 22 mm. It has twenty-seven poles and integrated end correctors and field clamps. The magnetic design for this device is pushed to a regime where few hybrid devices have operated. The very large peak field causes significant increase in the saturation of the vanadium permendur poles. The operating point also significantly impacts the transverse uniformity of the field and the magnet operating point. We discuss the magnetic design approach and the development of a mechanical structure which provides adequate strength and stability. The system is a complete stand-alone system with a fully integrated controls system and complete insertion device magnetics measurement system. The adjustment of the end compensation of the device with the presence of the field clamps requires particular attention. We present the distinctive elements of the design and the result of the magnetic and mechanical testing of the device. This wiggler is being delivered to the Synchrotron Radiation Research Center for installation during late summer of 1994.

Shigemi Sasaki and Shinya Hashimoto*

Department of Synchrotron Radiation Facility Project
Japan Atomic Energy Research Institute
Tokai-mura, Naka-gun, Ibaraki 319-11, Japan

Conventional periodic undulators generate the rational harmonics such as a third and a fifth harmonic radiation in the practical range of undulator use ($K=1$). These harmonics are not welcome in some experiments because the rational higher harmonics cannot be discriminated by crystal monochromators or conventional grating monochromators. The existence of higher harmonics increase the noise ratio in a signal.

A new undulator which never generates the rational higher harmonics was considered. This undulator consists of a quasi-periodic array of magnets. The order of array with positive and negative magnetic poles is determined in the way of Fibonacci series with two irrationally different spacing distances. This device generates irrational higher harmonics which can be discriminated by conventional monochromators.

Detailed discussion will be made in this conference on this undulator with respect to practical magnetic structures and undulator radiation spectra.

Shinya Hashimoto and Shigemi Sasaki : JAERI -M Report 94-055 (1994).

* On leave from Japan Synchrotron Radiation Research Institute

Position Monitor and Read-Out Electronics for Undulator and Focused Bending Magnet Beamlines

Wilfried Schildkamp, Claude Pradervand
Consortium for Advanced Radiation Sources,
The University of Chicago, Chicago, Illinois 60637

Third generation synchrotron radiation sources offer the opportunity to use undulators as insertion devices. The spectrum, spectral brightness and polarization of the narrow cone of undulator radiation vary strongly with the distance from the centroid and, therefore, experiments using radiation from undulators require unusually precise knowledge of the beam position in two dimensions. Since the energy dispersion of the undulator radiation changes when the undulator is tuned to a different energy, a position monitor must either be insensitive to energy or a different set of calibration curves has to be applied for different tunes. As the specific heat load of undulator radiation is in excess of 200 W/mm² a position monitor must either withstand the heatload without deformation or only a small fraction of the radiation interacts with the position monitor and is used to determine the position of the centroid of the undulator radiation. This position monitor is basically non-destructive and can be mounted directly upstream of the diffraction experiment. Similarly high specific heatloads can be achieved with focused radiation from wiggler sources on second generation machines.

A position monitor based on the principle of an ionization chamber can be used even for a high power density x-ray beam from an undulator. The choice of the right ionization gas and its density is crucial. The monitor has been used as a pure null instrument for large beam motions and as a differential monitor for small beam motions. In the first case the pair of translation stages or an optical table is used to bring the radiation into the electrical center of the monitor and the position was determined by the position of the stepping motors of the translation system. In both dimensions a bandpass of 1 kHz was achieved. The accuracy of the calibration curve was about 5 μ m when the monitor was used as a null instrument and depended largely on the positioning system, with a resolution of less than 1 μ m.

A position monitor and the read-out electronic of the presented kind is in use on NSLS beamline X26C with focused bending magnet radiation. This monitor uses a programmable pre-amplifier in combination with analog electronics read-out, suitable for studying the dynamics of x-ray beams. An alternative digital read-out electronics module, which matches the same preamplifiers, has been designed and build that resides in a VME crate and is hence easily computer readable.

TuE47

Design and manufacture of a 10-T superconducting wiggler magnet for the TERAS

S. Sugiyama, H. Ohgaki, T. Mikado, and T. Yamazaki
Electrotechnical Laboratory, 1-1-4 Umezono, Tsukuba City, Ibaraki 305, Japan

S. Isojima, H. Usami, C. Suzawa, T. Masuda, and Y. Hosoda
Sumitomo Electric Industries, Ltd., 1-1-3 Shimaya, Konohana-ku, Osaka 554, Japan

The 10-T wiggler is an iron-cored superconducting dipole magnet installed for the TERAS Electrotechnical laboratory's 800 MeV electron storage ring to provide x-ray synchrotron radiation¹⁾. The wiggler magnet is a three pole device designed to have a central field of 10 tesla and return fields of 6 tesla to lead to minimum integrated field errors. Design consideration of the wiggler was focused on making the wiggler magnet as compact as possible to insert the wiggler in 1.8-m long straight section of the storage ring. Three parallel dipoles with 30 mm gap being an assembly of racetrack conductor elements are arranged with coil straight sections transverse to the beam direction. The central coil consists of two parts separated into the high and low magnetic field regions in order to achieve a short field periodicity of 230 mm. The inner part of the coil is composed of 1.25 mm diameter Nb₃Sn wire wound onto soft iron pole piece and the outer part is wound with NbTi wire with 1.0 mm diameter around a partition wall between the two parts.

Construction experiments has been carried out to examine the feasibility of producing 10-T racetrack superconducting coils. Preliminary magnet test has been performed and showed that the training in the central coil started at 6 tesla proceeded to 7 tesla in some 10 quenches.

Afterward a lot of efforts have been made to achieve higher magnetic field by improving the constructive properties of the central coil. Experiments related to impulsive mechanical events resulted from compressive forces and shear stress fields has been carried out by using a specially designed measuring system and AE sensor with resonant frequency of 150 kHz. Additionally three-dimensional finite-element analysis has been utilized to calculate the magnetic force characteristic according with such variables as coil straight section length and hemispherical arrangement. The hemispherical arrangement formed in straight section was taken to increase the winding tension of superconducting wire. Experimental results indicates that sheared stress from the coil deformation in the straight section pay an important role in cracking of epoxy resin. The maximum magnetic field of 9 tesla is expected to be achieved by increasing the thickness of the partition wall in the central magnet of the wiggler. The 10-T superconducting wiggler in the final stage of manufacture is going to be installed in TERAS in the last quarter of 1994.

Reference

(1) S. Sugiyama, H. Ohgaki, M. Mikado, T. Noguchi, K. Yamada, M. Chiwaki, R. Suzuki, M. Koike, T. Yamazaki, T. Tomimasu, T. Keishi, H. Usami, and Y. Hosada, *Rev. Sci. Instrum.* 63,313(1992).

TuE48

Status of the Booster Synchrotron for SPring-8

Hiromitsu Suzuki, Hiroto Yonchara, Tsuyoshi Aoki, Norio Tani, Takayoshi Kaneda,
Yasuo Ueyama, Yasushi Sasaki, Teruyasu Nagafuchi, Soichiro Hayashi and Hideaki Yokomizo
JAERI-RIKEN SPring-8 Project Team
JAERI, Tokai-mura, Naka-gun, Ibaraki-ken, 319-11, Japan

abstract

The specification and the layout of the booster synchrotron for SPring-8 were decided. The synchrotron is designed to accelerate electron or positron beams from 1 GeV to 8 GeV with the repetition cycle of 1 Hz.

The construction of the synchrotron was started in 1993. Firstly one bending, one quadrupole and one sextupole magnet were made and the results of the magnetic field measurement were acquired. Two septum, one bump and one kicker magnets for the beam extraction have been made, the field measurement and a few improvement have progressed. The high power test of the first rf cavity was finished successfully. The calibration test of the button position monitor with the signal treatment circuits is advanced now. The residual components of the synchrotron are designed and constructed, and the commissioning of the synchrotron is started in 1996. This report presents the first measurement of each component.

Construction and beam experiment of a compact storage ring at MFLCO,

T.Nakanishi, K.Ikegami, I.Kodera, A.Maruyama, T.Matsuda, T.Nakagawa, S.Nakamura, S.Nakata, N.Oishi, S.Okuda, T.Takeuchi, H.Tanaka, C.Tsukishima, and T.Yamada, Mitsubishi Electric Corporation, 8-1-1 Tsukaguchi-honmachi, Amagasaki, 661 Japan.

A compact storage ring has been developed for industrial research such as x-ray lithography and material analysis. This machine is a racetrack type with two superconducting bending magnets and only two normal conducting quadrupole magnets. The circumference is as short as 9.2m. One quadrupole magnet per a cell contributes to make the smaller machine. The injector is a synchrotron and a full energy injection is performed. The bending magnets excite a field of 3.5T, and are operated in persistent current mode. The helium consumption is as low as 3 ℓ /hr/2 magnets where no liquefier is used. An iron shield of the magnet decreases a leakage flux to a terrestrial level at 3m.

The operation parameters are shown in Table 1. The critical wavelength is 1.53nm which is suitable for x-ray lithography. Any beam instabilities are not observed during beam injection up to 380mA in spite of no correction of the chromaticities. The chromaticities were measured $\xi_x = -0.92$ and $\xi_y = -1.07$, respectively, and agreed well with the calculated values. Beam emittances were obtained from measured beam sizes and were in good agreement with the calculated values. The coupling coefficient, ϵ_y/ϵ_x , is calculated around 0.04.

Table 1. Operation parameters

Maximum energy (MeV)	600	Betatron frequency ν_x	1.38
Injection energy (MeV)	600	ν_y	0.43
Maximum magnetic field (T)	3.5	Emittance $\epsilon_{x0}(\pi mm \cdot mrad)$	0.7
RF frequency (MHz)	130	Beam size $\sigma_x(mm)$	0.8
Circumference (m)	9.2	Beam current (mA)	380
Critical wavelength(nm)	1.53	Life time(hr) at 100mA	3

Studies of Beam Dynamics of a Compact Storage Ring using Superconducting Bending Magnets,
H.Tanaka and T.Nakanishi, Mitsubishi Electric Corporation, 8-1-1 Tsukaguchi-honmachi, Amagasaki, 661 Japan.

Construction of a compact storage ring has been completed in June 1993, and a beam test has been done. The ring is a racetrack-type consisting of two superconducting bending magnets, and the circumference and the beam energy are 9.2m and 600MeV, respectively.

Differences of calculated beam parameters from measured ones are studied using the compact ring. The beam parameters are calculated using a numerical integration of exact equations of motion and exact three-dimensional magnetic fields (B_x, B_y, B_z) measured[1]. Discussions are as follows: 1)betatron tunes and chromaticities, 2)the dynamic aperture in the vertical coordinate at the center of bending magnet, 3)the differences of closed orbit errors calculated with misalignment data of magnets from the measured ones, and 4)corrections of closed orbit errors. The measured values agree with the calculated ones as shown in Table 1.

[1] H.Tanaka and T.Nakanishi, Review of Scientific Instruments, 63, No.1, p777-780 (1992)

Table 1. Beam parameters measured and calculated

	horizontal		vertical	
	calculated	measured	calculated	measured
betatron tunes	1.383	1.380	0.440	0.441
chromaticities($\frac{\Delta\nu}{\Delta P/P}$)	-0.96	-0.92	-0.97	-1.07
dynamic aperture	-	-	28.8mm	28mm
COD(before correction)	2.2mm(1 σ)	3.0mm	4.9mm(1 σ)	6.7mm
COD(after correction)	0.2mm	0.1mm	0.1mm	0.1mm

Emittance Measurement at the ESRF

E. Tarazona, P. Elleaume
ESRF, BP 220, 38043 Grenoble Cedex France

A new kind of electron beam imaging set-up has been routinely operated at ESRF. It uses the X-ray beam from an undulator. The white beam is monochromatized by a Si 400 Bragg reflection at 30 keV. The monochromatic beam is sent to a fluorescent screen which is imaged by a CCD camera. The emittance of the electron beam is deduced from the size measured on the CCD image and the independent knowledge of the beta function at the source point. This set-up has been able to measure emittances in the range between 0.2 nm to 20 nm with a precision of 20%. The principal limitation appears to be the single electron emission angular pattern which probably limits the minimum detectable emittance to 0.1 nm.

The set-up has been routinely used for more than 1000 hours. It has been fully automatized resulting in a permanent display of the values of horizontal and vertical emittances without intervention of any operator.

EMITTANCE MONITORS BASED ON BRAGG-FRESNEL LENSES.

Ya.Hartman¹, E.Tarazona², P.Ellecaume², I.Snigireva², A.Snigirev².

¹ Institute of Microelectronics Technology Russian Academy of Sciences, 142432 Chernogolovka, Moscow district, Russia

² European Synchrotron Radiation Facility, BP220, F38043 Grenoble Cedex, France

Measuring the emittance of a third generation synchrotron radiation source is a non trivial problem. The existing emittance monitor at the ESRF is limited to emittances higher than 0.1-0.2 nm.rad. Imaging the source in the x-ray range is one of the solutions to measure lower emittances. Two emittance monitor setups based on Bragg-Fresnel lenses (BFL) have been tested on the so-called machine diagnostic beamline at the ESRF.

The first one is a two-lenses telescope : the source is imaged by a long focus BFL (1.25 m), this image is magnified by a short focus BFL (0.25 m). The magnification ratio of this system was 0.2. The image was then recorded by a high resolution CCD camera.

The second setup uses a single BFL (focal distance = 1.25 m) whose image is magnified in the vertical by an asymmetrically-cut crystal and recorded by using the same CCD camera. The magnification ratio was 0.6 in the vertical.

TuE53

DEVELOPMENT OF A FLUORESCENT X-RAY SOURCE FOR MEDICAL IMAGING

Fukai Toyofuku, Kenji Tokumori, Katsuyuki Nishimura, Tsuneo Saito, Masahiro Endo, Tohru Takeda, Yuuji Itai, Kazuyuki Hyodo, Masami Ando, Hiroaki Naito and Chikao Uyama
Kyushu University School of Health Sciences, 3-1-1 Maidashi, Higashi-ku, Fukuoka 812, Japan

Introduction

In medical imaging using synchrotron radiation, such as K-edge subtraction angiography and monochromatic X-ray CT, it is necessary to use high intensity monochromatic X-rays with different energies. There are several ways to produce such monochromatic X-rays. The most popular one is crystal diffraction, which has been used almost exclusively due to the fact that the energy spread is very narrow and the energy can be alternated continuously. In the United States as well as in Europe non-invasive coronary angiography of the line-scan method is presently undergoing clinical evaluation with positive results. However, in this method, it is difficult to obtain large area monochromatic X-rays with a rapid energy switching time.

The fluorescent X-rays, on the other hand, which are generated by irradiating the target materials with a white X-ray, offer a large beam size due to its divergent characteristics. The purpose of this study is to develop a fluorescent X-ray source, to investigate its fundamental characteristics, and to obtain separate contrast material images for both projection and CT imaging.

Materials and Methods

Fluorescent X-rays which range from about 20 keV to 70 keV are generated by irradiating several target materials with a white X-ray from 6.5 GeV SR-ring in Tsukuba (Fig.1). The intensity of fluorescent X-rays are $6.2 \times 10^5 \sim 3.0 \times 10^5$ photons / mm² · sec · mA at 30cm from the focal spot on the target.

The purity of the K_α X-rays are improved to better than 95% by using K_α attenuation filters. A phantom which contains three different contrast media (iodine, barium, gadolinium) is used for the K-edge energy subtraction subject.

Results

Projection Images for above and below each K-edge are obtained using imaging plates. By taking subtractions between images above and below each K absorption edge (33.17, 37.41, 50.23 keV), three separate contrast media images are successfully obtained. Monochromatic X-ray CT images are also obtained using a 64 channel CdTe array detector.

The fluorescent X-ray source using SR proved to be useful for quantitative, element selective imaging.

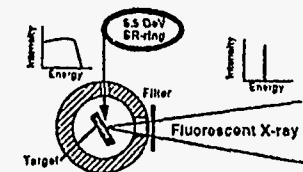


Fig.1 Fluorescent X-ray Source

TuE54

**The Optimisation of Multipole Wigglers as Sources of Polarised Radiation
for X-ray Experiments**

G.E. van Dorssen¹, H.A. Padmore²

¹DRAL Daresbury Laboratory, Warrington WA4 4AD, UK and NWO, P.O.
Box 93138, 2509 AC The Hague, The Netherlands

²Advanced Light Source, Lawrence Berkeley Laboratory, Berkeley CA 94720,
USA

The useful flux received in an experiment will depend both on the characteristics of the source and the characteristics of the experiment. It is therefore necessary when optimising the design of a synchrotron radiation source to take full account of the experimental requirements and not simply optimise the integrated flux or brilliance.

The method of optimisation used for multipole wigglers is described as applied to a proposed Medium Energy Source at Daresbury for absorption experiments using polarised radiation. The phase space of the source is first calculated [1], and then the phase space acceptance of the experiment is projected onto the source so that the flux in the overlap region can be calculated. The various parameters of the storage ring, electron energy, straight section length, emittance and beta functions as well as the magnetic structure of the radiation source can then be searched to find an optimum combination.

Results are presented for hybrid multipole wigglers [2] for both linear and circular polarised radiation in the photon energy range 500 - 5000 eV. For a 3 GeV electron energy it was found that the maximum length of the multipole wiggler is determined by the acceptable source broadening, due to the depth of the source. In the case of absorption spectroscopy in transmission or fluorescence mode a length of 10 m for the multipole wiggler at $B = 1.1$ T and period length of 93 mm is the maximum useful length. When the source characteristics are more important, specially the depth of the source, the maximum useful length reduces to 4 m.

References

1. R. Coisson, S. Guiducci and M.A. Preger, Nucl. Instrum. Meth. 201, 3 (1982).
2. K. Halbach, J. de Physique, Coll. C1 44, C1-211 (1983).

TuE55

LBL-35575A

**Performance of Photon Position Monitors for Undulator Beams
at the Advanced Light Source**

Tony Warwick
Lawrence Berkeley Laboratory, Berkeley, CA 94720, USA

Photon position monitors are installed at three undulator beamlines at the advanced light source. They operate using photocurrents from cooled metal blades which protrude into the photon beam and they are being used to monitor the stability of the electron beam in the storage ring. The measured performance will be described. The monitors are sensitive to motion of the undulator beams at the $1\mu\text{m}$ level, and are carefully engineered to be stable monuments for the facility.

These monitors are calibrated by being moved across the beam of photons and when they are used as a pair the detected motion of the photon beam can be extrapolated back to the center of the undulator as an angular and positional shift of the electron beam. Signals are large and there is relatively little sensitivity to the light from bend magnets.

When the undulator gap is changed the illumination pattern at the monitor changes. Careful positioning and calibration of the detectors is necessary to minimize any false information about beam motion when these changes occur. The calibration procedure and the results will be described in detail.

This work was supported by the Director, Office of Energy Research,
Office of Basic Energy Sciences, Materials Sciences Division of the U.S.
Department of Energy, under Contract No. DE-AC03-76SF00098

*This paper should be considered as a POSTER, contact:
Dr. Tony Warwick, 2-400 Lawrence Berkeley Laboratory,
Berkeley, CA 94720.
Tel. (510) 486 5819 Fax (510) 486 7696*

TuE56

THE LCLS - A 4th GENERATION LIGHT SOURCE USING THE SLAC LINAC

Herman Winick (for the LCLS Group) *

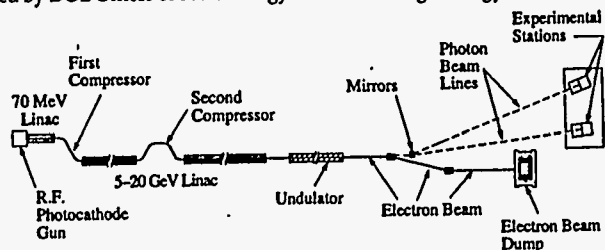
SSRL/SLAC, P.O. Box 4349, MS 69, Stanford CA 94309, USA

Recent technological developments make it possible to consider use of the SLAC linac to drive a Linac Coherent Light Source (LCLS) - an X-ray laser operating down to the Angstrom range. The LCLS operates on the principle of the Free Electron Laser (FEL); i.e., coherent, stimulated emission is achieved by inducing a bunch density modulation at the optical wavelength on a bright, relativistic electron beam as it passes through an undulator. However, in the LCLS this is achieved in a single pass, *without* the optical cavity resonator that is normally used in multi-pass, longer wavelength FELs. Thus, this approach, called Self-Amplified-Spontaneous-Emission (SASE), is extendable to wavelengths below the region in which reflectors can be used to make such a cavity.

The LCLS offers three or more orders of magnitude higher average brightness and nine or more orders of magnitude higher peak brightness than third generation synchrotron radiation sources. Furthermore, the radiation is diffraction limited, with full transverse coherence and with a longitudinal coherence length of ~1000 times the wavelength. The pulse duration is about 300 fs (FWHM) or less. The peak power during the pulse is 10-100 GW and the average power (at a 120 Hz repetition rate) is about 1 W or less. The radiation would normally be linearly polarized, but could also be circularly polarized. About 10^{13} coherent X-ray photons within a bandwidth of about 0.1% are produced per *sub-picosecond pulse*. By comparison, undulators on third generation X-ray sources such as the ESRF in Grenoble, the Advanced Photon Source at Argonne, and the Spring-8 facility in Japan will produce up to 10^9 - 10^{10} coherent X-rays *per second* within a similar bandwidth in the Angstrom range.

With present technology, an LCLS could be built to operate at wavelengths down to about 20 Angstroms. With improvements to technical components, it should be possible to extend this to wavelengths as short as a few Angstroms. The longer-wavelength region is of interest primarily for microscopy and imaging of biological samples. Though the intense, fast pulse of the LCLS could produce an image in a single shot, multiple images would be required to completely characterize a sample, and radiation damage to biological samples would be a major problem. There is more general scientific interest in the short-wavelength region. Here, the high coherence and ultra-short pulse capabilities of the LCLS would allow fundamentally new types of research to be carried out in chemistry, materials science, physics, and structural biology. Time-resolved studies of crystal lattice motions and fast chemical reactions would be possible. Enough coherent photons would be available to study nonlinear optical properties of materials in the X-ray region. Radiation damage is not seen as an insurmountable problem in this spectral region, due to greater X-ray penetration depths and more robust types of samples.

*Supported by DOE Offices of Basic Energy Science and High Energy & Nuclear Physics



TuE57

A Wire Scanning SR Position Monitor for Insertion Devices
Zhang Xiaowei, Hiroshi Sugiyama, Masami Ando, Xia Shaojian*,
Hideaki Shiwaku**
Photon Factory KEK, Japan, BESR IHEP, China, Spring-8 Team
JAERI, Japan

Precise monitoring of position of a SR beam from an insertion device is quite necessary not only for precision x-ray diffraction experiments, but also for operation of the next generation SR sources. Some ideas based on a pair of triangular photo-emission electrodes with an analogue electric arithmetic circuit to monitor the SR beam position have been applied at several facilities. Although they have been used successfully for bending magnet sources, they can not be applied to a SR beam from an undulator because of the following reasons. (1) It is technically difficult to design a pair of water cooled electrodes irradiated by a high-power-density beam, the position of which is to be monitored. (2) The beam position is detected through subtraction of photo-currents produced by the individual electrodes. When the deflection parameter of the undulator is changed, spatial (and spectral) distribution of the radiation is also changed. This change may generate a false signal of the change in the beam position. Therefore, this type monitor can be used for the undulator radiation only when its calibration is made precisely with respect to the deflection parameter which changes continuously.

On the basis of a different and new idea, we devised a wire-type beam position monitor for an x-ray undulator, and examined its feasibility and operational limitation in the beam line BL-NE3 in the AR by using radiation from the x-ray undulator U#NE3. Test result obtained by the wire-type position monitor is given in Fig. 1 which corresponds a result obtained by a graphite wire of 0.1-mm thickness and 0.5-mm width and the undulator gap of 20mm.

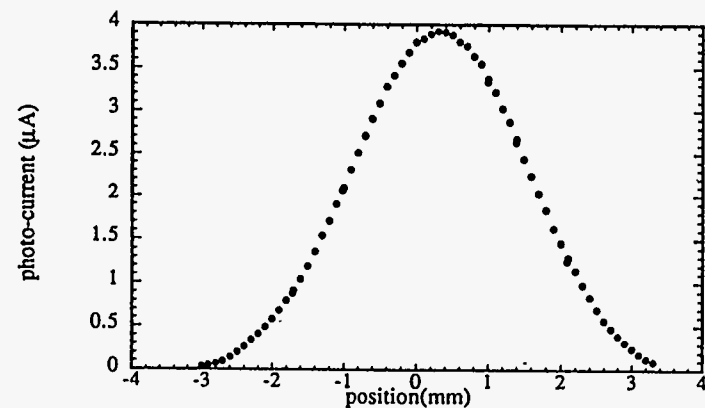


Photo-electron current versus wire position
the graphite wire of 0.1-mm thickness and 0.5-mm
width used in the condition of the electric shield
bias of 1000V and the undulator gap of 20 mm.

TuE58

Computer simulation study of undulator radiation

K.Yagi, M.Yuri, S.Sugiyama, and H.Onuki

Electrotechnical Laboratory, 1-1-4 Umezono, Tsukuba-shi, Ibaraki 305, Japan

A polarizing undulator with crossed and retarded magnetic field has been constructed and installed¹⁾ in the electron storage ring TERAS of ETL. Detailed specification of its design¹⁾ and absolute spectral intensity and polarization characteristics in the visible region²⁾ have already been published. The results indicate that even a four-period short undulator can produce extremely bright radiation and high degree of polarization. However, optimum use of the undulator radiation requires knowledge of spectral intensity and the polarization under the realistic condition.

We present calculations of the radiation from the four-period undulator¹⁾ by use of the general radiation equation and either numerical integration including the effect of electron beam emittance, energy spread, finite observation distance and collection angle. Methods of calculating the undulator radiation properties have been discussed widely and several different approaches put forward by many authors. Most of them use a simplified form of the radiation equation and an analytic formula for the electron trajectory in an ideal undulator. With this simplification, which is valid in most cases, the analytic formulae have been able to derive for the case of ideal electron trajectories. However, a numerical integration of the general radiation equation is necessary to calculate accurately the radiation properties of our four-period short undulator because actual form of magnetic field is not simple.

Despite the fact that some programs exist for such calculations, none of them include accurate electron beam properties. Realistic modeling of the electron beam including beam emittance effect and energy spread effect is essentially required for these calculations if accurate performance predictions are necessary. Thus electron beam profiles must be experimentally determined, even though it is difficult to do. We have recently overcome this difficulty to successfully calculate undulator radiation spectral intensity and degree of polarization. The undulator radiation was focused with a lens and the transverse beam profile was imaged on the detection surface of a CCD camera. The observed electron beam was modeled by a standard binary normal distribution. Using the Monte Carlo method, we can take into account the effect of electron beam emittance, energy spread, finite observation distance and collection angle. Fig. 1 shows measured and calculated spectral intensity. Fig. 2 displays comparison between measured and calculated Stokes parameters.

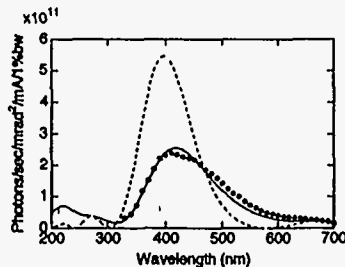


Fig. 1: Spectral intensity of the undulator radiation with $E=230\text{MeV}$, $K=1.0$. The dashed and solid curves are the spectra calculated for a zero-emittance electron beam and for actual electron beam, respectively. The dotted is measured spectrum.

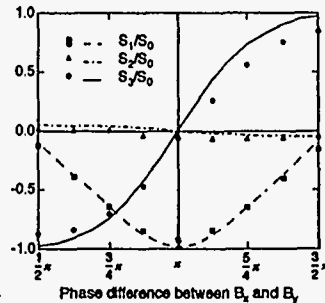


Fig. 2: Undulator phase dependence of Stokes parameters. Markers and lines indicate measured and calculated Stokes parameters, respectively.

1) H.Onuki, N.Saito, T.Saito, and M.Habu, Rev. Sci. Instrum. 60, 1838 (1989)

2) K.Yagi, H.Onuki, S.Sugiyama, and T.Yamazaki, Rev. Sci. Instrum., 63, 396 (1992)

A super-brilliant x-ray undulator for the Tristan Super Light Facility

Shigen YAMAMOTO, Tatsuro SHIOYA, Kimichika TSUCHIYA, and Hideo KITAMURA

Photon Factory, National Laboratory for High Energy Physics, KEK, Tsukuba Ibaraki 305, Japan

In the National Laboratory for High Energy Physics, KEK, various R&D studies are being carried out, in order to renew the Tristan Main Ring (MR) for high energy physics to a very low emittance accelerator with about $1\text{nm}\cdot\text{rad}$ and to convert it to a novel synchrotron light source, which is called the "Tristan Super Light Facility (TSLF)".

This source is characterized by extremely brilliant radiation and coherent radiation produced by the low emittance beam in undulators and free electron lasers (FEL's). When we optimize the MR for synchrotron-radiation experiments, three of four 200-m long straight sections of the present MR will be used for installing undulators by greatly reducing the number of RF cavities. Each straight section is bent slightly outward for the extraction of light beams to form a 200-m arc, and is divided into two long (70m) sections and two short (6m) ones; the 70-m and 6-m sections in an upper-stream half of the arc are to be used.

Since the total length of the undulators required for the TSLF amounts to 400m, it is not very practical to design and construct such undulators using a device-by-device policy, from both the view-points of design and construction costs as well as from that of man-power for commissioning and operation. Here, we propose a new scheme using a standardized unit undulator, in which: (1) three unit undulators are placed very precisely on a common frame for the short undulator (5.4m long); (2) for long undulators with about 70-m length, these short undulators will be connected longitudinally.

In accordance with the above-mentioned concept, we have been constructing a prototype of the short undulator (named XU#MR0; 4.5cm periodicity \times 120 periods) using permanent magnets in the pure type and out-of-vacuum configuration, and exploring and solving various mechanical problems, including thermal expansion and alignment issues, which will arise in the actual construction of standardized undulators for the TSLF in future. The XU#MR0 will further be used as the first undulator in a feasibility study for the TSLF planned in autumn, 1995. A calculation shows that it is able to produce quasi-monochromatic x rays as the first harmonic with a brilliance of 1.0×10^{18} [photons/s/mm²/mrad²/0.1% bandwidth] at 14.4keV in the case of $K=0.97$, when the MR is operated at 10GeV and 10mA.

Design of the ISI-800 for the Ukrainian National Synchrotron Center. V.BAR'YAKHTAR*, E.BULYAK, A.GEVCHUK, P.GLADKIKH, I.KARNAUKHOV, S.KONONENKO, V.MOLODKIN*, A.MYTSYKOV, V.NEMOSHKALENKO*, A.SHCHERBAKOV, A.SHPAK*, A.ZELINSKY
Institute of Physics and Technology, 310108 Kharkov, Ukraine.
*Metallophysics Institute of the Ukrainian Academy of Sciences, 252142 Kiev, Ukraine.

The synchrotron radiation source for the scientific and industrial applications is designed at Kharkov Institute of Physics and Technology. Main systems of the 800 MeV electron storage ring are described. Given are the principal characteristics of the storage ring magnet elements and the system of beam transport from the 120 MeV electron linac to the storage ring; production and positioning tolerances are also presented. The ring lattice is to provide low beam emittance ($2.5 \cdot 10^{-6} \text{ m}^2$), large enough dynamic aperture and to decrease sensitivity to the collective effects.

The construction of the complex is scheduled to start in 1994.

The Conference will correspond with A.SHCHERBAKOV
Address: KFTI, Akademicheskaya St., Kharkov 310108 Ukraine
Phone number (057-2) 3 51 993
FAX (057-2) 3 51 738
E-mail SASHA_PSRL%KFTI.KHARKOV.UA@RELAY.USSR.EU.NET

TuE61

A combined magnet lattice of the synchrotron light source ISI-800. I.KARNAUKHOV, S.KONONENKO, V.MOLODKIN*, V.NEMOSHKALENKO*, A.SHCHERBAKOV, A.SHPAK*, A.TARASENKO

Institute of Physics and Technology, 310108 Kharkov, Ukraine.
*Metallophysics Institute of the Ukrainian Academy of Sciences, 252142 Kiev, Ukraine.

The design of an electron storage ring for low emittance mode operation is presented. The parameter optimization is based on the spectrum and on beam source sizes and on general specifications for the machine performance such as dynamic aperture, lifetime. Superconducting magnets in the middle of a TBA cell with a high field are used in the storage ring.

The Conference will correspond with A.SHCHERBAKOV
Address: KFTI, Akademicheskaya St., Kharkov 310108 Ukraine
Phone number (057-2) 3 51 993
FAX (057-2) 3 51 738
E-mail SASHA_PSRL%KFTI.KHARKOV.UA@RELAY.USSR.EU.NET

TuE62

Time	WEDNESDAY, JULY 20, 1994
	SOURCES
	<p style="text-align: center;">WeA Staller Center Chairpersons: M. Kihara (PF); H. Winick (SSRL)</p> <p>8:30 A. Hofmann (CERN) <i>Accelerator based photon sources</i></p> <p>9:15 G. Mulhaupt (ESRF) <i>Particle beam stability</i></p> <p>9:35 D.E. Moncton (APS) <i>Operational stability</i></p> <p>9:55 A. Wrulich (ELETTRA) <i>Commissioning</i></p> <p>10:15 Coffee Break</p> <p>10:45 H. Kitamura (KEK) <i>Insertion devices</i></p> <p>11:05 Y.-C. Liu (SRRC) <i>Building a 3rd generation source</i></p> <p>11:25 S. Krinsky (NSLS) <i>Evolution of 2nd generation sources</i></p>
12:30	LUNCH
2-5:30	VISIT THE NSLS
6:00-10:00	BANQUET

Session WeA - Invited Talks

Review of accelerator based sources; A. Hofmann, CERN.

The development of storage rings for synchrotron radiation have now arrived at so-called third generation and have straight sections with optical functions optimized for undulators and electron beams of very small emittances. The beam optics of the ring is chosen as to minimize the quantum excitation of betatron oscillations which determines the emittance. This can be achieved with a ring containing many cells with a small bending angle and with strong focusing in each cell. The first point results in large and expensive rings and both points require strong sextupole magnets for the chromaticity correction which can limit the dynamic acceptance. The optimization of storage rings with these points in mind lead to lattices which have achromatic cells with two, three or more bending magnets. Studies for future rings consider further methods like the use of wigglers, combined function magnets, increased transverse damping partitions etc. in order to obtain even smaller emittances which approach the diffraction limit.

BEAM STABILITY IN THE 3RD GENERATION SR SOURCES

G.Mülhaupt

European Synchrotron Radiation Facility

After recapitulation of the principal sources for beam instability, the different ways to minimise beam instability at the design stage and during operation are discussed. The presently achieved beam stability data (presently a few percent of the beam sizes at the ESRF) and the limitations of beam position measurements are presented.

ACHIEVING HIGHER OPERATIONAL STABILITY AND RELIABILITY IN 3RD. GENERATION SOURCES

D. E. MONCTON

Advanced Photon Source, Argonne National Laboratory, Argonne, Illinois 60439

In order to maximize the scientific effectiveness of the high brilliance radiation provided by third generation x-ray sources, a high degree of operational reliability and stability must be achieved. Beyond the basic physics considerations of particle beam stability, a number of opportunities exist to improve performance from the users perspective. Perhaps the most exciting of these is the possibility to inject essentially continuously thereby effectively eliminating the decay of the particle beam, the associated thermal cycling of the machine and the beamline optics, and the need for injection downtime. Smaller undulator gaps and consequently higher photon beam are then possible since the decrease in beam lifetime is compensated. This and other examples of systems and instrumentation for enhancing stability and reliability will be described.

Commissioning of Third Generation Light Sources

A. Wrulich, Sincrotron Trieste

World-wide, four third generation light sources have been set in operation during the last few years, the ESRF, SRRRC, ALS and ELETTRA. An overview on the commissioning of these sources is given with the emphasis on the specific experience with ELETTRA.

Time	THURSDAY, JULY 21, 1994
	OPTICS
	<p style="text-align: center;">ThA Staller Center Chairpersons: M. Hart (Manchester); V. Saile (CAMD)</p> <p>8:30 C. Kunz (HASYLAB) <i>VUV Optics = Science</i></p> <p>9:00 M. Ando (KEK) <i>X-ray Optics = Science</i></p> <p>9:30 K-J Kim (LBL) <i>Phase space descriptions of sources</i></p> <p>9:50 T. Warwick (ALS) <i>Brightness conservation with UV optics</i></p> <p>10:10 Coffee Break</p> <p>10:30 L. Berman (NSLS) <i>Brightness conservation with X-ray optic</i></p> <p>11:00 J. Susini (ESRF) <i>Adaptive optics</i></p> <p>11:20 A. Snigirev (ESRF) <i>Bragg-Fresnel</i></p> <p>11:40 D. Bilderback (CHESS) <i>Capillary Optics</i></p> <p>12:00 W.B. Yun (APS) <i>Zone Plates</i></p>
12:30	LUNCH
2-5:30	OPTICS POSTERS (ThD)
6:00	DINNER
7:00-10:00	DETECTOR POSTERS (ThE)

Session ThA - Invited Talks

NEW XUV OPTICS - NEW SCIENCE

*Christof Kunz and Joachim Voß
II. Institut für Experimentalphysik
Universität Hamburg, Luruper Chaussee 149
22761 Hamburg, Germany*

Optical elements need to be developed at least at the same pace as synchrotron radiation sources of the third generation. The talk will deal with measurements of optical constants as the basis for the optimization of filters, coating of mirrors and gratings and multi-layer engineering. Efficiency performance of gratings with multi-layer coatings will be shown. Imaging with zone plates and capillary optics is mentioned only marginally. The same holds for the heat load problem and adaptive optics. The attempts made to obtain good imaging and light concentration for scanning microscopy with aspherical optics are described on the basis of our own microscopy project. Results are shown with photoemission and fluorescence as the imaging signal.

Several ways to circumvent aspherical optics with combinations of spherical mirrors are shown. The special case of an optimized non-concentric Schwarzschild objective is described and our first results are given. The results of other groups in this field are reviewed. Science being done with improved optics will produce revolutionary results only in rare cases, but will move rather gradually into new directions.

X-Ray Optics-----Science

---Trend and Trial Towards a Fourth Generation Light Source
Started from the PF Ring, the AR, Through the TRISTAN MR---

Masami Ando

Photon Factory, KEK, Oho 1-1, Tsukuba, Ibaraki 305. Japan

Relations between x-ray optics and its associated sciences are somewhat similar to a couple of wheels linked with the axle: one needs the other; a proper and smooth rolling is available only when both are fine tuned. The following items may provide some flavour of such progress of x-ray science and optics.

- (1)"A monolithic channel-cut monochromator for a fixed exit beam position" applied to powder diffractometry.
- (2)"A quasi-doubly bent crystal monochromator" applied to magnetic Compton scattering experiments.
- (3)"A skew monochromator" applied to polarization analysis of x-ray magnetic Kerr rotation of a Gd single crystal.
- (4)"A monolithic (+,+) monochromator" applied to precision measurement of absolute lattice spacing of GaAs single crystals.
- (5)"An asymmetric monochromator" applied to intravenous angiography.
- (6)"A cryogenic cooling double crystal monochromator" applied to production of Mossbauer photons and parametric scattering.
- (7)"A combination of channel-cut monochromators for high energy resolution beam" applied to inelastic scattering.
- (8)"An interferometer" applied to measurement of degree of coherence.

References:

- (1)P. Spieker, M. Ando and N. Kamiya: Nucl.Instr. & Meth.,222(1984)196-201 and R. Uno, H. Ozawa, T. Yamanaka, H. Morikawa, M. Ando, K. Ohsumi, A. Nukui, K. Yukino and T. Kawasaki: Aust.J.Phys.,41(1988)133-144.
- (2)H. Kawata, M. Sato, T. Iwazumi, M. Ando, N. Sakai, M. Ito, Y. Tanaka, N. Shiotani, F. Itoh, H. Sakurai, Y. Sakurai, Y. Watanabe and S. Nanao: Rev. Sci. Instr.,62-9 (1991) 2109-2114 and Y. Tanaka, N. Sakai, Y. Kubo, H.Kawata: Phys.Rev.Lett.70(1993)1537-1540.
- (3)K. Mori, K. Namikawa, Y. Funahashi, Y. Higashi and M. Ando: Rev.Sci.Instr.,64-7(1993)1825-1830.
- (4)K.Usuda,S.Yasuami, T.Fujii, Y.Higashi, H.Kawata and M.Ando: J.Appl.Phys.,69-1(1991)182-184.
- (5)H. Shiwaku, K. Hyodo, M. Ando: Jpn.J.Appl.Phys.,30-12A(1991)L2065-L2067 and S. Ohtsuka, Y. Sugishita, M. Kakihana, H. Watanabe, T. Takeda, Yuji Itai, K. Hyodo and M. Ando: submitted to J. Circulation.
- (6)X. Zhang, T. Mochizuki, H. Sugiyama, S. Yamamoto, H.Kitamura, T. Shioya, M. Ando, Y. Yoda, T. Ishikawa, C. K. Suzuki and S. Kikuta: Rev. Sci. Instrum., 63 (1992) 404 and S. Kikuta, Y. Yoda, Y. Hasegawa, K. Izumi, T. Ishikawa, X. Zhang, S.Kishimoto, H. Suigiyama, T. Matsushita, M. Ando, C. K. Suzuki, M. Seto, H. Ohno and H. Takei: Hyperfine Interactions 71 (1992) 1491-1494 and K. Namikawa, H. K. Uematsu, M. Ohi, X. Zhang, M. Ando and S. Itoh: to be submitted to Phys.Rev.Lett.
- (7)Y. Yoda, S. Kikuta, X. Zhang & others: in preparation.
- (8)K. Izumi, S. Kikuta, X. Zhang & others: in preparation.

Phase Space Description of Synchrotron Radiation Sources*

Kwang-Je Kim
Center for Beam Physics
Lawrence Berkeley Laboratory
Berkeley, California 94720

We review the phase space description of synchrotron radiation sources and its application. Approximate formulae for the phase space distributions for bending magnets, wigglers and undulators will be discussed, pointing out their different characteristics. These formulae are useful as an invariant characterization of the radiation strength as well as in deciding insertion device parameters for a particular application.

- This work was supported by the Director, Office of Energy Research, Office of Basic Energy Sciences, Materials Sciences Division, of the U.S. Department of Energy under Contract No. DE-AC03-76SF00098.

Implementation of VUV beamlines for high brightness, high flux and high resolution at third generation light sources.

Tony Warwick

Lawrence Berkeley Laboratory, Berkeley, CA 94720, USA

VUV beamlines at third generation synchrotrons must be carefully designed to deliver the bright light promised from these new sources. There are many ways in which the optical manipulations of the light in the line can degrade the brightness. Design decisions must be made with close regard for the type of experiment to be served, so that the most important parameters can be optimized. Beamline components must be carefully engineered, and the cooling of optics is critical. The geometrical and spectral properties of the undulator beams at the low emittance storage rings are very interesting and they impose new requirements on the coordination between the experiment, the beamline operation and the control of the accelerator. The cost of beamlines is higher than ever before so that ease of operation with multiple users is at a premium. These beamlines have become integrated systems, with the optical design influenced by engineering considerations and by the storage ring parameters.

Present and future designs of beamlines for VUV light will be described from this point of view. Features of operational lines will be illustrated, and lessons for the future will be discussed.

This work was supported by the Director, Office of Energy Research, Office of Basic Energy Sciences, Materials Sciences Division of the U.S. Department of Energy, under Contract No. DE-AC03-76SF00098

This paper should be considered as an INVITED TALK contact:

Dr. Tony Warwick, 2-400 Lawrence Berkeley Laboratory, Berkeley, CA 94720.

Tel. (510) 486 5819 Fax (510) 486 7696

warwick@lbl.gov

Preserving the High Source Brightness
with X-Ray Beam Line Optics

Lonny E. Berman
National Synchrotron Light Source
Brookhaven National Laboratory
Upton, NY 11973, USA

A first-order challenge facing developers of x-ray beam line optics at synchrotron sources lies in producing optics that faithfully deliver the brightness of the source, especially in the presence of adverse power loads. Considerable world-wide effort has been devoted to this problem. Once overcome, continued use of beam line optics in experiments often reveals a second-order challenge, that of preservation of the source brightness over time, especially as the electron beam current and other environmental conditions change. This requires maintaining stability, with beam line optics, of the widths and centroid positions of the various parameters that contribute to the brightness, the wavelength, position, and angle distributions of the delivered photon beam. As such a problem only becomes apparent over the course of time, so does the implementation of proper solutions. This problem spans all generations of synchrotron sources. A few ideas on the use of x-ray monochromators, mirrors, apertures, and position-sensitive monitors to stabilize the brightness parameter distributions, as well as methods to avoid or minimize transients in the first place, will be discussed. Appropriate examples based on experiences at the X25 wiggler beam line at the National Synchrotron Light Source (NSLS) will be presented.

This work was supported by DOE Contract No. DE-AC02-76CH00016.

Microbeam Generation with Capillary Optics - Donald H. Bilderback and Dan J. Thiel,
Cornell High Energy Synchrotron Source, Cornell University, Ithaca, New York, 14853,
USA

Tapered glass capillaries are very useful optical components for generating microbeams of x-rays on a micron scale. A capillary concentrator produces a small diameter beam from a large beam as it passes through a long hollow needle-like structure. The x-rays are compressed in cross sectional area as they successively totally reflect from the smooth inner wall of the glass tube. The beam compression can be efficient if reflection from the inner wall takes place at angles less than the critical angle of reflection. For hard x-rays and borosilicate glasses, the critical angle is about 3 milliradians at 10 keV.

Optics based on capillaries have a number of advantages. They have been shown useful to condense monochromatic or white (or very wide bandpass) beams down on a scale of from millimeter size to 50 nanometers. Intensity gains (x-rays/second/area) as high as 1000 have been observed with synchrotron radiation sources. Ideal optics calculations show that gains up to 100,000 may be possible in the future.

The output divergence of the optic depends on its energy of operation and the taper angle of the needle. We have constructed pipettes that produce anywhere from 2 to 8 milliradians of divergence from a CHESS bending magnet x-ray source where the natural divergence is 0.1 mrad for x-rays whose energy range from 5 to 25 keV.

We believe that capillary optics will have a wide impact on application areas such as x-ray crystallography, fluorescence, tomography, spectroscopy, high-pressure diffraction, etc. They may be of use where ever a very small beam is required. In this paper, we will review the general properties of capillary optics and a few of the first applications that have been made in crystallography and imaging.

Submitted by Donald Bilderback, 281 Wilson Laboratory, Cornell University, Ithaca, NY,
14853, USA, Ph: (607)-255-0916, Fax: (607)-255-9001, Email: dhb2@cornell.edu

Optics Posters

(Session ThD)

- ThD1 Alp, E.E., Toellner, T., Sturhahn, W., Mooney, T. X-Ray Optics Development for Nuclear Resonant Scattering Beamline at APS.
- ThD2 Assoufid, L., Lee, W.K., Mills, D.M. A Finite Element Analysis of Room Temperature Silicon Crystals for the APS Bending Magnet and Insertion Device Sources.
- ThD3 Bahrtd, J., Flechsig, U., Senf, F. Beamline Optimization Using Phase Space Transformation.
- ThD4 Belakhovsky, M. Mirror of Integrated Design for the CRG/IF Beamline at ESRF.
- ThD5 Bernstorff, S., Busetto, E., Colapietro, M., Savoia, A. A Fixed-Exit Double-Crystal Monochromator for the Crystallography Wiggler Beamline at ELETTRA: Concept of the Crystal Movements.
- ThD6 Lausi, A., Bernstorff, S. Light Choppers: A New Approach to the Problem of Heat Load on Samples and Optical Elements at ELETTRA Beamlines.
- ThD7 Bissen, M., Fisher, M., Rogers, G., Eisert, D., Kleman, K., Nelson, T., Mason, B., Middleton, F., Hochst, H. First Test Results of SRC's New High Energy Variable Line Density Grating Monochromator.
- ThD8 Blasdell, R.C., Macrander, A.T. Prototype Grooved and Spherically Bent Si Backscattering Crystal Analyzers for meV REsolution Inelastic X-Ray Scattering.
- ThD9 Busetto, E., Lausi, A., Bernstorff, S. The High Energy Monochromator for the ALOISA Beamline at ELETTRA.
- ThD10 Comin, F. A Cryogenically Cooled, Sagittal Focusing Scanning Monochromator for ESRF.
- ThD11 Cowan, P.L., Beno, M.A., Bedzyk, M., Jennings, G., Knapp, G.S., Montano, P.A., Ramanathan, M. Mirror First, A Heat Load Strategy for the BESSRC Undulator Beamline at the Advanced Photon Source.
- ThD12 Darovsky, A., Meshkovsky, I., Coppens, P. A Compact Monochromator for Multi-Purpose Synchrotron Beamlines.
- ThD13 Doing, P., Increased Throughput of a Heat Loaded Double Crystal Di(111) Monochromator by Roughening of the Second Crystal Surface.
- ThD14 Dolbnya, I.P., Zolotarev, K.V., Sheromov, M.A., Antonov, A.A., Grigoryeva, I.G. Parabolic Focusing Pyrolytic Graphite X-Ray Monochromator.
- ThD15 Ferrer, J.L., Roth, M., Fanchon, E., Simon, J.P., Berard, J.F. A Thermal Bilayer Monochromator Crystal for a High Resolution Multi-Wavelength Anomalous Diffraction Beam Line at the ESRF.
- ThD16 Yamaoka, H., Freund, A.K., Ohtomo, K., Krumrey, M. A Crystal Bender for Water-Cooled Monochromator in High Head Load Synchrotron Radiation Wiggler Beamline at ESRF.
- ThD17 Graessle, D.E., Fitch, J.J., Ingram, R., Zhang, J., Blake, R.L. A Reflectometer End Station for Synchrotron Calibrations of AXAF Flight Optics and for Spectrometric Research Applications.
- ThD18 Hahn, U., Gurtler, P. The Mirror Concepts of the New Wiggler and Undulator Beamlines at HASYLAB.
- ThD19 Hiraya, A., Matsuda, K., Hai, Y., Watanabe, M. Performance Check of β -Alumina as a Soft X-Ray Monochromator Crystal.
- ThD20 Hiraya, A., Nakamura, E., Hasumoto, M., Kinoshita, T., Sakai, K., Ishiguro, E., Watanabe, M. Construction of 15m Constant-Deviation Constant-Length Grazing Incidence Monochromator at UVSOR.
- ThD21 Howells, M.R., Irick, S.C., McKinney, W.R., Lowrey, W.H., Tonnessen, T.W., Anthony, F.M. Design for a High-Optical-Quality, Tunable-Radius X-Ray Mirror.

- ThD22 Hrdy, J. Distortions of the Exit Beam from Asymmetric and Inclined Double Crystal Synchrotron Radiation Monochromators.
- ThD23 Hung, H.H. Revised SHADOW Calculation for Asymmetrically Cut Monochromator.
- ThD24 Irick, S.C., Kaza, R.K., McKinney, W.R. Obtaining Three-Dimensional Height Profiles from a Two-Dimensional Slope Measuring Instrument.
- ThD25 Ishiguro, E., Kawashima, T., Yamashita, K., Kunieda, H., Yamazaki, T., Sato, K., Koeda, M., Nagano, T., Sano, K. Multilayer Coated Gratings for the Soft X-Ray Region.
- ThD26 Ishikawa, T. Applications of Extremely Asymmetric Diffraction in Synchrotron X-Ray Optics.
- ThD27 Yamaoka, H., Ohtomo, K., Ishikawa, T. Diamond Crystal Monochromator in a SPring-8 Undulator Beamline.
- ThD28 Ito, K., Morioka, Y., Ukai, M., Kouchi, N., Hatano, Y., Hayaishi, T. A High Flux 3-M Normal Incidence Monochromator at Beamline 20A of the Photon Factory.
- ThD29 Ito, K., Yoshino, K., Thorne, A.P., Smith, P.L., Murray, J.E., Parkinson, W.H. The Combination of a VUV Fourier Transform Spectrometer and Synchrotron Radiation.
- ThD30 Jark, W., Melpignano, P., DiFonzo, S., Bianco, A. Optimization of Spherical Grating Monochromators Operating With Variable Included Angle for Different Applications.
- ThD31 Jensen, B.N., Mancini, D.C., Nyholm, R. Thermal Effects of Undulator Radiation on Si Optics for a Plane Grating Monochromator.
- ThD32 Kamijo, N., Tamura, S., Suzuki, Y., Kihara, H. Fabrication and Testing of Hard X-Ray Sputtered-Sliced Zone Plate.
- ThD33 Khounsary, A.M., Yun, W. Contact Cooling for High Heat Load Synchrotron X-Ray Mirrors.
- ThD34 Kirkland, J.P., Elam, W.T. A UHV-Compatible Fixed-Exit Two-Crystal Monochromator.
- ThD35 Knapp, G.S., Rogers, C.S., Beno, M.A., Wiley, C.L., Jennings, G., Bedzyk, M.J., Cowan, P.L. A Cryogenic Monochromator as a Solution to Undulator Heat Loads at Third Generation Synchrotron Sources.
- ThD36 Koike, M., Chiwaki, M., Suzuki, I.H. A Helicon Plasma Sputtering System for Fabrication of Multilayer X-Ray Mirrors.
- ThD37 Koike, M., Namioka, T., High-Resolution Grazing Incidence Plane Grating Monochromator for Undulator Radiation.
- ThD38 Underwood, J.H., Malck, C.K., Gullikson, E.M., Krumrey, M. Multilayer Coated Echelle Gratings for Soft X-Rays and Extreme Ultraviolet.
- ThD39 Yamaoka, H., Freund, A.K., Ohtomo, K., Krumrey, M. Test of a Crystal Bender for a Water-Cooled Monochromator Crystal at a High Power Wiggler Beamline at ESRF.
- ThD40 Koronkevich, V.P., Kulipanov, G.N., Makarov, O.A., Mezentseva, L.A., Nazmov, V.P., Pindyurin, V.F., Churin, E.G. Preliminary Experience of Optical Elements Fabrication by X-Ray Lithography.
- ThD41 Kuroda, K., Kaneko, T., Itabashi, S. An Efficient Extraction Window for High-Throughput X-Ray Lithography Beamlines.
- ThD42 Senf, F., Lammert, H., Flechsig, U., Zeschke, T., Peatman, W.R. The Precision Demanded of a Rowland-Circle-Monochromator: Its Realisation.

- ThD43 Latimer, M.J., Rompel, A., Underwood J.H., Yachandra, V.K., Klein, M.P. A Simple In-Hutch Mirror Assembly for X-ray Harmonic Suppression.
- ThD44 Mancini, D.C., Nordgren, J., Wassdahl, N., Andersen, W., Nyholm, R. A Compact VLSG Monochromator for Enhanced Flux at MAX-Lab.
- ThD45 McKinney, W.R., Mossessian, D., Gullikson, E., Heimann, P. Efficiency and Stray Light Measurements and Calculations of Diffraction Gratings for the ALS.
- ThD46 Meron, M., Schildkamp, W., Doumas, J., Bender, J., Ewing, D. Design and Fabrication of a Conical Mirror for Hard X-Rays.
- ThD47 Miyahara, T., Kagoshima, Y. Importance of Wave-Optical Corrections to Geometrical Ray-Tracing for High Brilliance Beamlines.
- ThD48 Mochizuki, T., Zhang, X., Sugiyame, H., Zhao, J., Ando, M., Yoda, Y. Cooling of Silicon Monochromator Crystals for the High Heat Load Undulator Beamline NE3 of Tristan Accumulation Ring.
- ThD49 Mori, T., Sasaki, S. Improvement of Beam Divergence in Pseudo-Paraboloidal Bending of an X-Ray Mirror.
- ThD50 Nave, C., Gonzalez, A., Clarke, G., McSweeney, S. Use of Asymmetric Monochromators for X-Ray Diffraction on a Synchrotron Source.
- ThD51 Pauschinger, D., Becker, K., Ludewig, R., Garreis, R. Side Cooled 1200 mm Silicon X-Ray Mirror with Pneumatic Bender and In Situ, on Beamline Mirror Metrology.
- ThD52 Pflibsen, K.P., Stuppi, A., Goetz, A.J., McClain, D. Figure Sensing and Control of Synchrotron Radiation Mirrors.
- ThD53 Polack, F., Joyeux, D., Svatos, J. Applications of Wavefront Division Interferometers in Soft X-Rays.
- ThD54 Mercier, R., Fournet, P., Tissot, G., Marioge, J.P., Polack, F. Control at 11.4 nm of an XUV Schwarzschild Objective.
- ThD55 Qian, S., Jark, W., Takacs, P.Z. A Novel Scheme for the LTP (Long Trace Profiler) With Stationary Optical Head and Moving Penta-Prism.
- ThD56 Quintana, J.P., Dolin, Yu., Georgopoulos, P., Kushnir, V.I. Anticlastic Curvature Measurements on Unribbed Crystal Optics for Synchrotron Radiation.
- ThD57 Quintana, J.P., Hart, M., Bilderback, D., Henderson, C., Setterston, T., White, J., Hausermann, D., Krumerey, M. Adaptive Silicon Monochromators for High Power Insertion Devices; Tests at CHESS, ESRF and HASYLAB.
- ThD58 Ramanathan, M., Beno, M., Knapp, G.S., Jennings, G., Cowan, P., Montano, P.A. A Multipurpose Monochromator for the BESSRC CAT Beamlines at the APS X-Ray Facility.
- ThD59 Reininger, R., Severson, M.C., Hansen, R.W.C., Green, M.A., Trzeciak, W.S. VUV High Resolution and High Flux Beamline for the Aladdin Storage Ring.
- ThD60 Rode, A.V., Chapman, H.N. X-Ray Focusing of Synchrotron Radiation with Arrays of Reflectors.
- ThD61 Rogers, C.S., Assoufid, L. Design and Thermal Stress Analysis of High Power X-Ray Monochromators Cooled with Liquid Nitrogen.
- ThD62 Rowe, J.E., Malic, R.A., Chaban, E.E., Chiang, C.M., Smith, N.V. Photon Channeling in the Vacuum Ultraviolet Wavelength Range.

- ThD63 Rowen, M., Rek, Z.U., Tanaka, T., Wong, J. Characterization and Performance of YB66 as a Monochromator in the 1 to 2 keV Spectral Region.
- ThD64 Sanchez del Rio, M., Ferrero, C., Freund, A.K. Calculation of the Diffraction Pattern of a Set of Thin Perfect Crystals for a Bonse-Hart Camera.
- ThD65 Sanchez del Rio, M., Grubel, G., Als-Nielsen, J., Nielsen, M. Focussing Characteristics of Diamond Crystal X-Ray Monochromators. An Experimental and Theoretical Comparison.
- ThD66 Sasano, T., Ishiguro, E., Mitani, S., Tomimori, H. Reflectivities of CVD-Diamond Mirrors in the VUV Region.
- ThD67 Schildkamp, W. Modular Double Crystal Monochromator Design.
- ThD68 Schilling, P., Morikawa, E., Tolentino, H., Cusatis, C. Installation and Operation of the LNLS Double Crystal Monochromator at CAMD.
- ThD69 Schulte-Schrepping, H., Materlik, G., Heuer, J., Teichmann, T. A Novel Adaptive Directly Water Cooled Monochromator Crystal for High Heatload Wiggler Beamlines at HASYLAB.
- ThD70 Schulze, C., Chapman, D. PEPO - A Programme for the Calculation of the Reflectivity of Cylindrically Bent Laue Crystal Monochromators.
- ThD71 Senf, F., Methel, U., Peatman, W.B. Heat Load Problem of an Entrance Slit on an Undulator Beamline.
- ThD72 Siddons, D.P. Some Simple Bending Mechanisms for Bragg-Reflection X-Ray Optical Devices.
- ThD73 Smither, R.K., Fernandez, P.B. Focusing with Variable-Metric Crystals.
- ThD74 Snigirev, A.A., Suvorov, A.Y., Lequien, S. Backscattering Analyzer Geometry as a Straightforward and Precise Method for Monochromator Characterization at Third Generation Synchrotron Radiation Sources.
- ThD75 Snigirev, A.A. The Recent Development of Bragg--Fresnel Optics. Experiments and Applications at the ESRF.
- ThD76 Stephenson, J.D. Optimised Reflectivities from SR-Diamond-Laue-Monochromators.
- ThD77 Susini, J., Krumrey, M., Baker, R., Kvik, A. Adaptive X-Ray Mirror Prototype: First Results.
- ThD78 Susini, J., Laberge, D., Zhang, L. Compact Adaptive/Active X-Ray Mirror: Bimorph Piezoelectric Flexible Mirror.
- ThD79 Susini, J., Baker, R., Vivo, A. Optical Metrology Facility at the ESRF.
- ThD80 Suzuki, C.K., Zhang, X.W., Yoda, Y., Harami, T., Shiwaku, H., Izumi, K., Ishikawa, T., Ando, M., Ohno, H., Kikuta, S. SR Time Gate Quartz Device for Nuclear Resonant Scattering.
- ThD81 Takeshita, K. Chromatic Aberration of Asymmetrically-Cut Curved Crystal Due to Dynamical Diffraction Effect.
- ThD82 Tan, Z., MacDowell, A.A., Fontaine, B., Bjorkholm, J.E., Freeman, R.R., Himel, M., Tennant, D., Taylor, D., Wood II, O.R., Waskiewicz, W.K., Windt, D.L., White, D.L., Spector, S. At-Wavelength Metrology of 13 nm Lithography Imaging Optics.
- ThD83 Ulm, G., Wende, B. The Radiometry Laboratory of PTB at BESSY.
- ThD84 Fuchs, D., Krumrey, M., Muller, P., Scholze, F., Ulm, G. The New PTB Reflectometer at BESSY.
- ThD85 Uruga, T., Ohtomo, K., Yamaoka, H. Heat Load Analysis for Pre-Mirrors at SPring-8 Undulator Beamlines.

- ThD86 Uruga, T., Hashimoto, S., Kashihara, Y., Kimura, H., Kohmura, Y., Kuroda, M., Nagasawa, H., Ohtomo, K., Okui, K., Yamaoka, H., Matsuoka, S., Ishikawa, T., Ueki, T., Iwasaki, H. X-Ray Optics R&D's for SPring-8 Beamlines.
- ThD87 Furst, M.L., Graves, R.M., Canfield, L.R., Vest, R.E. Radiometry at the NIST SURF II Storage Ring Facility.
- ThD88 Wallace, J.P., Welnak, J.T., Cerrina, F. Design and Performance of a Schwarzschild Objective Mirror Positioning System for the SuperMAXIMUM X-Ray Microscope.
- ThD89 Wang, Z., Kuzay, T.M., Assoufid, L. Liquid-Metal Pin-Fin Pressure Drop by Correlation in Cross Flow.
- ThD90 Wang, Z., Kuzay, T.M., Dejus, R. X-Ray Optical Analyses with X-Ray Absorption Package (XRAP).
- ThD91 Wang, Z., Yun, W., Kuzay, T.M. Thermal and Deformation Analyses of a Novel Cryogenically Cooled Monochromator for the Advanced Photon Source Beamline.
- ThD92 Warwick, T., Shlezinger, M. A Variable Radius Mirror for Imaging the Exit Slit of an SGM Undulator Beamline at the ALS.
- ThD93 Welnak, J., Dong, Z., Solak, H., Wallace, J., Cerrina, F., Bertolo, M., Bianco, A., DiFonzo, D., Fontana, S., Jark, W., Mazzolini, F., Rosei, R., Savoia, A., Margaritondo, G. Super MAXIMUM: A Schwarzschild-Based, Spectro-Microscope for ELETTRA.
- ThD94 Wong, J., Rek, Z.U., Rowen, M., Tanaka, T., Schaefer, F., Mueller, B., George, G.N., Pickering, I.J., Via, G.H., DeVries, B., Brown, G.E. YB₆₆ Monochromator: New Opportunities in XAFS Spectroscopy in the 1-2 keV Region.
- ThD95 Xu, Z., Hulbert, S.L., McNulty, I. Cross Collimation: A New Scheme For Grating Monochromator Alignment.
- ThD96 Yang, B., Rivers, M., Schildkamp, W. GeoCARS Micro-Focusing Kirkpatrick-Baez Mirror Bender Development.
- ThD97 Yang, L., McNulty, I., Gluskin, E. An Intensity Interferometer for Soft X-Rays.
- ThD98 Yun, W., Lai, B., Krasnoperova, A.A., Cerrina, F., Fabrizio, E.Di., Luciani, L., Figliomeni, M., Gentili, M. X-Ray Zone Plates and Their Applications.
- ThD99 Gambitta, A., Poloni, C., Visintin, A., Zanini, F. Comparison of Numerical and Experimental Simulation of a Beryllium Window Under Intense Heat Load.
- ThD100 Wang, Q., Zhang, Y. A Simple Method for Wavelength Calibration of Monochromators with a Sine Drive.
- ThD101 Lai, B., Yun, W., Xiao, Y., Yang, L., Cai, Z., Krasnoperova, A., Cerrina, F., DiFabrizio, E., Luciani, L., Figliomeni, M., Gentili, M. Development of a Hard X-Ray Imaging Microscope.

X-RAY OPTICS DEVELOPMENT FOR NUCLEAR RESONANT SCATTERING BEAMLINE AT APS (*)

E. E. Alp, T. Toellner, W. Sturhahn, and T. Mooney

Advanced Photon Source, Argonne National Laboratory, Argonne, Illinois 60439

The construction of a dedicated beamline for nuclear resonant scattering studies prompted the development of various x-ray optical components. These include focusing and collimating mirrors, large angular acceptance nested crystal monochromators with meV-level energy resolution in the range of 6-30 keV, polarizer/analyzer monochromator to filter nuclear resonant radiation using optically active absorbers, and thin film optics in the form of GIAR films and multilayers. In this paper, we will provide a review of the current status of these developments.

(*) This work is supported by US-DOE, BES Materials Science, under contract No: W-31-109-ENG-38.

A Finite Element Analysis of Room Temperature Silicon Crystals for the APS Bending Magnet and Insertion Device Sources

Lahsen Assoufid, Wah-Keat Lee, and Dennis M. Mills

Advanced Photon Source
Argonne National Laboratory
9700 S. Cass Avenue
Argonne, IL 60439

Abstract

The third generation of synchrotron radiation sources, such as the Advanced Photon Source (APS), will provide users with a high brilliance x-ray beam with high power and power densities. At a ring energy of 7 GeV and a positron current of 100 mA, the APS Undulator A and Wiggler A will produce x-ray beams containing up to about 4 and 7 kW, respectively, with peak power densities of about 150 and 80 W/mm². In many cases, the first optical component to intercept the x-ray beam is a silicon crystal monochromator. Due to severe heat loading, the photon throughput and brilliance will be severely degraded if the monochromator is not properly designed (or cooled). This paper describes a series of finite element analysis performed on room temperature silicon for the three standard APS sources, namely the bending magnet, Undulator A, and Wiggler A. The modeling was performed with the silicon cooled directly with water or liquid gallium through rectangular channels. Both temperature distributions and thermally induced deformation are presented.

Beamline Optimization Using Phase Space Transformation

J. Bahrtdt, U. Flechsag, F. Senf
BESSY

Usually, the optical aberrations of mirrors and gratings (defocussing, coma, spherical aberrations etc.) are parametrized with respect to the coordinates of the optical element. This formalism is not expandable to a combination of several optical elements. Therefore, we have chosen the coordinates "displacement" and "slope" with respect to an optical axis to characterize a ray and derived a fourth order Taylor series expansion of the coordinates in the image plane with respect to the coordinates in the source plane using the algebraic code REDUCE (1). The formalism has been described in detail in (2).

The fourth order transformation for one optical element is represented by a 70x70 matrix and the matrix elements can be interpreted as optical aberrations. The transformation for a system of several optical elements is given by the multiplication of the transformation matrices of the individual elements yielding an analytic expressions for the transformation of phase space. It is thus straightforward to perform a complete phase space transformation from the source plane to the image plane. An integration of the phase space density in the image plane with respect to angles yields the intensity distribution.

The parametrisation of the focal shape in the image plane via the Fourier expansion coefficients allows for a very efficient beamline optimisation. One has to construct an appropriate cost function that consists of a weighted sum of the important optical aberrations. Minimizing the cost function yields the beam line parameters. Minimizing is done using the CERN routine MINUIT (3).

As an example we demonstrate the optimization procedure for a focussing spherical grating monochromator designed for a 49 mm period undulator at BESSY II. The monochromator covers the energy range from 130 eV up to 1500 eV with three gratings. The monochromator parameters (distances between the optical elements, deflection angles, radii and line densities) have been optimized with respect to high resolution. The cost function included optical aberrations, the finite slit width and the tangent errors of the optical components.

- (1) A. C. Hearn, REDUCE User's Man. 3.4 (Rand, Santa Monica, Cal. 1991)
- (2) J. Bahrtdt, to be published in Applied Optics
- (3) F. James, M. Roos, MINUIT, Routine no. D506, CERN library (1983)

MIRROR OF INTEGRATED DESIGN FOR THE CRG/IF BEAMLINE AT ESRF

M. BELAKHOVSKY
SP2M / Laboratoire de Physique des Interfaces
CENG-DRFMC 38054 Grenoble Cédex 9 -France

The CRG/IF beamline at ESRF, which is near completion, is a common CEA-CNRS venture. It is dedicated mainly to the physics and physicochemistry of interfaces.

The optics include a monochromator (cf abstract on the sagittal focusing, this conference) and a premirror for focusing/collimating and filtering.

The mirror (manufactured by PSI, USA) has an innovative integrated design : the substrate made of glidcop (strengthened copper) has a hollow brazed shape, incorporating both cooling channels (located beneath the surface) and a pair of piezo-actuated rods for variable curvature between 7 and 20 km.

Electroless Ni is deposited on the whole area of the upper surface (1m*0.29 m) and on top of it a thin Pt coating and a thick SiO₂ coating, each on one third of the width : hence, and using a transverse translation, the incoming photons at a fixed glancing angle of 2.9 mrd are reflected off one of 3 materials (SiO₂, Ni, Pt), with respective cutoff energies around 10, 20 and 30 keV.

The mirror assembly and its mechanics (manufactured by IRELEC, Grenoble) will be described, as well as the first tests on the beamline.

A Fixed-Exit Double-Crystal Monochromator for the Crystallography Wiggler-Beamline at ELETTRA: Concept of the Crystal Movements

S. Bernstorff, E. Busetto, M. Colapietro and A. Savoia
Sincrotrone Trieste, Padriciano 99, 34012 Trieste, Italy

A fixed-exit double-crystal X-ray monochromator has been constructed for use at the Macromolecular Crystallography Beamline at the Sincrotrone Trieste. For its design a new concept has been developed, which is based on a single rotational stage to control the Θ or Bragg angle for both the first and second crystal. The stage rotation axis lies in the centre of the surface of the first crystal, thus the incoming photon beam remains centred on it over the whole tuning range, which opens the possibility to e.g. optimise the crystal cooling system. The fixed-exit aspect of the monochromator is achieved by translating the second crystal on a slide forming an angle α with the surface of this crystal. In this way, the translation distance can be kept small thus minimising detuning effects of the monochromator due to not-perfect slides. The cost is, that during energy scans the beam footprint will wander somewhat on the second crystal surface. It is demonstrated that, by choosing a suitable angle α , both the translation distance T and the length of the second crystal can be reasonably minimised. In fact, for e.g. a monochromator having a vertical beam offset of 17 mm and an angular tuning range 5° - 30° , T can be kept as small as 25 mm by only doubling the length of the second crystal with respect to the first one.

ThD5

Light Choppers: a New Approach to the Problem of Heat Load on Samples and Optical Elements at ELETTRA Beamlines

A. Lausi and S. Bernstorff
Sincrotrone Trieste, Padriciano 99, 34012 Trieste, Italy

The Macromolecular Crystallography Beamline at ELETTRA is designed to serve two different types of experiments: diffraction experiments with monochromatized beam and Laue-type experiments with white (i.e. not monochromatized) beam. In this latter case the monochromator crystals are removed from the optical beam path, leading to the full power impinging onto the downstream focusing mirror, the Be-window at the end of the beamline and the sample. Even though a pyrolytic graphite power filter, situated upstream of all the optical elements, reduces the incoming power load by about a factor of two by absorbing all the lower photon energies that will not be used in experiments, the passing white beam carries still a total power load of up to 1.2 kW. Such a high power load would give rise to surface distortions of the water-cooled mirror which in turn would lead to an unacceptable increase of the beam divergence at the sample. Much worse however would be the situation for the small ($<1\text{mm}^3$) organic sample crystal situated in the beam focus. Its lifetime would be severely reduced due to the large impinging radiation dose.

We present here a new solution to this problem based on the use of an UHV-compatible light chopper positioned upstream of the focusing mirror. The chopper, which is used only during "white beam" experiments, acts as a beam shutter, blocking completely the photon beam when closed. Both the opening time and repetition rate can be varied over a large range according to the experimental needs. Compared to a beam shutter the use of a chopper offers the advantages of a greater flexibility in the selection of the time structure and of a higher mechanical reliability since long periods of frequent use are necessary. By means of the chopper the time-integrated heat load on downstream optical elements and the radiation dose on the sample can be greatly reduced, allowing to work with full source flux during data acquisition times only, while the beam will be shut off during e.g. detector dead times.

ThD6

First Test Results of SRC's new High Energy Variable Line Density Grating Monochromator

Mark Bissen, Mike Fisher, Greg Rogers, Dave Eisert, Kevin Kleman, Tom Nelson, Bill Mason⁺, Fred Middleton⁺ and Hartmut Höchst,
Synchrotron Radiation Center, University of Wisconsin-Madison
3731 Schneider Dr., Stoughton WI 53589.

and

⁺Physical Sciences Laboratory, University of Wisconsin-Madison
3731 Schneider Dr., Stoughton WI 53589.

During the last two years we built a new high resolution soft x-ray beamline utilizing a variable line density grating. In addition to the regular grating rotation the grating housing mechanism allows also a translation of the grating. The additional translational motion of the VLS grating can be used in such a way that grating aberration effects such as defocus, coma, and spherical aberrations are minimized over the entire scan range. The underlying principle and the basic optical design was discussed earlier.^{1,2}

In order to achieve the theoretical energy resolution which varies from 10^4 to $5 \cdot 10^3$ over the photon energy range 480-1180 eV. Extreme care had to be exercised in positioning and controlling the grating scan angle (<0.12 arcsec) and focus drive position ($<10 \mu\text{m}$). Using a spherical grating with figure error of <0.2 arcsec and $10 \mu\text{m}$ slits, we were able to experimentally reproduce our theoretical predicted energy resolution over a wide energy range

We present photo absorption data of the K-shell edges and associated Rydberg states of Ne, O₂, CO and Xe as well as the 2p absorption edges from several transition metals. Due to the high resolution our gas phase data reveal structures which were previously not seen or only poorly resolved. A detailed quantitative data analysis of the Ne absorption peak allows us to directly determine the intrinsic lifetime broadening of the Ne 1s state which is considerably smaller than previously estimated.

1. H. Höchst, M. Bissen, M.A. Engelhardt and D. Crossley, NIM A319, 121 (1992)

2. The monochromator utilizes the IFM principle which is covered by US. Patent No.4,991,934 and licensed to SRC by Hettrick Scientific Inc.

Prototype Grooved and Spherically Bent Si Backscattering Crystal Analyzers for meV Resolution Inelastic X-Ray Scattering.*

R. C. Blasdell and A. T. Macrander
Experimental Facilities Division
Advanced Photon Source, Argonne National Laboratory,
Argonne, IL 60439-4814

Abstract

The high order backscattering reflections from single crystals of silicon have mrad rocking curve widths that can be exploited to produce meV energy-resolution focusing analyzer crystals for use in inelastic X-ray scattering experiments at third generation synchrotron sources. We present here the results of calculations and tests of the performance of prototype analyzers made of spherically bent, (1,1,1) oriented, strain-relief grooved Si wafers. We examine the affect of slope errors on the focus spot size and energy resolution using ray-tracing and present the results of measurements of the spot size and slope errors of prototype analyzers.

*This work is supported by the U.S. DOE Contract No. W-31-109-Eng-38.

The High-Energy Monochromator for the ALOISA-Beamline at ELETTRA

E. Busetto, A. Lausi and S. Bernstorff
Sincrotrone Trieste, Padriciano 99, 34012 Trieste, Italy

Experiments at the ALOISA beamline at ELETTRA are foreseen with a monochromatized photon beam in the range 250 eV to 8 keV. Such a wide energy range will be provided by switching between a plane mirror / grating monochromator (PMGM) and a crystal monochromator - for the low and high energy range respectively - sharing the same beamline mirror optics. All dispersing elements are used in a collimated beam, which is focused downstream onto the sample by means of two aspheric mirrors. Therefore a "channel-cut" crystal-monochromator could be chosen where the use of only one rotational movement (for the energy tuning) allows for a simple and compact mechanical layout, while the centre of the light spot on the sample will still keep a fixed position over the whole energy tuning range. The size and shape of the light spot at the sample depends on the selected photon energy, since the vertical beam offset at the exit of the channel-cut crystal varies during energy scanning, thus leading to different "off-axis" conditions in the illumination of the downstream mirror optics. Extensive raytracing calculations performed for the whole optical system demonstrated that the variation of the geometry of the light spot remains within acceptable limits over the requested energy range.

The radiation source of the beamline is a wiggler / undulator insertion device, that will deliver up to 50 W into the narrow $140 \times 140 \mu\text{rad}^2$ (horiz. x vert.) central cone accepted by the beamline optics. Differently from the PMGM, which will reflect most of the incoming power, the absorbed power density on the first crystal surface will be as high as 3.4 W/mm^2 . Two different strategies have been adopted in order to cope with this incoming power load. First, the crystal will have an inclined cut where the Bragg planes form an angle of 60° with respect to the optical surface. This choice allows to spread the incoming power load sufficiently over the first reflecting crystal surface to allow for simple backside cooling. In addition the heat load will be reduced by means of a power filter which will be inserted upstream of the monochromator during the high-energy mode of the beamline, and which will absorb all the unused photons with energies $< 3 \text{ keV}$. Radiatively cooled Graphite multifoil-assemblies are commonly used for this purpose. However, since the closely following cooled mirror optics requires a very clean carbon-free UHV, a different, new solution has been preferred. The filter consists of a thin, water-cooled Be-disk which rotates around an axis parallel to the photon beam. With this design the effective absorbed power density in the filter is reduced by two orders of magnitude with respect to a static multifoil solution, resulting in a cool, clean, UHV-compatible device.

Both the layout of the crystal monochromator and the Be-filter will be presented.

ThD9

A cryogenically cooled, sagittal focusing scanning monochromator for ESRF
Fabio Comin, ESRF

A double crystal monochromator for fast scans on large energy ranges has been designed, constructed and tested at ESRF. The instrument is based on a drive unit operated in air that rotates a large wheel sitting in UHV and supporting the two crystal assemblies. The link between the drive and the wheel is realized by a differentially pumped feedthrough.

In order to withstand without noticeable deformations the full power of typical ESRF undulators, the first crystal is liquid nitrogen cooled via pipes hosted in the hollow core of the differentially pumped feedthrough.

The second crystal mount is based on an elastically deformable structure driven by piezoelectric and pneumatic actuators for precise angular adjustments.

In its basic version the relative distance between the first and second crystal is kept constant (channel cut type of design), but a nearly fixed beam at the focal plane can be obtained by the partial compensation, as the Bragg angle is changed, of two different effects: the vertical displacement of the exit beam typical of channel cut designs and its divergence with respect to the incoming one due to the difference in lattice spacing between the cool first crystal and the room temperature second one.

Horizontal focusing of the beam is achieved by sagittal bending of the second crystal.

The major drawbacks of crystal focusing, the necessity of changing the radius of curvature while scanning and the losses in throughput due to the anticlastic deformation experienced at high energy are circumvented by an appropriate choice of the crystal geometry and orientation.

ThD10

Mirror First, a Heat Load Strategy for the BESSRC Undulator Beamline at the Advanced Photon Source

Paul L. Cowan, Mark A. Beno, Michael Bedzyk, Guy Jennings, Gordon S. Knapp, Pedro A. Montano and Mohan Ramanathan,
Argonne National Laboratory, Argonne, IL 60439

The Basic Energy Sciences Synchrotron Research Center (BESSRC) of the Physical Research Divisions (Physics, Chemistry, Materials Science and Geosciences) of Argonne National Laboratory is a facility to exploit the unique characteristics of the Advance Photon Source (APS) for applications of x-ray techniques to a broad range of fundamental and applied physical research. The scientific programs which will be based on the undulator beamline in this facility include those for which the unprecedented brilliance of such a source is especially critical to the research program. The insertion device that best fulfills the experimental requirements of this project is a modification of Undulator A, which has a 4.1cm period with 56 poles. This undulator (designated as "Undulator P") will provide first harmonic tunability over the energy range of 2 to 10 keV and allow tuning to energies between 2 and 30 keV (with 1st and third harmonics) in the final phase of APS operations. To deal with the high heat loads and extremely high power densities of the undulator at closed gap, a three fold approach will be taken. All experiments on this line require a small well defined beam. A 4.1cm-period undulator permits operations exclusively using the high-brilliance central cone of the on-axis odd-numbered harmonics. The use of a pin-hole to limit the beam to the central cone will permit us to remove most of the unused spectrum from the undulator radiation, greatly reduce the total heat load on beamline optical elements. X-ray absorption filters will be used to reduce the total heat load on beamline optics, without significant attenuation at the photon energy of interest and also will reduce harmonic contamination of the beam. To reduce the problem of power density on the filter, we propose to operate filters composed of graphite (or diamond) at grazing incidence angles (roughly 6 degrees). The first optical element of the beamline will be a mirror¹ to eliminate higher harmonics, reduce the heat loads on other components of the beam line and focus the beam in the vertical direction. To effectively reduce the heat load and eliminate harmonics the mirror cut off energy must be set just above the harmonic energy this is accomplished by using a mirror which has a number of different coating with different cut-offs running parallel to the beam direction. Translating the mirror sideways allows the cut off energy to be varied without changing the reflected beam angle. Using a mirror as a first optical component has the major advantage of reducing the heat load on the monochromator by as much 80-90% depending on energy. The use of a mirror as the first optical element also simplifies the design of the Bremsstrahlung shielding and reduces beamline and hutch shielding requirements, since the extremely penetrating high energy x-rays are removed from the beam. The presence of the mirror will allow a simpler monochromator design, since heat load requirements are greatly reduced. An alternative approach to the heat load problems at undulator beamlines is the use of a cryogenically cooled thin crystal monochromator, discussed elsewhere². This approach also requires reductions in power resulting from use of the central cone and filters to reduce the fundamental contribution when using higher harmonics.

¹ A mirror first strategy was previously reported in the Conceptual Design Report for the SRI CAT at APS.

² G. S. Knapp, C. S. Rodgers, M. A. Beno, C. L. Wiley, G. Jennings, M. J. Bedzyk and P. L. Cowan, this conference.

Work at Argonne National Laboratory is supported by the US Department of Energy (DOE), Office of Basic Energy Sciences, Division of Material Sciences, under contract W-31-109-ENG-38.

A compact monochromator for multi-purpose synchrotron beamlines.

A. Darovsky

SUNY X3 beamline at the National Synchrotron Light Source, BNL, Upton NY, 11973, USA.

I. Meshkovsky

OPTOEL, Sablinskaya 14, St. Petersburg, 194101, Russia.

P. Coppens

Department of Chemistry, State University of New York at Buffalo, Buffalo, NY 14214-3094, USA

Abstract

A newly designed monochromator assembly for the State University of New York (SUNY) X3 beamline at National Synchrotron Light Source (NSLS) consists of two monochromators enclosed in a single vessel, and is positioned at 7813 mm from the source. It allows delivery of monochromatic radiation into two independent end stations. The first unit consists of a double crystal assembly reflecting in the vertical plane, and operating in a "channel-cut" mode. Triangular shaped first crystal can be bent by a piezoelectric driver to allow for vertical focusing or compensation for the "thermal bump". The second ribbed crystal provides for sagittal focusing of 12 mrad of incident beam by a four point bender mechanism. A fine alignment of the reflecting planes of the two crystals by the piezoelectric driver allows an active feedback system to be implemented.

The second unit utilizes the portion of the radiation fan left between the A and B branches of the SUNY X3 beamline by reflecting it at a fixed angle of $\Theta = 6^\circ$ into the sideways experimental station A1. Four interchangeable triangular crystals mounted on a rotary holder provide X-Rays of four different energies.

A position sensitive monitor intercepting a portion of the direct beam between the two monochromators is installed in the monochromator housing to allow for angular and positional control of the incident beam.

Increased Throughput of a Heat Loaded Double Crystal Si(111) Monochromator by Roughening of the Second Crystal Surface

Park Doing, Cornell High Energy Synchrotron Source
Ithaca, New York 14853, USA

In a double crystal monochromator, the first crystal absorbs the heat load and its lattice planes become distorted¹. This distortion allows the first crystal to pass x-rays with a larger energy spread and more angular divergence than the second crystal, which is not under a heat load, can accept. If the bandwidth of the second crystal can be increased, then more x-rays will pass through the system. At the F2 station at the Cornell High Energy Synchrotron Source, a test was done where the bandpass of the second crystal of a double crystal monochromator was increased by roughening its surface. In this test, the flux through the system was increased by a factor of 2.75 and the energy spread of the beam exiting the monochromator was increased by a factor of 2.5. For experiments where the energy spread is not a critical issue, this method can greatly alleviate the loss of flux associated with heat loaded optics.

¹Smither B., SPIE, Vol 1739, 1992

This work is supported by the National Science Foundation through CHES under grant No. DMR-90-21700

Parabolic focusing pyrolytic graphite X-ray monochromator

I.P. Dolbnya, K.V. Zolotarev, M.A. Sheromov, A.A. Antonov#, I.G. Grigoryeva#
Budker Institute of Nuclear Physics, 630090 Novosibirsk, Russia
*#Institute of Graphite Based Construction Materials (NIIGraphite),
111524 Moscow, Russia*

The results of the experimental testing of the parabolic focusing pyrolytic graphite X-ray monochromator (mono) on the wiggler (2 Tesla) synchrotron radiation (SR) beamline of the storage ring VEPP-3 are presented. The monochromatization and the focusing of X-radiation in both vertical and horizontal directions are provided by the optical properties of the parabolic surface of revolution of the properly shaped pyrolytic graphite crystal attached to the parabolic-machined brass support. A single crystal is a half of the parabolic surface of 160 mm long and 20 mm minimal focus length. The sagittal radii are changed from 10 to 30 mm. The available photon energy range is 7-20 keV on the first harmonic of reflection. The second order of reflection has a reasonably high intensity comparable with the first one, due to this fact the energy range can be extended up to 40 keV. The change of the energy of the monochromatized X-radiation is accomplished by the simple vertical shift of a mono, according to this shift the space location of the focal point is also vertically displaced.

For the study the mono was placed at a distance of ~16 m from the source point so the accepted horizontal divergence of the "white" SR beam was ~2 mrad. The mono was supplied with In-Sn conical collimator to prevent the parasitic scattering radiation and to avoid the possible undesirable characteristic emission X-ray lines in the working energy range mentioned above. X-ray imaging of different cross-sections (horizontal-vertical, horizontal-longitudinal, vertical-longitudinal) of the focal point space region was performed by the point-by-point scanning of NaI(Tl) scintillation counter supplied by the pinhole collimator of ~80 mm in diam made in the lead disc screen of 2 mm in a thickness. The achieved size of the focal spot of ~0.35(horizontal)×0.6(vertical) mm² is in a good coincidence with theoretical expectations and the preliminary computer modelling. In fact, the main role in an extending of the focal spot plays the large angular mosaic spread (~1 degree FWHM) of the used graphite crystal. The registration of Compton scattered radiation spectra from the acrylic cylinder of 5 mm in diam placed at the focus position by a Si(Li) liquid nitrogen-cooled solid-state detector was conducted to measure the behavior of spectrums of output monochromatic X-radiation with respect to the longitudinal location of the footprint of a primary SR beam on the parabolic surface of the graphite crystal.

The possible applications of the presented mono for the construction of a "middle" space resolution class of SR based X-ray fluorescence microprobes and other usages as a powerful concentrators of X-radiation are discussed and described

A THERMAL BILAYER MONOCHROMATOR CRYSTAL
FOR A HIGH RESOLUTION MULTI-WAVELENGTH ANOMALOUS
DIFFRACTION BEAM LINE AT THE E.S.R.F.

Jean-Luc FERRER⁽¹⁾, Michel ROTH⁽¹⁾, Eric FANCHON⁽¹⁾, Jean-Paul SIMON⁽²⁾, Jean-François BERAR⁽³⁾

⁽¹⁾Institut de Biologie Structurale, Grenoble, France,

⁽²⁾ENSEEG/Laboratoire de Thermodynamique et Physico-Chimie
Métallurgiques, Grenoble, France,

⁽³⁾CNRS/Laboratoire de Cristallographie , Grenoble, France.

High intensity for diffraction experiments with high energy resolution on an intense X ray beam, like the bending magnet beam lines at the E.S.R.F., requires a strict control of the curvature of the optical elements placed in the beam for geometrical focusing and for wavelength monochromatisation. Unwanted curvatures can come from heating of the first crystal of the monochromator, produced by the absorption of X rays. Indeed, because of the size of the crystal, only cooling from the rear is conceivable. This induce a front-to-rear thermal gradient and, as a consequence, a strong spherical curvature.

To design the CRG/D2AM beam-line, a new techniques was developed to control this effects^[1]. It can be shown by calculation that this curvature can be exactly compensated, whatever is the heat load power, by the thermal expansion of a metallic layer at the rear of the crystal, having a larger expansion coefficient than Si.

Such a crystal was tested on the CRG/D2AM beam-line. First results confirm predicted behaviour of the crystal but, in the other hand, show how sensitive is the technical problem of the fixation of this crystal on its cooling device.

[1] M ROTH, J-L FERRER, J-P SIMON, E GEISSLER, Nucl. Instrum. Methods 63, 1043 (1992).

**A crystal bender for water-cooled monochromator
in high heat load synchrotron radiation
wiggler beamline at ESRF**

H. YAMAOKA*, A. K. FREUND**, K. OHTOMO* and M. KRUMREY**

* JAERI-RIKEN Spring-8 Project Team,
The Institute of Physical and Chemical Research (RIKEN)
Hirosawa 2-1, Wako, Saitama 351-01, Japan

** ESRF, BP-220, F 38043, Grenoble Cedex, France

A crystal bender has been developed for a directly water-cooled monochromator. The performance of the bender was tested at the materials science wiggler beamline (BL2) of the ESRF (European Synchrotron Radiation Facility). The x-rays were reflected from a thin silicon wafer (600 μm) bonded onto a 40 mm thick silicon substrate with grooved cooling channels at the surface. The cooling channels of which the widths of the channel and of the fins were 500 μm and 1 mm, respectively. The input power on the monochromator crystal was measured using a Cu calorimeter. The heat load effects on the rocking curve width were about 1.5 arc-seconds at an input power of 1440 W using 13 keV x-rays and the Si (111) reflection. By using this bender system the crystal curvature was compensated and the rocking curve width decreased from 17 arc-seconds to 9.5 arc-seconds for the above conditions. Results of finite element analysis for the crystal bending are presented, too.

**A REFLECTOMETER END STATION FOR SYNCHROTRON CALIBRATIONS
OF AXAF FLIGHT OPTICS AND FOR SPECTROMETRIC RESEARCH
APPLICATIONS**

D.E. Graessle, J.J. Fitch, R. Ingram, J. Zhang
Smithsonian Astrophysical Observatory
Cambridge, MA 02138-1596

R.L. Blake
Los Alamos National Laboratory
Los Alamos, NM 87545

Preparations have been under way to construct and test a facility for grazing incidence reflectance calibrations of flat mirrors at the NSLS. The purpose is to conduct calibrations on witness flats to the coating process of the flight mirrors for NASA's Advanced X-ray Astrophysics Facility (AXAF). The X-ray energy range required is 50 eV to 12 keV. Three monochromatic beamlines (X8C, X8A, U3A) will provide energy tunability over this entire range. The goal is to calibrate the AXAF flight mirrors with uncertainties approaching 1%. A portable end station with a precision-positioning reflectometer has been developed for this work. We have resolved the vacuum cleanliness requirements to preserve the coating integrity of the flats with the strict grazing-angle certainty requirements placed on the rotational control system of the reflectometer. A precision positioning table permits alignment of the system to the synchrotron beam to within 10 arc seconds; the reflectometer's rotational control system can then produce grazing angle accuracy to within less than two arc seconds, provided that the electron orbit is stable. At 10-12 keV, this degree of angular accuracy is necessary to achieve the calibration accuracy required for AXAF. However the most important energy regions for the synchrotron calibration are in the 2000-3200 eV range, where the M-edge absorption features of the coating element, iridium, appear, and the 300-700 eV range of the Ir N-edges. The detail versus energy exhibited in these features cannot be traced adequately without a tunable energy source, which necessitates a synchrotron for this work.

An existing precision X-ray spectrometer was modified to meet the UHV and cleanliness requirements for mirror reflectometry. The improved hardware continues to function as a versatile synchrotron X-ray spectrometry system. It has been used to calibrate the energy scales of synchrotron monochromators, for spectrometric properties of crystals and multilayers, and for a research program to measure optical constants of reflecting materials.

Silicon PIN diodes are used to measure alternately the incident beam intensity and the reflected intensity, in a gated mode. Reflectance measurements have been made on test flat mirrors, with precisions approaching 0.1%. An uncertainty within 1% has been obtained in the best cases. Further procedural development is required to assure this accuracy for all measurements required by AXAF.

We present the mechanical designs, motion control systems, detection and measurement capabilities, selected procedures for our measurements, as well as reflectance data.

* This research is supported by the US D.O.E., and by NASA under contract NASS-36123.

ThD17

**The Mirror Concepts of the new Wiggler and Undulator Beamlines at
HASYLAB**

U. Hahn, and P. Gürtler

*Hamburger Synchrotronstrahlungslabor HASYLAB at DESY, D-22603 Hamburg, Federal
Republic of Germany*

After changing the storage ring DORIS II to DORIS III with a so-called "bypass" in one straight section, seven new wiggler and undulator beamlines are installed. All these beamlines have to cope with total radiation powers up to 7 kW at 100 mA current in the storage ring. In six of these beamlines mirrors are used for optical imaging and filtering. The major point in the mirror concept at all these beamlines is, that the first mirror acts as an energy low pass filter. Due to the very grazing incidence angle of the mirrors, most of the low energy radiation is reflected and only the high energy part of the spectrum is absorbed in the mirror and has to be dissipated by the cooling. Another aspect is the power density of the radiation on the surface. The first mirror is normally installed close to the source with a distance of about 19 m, where the power density of the radiation is about 36 W/mm². The grazing angle of the mirror reduces this value to about 0.1 W/mm². The mirror material is in all cases graphite with a SiC surface. The table gives the characteristics of the installed first mirrors.

Beamline	Mirror characteristics				
	Coating	Micro Roughness	Slope error	Shape	Deflection
BW1	Au	≤ 4 Å RMS	≤ 4°, Δ ≤ 5°	plane	8-14 mrad
BW2	Au	≤ 3 Å RMS	≤ 3°, Δ ≤ 9°	plane	8-14 mrad
BW3	Au/SiC/SiO ₂	≤ 4 Å RMS	≤ 0.15°, Δ ≤ 1.1°	plane	3.2°
BW4	Au	≤ 3 Å RMS	≤ 4°, Δ ≤ 5°	toroidal	14 mrad
BW6	Au	≤ 5 Å RMS	≤ 2°, Δ ≤ 5°	plane	0-8 mrad
BW7	Rh	≤ 4 Å RMS	≤ 1°, Δ ≤ 4°	plane	0-14 mrad

The second mirrors have in general a comparable angle of incidence and therefore the heat load is negligible. All have a toroidal shape to focus the beam onto the sample.

The contribution will inform about the experience with this mirror concept and will cover the following topics:

- mirror performance - mirror material, surface finish, mirror cooling
- mirror orientation, alignment and stability
- Compton scattering and thermal protection of the mirror
- vacuum

In the final section we will report about future improvements which are under construction now. We show an optimized solution for the beamline BW1 which is used by two experiments with different source distances.

ThD18

Performance Check of β -Alumina as a Soft X-ray Monochromator Crystal

Atsunari Hiraya, Kazunori Matsuda*, Yang Hai**, and Makoto Watanabe***

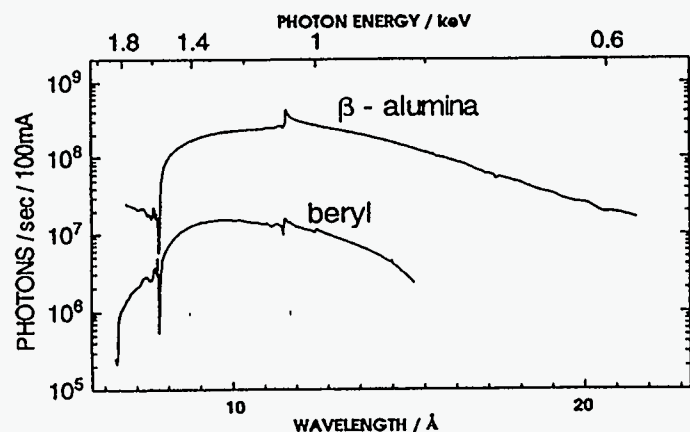
UVSOR, Institute for Molecular Science, Myodaiji, Okazaki 444, Japan

*Naruto University of Education, Naruto 772, Japan

**Institute of High Energy Physics, Beijing, China

***Research Institute for Scientific Measurements, Tohoku University, Sendai 980, Japan

In order to extend the available photon energy range of the double crystal monochromator (DXM) to the lower energy side than that with beryl crystal, a synthesized β -alumina ($\text{Na}_2\text{O} \cdot (\text{Al}_2\text{O}_3)_{11}$, $2d = 22.53 \text{ \AA}$) was tested as a monochromator crystal. The resolution and intensity of monochromatized x-ray with β -alumina were compared to those with beryl. β -alumina monochromator crystals were prepared from crystallized parts of a alumina firebrick (Toshiba Monoflux) by cleaving its flat area (ca. $2 \times 2 \text{ cm}^2$) and used without further polishing. Measurements were carried out by setting a pair of β -alumina crystals in the DXM at BL1A beamline in the UVSOR. Figure 1 shows the throughput spectra of the DXM obtained with β -alumina and with beryl crystals. The β -alumina crystal covers the energy region from 580 to 1740 eV (Bragg angle $71.5^\circ \sim 18.5^\circ$) with more than ten times higher intensity than beryl crystal. The resolution of the pair of β -alumina crystals used is estimated to be 0.75 eV at about 900 eV, which is wider almost twice than that of the beryl crystals (0.46 eV).

Fig. 1. Throughput spectra of DXM with β -alumina and beryl.

ThD19

Construction of 15m Constant-Deviation Constant-Length Grazing Incidence Monochromator at UVSOR

Atsunari Hiraya, Eiken Nakamura, Masami Hasumoto, Toshio Kinoshita, Kusuo Sakai, Eiji Ishiguro*, and Makoto Watanabe**

UVSOR, Institute for Molecular Science, Myodaiji, Okazaki 444, Japan

*Department of Applied Physics, Osaka City University, Osaka 558, Japan

**Research Institute for Scientific Measurements, Tohoku University, Sendai 980, Japan

A constant-deviation constant-length grazing incidence monochromator was constructed at the bending-magnet beamline 8B1 of the UVSOR. The monochromator has a scanning mechanism with fixed entrance and exit slits, as well as fixed directions of incident and exit photon beams. As shown in the inset of Fig. 1, the spherical grating travels parallel to the incident beam axis together with the plane pre-mirror, while being rotated by an arm of which free-end slides on a linear guide. Accordingly the constant deviation angle of the diffracted beam at the grating is canceled by that of the plane pre-mirror to give parallel exit beam to the incident beam. The monochromator was designed to cover the photon energy of 31-620 eV by three gratings: $>368\text{eV}$ by G1 (1080 lines/mm, $R=15\text{m}$), $>184\text{eV}$ by G2 (540 lines/mm, $R=15\text{m}$), and $>31\text{eV}$ by G3 (360 lines/mm, $R=7.5\text{m}$). The evaluated resolving power by ray-tracing is ~ 4000 at the lowest energy (E_{min}) of each grating and ~ 2000 at $2E_{\text{min}}$ with $10 \mu\text{m}$ slit width. All gratings are original laminar-type gratings fabricated on a synthetic quartz and coated with Au. Output spectrum of the monochromator with G1 grating (1080 lines / mm) obtained before the final adjustment was found to extend up to 1 keV with resolving power of ~ 1000 at 870 eV.

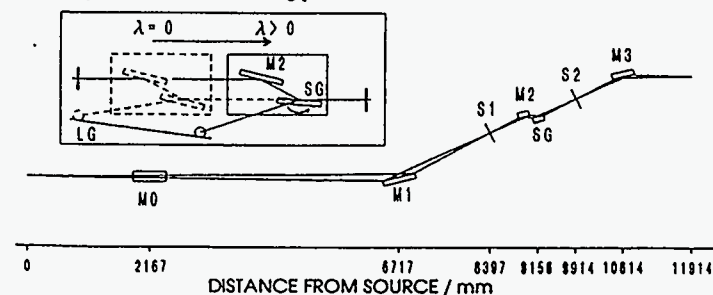


Fig. 1. Schematic layout of the monochromator. Optical elements are: M0, spherical mirror; M1, elliptic-cylindrical mirror; S1, entrance slit; M2, plane pre-mirror; SG, spherical grating; S2, exit slit; M3, toroidal mirror. Inset shows schematic scan mechanism. Grating chamber (M2 and SG) movement from $\lambda=0$ to $\lambda>0$ is shown: LG, linear guide for grating rotation.

ThD20

Design for a high-optical-quality, tunable-radius X-ray mirror

Malcolm R. Howells, Steven C. Inick and Wayne R. McKinney
Lawrence Berkeley Laboratory
University of California
1 Cyclotron Road
Berkeley, Ca 94720

William H. Lowrey and Thomas W. Tonnesen
Rockwell International Corporation,
Rocketdyne Division - Albuquerque Operations
2511 C Broadbent Pkwy. NE
Albuquerque, NM 87107

Frank M. Anthony
FMA Associates
103 Doncaster Road
Kenmore, NY 14217

The construction of a 265 mm long adaptive X-ray mirror is described. The radius of the mirror can be remotely tuned, with feedback from a linear position encoder allowing the mirror to operate in ultra-high vacuum. The design¹ of this monolithic bendable mirror has been carefully optimized so that the hinges which drive the bending introduce minimal errors to the surface shape.

This paper describes the design philosophy and lists construction parameters for the mirror. Achieved performance levels with respect to surface figure and finish are reported.

This work was supported by the Director, Office of Energy Research, Office of Basic Energy Sciences, Materials Sciences Division of the U. S. Department of Energy, Under contract No. DE-AC03-76SF00098.

1. Howells, Malcolm R. and David Lunt, "Design considerations for adjustable-curvature, high-power, X-ray mirrors based on elastic bending", *Optical Engineering*, August 1993, Vol. 32, No. 8, 1981-1989.

Distortions of the Exit Beam from Asymmetric and Inclined
Double-Crystal Synchrotron Radiation Monochromators

Jaromír Hrdý
*Institute of Physics, Czech Academy of Sciences, Na Slovance 2, 18040 Praha 8,
Czech Republic*

Edoardo Busetto and Sigrid Bernstorff
Sincrotrone Trieste, Padriciano 99, 34012 Trieste, Italy

Intense synchrotron X-ray beams from wigglers and undulators contain several kW of power and thus can severely impair the performance of monochromators and other optical elements in the beam. The use of upstream power filters or efficient cooling systems is often not fully satisfying. Another approach to reduce thermal deformations is by increasing the beam foot print and thus reducing the power density on an optical surface. In the case of crystal monochromators, this can be achieved by using asymmetric or inclined crystal cuts. While asymmetric crystals limit the tuneable energy range as compared to symmetric cut crystals, inclined crystals do not have this limitation. However, the vertical divergence of a photon beam impinging onto a double-crystal monochromator with asymmetric cut surfaces, and the horizontal divergence in an inclined double-crystal monochromator, cause an optical distortion of the exit beam. The consequence of this distortion is that a real point-like source is transformed into a virtual source which has a finite vertical dimension. This may manifest itself on the size of the focus when using conventional focusing optics after the monochromator. Thus, in order to determine the convenience of using asymmetric and inclined crystals for synchrotron X-ray monochromators, we decided to study these deformations and their consequences more in detail. For some real sources the sizes of the corresponding virtual sources are estimated, and it is shown that this effect is more serious in the case of the inclined monochromator. The theoretical results are confirmed by raytracing calculations. The raytracing allowed in addition to visualise another cause of virtual source deformations, namely the refraction of the X-ray beam at the crystal surface. This effect, which is increasing both with increasing source divergence and increasing inclination angle, has also been studied in detail.

Hsueh-Hsing Hung

Synchrotron Radiation Research Center, Hsinchu 30077, Taiwan, ROC

**Obtaining three-dimensional height profiles from a
two-dimensional slope measuring instrument**

Steven C. Irick, R. Krishna Kaza, and Wayne R. McKinney
Lawrence Berkeley Laboratory
University of California
1 Cyclotron Road
Berkeley, Ca 94720

Asymmetrically cut crystals are often used in synchrotron radiation monochromators. To calculate the monochromator reflectivity, the Darwin-Prins formalism has recently been implemented in the famous ray tracing code SHADOW.¹ However, the formulation of conventional dynamical theory of x-ray diffraction fails in extremely asymmetric Bragg case and needs some necessary modifications.² In this report, following our novel formulation³ which can result in both the intensity calculation of the Bragg diffraction rocking curve and specular reflectivity profile, we present the simulation for SRRC proposed asymmetrically cut monochromator.

References

1. M. S. del Rio and F. Cerrina, *Rev. Sci. Instrum.* **63** (1992) 936-940.
2. F. Rustichelli, *Philos. Mag.* **31** (1975) 1-12.
3. H.-H. Hung and S.-L. Chang, *Europhys. Lett.* **23** (1993) 415-420.

The Long Trace Profiler (LTP)^{1, 2} was developed in order to measure the mid- and long-period variations in optical components for beamlines of high-brightness synchrotron sources. The LTP is particularly useful for measuring aspherical or spherical surfaces which have a curvature-length product that makes the surfaces immeasurable with conventional metrology.

The LTP is a slope measuring instrument, and the optic is typically measured along a single tangential line, giving a two-dimensional profile. If a three-dimensional height profile (surface map) is desired, it is necessary to combine the integrated slopes of several measurements.

We describe a series of LTP measurements and a data processing method used to combine standard LTP data into a three dimensional height profile. Measurements of two synchrotron beamline mirrors and their three-dimensional height profiles are presented.

This work was supported by the Director, Office of Energy Research, Office of Basic Energy Sciences, Materials Sciences Division of the U. S. Department of Energy, Under contract No. DE-AC03-76SF00098.

1. Takacs, P. Z., and Qian, S, United States Patent 4884697, 1989.
2. Irick, S. C., "Advancements in one-dimensional profiling with a long trace profiler", Proc. SPIE, vol. 1720, (1992), 162.

Multilayer coated gratings for the soft X-ray region

E. Ishiguro¹, T. Kawashima¹, K. Yamashita², H. Kunicda², T. Yamazaki², K. Sato³, M. Koeda⁴, T. Nagano⁴ and K. Sano⁴

- 1) Dept. of Applied Physics, Osaka City University, Osaka 558, Japan
- 2) Dept. of Physics, Nagoya University, Nagoya 464-01, Japan
- 3) National Institute for Fusion Science, Nagoya 464-01, Japan
- 4) OE devices Dept., Shimadzu Corporation, Kyoto 604, Japan

Diffraction gratings with a multilayer structure on the surface are expected to become a new dispersive element for high efficiency and high resolution optics in the VUV and soft X-ray regions¹⁾. In this paper we report reflectivities of multilayer coated gratings measured in the soft X-ray region. Pt/C multilayers were deposited on a SiO₂ laminar grating by means of electron beam evaporation in a ultra-high vacuum. Fig.1(a) shows reflectivities at the photon energy of 1.2 keV for a multilayer reflection mirror and a 1200 l/mm multilayer diffraction grating with 10 pairs of Pt/C layers and a pair thickness of 53 Å. Increase of the reflectivities around the glancing angle of 6° is due to the bragg reflection of the multilayer. This region is enlarged in Fig.(b) for a comparison with results computed using a theory²⁾ for a multilayer grating. In the calculation, the groove depth of 106 Å and the groove land-to-period of 0.5 were used. Dependence of the reflectivities on the glancing angle are similar to the theoretical curves, but the absolute values are smaller than the calculated ones. The decrease of the reflectivities is probably caused from a surface roughness of the layers deposited on the grating which was observed with a AFM. The maximum reflectivities for m=0, +1 and -1 in the bragg reflection region were 6.6, 1.7, and 1.5 % at E=1.2 keV, 8.9, 1.5, and 2.1% at 1.7 keV, 6.5, 1.2 and 1.3 % at 2.0 keV, and 8.6, 1.4 and 1.1 % at 2.8keV.

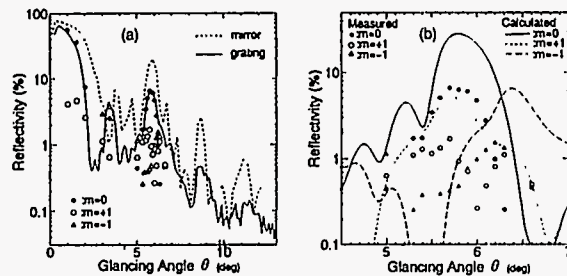


Fig.1 Reflectivities of a Pt/C multilayer grating

References

- 1) T.W. Barbee, Jr., Rev. Sci. Instrum., 60, 1588 (1989)
- 2) H. Berrouane, J-M. André, R. Barchewitz, T. Moreno, A. Sammar, C. Khan Malek, B. Pardo and R. Rivoira, Nucl. Instrum. and Methods in Phys. Research, A312, 521 (1992)

Applications of Extremely Asymmetric Diffraction in Synchrotron X-Ray Optics

Tetsuya Ishikawa

Department of Applied Physics, University of Tokyo,
Hongo 7-3-1, Bunkyo-ku, Tokyo 113, Japan

Tunable wavelength synchrotron radiation has made x-ray optics using extremely asymmetric diffraction more accessible. Easily obtainable (111)- or (001)-silicon plates can be used as an asymmetric diffraction device by choosing appropriate diffraction netplanes inclined to the surface at appropriate wavelength.

Beam expanding property of the asymmetric diffraction was applied to two-dimensional magnification of x-ray image up to 180 times. Limiting factors for spatial resolution is discussed.

Small and controllable penetration depth of extremely asymmetric diffraction leads to depth-selective diffraction imaging technique of near-surface and near-interface region. Using this, we observed localized strain field beneath an Al/Si interface, which is related to the spatial fluctuation of the Schottky barrier height. The small penetration depth also made it possible to characterize lattice imperfections in 1000Å thick epitaxial layer by x-ray topography.

Another characteristic of the asymmetric diffraction is the reduction of the power density on the crystal surface. A design of a water-cooled silicon monochromator for SPring-8 undulator beamline (power density of more than 1kW/mm²) using variable asymmetric diffraction is presented.

Diamond crystal monochromator in a SPring-8 undulator beamline

H. YAMAOKA, K. OHTOMO and T. ISHIKAWA

*JAERI-RIKEN SPring-8 Project Team,
The Institute of Physical and Chemical Research (RIKEN)
Hirosawa 2-1, Wako, Saitama 351-01, Japan*

Diamond crystal is one of the choices as monochromator to withstand high brilliance undulator beam owing to its better thermal characteristics compared to silicon crystal. Although it has been used at ESRF, thermal problem is more serious in SPring-8 beamlines. Here we describe analytical results to confirm potential of applicability to SPring-8 undulator beam. Typical insertion device of which parameters of $\lambda=3.2$ cm, $K_y=1.66$, $N=140$, and $L=4.5$ m is chosen and total power is estimated to be 5.56 kW. We can reduce the power by setting slit system of which size is 1 mm x 2 mm without losing the incident flux. This leads decrease of photon flux less than only about 20 %. The power is estimated to be about 465 W after 200 μ m graphite filter, 500 μ m Be window and the slit system. Pure heat power of a diamond crystal is calculated to be about 45 W by using OEHL (Optical Element Heat Load Analysis) program for a crystal of 300 μ m thickness at incident angle of 30°. Analytical solution gives thermal distortion of about 1 arc seconds under 50 W total power and 13 W/mm² power density. The relation between the crystal thickness and temperature raise by absorbing the x-rays indicates that thicker crystal gives lower temperature raise for indirectly edge cooled crystal. Three dimensional finite element analysis (ANSYS) for above condition indicates the result of about 0.6 arc seconds, and agrees with analytical one. It is concluded that a diamond crystal monochromator has potential for SPring-8 undulator beam from a thermal view point.

A HIGH-FLUX 3-M NORMAL INCIDENCE MONOCHROMATOR AT BEAMLINE 20A OF THE PHOTON FACTORY

K. Ito¹, Y. Morioka², M. Ukai³, N. Kouchi³, Y. Hatano³, and T. Hayaishi⁴

¹Photon Factory, Natl. Lab. for High Energy Physics, Tsukuba 305, Japan.

²Institute of Physics, University of Tsukuba, Tsukuba 305, Japan.

³Dept. of Chem., Tokyo Inst. of Technology, Meguro-ku, Tokyo 152, Japan.

⁴Institute of Applied Physics, University of Tsukuba, Tsukuba 305, Japan.

A high-flux 3-m normal incidence monochromator (3-NIM) has been installed at beamline 20A of the Photon Factory. The 3-m NIM can supply a high photon flux in the energy range of 10 - 40 eV, primarily because of a large horizontal acceptance angle of 28 mrad for the SR beam from bending magnet 20. A schematic view of the optical system is shown in fig. 1. A water-cooled SiC mirror of toroidal shape, M_1 , is installed as close as possible to the source point, P, in order to have a large acceptance angle for the SR. The SR beam is focused onto the entrance slit, S_1 , of the 3-m NIM with M_1 where the ideal 1:1 focusing condition PM_1S_1 is fulfilled. A bent-plane mirror of quartz, M_2 , is installed in order to facilitate the optical adjustment. The 3-m NIM consists of S_1 , a grating, G, and the exit slit, S_2 . For wavelength scanning, G is rotated and translated on the bisector line of the angle S_1GS_2 . A post-focusing system, composed of plane and toroidal mirrors, M_3 and M_4 , bring the SR to a focus point FP. The photon flux of the 3-m NIM was estimated to be $\approx 10^{12}$ photons/A/sec at ≈ 50 nm by measuring the photoemission current from a gold-coated surface. The resolving power with a 2400-grooves/mm grating was found to be $\approx 30,000$ at 85 nm from the autoionization profile of the Kr 8s' line. The 3-m NIM is mainly used for photoionization and photodissociation studies of simple molecules, some of which will also be presented.

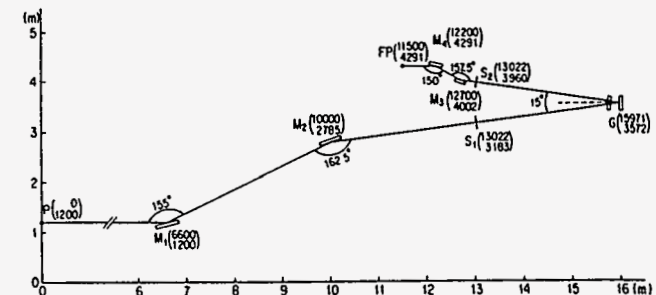


Figure 1. Schematic of the optical system of beamline 20A.

Optimization of spherical grating monochromators
operating with variable included angle for different
applications

P. Melpignano, S. Di Fonzo, A. Bianco and W. Jark,
SINCROTRONE TRIESTE, Padriciano 99, I-34012 Trieste, Italy

The Combination of a VUV Fourier Transform Spectrometer
and Synchrotron Radiation.

K. Ito¹, K. Yoshino², A.P. Thorne³, P.L. Smith²,
J.E. Murray³, and W.H. Parkinson²

¹Photon Factory, KEK, Tsukuba, Ibaraki 305, Japan

²Harvard-Smithsonian Center for Astrophysics, Cambridge, MA 02138

³Blackett Laboratory, Imperial College, London, SW7-2BZ, U.K.

Accurate determination of absorption cross sections requires spectrometers with instrument functions that are significantly narrower than the widths of the spectral features being studied. If low resolution spectrometers are employed to study narrow lines, the line profiles will be distorted and saturated and absorption features may be overlooked. Most of our high resolution measurements of VUV photoabsorption cross sections of aeronomically important molecules have been made with the 6.65-m grating spectrometers at the Center for Astrophysics or at the Photon Factory. These spectrometers have resolution of about 0.4 cm^{-1} , which is larger than the Doppler widths of simple molecules at room temperature (0.15 cm^{-1}).

The only VUV Fourier transform (FT) spectrometer is that developed at Imperial College¹. Maximum resolution is $\sim 0.03 \text{ cm}^{-1}$. We are now using this VUV-FT spectrometer for absorption cross section measurements of NO in the wavelength region 185-193 nm with resolution 0.06 cm^{-1} ($\lambda/\Delta\lambda \approx 10^6$).

For absorption measurements with an FT spectrometer, a bright, stable, and lineless background source with a limited wavelength extent is required. A hydrogen continuum has been used for the NO measurements above 185 nm, but can not be used for shorter wavelengths because the brightness decreases rapidly with wavelength and many lines (bands) start to appear. Below 185 nm, synchrotron radiation is the only choice for FT absorption spectroscopy. The zero dispersion predisperser on BL-12B at the Photon Factory provides the narrow range of wavelengths that we also require.

We will move the VUV-FT spectrometer from Imperial College to the Photon Factory. The VUV-FT spectrometer is small ($1.5\text{m} \times 0.3\text{m} \times 0.3\text{m}$) and light. We will measure photoabsorption cross sections of NO below 185 nm, and those of the Schumann-Runge (S-R) bands of O_2 with $v' \geq 12$. The S-R bands of O_2 with $v' = 13$ to the dissociation limit are only region in the entire oxygen spectrum remaining for which we can not now supply the absolute cross sections of atmospheric interest.

This work is supported by NASA under Grant No. NAGS-484 to the Smithsonian Astrophysical Observatory.

¹A.P. Thorne, C.J. Harris, I. Wynne-Jones, and R.C.M. Learner, J. Phys. E: Sci. Instrum. 20, 54 (1987).

The highest numbers for the resolving power of soft x-ray monochromators are reported up to now for spherical grating monochromators (SGM) and for the SX700 and modifications of this design. The latter instrument is a rather complex device, while the spherical grating monochromators are much simpler. This simplicity comes on the expense of a movable exit slit over rather significant distances. Such an operation is not desirable for several applications, which ask for fixed slit positions in order to focus optimally onto fixed samples without loosing the brightness of the beam from e.g. undulators at the third generation synchrotron radiation sources.

Padmore [1] could show that SGM's in which the deflection angle at the grating can be varied can be operated with minimal defocus (i.e. maximum resolution) with fixed slit distances. In order to do this without changing the direction of the beam in the monochromator section, one has to introduce an additional plane mirror in front of the grating - similar to a double crystal configuration. Typical applications of this scheme are in microscopy. At the SINCROTRONE TRIESTE we are constructing 3 beamlines which are based on this variable angle spherical grating monochromator concept.

In this paper we will discuss in how far we could optimize this type of monochromator for the quite different experimental requests. The applications are as diverse as small-numerical-aperture zone-plate microscopy in the photon energy range 200 eV to 1200 eV, large-numerical-aperture microscopy with multilayer coated Schwarzschild-objectives in the range 20 eV to 300 eV and photoemission studies from molecular gas beams with 20 eV to 1000 eV photon energy requiring a small spot with small divergence.

In any case we are using only one plane mirror in combination with 2 to 5 spherical gratings. The optimization dealt with the choice for the deflection angle, the grating parameters and mechanical details such as the position of the rotation axes.

[1] H.A. Padmore, Rev. Sci. 60, 1608 (1989)

Thermal effects of undulator radiation on Si optics for a plane grating monochromator

B. N. Jensen, D. C. Mancini,* and R. Nyholm

MAX-Lab, University of Lund, Box 118, S-221 00 Lund SWEDEN

*Department of Physics, Uppsala University, Box 530, S-751 21 Uppsala
SWEDEN

Insertion devices on the third generation electron storage ring MAX II will subject the grazing incidence mirrors and gratings of new soft x-ray beamlines to high thermal loads. These thermal loads will cause distortion in the optical surfaces which can be reduced to acceptable levels by the proper choice of substrate material and cooling. A finite element analysis of the temperature variation and thermal distortions are carried out for silicon plane mirrors and gratings under thermal load from the 66mm and 52mm period undulators planned for MAX II. The energy dependence of the reflectivity for coated and uncoated mirrors is taken into account. The minimum cooling requirements are determined for each of these optical elements in the beamline. The effect of the final induced figure errors on the performance of a plane grating monochromator are examined using ray tracing.

Fabrication and Testing of Hard X-ray Sputtered-Sliced Zone Plate

N. Kamijo*, S. Tamura*, Y. Suzuki** and H. Kihara***

* Osaka National Research Institute, AIST, Midorigaoka 1-8-31, Ikeda
Osaka 563 Japan

** Advanced Research Laboratory, Hitachi, Ltd., Hatoyama, Saitama 350-
03 Japan

*** Kansai Medical University, Uyama, Hirakata Osaka 573 Japan

Sputtered-sliced zone plates (which operate by diffraction) are the main focusing elements for hard X-rays. The improvement of their performances is essential for the development of hard X-ray microscopes,^{1,2)} small-area X-ray absorption fine structure spectroscopy and imaging techniques³⁾.

We are currently making sputtered -sliced zone plates by physical vapour deposition (DC magnetron sputtering technique), with alternating transparent (carbon) and opaque (silver) layers on a thin gold wire core of 50 $\mu\text{m}\phi$.⁴⁾ The zone width decreases gradually from 0.4 μm near the Au core to 0.25 μm on the outer edge. Subsequent sectioning, thinning, and polishing normal to the growth direction of the films along the wire axis are then made. The thickness obtained is assumed to be about 40 μm .

Preliminary test of the zone plate was performed at beamline 8C of the 2.5 GeV storage ring in the Photon Factory (Proposal No. 93-273). Using the monochromatized beam (8-KeV) the focused beam size thus obtained was 4.2 μm (vertically) \times 14 μm (horizontally) for the first order focusing beam of focal length $f=135\text{mm}$. Considering the fact that the contraction of size of the photon source is 1/207 (=135mm/28m), the measured spot size shows well the agreement with calculated values (4.4 $\mu\text{m}\times$ 13.5 μm). Further detailed test of this zone plate is scheduled.

References

- 1) K. Saitoh et al. Jpn. J. Appl. Phys., 27(1988)L2131.
- 2) R.M. Bionta, E. Ables, O. Clamp, O.D. Edwards, P.C. Gabriele, D. Makowiecki, L.L. Ott, K.M. Skulina and N. Thomas, Proc. SPIE 1160 (1989) 12.
- 3) S. Hayakawa, Y. Gohshi, A. Iida, S. Aoki and K. Sato, Rev. Sci. Instrum. 62(1991)2545.
- 4) S. Tamura, K. Ohtani and N. Kamijo, Applied Surface Science, to be published.

Contact Cooling for High Heat Load Synchrotron X-ray Mirrors*

A. M. Khounsary and W. Yun
Advanced Photon Source
Argonne National Laboratory, Argonne, IL 60439

Abstract

X-ray mirrors used as the first optical element on high heat load, insertion device beamlines can receive several kilowatts of thermal load with heat fluxes exceeding several watts per square millimeter. In order to reduce thermally induced slope errors to acceptable levels, it is necessary to use materials with a high thermal strain figure-of-merit, such as silicon, in combination with sophisticated internal cooling. Expertise and fabrication techniques developed in the past two decades in the design of high heat load laser mirrors are being utilized to develop synchrotron mirrors.

While heat loads on laser and synchrotron mirrors may be comparable, from a thermal point of view there is one particular difference that can lead to a much simpler design for synchrotron mirrors: because of the grazing angles of incidence in x-ray mirrors (a) the beam has typically a narrow-strip footprint, and (b) sagittal slope errors several times the tangential slope errors can be tolerated. Laser beams, on the other hand, have generally round footprints and wavefront distortion limitations are uniform across the clear aperture.

In this paper, we show that a simple, optimized *contact cooling* method can be used to cool high heat load synchrotron mirrors. Cooling is provided by flowing the coolant through optimally designed cold plates pressed against the long sides of the mirror. The substrate is simply a block of silicon. Design features will be described and key parameters affecting the performance of mirrors (time constant, cooling arrangements, flow rate, etc.) will be discussed. It is estimated that heat fluxes as high as a few W/mm² can be handled. As an example, our analyses show that the maximum tangential slope errors on a 1.2 m-long, contact-cooled mirror subjected to the APS Undulator A beam can be kept below 1 μ rad. The total heat load is 1200 W, and the peak heat flux on the mirror at a grazing incident angle of 0.15° is about 0.38 W/mm². Plans for the design of this mirror are underway.

Advantages of the contact cooling technique include simplicity of design (no internal channels, no bonding/brazing involving silicon), high reliability (no radiation damage concerns, use of proven materials and techniques, reduced leak potentials), UHV compatibility, low jitter, and reduced manufacturing costs.

*This work is supported by the Department of Energy, BES-Material Sciences, under contract no. W-31-109-ENG-38.

The submitted manuscript has been authorized by a contractor of the U.S. Government under contract No. W-31-109-ENG-38. Accordingly, the U.S. Government retains a nonexclusive, royalty-free license to publish or reproduce the published form of this contribution, or allow others to do so, for U.S. Government purposes.

ThD33

A UHV-Compatible Fixed-Exit Two-Crystal Monochromator

J.P. Kirkland
SFA Inc., 1401 McCormick Dr., Landover, MD 20785

W.T. Elam
Naval Research Laboratory, Condensed Matter
Physics Branch, Washington, DC 20375

Simplicity, symmetric design, variable energy range, and support for both sides of the crystals are features of a new fixed-exit crystal monochromator that we have designed, built and tested. It is less complex, therefore it is less expensive to build, easier to understand, and easier to maintain. The design is a variation of the Golovchenko-Cowan boomerang design. Most of the high precision surfaces are bars ground in parallel. Crystals are supported on both ends by carriages with high precision ball bearing wheels. These bearings roll along the bars to carry the crystals and to actuate the rotation of the crystals. By supporting crystals on both sides, water-cooling and dynamic crystal bender systems can be incorporated without adversely affecting the crystal stability. The system is highly symmetric, with no preferred orientation for entrance and exit beams. Angular ranges, and therefore energy ranges, for the system are easily varied by changing the length of the boomerang arms. The system is compact, with an angular range of 80° to 3.5° for theta fitting within a length of 840 mm. This angular range is equivalent to an energy range of 2.5 keV to 30 keV for Si(111).

ThD34

A HELICON PLASMA SPUTTERING SYSTEM FOR FABRICATION OF MULTILAYER X-RAY MIRRORS

M. KOIKE, M. CHIYAKI and I.H. SUZUKI
 Electrotechnical Laboratory
 1-1-4 Umezono, Tsukuba, Ibaraki, 305 Japan

A Cryogenic Monochromator as a Solution to Undulator Heat Loads at Third Generation Synchrotron Sources

G. S. Knapp*, C. S. Rogers**, M. A. Beno*, C. L. Wiley*, G. Jennings*, M. J. Bedzyk*† and P. L. Cowan***

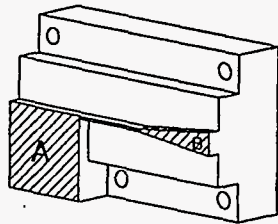
*Materials Science Division, Argonne National Laboratory, Argonne IL 60439

**Advanced Photon Source, Argonne National Laboratory, Argonne IL 60439

***Physics Division, Argonne National Laboratory, Argonne IL 60439 †also at, Dept. of Materials Science and Engineering, Northwestern University, Evanston, IL 60208

We have developed a new design for a cryogenically cooled monochromator employing a thin-crystal strategy which is capable of handling the central-cone power of the Advanced Photon Source's Undulator A at closed gap and at the full design current of 300 mA. The key to our approach is the recognition that both the central cone power not only increases strongly as the gap is closed, but also that much of the power comes from x-rays which have energies above 20 KeV. The absorption coefficient of Si becomes very small above 20 KeV therefore much of the power is transmitted through a reasonably thin crystal and not absorbed. We have calculated the power spectrum of Undulator A at a number of gaps using the program URGENT¹. A proposed design for the first crystal of a monochromator for undulator A is shown below. Two narrow channels, each 2.4 mm wide, are machined into opposite sides of a Si block. The thin central strip which diffracts the incident beam is approximately 15 mm long and 0.6 mm thick. For clarity we show only one half the crystal and we do not show details of the cooling geometry. The crystal strip will be reasonably strain free since it is supported by the square section A and the wedge-shaped section B. Section B is wedge shaped to allow both the reflected and the transmitted beams to miss the wedge-shaped section at low angles. The beam hits the crystal at the center of the thin section and

is 2.4 mm wide and 1.2 mm high at 30 mm from the source. This beam has 88% of the total central cone flux at closed gap. The proposed design has been analyzed by both approximate analytical calculations and by finite element analysis. For a beam produced by undulator A with APS operating at 100 mA the peak temperature is only 125 K. If we cut the beam and channel widths to 1.56 mm (70% of beam), APS could be run at 300 mA and the peak temperature would only be 131 K. These temperatures are near to the point where Si has a zero thermal expansion coefficient so there will be almost no thermal strain. Detailed structural finite element analysis calculations are currently being carried out to confirm this.



Perspective view of one half of the proposed crystal.

Work at Argonne National Laboratory is supported by the US Department of Energy, Office of Basic Energy Science, Division of Materials Sciences, under contract W-31-109-ENG-38.

1. R. P. Walker and B. Diviacco Rev. Sci. Instrum. 63 (1992) 392

A sputtering system which utilizes a pair of helicon plasma cathodes has been developed for fabrication of multilayer X-ray mirrors. The helicon plasma cathode, which has been developed by ULVAC Japan, Ltd.¹⁾, consists of a conventional DC magnetron cathode and an RF coil for a helicon wave (13.56MHz), as shown in fig.1. Because the helicon wave provides electromagnetic power to the plasma in addition to the magnetron power, the discharge is maintained locally around the target even under an ambient Ar gas pressure of $\sim 10^{-4}$ Torr (fig.2), which is one order lower than the pressure realized by the conventional method. This feature gives advantages for the fabrication of multilayer X-ray mirrors. (1) Because the spatial uniformity of the layer originates from the arrangement of the magnets in the cathode, the longer distance between target and substrate (T-S) gives the better uniformity. The T-S distance is adjustable from 150 to 400mm in the present system. (2) Because the kinetic energy loss of the sputtered material is lower under the lower gas pressure, the thicker and tighter layer can be obtained. The characteristics of the multilayers made by this system are discussed.

1) ULVAC Japan, Ltd., 2500 Hagisono, Chigasaki, Kanagawa, 253 Japan.

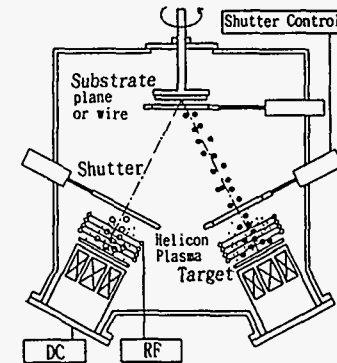


Fig. 1. Schematic drawing of the helicon plasma sputtering system.

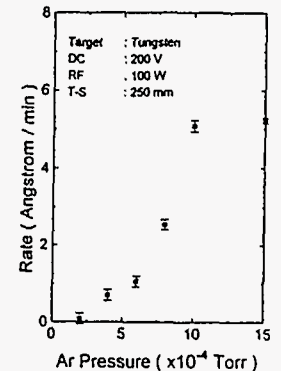


Fig. 2. Dependence of the tungsten sputtering rate on the Ar pressure.

J. H. Underwood, C. Khan Malek*, E. M. Gullikson

Center for X-ray Optics, Lawrence Berkeley Laboratory Berkeley, Ca. 94720, USA

M. Krumrey *

Physikalisch-Technische Bundesanstalt (PTB), D-10587 Berlin, Germany

High-resolution grazing incidence plane grating monochromator for undulator radiation

Masato Koike

Center for X-ray Optics, Lawrence Berkeley Laboratory, Berkeley CA 94720, USA

Takeshi Namioka

US Office of Naval Research, Asian Office, 7-23-17 Roppongi, Minato-ku, Tokyo 106, Japan

To meet the growing need for highly monochromatized soft-x-ray undulator radiation, we have designed a grazing incidence plane grating monochromator capable of providing a resolving power in excess of 10,000 over a wavelength range of 0.5 nm to 10 nm. Fig. 1 shows a schematic diagram of this monochromator. A fixed spherical mirror M1 accepts radiation from an undulator source US, which effectively forms the self-luminous entrance slit, and produces a converging beam incident onto a varied spacing plane grating G. Diffracted light of wavelength λ is focused on the fixed exit slit EX by M1 and G after being reflected by a movable plane mirror M2. The angle between this diffracted beam of λ and the beam incident onto G is referred to as the deviation angle. Wavelength scanning is carried out by combining simultaneous rotation and translation of M2 with simple rotation of G about its central groove, while the direction of exiting beam through EX is kept unchanged by the motion of M2. The principal role of M2 here is to maintain as much as possible the on-blaze property and suppression of higher orders by properly varying the deviation angle at G and the angle of incidence at M2, respectively.

With this rather complex scanning scheme it becomes very difficult to optimize the ruling parameters and the scanning parameters by a conventional design method, such as the one based on the light path function. This difficulty has been overcome in the present design by utilizing a hybrid method¹ which incorporates a ray tracing procedure into an analytic merit function which is related closely to the variance of an infinite number of ray-traced spots in the image plane. The hybrid method permits simultaneous optimization of the ruling parameters for varied spacing plane grating G and the scanning parameters for G and M2. The expected resolving power of the monochromator thus designed is 3×10^4 at 0.5 nm and 8×10^4 at 10 nm with a groove density of 2400 grooves/mm. It should be mentioned in passing that the monochromator can be used as a flat field spectrograph in a limited wavelength range.

This work was partly supported by the Director, Office of Energy Research, Office of Basic Energy Sciences, Material Science Division, of the Department of Energy under contract No. DE-AC03-76SF00098

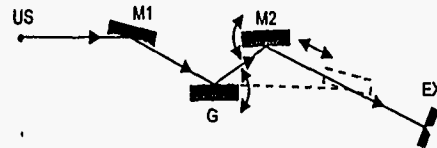


Fig. 1. Schematic diagram of the monochromator. US: Undulator source, M1: Spherical mirror, G: Varied spacing plane grating(rotation), M2: Plane mirror (translation and rotation), and Ex: Exit slit.

A number of groups have coated mechanically ruled or ion-etched blazed diffraction gratings with multilayer reflectors to increase their on-blaze efficiency in the soft x-ray and extreme ultraviolet (EUV) spectral regions. The quality of the groove facets produced by these conventional manufacturing techniques precludes the use of such gratings in very high spectral orders to achieve high resolving power, i.e. as echelles. However, coarse gratings fabricated in crystalline silicon by orientation-dependent etching have excellent groove profile and extremely smooth facets. These properties make them ideal for coating with multilayers for use as echelles at short wavelengths. Several such gratings were coated with tungsten-carbon multilayers for use in the 52nd order at a wavelength of 4.5 nm and were evaluated using both a reflectometer based on a laser-produced plasma source and with synchrotron radiation at the laboratory of the PTB at the storage ring BESSY. In an on-blaze scan through the 5 to 25 nm wavelength region, diffraction orders up to the 61st were observed, allowing the grating performance to be compared with theoretical predictions. Such multilayer coated echelles offer the possibility of extremely high spectral resolving power in the EUV and soft x-ray region.

* On leave from Laboratoire de Spectroscopie Atomique et Ionique, CNRS, Université Paris Sud, Orsay, France.

+ present address: European Synchrotron Radiation Facility, F-38043 Grenoble, France

1. M. Koike, R. Beguiristain, J. H. Underwood, and T. Namioka, to be published in Nucl. Instr. and Meth. A.

Test of a crystal bender for a water-cooled monochromator
crystal at a high power wiggler beamline at ESRF

H. YAMAOKA*, A. K. FREUND**, K. OHTOMO* and M. KRUMREY**

* JAERI-RIKEN SPring-8 Project Team,
The Institute of Physical and Chemical Research (RIKEN)
Hirosawa 2-1, Wako, Saitama 351-01, Japan

** European Synchrotron Radiation Facility, B.P. 220, F-38043 Grenoble Cedex, France

Abstract

A crystal bender has been developed for a directly water cooled monochromator crystal. The performance of the bender was tested at the materials science wiggler beamline (BL2) of the ESRF (European Synchrotron Radiation Facility). The X-rays are reflected in a thin (0.6 mm) silicon wafer bonded to a 40 mm thick silicon substrate with grooved cooling channels at the surface. These channels are 0.5 mm wide and 2 mm deep with 1 mm fins in between. The input power on the monochromator crystal was measured using a Cu calorimeter. The broadening of the rocking curve due to heat load effects was about 1.5 arc-seconds at an input power of 1440 W using 13 keV x-rays and the Si (111) reflection. By using this bender system the crystal curvature was compensated and the rocking curve width decreased from 17 arc seconds to 9.5 arc seconds for the above conditions. Results of finite element analysis for the crystal bending are presented, too.

ThD39

Preliminary experience of optical elements fabrication by
X-ray lithography

V.P.Koronkevich (*), G.N.Kulipanov, O.A.Makarov, L.A.Mezentseva, V.P.Nazmov,
V.F.Pindyurin, E.G.Churin (*)
Budker Institute of Nuclear Physics, 630090 Novosibirsk, Russia
(*) Institute of Automation and Electrometry, 630090 Novosibirsk, Russia

An X-ray lithography using SR from the VEPP-3 storage ring was applied for fabrication of test specimens of some optical elements such as Fresnel lenses and arrays of optical elements for visible light.

The promising advantage of application an X-ray lithography is the possibility of micron scale patterning on curved surfaces, for example, the formation of Fresnel-like zones on the lens surface for correction of some aberrations.

The use of PMMA as material for optical elements enables to produce diffraction pattern quite simply, as PMMA is an excellent X-ray resist.

Patterns of Fresnel-like structures were generated by the annular laser photoplotter (1) for fabrication of an X-ray mask on 2 micron thick silicon membrane with 0.6 micron thick gold absorber. The X-ray lithography station at the VEPP-3 storage ring (2) was used for deep X-ray lithography.

Preliminary results of testing these optical elements are given.

1. V.P.Koronkevich, et.al. Fabrication of kinoform optical elements. *Optic*, 1984, v.67, No.3, p.257- 266.

2. L.D.Artamonova, A.N.Gentselev, G.A.Deis, A.A.Krasnoperova, G.N.Kulipanov, L.A.Mezentseva, E.V.Mikhalyov, V.F.Pindyurin and V.S.Prokopenko. X-ray lithography at the VEPP-3 storage ring. *Rev. Sci. Instruments*, 1992, vol.63, No.1(Part 2A), p 764-766.

ThD40

An Efficient Extraction Window for High-throughput X-ray Lithography Beamlines

Kenichi KURODA, Takashi KANEKO, and Seiichi ITABASHI
NTT LSI Labs.

3-1, Morinosato-Wakamiya, Atsugi-shi, Kanagawa, 243-01, JAPAN

An X-ray extraction window separates the vacuum in the synchrotron radiation (SR) ring from the atmospheric environment in an exposure apparatus. It should have high transmittance so as to introduce enough X-ray power on wafers. In our beamline at the Super-ALIS SR ring (located in Atsugi, Japan), we have been using a beryllium (Be) extraction window¹⁾, but a recent increase in storage currents²⁾ has caused thermal damage on the Be film. Therefore, we investigate pressure and thermal tolerance of Be films and circumvent a double-window extraction setup by combining a diamond film and a thin Be film.

Figure 1 shows results of the pressurizing test conducted at room temperature for various cylindrical frames with 20-, 45- and ∞-mm (flat) radii with openings of 30 x 20 mm². The axis of cylinder is along a longer side of the opening. The simple cylindrical shell model predicts that 1-atm pressure induces 40 and 100 kg/mm² of tensile stress in the 5-μm-thick Be film for 20-mm- and 45-mm-radius cylindrical frames, respectively. The flat-framed film burst at 150 Torr and the 45-mm R-framed film burst at 550 Torr. The 20-mm R-framed film is stable under 760 Torr. Though a smaller-radius cylindrical frame ensures a thinner Be film, a 20-mm R frame is realistic for the above opening area.

Thermal tolerance of the 1-atm-pressurized Be film is evaluated by displacement under local heating with a quartz-rod IR heater. The result is shown in Fig. 2. Displacement drastically increases during a fixed period above 250°C, which suggests that plastic deformation occurs during short periods above this critical temperature. Be films under pressure should be used below that temperature.

The temperature of a single 25-μm-thick Be window, cooled by 1-atm helium (He) of our beamline, was measured using a thermoviewer (AVIO-2100ST). The measured temperature at 500mA of the storage current is about 300°C, which is higher than the critical temperature in Fig. 2. Thicker Be films are needed to keep a low-enough temperature at the sacrifice of X-ray transmittance. Instead, heat-resistant thin films such as diamond or silicon-carbide positioned on the upstream side can be used as thermal protectors for the Be windows behind them. This protection window transmits short-wavelength components from the SR source and absorbs longer-wavelength components, which reduces the thermal load on the Be film.

Based on the above experiments and discussion, we employ a double-window setup for our beamline. A 1-μm-thick diamond membrane (40-mm dia) is set at the upstream side of the 15-μm-thick Be film framed on a 20-mm R frame. The minimum thickness of available vacuum-tight Be films is 15 μm. Though the temperature of the diamond film in vacuum is found to be 700°C, that of the Be film cooled by 1-atm-He rises by only a few degrees even at a 500-mA storage current. Combining 1-μm-thick diamond and 15-μm-thick Be films has improved the reliability and efficiency of the X-ray extraction window.

1)T. Kaneko et al., SPIE 1720 (1992), p 238.

2)T. Hosokawa, Synchrotron Radiation News, 6-6 (1993), p 16.

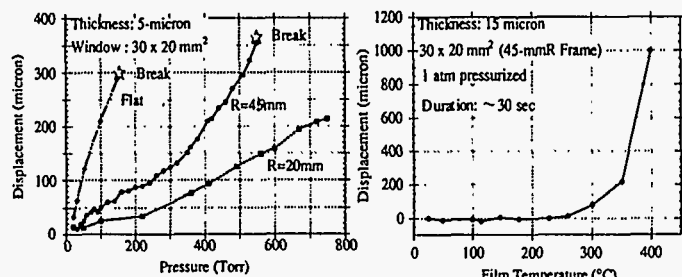


Fig.1 Pressurizing test

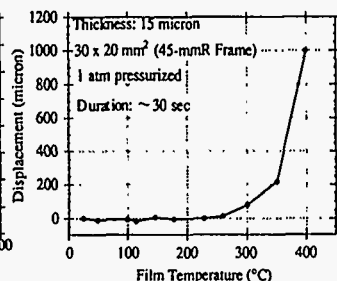


Fig.2 Temperature vs. displacement

ThD41

The Precision Demanded of a

Rowland-Circle-Monochromator: Its Realisation

F. Senf, H. Lammers, U. Flechsig, T. Zeschke, W.B. Peatman
BESSY GmbH, Lentzeallee 100, D 14195 Berlin, Germany

The development of high resolution monochromators for undulator beamlines at BESSY II led to a new design presented at the SRI-91 [1]. It consists of a spherical grating and a plane mirror mounted together on a carriage between fixed entrance and exit slits. An energy scan is made by rotating the grating while linearly translating the grating-mirror arrangement between the fixed slits. Since this type of monochromator works on or very close to the Rowland Circle a high energy resolution can be achieved with the advantages of having the incident beam and entrance slit as well as the exit beam and exit slit fixed. Hence, a pre-focussing and re-focussing mirror system can be employed without any changes during the energy scan of the monochromator. On the other hand, a high energy resolution of $E/\Delta E = 15000$ demands the highest possible control over the rotation of the grating and the translation of the grating-mirror assembly. For achieving this resolution an accuracy of 0.05 arcsec is required on the angular position of the grating on its moveable carriage with reference to the axis of the undulator beam. This accuracy is required over the entire scanning range of the monochromator. A prototype is being built at BESSY and most of the main components have been characterized.

For realisation of the 1.2 m long travel of the grating vessel/carriage between the fixed slits an air bearing system was employed. The carriage consists of a compact granite block and is driven by a controlled DC-motor. Decisive is the variation of the tilt of the carriage about a horizontal axis, $\Delta\theta$ (s), perpendicular to the direction of motion, here defined as "Difline". The Difline data include all differences of angle of the carriage resulting from non-straightness of the horizontal air bearing plane and from the transmission characteristics of the drive unit. The Difline data were determined with an autocollimator with a reproducibility 0.07 arcsec rms. The dependence of $\Delta\theta$ on the variation of the temperature gradient is shown along the 0.8 m high and 2.2 m long granite block. A change of the vertical temperature gradient of 1°K/m produces a Difline of 1.4 arcsec per meter of travel path. This is time dependent. The temperature gradient is measured with sensors on the granite block.

The grating positioning and measuring unit requires an accuracy of < 0.05 arcsec. A design with a measuring head on the linear drive unit pushing on a lever arm is too far removed from the actual axis to be measured and has an unacceptable accumulation of errors. For this reason an incremental angle measuring system with a resolution of 0.035 arcsec has been mounted directly on the grating rotation axis. With this angle measuring system the position is controlled with resolution of ± 0.018 arcsec. The accuracy of this angle measurement is of the order of 0.05 arcsec. The accuracy of the angular measuring system can be improved to 0.01 arcsec.

The calibrated values of the angle measuring system and the experimentally investigated Difline data permit a compensation of angular deviations which can be included in the grating drive software, so that the time dependent and the temperature independent influences are corrected for. Such an effort is required over the entire scanning range for monochromators with an energy resolution $E/\Delta E = 15000$.

Reference

[1] F. Senf, F. Eggenstein and W.B. Peatman, Rev. Sci. Instr. 63,1326 (1992)

ThD42

A compact VLSG monochromator for enhanced flux at MAX-Lab

A Simple In-hutch Mirror Assembly for X-ray Harmonic Suppression

Matthew J. Latimer,^{1,§} Annette Rompel,^{1,§} James H. Underwood,[‡] Vittal K. Yachandra,[‡] and Melvin P. Klein[§]

Department of Chemistry,¹ Structural Biology Division,[§] Lawrence Berkeley Laboratory and Center for X-ray Optics,[‡] Lawrence Berkeley Laboratory, University of California, Berkeley, CA 94720

Harmonic contamination of a monochromatized beam can result in serious distortions of the data in an X-ray absorption experiment. In experiments at the manganese K-edge ($>6.5\text{KeV}$) we have encountered a particularly troubling case of harmonic contamination in samples containing considerable amounts of bromine. We observed a drop in Mn fluorescence midway through a Mn EXAFS (Extended X-ray absorption fine structure) scan due to absorption of the harmonic energy X-rays by Br (K-edge 13.47KeV).

There are several ways to minimize harmonic content of the beam; Si $\langle 111 \rangle$ crystals will not pass this harmonic, but they possess an unacceptable glitch pattern for our experiments. We use Si $\langle 220 \rangle$ which also pass this harmonic. Monochromator detuning by rocking one crystal relative to the other results in reduction of harmonics due to the narrower rocking curve of the harmonic relative to the fundamental. However, we were unable to achieve sufficient harmonic rejection through detuning to 10% of the maximum flux and our extremely dilute Mn samples made further reductions in flux untenable. Finally, harmonics can be suppressed through the use of an X-ray mirror, but the beamline used, VII-3 at Stanford Synchrotron Radiation Laboratory, does not have a mirror.

To circumvent these problems we have designed and built a simple tabletop double mirror harmonic suppressor to be used in the X-ray hutch. Each mirror is a 285×25.4 mm strip of float glass coated with gold. The two mirrors are mounted in a face-to-face ("periscope") orientation spaced 1 mm apart and are further offset to allow a vertical entrance aperture of 2 mm at a glancing reflection angle of 0.4 degrees. This angle was chosen to achieve an optimum balance between second harmonic suppression and fundamental transmission through the use of the critical angle cutoff for gold. The double mirror design results in a vertical displacement of the beam, but the exit beam remains parallel to the entering beam. We have demonstrated that the mirror apparatus described here is much more effective than monochromator detuning, allowing much greater rejection of harmonics without a drastic reduction in flux of the fundamental. The harmonic suppressor can be used over a range of energies by rotating it to new angles and is generally useful for a variety of applications.

This work was supported by grants from the National Science Foundation (DMB91-04104) and by the Director, Division of Energy Biosciences, Office of Basic Energy Sciences, Department of Energy, under contract DE-AC03-76SF00098. Synchrotron radiation facilities and additional technical assistance were provided by the Stanford Synchrotron Radiation Laboratory which is supported by the U.S. Department of Energy.

ThD43

Derrick C. Mancini, Joseph Nordgren, Nial Wassdahl
*Department of Physics, Uppsala University, Box 530,
S-751 21 Uppsala SWEDEN*

Walther Andersén
*Spectra Konstruktion, Eklundshofsvägen 1,
S-752 37 Uppsala SWEDEN*

Ralf Nyholm
MAX-Lab, Lund University, Box 118, S-221 00 Lund SWEDEN

The bending magnets of the 550 MeV electron storage ring at MAX-Lab are an intense source of photons in the 30-700 eV energy range. For soft x-ray fluorescence spectroscopy with selective energy excitation, it is desirable to have maximum flux at moderate resolution. A plane grating monochromator with varied line spacing can provide moderate resolution with a large collection angle and only two reflecting surfaces. We have determined the parameters for a varied line space grating that, when coupled to the existing focusing mirror, will provide monochromatic light in the 200-900eV range. We model the throughput and resolution for this type of monochromator. The results of the modeling are discussed with respect to our experimental requirements. A novel mechanical design has been implemented for the construction of the monochromator in a compact form with few moving parts and easy alignment. This design allows the use of a second grating which is moved into position by extending the rotation of the first grating.

ThD44

Efficiency and Stray Light Measurements and Calculations
of
Diffraction Gratings for the ALS

Wayne R. McKinney, Dmitri Mossessian, †Eric Gullikson,
and Philip Heimann

Accelerator and Fusion Research Division
Advanced Light Source
Lawrence Berkeley Laboratory

†Materials Science Division
Center for X-Ray Optics
Lawrence Berkeley Laboratory

Water cooled gratings manufactured for spherical grating monochromators of the Advanced Light Source beamlines 7.0, 8.0 and 9.0 were measured with the laser plasma source and reflectometer in the Center for X-Ray optics at LBL.¹ The square wave gratings are ion-milled into the polished electroless nickel surface after patterning by holographic photolithography.² Absolute efficiency data are compared with exact electromagnetic theory calculation.³ Inter-order stray light and groove depths can be estimated from the measurements.

¹Gullikson, E. M., Underwood, J. H., Batson, P. C., and Nitikin, V., "A Soft X-Ray/EUV Reflectometer Based on a Laser Produced Plasma Source," *Journal of X-Ray Science and Technology*, 3, 283-299 (1992)

²McKinney, Wayne R., Shannon, Clayton L, and Shults, E., "Water-Cooled Ion-Milled Diffraction Gratings for the Synchrotron Community," 8th National Conference on Synchrotron Radiation Instrumentation, Gaithersburg, MD, August 23-26, 1993, to be published in *Nuclear Instruments and Methods in Physics Research*. (LBL#34670)

³Valdes, Vicentica S., McKinney, Wayne R., and Palmer, Christopher, "The Differential Method for Grating Efficiencies Implemented in Mathematica," 8th National Conference on Synchrotron Radiation Instrumentation, Gaithersburg, MD, August 23-26, 1993, to be published in *Nuclear Instruments and Methods in Physics Research*. (LBL#34543)

Design and Fabrication of a Conical Mirror
for Hard X-Rays

Mati Meron and Wilfried Schildkamp
Consortium for Advanced Radiation Sources,
The University of Chicago, Chicago, Illinois 60637

Jerry Doumas
Applied Physics Technologies Corporation
Stony Brook, NY 11790

John Bender and Donald Ewing
Rocketdyne Albuquerque Operations
Rockwell International, Albuquerque, NM 87107

High energy synchrotron radiation sources such as the Advanced Photon Source (APS) require the first optical components to be positioned in excess of 25 meters from the source. In order to use a single crystal monochromator in Rowland geometry requires either similarly long secondary focal lengths or very asymmetric cut focusing crystals with their intrinsically narrow tunability range and an inherent loss of integrated reflecting power. This disadvantage can be overcome by generating an image of the source closer to the monochromator and by using a symmetric monochromator crystal. This imaging process can be performed by a toroidal mirror; however, if asymmetric focusing conditions are desired (e.g., for floor space limitations), this method suffers from aberrations produced by the toroidal reflecting surface. As an alternative a bendable conical mirror adjustable to any applicable radius can avoid these aberrations and maintain the brilliance of the source. At the APS we plan to use such a mirror to generate a horizontal image of the source at a focusing ratio of 25 to 16.5 meters, while a vertical image will be generated at a more symmetric focusing ratio.

In an effort to develop a suitable procedure for fabrication of this optical surface a prototype mirror was fabricated from a 300 mm long, 75 mm wide silicon block. A conical surface having a larger than anticipated cone angle of 3 milliradians and a sagittal radius of 76 mm was generated. Polishing procedures capable of maintaining the desired cone angle were conceived and demonstrated. This paper discusses the details of optical design and use for such a mirror and presents the results obtained while developing a fabrication process capable of producing an optical element of one meter length.

Importance of wave-optical corrections to geometrical ray-tracing for high brilliance beamlines

Tsuneaki Miyahara and Yasushi Kagoshima

Photon Factory, National Laboratory for High Energy Physics,
Oho-machi, Tsukuba-shi, Ibaraki-ken 305 JAPAN

We demonstrate that wave-optical corrections to geometrical ray-tracing are not negligible for high brilliance beamlines, where the phase-space acceptance is comparable to the diffraction limit. We start from an example of a very simple focussing system with a thin lens. The focussing is expressed in the phase space by the following matrix equation;

$$\begin{bmatrix} 1 & b \\ 0 & 1 \end{bmatrix} \begin{bmatrix} 1 & 0 \\ 1/f & 1 \end{bmatrix} \begin{bmatrix} 1 & a \\ 0 & 1 \end{bmatrix} = \begin{bmatrix} -b/a & 0 \\ -1/f & -a/b \end{bmatrix}$$

, where a , b , and f are the distance between the object and the lens, the distance between the *geometrical* image and the lens, and the *geometrical* focal length of the lens with a relation, $1/f = 1/a + 1/b$, respectively. Apparently the final matrix is not diagonal, which indicates that the above focal point is not the waist of the Gaussian beam. In fact a "light source" is expressed by an ellipse in the phase space as,

$$kx_0^2 + x_0^2 = A.$$

Then the distance between the geometrical and the wave-optical focal points are expressed by

$$\Delta l = (1/2)[-(bf/a) + \{(b^2 f^2/a^2) - 4k^2\}^{1/2}].$$

The above effect is usually negligible when the phase volume of the beam is much larger than the diffraction limit, $\lambda/(4\pi)$. However recent development of the high brilliance beamlines and the low-emittance technology allows us to handle a diffraction limited beam and makes the effect non-negligible.

We will discuss a new possibility to make reasonable wave-optical corrections to the current geometrical ray tracing with an example of a grating monochromator.

ThD47

Cooling of silicon monochromator crystals for the high heat load undulator beamline NE3 of Tristram Accumulation Ring

Tetsuro Mochizuki, Xiaowei Zhang, Hiroshi Sugiyama, Jiyong Zhao, and Masami Ando

Photon Factory, National Laboratory for High Energy Physics, Oho, Tsukuba, Ibaraki 305, Japan

Yositaka Yoda

Department of Applied Physics, Faculty of Engineering, The University of Tokyo, Hongo, Bunkyo, Tokyo 113, Japan

Water cooling system and liquid cooling system of the first monochromator crystal are designed and installed in the undulator beamline NE3 of the 6.5 GeV TRISTAN Accumulation Ring (AR). The first crystal is heated with 40 W/mm^2 of peak power density at normal incidence and 1 kW of total power. In a series of experiments at the NE3 beamline the crystals are tilted at 7.9 degrees to diffract 14.4 keV photons, consequently the maximum power density on the crystal surface decreases to 5.5 W/mm^2 . The water cooled crystals with slots cut just below the surface as coolant channels are adopted for high heat load beamlines with insertion device in the Photon Factory. The water cooled crystals performed well with the power densities of up to 1.0 W/mm^2 and total power of up to 185W. At the power density of 2.3 W/mm^2 , the width of rocking curve of the second crystal increased to twice at that of 0.7 W/mm^2 . Our experiments shows that the water cooling Si crystal performs well only at the peak power density of up to 1.0 W/mm^2 .

Thermal conductivity of Si crystal at the low temperature (100-110K) is 6 times higher than that at room temperature and thermal linear expansion of Si crystal decreases, therefore thermal deformation decreases to 1/10 or less. A series of experiments showed that LN2 cooled Si crystal performed well with maximum peak power of 4.3 W/mm^2 on the Si crystal surface and maximum beam power of 815W. No change was observed in width of rocking curve and pattern of the topography of the diffraction. As our estimation, LN2 cooling Si crystal performs well at the peak power density of up to 3.0 W/mm^2 .

ThD48

Improvement of beam divergence in pseudo-paraboloidal bending of an X-ray mirror

Takeharu Mori and Satoshi Sasaki¹

Photon Factory, National Laboratory for High Energy Physics, Tsukuba 305, Japan.

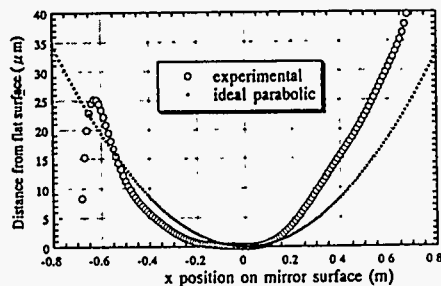
¹Research Laboratory of Engineering Materials, Tokyo Institute of Technology, Nagatsuta, Yokohama 227, Japan.

Paraboloidal mirrors act as collimators by making divergent synchrotron X-rays parallel. In Photon Factory BL-3A, we have tried to bend a flat mirror in pseudo-paraboloidal surface, leading to match the source divergence to the optical condition of monochromator crystals. Our ray-trace analysis using ideal paraboloid suggests that beam divergence can be minimized from 0.4 to 0.026 mrad.

A Pt coated fused quartz mirror is of 1.5 m flat-plate type (1.2 to 2.6 Å rms roughness). The mirror system (M1) consists of an H-beam steel holder, a pair of benders, two-plus-two supporters and height adjustment.¹⁾ The mirror blocks are clamped with spacer on the bottom of the holder. A pair of rods placed at both ends of the holder act as two fulcrums of moment.

The performance tests were made with a triple-axis/four-circle diffractometer.²⁾ With the M1 mirror set at a grazing angle, 3.4 mrad ($E_c = 25$ keV), we performed to establish the bending technique and to evaluate the optical quality of the mirror. [1] The degree of angular divergence was measured as a function of vertical beam size in the +, -, setting of large flat Si(111) crystals at $\lambda = 0.8$ and 1.38 Å. The degree of collimation (FWHM) for total beams was 14.1 arcsec at $\lambda = 0.8$ Å in contrast to 42.7 arcsec in off-mirror. The deviation from paraboloid was observed at various vertical beam-positions as follows. To select a part of beam, the slit placed in front of the mirror was scanned vertically. In each scan, the beam-profile was measured by rocking the third Si crystal. The deviation of the peak position (θ) in each profile gives mirror curvature at individual points of the mirror surface (Fig. 1). [2]

The efficiency of the M1 mirror was evaluated at $\lambda = 1.38$ Å using CeO₂ NIST powder crystals. The insertion of M1 mirror worked to reduce the reflection width and increase the peak intensity.



1) Sasaki et al.: Rev. Sci. Instrum., 63, 1047 (1992).
2) Kawasaki et al.: Rev. Sci. Instrum., 63, 1023 (1992).

Fig. 1, Observed mirror surface.

Use of Asymmetric Monochromators For X-ray Diffraction on a Synchrotron Source

Colin Nave, Ana Gonzalez, Graham Clarke and Sean McSweeney - DRAL Daresbury Laboratory, UK

Stuart Cummings and Michael Hart - University of Manchester, UK

Crystals of germanium or silicon are commonly used to provide monochromatic radiation on synchrotron radiation beamlines. By using asymmetrically cut crystals it is possible to alter the properties of the beam in position, angle, wavelength space. Here, the results obtained from using two types of asymmetrically cut monochromators are compared with theory.

Bent single crystals of silicon or germanium both monochromatise and focus the X-ray beam. With asymmetric cut crystals it is possible to compress the beam and alter the focusing conditions (Lemonnier, Fourme, Rousseaux and Kahn, Nucl. Instr. and Meth. 152, 173-177, 1978). The focusing properties of these monochromators have been extensively described in the literature. However, there is confusion as to the size of focal spot which can be expected when imaging a source of white radiation with an asymmetric monochromator of this type (see for example Fang, Li and Xian, Nucl. Instr. and Meth. A290, 597-602, 1990; Sanchez del Rio and Cerrina, Nucl. Instr. and Meth. A301, 589-590, 1991). This is particularly important when using a synchrotron with a small source size. The behaviour of these crystals for monochromatic (Matsushita and Kaminaga, J. Appl. Cryst. 13, 465-471, 1980) and white (Matsushita and Kaminaga, J. Appl. Cryst. 13, 472-478, 1980) radiation from point and extended sources needs to be understood in order to predict the focal spot sizes which are obtained. A comparison with the results obtained on one of the beamlines on the SRS will be made.

With double crystal or channel cut monochromators it is possible to rapidly change the wavelength with minimal change in the position of the diffracted beam. Asymmetric crystals can be used to broaden the bandpass and obtain increased flux (Kohra, Ando, Matsushita and Hashizume, Nucl. Instr. and Meth. 152, 161-166, 1978) at the expense of reduced tunability. The incident beam is also spread out over a greater surface area thereby reducing thermal problems. However, these monochromators do not appear to be in common use on synchrotron sources. Monochromators of this type require careful construction as the rocking width for reflection between the two crystals is narrowed by the square root of the asymmetry factor. Channel cut monochromators of this type have been tested at the SRS on focused and unfocused beamlines. Improvements in flux of 3-4 times were obtained when compared to the flux obtained from a symmetric cut Si(111) monochromator. Possibilities for improving the design to give even more flux will be described.

ThD50

ThD49

Side Cooled 1200 mm Silicon X-Ray Mirror with Pneumatic Bender and In Situ, on Beamline Mirror Metrology

D. Pauschinger, K. Becker, R. Ludewig, R. Garreis
Carl Zeiss
73446 Oberkochen, Germany

The high heat loads together with the high brilliance of third generation synchrotrons require for beamline optical components new solutions. In principal there are two approaches (apart from the implementation of sophisticated materials) to deal with the deformations due to heat loading:

1. Sophisticated internal cooling schemes to prevent any deformation of the mirror surface in the first place
2. Active correction of possible mirror surface deformations by a closed loop adaptive system within a very moderate band width (≈ 0.1 Hz)

Within this paper a closed loop adaptive synchrotron mirror system with one actuator for the adjustment of the meridional radius of curvature will be proposed. The basis for this proposal is the successful design, fabrication and testing of several side cooled Silicon synchrotron mirrors which will be delivered to ESRF in July 1994. The mirrors are equipped with a support structure which allows the mirror to be bent meridionally to cylinders with radii from infinity to 5000 m. For a complete adaptive mirror system an in situ on beamline mirror surface metrology system is required. The proposed system consists essentially of the Zeiss wavefront sensor DETECT 16 and a respective probe beam guiding system. Both the mirror bending mechanism and the wavefront sensor provide together with the respective software a closed loop adaptive synchrotron mirror system with one actuator for the adjustment of the radius of curvature. Advantages of a closed loop adaptive mirror system:

1. The mirror surface is continuously monitored during operation
2. The mirror surface is actively kept in the required shape (e.g. flat) independent of environmental impacts such as e.g. thermal loads
3. The measuring frequency is about 0.1 Hz.

Detailed metrology and specifications will be presented for the individual components, i.e. for the mirror bending system and the wavefront sensor. In addition first results of a laboratory experiment with the closed loop will be discussed.

Figure Sensing and Control of Synchrotron Radiation Mirrors

K. P. Pflibsen, A. Stuppi, A. J. Goetz, D. McClain
EOC, Kaman Aerospace Corporation, Tucson, Az

Advances in the fabrication of synchrotron radiation optics now make possible spectral and spatial resolutions which were not previously attainable. High thermal loads and the desire to maintain high performance over a large range of operating parameters have led to the development of bendable, higher order adaptive, and segmented synchrotron mirrors. Closed loop figure control makes it possible to compensate for a variety of changing mirror environments, such as source beam pointing variations, thermal loads, and experiment configuration changes.

Surface figure and control methods have been developed for adaptive optics applications in high power lasers and atmospheric turbulence compensation. These techniques have been translated to synchrotron optics applications. The mirror figure and position sensing requirements for bendable, higher order adaptive, and segmented mirrors will be discussed and sensing methods presented and evaluated. In particular, experience with the Wavefront Control Experiment (bendable mirror adaptive optics) and PAMELA (segmented mirror adaptive optics) systems will provide the foundation for developing alternative control architectures and evaluating their relative merits.

Control at 1.4nm of an XUV Schwarzschild objective

Applications of wavefront division interferometers in soft X-rays

François Polack, LURE, Université Paris XI, Orsay (France)

Denis Joyeux, Jan Svatoš, Institut d'Optique, Université Paris XI, Orsay (France)

Soft X-ray synchrotron sources are now attaining a very high spectral brightness which allows to isolate a spatially coherent beam while keeping a substantial part of the spectral flux. With such beams, the realization of wavefront division interferometers become possible. Such interferometers require no beam splitter; furthermore they can be done with grazing incidence plane mirrors allowing high precision interferometric measurement to be performed in a wide spectral range.

These interferometers could have numerous applications, a few of which have been proposed or tested up to now :

1. Direct measurements of soft X-ray index of refraction. Interferometric measurements of indices are not affected by absorption and they can be performed near the edges. Precise index values in the edge regions could have theoretical and experimental applications in atomic and solid state physics. The multilayer fabrication and optimization could benefit from accurate measurement of refractive index of actual layers.

2. It has been recently suggested that XUV absorption spectra could be measured by Fourier Transform spectroscopy with resolution over 20,000 λ . No new technological development is needed if such interferometers are to be built on the wavefront division principle.

3. Wavefront division interferometers can produce probe beams divided into very narrow fringes (period $> 10\text{nm}$). Such probes could be applied to the measurement of spatial resolution of detectors, to the control of very small structures ...

4. Interferential devices can be included in soft X-ray microscopes to detect phase objects. They can also be applied to perform an interferometric control of XUV optical elements at their working wavelength.

1 M. R. Howells *et al.* "Toward a soft X-ray Fourier Transform Interferometer" to appear in the proceedings of SRM 93, Gaithersburg MD, Aug. 93

The Schwarzschild configuration (with normal incidence multilayer coatings) gives well corrected optical systems at appreciable apertures. It only requires two *spherical* mirrors, allowing the best optical quality and yielding submicron foci in XUV.

In the course of fabrication, the optical control of individual components and the alignment may only be done in visible light. However, the tolerances imposed on X-ray optics are at the limit of the possibilities of visible light controls. Furthermore, the final optical quality also depends upon the multilayer coatings. It is therefore necessary to make a final control of the complete assembly at the working wavelength.

Of all the possible methods, Foucault type control yields to our mind three advantages:

- evaluation *and* interpretation of geometric aberrations
- measurement of the point spread function width *and* of the scattering with the same experimental set-up
- the required accuracy may be achieved with nowadays technology

In order to obtain all the possible information, it is necessary to record the evolution of the exit pupil shadows for various positions of a knife edge intercepting the light beam in the neighbourhood of the image of a point source. We shall present the set-up that was used for a preliminary experience, in which only the point spread function was measured. Spatially resolved observation of the pupil was replaced by integration of the transmitted flux on a photo diode.

We shall present and discuss the experimental results obtained so far

Raymond Mercier, Pierre Fournet, Gérard Tissot, Jean-Paul Maréchal,
Institut d'Optique Théorique et Appliquée, Université Paris XI, Orsay (France)

François Polack, LURE, Université Paris XI, Orsay (France)

A novel scheme for the LTP (long-trace-profiler)
with stationary optical head and moving penta-prism.

S. Qian, W. Jark

SINCROTRONE TRIESTE, Padriciano 99, I-34012 Trieste, Italy

and P. Z. Takacs

Brookhaven National Laboratory, Upton, New York 11 973, USA

The accuracy achievable in the measurement of the rms slope error of optical surfaces by use of the long-trace-profiler LTP [1] is significantly affected by mechanical problems. The major drawback of the concept is the need to move a complete interferometer along the trace length of up to 1 m. Up to now the theoretical limits have rarely been approached in existing instruments of this type.

Most of the problems can be by-passed if one succeeds to keep the optical head (the interferometer) stationary. This is possible in a configuration which moves a penta-prism along the test mirrors. Independently of the angle of incidence this prism will always deflect the test beam by exactly 90 degrees. This way the LTP should become almost insensitive to a possible non-straight motion of this prism along the trace length.

We constructed a prototype of this configuration utilizing the components of a standard LTP II. We will present experimental results which show that one can now measure repeatably slope errors with an accuracy of less than 0.2 urad without any need for sophisticated reference measurements. Even by using standard translation slides the measuring accuracy is very high, which allows to realized the presented concept also in a rather economic way. In contrast to the standard LTP this new concept allows in a simple way to position the sample surface also in the vertical and other orientations. Consequently it offers the possibility to examine any mirror in its operation orientation or in such a way that gravity will not introduce any significant distortion because of not appropriate mirror mounting.

[1] P.Z.Takacs and Shinan Qian, "Design of a long trace surface profiler", Proc. of SPIE, Vol. 749, 59 (1987)

Anticlastic Curvature Measurements on Unribbed Crystal Optics for Synchrotron Radiation

J.P. Quintana, Yu. Dolin, P. Georgopoulos
DND-CAT Synchrotron Research Center
APS/ANL Sector 5, Bldg. 400,
9700 South Cass Ave, Argonne, IL 60439
and

V.I. Kushnir
APS/XFD, Bldg 362,
9700 South Cass Ave, Argonne, IL 60439

Various methods have been proposed for measuring the distortion in perfect crystals using double crystal methods. The majority of these methods rely on making comparisons between double crystal rocking curve measurements under the spatial extent of an extended x-ray beam. Unless the beam is large and parallel (such as at a synchrotron bending magnet), these methods are not easily scalable to large crystals (e.g. crystal focussing elements for synchrotron beamlines) due to the mechanical inaccuracies inherent in moving the various optical components. We present a method based on a scanning source which simplifies the problems in scaling double crystal methods to large optics. In addition, results using this method are presented on a sagittal focusing Si(111) crystal designed using the "golden value method"[1] demonstrating that the anticlastic deviation can be made to be less than ± 1 second of arc over a 1 cm long section parallel to the sagittal axis.

[1] V.I. Kushnir, J.P. Quintana, and P. Georgopoulos, Nuc. Inst. & Meth. A328 (1993) 588-591

**Adaptive silicon monochromators for high power insertion devices;
tests at CHESS,ESRF and HASYLAB**

J P Quintana DND-CAT, 1033 University Place, Suite 140, Evanston, Illinois 60201, USA.

M Hart Department of Physics, Schuster Laboratory, The University, Manchester M13 9PL, UK.

D Bilderback, C Henderson, T Setterston and J White. Cornell High Energy Synchrotron Source,CHESS, Cornell University, Ithaca, New York 14853-8001, USA.

D Hausermann and M Krumerey European Synchrotron Radiation Facility, ESRF, BP 220, F38043 Grenoble cedex, France.

H Schulte-Schrepping Hamburger Synchrotronstrahlungslabor HASYLAB at Deutsches-Elektronen-Synchrotron DESY, Notkestrasse 85, D-2000 Hamburg 52, Germany.

ABSTRACT

X-ray wigglers which produce tens of kiloWatts of photon power within the white beam will soon become available at third generation sources of synchrotron radiation. Insertion devices that produce several kiloWatts already exist and we have used those at CHESS, ESRF and HASYLAB to test and develop an adaptive 111 silicon water jet-cooled monochromator at up to 2 kW total incident beam power. This development of earlier work at the Brookhaven National Synchrotron Light Source (NSLS) uses the pressure in the water coolant to provide active compensation of the strainfield in the thermal footprint, nulling it's effect to within residual variations in Bragg angle of only a few seconds of arc. The design is robust, vacuum compatible and uses no moving mechanical parts.

ThD57

**A MULTIPURPOSE MONOCHROMATOR FOR THE BESSRC CAT
BEAMLINES AT THE APS X-RAY FACILITY**

Mohan Ramanathan, Mark A. Beno, Gordon S. Knapp, Guy Jennings,
Paul Cowan and Pedro A. Montano
Argonne National Laboratory, Argonne, IL 60439

The Basic Energy Science Synchrotron Radiation Center (BESSRC) Collaborative Access Team (CAT) will construct x-ray beam lines at two sectors of the Advanced Photon Source facility. These sectors will include Undulator and Elliptical Multipole Wiggler insertion device beam lines along with three bending magnet beam lines. In most of the beam lines the first optical element will be a monochromator, so that a standard design is advantageous. A monochromator has been designed for UHV operation, thereby allowing windowless operation of the beamlines. The monochromator is a double crystal, fixed exit design with a constant 35 mm offset between the incident and exit beams. In this design, both the crystals are mounted on a turntable with the first crystal at the center of rotation. A mechanical linkages is used to correctly position the second crystal and maintain a constant offset. The monochromator design also includes an option for the positioning of the second crystal by a drive mechanism. This scheme has the advantage of optionally locking the motion of the second crystal during energy scans, thereby allowing the beam to walk on the second crystal while maintaining the fixed exit beam offset. The main drive for the rotary motion is provided by a vacuum compatible Huber goniometer. The turntable on which the crystals are mounted is rigidly connected to a Huber goniometer with a stainless steel hollow shaft. The monochromator does not employ a rotary vacuum seal which is a major component of current commercially available monochromators. Instead, rotary motion of the primary monochromator stage is accomplished by using two adjacent vacuum chambers connected only by the small annular opening around the rotary shaft. Both chambers will be pumped with ion pumps. This design allows true UHV operation of the monochromator since it is possible to maintain 10^{-10} Torr on the monochromator side while maintaining only 10^{-6} Torr in the goniometer vacuum chamber. The central shaft also allows for passage of crystal cooling lines from UHV chamber to the low vacuum side and then into the atmosphere. The design of the monochromator is such that it can accommodate water, gallium or liquid nitrogen for cooling the crystal optics. This monochromator design is mechanically simple, and therefore easy to construct and align.

Work at Argonne National Laboratory is supported by the US Department of Energy (DOE), Office of Basic Energy Sciences, Division of Material Sciences, under contract W-31-109-ENG-38.

ThD58

X-Ray Focusing of Synchrotron Radiation with Arrays of Reflectors

VUV High Resolution and High Flux Beamline for the Aladdin Storage Ring

R. Reininger, M.C. Severson, R.W.C. Hansen, M.A. Green and W.S. Trzeciak

Synchrotron Radiation Center, University of Wisconsin-Madison, Stoughton, WI 53589

In response to user requirements for a high flux and high resolution beamline in the VUV spectral range, we have designed a low-cost beamline based on an undulator and an improved version of the 4 m NIM already operational at our facility [1]. The existing bending magnet beamline is in extremely high demand and routinely attains a resolving power in excess of 29,000 [2]. The energy range of the new monochromator, 6-40 eV, can be covered by a simple 3.5 m electromagnetic undulator with a 10.9 cm period. The improved monochromator is expected to achieve a resolving power higher than 5×10^4 in first order between 7 and 23 eV using 1800 and 3600 line/mm gratings and 10 micron entrance and exit slits. The flux at the sample position is calculated to be greater than 3×10^{11} photons/sec with a resolving power of 3×10^4 in the energy range 6-35 eV. The ray-traced light spot at the focus of the exit mirror is less than 0.05 mm x 0.5mm (vertical x horizontal).

1. P. R. Woodruff, C. H. Pruett, F. H. Middleton, Nucl. Instr. and Meth. 172, 181 (1980).
2. M. O. Krause, C. D. Caldwell, Y. Azuma, Synchrotron Radiation News 5, 25 (1992).

A.V. Rode

Laser Physics Centre,

Research School of Physical Sciences and Engineering,

Australian National University,

Canberra, ACT 0200, Australia

H. N. Chapman

Department of Physics

SUNY at Stony Brook,

Stony Brook, NY 11974, USA

Abstract

The x-ray focusing performance of spherically curved arrays of reflectors is presented. It is shown that this type of array is able to condense synchrotron x-ray radiation with a high increase of intensity in a focal spot of about 200 microns in size.

The focusing performance of arrays of reflectors depends upon alignment of the reflectors and their reflective properties. The arrays were made using thin polished Si wafers and Ni-coated glass microscope slides. The arrays that were studied had a channel width of 100 to 250 micron and a radius of curvature of 10 to 200 cm. These arrays are useful for increasing the incident x-ray intensity on to samples, for example, for elemental and chemical analysis of bulk materials.

Design and Thermal Stress Analysis of High Power X-ray Monochromators Cooled with Liquid Nitrogen.*

C. S. Rogers and L. Assoufid
Argonne National Laboratory
Advanced Photon Source
Argonne, IL 60439, USA

Cryogenically-cooled, single-crystal silicon, x-ray monochromators offer better thermal performance than room temperature silicon. The improved performance can be quantified by a figure-of-merit equal to the ratio of the thermal conductivity to the coefficient of thermal expansion. This ratio increases by about a factor of 50 as the temperature is decreased from 300 K to 100 K. An extensive thermal and structural finite element analysis is presented for a liquid nitrogen cooled monochromator crystal diffracting 4.2 keV photons from undulator A at the Advanced Photon Source. The undulator beam was slitted down to accept 50 μ rad vertically and 120 μ rad horizontally. The peak power density at normal incidence to the beam is 148 W/mm² and the total power is 750 W. The crystal was oriented in the inclined geometry with an inclination angle of 80°. A comparison is made between the predicted performance of a monochromator crystal with porous-media enhanced cooling channels and an unenhanced crystal.

*This work is supported by the U.S. DOE Contract No. W-31-109-Eng-38.

PHOTON CHANNELING IN THE VACUUM ULTRAVIOLET WAVELENGTH RANGE

J. E. ROWE, R. A. MALIC, E. E. CHABAN, R. J. CHICHESTER, C.-M. CHIANG and N. V. SMITH^(a)

AT&T Bell Laboratories, Murray Hill, NJ 07974.

ABSTRACT

Experimental measurements in our laboratory have shown a new type of focusing of far ultraviolet light, $\lambda < 1000 \text{ \AA}$, using tapered capillary tubes similar to those first developed for the near-field scanning optical microscope (NSOM) which we call photon channeling. We have tested silica tubes with taper-half-angles of -0.5° to 6° .

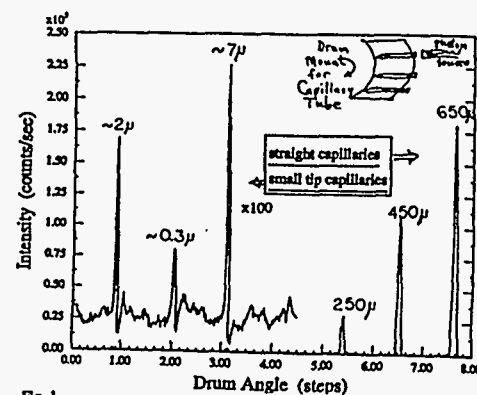


Fig. 1

Figure 1 shows the schematic idea of an array of capillaries mounted on a rotatable drum placed in front of a collimated photon source obtained from a rare-gas discharge lamp. By rotation of the drum, successive capillaries can be brought into alignment, and the photoemission detected by a channeltron-grid detector. The straight capillary intensity (shown on the right as dotted lines) shows no significant light guide effect; it simply decreases as the area of the capillary.

However, the tapered capillaries show an enhanced transmission (or photon channeling effect). In quantitative agreement with simple numerical estimates [1] we find that the transmission enhancement factor varies from ~ 10 -500 times the collimated transmission of a pinhole aperture of the same dimensions with an approximately linear dependence of channeling factor on inverse of the half angle. Useful intensity suitable for photoelectron energy analysis with capillary openings of $\sim 0.7 \mu$ has been demonstrated. The expected spatial resolution is comparable to that obtained with more complex lithographically formed Fresnel zone plates and has the important advantage that the image probe size is independent of photon wavelength. A scanning stage has been developed to form spectral energy-resolved images and requires a tip approach feedback control different from that of NSOM to operate in high vacuum. Preliminary calibration measurements and scanning tests will be presented.

(a) Present address: Advanced Light Source, Lawrence Berkeley Laboratory, Berkeley, CA 94720

[1] N. V. Smith, W. A. Royer and J. E. Rowe, Rev. Sci. Instr. 65, (1994) in press.

CHARACTERIZATION AND PERFORMANCE OF YB_{66} AS A
MONOCHROMATOR IN THE 1 TO 2 KEV SPECTRAL REGION
H. Rowen¹, Z.U. Rek¹, T. Tanaka², Joe Wong³

1)SSRL, P.O. Box 4349, Stanford CA 94309

2)National Institute for Inorganic Materials, Tsukuba, Ibaraki, 305 Japan

3)Lawrence Livermore National Laboratory, P.O. Box 808 Livermore CA 94551

YB_{66} cubic crystal with no intrinsic absorption by constituent elements in the region 1 to 2 keV has been characterized and is now operating as a practical monochromator at SSRL. The (400) reflection with a 2d spacing of 11.75Å can be used to cover the spectral range from the K -edge to just below the $Y L_3$ -edge. Undoped and Sc doped crystals grown in both the $\langle 011 \rangle$ and $\langle 001 \rangle$ directions^{1,2} have been characterized by x-ray white and monochromatic topography and rocking curve measurements. Three pairs of crystals were selected for further study at soft x-ray wavelengths in the JUMBO monochromator. Absolute flux measurements show that YB_{66} has a lower throughput than Beryl or InSb, but measured resolution from all the YB_{66} crystals studied is superior to both. In these YB_{66} crystals a mosaic structure of sub-grains limits resolution. With the best crystals the FWHM of the rocking curves, integrated over the beam foot print, are from 0.25 to 0.72 eV over the 1150 to 2000 eV range. This is several times the predicted resolution³. Two positive flux anomalies observed at 1385 and 1438 eV in all the crystals studied are attributed to anomalous diffraction from the normally forbidden (600) planes at the Bragg angles for the energies just below the $Y L_3$ and L_2 edges. YB_{66} is radiation stable in the synchrotron beam with no observed damage after several months of continuous operation. Shifts in energy and changes in resolving power correlate with ring current. Thermal distortion of the first crystal was anticipated, since YB_{66} has a low thermal conductivity and there is no cooling of the crystals in the JUMBO monochromator. The YB_{66} is now regularly used to measure high resolution EXAFS and NEXAFS K -edge spectra of Mg (1303 eV), Al (1559 eV) and Si (1839 eV) as well as some of the L -edges of 4p elements.

[1] T.Tanaka, S. Otani, Y. Ishizawa, J. Crystal Growth, 73 (1985) 31

[2] Y. Kamimura, T. Tanaka, S. Otani, Y. Ishizawa, Z.U. Rek, J. Wong, J. Crystal Growth, 128 (1993) 429

[3] J. Wong, G. Shimkaveg, W. Goldstein, M. Eckart, T. Tanaka, Z.U. Rek, H. Tompkins, Nucl. Instr. and Meth. A291 (1990) 243

Calculation of the Diffraction Pattern of a Set of Thin Perfect Crystals for a Bense-Hart Camera

M. Sánchez del Río, C. Ferrero and A. K. Freund

European Synchrotron Radiation Facility, B.P. 220, 38043 Grenoble Cedex (France)

The combination of several perfect single crystals is often used in x-ray optics to achieve an optimum matching of source parameters and experimental requirements. A set of two (or more) grooved (channel cut) crystals are applied to very high resolution x-ray small-angle scattering. In this arrangement, the so-called Bense-Hart camera, each grooved crystal allows multiple beam reflections in order to decrease the intensity of the wings of the diffraction curve. The last channel cut is rotated, acting as an analyzer. The resulting multi-reflection profiles can be exactly calculated by the dynamical theory of diffraction, if only coherent elastic scattering is considered. Although the profiles calculated in such a way give a general idea of the performances of the optical device, experiments show a strong effect of incoherent Compton scattering (ICS) and thermal diffuse scattering (TDS) contributions. In particular, the later contribution is important when performing small angle scattering experiments where intensities in an interval of up to ten orders of magnitude are recorded.

Very thin (few micrometer) crystals may decrease the TDS and ICS components, thus increase the performances of the Bense-Hart device. This argument and the advantage of the special Pendellösung features exhibited by thin crystals motivated the present theoretical study. We present here calculations of the optical performance of a set of very thin perfect channel-cut silicon crystals in a Bense-Hart camera arrangement. Calculations were performed in order to predict the reflectivity curves produced by multiple diffraction. The aim was to study the possible elimination of Pendellösung fringes produced by thin crystals by angularly offsetting one crystal with respect to the others. Adjusting the offset value, destructive interference between the Pendellösung oscillations are produced, thus reducing their contribution. Usually, crystals reflect in Bragg geometry but for comparison analogous investigations were conducted in Laue geometry.

Focussing characteristics of diamond crystal x-ray monochromators. An experimental and theoretical comparison.

M. Sánchez del Río*, G. Grübel*, J. Als-Nielsen*⁺ and M. Nielsen⁺

* European Synchrotron Radiation Facility, BP220 3843 Grenoble-Cedex (France)

⁺ Risø National Laboratory, DK 4000 Roskilde, Denmark

Diamond perfect crystals in transmission geometry are currently been considered as an interesting alternative to the conventional double crystal silicon monochromators. Between the reasons for such a choice one may find: i) The extremely good thermal qualities of diamond as thermal conductivity ($23 \text{ W.cm.K} @ 300\text{K}$ for C and 1.5 for Si) and thermal expansion coefficients ($1.18 \cdot 10^{-6}/\text{K}$ for C and $2.35 \cdot 10^{-6}/\text{K}$ for Si). ii) The availability of almost perfect synthetic or natural monocrystals, with high transparency or low absorption to the x-rays. iii) The possibility of using not only the diffracted monochromatic beam, but also the transmitted white beam for successive experimental stations operating at a different photon energy. The last concept is the fundamental idea of the Troika beamline at ESRF, a multi-station undulator beamline, working with a series of transmission monochromators. The first station, Troika I, operating with one diamond crystal, is already completed and will be open to users in late 1994.

Perfect crystals in transmission geometry present interesting effects in focussing the white x-ray beam. This effect is just a consequence of the theory of the dynamical diffraction applied to transmission crystals. We have measured at the Troika beamline the beam size of the monochromatic photon beam after the diffraction from the diamond monochromator, for different positions downstream the monochromator. We observe an interesting change in the beam size evolution (convergent or divergent) depending on the aperture of an entrance slit. These results are compared with ray tracing calculations made with the package SHADOW, with very good agreement. This comparison permits to correctly understanding the focussing properties of transmission crystals under undulator synchrotron radiation beams.

ThD65

Reflectivities of CVD-Diamond Mirrors in the VUV Region

Tomohiko Sasano, Eiji Ishiguro, Shichiro Mitani* and Hiroshi Tomimori**

Dept. of Applied Physics, Osaka City University, Sumiyoshi-ku, Osaka 558, Japan

*Faculty of Engineering, Doshisha University, Tanabe-cho, Kyoto 610-03, Japan

**R&D Division, Osaka Diamond Industrial Co., LTD, Sakai, Osaka 593, Japan

Chemical Vapor Deposition (CVD)-Diamond mirrors are expected as the optical element for the high power VUV radiation such as the high brilliance Synchrotron Radiation (SR). The advantages of the mirror are excellent heat resistance and chemical stability. Besides, a large area diamond mirror can be fabricated with CVD method.

We measured the reflectivities of a CVD-diamond mirror in the VUV region. The diamond thin film with a thickness 20-25 μm was deposited on a Si_3N_4 substrate by means of the hot filament. The surface was polished by grinding with diamond wheels. The RMS surface roughness was about ten \AA which was measured by using a LASER interferometer(Zygo Maxim-3D). The size of the mirror was 40mm(l) \times 30mm(w) \times 5mm(t).

Figure 1 shows the reflectivities of the CVD-diamond mirror for the p-polarized light as a function of the incidence light wavelength for the incidence angles of 80°, 70°, and 30°, along with those of SiC, gold coated SiC, which were measured by using SR at Okazaki, Japan.

The CVD-diamond mirror shows high reflectivities in the wavelength range from one hundred \AA to four hundred \AA both at a grazing incidence and at a nearly normal incidence. In this region it is higher than that of SiC which is well known as one of the best mirror for SR.

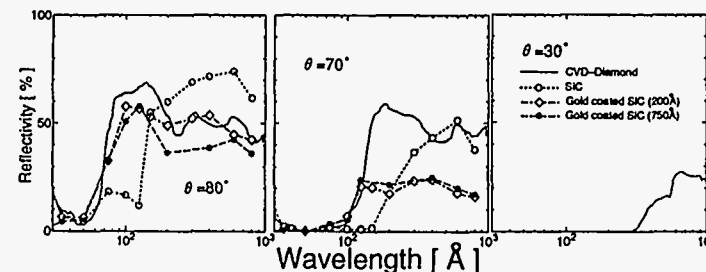


Fig. 1 Reflectivities of CVD-diamond, gold coated SiC and SiC.

ThD66

Modular Double Crystal Monochromator Design

Wilfried Schildkamp

Consortium for Advanced Radiation Sources,
The University of Chicago, Chicago, Illinois 60637

The CARS double crystal monochromators are mechanical devices with modular structure. Some monochromators are used with sagittal focusing second crystals, others use flat crystals. All first crystals are internally cooled with high efficiency heat exchangers and can be a symmetric Bragg crystal, an asymmetric crystal, or a Laue crystal. The design is of fixed exit type, and can accommodate varying accelerator orbit positions within limits. All stepping motors are directly attached to turntables and translation stages and are equipped with cooling sleeves.

The monochromators normally operate in a fine vacuum produced by vapor resistant turbo-molecular pumps, directly mounted to the tank, hence, avoiding typical UHV technology, like air guards around coolant channels. Virtual leaks are avoided wherever possible. The wiring material for motors and mechanical limit switches / home switches is radiation hard up to 100 Mrad.

Both first and second axis are equipped with fine tuning stages, absolute angle encoders, and with azimuthal rotation stages. The first axis resides on a vertical translation stage, and the second axis rides on a horizontal translation stage. Energy scans are performed by coupled motions under computer control. The angular range is typically from 4° to 28° with a slewing speed of 0.5°/sec and a settling time of less than 1 second. For increased energy stability an energy feedback stabilizer consisting of a channel cut crystal in energy dispersive arrangement can be coupled to the fine tuning stage of the first crystal, which should achieve a typical stability of 2×10^{-5} @ 12 keV. The emitted intensity can be stabilized by the fine tuning stage of the second crystal. Inclined crystal geometry and cryogenic first crystal design can be retrofitted at the expense of the azimuthal rotation stage. The monochromators are housed in a 36" diameter stainless steel tank, 31" deep, with a flange-to-flange distance of 1100 mm.

ThD67

Installation and Operation of the LNLS Double Crystal Monochromator at CAMD*

Paul J. Schilling and Eizi Morikawa

*The J. Bennett Johnston, Sr. Center for Advanced Microstructures and Devices,
Louisiana State University, Baton Rouge, Louisiana 70803*

Hélio Tolentino

Laboratório Nacional de Luz Síncrotron, LNLS/CNPq, Campinas, 13081, Brazil

Cesar Cusatis

Depto. de Física, Universidade Federal do Paraná, Curitiba, 81531, Brazil

A new x-ray beamline has been installed at CAMD utilizing a two-crystal monochromator designed and built at LNLS.¹ The beamline will operate in the 2-10 keV range using 4 mrad of dipole radiation from the CAMD storage ring. The monochromator maintains a fixed exit beam and fixed positions of the beam on the two crystals using mutually perpendicular elastic translations. The calculated values for energy resolution ($\Delta E/E$) using Si(111) crystals are $< 1.5(10^{-3})$ with no collimating optics. Ray tracing was performed to simulate the beamline performance at various photon energies. An optimum photon flux was predicted at about 4 keV, with approximately $7.5(10^{11})$ photons/sec entering the experimental hutch, under operating conditions of 1.5 GeV and 160 mA. The beamline is equipped with an XAFS endstation and will also be used for other x-ray applications at CAMD. First results are presented.

*Supported by CNPq and the State of Louisiana

¹M.C. Corrêa, H. Tolentino, A. Craievich, and C. Cusatis, Rev. Sci. Instrum. 63 896-898 (1992).

ThD68

A novel adaptive directly water cooled monochromator crystal for high heatload wiggler beamlines at HASYLAB

**H. Schulte-Schrepping, G. Materlik
J. Heuer, T. Teichmann**

**Hamburger Synchrotronstrahlungslabor HASYLAB
am Deutschen Elektronen-Synchrotron DESY
Notkestr. 85, 22603 Hamburg, Germany**

The performance of large area directly cooled monochromator crystals at high power wiggler beamlines is degraded by the heatload from the insertion device and by the pressure of the cooling agent.

Based on the gained experience with directly water cooled monochromator crystals at HASYLAB, a new adaptive crystal with matching remote controllable crystal bender was designed.

Finite element calculations of the crystal shape confirm the potential of the design to compensate the heat-load and water pressure induced bending.

The whole crystal setup is vacuum compatible in order to be used in a windowless beamline.

Positive results from the characterization of the first new Si(111) crystal under different heatload conditions at the HASYLAB high power wiggler beamline BW2 are presented.

ThD69

PEPO - A Programme for the Calculation of the Reflectivity of Cylindrically Bent Laue Crystal Monochromators

C. Schulze

European Synchrotron Radiation Facility, BP 220, 38043 Grenoble Cedex, France

D. Chapman

National Synchrotron Light Source, Brookhaven National Laboratory, Upton, NY 11973-5000, USA

Cylindrically bent Laue crystal monochromators combine the advantages of low absorbed power with either a polychromatic focusing of the beam or, in Cauchois geometry, a very small energy bandwidth. The broadening of the reflectivity curve induced by the deformation of the crystal results in a substantial gain in integrated reflectivity and hence in flux as compared to flat monochromators. Moreover the maximal reflectivity of bent Laue crystals exceeds by far the value of 0.5 known from the dynamical theory of diffraction for their flat analogues: in fact, reflectivities surpassing 0.9 can be attained.

PEPO is a programme for the calculation of the reflectivity profiles of cylindrically bent Laue crystal monochromators based on the Penning & Polder theory of X-ray diffraction in slightly strained crystals [1,2]. The creation of new wave fields as well as an anisotropic model for the crystal deformation has been added to the original theory [3]. The programme is widget-based and runs under the computing environment IDL [4]. The calculation of perfect flat crystal reflectivity curves in Bragg and Laue geometry using the formulae presented by Zachariasen is included [5].

The agreement with experimental results is excellent allowing the derivation of focal properties from the calculated reflectivity curves.

1. P. Penning and D. Polder, Philips Res. Repts. 16, pp. 419-440 (1961).
2. P. Penning, thesis, Delft, Netherlands (1966).
3. For details see thesis, C. Schulze, Hamburg, Germany (in preparation).
4. IDL, Interactive Data Language, Research Systems, Inc., Boulder, CO, USA.
5. W.H. Zachariasen, "Theory of X-Ray Diffraction in Crystals", John Wiley & Sons (1945).

This work was supported by the US Department of Energy Contract No. DE-AC02-76CH00016.

(Submitted for International Synchrotron Radiation Instrumentation Conference SRI'94; July 18-22, 1994)

ThD70

Heat load problem of an entrance slit on an undulator beamline

F. Senf, U. Menthel, W.B. Peatman
BESSY GmbH, Lentzeallee 100, D 14195 Berlin, Germany

For the first undulator beamline to be built in 1997 at BESSY II a spherical grating monochromator (SGM) has been optimized. The preoptics of this SGM simply consists of one, cylindrical mirror which focusses the source vertically onto an entrance slit. The use of only one premirror increases the heat load at the entrance slit.

In this study the heat load is numerically calculated for the undulator beamline U49 ($\lambda_0 = 49$ nm, $N = 84$) at the storage ring BESSY II running at 1.7 GeV electron energy and 200 mA stored current. For a wiggler parameter of $K = 2.5$ a maximum total power of 450 watts is emitted towards the cylindrical premirror of the SGM.

Keeping the length of the mirror limited allows us to collect almost all of the photons from the odd harmonics of the undulator between 135 eV to 1500 eV, but, accepting only a quarter of its total power. The absorbed and reflected heat load has been determined by taking the variation of the spectral power distribution of the undulator and the reflectivity of the gold coating of the mirror into account. The power reflected towards the entrance slit is calculated to be almost 50 watts. This is vertically focussed to a strip of about 30 μm in height with 2 mm horizontal extent.

For our finite element method (FEM) analysis we assumed the worst case, that most of the power (40 watts) hits the upper (or lower) blade of the slit at the edge. The very high power density in the focus then peaks up to about 700 watts/ mm^2 at the edge.

Despite employing watercooling at the backside of each blade in our model and using Glidcop as a material with high heat conductivity a local overheating - more than 400 K - occurs. As a result of this "hot spot" the center of the slit edge expands itself by several micrometers towards the edge of the opposite slit blade, leading to a partial, or, depending on the slit width, to a total closure of the slit.

The study presented shows that changes in the geometry of the edge and the cooling will not significantly prevent the closure of the slit in the center of the focus.

Some simple bending mechanisms for Bragg-reflection x-ray optical devices

D. P. Siddons

*National Synchrotron Light Source, Brookhaven National Laboratory,
Upton, New York 11973*

Abstract

Bragg-reflection x-ray optical systems frequently require well-controlled, stable rotations of sub-arc-second order. These are quite difficult to engineer using conventional design techniques. This paper will show that it is frequently better to take advantage of the excellent mechanical properties of silicon, and to engineer the rotations using flexural designs in silicon combined with force transducers. Designs for 2- and 4- reflection monochromators and for bent-crystal focussing monochromators will be presented.

FOCUSING WITH VARIABLE-METRIC CRYSTALS

Robert K. Smither and Patricia B. Fernandez
Argonne National Laboratory, Argonne, IL 60439, USA

Abstract

A Variable-Metric (V-M) crystal is one in which the spacing between the crystalline planes changes with position in the crystal.¹ This variation can be either parallel to the crystalline planes or perpendicular to the crystalline planes of interest and can be produced by either introducing a thermal gradient in the crystal or by growing a crystal made of two or more elements and changing the relative percentages of the two elements as the crystal is grown. A series of experiments were performed in the laboratory to demonstrate the focusing properties of the Variable-Metric crystals and their potential use in synchrotron beam lines. Experiments were performed to show how one can convert a normally divergent x-ray beam into a beam that is both monochromatic and parallel to a high degree. The experiment used a crystal which was both bent and subjected to an applied thermal gradient in the direction of the incident beam. The bending radius is given by $R = 2D \sin\theta$, where D is the distance from the source to the crystal and θ is the Bragg diffraction angle. A thermal gradient ($\Delta T / \Delta L = \cos\theta / (2\alpha D)$, where α is the thermal coefficient of expansion) is applied to the crystal so that the Bragg condition, $n\lambda = 2d \sin\theta$ is met at all points on the surface. The resultant x-ray beam is both monochromatic and parallel and can be diffracted by a flat crystal with a very small d -spacing for experiments that require very highly monochromatic and parallel beams with a very narrow band width.

¹ R Smither and P. Fernandez, Rev. Sci. Instrum. 63 (1992) 1755

*This work is supported by the U.S. DOE Contract No. W-31-109-Eng-38.

ThD73

BACKSCATTERING ANALYZER GEOMETRY AS A STRAITFORWARD AND PRECISE METHOD FOR MONOCHROMATOR CHARACTERIZATION AT THIRD GENERATION SYNCHROTRON RADIATION SOURCES

A. A. SNIGIREV¹, A. Yu. SUVOROV², S. LEQUIEN¹

¹ESRF, B.P. 220, F-38043 Grenoble, France

²Institute for Microelectronics Technology, Russian Academy of Sciences, 142342 Chernogolovka, Moscow Region, Russia

With the assessment of the third generation of synchrotron radiation sources, insertion devices (ID) are going to become extensively used. The choice of the ID field configuration allows the optimization of the photon flux at the desired energy. This attractive situation results in a much higher flux on optical elements, mainly on monochromators for which new cooling schemes have to be developed. These latter must be characterized under operating conditions and generally, the figure of merit for monochromators is the rocking curve (RC) measurement. By varying the ID field the monochromator may be fully characterized with regards to the heat load. To achieve this aim, we have proposed and tested double crystal setup where a Si analyzer crystal installed in backscattering geometry (BSG) is coupled with a silicon PIN photodiode as the detection system (Fig.1).

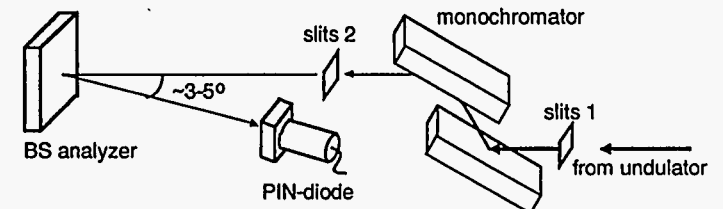


Fig.1 Backscattering analyzer setup for monochromator testing.

The analyzer was a standard Si wafer (111)-orientation, from which we used the following Bragg reflections : 333, 444, 555, 777, 888, 999 ... to measure the RCs of monochromators keeping the analyzer fixed. We were then able to probe the formers at the respective energies 5.9, 7.9, 9.9, 13.8, 15.8, 17.8keV etc.

Setting the analyzer crystal in BSG we get several fold benefits from the method:

- a very good angular resolution ($\sim 10^{-6}$ rad) when one combines the BSG analyzer with narrow slits ($\sim 100\mu\text{m}$).
 - a high energy resolution yielding to a calibration of the monochromator with an accuracy better than 1eV.
 - the analyzer crystal attenuates the reflected intensity which avoids the use of any scatterer foil to count the number of photons. We directly used photodiodes which are well known to respond linearly to radiation intensities and to have a high dynamic range (more than 6 decades).
 - no fine mechanics is needed for the analyzer, just a simple manual turn table can be used to set the analyzer in BSG through the utilization of a laser beam.
- Results on different tests for operating liquid N₂ cooled channel-cut monochromators at Microfocus and High brilliance beamlines will be presented and discussed.

We gratefully acknowledge the support of the ESRF EDS group, especially C. Riekel, P. Engström, I. Snigireva, M. Kocsis, P. Bösecke and O. Diat.

ThD74

THE RECENT DEVELOPMENT OF BRAGG-FRESNEL OPTICS .
EXPERIMENTS AND APPLICATIONS AT THE ESRF

A. A. Snigirev

ESRF, B.P. 220, F-38043 Grenoble, France

Presently there are three types of x-ray optics that are striving for sub-micrometer beam generation and application at the energy higher than 6keV: Fresnel zone plates [1], capillaries [2] and Bragg-Fresnel Optics (BFO). The youngest one BFO was put forward in Institute of Microelectronics Technology Russian Academy of Sciences almost ten years ago and first experiment was reported in 1986[3]. Since that time a lot of experimental and theoretical researches have been done on the BFO performance. Now it is evident that a combination of microfocusing x-ray optics with the high brilliance x-ray beams provided by the third generation synchrotron radiation sources like ESRF opens up new capabilities to develop hard x-ray microimaging and microprobe techniques.

Bragg-Fresnel optics is based on a superposition of Bragg diffraction by a crystal (or multilayer) and dispersion by a Fresnel structure, either linear or planar which is grooved into the crystal (or multilayer). Its main advantage is that the various possibilities of beam transformation arising from the specific properties of Fresnel structures now become accessible to the high energy x-ray range.

The performance and applications of the BFO was studied at the undulator and bending magnets beamlines at the ESRF. Optical properties of Bragg-Fresnel lenses (BFL) experimentally measured are the following:

- energy tunability
 - for linear BFL - 6-60keV (efficiency ~40%)
 - for circular BFL - 6-18keV (efficiency ~10-40%)
- a sub- μm resolution
 - 0.8 μm resolution was measured for linear BFL at 15keV and 0.7 μm for circular BFL at 8keV using fluorescence knife-edge technique
- a high thermal resistivity and stability
 - heat load test was done in white undulator beam at maximum power
- well defined shape of the focused beam and high degree of azimuthal symmetry of the intensity distribution, that is very desirable for microdiffraction (small angle scattering) technique.

The following applications have been realized:

- a sub-micrometer fluorescence microprobe;
- a linear and 2D microprobes for microdiffraction- a small-angle scattering camera;
- 2D imaging of the undulator source - a beam emittance monitor.

Test experiments on phase contrast imaging are very promising for developing a phase contrast microscopy and holography. Crystal BFO is of particular interest for microtopography and microtomography techniques as well.

[1] B.Lai, B.Yun, D.Legnini, Y.Xiao, J.Chrzas, P.J.Viccaro, V.White, S.Bajikar, D.Denton, F.Cerrina, E.Di.Fabrizio, M.Gentili, L.Grella, and M.Bacocchi, "Hard x-ray phase zone plate fabricated by lithographic techniques", Appl. Phys. Lett. 61 (16), 1992,1877.

[2] D.Bilderback, S.A.Hoffman, D.J.Thiel, "Nanometer spatial resolution achieved in hard x-ray imaging and Laue diffraction experiments", Science, vol.263, 1994, 201.

[3] V.V.Aristov, A.A.Snigirev, Yu.A.Basov, A.Yu.Nikulin, "X-ray Bragg optics", AIP Conf. Proc., 147, 1986, 253.

Optimised Reflectivities from
SR-Diamond-Laue-Monochromators

By J.D.Stephenson

Div.6.22 Federal Inst. for Materials Research and Testing,
Unter den Eichen 87, 12205 Berlin, FRG.

Theoretical monochromator crystal thickness's for diamond and silicon are determined for optimum Laue-diffracted intensities in the Troika¹ configuration. 111- and 220-diffractions are considered in both symmetric- and asymmetric- Laue diffraction. The influence of the 'effective structure factor' on these results is used to determine the degree of (point defect) SR-damage, accumulated when used as first monochromator crystals in high intensity third generation rings such as the ESRF (Grenoble).

Fig.1 shows typical (symmetrical) Laue 111-reflectivity oscillations vs crystal thickness (for 8KeV radiation) from a nearly perfect ($\bar{1}10$) diamond crystal. Both σ - and π -polarization states are given and exhibit the influence of a reduced 'effective structure factor' on the peak reflectivity values. Further reductions in reflectivity (due to increased point defect) radiation damage follow from these calculations.

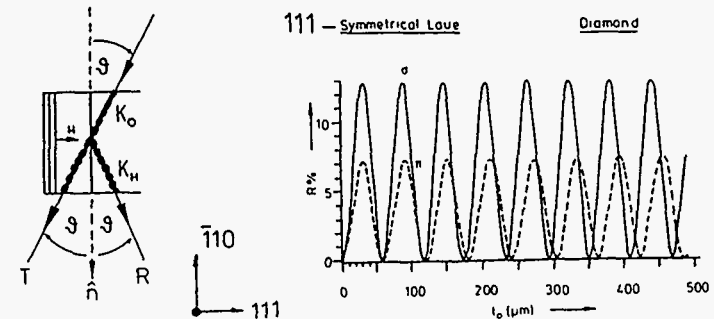


Figure 1: (Sym.) Laue 111-reflectivity oscillations in ($\bar{1}10$) diamond vs. crystal thickness (μm).

¹ESRF Beamline Handbook, p41, Aug 1993

Adaptive X-Ray Mirror Prototype: First results

J. Susini, M. Krumrey, R. Baker and Å Kwick

European Synchrotron Radiation Facility, BP 220, 38043 Grenoble Cedex, France

The substantial increase of the brilliance by the third generation synchrotron sources calls for equivalent progress in the beamline instrumentation. In particular, these characteristics bring the double challenge of requiring more precise focusing while collecting more photons. Therefore, very improved, if not totally new, designs of optical components are necessary. A best compromise must be found among three orthogonal requirements: versatility, high quality and stability under severe working conditions. For a long time, the straightforward solution was to make the surfaces from a rigid material such as metal, glass and other ceramics and then to rely on the dimensional stability of the material to provide acceptable performance during the life of the device. While fixed optical elements are satisfactory for the majority of applications in which the operating conditions can be controlled or at least adequately specified, there is an increasing number of applications in which environmental stress and random processes may dominate the performance of the optical system. In the x-ray optics field, the concept of adaptive systems is very recent and is based on the experience and expertise gathered in developments for astronomy applications.

A first adaptive x-ray mirror prototype was built in 1992 and is now installed on the ESRF beamline BL2 (Materials Science). This system consists of 1m long Pt-coated mirror, water cooled, supported by 2 rows of 11 piezo-electric actuators. The shape of the mirror is continuously inspected by an optical analyzer and its output is used by a feedback loop in a real-time algorithm. The mirror blank made of silicon single crystal shows a micro-roughness and slope errors of 1Å rms and 3µrad rms, respectively. Because of its simplicity, compactness and achromaticity, a Shack-Hartmann sensor is used for inspecting the shape of the reflecting surface. With suitable electronics, the accuracy of such a device is better than $\pm 0.1\mu\text{rad}$ over a 0.5µrad-1mrad range. For optimum performance this optical device has to be completely independent from the vacuum chamber. A workstation associated to real-time electronics calculates the relevant parameters for steering the actuators as a function of both the desired shape and the possible thermal deformation due to the incident beam.

Preliminary experiments carried out on the wiggler beamline showed that the system runs correctly: the feedback loop permits a control of the mirror shape on the µrad level at a frequency of 10Hz. Various shapes (cylinder, parabola or ellipse) can be produced at will to within the above accuracy. The different components of the device are described and the alignment and calibration procedures are discussed. The first results dealing with the properties of the reflected beam (size, divergence and shape) versus both the calibration quality and the incoming power are presented.

ThD77

Compact adaptive / active x-ray mirror: bimorph piezoelectric flexible mirror

J. Susini, D. Labergerie, L. Zhang

European Synchrotron Radiation Facility, BP 220, 38043 Grenoble Cedex, France

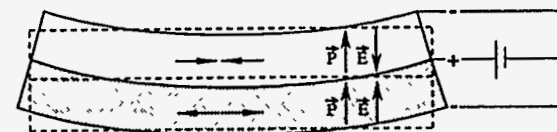
A new concept of bender for optical elements is being under development at the ESRF: a very compact active/adaptive x-ray mirror based on properties of bimorph piezoelectric devices have been manufactured and successfully tested. The system under investigation consists of two pairs of bilayers made of silicon and piezo-electric zirconate lead titanate (PZT). On the interface PZT-PZT a continuous conducting electrode (control electrode) was deposited while both Si/PZT interfaces contain the ground electrodes. As the PZT ceramics are polarized normal to their surfaces, the lateral dimensions of the piezo-electric plates change when a voltage is applied to this system: one plate expands while the other shrinks. This opposing expansion-contraction results in a bending of the bimorph composite like a bimetallic strip (see figure). Due to its symmetry, the Si-PZT-PZT-Si system is less sensitive to temperature variations and maintains constant thickness. PZT was chosen as material because of its high coupling factors, a high piezoelectric constant over extended temperature and stress amplitude ranges. Such a device exhibits several advantages over other benders:

- It is a low cost device: It is mechanically very simple, easy to manufacture and allows large strokes for low applied voltages; thus there is no need of sophisticated power supplies even with high temporal bandwidth.

- It is a versatile device: a multi-electrode system provides the possibility of an adaptive mirrors where the figure can be controlled locally for both meridional and sagittal curvatures. By changing the sign of the voltage one can swap between convex and concave shapes. Therefore the same system can be used either as a focusing mirror or as a beam expander.

As a test, a focused white beam of 35µm FWHM was achieved on a bending magnet beamline, this corresponds to a demagnification of $M=1/17$.

Because of the strong coupling between mechanical and electrical properties of the system, the assessment of the relationship between applied voltage distribution and the resultant deformation is very complex. A theoretical model of the behavior of such a system is presented and compared to both finite element analysis studies and experimental results. Laser interferometry and x-ray measurements allowed complete characterization of these mirrors. Finally, potentialities and perspectives of more advanced devices are discussed.



ThD78

Optical Metrology Facility at the ESRF

L. Susini, R. Baker, A. Vivo

European Synchrotron Radiation Facility, BP 220, 38043 Grenoble Cedex, France

One of the major mirror R&D activities at the ESRF is building a well equipped metrology laboratory for fast and accurate evaluation of the optical quality of beamline components. This paper gives a theoretical and technical overview of problems related to this field:

- Reflection by a non ideal surface can be assessed by calculating the amount and the angular distribution of the scattered light, which leads to a blurring of the ideal image. The rms roughness normally used to characterize surface finish is not related directly to the mirror performance because of bandwidth effects. The measured surface roughness can be described as a Fourier superposition over this range of spatial frequencies of which each component frequency could be defined as a sinusoidal diffraction grating. The spatial periods relevant to the scattering process of x-ray beams in grazing incidence range from several millimeters down to microns. A simple rms roughness value does not give enough information on the spatial periodicity of the reflecting surface, thus a new standard is needed for defining the optical quality of x-ray mirrors. The relevant parameter appears to be the Power-Spectral-Density-Function (PSDF) which is defined as the frequency spectrum of the surface roughness measured in inverse length units. This outlines the need for "PSDF oriented" metrology instrumentation able to cover the relevant spatial period range.

- Secondly, because of their focusing properties, the beamline designer often chooses elliptical or toroidal mirrors. However, such aspheres are very difficult to test by conventional interferometric methods. The manufacturer cannot control the mirror quality during fabrication nor can the user test the efficiency of the optical device before installation on the beamline. This explains why the procurement of suitable grazing incidence optics has been hindered by the lack of adequate standards and testing methods.

To overcome these difficulties, the Optics Group has devoted time and effort in defining and building a complete metrology laboratory. This facility is installed in a Class 1000 clean room, and is equipped with four optical instruments for different and complementary purposes:

- i) The *Micro-Profilometer* (WYKO TOPO 2D/3D) is a phase-measuring interferometer based on the heterodyne principle. A software package allows surface reconstruction and statistical analysis. Microroughness measurements down to the Å level (rms values) with a repeatability of 0.5Å can be achieved within the range 1Å-15µm.

- ii) The *Fizeau Interferometer* (WYKO 6000) is used for measuring figure errors of x-rays optics and thus for testing smaller bending devices for optical elements. This system is equipped with a stabilized single mode HeNe laser ($\lambda=632\text{nm}$) and has an aperture of 150mm. Accuracy and repeatability are $\lambda/100$ and $\lambda/200$, respectively.

- iii) A *Long Trace Profiler* (LTP) serves for absolute measurements of figure errors and of the radius of curvature of long flat or curved mirrors. Our system is an improved version of the LTP designed and built by P.Z. Takacs at Brookhaven National Laboratory. This system is based on a two beam interferometer in which the intensity pattern is recorded by a CCD detector. The optical path difference is related to the slope error which is in turn converted to surface height profile by a Fourier filtering technique. The optical head is mounted on a high precision air bearing stage and is driven by a linear DC motor (non contact drive) along a 2m ceramic beam. This assembly allows both tunable speed (up to 200mm/s) and pitch repeatability of 1µrad. Slope measurements with a resolution of 1 µrad in the tangential direction over spatial wavelengths from a few mm to nearly the length of the tested optical element have been achieved.

- iv) A *Shack-Hartmann* (SH) sensor allows fast and easy dynamical measurement of bent optical elements: After being reflected by the mirror under test, a plane wave produced by a HeNe Laser source, is split into 256 partial beams by an array of microlenses (16x16). This produces a pattern of light spots in the focal plane of the microlens array. This spot pattern is recorded by a CCD camera, from which a PC computer calculates the 2D-mirror shape and related slope errors. Such a device can be routinely used as an *in-situ* optical surface evaluation system.

ThD79

SR Time Gate Quartz Device for Nuclear Resonant Scattering

C.K. Suzuki^{a)}, X.W. Zhang^{b)}, Y. Yoda^{c)}, T. Harami^{d)}, H. Shiwaku^{d)}, K. Izumi^{c)}, T. Ishikawa^{c)}, M. Ando^{b)}, H. Ohno^{d)}, and S. Kikuta^{c)}

a) UNICAMP, University of Campinas, Faculty of Engineering, C.P. 6122, 13084-100 - Campinas, SP, Brazil

b) Photon Factory, National Lab. for High Energy Physics, Tsukuba, Ibaraki305, Japan

c) Department of Applied Physics, Faculty of Engineering, The University of Tokyo, Bunkyo-ky, Tokyo 113, Japan

d) Japan Atomic Energy Research Institute, Office of Synchrotron Radiation Facility Project, Tokai, Ibaraki 319-11, Japan

Very recently, the nuclear resonant scattering with SR, which delivers an intense time delayed and electronic scattered prompt (zero time) photons, has originated a new problem on photon detection technology, the saturation effect of time delayed photons. For any type of detector presently in use, there is a lack of counting the time delayed photons. This problem has been critical for nuclear forward scattering [1] conducted at AR-NE3 beamline of TRISTAN Accumulation Ring [2], and it will certainly be for any other high brilliance beamline. Another useful situation is concerned with experiments of nuclear Bragg scattering with single crystals that do not present forbidden reflections for electronic scattering.

We have then constructed a time gate using a quartz resonator with the objective to discriminate the prompt beam by diffraction on oscillating crystal lattices. The principle of this technique is to use an X-cut quartz resonator crystal with the same frequency of SR single bunch mode. In order to take the same phase, the resonator function generator is synchronized with the synchrotron RF trigger. Fig. 1 shows the SR time modulation diffracted by a 766.95 kHz quartz resonator for the alignment set at $\Delta\theta=4.5\text{arcsec}$ from the peak position of the rocking curve. The X-ray optics consisted of a high order reflection $\text{SiO}_2(16\ 8\ 8\ 0)$ combined with $\text{Si}(16\ 8\ 0)$ and the double crystal $\text{Si}(111)$. An interesting feature is the possibility of adjusting the modulation width and the decay time by changing the value of $\Delta\theta$.

The signal to back-ground rate can be improved by using lower amplitudes of the field V applied to the resonator. Fig. 1 was observed for $V=40\text{v}$, but for $V=3\text{v}$, the signal to back-ground rate increases approximately by a factor of 5. Other procedures can be applied to increase the signal/back-ground rate, for example, the use of double oscillating crystals in a parallel (+,-) setting [3].

An SR time gate with 794.6575 kHz that fits exactly to the AR single bunch frequency shows that this technique is quite viable, even though the signal/back-ground rate has still to be improved.

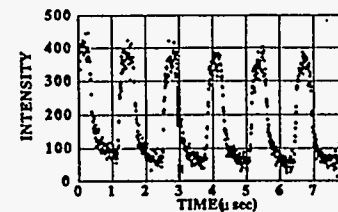


Fig. 1. SR time modulation by diffraction on 766.95 kHz quartz resonator.

[1] S. Kikuta et al., Hyperfine Interactions 71, 1491 (1992).

[2] X.W. Zhang et al., Rev. Sc. Instrum. 63, 404 (1992).

[3] P. Mikula et al., phys. stat. sol. (a) 26, 691 (1974).

ThD80

Chromatic aberration of asymmetrically-cut curved crystal due to dynamical diffraction effect

Kunikazu Takeshita

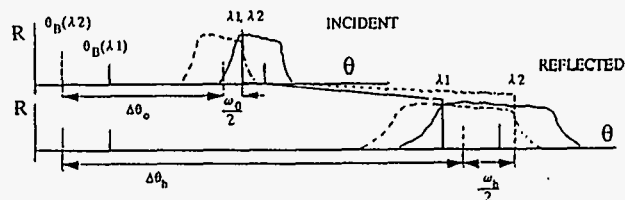
Photon Factory, National Laboratory for High Energy Physics, 1-1 Oho Tsukuba Ibaraki 305, Japan

Asymmetrically-cut curved crystal monochromators are widely used to obtain demagnified images of the sources at many synchrotron radiation facilities. In the case of a relatively large source as is the case for the 2nd generation storage rings, the focus width decreases in inverse-proportion to the asymmetry factor b .

In the present paper, we point out that a very small focal spot size is not obtained even for a point source because of chromatic aberration caused by the dynamical diffraction effect.

We assume that the dynamical diffraction occurs in a curved crystal having a radius of curvature larger than a few tens meters. For polychromatic incident beams emitted from a point source located on the Rowland circle, X-rays with a finite wavelength spread are reflected at every point on the curved crystal monochromator because of the finite Darwin width. For the case of an asymmetrically-cut crystal, X-rays having different wavelengths with the same incident angle are reflected toward slightly different directions. This situation is illustrated by the figure: X-rays with wavelength λ_1 (represented by solid line) are reflected toward $\theta_B(\lambda_1) + \Delta\theta_h(\lambda_1) - \omega_h(\lambda_1)/2$, while X-rays with wavelength λ_2 (represented by dotted line) are reflected toward $\theta_B(\lambda_2) + \Delta\theta_h(\lambda_2) + \omega_h(\lambda_2)/2$.

The broadening of the focal spot size due to this effect is approximately given by $R \cdot (b-1) \cdot \omega_0 \cdot \sin(\theta_B + \alpha)$, where R is the radius of Rowland circle. This broadening is estimated to be 0.7mm even for a point source with the optics being presently used on small angle scattering beam line (BL-15A) at the Photon Factory. Results of ray tracing calculations for BL-15A will be presented. It is important to take this effect into account in the designing of a demagnifying optics using a curved crystal.



ThD81

At-Wavelength Metrology of 13 nm Lithography Imaging Optics

Z.Tan, A.A.MacDowell, B.La Fontaine

AT&T Bell Laboratories, 510E Brookhaven National Laboratory, Upton, NY 11973

J.E.Bjorkholm, R.R.Freeman, M.Himel, D.Tennant, D.Taylor, O.R.Wood II,
AT&T Bell Laboratories, 101 Crawfords Corner Road, Holmdel, NJ 07733

W.K.Waskiewicz, D.L.Windt, D.L.White

AT&T Bell Laboratories, 600 Mountain Avenue, Murray Hill, NJ 07974

S. Spector

State University of New York at Stony Brook, Stony Brook, NY 11794

We discuss the development of an extreme ultraviolet (EUV) interferometer for testing EUV lithography systems operating at 13 nm wavelength using the UI3U undulator beam line at the NSLS. The design strategy and implementation for lateral shearing interferometry and knife edge tests will be described. We will present initial results of testing of a 10x Schwarzschild camera that is designed to image feature sizes as small as 0.10 μm with light of 13nm wavelength.

Work in part supported by Advanced Technology Program Cooperative Agreement #70NANB1H1115.

ThD82

The Radiometry Laboratory of PTB at BESSY

G. Ulm and B. Wende

Physikalisch-Technische Bundesanstalt, Abbestr. 2 - 12, D-10587 Berlin, Germany

The Physikalisch-Technische Bundesanstalt (PTB), the German national institute of science and technology in the field of metrology, operates a laboratory for VUV radiometry at the electron storage ring BESSY. The basic tasks of the laboratory are the realization and dissemination of radiometric units and the characterization of radiation sources, detectors and optical components in the VUV. Now, after more than ten years of BESSY operation, six calibration and testing stations on four beamlines are used for different objectives and spectral regions.

BESSY is optimized for use as a primary radiometric standard source in a broad spectral range from about 1 eV to 15 keV, i.e. as a source of calculable spectral photon flux.

Radiation source calibration is performed by comparing the unknown spectral photon flux of the source under investigation with the calculable spectral radiant flux of BESSY. Different transfer source standards (e.g. deuterium lamps, hollow cathode sources) are calibrated at three experimental stations in the spectral range from 2 eV to 1.8 keV, each consisting of an imaging mirror, a monochromator and a detector system.

Detector calibration is performed at three experimental stations (spectral range 3 eV to 1.8 keV) by comparing the response of a detector to monochromatic radiation with the response of a primary detector standard of known efficiency. For doing this spectral purity of the monochromatized radiation (low contributions due to stray light and higher orders) and high radiant powers are most important. We have recently begun to use electrically calibrated cryogenic radiometers as primary detector standards. Most of our work up to now concerned the calibration of semiconductor photodiodes. At one beamline the undispersed calculable synchrotron radiation is used for e.g. the determination of the absolute detection efficiency of Si(Li) detectors.

Characterization of optical components, e.g. determination of the reflectance of mirrors or the transmittance of filters and measurement of the diffraction efficiency of gratings, is performed at two reflectometers which are operated behind a SX700 or a TGM monochromator in the spectral range from about 30 eV to 1500 eV.

We describe in detail the experimental stations and the calibration instrumentation of PTB at BESSY. Furthermore, examples of very recent work (e.g. development of transfer source standards for the radiometric calibration of VUV telescopes, characterization of soft X-ray detectors, reflectance measurements of soft X-ray multilayer mirrors) will be presented.

ThD83

The new PTB reflectometer at BESSY

D. Fuchs, M. Krumrey*, P. Müller, F. Scholze, G. Ulm

*Physikalisch-Technische Bundesanstalt (PTB), Berlin,
Abbestr. 2-12, D-10587 Berlin, Germany*

At the radiometry laboratory of the PTB at BESSY a reflectometer for the VUV/soft x-ray spectral region is operated for several years utilizing monochromatic radiation from a toroidal grating monochromator (TGM) or from a high resolution plane grating monochromator (SX 700 type) /1/. The monochromators provide - as a prerequisite for precision reflectometry - a well collimated beam of high spectral purity in the energy region from 30 eV to 250 eV (TGM) and 40 eV to 1500 eV (SX 700). The development of more and more sophisticated optical elements for the VUV/soft x-ray spectral region, e.g. multilayer mirrors with curved surfaces and a gradient in layer thickness, for various applications ranging from x-ray microscopy to astronomy led to the design of the new reflectometer with advanced capabilities aimed at

- performing accurate $\theta / 2\theta$ -scans,
- positioning of the sample relative to axis of rotation,
- the ability to accommodate even large samples,
- minimum time for sample exchange.

Special double concentric ball bearings are used to guarantee that the axes of sample and detector rotation coincide. Both allow - independent of each other - simultaneous linear motions and rotations providing the necessary precision for $\theta / 2\theta$ -scans. The goniometers and linear motions for both the sample and the detectors are located outside the vacuum. A goniometer head carrying the sampleholder is operated in vacuum. It provides a positioning of the sample relative to its axis of rotation. This feature is of particular importance for figured and complex optics. The system can accommodate specimen with dimensions of up to 200 mm which can be interchanged through a vacuum interlock. Two kinds of detectors are used: a semiconductor photodiode (GaAsP-Schottky type) as a large area detector and a channel electron multiplier. A long detector-sample distance and the well collimated photon beam provide an angle resolution of less than 1 mrad in the reflected beam. Measurements can be performed in the range from near-normal incidence ($\theta < 1^\circ$) to grazing incidence angles. A detailed description of the reflectometer as well as some typical experimental results are presented.

/1/ M. Krumrey, M. Kühne, P. Müller, F. Scholze, Proc. SPIE 1547, 136 (1991)

*present address: ESRF, B.P. 220, F-38043 Grenoble Cedex, France

ThD84

Heat Load Analysis for Pre-Mirrors at SPring-8 Undulator Beamlines

T. Uruga, K. Ohtomo and H. Yamaoka

*JAERI-RIKEN SPring-8 Project Team
Hirosawa 2-1, Wako, Saitama, Japan*

Large heat power will be loaded on the pre-mirrors from undulator at the SPring-8 beamlines. It is required to design the effective cooling and reforming devices to correct the thermal deformation of mirror surface figure. As the first step, we have examined the simulation for these problems by the finite element analysis.

For the simulation, the incident beam flux and spectrum are calculated by using SPECTRA and OEHL. The typical high power density undulator of which first harmonic energy is 8 keV gives absorbed power density of 1.1 W/mm² on the mirror surface at the glancing angle of 5 mrad placed at 33 m from the source.

The thermal structural analysis including the effect of gravity is performed for direct or indirect water cooling mirrors by using ANSYS. The direct cooling mirrors have cooling channels in the longitudinal direction in the substrate. The indirect cooling mirror is designed to have cooling blocks as close as possible to the irradiated surface. The interface between the substrate and cooling blocks is filled with In-Ga. Si, SiC and Glid-Cop are chosen as the mirror substrate. The indirect cooling system has similar cooling efficiency to the direct one and hold the temperature raise of about 35 degree. The mirror surface is deformed to parabolic figure in the longitudinal direction. In the meridional direction, the deformation is negligibly small. Si is the most promising material as pre-mirror substrate among above three materials because of its better figure of merit.

The longitudinal deformation of the mirror surface can be corrected by a simple bending device such as 4 points force loading type. The device gives the cylindrical shape of which radius of curvature is several km to focus the beam under the heat load.

ThD85

X-Ray Optics R&D's for SPring-8 Beamlines

T. Uruga¹, S. Hashimoto², Y. Kashihara², H. Kimura¹, Y. Kohmura¹,
M. Kuroda¹, H. Nagasawa³, K. Ohtomo¹, K. Okui⁴, H. Yamaoka¹,
S. Matsuoka¹, T. Ishikawa¹, T. Ueki¹ and H. Iwasaki¹

1. *JAERI-RIKEN SPring-8 Project Team, Hirosawa 2-1, Wako, Saitama, Japan*
2. *JASRI, Minatoshimanakamachi 6-9-1, Chuo-ku, Kobe, Japan*
3. *Seikei University, Kichijojikitamachi 3-3-1, Musashino, Tokyo, Japan*
4. *The University of Tokyo, Hongo 7-3-1, Bunkyo-ku, Tokyo, Japan*

Toward the first operation of SPring-8 envisaged in 1997 fiscal year, several R&D programs for beamline optics have been carrying out. An overview of the present status of these R&Ds is presented. These include optical instruments and elements (monochromators, mirrors, multilayers, micro-beam generation, x-ray phase retarders, x-ray interferometers) for beamlines, off-line characterization station for optical elements, design-aid utilities such as software for ray-tracing, thermal stress analysis and diffraction optics.

ThD86

Radiometry at the NIST SURF II Storage Ring Facility

M. L. Furst, R. M. Graves, L. R. Canfield, and R. E. Ycsf
National Institute of Standards and Technology*
Gaithersburg, MD 20899

Abstract

SURF II, the 300 MeV circular electron storage ring at the National Institute of Standards and Technology (NIST) Gaithersburg, MD facility is the site of the NIST radiometry programs in the far ultraviolet. Continuum radiation from SURF II extends from the visible to about 310 eV, and is being productively used as a standard for the calibration of integrated optical systems, particularly space experiments. A dedicated beamline offers facilities for all necessary translations of the calibration object, either in a 3500 l vacuum tank, or through a bellows coupling on the beamline. The SURF II facility is also used for a large portion of the NIST far ultraviolet transfer detector standards program, in which spectrally calibrated photodiode radiation detector standards are available for the 5-248 eV range of photon energies. One of the most recent uses of the instrument calibration beamline has been with a new apparatus designed to qualify working standards for calibration of the NIST MgF₂-windowed far ultraviolet transfer standards (4.9-10.7 eV). In addition to these and other NIST photoemissive standards, available for many years, new radiometric quality silicon photodiodes have now been developed. These detectors offer several improvements, including much higher sensitivity, relative immunity to radiation-induced degradation, lower sensitivity to surface contamination, and they can be produced with spectrally-selective characteristics.

Design and Performance of a Schwarzschild Objective Mirror Positioning System for the SuperMAXIMUM X-ray Microscope

J.P. Wallace, J.T. Welnak, F. Cerrina
Center for X-ray Lithography
University of Wisconsin
Madison, WI 53706

SuperMAXIMUM is a second generation scanning spectroscopic X-ray microscope being developed by the University of Wisconsin. This work is in collaboration with and will be installed at ELETTRA in Trieste, Italy. In this paper we will discuss the mechanics designed to align the microscope.

The X-ray focusing element of the microscope is a multi-layer coated Schwarzschild Objective. This is a normal incidence spherical optic system containing two mirrors which need to be precisely positioned relative to each other. The microscope will provide a 50X demagnification. To achieve a 1000 Å spot size, the angular positioning accuracy between the mirrors must be better than 1 arcsec. Spacing between the mirrors must be positioned better than 100 μm. We will have the capability to index between three separate objectives, each coated for a specific energy. The entire system must reside in a UHV vacuum chamber capable of obtaining 10⁻¹¹ torr operating pressure.

To align the Schwarzschild Objective we have designed an all flexural hinge, single piece construction stage. This stage will give us the ability to change *in-situ* the tilt of the secondary mirror relative to the primary, and change the mirror spacing. To actuate the stage we will be using fired construction piezo stacks. For position feed back, in house designed capacitance gauges will read the position of the secondary mirror surface relative to the primary mirror mount. The stage design for indexing between the three gratings will also be discussed.

This paper will also present preliminary results from optical bench testing, including knife edge test and Ronchi grating tests. The final microscope assembly and operation is expected in July 1995.

* Electron and Optical Physics Division, Physics Laboratory, Technology Administration, U. S. Department of Commerce

Liquid-Metal Pin-Fin Pressure Drop by Correlation in Cross Flow

Zhibi Wang, Tuncer M. Kuzay, and Lahsen Assoufid

Experimental Facilities Division
Advanced Photon Source
Argonne National Laboratory
9700 South Cass Avenue
Argonne, IL 60439

The pin-fin configuration is widely used in high heat flux applications. Recently, the pin-fin design with liquid metal coolant are also applied to synchrotron-radiation beamline devices.

This paper investigates the pressure drop in pin-post mirror with liquid gallium as the coolant. Because the pin-post configuration is a relatively new concept, information in the literature on pin-post mirrors or crystals is rare, and information on the pressure drop in pin-post mirrors with liquid metal as the coolant are even rarer. Because the cross flow in cylinder arrays geometry is very similar to that of the pin-post, the pressure drop correlation for the cross flow of fluid with various fluid characteristics or properties through a tube bank are studied so that the results can be scaled to the pin-fin geometry with metal as coolant. The emphasis of this paper is on the influence of two variables on the pressure drop: fluid characteristics, especially viscosity and density, and the relative length of the posts. The difference and correlation of the pressure drop between long and short posts and the predication of the pressure drop of liquid metal in the pin-post mirror and comparison with a existing experiment are addressed.

This work is supported by the U.S. Department of Energy, BES-Materials Sciences, under contract no. W-31-109-ENG-38.

ThD89

X-Ray Optical Analyses with X-Ray Absorption Package (XRAP)

Zhibi Wang, Tuncer M. Kuzay, Roger Dejus

Experimental Facilities Division
Advanced Photon Source
Argonne National Laboratory
9700 South Cass Avenue
Argonne, IL 60439

XRAP is a computer code developed for analysis of optical elements in synchrotron radiation facilities. Two main issues are to be addressed: 1) generating BM (bending magnet) and ID (Insertion Device) spectrum and calculate their absorption in media, especially in such structural forms as variable thickness windows/filters and crystals; and 2) providing a finite difference engine for fast but sophisticated thermal and stress analyses for optical elements. Radiation cooling, temperature-dependent material properties such as thermal conductivity, thermal expansion coefficient, etc. are included. For very complex geometries, an interface is provided directly to a finite element code such as ANSYS. Some of the present features built into XRAP include: (1) generation of BM and ID spectra; (2) photon absorption analysis of optical elements including filters, windows and mirrors, etc.; (3) buckling check of the optics and filters/windows under thermal loading from the absorbed power; (4) user friendly graphical interface that is based on the state-of-the-art technology of GUI and X-window systems, which can be easily ported to other computer platforms; (5) postscript file output of either black/white or colored graphics for total/absorbed power, temperature, stress, spectra, etc.

This work is supported by the U.S. Department of Energy, BES-Materials Sciences, under contract no. W-31-109-ENG-38.

ThD90

**Thermal and Deformation Analyses of a Novel Cryogenically Cooled
Monochromator for the Advanced Photon Source Beamline**

Zhibi Wang, Wenbin Yun, and Tuncer M. Kuzay

Experimental Facilities Division
Advanced Photon Source
Argonne National Laboratory
9700 South Cass Avenue
Argonne, IL 60439

The analytical results and design considerations for a novel cryogenically cooled Advanced Photon Source (APS) monochromator are presented. Because the monochromator uses silicon crystal, cryogenic cooling enables one to take advantage of the high conductivity and low thermal expansion coefficient of silicon at cryogenic temperatures. The APS monochromator features a machined slot with variable thickness below the surface. With this configuration, only a fraction of the total undulator power is absorbed by the crystal; the remaining power is transmitted through the crystal and is absorbed by a second element that can be cooled by standard cooling techniques. A variety of analyses has been performed with different parameters and configurations to maximize the performance of the monochromator and minimize the total absorbed power by the crystal.

This work is supported by the U.S. Department of Energy, BES-Materials Sciences, under contract no. W-31-109-ENG-38.

ThD91

LBL-35577A

**A Variable Radius Mirror for Imaging the Exit Slit of an SGM
Undulator Beamline at the ALS.**

Tony Warwick
Lawrence Berkeley Laboratory, Berkeley, CA 94720, USA
and
Meir Shlezinger
ADA, Haifa-31021, Israel

Adjustable radius cylindrical mirrors have been built for refocusing the light which diverges from the monochromator exit slit in two undulator beamlines at the Advanced Light Source. The spherical grating monochromators have exit slits which move up and down the beamline to stay at the focus of the grating as it rotates. The mirrors have adjustable focal lengths, accomplished by means of an integral bending mechanism¹ driven by a UHV piezo-electric transducer, to keep the image of the moving slit (10 μ m FWHM) focussed at various locations in the end-stations. Because of the high brightness of the source, the slope tolerances on the mirrors are very tight (1 μ rad). Figure deformations caused by bending are modeled by finite element calculations and compared to slope error measurements of the polished surface, as the radius is changed. The mirrors are designed to develop these errors only as the magnification varies from unity, and the effect of the bending deformations is of magnitude comparable to that of the third order aberration from the cylindrical surface.

1. M.R. Howells, D.Lunt, Opt. Eng., to be published.

This work was supported by the Director, Office of Energy Research, Office of Basic Energy Sciences, Materials Sciences Division of the U.S. Department of Energy, under Contract No. DE-AC03-76SF00098

*This paper should be considered as a POSTER, contact:
Dr. Tony Warwick, 2-400 Lawrence Berkeley Laboratory,
Berkeley, CA 94720.
Tel. (510) 486 5819 Fax (510) 486 7696*

ThD92

**SuperMAXIMUM:
A Schwarzschild-Based,
Spectro-Microscope for ELETTRA**

J. Welna^k, Z. Dong, H. Solak, J. Wallace, and F. Cerrina
University of Wisconsin—Center for X-ray Lithography
3731 Schneider Drive, Stoughton, WI 53589

M. Bertolo, A. Bianco, S. Di Fonzo, S. Fontana, W. Jark, F. Mazzolini, R. Rosei and
A. Savoia
Sincrotrone Trieste, Padriciano 99, I-34012 Trieste, Italy

G. Margaritondo
Institut de Physique Appliquée, Ecole Polytechnique Fédérale, CH-1015 Lausanne,
Switzerland

X-ray microscopy excels on high-brightness sources, such as the ALS and ELETTRA, where there is a good match between the source and optics phase spaces. In these conditions, diffraction-limited operation becomes possible with large flux.

We will discuss the development of a second-generation X-ray scanning spectro-microscope; an evolution of the MAXIMUM project at the University of Wisconsin. The new tool is called SuperMAXIMUM and will be installed on ELETTRA in Trieste, Italy.

The monochromator consists of a rotatable plane mirror and a set of three interchangeable spherical gratings covering the photon energy range from 20 eV to 300 eV. This monochromator design was chosen to approximately preserve the Rowland circle condition without changing the slit position or the beam direction. A focused image of the radiation coming from the undulator is formed at a pinhole placed at the end of the beamline. At that position, the radiation spot from the undulator is demagnified by a factor of 60 in both the vertical and the horizontal direction by means of a pair of focusing and a pair of refocusing mirrors placed before and after the monochromator.

The microscope design is based on MAXIMUM¹. Both microscopes use multilayer-coated Schwarzschild objectives for their reduction optics. The planned enhancements over MAXIMUM include a higher demagnification (50x compared to 20x), multiple objectives changeable *in situ*, a novel flexure pinhole stage, a unique Schwarzschild positioner and combination coarse/fine scanning stage. An electrostatic analyzer with multiple detectors will also be used to increase the data acquisition rate. We will discuss these improvements as well as our new experimental control software and a custom data display and analysis program developed by our group.

¹High Resolution Nanospectroscopy with MAXIMUM: Photoemission Spectroscopy Reaches the 1000 Å Scale. W. Ng et al., Nuclear Instruments & Methods (A) (1994) In press.

**YB₆₆ Monochromator: New Opportunities in XAFS Spectroscopy in the
1-2 keV Region.**

Joe Wong^a, Z.U. Re^k, M.Rowen^b, T. Tanaka^c, F. Schaefer^d, B. Mueller, G.N. George^b, I.J. Pickering^b, G.H.Via^e, B.DeVries^e, and G.E. Brown, Jr.^f, ^aLawrence Livermore National Laboratory, University of California, PO Box 808, Livermore, CA 94551, ^bStanford Synchrotron Radiation Laboratory, PO Box 4349, Stanford, CA 94309, ^cNational Institute for Reseach in Inorganic Materials, 1-1 Namiki, Tsukuba, Ibaraki 305, Japan, ^dBESSY, 1000 Lenzallee, Berlin, Germany, ^eExxon Research and Engineering Company, Route 22 Est, Annadale, NJ 08801, ^fDepartment of Geological and Environmental Sciences, Stanford University, Stanford, CA 94305.

Until recently XAFS measurements in the 1-2 keV region remained a challenging experimental task. This was primarily due to the lack of an adequate monochromator crystal that possesses both the required x-ray and materials properties, such as large d-spacing, high resolution and reflectivity, UHV compatibility, damage resistance in a synchrotron radiation beam, absence of constituent element absorption edges and stability, both thermal and mechanical. A recent successful development of a new YB₆₆ monochromator material obviates a number of these earlier experimental difficulties. In this paper the crystal structure and properties of YB₆₆ relevant to the use of soft x-ray monochromator will be reviewed. The XAFS spectra of a number of selected model compounds containing Mg, Al and Si will be presented. Future monochromator development and prospect of XAFS experiments with YB₆₆ for high Z L- and M- edges will also be discussed.

References

1. Joe Wong et al., Nucl. Instrum. Meth. A291, 243 (1990).
2. F. Schaefer et al., Synchrotron Radiation News, 5(2) 28 (1992).
3. M. Rowen et al., Synchrotron Radiation News, 6(3), 25 (1993).

CROSS COLLIMATION: A NEW SCHEME
FOR GRATING MONOCHROMATOR ALIGNMENT

Z. Xu,* S. L. Hulbert,** and I. McNulty*

*Advanced Photon Source, Argonne National Laboratory
Argonne, IL 60439

**National Synchrotron Light Source, Brookhaven National Laboratory
Upton, NY 11973

A simple scheme for precision alignment of grating monochromators is presented. The achievable resolution and limitations of the scheme are also discussed. By requiring each of two laser beams to be normal to the grating surface and collinear with the reflected beam from the other laser, the grating surface normal can be accurately made orthogonal to the monochromator spindle axis (roll adjustment). With the lasers set 150° apart and 5 meters away from the grating, the alignment resolution of the roll axis is of the order of 2 arc seconds. The grating grooves and the monochromator spindle axis can be made parallel (yaw adjustment) then by aligning all the diffracted beams of different orders (including zeroth order). A screen 5 meters away from the grating yields a yaw resolution of the order of 10 arc seconds. This scheme has been used to align the monochromators at X13A and U13U beamlines at the National Synchrotron Light Source.

This research was supported by the U.S. Department of Energy, BES Materials Sciences, under contracts No. W-31-109-ENG-38 and DE-AC02-76CH00016.

ThD95

GeoCARS Micro-Focusing Kirkpatrick-Baez Mirror Bender
Development

Bingxin Yang¹, Mark Rivers and Wilfried Schildkamp

Consortium for Advanced Radiation Sources,
The University of Chicago, Chicago, Illinois 60637

We present the design and initial test data on the GeoCARS microfocusing Kirkpatrick-Baez Mirror Bender. The bent mirror design is based on a Taylor series approximation of the ideal ellipse shape. The mirror has a focal length is 15 cm with a working length of 8 cm. It is designed to work in the range of grazing incidence angle of 3 to 8 mrad with the shaping adjusted dynamically. Results of the shape measurement with a long trace profiler will be presented.

1) Present address: APS Argonne National Lab.

ThD96

An Intensity Interferometer for Soft X-rays

L. Yang, I. McNulty, and E. Gluskin
Advanced Photon Source,
Argonne National Laboratory
Argonne, IL 60439

We designed and built an intensity interferometer to characterize the spatial coherence of a soft x-ray undulator beam. The source size and shape can be determined from the measured coherence function. We anticipate that when this technique is mature, it will provide a useful diagnostic for high brightness x-ray beams. The instrument is 400 mm long and is mounted on a standard 204 mm diameter flange. This compact design is readily adaptable to other beam lines with sources of sufficient spectral brightness. Details of the interferometer design and performance are presented.

X-RAY ZONE PLATES AND THEIR APPLICATIONS

W. Yun, B. Lai
Advanced Photon Source, Argonne National Laboratory, Argonne, IL 60439

A. A. Krasnoperova, F. Cerrina
Center for X-Ray Lithography, University of Wisconsin-Madison, Stoughton,
WI 53589

E. Di. Fabrizio, L. Luciani, M. Figliomeni, and M. Gentili
CNR-IESS, Via Cineto Romano 42, 00156 Roma, Italy

In recent years, zone plates have been shown to be among the most promising x-ray focusing devices over a large spectral region. Many types of x-ray microprobes using zone plate as a focusing device are been developed. These techniques can be used to map spatial distributions of trace elements, crystal strains, crystall orientation, chemical states, and to image an object with submicron spatial resolution in all three directions.

In this presentation, we will review the current status of zone plate development and discuss future possibilities. The focusing properties of a zone plate and their applications will be discussed in general and compared with other types of focusing optics. The development of a zone plate based microprobe and its applications for study of various material systems will be presented.

* This work is supported in part by the Dept. of Energy, BES-Materials Science, under contract no. W-31-109-ENG-38.

* Supported by the U.S. Department of Energy, BES-Material Sciences, under contract W-31-109-ENG-38.

ThD97

The submitted manuscript has been authored
by a contractor of the U. S. Government
under contract No. W-31-109-ENG-38.
Accordingly, the U. S. Government retains a

The submitted manuscript has been authored
by a contractor of the U. S. Government
under contract No. W-31-109-ENG-38.
Accordingly, the U. S. Government retains a
nonexclusive, royalty-free license to publish
or reproduce the published form of this
contribution, or allow others to do so, for
U. S. Government purposes

ThD98

COMPARISON OF NUMERICAL AND EXPERIMENTAL
SIMULATION OF A BERYLLIUM WINDOW
UNDER INTENSE HEAT LOAD

A. Gambitta¹, C. Poloni², A. Visintin² and F. Zanini^{1,3}

¹ Sincrotrone Trieste, Trieste (Italy)

² Dip. di Energetica, Università Di Trieste, Trieste (Italy)

³ I.N.F.N., Sezione di Trieste, Trieste (Italy)

Beryllium windows are widely used in synchrotron radiation beamlines as filters to absorb photons in the lower energy region or used as an interface between two different vacuum environments. In the X-Ray Diffraction beamline at Elettra the UHV environment of the front-end is decoupled from the high vacuum of the beamline by means of two different beryllium windows. The first one acts as a prefilter and will absorb most of the heat load, while the second is a safety, bent window against a possible overpressure due to accidental venting in the high-vacuum part of the beamline. We focalize our attention on the first window to evaluate its resistance to thermal loads by means of a finite element method analysis and an experimental test with an electron gun assembly. This subject has already been studied by some research groups who have usually found a large discrepancy between experimental results and theoretical predictions, finding a higher resistance to thermal loads. To overcome this discrepancy, non-linear analysis in the plastic region of the material is developed taking into account the behaviour of the material as a function of temperature.

A Simple Method for Wavelength Calibration of
Monochromators with a Sine Drive

Qiuping WANG, Yunwu ZHANG
NSRL, Univ. of Sci & Tech of China, Hefei, Anhui 230026, P R. China

1. Introduction

A sine drive, converting the linear displacement to axis rotation, is widely used in spectroscopy for wavelength scanning. Its simplicity and possibility to make the wavelength proportional to the displacement are the main advantages.

For the SR beamline, generally there are several gratings which can be interchangeable in UHV. It is a laborious task that making all gratings have the linear relation between the wavelength and the displacement. From the practical point of view, it is not necessary to do so. In this paper, we give out in which case we can realize the linear relation of λ -X and how to calibrate the monochromator which has more than one grating by the fitting method, which has been used successfully in the wavelength calibration of two monochromators at NSRL.

2. Errors in Sine drive and its characteristics

If the sine bar is not perpendicular to the direction of displacement, the error is θ_1 and the driving plate is not perpendicular to the direction of displacement, the error θ_2 . It is easy to get the expression for displacement X and its rotation angle α :

$$X = L_e(\sin(\alpha - \theta) + \sin\theta) \quad (1)$$

$\theta = \theta_1 - \theta_2$ means the angle between sine arm and driving plate at $X=0$, $L_e = L/\cos\theta_2$ is the effective sine arm length, L is the sine arm length. This is the intrinsic relation between the displacement and angle in a sine drive.

3. Wavelength calibration

According to the grating equation for the 1st inside spectrum,

$$\lambda = C \sin\alpha \quad (2)$$

in which C: $= 2d \cos k$ λ : monochromatic wavelength behind the exit slit d: grating ruling separation k: half extending angle of the grating α : grating angle turned from zero order. From (1) and (2), we have

$$\lambda/X = (C/L_e)(\cos\theta - \sin\theta \tan(\alpha/2)) \quad (3)$$

As shown above, if the extending angle $2k$ of the grating is constant for the whole wavelength, the only way to obtain linear λ -X relation is to make $\theta=0$.

Indeed, it is a simple matter to get λ -X in linear relation for one grating. But in SR beamline, often there are more than one grating adopted in monochromator. It is arduous to obtain the linear λ -X relation for every grating at the same time. We must do the adjustment and measurement repeatedly for all gratings.

In fact, (2) and (3) are the basic relations of wavelength and the displacement. After we measured at the known wavelength λ_i and its displacement X_i ($i \geq 3$), the variable parameters θ , C and L_e in (2) and (3) can be determined completely.

$$\text{Let } F(\theta, C, L_e) = \sum (X_i - X_i')^2, \quad i \geq 3 \quad (4)$$

where $X_i' = L_e(\sin(\alpha_i - \theta) + \sin\theta)$, $\alpha_i = \sin^{-1}(\lambda_i/C)$, X_i and λ_i are measured values of displacement and wavelength. By iterating the variable parameters of θ , C and L_e , it is possible to reduce (4) to a minimum. Substituting the above parameters into (1) and (2), the wavelength λ at any position X of the sine drive is determined. Thus we only need to measure a set of λ_i and X_i one time for each grating. This method is suitable for all monochromators utilizing a sine drive as the wavelength scanning apparatus, whether or not the angle k is constant. If k is wavelength dependent, the λ -X has no linear relation even for the case $\theta=0$. The fitting method is viable, too

Development of a Hard X-Ray Imaging Microscope

B. Lai, W. Yun, Y. Xiao, L. Yang, and Z. Cai
Advanced Photon Source, Argonne National Laboratory, Argonne, IL 60439

A. Krasnoperova and F. Cerrina
Center for X-Ray Lithography, University of Wisconsin-Madison, Stoughton, WI 53589

E. DiFabrizio, L. Luciani, M. Figliomeni, and M. Gentili
CNR-IESS, Via Cineto Romano 42, 00156 Roma, Italy

Abstract

An imaging microscope using a phase zone plate for hard x-rays has been developed and tested. The zone plate, with a 5-cm focal length and 0.2 μm smallest linewidth, was used to image 8 keV x-rays from the samples. Compared to scanning probe, imaging microscope can offer advantages such as parallel detection, easily adjustable magnification, nearly diffraction-limited resolution over the entire field, and reduced sensitivity to source size and source motions. In the simple case, an imaging microscope can be set up with a small divergence beam and a CCD camera. For more divergent beam, condenser optics can be used upstream of the sample. We had tested both geometries and resolution better than 0.5 μm was obtained in either case. The images were all obtained with an exposure time of less than one minute, for a magnification factor of 20-30 for the x-rays. Another magnification of 7 times was obtained by converting the x-rays into visible light and then using a lens system coupled to the CCD camera. The results from both arrangements of the imaging microscope will be discussed and possible applications will be assessed.

• This work is supported in part by the Dept. of Energy, BES-Materials Science, under contract no. W-31-109-ENG-38.

The submitted manuscript has been authored by a contractor of the U.S. Government under contract No. W-31-109-ENG-38. Accordingly, the U.S. Government retains a nonexclusive, royalty-free license to publish or reproduce the published form of this contribution, or allow others to do so, for

ThD101

Detector Posters

(Session ThE)

- ThE1 Amemiya, Y., Yagi, N., Ito, K., Asano, Y., Wakabayashi, K., Ueki, T., Endo, T. Development of X-Ray TV Detectors with Image Intensifiers for Diffraction Experiments.
- ThE2 Aulchenko, V., Baru, S., Velikzanin, Yu., Dubrovin, M., Ponomarev, S., Usov, Yu. Fast One Coordinate X-Ray Detector.
- ThE3 Capel, M.S., Smith, G.C., Yu, B. One and Two-Dimensional Xray Detector Systems at NSLS Beam Line X12B, for Time Resolved and Static Xray Diffraction Studies.
- ThE4 Cho, T., Kohagura, J., Hirata, M., Sakamoto, Y., Yatsu, K., Tamano, T., Miyoshi, S., Hirano, K., Yagishita, A., Maezawa, H., Saitoh, Y., Sato, K., Miyahara, S., Kondoh, T., Tanaka, S., Snider, R. Experimental Verification of the Three-Dimensional Diffusion Effect of X-Ray Produced Charges in Semiconductor X-Ray Detectors on the Quantum-Efficiency Enhancement.
- ThE5 Crowder, T., Ade, H. A Low Pressure Parallel Plate Proportional Counter Optimized for Detection of Nitrogen Fluorescence.
- ThE6 Dent, A.J., Derbyshire, G.E., Derst, G., Farrow, R.C. Dead Time Correction and Io Normalisation in Germanium Solid State Detector Systems Using an Incoming Count Rate Monitor.
- ThE7 Dolbnya, I.P., Makarov, O.A., Mezentsev, N.A., Pindyurin, V.F., Subbotin, A.N. Measurements of an Absolute Spectral Sensitivity of X-Ray Semiconductor Detectors in the Photon Energy Range of 1.5-15 keV with the Use of "White" SR Beam of the Storage Ring VEPP-3.
- ThE8 Dolbnya, I.P., Pindyurin, V.F., Subbotin, A.N. Measurements of Time Parameters of X-Ray Semiconductor Detectors With the Use of Synchrotron Radiation of the Storage Ring VEPP-3.
- ThE9 Farrow, R., Derbyshire, G.E., Dobson, B.R., Dent, A.J., Bogg, D., Headspith, J., Lawton, R., XSPRESS X-Ray Signal Processing Electronics for Solid State Detectors.
- ThE10 Fedotov, M.G., Panchenko, V.E. The Experimental Photodiode-Array Unit for Ultrahigh-Resolution Recording of X-Ray Images.
- ThE11 Fedotov, M.G., Panchenko, V.E. The System of Fast One-Dimensional X-Ray Cinema with Direct Registration and Storage of Images by the Matrix CCD.
- ThE12 Fischetti, R.F., Rosenbaum, G., Blasie, J.K. Multi-Element Detector for Sub-Millisecond Time-Resolved X-Ray Diffraction: Fast Plastic Scintillator Fiber Array with Parallel Read Out.
- ThE13 Hammersley, A.P., Svensson, S.L., Thompson, A. Generalised Calibration and Correction of Distortions in 2-D Detector Systems with Application to the Molecular Dynamics™ Imaging Plate Scanner and the ESRF X-Ray Image Intensifier/CCD Detectors.
- ThE14 Hirata, M., Cho, T., Kohagura, J., Yatsu, K., Tamano, T., Kondoh, T., Saitoh, Y., Sato, K., Miyahara, S., Hirano, K., Maezawa, H., Miyoshi, S. A Newly Developed Multilayer Semiconductor X-Ray Detector for the Observations of Wide Energy-Range X-Rays.
- ThE15 Kishimoto, S. Recent Developments in the Avalanche Photodiode (API) X-Ray Detector for Timing and Fast Counting Measurements.

- ThE16 Kohagura, J., Cho, T., Hirata, M., Yatsu, K., Tamano, T., Yagishita, A., Maezawa, H. Detection Characteristics of an Ultra-Low-Energy-Measurable Pure-Germanium Detector for a Pulse-Hight-Analysis and a Current-Mode Observation in the 100 ev Photon-Energy Region.
- ThE17 Korde, R., Canfield, L.R., Vest, R., Pearson, D., MacKay, J., Gullikson, E. Absolute XUV Silicon Photodiodes for Synchrotron Radiation Applications.
- ThE18 Dolbnya, I.P., Kulipanov, G.N., Lyakh, V.V., Makarov, O.A., Pindyurin, V.F., Gorin, G.B., Gyunsburg, K.E., Zvezdova, N.P., Kochubey, V.I. Micron Spatial Resolution X-Ray Image Plates with Non-Erasing Reading.
- ThE19 Yoo, S.S., Rodricks, B., Sivananthan, S., Faurie, J.P., Montano, P.A. MBE Grown CdTe Photoconductor Array Detector for X-Ray Measurements.
- ThE20 Naday, I., Ross, S., Kanyo, M., Westbrook, M.L., Westbrook, E.M., O'Mara, D., Stanton, M., Phillips, W.C., Belamy, H., Cox, A., Tsuruda, H., Phizackerley, P. The Gold Detector: Modular CCD Area Detector for Macromolecular Crystallography.
- ThE21 Chernov, V.A., Nikitenko, S.G., Dementyev, E.M., Drobyazko, I.B. The Applications of Gas Electroluminescence Detectors for Fluorescence and Quick-Scanning XAFS Measurements.
- ThE22 Lau-Frambs, A., Kroth, U., Rabus, H., Tegeler, E., Ulm, G. The New PTB Detector Calibration Facility Based on an Electrical Substitution Radiometer for the Wavelength Range 35-400 nm.
- ThE23 Menk, R.H., Besch, H.J., Grobmann, U., Langer, R., Lohmann, M., Schenk, H.W., Wagener, M., Walenta, A.H., Dix, W.R., Graeff, W., Illing, G., Reime, B., Schildwachter, L., Tafelmeier, U., Kupper, W., Harron, C., Rust, C. A Dual Line Multi Cell Ionization Chamber for Transvenous Coronary Angiography with Synchrotron Radiation.
- ThE24 Meyer, M. Construction of a Small Area Position Sensitive Detector for Measurement of Low Intensity Bragg Reflections.
- ThE25 Milne, J.C., Johnson, E.D., Smith, G.C. Low-Pressure Multistep Gaseous Primary Ion Counting.
- ThE26 Smith, A.D., Derbyshire, G.E., Farrow, R.C., Martini, M. Solid State Detector for Soft Energy EXAFS.
- ThE27 Sturhahn, W., Toellner, T., Alp, E. APDs - Large Dynamic Range Detectors for Hard X-Rays.
- ThE28 Suzuki, M., Awaya, Y., Oura, M., Mizogawa, T., Masuda, K. Development of a Proportional Scintillation X-Ray Imaging Chmber for Synchrotron Radiation Experiments.
- ThE29 Wentink, R.F., VanGorden, S., Zarnowski, J., Aloisi, D., MacDonald, C.A., Gibson, W.M., Fields, R.E., Denton, M.B. Advances in Radiation Hardened Charge Injection Devices (CIDs) as Direct X-Ray Imaging and Energy Dispersive Detectors.
- ThE30 Zinin, E.I. Dissector with 2 Picosecond Time Resolution
- ThE31 Beck, L., Bizeuil, C., Soullie, G. Absolute Calibration of a Photodiode Array with the Synchrotron Radiation (1.5-10 keV)

Development of X-ray TV Detectors with Image Intensifiers for Diffraction Experiments

Y. Amemiya¹, N. Yagi², Y. Asano³, K. Ito¹, S. Kishimoto¹,
K. Wakabayashi⁴, T. Ueki⁵, and T. Endo⁶

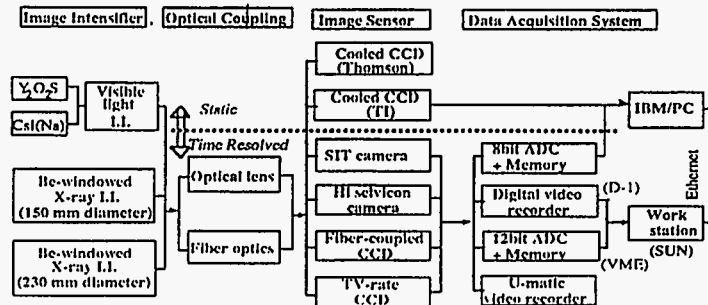
¹ Photon Factory, KEK ² Tohoku Univ. ³ JAERI
⁴ Osaka Univ. ⁵ Riken ⁶ Hamamatsu Photonics K.K.

Although the imaging plate has excellent performance as an X-ray area detector, it is neither suited to time-resolved nor real-time measurements. The advantage of the X-ray TV detector is that 1) it is well suited to time-resolved and real-time measurements, 2) it is free from count-rate limitation unlike gas area detectors such as MWPC, and that 3) the related technologies which have been long accumulated are expected to develop further in the near future.

The X-ray TV detector consists of i) an image intensifier, ii) an optical coupling, iii) an image sensor (camera), and iv) a data acquisition system. An X-ray image is converted to intensified and de-magnified visible-light image by the image intensifier. Then the visible-light image is viewed by the image sensor such as a cooled CCD camera or a TV-rate (30 frames/second: NTSC mode) CCD camera through the optical coupling. The output from the image sensor is digitized and stored in the data acquisition system. The role of the image intensifier is 1) to enlarge the active area size of the TV detector, 2) to improve the detective quantum efficiency (DQE), and 3) to improve the dynamic range for the X-ray detection. Figure shows the diagram of our X-ray TV detectors which have been developed under the R & D project.

One of the major developments in the project is concerned with the fabrication of a large aperture X-ray image intensifier (I.I.) which has a beryllium (Be) entrance window. It has an aperture of 150 mm ϕ or 230 mm ϕ with a 1-mm thick Be window. The CsI:Na phosphor of 150 μ m thickness is attached directly on the inner surface of the Be window. The CsI:Na crystals are made in a columnar shape along the direction normal to the phosphor surface so that the undesired light scattering within the phosphor in the lateral direction is minimized. A bi-alkali (RbCsSb) photo-cathode is evaporated onto the inner surface of the CsI:Na phosphor. Incident X-rays are efficiently transmitted through the Be window (80 % for 8 keV X-rays), and are converted to visible photons by the phosphor. Then they are converted to photoelectrons with the photo cathode. The photoelectrons are accelerated so as to produce an intensified visible image on an output phosphor. Owing to the photon gain of the X-ray I.I., as many as 550 visible photons per an 8 keV photon are incident to the CCD. This value is large enough to employ a TV-rate CCD camera with its noise quantum-limited. This enables us to record time-resolved diffraction patterns at a rate of 30 frames/second. The dynamic range of the Be-windowed X-ray I.I. is of 4 orders of magnitude. The X-ray TV detector has the non-uniformity of response and the image distortion to be corrected by software.

The detailed performance of the X-ray TV detectors will be described together with preliminary applications to time-resolved X-ray diffraction experiments.



The1

FAST ONE COORDINATE X-RAY DETECTOR

V.Aulchenko, S.Baru, Yu.Velikzanin, M.Dubrovin,
S.Ponomarev, Yu.Usov
Budker Institute of Nuclear Physics
Novosibirsk, Russia

The new detector OD-3 is under testing now. The multiwire proportional chamber and electronics of OD-3 differ essentially from those of the old OD-2 /1/. The MWPC of OD-3 has a drift volume and the coordinate of quantum along the anode wire is detected by measuring the charge induced on the strips of the lower cathode plane directed to the object under investigation for parallax elimination.

The signals from the strips preliminary amplified and shaped by the low noise front-end electronics are transmitted to the Main Crate via screened twisted pairs and after additional amplification and shaping are continuously digitized by FLASH ADC's under 40MHz common clock control.

Detection and selection of the signals from the certain quanta is realized in the logic part of the electronics using pulse height, time and coordinate cuts. All main transformations of data are realized in the Processor Unit using tables written in the RAM.

There are several modes of operation which allow one successively accumulate in the incremental RAM 16, 32 or 64 frames by 4, 2 or 1K channels respectively. The frame can contain full scale, any part or several parts of scale. The frame time is controlled by external Timer and it's minimum duration is 1mks. The Incremental RAM consists of fast and slow parts with common size 64kx29 bits and 10MHz operation rate.

Main design parameters of OD-3 detector

- inlet window (beryllium) 200x10mm*2;
- detection angle 30 degree;
- scale 3200 channels;
- channel width 1.6x10E-4 rad (60mkm);
- coordinate resolution (F.W.H.M.) 4.5x10E-4 rad;
- differential nonuniformity (R.M.S.) 1.5%;
- counting rate (50% losses) 10E7 events/sec;
- energy range 3-20 keV;
- excessive pressure in chamber 0--3 atm.

1. V.M.Aulchenko, I.G.Feldman et al. One coordinate X-ray detector OD-2. Nucl. Instr. and Meth. in Phys. Research, v.A261(1987),78-81.

The2

ONE- AND TWO-DIMENSIONAL X-RAY DETECTOR SYSTEMS AT NSLS
BEAM-LINE X12B, FOR TIME RESOLVED AND STATIC X-RAY
DIFFRACTION STUDIES

M. S. Capel, G.C. Smith and B. Yu
Brookhaven National Laboratory
Upton, NY11973-5000

Abstract

X-ray detector systems, both one- and two-dimensional, have been designed and built according to gas proportional chamber principles for small angle scattering studies of biological and polymer samples. The major instrument, a two-dimensional detector with delay-line readout on both axes, has count rate capabilities approaching 10^6 s^{-1} , very low differential non-linearity, position resolution of about $100 \mu\text{m}$ for X-ray energies from 5 to 15 keV, and exceptional stability in the position response. It has been operating almost continuously for the last two years. We present a description of the detector design philosophy, the characteristics of the TDCs which were specifically designed for the position readout, and the data acquisition. We emphasize particularly those aspects of the system which require careful design to ensure these detectors are capable of operating stably at very high rates for long periods of time, and therefore result in devices which are generally superior in performance to those available commercially.

Results are presented from dynamic and static studies carried out at beam line X12B which illustrate the benefits that gas proportional detectors possess, compared to other types of detector, for specific experiments, particularly those concerned with time resolved phenomena.

An outline is presented of plans for future, higher rate detectors (in the region of 10^8 s^{-1}), with emphasis directed to dynamic studies with biological molecular structures. These new systems are based on position encoding techniques that are presently being developed for high rate, high multiplicity, particle experiments in high energy and nuclear physics. Sophisticated interpolating cathode structures will be used, together with multi-channel front-end electronics designed in monolithic form.

Experimental verification of the three-dimensional diffusion
effect of x-ray-produced charges in semiconductor
x-ray detectors on the quantum-efficiency enhancement

T. Cho, J. Kohagura, M. Hirata, Y. Sakamoto, K. Yatsu, T. Tamano,
S. Miyoshi, K. Hirano^{a)}, A. Yagishita^{a)}, H. Maezawa^{a)}, Y. Saitoh^{b)},
K. Satoh^{b)}, S. Miyahara^{c)}, T. Kondoh^{d)}, S. Tanaka^{e)}, R. Snider^{f)}

Plasma Research Centre, University of Tsukuba, Ibaraki 305, Japan

^{a)}Photon Factory, National Institute for High Energy Physics,
Tsukuba, Ibaraki 305, Japan

^{b)}Seiko Instruments Inc. ^{c)}Seiko EG&G Co. Ltd.

^{d)}Japan Atomic Energy Research Institute, Naka Fusion Research
Establishment, Ibaraki, Japan

^{e)}Fukui National College of Technology, Fukui, Japan

^{f)}General Atomics, San Diego, California 92186

We proposed a new theory on the x-ray energy response of a semiconductor x-ray detector [1]; this theory provided the interpretations of the recent finding of a contradictory evidence against the conventional understanding of the semiconductor x-ray-sensitive layer (*i.e.* the depletion layer) [2].

The essential physics principle of this theory is based on the three-dimensional diffusion effect of x-ray produced charges in a semiconductor field-free substrate region. It is found and reported in this paper that the quantum efficiency of a semiconductor x-ray detector is enhanced when this phenomenon is taken into account, and the data on the semiconductor detector using monochromatized synchrotron radiation from a 2.5-GeV positron storage ring at the Photon Factory of the National Institute for High Energy Physics are well fitted by the theory. Using this theory, we fabricated a new detector in a commonly employed "photodiode" shape for the experimental verification of this theory; the enhanced quantum efficiency of 50 % at 20 keV compared with that for a commercially available silicon-surface-barrier (SSB) detector is demonstrated using the same thickness of the depletion layers.

In addition to such an improvement of quantum efficiency of the x-ray detector, we measure the diffusion length of the detector using a precisely collimated x-ray narrow beam and a multichannel detector array having μm -order position controller mechanisms (the x, y, z, and θ -direction controller). Verification of the consistency between the value of the diffusion length from this direct observation and the predicted value of the diffusion length from our theory on the quantum efficiency, as well as its observed value from the photoluminescence method using a laser beam has been attained for the first time.

[1] T. Cho *et al.*, Nucl. Instrum. Method A (to be published).

[2] W. J. Price, *Nuclear Radiation Detection*
(McGraw-Hill; New York, 1964).

A low pressure parallel plate proportional counter optimized for detection of Nitrogen fluorescence.

T. Crowder and H. Ade

Department of Physics, North Carolina State University, Raleigh, NC 27695

Detection of Nitrogen fluorescence at 400 eV has been difficult with proportional counters using polymer windows due to the low transmission of photons at this energy by carbon based compounds. Typically two polypropylene films in a differentially pumped arrangement are used [1]. We have chosen a single 230 μm silicon nitride film as a window. It can withstand atmospheric pressure and has extremely low gas leakage. It is therefore possible to operate the detector in a UHV environment. The Si_3N_4 window has the further advantage of efficient N fluorescence detection, while effectively filtering lower energy fluorescence. Energy resolution at the nitrogen fluorescence energy will be discussed as will applications.

Acknowledgments: We thank Graham Smith and Erik Johnson of Brookhaven National Labs for their advice and stimulating conversations.

References

[1] D.A. Fischer et al., Proc. SPIE 733 (1986) 504.

Dead time correction and I_0 normalisation in germanium solid state detector systems using an incoming count rate monitor.

A.J. Dent, G.E. Derbyshire, G. Derst, R.C. Farrow.
EPSRC Daresbury Laboratory.

Abstract

The rate limitation of a photon counting germanium solid state detector system is largely determined by the shaping time of the amplifier, which is in turn set by the required system resolution. This rate limitation arises because when an event passes into the shaping amplifier it is paralysed for a time referred to as the dead time, which is a function of the shaping time. If any further events pass into the shaping amplifier during this time, one or both events may be corrupted or lost. This phenomenon is known as pulse pile-up. However, if we use an incident count rate monitor (ICR) which gives an accurate indication of the incident photon rate but no energy information, we can correct for any pulses lost in the shaping amplifier due to pile-up. This allows us to run the detector system at higher rates and still retain throughput linearity. This has been shown by the work of Zhang *et al* [1]. The authors also showed that with respect to EXAFS, the loss of linearity due to pulse pile-up at high rates has two main effects: 1) The EXAFS oscillations and edge step height are reduced and 2) noise and glitches present in I_0 do not normalise out.

We have extended this work to higher input count rates and in addition to using the paralysable model to correct for the loss of throughput linearity as the input rate increases, we have also used the ICR monitor to give us an I_0 value which when itself corrected can give improvements over an ion chamber I_0 in normalising noise and glitches out. Data has been taken with station 9.3 on the SRS at Daresbury Laboratory using 18mM CuNO_3 solution at ICR values of 20,47,84,120 and 180kHz. In addition data has also been taken for 0.02 at% As implanted to 1 μm depth in a-Si using reflexafs. This data was collected at 120kHz as opposed to the usual 40kHz and normalised using these techniques.

We will show using this data that using pile-up correction and an ICR I_0 , the linearity of the system can be retained at higher count rates and thus significant improvements in the signal to noise ratio can be gained.

Measurements of an absolute spectral sensitivity of X-ray semiconductor detectors in the photon energy range of 1.5-15 keV with the use of "white" SR beam of the storage ring VEPP-3

I.P. Dolbnya, O.A. Makarov, N.A. Mezentsev, V.F. Pindyurin, A.N. Subbotin#
Budker Institute of Nuclear Physics, 630090 Novosibirsk, Russia
#Institute of Experimental Physics, 607200 Arzamas-16, Russia

The results of measurements of an absolute spectral sensitivity of silicon semiconductor detectors (SSD) in the X-ray quanta energy range of 1.5-15 keV are presented. The detectors under calibration procedure have been placed into the direct "white" synchrotron radiation (SR) beam from the bending magnet (1.7 T) of the storage ring VEPP-3. The spectrum of X-radiation has been changed with the using of sets of filters made from lavsan (mylar), polychlorvinil and aluminium foils. The spectrum could be also changed by the tuning the energy of electrons in the storage ring. The possibility of exact calculation of SR spectrum on the calibrated detector under its irradiation in different conditions allows to resolve a system of Fredholm integral equations of the first kind on the dependence of unknown spectral sensitivity with respect to detector's currents registered [1]. The solution of such a system has been found in a parametric form. The correction of the kernel of integral equations (SR spectrum) with the regarding to the vertical angular spread of electrons has been carried out in assumptions that the function of the angular spread of electrons has the Gaussian type and the resulting vertical angular dependence of SR spectrum is a convolution integral of the angular-energy own function of SR source and the electron's angular spread function. Such a correction can be made (without the solution of integral equations) by simple measurement of a dependence of a signal from the detector vs. its vertical angular position in a conditions when this dependence is mainly determined by electron's angular spread function than the own SR angular spread function. These demands are satisfied when the hard part of SR spectrum is only registered, i.e. that the proper thick absorber is located before the detector.

The measurements of the vertical angular spread of electrons in the bending magnet and in the wiggler-magnet have done. The Mo-absorber with a thickness of 0.1 mm and SSD were used in measurements for the bending magnet source (the electron's energy of 1.2 GeV). The same Mo-absorber, Al-absorber with a thickness of 1 cm and ionization chamber filled with nitrogen under normal pressure were applied in measurements for the wiggler-magnet (2 T) source (2 GeV).

The analysis of possible experimental errors on the result of the restoration of SSD absolute spectral sensitivity are carried out and described. The achieved error of measurements for an energy and a current of electrons in the storage ring, the bending radius and the angular spread of electrons on the orbit in a source point, the transmission of SR through the filters, geometrical sizes, etc. allowed to restore the SSD absolute spectral sensitivity with the resulting error of not worse than 10% in the total photon energy range under the study.

References

- 1 I.P. Dolbnya, N.A. Mezentsev, V.F. Pindyurin, K.P. Romanenko, A.N. Subbotin, *Rev. Sci. Instrum.* 63, No.1 (part 2A) 685-688(1992)

Measurements of time parameters of X-ray semiconductor detectors with the use of synchrotron radiation of the storage ring VEPP-3

I.P. Dolbnya, V.F. Pindyurin, A.N. Subbotin#
Budker Institute of Nuclear Physics, 630090 Novosibirsk, Russia
#Institute of Experimental Physics, 607200 Arzamas-16, Russia

The method of measurements of time parameters of X-ray detectors with the use of specific pulse peculiarities of synchrotron radiation (SR) is introduced and developed. The results of measurements of time characteristics of pulse silicon semiconductor X-ray detectors (SSD) with the using of the "white" SR beam produced by the wiggler-magnet (2 Tesla) of the storage ring VEPP-3 are presented. The stroboscopic oscilloscope was employed to register X-radiation flashes. The signals from the oscilloscope for the further data processing have been delivered to the PDP-11/73 computer via CAMAC modules. The preliminary amplitude and time calibration of the oscilloscope was performed with the using of generators of precise amplitude and precise frequency, respectively. The comparison of results with independent measurements on the powerful pulse X-ray tube MIRA-2D was carried out. The comparison of impulse and static regimes of the SSD operation has been performed for the aim of absolute spectral calibration. It was shown that if the time dependence of SR flash, impulse time characteristic function of the detector and distortions of the cable registration track are taken into account then there is possible to obtain the pulse parameters of X-ray detectors with the time resolution of not worse than 0.5 nsec.

XSPRESS

X-RAY SIGNAL PROCESSING ELECTRONICS FOR SOLID STATE DETECTORS

R. Farrow, G.E. Derbyshire, B.R. Dobson, A.J. Dent, D. Bogg, J. Headspith, R. Lawton.
EPSRC Daresbury Laboratory.

M. Martini, K. Buxton.
EG&G ORTEC Ltd.

Abstract

With recent improvements in synchrotron sources and X-ray optics great pressures have been placed on detector systems to produce higher count rates and better resolutions. Present high performance 13 element germanium detector systems can give reasonable count rates with good resolution ($\sim 10^4 - 10^5$ kHz per channel and ~ 250 eV FWHM @ Fe^{55} with 0.5uS shaping time). However, these systems are restricted by limitations in both the detector and in the analogue pulse processing after the detector. With respect to the detector, increasing the number of channels without degrading the energy resolution is a great challenge due to increased crosstalk and capacitance. The analogue pulse processing electronics are significantly limited by the dead time introduced by the shaping amplifier. This dead time causes pulse pile-up at higher rates which leads to non-linearity and poor resolution.

This paper describes the XSPRESS system which has been developed at Daresbury Laboratory for the new Wiggler II beamline 16. This system overcomes previous limits in both signal processing and detector fabrication to give great improvements in system performance. The signal processing electronics departs from standard analogue processing techniques and employs sophisticated adaptive digital signal processing hardware to reduce the dead time associated with each event to a minimum. This VME based technology allows us to vastly increase the count rate for each channel yet still retain the ability to gain very good resolution. The detector has been developed through a collaborative agreement with EG&G ORTEC and packs an unprecedented 30 germanium crystals into an extremely small area whilst still retaining the energy resolution of smaller arrays.

This system has increased throughput rate by an order of magnitude per channel and when all channels are implemented, an increase of at least two orders of magnitude for the whole array should be seen.

Data has been taken using this system on the SRS at Daresbury Laboratory and these results will be given along with a detailed explanation of the operation of this system.

The experimental photodiode-array unit for ultrahigh-resolution recording of X-ray images

Fedotov M. G. and Panchenko V. E.
Institute of Nuclear Physics,
630090 Novosibirsk, Russia

The solid-state X-ray imagers (photodiode arrays, PDA, and charge-coupled devices, CCD) which are now used have a geometrical resolution defined by their sensitive-pixel sizes and being from 10 up to 20 microns that is considerably worse than the resolution of photoemulsions (0.1 - 1 micron).

There is description of attempt to create the recording unit with the spatial resolution comparable to that of photoemulsions; the first results of testing of the unit are described. The last has been done on the basis of the PDA containing 1024 sensitive pixels which have 150-microns height and are positioned with 25-microns step. The feature of given PDA consists in presence of the individual charge-sensitive amplifier in each pixel. This allowed to realize an algorithm of the digital double correlated sampling and to remove KTC noise which, under ordinary conditions, limits the PDA sensitivity. For diminishing the noise level, the unit is provided with the double-correlated-sampling analogous chain, which removes 1/f noises of the on-chip read preamplifiers as well as possesses the LF-filter qualities, and with cooling of the PDA by means of the two-stage battery of Peltier cells.

The unit has been tested in the mode of the integrating X-ray imager. It is expected, by corresponding computer processing of the separate X-ray photon absorption events, one will succeed in determining of each event coordinate while allowing for the signal charge distribution between pixels due to charge diffusion in the PDA substratum.

The system of fast one-dimensional X-ray cinema with direct registration and storage of images by the matrix CCD

Fedotov M. G. and Panchenko V. E.
Institute of Nuclear Physics,
630090 Novosibirsk, Russia

A recording system on the basis of the matrix CCD and first results of its testing are described. The system is intended for fast registration (from 10 up to 100 microseconds per an image) of limited series (100 through 500) of one-dimensional X-ray images. Here the CCD is used for direct registration of X-rays as well as for accumulation and short-time holding of one-dimensional-images bulk. After completion of registration, stored images are transformed into electric signal, digitized and transmitted to a computer.

There is consideration of the system speed main restrictions conditioned by both matrix-CCD electric parameters and charge-diffusion effects in substratum; the methods which allow to diminish these restrictions are considered too.

Multi-Element Detector for Sub-Millisecond Time-Resolved X-ray Diffraction: Fast Plastic Scintillator Fiber Array with Parallel Read Out.

R.F. Fischetti, G. Rosenbaumt and J.K. Blasiç†

Biostructures Institute, University City Science Center and †Department of Chemistry, University of Pennsylvania, Philadelphia, PA

† Current Address: Structural Biology Center, Argonne National Laboratory, Argonne, IL

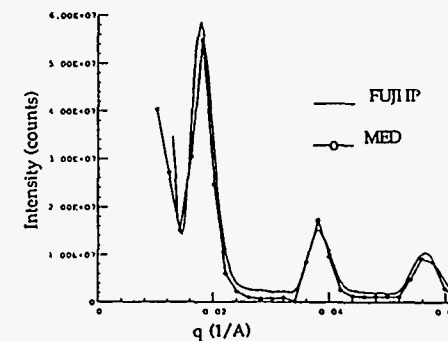
Time resolved X-ray diffraction experiments require the high flux available at synchrotron radiation sources in order to record data of high statistical quality on submillisecond and longer time scales. There presently is no two-dimensional position sensitive X-ray detector that can both record the high flux available and time slice on submillisecond time frames. The Multi-Element Detector (MED) was designed to bridge the gap between detectors such as CCDs and proportional wire detectors for time-resolved X-ray diffraction experiments.

The design of the MED incorporates 128 independent channels of fast plastic scintillator fibers which are read out in parallel via photon counting electronics. We are presently using scintillator fibers (BCF-10, Bicon Corp.) of 1 x 1 mm cross section which are arranged to form a linear position sensitive detector with an active area of 1 mm by 128 mm. An advantage of this design is that the X-ray sensitive front end is constructed of relatively inexpensive materials, and one can exchange the front end to match the detection geometry of a particular experiment.

The maximum useful count rate is limited to ~10 MHz per channel at a 10% dead time loss. Thus the electronic dynamic range can exceed six orders of magnitude due to the low dark counts of the 1/2 inch diameter PMTs. Diffraction patterns can be recorded in up to 1024 contiguous time frames of 16 microsecond minimum duration with only 200 nsec blind time between frames. Noncontiguous time frames of 1 μ sec minimum duration can be spaced as closely as 16 μ sec. The scintillation efficiency coupled with the numerical aperture of the fibers and the photocathode efficiency results in an overall quantum efficiency of ~50%.

Figure 1 shows diffraction patterns obtained with the 16-channel prototype detector and FUJI Imaging Plates for comparative purposes. The meridional diffraction patterns were obtained by stepping the grazing angle of incidence, ω and recording the intensity as a function of 2θ . The maximum intensity of the (001) reflection at $q = 0.0181 \text{ \AA}^{-1}$ was 3.4×10^6 cps. Optical cross talk on the order of a few percent exists between adjacent channels. Thus the MED data shown have been corrected for cross talk and uniformity of response. These diffraction patterns clearly demonstrate the ability of the MED detector for recording X-ray diffraction patterns at high incident rates. The full 128-channel version of the detector will be constructed from such 16-channel segments as soon as the cross talk problem has been resolved.

Figure 1. Meridional X-ray diffraction patterns recorded from 5-bilayer Langmuir Blodgett multilayer films of Ba-arachidate as function of $q = 2\sin(\theta)/\lambda$. The 16 channels of the MED were positioned at two different 2θ values, and the patterns were appended together to provide the 32 channel pattern. The pattern obtained with the FUJI IP was scaled to approximately the same intensity of the maxima of the pattern recorded with the MED.



This work was performed on beamline X9B at NSLS and is supported by NIH grant RR01633.

A newly developed multilayer semiconductor x-ray detector for the observations of wide energy-range x rays

M. Hirata, T. Cho, J. Kohagura, K. Yatsu, T. Tamano, T. Kondoh^{a)}, Y. Saitoh^{b)}, K. Satoh^{b)}, S. Miyahara^{c)}, K. Hirano^{d)}, H. Maizawa^{d)}, and S. Miyoshi

Plasma Research Centre, University of Tsukuba, Ibaraki 305, Japan
a) Japan Atomic Energy Research Institute, Naka Fusion Research Establishment, Ibaraki, Japan
b) Seiko Instruments Inc. c) Seiko EG&G Co. Ltd.
d) Photon Factory, National Laboratory for High Energy Physics, Ibaraki 305, Japan

For the purpose of the developments of wide-energy-range-sensitive x-ray detectors, we design and fabricate a new-type multilayer semiconductor x-ray detector using our new theory on a semiconductor x-ray detection efficiency [1]. This new-type detector is characterized using synchrotron radiation from a 2.5-GeV positron storage ring at the Photon Factory of the National Laboratory for High Energy Physics (KEK) [2]. This new detector is essentially composed of the multilayers of 4 or 6 commercially available photodiodes. Each photodiode is made by a 300- or a 515- μm thick, and a 10 \times 10-mm² or a 20 \times 20-mm² square-shaped wafer. For the common use of these individual photodiodes, the quantum efficiency η begins to decrease from (8-10) keV, and then η decreases down to a few tens % at 20 keV.

On the other hand, for our newly designed detector a significant improvement of $\eta \sim 100$ % in the 10-20-keV energy regime (Beam Line 15C at the Photon Factory) is observed, and even at 100 keV $\eta > 30$ % is still anticipated. This new x-ray detector has the following various characteristic advantages: (i) compactness being available to a multichannel-detector array, (ii) an outgas-free detector for a high-vacuum use, (iii) high degree of immunity to ambient magnetic fields, (iv) no need of new technologies and new devices for the fabrication of this special-shaped multilayer detector. Furthermore, (v) the combination of the x-ray-signal output from each layer provides the information on the electron energies. These advantages lead to make a new x-ray-tomography detector array under a high-vacuum and a strong magnetic-field conditions particularly for the identifications of wide-band x-ray-emitting electron distributions including high-energy plasma-electron distributions. The detailed structure and the detailed x-ray response of the new-type detector are presented at the conference.
[1] T.Cho, M.Hirata *et al.*, Nucl. Instrum. Method A (to be published).
[2] M.Hirata *et al.*, Nucl. Instrum. Method B 66, 479 (1992).

Generalised Calibration and Correction of Distortions in 2-D Detector Systems with Application to the Molecular DynamicsTM Imaging Plate Scanner and the ESRF X-Ray Image Intensifier/ CCD Detectors

A P Hammersley, S O Svensson, A Thompson

Abstract

A flexible modular system has been developed for the calibration and correction of: spatial distortion, intensity linearity, uniformity of response, and image plate decay, in area detector systems. The "system" consists of both a variety of calibration techniques and software. The approach has been applied in detail to two different types of detector system which present appreciable distortions: the Molecular DynamicsTM Imaging Plate scanner, and the ESRF developed X-ray Image Intensifier/ CCD read-out detector system [1]. Some of the techniques have also been applied to other imaging plate scanners and other detector systems.

A. The Molecular DynamicsTM Imaging Plate Scanner (Model 400E): With suitable calibration and application of corrections to scientific data the MD scanner system has been shown to give comparable scientific results to the MarResearchTM scanner in laboratory protein crystallography test experiments. With this success the MD scanner has been used in a variety of synchrotron radiation scientific experiments. Both the calibration methods and the scientific results will be presented.

B. The ESRF X-Ray Image Intensifier/ CCD Detector: This type of detector is potentially a very important development in X-ray detectors, but one which inherently causes very large spatial and uniformity of response distortions. The success of this detector depends on calibration and correction of scientific data. With the addition of non-magnetic calibration grids, the same techniques have been applied to these detectors. A laboratory experiment has shown that data from a protein crystal (tetragonal lysozyme) can be successfully corrected and integrated, and further synchrotron radiation experiments are being performed. Both the calibration methods particularly important for these systems and the scientific results will be presented.

[1] A P Hammersley, S O Svensson, and A Thompson, "Calibration and correction of spatial distortions in 2D detector systems", *Nucl. Instr. Meth. Section A*, 1994, In Press

Recent developments in the avalanche photodiode (APD) X-ray detector for timing and fast counting measurements

Shunji KISHIMOTO

Photon Factory, National Laboratory for High Energy Physics
Oho 1-1, Tsukuba-shi, Ibaraki-ken 305, Japan

An APD detector using a new silicon device has been developed for X-ray timing measurements. The device, S5343, developed by Hamamatsu Photonics, has an excellent time resolution of 100 ps and has only a short tail, or a width of 1.4 ns at 10^{-5} maximum. Its depletion layer is 10 μm thick and the detection area is 1 mm in diameter. A small peak adjacent, 2 ns apart, to the main peak can be clearly resolved by using the detector in observing the bunch structure of the Photon Factory ring. A measurement of the purity between the main bunch and the second one to the order of 10^{-9} was successfully executed with the detector as an application to the bunch-purity monitor. As another application of the device, an APD detector of 4-ch multi-array type has been tested for X-ray timing measurements, which needs a sub-nanosecond time resolution and a tail as short as possible in the response function of the detector.

The APD detector has also a property for fast counting to the order of 10^8 counts per second because its output width is shorter than a few nanoseconds. The count-rate property has been examined by using synchrotron radiation beam and an APD device of C30817E (EG&G Optoelectronics), which has a depletion layer of 100 μm thick and a detection area of 1 mm in diameter. The result shows that the count-rate response can be expressed by a paralyzable model of $k=2$ in the pulsed beam counting, given by

$$m = f(1 - \exp(-\epsilon \cdot n/f)) \exp(-(k-1)\epsilon \cdot n/f),$$

where m is the observed rate, n is the true rate, f is the frequency of the pulsed beam and ϵ is the efficiency of the detector. The number of $k(=1, 2, \dots)$ is determined by a dead time, τ in the counting system, i.e., $\tau < (k/f)$. A tandem-type detector (4-ch, arranged in parallel with the beam direction) using thicker devices and a CAMAC counting system is prepared to detect X-rays to a high count-rate of 10^8 cps with an efficiency larger than 80% at 17.5 keV.

Detection characteristics of an ultra-low-energy-measurable pure-germanium detector for a pulse-height-analysis and a current-mode observation in the 100-eV photon-energy region

J. Kohagura, T. Cho, M. Hirata, K. Yatsu, T. Tamano,
A. Yagishita*, and H. Maezawa*

Plasma Research Centre, University of Tsukuba, Tsukuba,
Ibaraki 305, Japan

* Photon Factory, National Laboratory for High Energy
Physics, Tsukuba, Ibaraki 305, Japan

In the energy range from one keV down to a few hundred eV, a newly developed "ultra-low-energy-measurable" pure-germanium detector for a pulse-height-analysis and a current-mode observation has been characterized using synchrotron radiation monochromatized by a grasshopper monochromator [1] at the Photon Factory of the National Laboratory for High Energy Physics (KEK) for the first time.

X-ray observations in this low-energy region were previously tried to be carried out using several types of "windowless" Si(Li) detectors for the necessity of these photon observations. These detectors, however, unfortunately had several troubles including temporal variations in the quantum efficiencies because of their detector-surface deteriorations due to various impurities in vacuum.

Our pure-germanium detector has a 3000- \AA thick polymer window metalized by a 400- \AA thick aluminum supported by a 100- μm apart silicon-ribbed structure. However, for this liquid-nitrogen-cooled detector with the special window, its actual energy-response data are not available at this time. Therefore, the detailed studies of its characteristics are reported particularly for the purpose of the reliable realization of pulse-height-analyses in such a low-energy photon regime. The present report includes (i) the experimental data on the quantum efficiency in the 100-eV energy regime, and (ii) the energy resolution data at the 600 eV photons in a pulse-height-analysis mode, including the information on the system noise level.

This detector is essentially useful for resolving problems on the formation mechanisms of plasma electron-velocity distribution functions [2] including a key issue of rf plasma current sustainments [3] for steady-state operations in future nuclear-fusion devices.

[1] T. Cho *et al.*, Nucl. Instrum. Method A **282**, 317 (1990).

[2] T. Cho *et al.*, Phys. Rev. Lett. **64**, 1373 (1990).

[3] T. Cho *et al.*, Nucl. Fusion **26**, 349 (1986).

ABSOLUTE XUV SILICON PHOTODIODES
FOR SYNCHROTRON RADIATION APPLICATIONS

Raj Korde
International Radiation Detectors, Torrance CA 90505-5229
L. R. Canfield and Robert Vest
NIST, Gaithersburg MD 20899-0001
David Pearson and James MacKay
SRC, University of Wisconsin-Madison, Stoughton WI 53589
Eric Gullikson
Lawrence Berkeley Laboratory, Berkeley CA 94720

This paper reviews design, fabrication, characterization and application aspects of a unique class of p-n junction silicon photodiodes developed during the past few years for vacuum ultraviolet, extreme ultraviolet and soft X-ray (XUV) spectral region. The quantum efficiency of these unique devices (AXUV photodiodes) can be predicted using well-known theoretical expression. This has resulted into their use as absolute photodiodes for the XUV. This self calibration process leads to quantum efficiency uncertainties about 4%, far superior compared with 7 to 15 % uncertainties of the calibrated secondary standards.

Recently developed AXUV diodes have shown unparalleled radiation hardness when exposed to 10 to 100 eV photons. Radiation hardness of these devices was 1 G-rad (SiO_2), about 10,000 times the hardness of the commonly used silicon photodiodes. This is the highest hardness which is known to exist in any silicon device. With the increased brightness of third generation synchrotrons, this radiation hardness aspect will be of great importance to many workers in this area.

Quantum efficiency stability and uniformity of discrete devices with areas up to 3 cm² will be described. The audience will be introduced to a novel AXUV quadrant diode with a 0.5 mm hole in the center designed specifically for beam intensity monitoring and position sensing. This device will be of particular interest to scientists since large errors in the experimental data often occur owing to the unstable nature of the synchrotron radiation beams.

Performance of the developed visible blind AXUV photodiodes with integrated thin film filters will also be described. As these filtered diodes have orders of magnitude blocking for the out-of-band radiation, they will be quite useful in applications where spurious radiation is a problem.

Design and fabrication of one and two dimensional arrays being developed for spectroscopy and imaging applications will also be discussed. These arrays are expected to have 100% quantum efficiency for XUV and about 10,000 times more radiation hardness compared with the present CCDs and self-scanned photodiode arrays.

Applications of the developed AXUV diodes in X-ray scattering experiments, beam position and intensity monitoring and in plasma diagnostics will also be presented.

Micron spatial resolution X-ray image plates with non-erasing reading

I.P.Dolbnya, G.N.Kulipanov, V.V.Lyakh, O.A.Makarov, V.F.Pindyurin
Budker Institute of Nuclear Physics
630090 Novosibirsk, Russia
D.I.Kochubey
Institute of Catalysis, 630090 Novosibirsk, Russia
G.B.Gorin, K.E.Gyunsburg, N.P.Zvezdova, V.I.Kochubey
Institute of Physics and Mechanics,
Saratov University, Saratov, Russia

It is well known and widely used last years special area detectors - Imaging Plates (1). Unfortunately, a spatial resolution of the Imaging Plates which is typically of about 150 microns now and, in principle, may be up to several tens of microns, confines their using for the purposes of X-ray microscopy, holography, diffraction experiments.

The authors have been proposed and examined, as an X-ray area detector, the silverless radiophotoluminescence substances LiF(In) and NaCl(In). A stored X-ray image is read out by measuring the intensity of photoluminescence with a wavelength of $\approx 530 - 560\text{nm}$ under the excitation by ultraviolet light with a wavelength of about 365 nm. In opposite to the conventional Imaging Plates, a stored image is not erased under the reading therefore a read out process can be repeated many times. For a complete erasure of an image the substances must be heated for 0.5 hour at a temperature of 400 degrees centigrade.

A study of these substances with 6-30 keV photons using synchrotron radiation from the storage ring VEPP-3 (Budker Institute of Nuclear Physics) showed their high sensitivity to X-rays and a wide dynamic range of about $6 \cdot 10^3$. Preliminary results indicate that a spatial resolution of the substances is not worse than 2 microns. A degradation of the image luminescence intensity after one year keeping of the substance is not observed.

The obtained results show that these substances may be promising for registration of X-rays in the X-ray imaging experiments (2).

References:

1. Y.Amemiya. Imaging plate - X-ray area detector based on photostimulable phosphor. Synchrotron Radiation News, V.3, No.2, 1990, p.21.
2. I.P.Dolbnya, et al. Radiophotoluminescence area detectors with micron spatial resolution for registration of x-ray images. Will be published in Proceedings of XRM-93. (September 20-24, 1993, Chernogolovka, Russia)

MBE GROWN CdTe PHOTOCONDUCTOR ARRAY DETECTOR FOR X-RAY MEASUREMENTS

S. S. Yoo¹, B. Rodricks², S. Sivanathan¹, J. P. Faurie¹, and P. A. Montano^{1,3}
¹Microphysics Laboratory, Department of Physics, University of Illinois at Chicago
Chicago, IL 60607; ²Advanced Photon Source, and ³Materials Science Division, Argonne
National Laboratory, Argonne, IL 60439

A photoconductor array was made using Molecular Beam Epitaxially (MBE) grown CdTe. CdTe has been found to be an excellent material for high energy photon detection. Our objective is to develop an array detector with high efficiency and fast response towards x-rays. There is considerable interest in the development of new x-ray detectors for use in the new synchrotron radiation sources. We have fabricated photoconductor arrays with gaps ranging in 5 to 50 μm between elements and 100 μm pitch size. The temporal response of the detectors was measured using 100fs Ti: Sapphire laser pulses. The temporal response of the photoconductor arrays is as fast as 21 psec rise time and 38 psec Full Width Half Maximum (FWHM). Spatial and energy responses were obtained using x-rays from rotating anode (ANL) and synchrotron radiation sources (NSLS, beam line X-18 B). Because of its small thickness 10 μm , and small size sensing area, the spatial resolution of the photoconductor obtained was 75 μm FWHM, for a 50 μm beam size. The best results were obtained for those arrays with the best crystal qualities. We observed linear response up to an energy of 15 KeV. We observed that a substantial number of x-ray photons were effectively absorbed within the MBE CdTe layer. The array detector did not show any evidence of radiation damage after x-ray exposure of several days. These results demonstrate that MBE grown CdTe is a suitable choice to meet the detector requirements for synchrotron radiation applications.

This work was supported by the U.S. Department of Energy, BES-Materials Science under contract No. W-31-109-ENG-38.

The Gold Detector: Modular CCD Area Detector for Macromolecular Crystallography

I. Naday, S. Ross, M. Kanyo, M. L. Westbrook, E. M. Westbrook: Argonne
National Laboratory

D. O'Mara, M. Stanton, W. C. Phillips, Brandeis University

H. Belamy, A. Cox, H. Tsuruda, and P. Phizackerley, Stanford Synchrotron
Radiation Laboratory

We have designed, fabricated, and tested a modular CCD area detector system for macromolecular crystallography at synchrotron x-ray sources, code-named the "gold" detector system. The sensitive area of the detector is 150mm x 150mm, with 3,072 x 3,072 pixel sampling, resulting in roughly a 50 μm pixel raster. The x-ray image formed on the face of the detector is converted to visible light by a thin phosphor layer. This image is transferred optically to nine CCD sensors by nine square fiberoptic tapers (one for each CCD), arranged in a 3x3 array. Each taper demagnifies the image by a factor of approximately 2. Each CCD has a 1,024 x 1,024 pixel raster and is read out through two independent data channels. After each x-ray exposure period the x-ray shutter is closed and the electronic image is digitized (16-bit) and read out in 1.8s. Alternatively, the image may be binned 2x2 during readout, resulting in a 1,536x1,536 raster of 100 μm pixels; this image can be read out in 0.4s. The CCD sensors are operated at -40°C to reduce electronic noise. The detector is operated under full computer control: all operational parameters (readout rates, CCD temperature, etc.) can be adjusted from the console. The image data (18 MByte/image) are transferred via a fast VME system to a control processor and ultimately to disk storage.

During April, 1994 we carried out a complete set of measurements at SSRL for a full characterization of the gold detector. Characterization includes quantitative evaluation of the instrument's conversion gain (signal level/x-ray photon); detective quantum efficiency (DQE); point-spread function; sensitivity as a function of x-ray energy; geometrical distortion of images; spatial uniformity; read noise; and dark image and dark image noise. Characterization parameters derived from these measurements will be presented.

This work has been supported by U.S. DOE/OHER under Contract W31-109-ENG-38 and by NIH/NCRR under grant P41 RR06017.

THE APPLICATIONS OF GAS ELECTROLUMINESCENCE DETECTORS
FOR FLUORESCENCE AND QUICK-SCANNING XAFS MEASUREMENTS

V. A. Chernov, S.G. Nikitenko, E.M. Dementyev, I.B. Drobyazko

Institute of Catalysis, Siberian SR Centre at the Budker Institute of Nuclear Physics.

* Budker Institute of Nuclear Physics.
Lavrentyev pr 5, Novosibirsk, 630090, Russia.
Telex: 133116 ATOM SU. Fax: (3832)35-21-63

In this paper we have presented results on applications of gas scintillation proportional counters that was obtained for XAFS measurements in few last years. This detector type has, as compared with conventional gas scintillation proportional counter, the such advantages as better energy resolution and higher throughput [1,2]. The detector has a sealed cell filled with Xe. A 25 mm diameter entrance beryllium window provides a good solid angle subtended by the detector. At maximum count rates of about $9 \cdot 10^4$ counts/sec, the detector has an energy resolution of 9 % at 5.9 keV (Fe^{2+}). The useful energy range of the detector extends from 3 to 13 keV in the count mode. Moreover, this detector can be used in the nontraditional current mode like a "ion chamber with internal amplification" with a very high sensitivity. Using this detector good quality fluorescence yield XAFS spectra of thin films have been recorded with total time about 10 minutes. This detector is very suitable for XAFS measurements at concentrations of the element to be examined of above 10^2 ppm. Besides this detector in current mode is preferential, as opposed conventional gas ionization chamber, to be used for quick-scanning XAFS measurements (QEXAFS) [3]. In the QEXAFS mode the data point is integrated for typically 0.01 to 0.05 s. However, with a beam of $10^{11} - 10^{12}$ ph/s, it is feasible to measure microsecond resolved absorption. In this case, the time resolution is limited by the noise of the wide-band current preamplifier of the chamber. To overcome this limitation, it is desirable to increase the output current of the chamber. Due to the internal conversion/amplification process the "gas ionization chamber with electroluminescence amplification" has advantages of high sensitivity, very low noise, large dynamical range in compare with ordinary gas ionization chamber. Using this detector good quality XANES and EXAFS spectra have been recorded with integration times of 1 to up 10 ms at the point. Currently 5 s are sufficient to get a high quality spectrum and this time is limited by the monochromated photon flux incident upon a sample. However, with the availability of high brightness monochromator and SR from the VEPP-4 storage ring it could be possible to record the each point of the spectrum in the one-bunch mode. Some experimental results of XAFS measurements obtained by alternative techniques are illustrated for comparison.

1. A. J. P. L. Pollicarpo, in "X-ray microscopy", Springer-Verlag, New-York, 1984
2. A. Smith, M. Bavdaz, Rev. Sci. Instrum., 63, 689 (1992)
3. R. Frahm, Rev. Sci. Instrum. 60, 2515 (1989)

The new PTB detector calibration facility based on an electrical substitution radiometer for the wavelength range 35-400nm

A. Lau-Främbis*, U. Kroth, H. Rabus, E. Tegeler, G. Ullm
Physikalisch-Technische Bundesanstalt, Abbestraße 2-12, 10587 Berlin, Germany

The Physikalisch-Technische Bundesanstalt (PTB) is operating a radiometric laboratory at the Berlin electron storage ring BESSY. In this laboratory a new instrumentation has been set up for the calibration of transfer detectors, e.g. semiconductor photodiodes, in the wavelength range from 35 to 400 nm with an aspired uncertainty < 1%. The primary detector standard is an electrical substitution radiometer (ESR) operated at liquid helium temperature. The unknown spectral responsivity of a detector under investigation is determined by comparison with the known responsivity of the ESR using monochromatized synchrotron radiation.

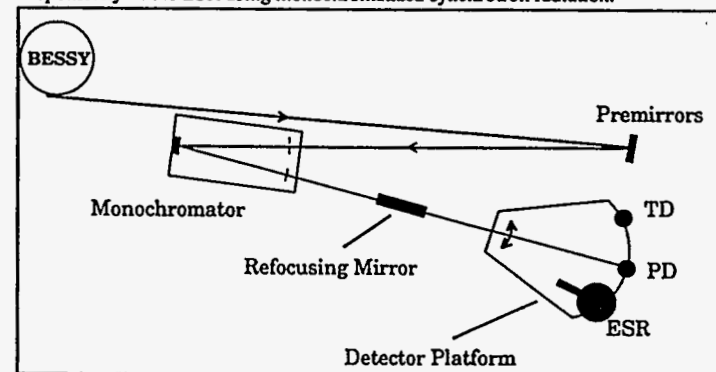


Fig. 1: Schematic drawing of the new detector calibration facility, TD: transfer detector, PD: photodiodes, ESR: electrical substitution radiometer

The new detector calibration facility (see fig. 1) consists of a premirror, a monochromator, a refocusing mirror and a detector platform. The normal incidence premirror (170° deviation angle) focuses the radiation into the entrance slit of the monochromator by 1:3 demagnification. Three differently coated mirrors exchangeable under vacuum are available. The monochromator is a 1m, 15° McPherson-type instrument with three differently coated gratings. A SiC premirror - SiC grating combination is used to suppress higher diffraction orders in the critical wavelength range from 60-110 nm. The Ir refocusing mirror focuses the beam to an area of 3 mm (horizontally) and 1.5 mm (vertically). The radiant power within a bandwidth of $\Delta\lambda = 3.3\text{nm}$ is between 1 and 6 μW depending on wavelength. The detector platform at the end of the beamline bears the ESR primary detector and two setups for transfer detectors. The three detectors can be positioned in the beam path by swinging the platform.

The performance of the instrumentation and first calibration results of semiconductor photodiodes will be presented.

* Permanent guest from BESSY GmbH, Lentzeallee 100, 14195 Berlin, Germany

A Dual Line Multi Cell Ionization Chamber for Transvenous Coronary Angiography with Synchrotron Radiation

Menk R.H.³, Besch H.J.¹, Großmann U.¹, Langer R.¹, Lohmann M.¹, Schenk H.W.¹, Wagener M.²,
Walentz A.H.¹

Dix W.R.³, Graeff W.³, Illing G.³, Reime B.³, Schildwächter L.³, Tafelmeier U.³,

Kupper W.⁴, Hanun C.⁵, Rust C.⁵

¹ University GHS Siegen Germany

² University GHS Siegen now at PSI Villigen Switzerland

³ HASYLAB at DESY Hamburg Germany

⁴ Herz Kreislauf Klinik Bad Bevensen Germany

⁵ UKE Hamburg Eppendorf Germany

ABSTRACT

A position sensitive one dimensional x-ray detector with a large dynamic range ($> 2^{14}$) for high photon fluxes with fast image recording sequence has been developed for intravenous coronary angiography. Due to the weak density of contrast media in the coronary vessels two x-ray images with slightly different energies near the K-absorption edge of iodine have to be taken in less than 300 msec and subtracted logarithmically [1],[2],[3]. The beams are generated by two Laue-monochromators of the white synchrotron beam of HASYLAB at DESY.

A position resolution of 430 μ m FWHM [4] and a detective quantum efficiency (DQE) of at least 58% (for 20 000 photons per pixel) could be achieved for 33keV photons in a Xe-CO₂ gas mixture at 20bars [6],[10]. The use of Kr-CO₂ as conversion gas provides a better contrast of the weak iodine signal than Xe-CO₂ or Si respectively for a fraction of 2% of the third harmonics of the used synchrotron beam.

At the same time the setup allowed the investigation of saturation effects beyond the intensity range used for angiography but of possible interest for other applications. A quantitative dynamic model has been developed and compared with measurements.

- [1] E B Hughes et al. 'Prospects for non-invasive coronary angiography' NIM B10/11 (1985),p.323-328
- [2] Thomlinson W. 'Medical applications of synchrotron radiation' NIM A319 (1992), p. 295-304
- [3] Dix et al. 'Coronary Angiography at HASYLAB' BSR92 Proceeding of the conference 'Synchrotron Radiation in Life-Science' Tsukuba Japan, will be published in Oxford University Press
- [4] Besch et al. 'A high precision, high speed x-ray ...' Physica Medica International Journal devoted to the Applications of Physics to Medicine and Biology Volume 6 No. 3-4 dec.1990
- [5] Besch et al. NIM A310, 1991 p.445
- [6] Besch et al. 'Proceeding of the 4th. Intern. Conf. on Appl. of Phys. in Med. and Biology 21-23 Sep. 92, Trieste, to be published in Physica Medica
- [7] Schenk W. 'Optimierung eines bildgebenden ...' Promotion Universität Siegen 1991
- [8] Langer R. 'DQE', Diplomarbeit Universität Siegen, 1993
- [9] Wagener M. 'Rekombination', Diplomarbeit Universität Siegen, 1992
- [10] Menk R.H. 'Eine Vielkanal Ionisationskammer' Promotion Universität Siegen 1993

CONSTRUCTION OF A SMALL AREA POSITION SENSITIVE DETECTOR FOR MEASUREMENT OF LOW INTENSITY BRAGG REFLECTIONS.

Mathias Meyer, Université de Lausanne, Institut de
Cristallographie, BSP Dorigny, CH-1015 Lausanne, Switzerland

Background assignment is an accuracy limiting factor when measuring weak reflections in point detector diffractometry. The weak satellites in incommensurate phases mainly encode the information about the deformation field active in these phases. To enhance the measurement precision for these reflections without unnecessary increase of measurement time we want to apply a recently proposed scan procedure (Mathieson (1982), Acta Cryst. A38, 378-387) that clearly defines the background locus, but needs a 1D or 2D position sensitive detector for practical handling. We will present a detector design with an active area of less than 1cm² based on CCD-technology, which is intended for the optimized measurement of incommensurate satellites using sealed tubes or rotating anodes as x-ray sources.

Solid State Detector for Soft Energy EXAFS

A.D.Smith, G.E.Derbyshire, R.C.Farrow, M.Martini*.

Title: Low-Pressure Multistep Gaseous Primary Ion Counting

Author: J. Christopher Milne

Collaborators: Erik D. Johnson, G. C. Smith -- Brookhaven National Laboratory

Abstract:

We are investigating the use of primary ion counting as an alternative to the parallel plate avalanche chamber we have previously utilized in soft x-ray scattering measurements. Energy resolution in conventional proportional counters is a function of the number of primary ion pairs created per incident photon and the fluctuation in single-electron multiplication. In the proportional regime, the rms resolution may be expressed as

$$\sigma_{\epsilon}/E = [(F+B)/N_0]^{1/2}$$

where the Fano factor F (~0.2) characterizes the fluctuation in the number of primary ion pairs created per incident photon, the factor B (~0.6) represents the gain fluctuation in single-electron multiplication, and N_0 is the average number of electrons created per incident photon. If one is able to remove the gain fluctuations, one sees from the preceding expression that the energy resolution will be improved by a factor of two. The technique presented here, primary ion counting, is implemented by allowing the electron cloud created by the incident photon to disperse in a well defined low electric drift field. If the cloud is well dispersed, individual electrons will enter a two stage amplification region where they avalanche, and are then counted. The detector design and progress to date will be described.

Daresbury Laboratory
Keckwick Lane, Warrington, Cheshire WA4 4AD
United Kingdom

* EG&G Ortec
100 Midland Road, Oak Ridge, TN37830
United States of America

Following the success of solid state detector systems for EXAFS studies at high X-ray energies, there is now an increasing demand for similar devices capable of operating in the soft X-ray energy range below about 3keV. Recent developments in sophisticated detector fabrication techniques now make the construction of specialised devices, suitable for high quality spectroscopy in this energy range, a practicable proposition.

We present the results of extensive testing of a new detector developed specifically for use in the sub-3keV energy range. We have measured energy resolutions of less than 150eV FWHM at sulphur and silicon $K\alpha$ energies and the ability of the detector to achieve this resolution at the copper $L\alpha$ line has also been shown. Finally we demonstrate the potential of this device in a study of trace dopants in bulk silicon based quantum dot glasses.

Development of a Proportional Scintillation X-ray Imaging Chamber for Synchrotron Radiation Experiments

M.Suzuki, Y. Awaya¹⁾, M.Oura¹⁾, T.Mizogawa²⁾, and K.Masuda³⁾

Japan Synchrotron Radiation Research Institute, Minatogima, Nakamachi, Kobe, Hyogo 650, Japan.

1) RIKEN, Hirosawa, Wako, Saitama 351-01, Japan.

2) Nagaoka College of Technology, Kamitomioka, Nagaoka, Niigata 940-1, Japan.

3) Saitama College of Health, Kamiokubo, Urawa, Saitama 338, Japan.

The proportional scintillation x-ray imaging chamber program has been one of the most challenging plan among the SPring-8 area-detector R&D projects, since it is based upon a new chamber technique [1]. The detector system consists of a rare gas proportional scintillation chamber and an image-intensifier-associated CCD camera. The prototype constructed has demonstrated that this novel detector is capable of imaging the spatial pattern of incoming x rays either by recognizing the location of each x-ray photon at low counting region (digital mode) or by detecting the local intensity of superimposed x-ray photons at high counting region (analogue mode) [2]. Recently we have confirmed that the prototype can image a time-varying x-ray pattern with a time resolution of 1/30 sec (see Fig.1). We will introduce this new device and report recent attainments at the conference.

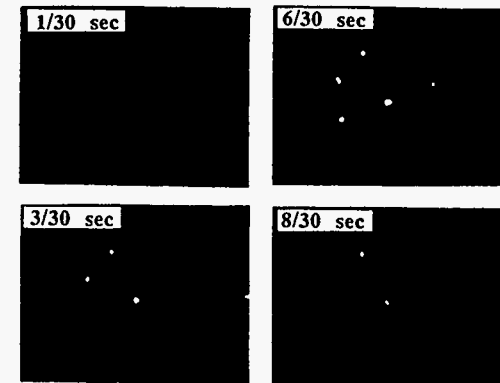


Fig. 1 Time-varying x-ray pattern observed with the prototype.

References

[1] G.Charpak *et al.*, *Nucl. Instr. and Meth.*, A258(1987)177.

[2] M.Suzuki *et al.*, in *Proceedings of Third London Conference on Position-Sensitive Detectors*, September 6-10, 1993.

APDs – Large Dynamic Range Detectors for Hard X – Rays
W. Sturhahn, T. Toellner, and E. Alp
Advanced Photon Source, Argonne National Laboratory
Argonne, IL, 60439

The ultra high brilliance of the third generation synchrotron radiation sources will increase count rates by several orders of magnitude if compared to existing synchrotron radiation sources. Detectors that allow to exploit this advantage should have a linear range of operation that reaches from very high count rates to their intrinsic noise level. We investigated APDs (Avalanche Photo Diodes) with respect to linearity, efficiency, time resolution, and dynamic range by the use of 8.4 keV and 14.4 keV synchrotron radiation. We observed linear behaviour up to count rates of 10^8 Hz. The intrinsic noise level was below 10^{-2} Hz. Efficiencies of about 50 % at 8.4 keV and about 14 % at 14.4 keV were achieved. The time resolution was about 1 ns. We will present the experimental data and discuss the performance of APD detectors.

This work is supported by US-DOE, BES Materials Science, under contract No: W-31109-ENG-38.

Abstract for SRI 94
International Synchrotron Radiation Conference

Advances in Radiation Hardened Charge Injection Devices (CIDs)
as Direct X-ray Imaging and Energy Dispersive Detectors

R. E. Wentink⁺, S. VanGorden⁺, J. Zarnowski⁺, D. Aloisi⁺,
C. A. MacDonald[#], W. M. Gibson[#], R. E. Fields^{**}, and M. B. Denton^{**}

⁺ CID Technologies Inc., 101 Commerce Blvd., Liverpool, NY 13088

^{*} X-Ray Optical Systems, Inc., 1400 Washington Ave, Albany, NY 11222

[#] Center for X-Ray Optics, University at Albany, SUNY, Albany NY 12222

^{**} Dept. of Chemistry, The University of Arizona, Tucson, AZ 85721

Charge Injection Device detectors have shown unique properties for imaging of photons in the UV-visible region. Together with good resolution and broad spectral response characteristics, CID array detectors have traditionally offered exceptionally large pixel charge capacity, non-destructive pixel readout, random pixel addressibility and two-dimensional, high speed windowing (sub-array readout). These features can be used to dramatically extend the dynamic range (greater than 10^8), eliminate blooming effects, allow real-time monitoring and dynamic adaptation of exposure time, improve signal-to-noise by random background integration and permit the readout of small pixel sub-arrays at exceptionally fast rates.

Recent developments in process technology and new array design techniques have facilitated the development of a radiation hardened CID detector capable of withstanding more than a megarad (gamma Si) of ionizing radiation. These detectors show great promise for direct imaging of x-radiation in the low to medium energies (1 KeV - 20 KeV) and appear to offer significant advantages over the CCD detector.

Preliminary data will be presented showing response to various energy x-rays. Conceptual thoughts will be presented for use of the CID as an x-ray imaging detector as well as an energy dispersive detector.

DISSECTOR WITH 2 PICOSECOND TIME RESOLUTION

Zinin E.I.

Budker Institute of Nuclear Physics
Novosibirsk, Russia

The new dissector are developed for the operation in stroboscopic regime with the characteristics:

Time resolution:

better than 2 ps (wavelength range >600 nm)

Spectral response sensitive wavelength range:

120-820 nm

Dynamic range: more than 10 in power 5

RF sweep frequency: up to 1 GHz

RANGE OF APPLICATIONS:

SYNCHROTRON RADIATION EXPERIMENTS

Damping kinetics measurement

Time-resolved spectra measurement

EXAFS spectroscopy with the detection in
optical spectral region

Experimental observation of quantum beats

Stationary luminescence spectra measurement

ACCELERATOR PHYSICS

Bunch length measurement

Investigation of the coherent motion of a bunch
at fixed point of phase space

FREE ELECTRON LASER

Adjustment of a length of optical cavity

Investigation of time evolution of lasing

Feedback for the stabilization of lasing

MODE-LOCKED LASERS

Investigation of the phase characteristic and
pulse shape

Absolute calibration of a photodiode array with the synchrotron radiation (1.5-10 keV)

L. BECK, C. BIZEUIL et G. SOULLIE
CEA/ Service CEM
BP 12
91680 Bruyères-le-Châtel
FRANCE

Abstract

The silicon photodiode array Hamamastu was primarily developed for the visible-UV spectral range, mainly for photon wavelengths between 200 and 1100 nm. By utilizing it without quartz window, we demonstrate that this sensor can be used for X-rays and particularly in the 1-10 keV range. This device consists of 1024 silicon pixels of 25 μm by 2.5 mm.

We present experimental measurements of the absolute detection efficiency and spatial resolution of our photodiode array between 1.5 and 8 keV. We performed the experiment on the beamline SB3 at the Super ACO storage ring (LURE-Orsay). In the BL-SB3 we can select several types of double-crystal monochromators; we used InSb crystals to study the silicon absorption K-edge of the sensor and Si crystals to work at upper energies.

The spectral efficiency measured is compared with the results of a simple model calculation based on the data given in a Hamamastu note for a device with a thinned silicon dioxide passivation layer of 1 μm . The simulation is in a good agreement with the experimental data for a active depth of silicon of 6 μm . The spatial resolution is estimated at 120 μm .

1.

The31

Time	FRIDAY, JULY 22, 1994
	DETECTORS
	<p style="text-align: center;">FrA Staller Center Chairpersons: R. Madden (SURF II); H. Kamitsubo (SPring-8)</p> <p>8:30 H. Kraner (BNL) <i>Si-based detectors</i></p> <p>9:00 G. Smith (BNL) <i>Gas detectors</i></p> <p>9:30 S. Gruner (Princeton) <i>CCDs</i></p> <p>10:00 Coffee Break</p> <p>10:30 A. Harrison (Edinburgh) <i>Physics of Image Plates</i></p> <p>11:00 S. Loken (LBL) <i>Computing Environments for SR Experiments</i></p> <p>11:30 Yves Petroff (ESRF) <i>Conference Summary</i></p> <p>12:00 <i>Closing remarks by the Chairperson of the next International SRI Conference</i></p>
12:30	LUNCH

Session FrA - Invited Talks

The Physics of Image Plates

Andrew Harrison* and Richard Templar

*Department of Chemistry, University of Edinburgh, Scotland

Department of Chemistry, Imperial College, University of London, England

In recent years, two-dimensional x-ray detectors have been developed that are based on the use of a BaFBr:Eu²⁺ phosphor. The phosphor stores the x-ray image in the form of trapped charge, the charge having been produced by the x-ray ionisation. The image may be read by exposing the plate to red light from a HeNe laser, and observing the stimulated, blue luminescence. Research on the mechanism of photostimulated luminescence in this material indicates that one of the trapped charge species may migrate through the lattice until it is close to a recombination centre. Charge recombination may then occur through photostimulation. The lattice migration affects the stability of the image, the effective sensitivity of the detector and the ability to erase the image. These effects are described, and their implications for the construction of high-resolution x-ray detectors with high photometric accuracy are discussed.

Author Index

Abernathy, D.	MoE7, TuD25	Asfaw, A.	TuD4
Abrami, A.	TuD1	Assoufid, L.	ThD2, ThD61, ThD89
Adachi, S.	TuD81, Inv. (MoB)	Astaldi, C.	TuD53
Ade, H.	MoD44, MoD46, ThE5, MoD17	Atkinson, P.A.	TuD46
Agui, A.	MoE39	Attwood, D.	MoD39
Aizawa, K.	MoD63	Aulchenko, V.	ThE2
Akatsuka, T.	MoD34, MoD73	Awaya, Y.	ThE28
Akre, J.	TuE19, TuE20	Bahr, D.	MoE14
Aksela, S.	TuD2	Bahrtdt, J.	ThD3, TuD64
Aleksandrov,	MoE24	Bajt, S.	MoE1, MoE2, MoD71
Allinson, N.M.	Inv (MoB)	Baker, T.	TuD44
Aloisi, D.	ThE29	Baker, R.	ThD77, ThD79
Alp, E.E.	ThD1, TuD8, ThE27, MoD76, TuD68, TuD69	Bandyopadhyay, P.	TuE3
Als-Nielsen, J.	MoE7, TuD25, ThD65	Barba, L.	TuD15
Alves, O.L.	MoD15	Barbiellini, G.	MoD7
Amamoto, H.	TuD62	Barbosa, L.C.	MoD15
Amano, D.	Fac.	Bark, M.	MoD23
Amemiya, Y.	ThE1	Barnaba, M.	TuD1
Amenitsch, H.	TuD3	Barraza, J.	TuD5, TuD70, TuD67
Anashin, V.V.	TuE1	Baru, S.	ThE2
Andersen, J.N.	Inv. (TuC)	Baryakhtar, V.	TuE61
Andersen, W.	ThD44	Batterman, B.W.	MoE38
Anderson, E.H.	MoD55, MoD46, MoD39	Battistello, L.	TuD1
Andersson, A.	TuE2	Baudelet, F.	Inv (TuC), MoE25
Ando, M	MoD34, MoD39, MoD63, ThD48, MoE19, TuE54, ThD80, Inv. (ThA)	Beck, L.	MoE47, ThE31
Andrault, D.	Inv (TuC)	Becker, U.	MoE3
Angot, T.	MoE11	Bedzyk, M.J.	ThD35, TuD87, MoE4, ThD11
Anthony, F.M.	ThD21	Belakhovsky, M.	ThD4
Antonini, A.	TuD53	Belamy, H.	ThE20
Antonov, A.A.	ThD14	Bellamy, S.J.	MoD6
Aoki, S.	MoD39, MoE19	Belsky, A.N.	MoD67
Aoki, T.	TuE49	Belyakov, V.A.	MoE5, MoE6, MoE44
Archer, D.W.	MoD68	Bender, J.	ThD46
Arfelli, F.	MoD7	Beno, M.A.	MoD52, ThD35, ThD58, MoD1, TuD87, ThD11
Armand, P.	MoD1	Berard, J.F.	ThD15
Artamonova, L.D.	MoD50	Bergevin, F.de.	MoE25
Asano, Y.	ThE1	Berman, L.	Inv. (ThA)
		Bernstorff, S.	ThD5, ThD6, ThD9 TuD3, TuD15
		Berry, B.	TuD44
		Bertolo, M.	ThD93

Besch, H.J.	ThE23	Butorin, S.	MoE29
Bessergenev, A.V.	MoD77	Cai, Z.	ThD101, TuE23, TuE5
Beutler, A.	TuD45	Calcott, T.A.	MoD37, TuD4
Bianco, A.	ThD30	Caliebe, W.	MoE15
Bianco, A.	ThD93	Calvani, P.	TuE35
Bijleveld, J.H.M.	TuD78	Camalli, M.	TuD15
Bilderback, D.H.	Inv. (ThA), ThD57, MoD75	Canfield, L.R.	ThE17, ThD87
Bilsborrow, R.L.	TuD6	Cantatore, G.	MoD7
Biscardi, R.	TuE4	Capel, M.S.	ThE3
Bissen, M.	TuD18, ThD7	Capozi, M.	TuD53
Bizeuil, C.	MoE47, ThE31	Carlisle, J.A.	MoD37
Bjorkholm, J.E.	MoD95, ThD82	Carr, G.L.	MoE8, TuD9, MoD91
Bjorneholm, O.	TuD45	Carr, R.	TuE6, TuE7
Blake, R.L.	ThD17	Cassetta, A.	TuD15
Blasdell, R.C.	ThD8, MoE23	Castelli, E.	MoD7
		Castelli, C.	Inv. (MoB)
		Cautero, G.	TuD1
Blasie, J.K.	ThE12	Cerino, J.	TuD10
Bliss, N.	TuD6, MoD2	Cernik, R.J.	TuD6
Blume, M.	MoE22	Cerrina, F.	ThD101, MoD60, ThD88, ThD93, ThD98
Bogg, D.	ThE9		ThD62
Bonivert, W.	MoD94	Chaban, E.E.	ThD62
Bordas, J.	TuD6, MoD2	Chang, S.L.	MoE17
Borovikov, V.M.	TuE39	Chang, C.-N.	TuD13, TuD14, TuD76
Bosecke, P.	TuD7	Chang, J.	TuD11
Bouchard, R.	Inv. (TuB), MoE35	Chantler, C.T.	TuD12
Bourgeois, D.	TuD38	Chapman, D.	MoD8, MoD24, MoD18
Boyanov, B.	TuE3		ThD70
Bradshaw, A.M.	MoE18	Chapman, H.N.	MoD9, ThD60
Bras, W.	MoD3	Chavanne, J.	TuE8
Brasher, D.	TuD66	Chen, C.-I.	TuD14
Brauer, S.	MoE7	Chen, J.H.	MoD10, MoD35
Brena, B.	TuD1	Chen, Z.	MoD18
Brennan, S.	Inv. (MoC), MoD53	Chen, C.-C.	TuD13, TuD76
Brennen, R.	MoD94	Chen, C.-I.	TuD13, TuD76
Brister, K.	MoD4	Chen, J.-R.	TuD75
Brite, C.	TuD8, TuD68, TuD70	Cherkov, G.A.	MoD50
Brown, G.E.	ThD94	Chernov, V.A.	MoD11, ThE21
Bruckel, T.	Inv. (TuB), MoE35	Chesnokov, V.V.	MoD50
Bucher, J.	MoD16	Chevallier, P.	MoD69
Buckley, C.J.	MoD6	Chiang, C.M.	ThD62
Buffey, S.G.	TuD46	Chin, J.	TuE20
Bulicke, P.	MoE46	Chiwaki, M.	ThD36
Bulyak, B.	TuE61	Chkhalo, N.I.	MoD11
Bunker, G.	TuE3	Cho, T.	ThE16, ThE4, ThE14
Burkel, E.	MoE37	Chu, B.	MoD90
Busetto, E.	TuD15, ThD5, ThD9		

Chuang, J.-M.	TuD13, TuD76	Deis, G.A.	MoD50
Chubar, O.V.	TuE9	Dejus, R.	TuE5, TuE10, ThD90
Chung, S.-C	TuD13, TuD14, TuD76	Delaney, J.S.	MoE2
Chung, Y.	TuD54	Dementyev, E.M.	ThE21
Churin, E.G.	ThD40	Deng, J.F.	MoD88
Clark, S.M.	TuD6, MoD12, MoD13, MoD14	Denlinger, J.D.	MoD16, MoD17
Clark, G.F.	TuD6	Dennison, J.R.	MoE11
Clarke, G.	ThD50	Dent, A.J.	ThE6, ThE9
Cocco, D.	TuD1	Denton, M.B.	ThE29
Coffman, F.	TuE6	Derbyshire, G.E.	ThE6, MoD3, ThE9, ThE26
Colapietro, M.	TuD15, ThD5	Derossi, A.	TuD37
Collins, S.P.	TuD6	Derst, G.	ThE6
Collins, S. J.	TuD91	Derst, G.	MoD80
Collins, J.	TuD68, TuD69	Dervan, J.P.	MoD8
Comelli, G.	TuD1	DeVries, B.	ThD94
Comin, F.	ThD10, TuD16, TuD19	Dhanak, V.R.	TuD58
Contrino, S.	TuD1	Dierker, S.	MoE7
Cookson, D.J.	TuD22, TuD23, MoD22	DiFabrizio, E.	ThD101
Cookson, D.	MoD83	DiFonzo, S.	MoE10, TuD1, ThD30
Coppens, P.	ThD12	DiFonzo, D.	ThD93
Cowan, P.L.	ThD11, TuD87, ThD35	Dilmanian, F.A.	MoD18
Cowan, P.	ThD58	Dilmanian, F.A.	MoD68
Cox, A.	ThE20	Diviacco, B.	TuE11
Craievich, A.F.	MoD15	Dix, W.R.	MoD32, ThE23
Creagh, D.C.	TuD23	Dobson, B.R.	TuD6, ThE9
Cronauer, J.	Inv. (MoC)	Dohrmann, R.	Inv. (MoC)
Crotti, C.	TuD53	Doing, P.	ThD13
Crowder, T.	ThE5	Dolbnya, I.P.	ThE7, ThE18, ThE8, ThD14
Cunis, S.	MoD23	Dolin, Y.	ThD56
Cusatis, C.	ThD68, TuD73	Dong, Z.	ThD93
D. Becker, K.	ThD51	Doumas, J.	ThD46
D'Addato, S.	TuD58	Downes, S.	MoD6
Dai, P.	MoE11, MoD86, MoD87	Dozier, C.M.	MoD43
Daimon, H.	MoE9	Dragun, G.N.	MoD19
Dalla Palma, L.	MoD7	Drobayzko, I.B.	ThE21
Dann, T.-E.	TuD13, TuD14, TuD75, TuD76 TuD76	Drube, W.	Inv. (TuC), TuD17
Darovsky, A.	ThD12, MoD90	Dubrovin, M.	ThE2
Dartyge, E.	MoE25, Inv. (TuC)	Dubuisson, J.M.	Inv. (TuC)
Davey, P.	TuD22	Duda, L.C.	MoE29
Deacon, A.	Inv. (MoB)	Duke, E.M.H.	TuD46
deBergevin, F.	MoE13	Durr, J.	TuD73
DeBona, F.	TuD42, TuD1	Ealick, S.E.	MoD75
		Earnest, T.	TuD48
		Edelstein, N.	MoD16
		Ederer, D.	MoD37

Ederer, D.L.	TuD4	Fischer-Colbrie, A.	Inv.
Egawa, K.	TuE25	Fischetti, R.F.	ThE12
Ehrlich, S.N.	MoE11, MoD87, MoD86	Fisher, M.V.	TuD18
Eikenberry, E.F.	MoD75	Fisher, M.	ThD7
Eisert, D.E.	TuD18	Fitch, J.J.	ThD17
Eisert, D.	ThD7	Flaherty, J.	MoD14
Elam, W.T.	TuD33, ThD34	Flechsigt, U.	ThD3, ThD42
Elkaim, E.	MoD97	Flemming, R.	MoE7
Elleauime, P.	TuE8, TuE52, TuE53	Fontaine, A.	Inv. (TuC), MoD97, MoE25
Ellis, A.W.	MoD37	Fontaine, B.	ThD82
Emerich, H.	TuD91	Fontana, S.	ThD93
Endo, T.	ThE1	Foran, G.	MoD83, TuD23
Endo, M.	TuE54	Foran, G.J.	MoD22
Englund, C.J.	MoE29	Fossing, F.	TuD45
Engstrom, P.	MoD20, MoD69	Fournet, P.	ThD54
Erg, G.	TuE14, TuE31	Frahm, R.	MoE12, TuD20
Eriksson, M.	TuE2	Franchon, D.	TuD87
Evans, J.S.O.	MoD13	Francis, R.J.	MoD13
Evdokov, O.V.	TuD24, MoD21	Frank, K.D.	MoE32
Evstigneev, A.B.	TuE1	Freeman, R.R.	ThD82
Ewing, D.	ThD46	Freund, A.K.	ThD16, ThD39
Fabrizio, E.Di.	ThD98	Freund, A.	MoE25
Fajardo, P.	TuE12, TuE13, TuD57	Freund, A.K.	ThD64
Fanchon, E.	ThD15	Friedman, A.	TuE14
Farges, F.	Inv. (TuC)	Froba, M.	MoE12
Farrow, R.C.	ThE6, ThE26	Fuchs, D.	ThD84
Farrow, R.	ThE9	Fujii, Y.	MoD20
Faurie, J.P.	ThE19	Fujisawa, T.	TuD85
Fava, C.	TuD42, TuD1	Fujisawa, M.	MoE39
Federmann, F.	TuD45	Fukui, K.	MoD20
Fedotov, M.G.	ThE10, ThE11	Fukuma, H.	TuE25
Fedurin, M.G.	TuE39	Fullerton, E.	MoD76
Feldhaus, J.	MoE18	Furst, M.L.	ThD87
Fell, B.D.	TuD6, MoD2	Furuya, T.	TuE25
Fernandez, P.B.	ThD73	Gabriel, K.J.	MoE37
Ferrand-Tanaka, L.	MoE40	Galimberti, A.	TuD1
Ferrer, S.	TuE13, TuD19, TuE12	Gambitta, G.	TuD42
Ferrer, J.L.	ThD15	Gambitta, A.	TuD1, TuD21, ThD99
Ferrero, C.	ThD64	Gaponov, Yu.A.	MoD21
Fiedler, S.	MoD20	Garreau, Y.	MoD97
Fields, R.E.	ThE29	Garreis, R.	ThD51
Figliomeni, M.	ThD98, ThD101	Garrett, R.F.	MoD22, TuD22, TuD23,
Finetti, P.	TuD1, TuD58	Gashtold, V.N.	MoD50
Finkelstein, K.D.	Inv. (TuB), MoE38	Gath, W.	TuE20
Fiquet, G.	Inv. (TuC)	Gaupp, A.	MoE10
Fischer, Th.	MoE36		

Gavrilov, N.	TuE14	Guckel, H.	MoD93
Gavrilov, N.G.	TuD24, MOD78	Gudat, W.	MoD28
Gebbers, J.O.	MoD68	Gullikson, E.	TuE16, ThD38, ThD45, ThE17
Gehrke, R.	MoD23	Gunshor, R.L.	MoD54
Gentili, M.	ThD98, ThD101	Guo, J.H.	MoD16, MoE29
George, G.N.	ThD94	Gurtler, P.	ThD18
Georgopoulos, P.	ThD56	Gyunsburg, K.E.	ThE18
Gevchuk, A.	TuE61	Habash, J.	Inv. (MoB)
Giacomini, J.	MoD8	Hachman, J.	MoD94
Gibson, W.M.	MoD43, ThE29	Haddad, W.S.	MoD55
Giles, C.	MoE13, MoE25	Hadener, A.	Inv. (MoB)
Gilfrich, J.V.	MoD43	Haeffner, D.	TuD8
Giorgetti, C.	Inv. (TuC)	Haeffner, D.R.	TuD68, TuD69
Giuressi, D.	TuD1	Hagelstein, M.	MoD97
Gladkikh, P.	TuE61	Hagiya, K.	MoD62
Glastra van Loon, D.	TuD78	Hahn, U.	TuD45, ThD18
Gluskin, E.	TuE10, TuD56, TuD87, TuE23, TuE5, TuE14, ThD97, TuD83, TuD74	Hai, Y.	ThD19
Gmur, N.F.	MoD8, MoD24	Haibin, P.	MoD89
Godnig, R.	TuD1	Hamada, K.	TuD31
Goetz, A.J.	TuD88, ThD52, TuD43	Hamalainen, K.	MoE15, TuD30
Goetz, F.	TuE22	Hammersley, A.P.	ThE13
Gog, Th.	MoE14, MoD61	Han, K.S.	Fac.
Goirand, L.	TuD40	Hanfand, M.	TuD9
Gonzales, A.	TuD46, ThD50, Inv. (MoB)	Hanmura, K.	MoE41
Gordon, H.	MoD8	Hansen, R.W.C.	ThD59
Gorin, G.B.	ThE18	Hanson, A.L.	MoE1
Goto, Y.	TuE27, MoE43	Hanyu, T.	MoE27
Gottschalk, S.C.	TuE15, TuE45	Harami, T.	TuD62, TuD63, ThD80
Goulon, J.	MoE25	Harney, P.J.	MoD90
Graafsma, H.	TuD59	Harris, N.W.	MoD2, TuD6
Graeff, W.	ThE23, MoD32	Harrison, A.	Inv. (FrA)
Graessle, D.E.	ThD17	Harron, C.	ThE23
Grant, A.F.	TuD6	Harrop, S.J.	Inv. (MoB)
Graves, R.M.	ThD87	Hart, M.	ThD57
Greaves, G.N.	MoD80	Hartman, Ya.	TuE53
Green, M.A.	ThD59	Hasegawa, M.	MoD25
Griebenow, M.	MoD61	Hashimoto, S.	ThD86, TuE46
Grigoryeva, I.G.	ThD14	Hashizume, H.	MoD26, MoD83
Grobmann, U.	ThE23	Hassenzahl, W.V.	TuE20
Grossi, F.	MoE13	Hastings, J.B.	MoE15, TuD30
Grubel, G.	MoE13, TuD25, MoE7, ThD65	Hasumoto, M.	MoD20, ThD20
Gruner, S.M.	MoD75	Hatano, Y.	ThD28
Gu, X.	TuD82	Hatano, T.	MoE27
		Hausermann, D.	ThD57
		Hayaishi, T.	ThD28
		Hayakawa, T.	TuD65

Hayashi, S.	TuE49	Humphries, D.	TuE19, TuE20,
Headspith, J.	ThE9		TuE22
Hecht, M.,	MoD94	Hung, H.H.	MoE17, ThD23
Heimann, P.	TuE16	Hunter, W.N.	Inv. (MoB)
Heimann, P.	TuD80, ThD45	Hyodo, K.	MOD34, MoD63,
Heintze, G.	TuE42		MoD73, TuE54
Heinzmann, U.	MoE3	Ichikawa, K.	MoD20
Helliwell, J.R.	Inv. (MoB)	Ieiri, T.	TuE25
Helsby, W.I.	MoD2	Igarashi, K.	MoD79
Henderson, C.	ThD57	Iida, A.	MoD30
Hentschel, M.P.	MoD70	Ikegami, K.	TuE50
Hergenbahn, U.	MoE3	Ikemizu, S.	Inv. (MoB)
Hermes, C.	TuD77	Iketaki, Y.	MoD31, MoD82
Heuer, J.	MoD32, ThD69	Ikeura, H.	MoD74
Hideaki, S.	TuE58	Ilinski, P.	TuE5, TuE23
Higashi, T.	Inv. (MoB)	Illing, G.	MoD32, ThE23
Hille, A.	MoE14	Imada, S.	MoE9
Himmel, M.	ThD82	Imafuku, M.	TuD72
Himpsel, F.J.	MoD37	Imamura, M.	TuD65
Hirano, K.	MoD30, ThE4, ThE14,	Ingram, R.	ThD17
	Inv. (TuB)	Inoue, Y.	TuD85
Hirata, M.	ThE4, ThE14, ThE16	Inui, M.	MoD33
Hiraya, A.	MoD20, ThD19,	Irick, S.C.	ThD21, ThD24
	ThD20, MoE16	Irvine, P.	MoD14
Hirosi, S.	TuE58	Isawa, M.	TuE25
Hirsch, G.	MoD27	Ishiguro, E.	MoD20, ThD20,
Hirschmugl, C.J.	MoD85		ThD25, ThD66
Hochst, H.	Inv. (TuC), TuD18,	Ishii, T.	Fac., MoE39
	ThD7, MoE46	Ishikawa, T.	ThD27, ThD26, Inv.
Hodeau, J.L.	MoD97		(TuB), MoD47, TuD31,
Hoffner, C.	MoD84		ThD86, TuD63,
Hofmann, A.	Inv. (WeA)		TuD85, ThD80
Holldack, K.	MoD28, TuE17	Ishizaka, S.	MoD92
Hoppner, K.	MoE36	Isojima, S.	TuE48
Hori, Y.	TuE18	Itabashi, S.	ThD41
Horii, Y.	MoD29	Itai, Y.	MoD34, MoD56,
Hosoda, Y.	TuE48		MoD73, TuE54
Howells, M.R.	ThD21	Itchkawitz, B.S.	MoE18
Hoyer, E.	TuE19, TuE20, TuE21	Itie, J.P.	Inv. (TuC)
Hrady, J.	ThD22	Ito, K.	ThD28, ThD29, ThE1
Hsieh, T.-F.	TuD14, TuD76	Ito, T.	MoD73
Hu, Y.	TuD86	Ivanov, P.M.	TuD87
Huang, L.-R.	TuD13, TuD76	Ivanov, P.	TuE14
Huang, K.G.	TuD26	Ivanov, S.N.	MoE28
Hudson, E.A.	MoD37	Iwasaki, H.	MoD40, TuD31,
Hulbert, S.	MoD46, MoD95,		MoD35,
	ThD95		TuD85, ThD86

Iwazumi, T.	TuD27	Katoh, T.	Fac.
Izawa, M.	TuE24, TuE32	Katoh, M.	TuE18
Izumi, K.	ThD80	Katsura, T.	TuE25
Jacob, J.	MoD24	Kawado, S.	MoD47
Jacobsen, C.	MoD9, MoD44	Kawano, Y.	TuD31
Jander, D.R.	TuE44, TuE45	Kawasaki, K.	MoD40
Janky, S.	TuD22	Kawashima, T.	ThD25
Jark, W.	MoE10, TuD1, ThD30, ThD55, ThD93	Kawata, H.	MoD41, TuD63
Jean, Y.-C.	TuD75	Kaza, R.K.	ThD24
Jennings, G.	MoD36, MoD52, ThD11, ThD35, ThD58	Kazama, M.	MoD34, MoD73
Jennings, J.	TuD87	Kazimirov, A.Y.	MoD42
Jensen, B.N.	ThD31	Kelly, L.A.	MoD96
Jia, J.J.	MoD37, TuD4	Kemppens, B.	MoE18
Jia, C.Z.	MoD88	Kennedy, B.J.	MoD22
Jiang, X.	Fac., TuD28	Kenny, T.	MoD94
Jin, M.	TuD82	Kern, D.	MoD39
Jing, Y.	TuD28	Kevan, S.K.	MoD16
Job, P.K.	TuD11	Khaleque, N.	MoD6
Johansson, U.	MoD38	Khlestov, B.V.	TuE40
Johnson, E.D.	ThE25, MoD46, MoD93, MoE45, TuD83	Khounsary, A.M.	ThD33
Jones, G.	TuD51, TuD52	Kihara, H.	MoD39, ThD32
Joyeux, D.	ThD53	Kikegawa, T.	MoD10, MoD35
Kachel, T.	MoD28	Kikuchi, T.	TuD32, TuD72
Kagoshima, Y.	MoE9, ThD47, MoD39, TuD29, MoE19, MoE27	Kikuta, S.	Inv. (TuB), ThD80
Kalb (Gilboa), A.J.	Inv. (MoB)	Kim, D.E.	TuE40
Kamada, M.	MoD20	Kim, B.	TuD54
Kamada, S.	TuE25	Kim, Y.S.	Fac.
Kamijo, N.	ThD32	Kim, S.H.	TuD48
Kamiya, N.	TuD31	Kim, H.	Fac.
Kamiya, Y.	TuE24, TuE26, TuE32	Kim, K.J.	Inv. (ThA)
Kanazawa, K.	TuE25	Kimura, A.	MoD57
Kaneda, T.	TuE49	Kimura, S-I.	MoD20
Kaneko, M.	Inv. (MoC)	Kimura, H.	TuE27, TuD31, TuE28, TuD63, TuD85, TuD62, ThD86
Kaneko, T.	ThD41	Kincaid, B.	TuE20
Kang, T.H.	TuD54	Kinder, S.H.	TuD46
Kanyo, M.	ThE20	Kinoshita, T.	ThD20
Kao, C.C.	MoE15, TuD30	Kirikova, N.Yu.	MoE24
Kaprolat, A.	MoE36, MoE37	Kirkland, J.P.	MoD43, TuD33, ThD34
Karlin, B.A.	TuD52	Kirz, J.	MoD44, MoD46
Karnaukhov, I.	TuE61, TuE62	Kishi, K.	MoD73
Kashihara, Y.	TuD31, TuD63, ThD86	Kishimoto, S.	ThE15
		Kitajima, Y.	MoD45

Kitamura, H.	TuE18, TuE28, TuD29, TuE29, TuD31, TuE36, TuD62, TuD63, TuE60, TuD85	Kramer, S.L.	TuE33
Kivimaki, A.	TuD2	Krasnoperova, A.	ThD98, ThD101
Klein, M.P.	ThD43	Krinsky, S.	Inv., TuE14
Kleman, K.	ThD7	Krisch, M.	TuD30
Klimenko, V.E.	MoE24	Krisch, M.	MoE15
Knapp, G.S.	ThD35, TuD34, ThD58, MoD52, MoD1, ThD11,	Kronenburg, M.	TuD78
Ko, C.H.	MoD46	Kroth, U.	ThE22
Kobayakawa, H.	TuE18	Krumrey, M.	ThD57, ThD16, TuD36, ThD39, ThD38, ThD84, ThD77
Kobayashi, M.	MoE41, TuE25	Krui, T.L.	TuD41
Kochubey, V.I.	ThE18	Kubo, T.	TuE25
Kodera, I.	TuE50	Kudo, H.	TuE26
Koeda, M.	ThD25	Kudo, Y.	MoD47
Kohagura, J.	ThE4, ThE14, ThE16	Kulipanov, G.N.	MoD50, ThD40, MoD49, TuE14, ThE18, TuE40, MoD67
Kohler, T.	Inv. (TuB)	Kunieda, H.	ThD25
Kohmura, Y.	ThD86	Kuntze, R.	MoE3
Kohzu, H.	TuD32	Kunz, K.	Inv. (ThA)
Koide, T.	TuE30	Kupper, W.	ThE23
Koike, M.	ThE36, ThD37	Kuroda, K.	ThD41
Kojima, S.	MoD47	Kuroda, M.	ThD86
Kolber, Z.S.	TuE33	Kurokawa, S.	TuE25
Kolesnikov, K.A.	MoD19	Kushnir, V.I.	ThD56
Kolobanov, V.N.	MoE24	Kushnir, V.I.	MoE23
Komiya, S.	MoD29	Kuzay, T.M.	TuD41, TuD8, TuD92, TuD47, TuD11, TuD67, ThD89, TuD68, TuD66, TuD79, ThD90, ThD91, TuD69
Kondoh, T.	ThE4, ThE14,	Kuzin, M.V.	MoD19
Konishi, H.	TuD35	Kvick, A.	TuD36, TuD59, ThD77
Konishi, T.	TuD62	Labergerie, D.	ThD78
Kononenko, S.	TuE61, TuE62	Lacoursiere, J.	MoE26
Koo, Y.M.	TuE40	Laderman, S.S.	Inv. (MoC)
Koppe, H.M.	MoE18	LaFontaine, B.	MoD95, TuE34
Korchuganov, V.	Fac., TuE31	Laggner, P.	TuD3
Korde, R.	ThE17	Lai, B.	TuE23, TuE5, ThD101, ThD98, TuD67, MoD68
Koronkevich, V.P.	ThD40	Laissue, J.A.	MoD68
Kortright, J.B.	Inv. (MoC), TuE6, MoE32	Lama, F.	TuD37
Koseki, T.	TuE32, TuE24, TuE26, MoE41	Lamble, G.M.	MoD51
Kouchi, N.	ThD28		
Kovalchuk, M.V.	MoD42, MoD48, MoD81		
Kovantsev, V.E.	MoD43		
Kownacki, P.	TuE22		
Koyama, A.	TuD27		

Lammert, H.	ThD42	Lowrey, W.H.	ThD21
Lang, J.C.	MoE21	Lu, E.	MoD89
Lange, A.	MoD70	Lu, E.D.	TuD84
Langer, R.	ThE23	Luciani, L.	ThD98, ThD101
Larsson, C.	TuD45	Ludewig, R.	ThD51
Latimer, M.J.	TuD90, ThD43	Lyakh, V.V.	ThE18
Lau-Frambs, A.	ThE22	Lysenko, A.P.	TuE1
Lauriat, J.P.	MoD97	Ma, Y.	MoE22, MoE29
Lausi, A.	TuD15, ThD6, ThD9,	MacDonald, C.A.	ThE29
Lavender, W.	MoD8	MacDowell, A.A.	MoD95, ThD82
Lavollee, M.	MoE40	MacDowell, A.	TuE34
Lawton, R.	ThE9	MacKay, J.	ThE17
Lee, P.L.	MoD36, MoD52	Macrander, A.T.	MoE23, ThD8
Lee, K.B.	TuD54	Madden, M.	Inv. (MoC)
Lee, T.N.	Fac.	Maeda, T.	MoD34, MoD73
Lee, K.-B.	TuD39	Maezawa, H.	ThE4, ThE14, ThE16
Lee, W.K.	ThD2	Mahadev, V.	MoD54
Lee, C.-H.	TuD75	Makarov, O.A.	MoD50, ThE18,
Lee, K.-D.	TuD76		MoD49, ThD40, ThE7
Legrand, F.	MoD69, MoE47	Makhov, V.N.	MoE24
LeGrand, A.D.	TuD38	Malck, C.K.	ThD38
Leonard, G.A.	Inv. (MoB)	Malgrange, C.	MoE25, MoE13
Lequien, S.	TuD40, ThD74	Malic, R.A.	ThD62
Lesimple, F.	TuD40	Malloy, N.	MoD24
Lessmann, A.	MoD53	Malyshev, O.B.	TuE1
Levender, W.M.	MoD24	Mancini, D.C.	ThD44, ThD31
Levichev, E.	TuE31	Mangano, J.	MoD24
Levine, Y.K.	TuD78	Manion, S.	MoD94
Lewin, D.	MoD23	Mant, G.R.	MoD2, MoD3
Li, Y.	MoD90, TuD68,	Marcelli, A.	TuE35
	TuD66, TuD69	Marchang, S.A.	TuD4
Li, C.	TuD82	Mardalen, J.	TuD91
Lidia, S.	TuE6, TuE7	Marechai, X.	TuD63
Liedl, G.L.	MoD54	Marechal, X.M.	TuE36
Lin, H.-F.	TuD13, TuD14, TuD76	Marechal, X.	TuE28, ThD29
Lin, H.-J.	TuD14	Margaritondo, G.	ThD93
Lin, L.	TuD4	Marioge, J.P.	ThD54
Linderholm, J.	TuD59	Marks, S.	TuE37, TuE20, TuE22,
Lindgren, L.J.	TuE2		TuE21, TuE19, TuE16
Lindle, D.W.	TuD51, TuD52	Martini, M.	ThE26
Lippert, M.	Inv. (TuB), MoE35	Martoglio, P.A.	Inv. (MoC)
Liu, J.Y.	MoE17	Maruyama, A.	TuE50
Liu, G.	TuD28	Masami, A.	TuE58
Liu, C.	TuD41	Mason, B.	ThD7
Lizzit, S.	TuD1	Masuda, K.	ThE28
Lohmann, M.	MoD32, ThE23	Masuda, T.	TuE48
Longo, R.	MoD7	Masui, S.	Fac.

Materlik, G.	MoD61, MoD53, MoE14, TuD20, Inv. (TuC), TuD17, ThD69	Mishnev, S.I.	MoD50
Matsubayashi, N.	TuD65	Misu, A.	MoE41
Matsuda, K.	ThD19	Mitani, S.	ThD66
Matsuda, T.	TuE50	Mitrovic, V.	TuE3
Matsumura, T.	Inv. (MoC)	Mitsubishi, T.	TuE25
Matsuoka, S.	ThD86	Mitsunobu, S.	TuE25
Matsushita, T.	MoD47	Miyahara, T.	MoE9, TuD29, TuE30, MoD39, MoE19, ThD47, MoE27, E27
Matteucci, M.	TuD53	Miyahara, S.	ThE4, ThE14
Mayama, K.	TuE27	Miyamoto, M.	MoD62
Mazzaro, I.	TuD73	Miyano, K.E.	TuD4
Mazzolini, F.	TuD1, TuD42, ThD93	Miyata, H.	MoD30
McClain, D.B.	TuD43	Miyazaki, K.	Inv. (MoC)
McClain, D.	TuD88, ThD52	Miyoshi, S.	ThE14, ThE4
McCutcheon, S.	MoD16	Mizogawa, T.	ThE28
McKinney, W.R.	ThD24, ThD45, ThD21	Mizuno, H.	TuE25
McKinney, W.	TuE37	Mizutani, T.	TuD72
McMillin, P.	TuD44	Mochizuki, T.	ThD48
McNulty, I.	MoD55, ThD97, ThD95, TuD83	Mochrie, S.G.J.	MoE7
McSweeney, S.	ThD50, Inv. (MoB),	Moller, T.	TuD45
McSweeney, S.M.	TuD46	Molodkin, V.	TuE61, TuE62
Medvedko, E.	TuE14	Momose, A.	MoD56
Melczer, M.E.	TuE38	Moncton, D.E.	Inv. (WeA)
Melpignano, P.	ThD30, TuD1	Montano, P.A.	ThD11, TuD87, TuD55, TuD26, ThD58, ThE19
Menk, R.H.	ThE23	Monteleone, D.C.	TuE33
Mercier, R.	ThD54	Moog, E.G.	TuE41
Meron, M.	ThD46, MoE33	Moog, E.R.	TuD87
Meshkovsky, I.	ThD12	Mooney, T.	ThD1
Methel, U.	ThD71	Moor, E.R.	TuE10
Meyer, M.	ThE24, MoE26	Mori, T.	ThD49, TuD32, TuD72
Meyer, G.	TuD20	Mori, K.	MoD41
Mezentsev, N.A.	ThE7, TuE40, MoD19, TuE39, MoD77	Morikawa, E.	TuD4, ThD68
Mezentseva, L.A.	ThD40, MoD49, MoD50	Morin, P.	MoE26, MoE40
Middleton, F.	ThD7, MoE46	Morioka, Y.	ThD28
Mikado, T.	TuE48	Moriyama, H.	TuD31
Mikhailin, V.V.	MoE28, MoD67	Moryakov, V.P.	MoE28
Mikheeva, M.N.	MoE28	Mossessian, D.	ThD45, TuE16, TuD80
Miki, K.	TuD31	Motohashi, H.	TuD35
Mills, D.M.	ThD2	Mueller, B.	ThD94
Milne, J.C.	ThE25	Mulhaupt, G.	Inv. (WeA)
Milyokhin, A.G.	MoD49	Muller, B.R.	MoE10
Mimashi, T.	TuE25	Muller, N.	MoE3
Minamihara, Y.	TuE19	Muller, P.	ThD84
		Murata, T.	MoD57

Murray, J.E.	ThD29	Nishimura, K.	TuE54
Murray, P.K.	TuD91	Noma, T.	MoD30
Muto, S.	TuD29, MoE27	Nommiste, E.	TuD2
Mystykov, A.	TuE61	Nordgren, J.	MoD16, ThD44,
Mytnichenko, S.V.	MoD11		MoE29
Naday, I.	ThE20	Novikov, D.V.	MoD61
Nagafuchi, T.	TuE49	Novikova, N.N.	MoD48
Nagano, T.	ThD25	Nucara, A.	TuE35
Nagasawa, H.	ThD86	Nyholm, R.	MoD38, ThD44,
Nagatsuka, T.	TuE26		ThD31
Naito, H.	TuE54	O'Hare, D.	MoD13
Nakagawa, A.	Inv. (MoB)	O'Mara, D.	ThE20
Nakagawa, K.	MoD20, MoD57,	Ogata, A.	TuE25
	TuD81, TuE50	Ogata, C.M.	MoD52
Nakajima, T.	MoD59, MoD58	Ohara, S.	MoD20
Nakajima, K.	TuE25	Ohgaki, H.	TuE48
Nakamura, N.	TuE25, TuE26, TuE18	Ohmasa, M.	MoD62
Nakamura, E.	ThD20	Ohmi, K.	TuE25
Nakamura, S.	TuE50	Ohno, H.	TuD35, MoD79,
Nakamura, A.	TuD62		ThD80
Nakanishi, T.	TuE51, TuE50	Ohsumi, K.	MoD62
Nakasako, M.	TuD85	Ohtomo, K.	ThD39, ThD16,
Nakata, S.	TuE50		ThD27, TuD63,
Nakatani, T.	MoE9		ThD86, ThD85
Namioka, T.	ThD37	Oikawa, Y.	TuD62
Namkung, W.	Fac.	Oishi, N.	TuE50
Naumov, I.V.	MoE28	Oku, Y.	MoD63
Nave, C.	ThD50, TuD46	Okuda, S.	TuE50
Naves de Brito, A.	TuD2	Okui, K.	ThD86
Nazin, V.G.	MoE28	Olivi, L.	TuD15
Nazmov, V.P.	ThD40, MoD50,	Onuki, H.	MoD92, MoE42,
	MoD49		MoE33
Nelson, T.	ThD7, MoE46	Osborn, K.	TuD4
Nemoshkalenko, V.	TuE61, TuE62	Osipov, V.N.	TuE1
Nesterov, S.I.	MoD19	Otoda, N.	MoD57
Neumann, H.B.	Inv. (TuB), MoE35	Ottaviani, C.	TuD53
Ng, W.	MoD60	Oura, M.	TuD62, ThE28
Nian, H.L.T.	TuD92, TuD47	Oversluizen, T.	TuD30, TuD83
Nian, T.	TuD11, TuD8, TuD68,	Padmore, H.	TuE37, TuE16, TuD80
	TuD69	Padmore, H.A.	--TuD48, TuE55, MoD80
Nield, A.	MoD13	Pahl, R.	MoE30
Nielsen, W.	TuD41	Panchenko, V.E.	ThE10, ThE11, TuD49
Nielsen, M.	ThD65	Paolucci, G.	TuD1
Nikitenko, S.G.	ThE21	Park, Y.-J.	TuD39
Nikulin, A.Yu.	MoD83	Park, S.Y.	MoE27, TuD29
Ninomiya, K.	MoD25	Park, B.-J.	TuD39
Nishijima, A.	TuD65	Parkinson, W.H.	ThD29

Parry, R.	TuD8	Prokopenko, V.S.	MoD50
Pattison, P.	TuD91	Prosperi, T.	TuD37
Paul, D.F.	TuD50	Pugliese, R.	TuD1
Pauschinger,	ThD51	Pustovarov, V.A.	MoD67
Pearson, D.	ThE17	Qian, S.	ThD55
Peatman, W.	TuE17	Qian, S.N.	TuD1
Peatman, W.R.	ThD42	Quaresima, C.	TuD53
Peatman, W.B.	ThD71	Quimby, D.C.	TuE15, TuE45
Perera, R.C.C.	TuD51, MoD37, TuD52	Quimby, D.C.	TuE44
Perfetti, P.	TuD53	Quinn, F.M.	MoE31
Petersen, H.	TuD64	Quintana, J.P.	ThD56, ThD57
Peterson, M.	Inv. (MoB)	Rabedeau, T.	TuD10
Petrov, S.	TuE14	Rabus, H.	ThE22
Pflibsen, K.P.	TuD88, ThD52, TuD43	Rah, S.-Y.	TuD39
Pflugger, J.	TuE42	Rah, A.Y.	TuD54
Philipchenko, A.	TuE31	Rakowsky, G.	TuE14
Phillips, W.C.	ThE20	Ramanathan, M.	ThD11, TuD55, ThD58, TuD26, TuD87
Phizackerley, P.	ThE20	Ramirez, G.	TuE4
Piacentini, M.	TuD37	Randall, K.J.	TuD56, TuD83
Pianetta, P.	Inv. (MoC), MoD94	Rarback, H.	MoD65
Pickering, I.J.	ThD94	Rathbone, T.	MoD14
Pifferi, A.	TuD15	Redin, O.A.	MoD50
Pinayev, I.V.	TuE43	Reffner, J.A.	Inv. (MoC)
Pindak, R.	MoE7	Reime, B.	MoD32, ThE23
Pindyurin, V.F.	MoD49, ThE7, ThE8, ThD40, MoD19, ThE18, MoD50	Reininger, R.	ThD59
Pipersky, P.	TuE21, TuE20, TuE19	Rek, Z.U.	ThD94, ThD63
Pizzini, S.	Inv. (TuC), MoE25	Rey-Bakaikoa, V.	TuD57
Plate, D.	TuE19, TuE20	Reznikova, E.F.	MoD50
Plodstrom, A.	MoD38	Rice, M.	TuE6, MoE32
Polack, F.	ThD53, ThD54	Riechert, H.	MoD53
Polewski, K.	TuE33, MoD96	Rieck, A.	TuD45
Polian, A.	Inv. (TuC)	Riekel, C.	MoD20
Poloni, C.	TuD21, ThD99	Rinaldi, S.	TuD53
Ponomarev, S.	ThE2	Rivers, M.	MoD44, ThD96
Popik, V.	TuE14	Rivers, M.L.	MoD65, MoD64
Popik, V.M.	TuE43	Robinson, I.K.	MoE7, TuD59
Poropat, P.	MoD7	Robinson, K.E.	TuE15, TuE45, TuE44
Portalone, G.	TuD15	Robinson, A.	TuD48
Portmann, G.	TuE20	Robinson, A.W.	TuD58
Poulsen, H.F.	Inv. (TuB), MoE35	Rode, A.V.	ThD60
Pradervand, C.	TuD38, TuE47	Rodricks, B.	ThE19, MoD66
Prat, A.	MoD97	Rogalev, A.L.	MoD67
Price, D.L.	MoD1	Rogers, G.	ThD7
Prince, K.	TuD53	Rogers, C.S.	ThD35, ThD61
		Rojsel, P.	TuE2
		Rompel, A.	ThD43

Roper, M.	MoD80	Savoia, A.	TuD15, TuD53, TuD1, ThD5, ThD93
Rosei, R.	MoD7, TuD1, ThD93	Sawatzky, G.A.	Inv. (TuA)
Rosenbaum, G.	ThE12, TuD60	Scalia, K.	MoD24
Ross, S.	ThE20	Schaefers, F.	ThD94
Rotenberg, E.	MoD16	Schafers, F.	MoE10, TuD64
Roth, M.	ThD15	Schell, N.	MoE37
Rousseau, J.	MoD90	Schenk, H.W.	ThE23
Rowe, J.E.	ThD62	Schildkamp, W.	ThD46, TuD38, ThD96, ThD67, TuE47
Rowen, M.	ThD63, ThD94	Schildwachter, L.	ThE23, MoD32
Ruan, Y.	TuD61	Schilling, P.	ThD68
Rubenstein, E.	MoD8	Schlueter, R.	TuE22, TuE20, TuE19, TuE21
Rust, C.	ThE23	Schmidt, H.-G.	TuD17
Rutt, U.	Inv. (TuB), MoE35	Schmidt, T.	Inv. (TuB), MoE35
Ruvinsky, S.G.	TuE40	Schneider, J.R.	Inv. (TuB), MoE35
Ryan, A.J.	MoD3	Scholze, F.	ThD84
Ryce, S.	TuD52	Schroeter, Th.	TuE17
Ryding, D.	TuD66, TuD68, TuD69	Schulke, W.	MoE36, MoE37
Sabersky, A.	TuD10	Schulte-Schrepping H	TuD17, ThD69
Sabine, T.M.	MoD22	Schulze, C.	MoD8, ThD70
Saboungi, M.-L.	MoD1	Schulze, D.	MoD71
Saffarnia, A.	TuE38	Schuster, M.	MoD53
Sairanen, O.-P	TuD2	Schwegle, W.	TuD36
Saito, T.	MoE33, TuE54	Seddon, E.A.	MoE31
Saitoh, Y.	ThE14, ThE4	Sekiguchi, T.	MoD74
Sajev, V.	TuE31	Sekitani, T.	MoD74
Sakabe, K.	Inv. (MoB)	Senf, F.	ThD3, ThD42, TuD64 ThD71
Sakabe, N.	TuD81, Inv. (MoB)	Sergo, R.	TuD1
Sakae, H.	TuD62	Sessa, M.	MoD7
Sakai, K.	ThD20, MoD20	Sette, F.	MoE15
Sakai, N.	TuD63	Setterston, T.	ThD57
Sakamoto, Y.	ThE4	Severson, M.C.	ThD59
Sakanaka, S.	TuE25	Shaftan, T.V.	TuE43
Sakata, O.	MoD26	Sham, T.K.	MoE16
Sakurai, Y.	TuD27, TuD62, TuD63	Shang, L.	MoD88
Samant, M.G.	MoD37	Shastri, S.D.	MoE38
San Miguel, A.	Inv. (TuC)	Shastri, S.	Inv. (TuB)
Sanchez del Rio, M.	TuE35, ThD65, ThD64	Shcherbakov, A.	TuE61, TuE62
Sanchez, T.	TuD70	Shen, Q.	Inv. (TuB), MoE38
Sandrin, G.	TuD42, TuD1	Sheng, I.C.	TuD92
Sano, K.	ThD25	Sheng, W.	TuD82
Sasaki, K.	Inv. (MoB)	Shenoy, G.K.	TuD87
Sasaki, S.	TuD32, ThD49, TuD72, TuE46, MoE34	Shepel, G.T.	MoD67
Sasaki, Y.	TuE49	Sheromov, M.A.	ThD14, MoD77
Sasano, T.	ThD66		
Sato, K.	ThE4, ThD25, ThE14		
Sato, T.	TuD65		

Sheu, H.S.	MoE17	Snigirev, A.	MoD69, TuE53
Shi, C.	TuD86	Snigireva, I.	MoD69, TuE53
Shidara, T.	TuE30	Soda, K.	MoD20
Shimada, H.	TuD65	Sohn, Y.U.	TuE40
Shimazaki, A.	Inv. (MoC)	Sokolov, A.S.	TuE43
Shimomura, O.	MoD10, MoD79	Solak, H.	MoD60, ThD93
Shin, S.	MoE39	Song, Y.-F.	TuD13, TuD14, TuD76
Shinoe, K.	TuE26	Sospheonov, A.N.	MoD48
Shinohara, K.	MoD39, MoD79	Sostero, G.	TuD1
Shiotani, N.	TuD63	Soullie, G.	MoD69, ThE31
Shioya, T.	TuE60	Spagna, R.	TuD15
Shiwaku, H.	ThD80, TuD62	Spanne, P.	MoD68
Shkaruba, A.	TuE40	Spector, S.	TuE34, ThD82
Shkaruba, V.A.	TuE39	Srajer, G.	MoE21
Shleifer, M.	MoD18	Staicu, F.A.	MoD18
Shlezinger, M.	ThD92	Stanton, M.	ThE20
Shpak, A.	TuE61, TuE62	Staudenmann, J.-L.	TuD12
Shu, D.	TuD5, TuD11, TuD47, TuD8, TuD41, TuD92, TuD70, TuD68, TuD66, TuD69, TuD67	Stavola, T.	MoD8
Shuh, D.K.	MoD37	Stemmler, P.	MoE47
Shuh, D.	MoD16	Stephenson, G.B.	MoE7
Siddons, D.P.	TuD30, ThD72, MoD90, MoD93	Stephenson, J.D.	MoD70, ThD76
Simmons, R.O.	MoE37	Stevenson, A.W.	MoD83
Simon, M.	MoE26, MoE40	Stohr, J.	MoD37
Simon, J.P.	ThD15	Stott, J.P.	TuD18
Singh, S.	MoD60	Stowe, T.	MoD94
Sinkovic, B.	Inv. (TuC)	Stuppi, A.	ThD52
Sinyukov, M.P.	MoD49	Sturhahn, W.	ThD1, MoD76, ThE27
Sivananthan, S.	ThE19	Subbotin, A.N.	ThE7, ThE8
Skrinsky, A.N.	MoD50	Suchorukov, A.V.	MoD78
Skytt, P.	MoD16, MoE29	Suga, S.	MoE9
Slatkin, D.N.	MoD18, MoD68	Sugiyama, S.	TuE48
Smith, G.C.	ThE25, ThE3	Sugiyama, H.	TuD89
Smith, R.	Inv. (MoC)	Sugiyame, H.	ThD48
Smith, W.	MoD2, TuD6	Sukhanov, S.V.	TuE39, TuE40
Smith, W.S.	TuD4	Sukhorukov, A.V.	MoD21
Smith, P.L.	ThD29	Suortti, P.	TuD71
Smith, N.V.	ThD62	Susini, J.	ThD78, ThD79, ThD77
Smith, A.D.	ThE26	Sutherland, J.C.	TuE33, MoD96
Smither, R.K.	ThD73	Sutton, M.	MoE7
Snell, G.	MoE3	Sutton, S.R.	MoE2, MoD71, MoD64, MoD65
Snider, R.	ThE4	Suvorov, A.Y.	ThD74
Snigirev, A.A.	ThD74, ThD75	Suvorov, A.	MoD69
		Suzawa, C.	TuE48
		Suzuki, T.	MoD58
		Suzuki, H.	MoD58, MoD58, TuE49
		Suzuki, I.H.	ThD36

Suzuki, Y.	ThD32, MoD72	Thissen, R.	MoE40
Suzuki, M.	ThE28, MoE41	Thomlinson, W.	MoD8, MoD18, MoD24
Suzuki, C.K.	ThD80	Thompson, A.	ThE13, TuD46
Svatos, J.	ThD53	Thompson, A.C.	MoD24, TuD48, MoD8
Svensson, S.L.	ThE13	Thompson, A.W.	Inv. (MoB)
Svishchev, A.V.	MoE28	Thorne, A.P.	ThD29
Syrejshchikova, T.I.	MoE24	Thornton, G.	TuD58
Tafelmeier, U.	ThE23	Tinone, M.C.K.	MoD74
Takacs, P.Z.	ThD55	Tissot, G.	ThD54
Takagi, Y.	TuD32, TuD72	Tobin, J.G.	MoD16
Takaki, H.	TuE26	Tobiyama, M.	TuE25
Takaura, N.	Inv. (MoC)	Toellner, T.	ThD1, ThE27, MoD76
Takeda, T.	MoD34, MoD56, MoD73, TuE54	Tokumori, K.	TuE54
Takehira, K.	TuD65, ThD81	Tokunaga, T.	MoD71
Takeuchi, T.	TuE50	Tolentino, H.	Inv. (TuC), TuD73, ThD68
Tamano, T.	ThE4, ThE14, ThE16	Tolochko, B.P.	MoD21, MoD78, MoD77
Tamura, S.	ThD32	Tomimori, H.	ThD66
Tamura, K.	MoD33	Tomita, H.	MoD29
Tan, Z.	MoD95, ThD82	Tommasini, R.	TuD1
Tanaka, T.	TuE29, TuE36, TuE28	Tompkins, W.	Inv. (MoC)
Tanaka, N.	TuD31	Tonner, B.P.	MoD16, MoD17, Inv. (MoC)
Tanaka, S-I.	MoD20	Tonnessen, T.W.	ThD21
Tanaka, S.	ThE4	Tornevik, C.	MoD38
Tanaka, H.	TuE51, TuE50	Towns-Andrews, E.	MoD2, TuD6
Tanaka, K.	MoD74, TuD65	Toyofuku, F.	TuE54
Tanaka, T.	TuD85, ThD63, ThD94	Toyomasu, T.	TuE24
Tanaka, Y.	TuD63	Toyoshima, A.	TuD65
Tang, E.	Fac.,	Trakhtenberg, E.	TuD87, TuE14, TuD74
Tani, N.	TuE49	Trebes, J.	MoD55
Tarasenko, A.	TuE62	Treusch, R.	TuD17, Inv. (TuC)
Tarasov, Y.F.	MoE28	Tromba, G.	MoD7
Tarazona, E.	TuE53, TuE52	Trunk, G.	TuE33
Taub, H.	MoE11, MoD87, MoD86	Trunk, J.G.	MoD96
Taylor, G.N.	MoD95	Trzeciak, W.S.	ThD59
Taylor, D.	ThD82	Tsang, K.-L.	TuD14, TuD13, TuD76, TuD75
Tcheskidov, V.	TuD70	Tschentscher, Th.	TuD71
Tegeler, E.	ThE22	Tseng, P.-C	TuD13, TuD14, TuD76
Teichmann, T.	ThD69	Tsetlin, M.B.	MoE28
Tejima, M.	TuE25	Tsheskidov, V.	TuD69
Templer, R.	Inv. (FrA)	Tsuchiya, K.	TuE60
Tennant, D.M.	MoD95	Tsukishima, C.	TuE50
Tennant, D.	ThD82	Tsuruda, H.	ThE20
Terminello, L.J.	MoD37		
Tezuka, Y.	MoE39		
Thiel, D.J.	Inv. (ThA), MoD75		

Tudor, M.	TuD1	Vobly, P.D.	TuE39
Turner, L.	TuE14	von Zimmermann M.	MoE35, Inv. (TuB)
Turner, L.R.	TuD87	Vorobyov, P.V.	TuE43
Uchida, A.	MoD34	Wagener, M.	ThE23
Uchida, F.	MoD72	Wakabayashi, K.	ThE1
Udron, D.	TuD73	Walenta, A.H.	ThE23
Ueki, T.	TuD31, ThE1, ThD86, TuD85	Walker, R.P.	TuE11
Ueyama, Y.	TuE49	Walko, D.A.	MoE38
Ukai, M.	ThD28	Wallace, J.	ThD93
Ulm, G.	ThE22, ThD84, ThD83	Wallace, J.P.	ThD88
Umesaki, N.	MoD79	Walter, R.L.	MoD75
Umezawa, K.	MoD43	Wang, C.	TuE16
Underwood II, J.	ThD43	Wang, J.	MoD39, TuD29, MoE19
Underwood, J.H.	ThD3, MoE10	Wang, Z.	TuD8, TuD79, ThD89, ThD90, ThD91
Urakawa, S.	MoD79	Wang, S.K.	MoE11
Uruga, T.	TuD31, TuD85, ThD86, ThD85	Wang, K.	TuD82
Usami, H.	TuE48	Wang, W.	TuD82
Ushakov, V.	TuE31	Wang, G.Q.	MoD88
Usov, Yu.	ThE2	Wang, Q.P.	TuD84
Usui, T.	TuD62	Wang, Q.	ThD100
Uyama, C.	TuE54	Warwick, A.	TuE16
Vacchi, A.	MoD7	Warwick, T.	MoD17, MoD16, ThD92, TuE56, TuD80, Inv. (ThA)
Vacinova, J.	MoD97	Waskiewicz, W.K.	ThD82
Valla, A.S.	TuE45	Wassdahl, N.	MoE29, ThD44
van der Heide, U.A.	TuD78	Watanabe, M.	ThD20, ThD19, MoE16
van Silfhout, R.G.	TuD77	Watanabe, N.	MoD39, TuD81, Inv. (MoB)
van Dorssen, G.E.	TuE55, MoD80	Watanabe, T.	MoD31, MoD82
VanGorden, S.	ThE29	Weber H.-P.	TuD91
Vartanyants, I.A.	MoD81	Wehlitz, R.	MoE3
Vasillev, A.N.	MoD67	Wei, W.	TuD82
Vasserman, I.	TuE14, TuE10, TuE41, TuE42	Weigelt, J.	TuD20
Vasserman, I.B.	TuD87	Welnak, J.T.	ThD88
Velikzanin, Yu.	ThE2	Welnak, J.	ThD93
Vest, R.	ThE17	Wende, B.	ThD83
Vest, R.E.	ThD87	Wentink, R.F.	ThE29
Vettier, C.	MoE25, MoE13	Werin, S.	TuE2
Via, G.H.	ThD94	Westbrook, E.M.	ThE20, TuD60
Viefhaus, J.	MoE3	Westbrook, M.L.	ThE20
Vinokurov, N.	TuE14	Wherry, D.C.	Inv. (MoC)
Vinokurov, N.A.	TuE43	White, D.	TuE34
Visintin, A.	TuD21, ThD99	White, J.	ThD57
Visser, G.	MoD16	White, D.L.	MoD95, ThD82
Vivo, A.	ThD79		
Vlieg, E.	TuD78		

Wiley, C.L.	ThD35	Yamamoto, S.	TuD29, TuE60
Wilkins, S.W.	MoD22, TuD23, TuD22, MoD83	Yamaoka, H.	TuD31, ThD39, ThD16, ThD27, ThD86, TuD85, ThD85, TuD63
Will, G.	MoD84	Yamashita, K.	ThD25
Williams, S.	MoD44, MoD9	Yamazaki, T.	ThD25, TuE48
Williams, G.P.	Inv. (MoC), TuD9, TuE4, MoD85	Yanagihara, M.	TuE27, MoE43
Windt, D.L.	ThD82	Yang, L.	ThD101, MoD55, TuD83, ThD97
Winick, H.	TuE57	Yang, F.	MoD89
Wirick, S.	MoD44	Yang, B.	ThD96
Wobly, P.D.	TuE40	Yaoita, K.	MoD10
Wohlert, F.	MoE36	Yatsu, K.	ThE16, ThE14, ThE4
Woicik, J.C.	TuD52	Yeh, F.	MoD90
Wolfers, P.	MoD97	Yoda, Y.	ThD48, ThD80
Wong, J.	MoE12, ThD94, ThD63	Yokomizo, H.	TuE49
Wood III, O.R.	MoD95	Yokoyam, A.	TuD35
Wood, O.	TuE34	Yonehara, H.	TuE49
Wood II, O.R.	ThD82	Yoo, S.S.	ThE19
Wrulich, A.	Inv. (WeA)	Yoshimura, Y.	TuD65
Wu, X.Y.	MoD18	Yoshino, K.	ThD29
Wu, J.	MoD34, TuD28	Yoshioka, K.	TuE25
Wu, Z.	MoD87, MoD86	Yoshizawa, M.	MoD59
Wu, J.	TuD82, MoD73	You, H.	TuD34
Wulff, M.	TuD38	Young, A.	TuE37
Wutz, C.	Inv. (MoC)	Yu, B.	ThE3
Xia, S.	TuE58	Yu, X.J.	TuD84
Xia, A.	MoD89	Yu.M.	MoE24
Xian, D.	Fac.	Yuasa, T.	MoD34, MoD73
Xiao, Y.	ThD101	Yun, W.	TuE23, ThD101, TuE5, ThD33, TuD68, TuD67, ThD98, ThD91
Xiao, Q.F.	MoD43	Yuri, M.	TuE30, MoD92, MoE42, MoE33
Xie, X.S.	MoD88	Yurkas, J.	MoD37
Xie, X.	TuD86	Zacchigna, M.	TuD53
Xu, Z.	TuD56, ThD95, TuD83	Zachmann, H.G.	Inv. (MoC)
Xu, S.	TuD74	Zanini, F.	TuD15, TuD1, TuD21, ThD99
Xu, S.H.	TuD84	Zarnowski, J.	ThE29
Xu, P.	TuD86, MoD89	Zarodyshev, A.V.	MoD49
Xu, P.S.	TuD84	Zelentsov, E.L.	MoD19
Yachandra, V.K.	ThD43	Zelinsky, A.	TuE61
Yagi, N.	ThE1	Zema, N.	TuD37
Yagi, K.	TuE59, MoE42	Zeschke, T.	ThD42
Yagishita, A.	ThE4, ThE16	Zhadenov, I.V.	MoE6
Yakimenko, M.N.	MoE24		
Yamada, H.	Fac.		
Yamada, T.	TuE50, MoD92		
Yamaguchi, N.	MoE41		
Yamamoto, M.	TuE27, TuD31, TuD85		

Zhang, J.	ThD17
Zhang, X.	MoD44, MoD6, ThD48, Fac., TuE58, MoD89
Zhang, W.	TuD28
Zhang, Y.	Fac., ThD100, TuD86
Zhang, L.	ThD78
Zhang, X.W.	ThD80
Zhang, J.Y.	MoD88
Zhao, J.	ThD48
Zhao, Y.F.	MoD88
Zhao, F.	TuD82
Zhao, N.	TuD82
Zheludeva, S.I.	MoD48
Zheng, D.	TuD82
Zhou, L.	TuD4
Zinin, E.I.	MoD67, ThE30
Zolotarev, K.V.	ThD14
Zvezdova, N.P.	ThE18